Title
Proceedings of the XIVth Combustion Research Conference

Authors
Ashurts, W.T.
Barr, P.K.
Kerstein, A.R.
et al.

Publication Date
1992-06-01

LBL-32408
UC-401

XIVth Combustion Research Conference

Granlibakken Conference Center
Tahoe City, California

June 14–17, 1992

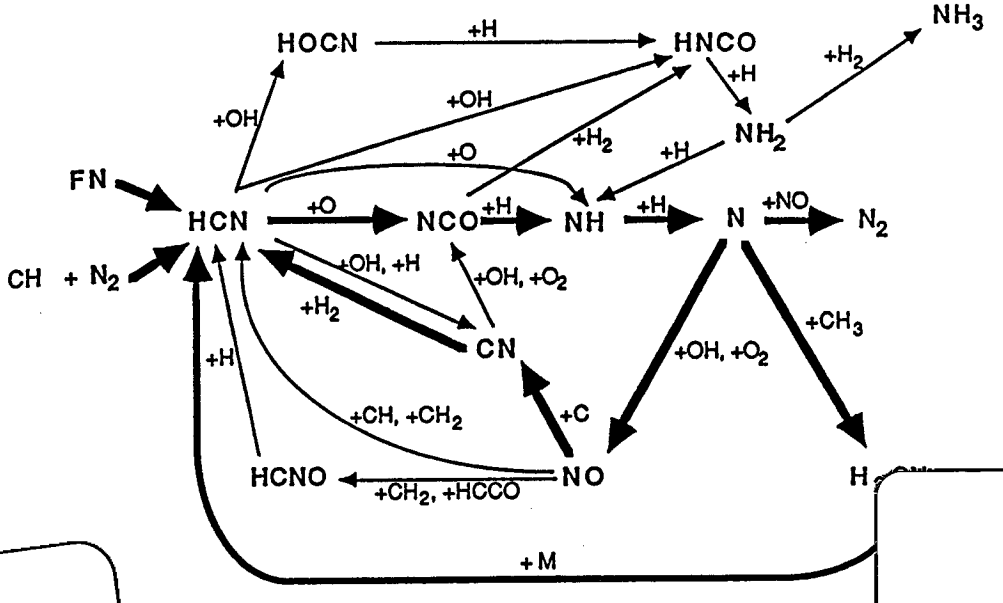

Sponsored by:
Division of Chemical Sciences
Office of Basic Energy Sciences
Department of of Energy

and

Chemical Sciences Division
Lawrence Berkeley Laboratory

DISCLAIMER

LBL-32408
UC-401

XIVth Combustion Research Conference

Granlibakken Conference Center
Tahoe City, California

June 14–17, 1992

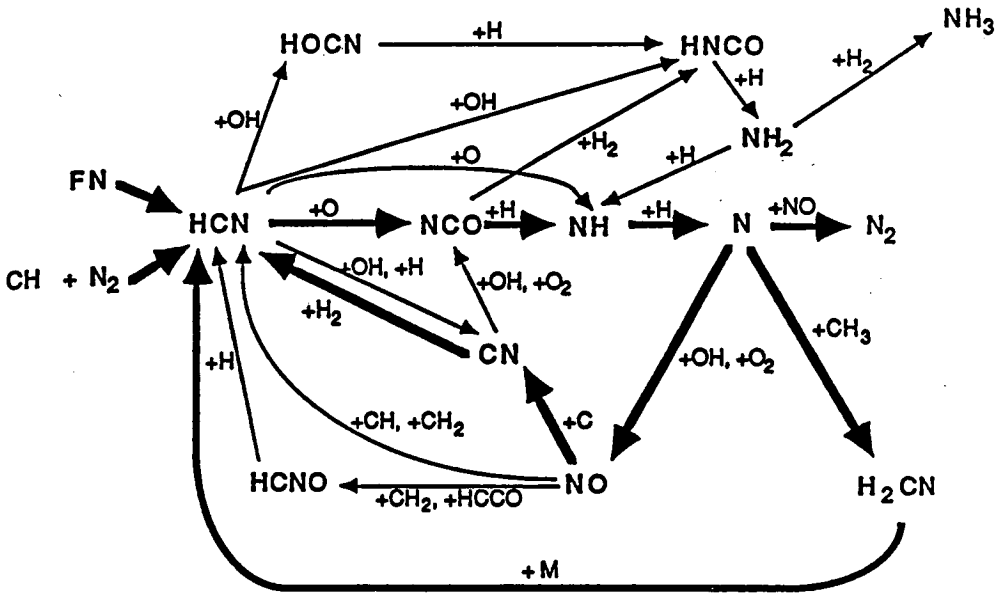

Sponsored by:
Division of Chemical Sciences
Office of Basic Energy Sciences
Department of of Energy

and

Chemical Sciences Division
Lawrence Berkeley Laboratory

FOREWORD

The Fourteenth Combustion Research Meeting is being hosted this year by the Chemistry Division, Lawrence Berkeley Laboratory and held from June 14, 1992, through June 17 at the Granlibakken Conference Center, Tahoe City, California.

As in the past, the purpose of this meeting is to foster collaboration, cooperation, and exchange of current research ideas among those grantees and contractors of the Chemical Sciences Division whose research is related to the general area of combustion. This meeting affords a singular opportunity for the scientific community most directly involved with the chemistry and dynamics underlying combustion processes to contribute to the evaluation and direction of the DOE basic research effort in combustion. Because the combustion-related effort of the Chemical Sciences Division covers a broad spectrum of activities ranging from direct work with combustion systems to theoretical aspects of chemical dynamics, this meeting brings together scientists who might not otherwise have occasion to communicate directly with each other. To this end, time that might have otherwise been assigned to additional presentations has been set aside for participants to discuss and plan work of mutual interest. To this end also, the extended abstracts are made available at the start of the meeting and serve in place of poster sessions.

It should be noted that the program this year includes abstracts and presentations by individuals supported by the Chemical Engineering Sciences Program of the Chemical Sciences Division. Research in this program is concerned primarily with interaction between chemistry and fluid flow in combustion.

This book of abstracts contains, in addition to the extended abstracts of all projects supported by the DOE Division of Chemical Sciences of the Office of Basic Energy Sciences and related to combustion, the agenda for the meeting and the list of invitees. The abstracts, including those corresponding to this year's formal presentations, are in alphabetical order according to principal investigator or, if more than one, by the name of the first author on the abstract.

The success of this meeting is due in large measure to your willingness to participate as speakers or to be present for discussions with those in the program who may need your particular expertise or viewpoint.

Special thanks are due to Daniel Neumark and Daina Tekorius of the Lawrence Berkeley Laboratory for the organization of this year's meeting.

William H. Kirchhoff
Fundamental Interactions Branch
Division of Chemical Sciences
Office of Basic Energy Sciences
U.S. Department of Energy

Monday Morning Agenda ***Daniel M. Neumark, Chair*** ***June 15, 1992***

7:30 am *Breakfast Buffet*

8:30 am Opening Remarks, William H. Kirchhoff

8:45 am Plenary Lecture, "Rationalizing Dissociation-Recombination Rate Data in Combustion: Where are the Problems?", Professor Jurgen Troe of the Institut für Physikalische Chemie der Universität Göttingen, West Germany

9:45 am *Break*

10:00 am "High Resolution Raman Spectroscopy of Complexes and Clusters in Molecular Beams", Peter M. Felker.....(89)

10:30 am "Time-Resolved Fourier-Transform IR Fluorescence Spectroscopy", Jack M. Preses.....(255)

11:00 am "Vacuum Ultraviolet Photoionization and Photodissociation of Molecules, Clusters, and Radicals", Cheuk-Yiu Ng.....(242)

11:30 am "A High Resolution Infrared Double Resonance Technique for Molecular Eigenstate Spectroscopy in a Free Jet", David S. Perry.....(247)

Monday Afternoon/Dinner Agenda ***June 15, 1992***

12:30 pm Luncheon at Squaw Valley (until 2:30?)

2:30 pm *Available for Informal Discussions*

5:30 pm *Refreshments available*

6:00 pm *Western Barbeque*

Monday Evening Agenda ***Henry F. Schaefer III, Chair*** ***June 15, 1992***

7:30 pm "Single-Collision Studies of Hot Atom Energy Transfer and Chemical Reaction", James J.Valentini.....(311)

8:00 pm "Quantum Dynamics of Fast Chemical Reactions", John C. Light .....(205)

8:30 pm "Time-Resolved Diode Laser Studies of Energy Transfer from Vibrationally Excited Molecules", Ralph E. Weston.....(325)

9:00 pm *Break*

9:15 pm "Theoretical Studies of the Dynamics of Chemical Reactions", Michael J. Davis...(314)

9:45 pm "Reactions of Small Molecular Systems", Curt Wittig.....(332)

10:15 pm Informal Discussion

Tuesday Morning Agenda ***Terrill A. Cool, Chair*** ***June 16, 1992***

7:30 am *Breakfast Buffet*

8:30 am "HTP Kinetics Studies on Isolated Elementary Combustion Reactions over Wide Temperature Ranges", Arthur Fontijn.....(101)

9:00 am "Comprehensive Mechanisms for Combustion Chemistry: Experiment, Modeling, and Sensitivity Analysis", Frederick L. Dryer .....(71)

9:30 am "Analysis of Forward and Inverse Problems in Chemical Dynamics and Spectroscopy", Herschel A. Rabitz.....(259)

10:00 am "Kinetics of Combustion Related Processes at High Temperatures", John H. Kiefer.....(170)

10:30 am *Break*

10:45 am "Shock Tube Studies of Fuel Pyrolyses", Ralph D. Kern, Jr.....(166)

11:15 am "Photochemical Reaction Dynamics", C. Bradley Moore.....(229)

11:45 am "Flash Photolysis-Shock Tube Studies of Bimolecular Reactions", Joseph V. Michael.....(218)

Tuesday Afternoon/Dinner Agenda ***June 16, 1992***

12:30 pm *Lunch (served until 1:30 pm)*

2:00 pm *Available for Informal Discussions*

5:30 pm *Refreshments available*

6:00 pm Banquet

Tuesday Evening Agenda ***George W. Flynn, Chair*** ***June 16, 1992***

7:30 pm "Investigation of Degenerate Four-Wave Mixing for Quantitative Detection of Nitric Oxide", Roger L. Farrow .....(85)

8:00 pm "Elementary Reaction Rate Measurements at High Temperatures by Tunable-Laser Flash-Absorption", Jan P. Hessler.....(144)

8:30 pm "Infrared Absorption Spectroscopy and Chemical Kinetics of Free Radicals", Robert F. Curl, Jr. and Graham P. Glass .....(63)

9:00 pm *Break*

9:15 pm "Laser Spectroscopy of Hydrocarbon Radicals", Peter Chen .....(44)

9:45 pm "Unimolecular Reaction Dynamics and Vibrational Overtone Spectroscopy of Highly Vibrationally Excited Molecules", F. Fleming Crim.....(56)

10:15 pm Informal Discussion Session

Wednesday Morning Agenda ***Hanna Reisler, Chair*** ***June 17, 1992***

Wednesday Afternoon Agenda ***June 17, 1992***

11:45 am *Lunch (served until 12:30 pm)*

TABLE OF CONTENTS

ABSTRACTS

Analysis of Turbulent Reacting Flows

W. T. Ashurst, P. K. Barr & A. R. Kerstein
Combustion Research Facility
Sandia National Laboratories
Livermore, California 94551-0969

Program Objective

Numerical simulations that treat one aspect of combustion in great detail, but treat other aspects more crudely, have been developed in order to highlight various aspects of combustion. Thus, the full computer power is devoted to a single feature in each model, and does that feature well, rather than poorly representing all features. *Direct simulations* of constant density Navier-Stokes turbulence are used to determine premixed flame geometry. *Vortex rings* are used to simulate the unsteady entrance flow in a pulse combustor and the impact of strain-rate quenching on premixed flame propagation is revealed in the heat release rate. *Front-tracking algorithms* applied to constant-speed propagation through idealized flow fields are used to confirm a scaling hypothesis concerning the turbulent burning velocity.

Our goal of detailed viewpoints of combustion will allow other researchers to focus their work based on insights gained from our work. In particular, our group has not yet included detailed chemical kinetics but our results point out which chemical-flow configurations are of interest in turbulent combustion. From detailed or reduced chemical analysis our specialized simulations could be extended beyond the current limitations.

Geometry of Premixed Flames in Three-Dimensional Turbulence

Constant density premixed flame propagation in three-dimensional Navier-Stokes turbulence has been simulated. A zero-thickness flame model with specified flame speed in terms of flame stretch has been used, as represented by the evolution of a continuous scalar G according to

$$\frac{\partial G}{\partial t} + \mathbf{u} \cdot \nabla G = u_F |\nabla G|.$$

As one possible choice for flame stretch we use $u_F = S_L \exp(-L_M \kappa)$ where S_L is the planar, laminar flame speed, L_M is the Markstein length and κ is the local flame stretch (strain rate plus curvature). Because the flame is a passive scalar, the continuous scalar G contributes statistical information on flame propagation at each numerical grid point within the computational domain. Thus, a small system of only 32^3 yields results comparable to larger systems in which a flame with finite thickness occupies only a small fraction of the total volume. Comparison of small-scale strain rate and shape of the strain rate tensor in this driven 32^3 system shows good agreement with previous results in larger systems of 128^3. The advantage of this constant energy simulation is that the statistics of flame propagation are gathered in a statistically steady turbulent flow.

From first and second spatial derivatives of the scalar G the two eigenvectors of curvature are determined at each grid point. The sampled distribution of curvature indicates vanishing probability for a spherical shape, finite probability for a saddle shape and the largest probability for a cylindrical shape.

The orientation, or alignment of the curvature eigenvectors is determined by taking dot products of unit vectors of the three components of strain rate and of the vorticity vector. Previous investigation of turbulence revealed that vorticity aligns with the intermediate strain rate direction, and the probability of alignment increases as the strain magnitude increases. The flame normal direction shows alignment with the most compressive strain direction, similar to that observed for diffusive, passive scalars in previous work. The flame curvature indicates alignment of the smallest curvature with the vorticity direction. Thus, when the flame surface has a cylindrical shape, the cylinder axis is in the direction of the vorticity vector. This occurs because the most intense vorticity has a rod-like shape and the flame surface becomes wrapped around the vortex rod.

The implication of this constant density flame propagation simulation is that realistic chemical reactions in a flame-vortex interaction may be simulated in two-dimensions and this configuration will represent a large fraction of flame geometry in three-dimensional turbulence. Furthermore, comparison of computed flame curvature in two and three-dimensional representations indicates that measurements in only a two-dimenisonal plane do yield a good statistical description of the actual flame curvature.

Future work will examine the effect of thermally induced density variations on flame geometry.

Vortex Simulation of Periodic Reacting Flow

The vortex technique has been used to simulate the periodic reacting flow that occurs in a pulse combustor. The vorticity introduced during injection dominates the flow field and so the vortex dynamics technique is ideally suited for this application. The pulse combustion research has both fundamental and applied aspects. There is considerable interest in pulse combustors because they take advantage of combustion oscillations, and their attractive characteristics include enhanced heat transfer and low NOx levels in the exhaust, with few, if any, moving parts. Many new applications exist for pulse combustors, from home heaters to large commercial boilers.

Preliminary results have answered many questions about mixing and ignition occurring in the combustion chamber. Our model reveals that during each cycle the injected cold reactants form a large-scale toroidal vortex. Both the simulation and experimental results show that this large toroidal structure convects the unburned gas far into the burned gas, where it is mixed with the hot products from previous cycles and undergoes reaction. The mechanism of ignition is believed to be thermal and/or radical. Although reactants injected during one cycle may still be burning during the next cycle, they are too far from the fresh

charge to be the source of ignition. For premixed combustion the numerical model shows that large strain rate in the early injection phase reduces the reaction, thereby allowing penetration of reactants into the chamber much farther than would be estimated by models that ignore strain-rate effects. This delay of reaction allows the energy release to occur after injection, a delay that is necessary to satisfy Rayleigh's criterion for combustion-driven oscillations.

Both computational and experimental results have indicated that flame extinction by strain rate plays a dominant role in many periodic reacting flow conditions. The next step is to investigate the importance of fluid strain in nonpremixed combustion conditions. Many of the combustors that experience combustion oscillations are operated with separate fuel and air injection. Development of a new model will be strongly tied to an experimental study, funded by the DOE Advanced Industrial Concepts Division. The model used for this study will be two-dimensional and planar, selected to be compatible with the new experimental combustor presently under design. This geometry will allow for orthogonal injection of the fuel and air streams in a relatively simple configuration that is amenable to study by both experiments and modeling.

Front Propagation through Weak Turbulence

The mechanism determining the premixed flame speed in a turbulent medium is generally regarded to be best understood in the weak-turbulence limit $u' \ll S_L$, where u' is the root-mean-square velocity fluctuation and S_L is the laminar flame speed. In this limit, a quadratic dependence of $u_T - S_L$ on u'/S_L has been derived, where the turbulent flame speed u_T is operationally defined as the surface area of the wrinkled flame per unit projected transverse area.

The present work began with a simple scaling analysis which implied that the quadratic dependence holds only for atypical cases such as periodic flow. The general result for randomized flow fields is $u_T - S_L \sim (u'/S_L)^{4/3}$.

In the analysis, the flame is regarded as an interface that propagates normal to itself toward the unburned fuel at a constant speed S_L. In addition, the interface is convected by a flow field whose longitudinal and transverse components are denoted as u and $\mathbf{v}$ respectively. The interface is treated as dynamically passive, e.g., the impact of heat release on the flow field is neglected. In the weak-turbulence limit, flow-induced wrinkling is a small perturbation of the initially planar flame, so the longitudinal location h of the flame is a single-valued function of transverse location, denoted $\mathbf{x}$. In this limit, geometrical considerations lead to the flame propagation equation $\partial h/\partial t + \mathbf{v}\cdot\nabla h = S_L + (S_L/2)(\nabla h)^2 + u$ and the turbulent flame speed formula $u_T = \langle \partial h/\partial t \rangle = S_L + (S_L/2)\langle (\nabla h)^2 \rangle$, where ∇ is the gradient with respect to $\mathbf{x}$.

Numerical simulations of interface propagation in two and three-dimensional flows confirm this prediction and the additional prediction that the time scale for transition of

an initially planar flame to statistically steady propagation is of order $(u'/S_L)^{1/3}(L/u')$, where L is the turbulence integral scale. The simulations track fronts propagating with local speed S_L through orthogonal arrays of finite-range vortices of identical structure but with randomized orientations. When the orientations are constrained to enforce periodicity, quadratic dependence of $u_T - S_L$ on u' is obtained, in accordance with the previous analysis.

Implications of these results concerning the premixed flame speed in strong turbulence will be investigated in future work.

Recent Publications Supported by the Chemical Sciences Division

1. W. T. Ashurst, "Spin a Tsuji-Burner and Create a Steady, Wrinkled, Strained Diffusion Flame?" *Combustion Science and Technology* **70**, 75 (1990).
2. W. T. Ashurst and F. A. Williams, "Vortex Modification of Diffusion Flamelets," *Twenty-Third Symposium (International) on Combustion*, p. 543 (1990).
3. P. K. Barr, "Acceleration of a Flame by Flame-Vortex Interactions," *Combustion and Flame* **82**, 111 (1990).
4. P. K. Barr and J. O. Keller, "Premixed Combustion in an Oscillating / Resonant Flow Field. Part II: Modeling the Periodic Reacting Flow," in *Thermo-Physical Aspects of Energy Conversion*, ASME Publication No. AES-Vol. 16 (1990).
5. J. O. Keller, R. S. Gemmen, and P. K. Barr, "Premixed Combustion in an Oscillating / Resonant Flow Field. Part I: Experimental Investigation," in *Thermo-Physical Aspects of Energy Conversion*, ASME Publication No. AES-Vol. 16 (1990).
6. A. R. Kerstein, "Linear-Eddy Modeling of Turbulent Transport. Part 3. Mixing and Differential Molecular Diffusion in Round Jets," *Journal of Fluid Mechanics* **216**, 411 (1990).
7. W. T. Ashurst and G. I. Sivashinsky, "On Flame Propagation Through Periodic Flow Fields," *Combustion Science and Technology* **80**, 159 (1991).
8. A. R. Kerstein, "Linear-Eddy Modeling of Turbulent Transport. Part 5. Geometry of Scalar Interfaces," *Physics of Fluids A* **3**, 1110 (1991).
9. A. R. Kerstein, "Fractal Dimension of Propagating Interfaces in Turbulence," *Physical Review A* **44**, 3633 (1991).
10. A. R. Kerstein and W. T. Ashurst, "Propagation Rate of Growing Interfaces in Stirred Fluids," *Physical Review Letters* **68**, 934 (1992).
11. A. R. Kerstein, "Linear-Eddy Modeling of Turbulent Transport. Part 4. Structure of Diffusion Flames," *Combustion Science and Technology* **81**, 75 (1992).
12. A. R. Kerstein, "Linear-Eddy Modeling of Turbulent Transport. Part 7. Finite-Rate Chemistry and Multi-Stream Mixing," *Journal of Fluid Mechanics*, in press (1992).

THE ENERGETICS AND DYNAMICS OF FREE RADICALS, IONS, AND CLUSTERS

Tomas Baer
Department of Chemistry
University of North Carolina
Chapel Hill, NC 27599-3290

The structure and energetics of free radicals, ions, and clusters have been investigated by photoelectron photoion coincidence (PEPICO) and analyzed with *ab initio* molecular orbital and statistical theory RRKM calculations. In these experiments, molecules are prepared in a molecular beam so that their internal as well as translational energies are cooled to near 0 K. The coincidence condition between energy analyzed electrons and their corresponding ions insures that the ions are energy selected. The primary experimental information includes ionization and fragment ion appearance energies, and the ion time of flight (TOF) distributions. The latter are obtained by using the energy selected electron as a start signal and the ion as the stop signal. These types of experiments allow us to measure the ion dissociation rates in the 10^4 to 10^7 sec^{-1} range. Such ions are commonly referred to as metastable ions. In addition, the TOF peak widths are related to the release of translational energy in the ion dissociation process.

Summary of Major Results:

Perhaps the most important advance during the past year has been in the study of cluster photoionization. We have developed an experimental method for differentiating similar mass cluster ions produced by the reactions:

$$(ABn \rightarrow (AB)_n^+ \qquad (1)$$
$$(Ab)n+m \rightarrow (AB)_n^+ + (AB)_m \qquad (2)$$

This method is based on the kinetic energy of the ions measured by TOF.

One of the major problems in the study of clusters is the determination of the size distribution. Aside from spectroscopic identification of clusters which works well for dimers and trimers, mass analysis by mass spectrometry is virtually the only method for obtaining this information. However, there is a fundamental problem in this analysis which is that cluster ions can dissociate in the ionization process and produce ionic clusters of lower mass. This is a particularly severe problem in electron impact ionization in which the electron energy is ill defined. However, the problem also exists in photoionization where the photon energy is narrow and variable. Thus, the cluster ion distribution may not reflect the neutral size distribution. The problem is particularly difficult to deal with when the ion dissociates by loosing one of the neutral molecular units, because then the $(AB)_n^+$ ions from reactions (1) and (2) cannot be distinguished.

The method for distinguishing the production of a cluster ion, $(AB)_n^+$, from either the parent (AB)n, or the higher order cluster, say $(AB)_{n+1}$, by dissociative ionization is based on the kinetic energy of the ion. Cold molecules and clusters produced in a skimmed molecular beam have exceedingly low translational energies in a direction perpendicular to the molecular beam

axis. Thus, the ion time of flight distribution of an ion produced from such a cold precursor molecule is exceedingly narrow. On the other hand, dissociative ionization is invariably associated with the release of translational energy, which is often distributed isotropically. Thus, TOF peaks of such ions are broad. We have found that the TOF peak of an $(AB)_n^+$ cluster ion produced by dissociative ionization from a higher order neutral cluster is at least an order of magnitude broader than a similar mass ion produced by non-dissociative ionization.

Figure 1 shows the TOF distributions for acetylene ion monomers, dimers and trimers. The monomer ion signal is narrow. Its width of 13 ns indicates that the temperature of the molecular beam in direction perpendicular to the beam axis is about 4 K. On the other hand, the dimer and trimer ion peaks are broad because of the translational energy released in the dissociative ionization of higher order clusters. The translational temperatures of the dimer and trimer ions, assuming Maxwell-Boltzmann distributions of translational velocities, are 80 and 100 K, respectively. The Gaussian TOF distribution is, in fact, good evidence that the translational energy release is statistical and well described by a translational temperature.

The TOF spectra in Figure 1 indicate that no acetylene clusters are ionized directly to the corresponding ion. Rather, all are produced by dissociative ionization of higher order clusters. This is true even at the very lowest photon energies investigated.

Studies on several other systems, including ethylene clusters, methylchloride clusters, and methanol clusters indicate that essentially 100% of the cluster ions produced at or near the ionization onset come from dissociative ionization of higher order clusters. This means that determinations of, for instance, ionization energies of clusters by measuring the photoionization onset are unreliable. They represent only upper limits.

The non-observation of direct ionization of clusters lies in the structures of the neutral and ionic clusters, that is, in the Franck-Condon factors associated with the ionization process. This has been discussed by a number of workers. We have carried out, as others have, *ab initio* calculations on some of these clusters and their corresponding ions. In the case of acetylene, we have found that the trimer ion is totally unstable when we begin with a geometry corresponding to that of the neutral. The ion dissociates to a dimer ion, which has a structure that is neither dimer like, nor like any other $C_4H_4^+$ ion known so far.

Other studies in our laboratory are dealing with the role of rotational energy in the dissociation process. The cold samples make possible the study of rotational effects in dissociation reactions. The dissociation onset for a reaction is shifted to higher energies when the molecule is cooled to 0 K. The shift is equal to the internal vibrational energy plus any rotational energy that can be used to overcome the dissociation onset. Loose and tight transition states are thought to differ in the number of rotational degrees of freedom that can contribute. However, quantitative data for this effect are lacking.

Future Studies:

We plan to extend the study of cluster photoionization to determine which, if any, clusters can be directly ionized. For instance, one might expect that non-polar, spherical molecules such as $(CH_4)_n$ clusters might form the corresponding cluster ions. Similarly, NO dimers are thought to ionize directly, but this has so far not been confirmed. In addition, the role of rotations in the dissociation process will be investigated in detail. Experiments on the loss of CH_4 from isobutane ions have shown that all three rotational degrees of freedom are involved in the dissociation, that is, all three rotations are active. But what about the dissociation such ions as CH_3I which looses the I atom? The C_{3v} symmetry of the molecule is maintained throughout the dissociation so one would expect the K rotor (rotation about the symmetry axis) to remain non-active, or conserved.

Research Publications 1990, 1991, 1992:

J.S. Riley, T. Baer and G.D. Marbury, "Sequential Ortho Effects: Characterization on Novel $[M-35]^+$ Fragment Ions in the Mass Spectra of 2-alkyl-4,6-Dinitrophenols," J. Am. Soc. Mass Spectrom. 2 69 (1991).

K.M. Weitzel, J. Booze and T. Baer, "Shifts in Photoionization Fragmentation Onsets; A Direct Measure of Cooling in a Supersonic Molecular Beam," Chem. Phys. 150 263 (1991).

T. Baer, K.M. Weitzel and J. Booze, "Photoelectron Photoion Coincidence Studies of Ion Dissociation Dynamics" in Vacuum Ultraviolet Ionization and Dissociation of Molecules and Clusters, World Scientific, Inc., C.Y. Ng, Ed. (1991) p259-296.

T. Baer, "The Measurement and Interpretation of Onset Energies," NATO ASI Series, K. Jennings, Ed. (1991).

J.A. Booze, K.M. Weitzel and T. Baer, "The Rates of HCl Loss from Energy Selected Ethylchloride Ions: A Case of Tunneling Through an H-Atom Transfer Barrier," J. Chem. Phys. 94 3649-3656 (1991).

K.M. Weitzel, J.A. Booze and T. Baer, "TPEPICO Study of the Ethane Loss from Energy Selected n-Pentane Ions Cooled in a Supersonic Expansion," Int. J. Mass Spectrom. Ion Proc. 107 301 (1991).

K.M. Weitzel, J.A. Booze and T. Baer, "The Metastable Formation of diethylchloronium Ions from Ethylchloride Dimers in a Seeded Molecular Beam," Z. Phys. D. 18 383 (1991).

J. Riley and T. Baer, "Dissociation Dynamics of Phenetole Cations by Photoelectron Photoion Coincidence," J. Am. Soc. Mass Spectrom. 2 464 (1991).

O. Dutuit and T. Baer, "Isotope Effect in the Dissociation of Partially Deuterated Dimethyl Ether, $CH_3OCD_3^+$ Ions," Int. J. Mass Spectrom. Ion Proc. 110 67 (1991).

T. Baer and J.A. Booze, "Long Lived Ion Complexes," in Ion-Molecule Collision Complexes, W. Hase Ed. JAI Press (1992), in press.

J.A. Booze and T. Baer, "On the Determination of Cluster Properties by Ionization Techniques," J. Chem. Phys. (in press).

J.A. Booze and T. Baer, "*Ab initio* Study of $C_3H_8O^+$ Ions," J. Phys. Chem. (in press).

J.A. Booze and T. Baer, "Dissociation Dynamics of Energy Selected $CH_3CH_2CH_2OH^+$ and $CH_3CH_2CH_2OH^+$ Ions," J. Phys. Chem. (in press).

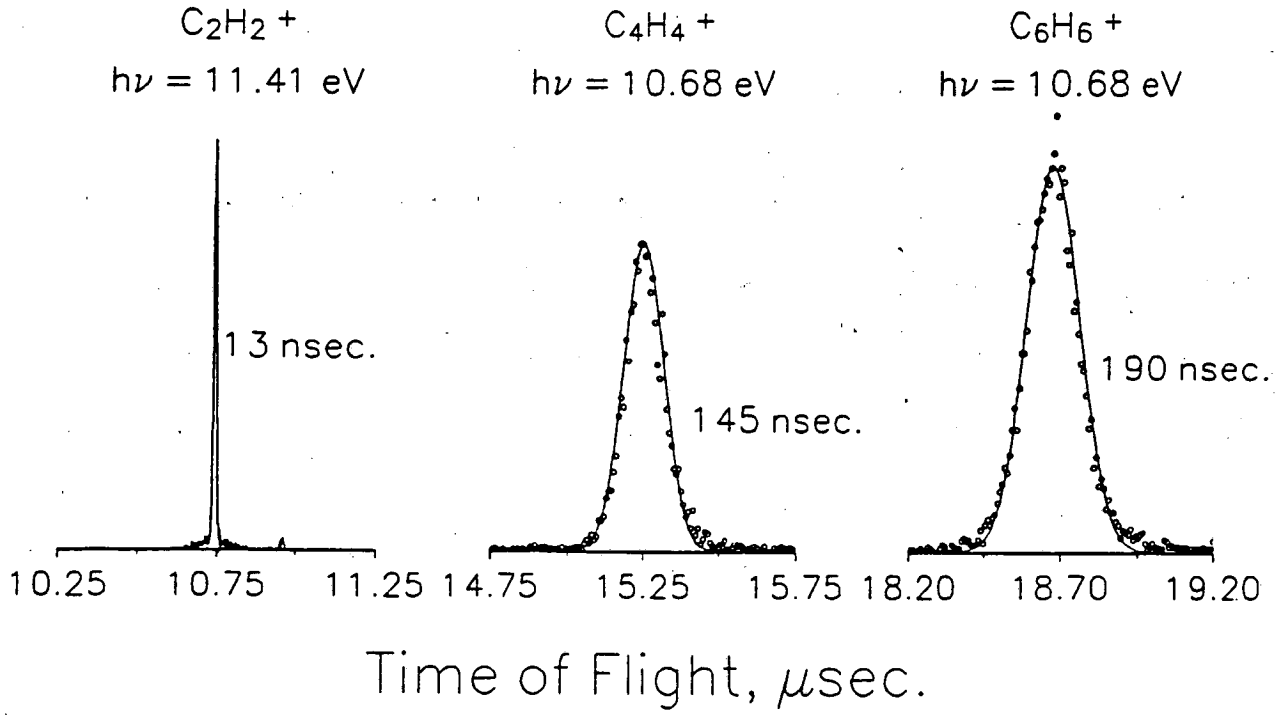

Figure 1

ENERGY TRANSFER PROPERTIES AND MECHANISMS

John R. Barker

Department of Atmospheric, Oceanic, and Space Sciences
Space Physics Research Laboratory
and Department of Chemistry
The University of Michigan
Ann Arbor, Michigan 48109-2143
[Internet: usergblg@um.cc.umich.edu]

Many chemical reaction systems are dominated by energy transfer. The principal motivation for this research is to characterize energy transfer processes in highly vibrationally excited molecules of moderate size, where individual states cannot be resolved.

I. Polyatomic Molecule Energy Transfer

In previous work, we investigated energy transfer in azulene and in benzene, where it was found that $\langle\langle\Delta E\rangle\rangle$, the bulk average energy transferred per collision, increases approximately linearly with the average vibrational energy. Recently, we have extended this work to other benzene derivatives (toluene, toluene-d8, and benzene-d6) and have worked to improve our data analysis and experimental techniques. In all cases investigated so far, the results show the same approximately linear energy dependence at low energy and there is a distinct tendency for $\langle\langle\Delta E\rangle\rangle$ to become less dependent on energy at higher internal energies. In this work, we have utilized a least-squares data analysis method that enables us to extract directly the functional form of $\langle\Delta E\rangle_d$ (step size for deactivating collisions), which is the most useful energy transfer property for Master Equation calculations. Analysis was also carried out to determine to what extent "supercollisions" may participate in energy transfer involving toluene, and it was found that the contributions suggested by Luther and coworkers [for example: K. Luther and K. Reihs, Ber. Bunsenges. Phys. Chem., 92, 442 (1988)] are not inconsistent with the present results.

In other experiments that are currently underway, we are investigating the time-dependent infrared spectrum of highly vibrationally excited benzene as it undergoes collisional deactivation. The aim of the these experiments is to determine how the population distribution evolves during the deactivation process. This work is still in progress, but it appears that the evolving distribution is similar to those produced in Master Equation calculations with an exponential model. Measurements of the C-H stretch overtone emission are also consistent with that picture. However, small contributions from supercollisions may still be present.

In Figure 1, the emission spectrum of highly excited benzene is shown along with the absorption spectrum which was measured with the same circular variable filter apparatus. The three components of the emission are due to $\Delta v = -1$

transitions originating from v = 1, 2, and 3. The relative intensities agree with statistical theory within ~10%. An interesting and important feature of the spectrum is the anharmonic red-shift of the main emission peak away from the absorption peak. This shift will affect the way researchers must go about identifying the emitters responsible for the infrared emission bands observed in interstellar dust clouds [Brenner and Barker, 1992].

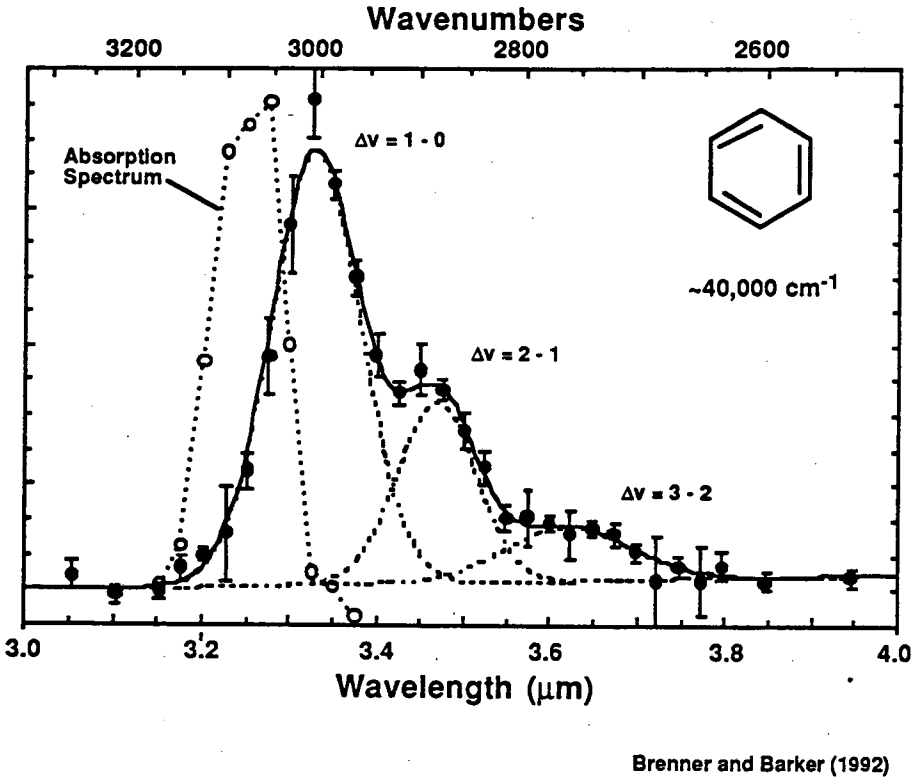

Figure 1. Infrared emission spectrum of benzene at ~40,000 cm^{-1}. The absorption spectrum is also shown.

In other research related to the deactivation of polyatomic species, the effect of infrared emission itself was investigated. In radical recombination reactions, the excited species produced is usually deactivated by collisions. At low pressures and at low temperatures, however, infrared emission deactivation may dominate. This process would be important in molecular beams, free jets, and in the interstellar medium. Master Equation simulations of several representative radical recombination reactions show that *for many reactions at moderate temperatures there is no pressure fall-off, because infrared emission is essentially completely effective and collisions are not necessary.* The results of these calculations [Barker,

submitted] are presented in Figure 2 as the ratio of rate constant for recombination in the complete absence of stabilizing collisions (k_0^0) divided by k_∞.

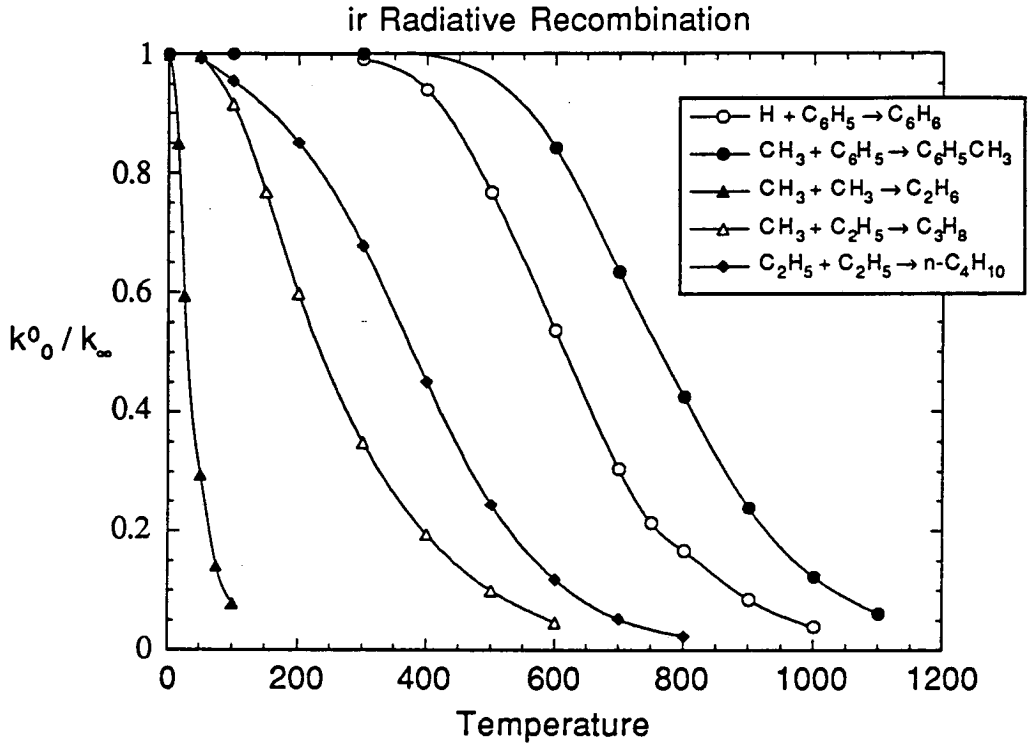

Figure 2. Infrared radiative recombination in the absence of stabilizing collisions.

II. Triatomic Molecule Energy Transfer

Our recent thermal lensing experiments on NO_2 indicated that the strongly coupled and doubly degenerate excited electronic states in that molecule strongly affect collisional energy transfer. We are currently investigating CS_2, which has strongly coupled, but singly degenerate, electronic states, in order to determine whether it is the strong coupling, or the degeneracy, which makes the larger difference. The experimental phase of the work is complete and the analysis is still underway.

III. Recent Publications Supported by DOE

Published or Accepted for Publication

"Incubation in Cyclohexene Decomposition at High Temperatures," Jichun Shi and John R. Barker, Int. J. Chem. Kinetics, **22**, 187 (1990).

"Time Dependent Thermal Lensing Measurements of V-T Energy Transfer From Highly Excited NO_2," Beatriz M. Toselli, Theresa L. Walunas, and John R. Barker, J. Chem. Phys., **92**, 4793-804 (1990).

"Collisional Deactivation of Highly Vibrationally Excited Benzene Pumped at 248 nm," Murthy L. Yerram, Jerrell D. Brenner, Keith D. King, and John R. Barker, J. Phys. Chem., **94**, 6341-50 (1990).

"Emission from Ozone Excited Electronic States," Jichun Shi and John R. Barker, J. Phys. Chem., **94**, 8390-3 (1990).

"Kinetic Studies of the Deactivation of $O_2(^1\Sigma_g^+)$ and $O(^1D)$," Jichun Shi and John R. Barker, Int. J. Chem. Kinetics, **22**, 1283-1301 (1990).

"Quantum Effects in Large Molecule Collisional Energy Transfer?", Beatriz M. Toselli and John R. Barker, Chem. Phys. Letters, **174**, 304-8 (1990).

"Vibrational Relaxation of Highly Excited Toluene," Beatriz M. Toselli, Jerrell D. Brenner, Murthy L. Yerram, William E. Chin, Keith D. King, and John R. Barker, J. Chem. Phys., **95**, 176 (1991).

"Polycyclic Aromatic Hydrocarbon Optical Properties and Contribution to the Acceleration of Stellar Outflows," Isabelle Cherchneff, John R. Barker, and Alexander G. G. M. Tielens, Astrophys. J., **377**, 541-552 (1991).

"Excitation of CO_2 by energy transfer from highly vibrationally excited benzene derivatives," Beatriz M. Toselli and John R. Barker, J. Chem. Phys., **95**, 8108 (1991).

"Infrared Emission Spectra of Benzene and Naphthalene: Implications for the Interstellar PAH Hypothesis," Jerrell D. Brenner and John R. Barker, Astrophys. J. (Letters), **388**, L39-L43 (1992).

"Polycyclic Aromatic Hydrocarbons and Molecular Equilibria in Carbon Rich Stars," Isabelle Cherchneff, John R. Barker, and Alexander G. G. M. Tielens, Astrophys. J., to be published August 20, 1992.

Submitted for publication

"Polycyclic Aromatic Hydrocarbon Formation in Carbon Rich Stellar Envelopes," Isabelle Cherchneff, John R. Barker, and Alexander G. G. M. Tielens, Astrophys. J., submitted.

"Isotope Effects in the Vibrational Deactivation of Large Molecules", Beatriz M. Toselli and John R. Barker, J. Chem. Phys., submitted.

"Radiative Recombination in the Electronic Ground State," John R. Barker, J. Phys. Chem., submitted.

Turbulence-Chemistry Interactions in Reacting Flows

R. S. Barlow
Combustion Research Facility
Sandia National Laboratories
Livermore, California 94551

Interactions between turbulence and chemistry in nonpremixed flames are investigated through the use of multispecies measurements. Simultaneous point measurements of CH_4, N_2, O_2, H_2O, CO, CO_2, H_2, OH, temperature, density, and the mixture fraction f are obtained by combining spontaneous Raman scattering, Rayleigh scattering, and laser-induced fluorescence (LIF). Corrections for the effects of collisional quenching are applied to the linear OH LIF signals for each laser shot, making the OH concentration measurements quantitative. Measured chemical states in the turbulent flames are compared to results from strained laminar flame calculations, perfectly stirred reactor (PSR) calculations, and Monte Carlo simulations using reduced chemical mechanisms.

Lifted Flame Experiments: Simultaneous point measurements of major species concentrations, temperature, and hydroxyl radical concentration were obtained in the stabilization region of a lifted natural gas flame. A natural gas jet issued from the vertical burner tube (7.2-mm diameter) at Reynolds number 28,600 into still air. The jet exit velocity was approximately 80 percent of the blowout velocity, and the flame stabilized at x/D~20, where x is the streamwise coordinate and D is the nozzle diameter. The multi-species point measurements in this flame complement imaging results obtained in lifted flames by R. W. Schefer (see abstract in this volume) and allow a critical evaluation of competing theories regarding the stabilization mechanism for lifted flames.

Measurements were made at locations shown in Fig. 1. Results show that the lifted flame stabilizes somewhat outside the mean stoichiometric contour, where the flow is intermittent and the turbulence level is low. There is evidence in the data of premixed burning at the flame base. However, there is also clear evidence of intermittency and wide excursions of the mixture fraction outside the flammability limits. The latter results run counter to the concept of the lifted flame base being a turbulent premixed flame front propagating steadily into the approach flow. On the other hand, the data provide no direct evidence of quenching at the flame base. Thus, diffusion flamelet quenching does not appear to be a dominant mechanism controlling flame stabilization. These experiments indicate that the lifted flame stabilization region includes both premixed and diffusion flame structures and that flame stabilization involves a combination of mechanisms.

Methane Flame Calculations: Previous experiments in laminar, transitional, and turbulent methane jet flames showed that turbulent mixing leads to OH mass fractions that are higher than predicted by steady strained laminar flame calculations. Furthermore, the experiments showed that this effect cannot be attributed to a local extinction/re-ignition process. These results are summarized in Fig. 2, which shows pdfs of OH mass fraction for data in the reactive range of mixture fraction where the maximum OH concentrations occur. A series of parametric laminar flame calculations were performed to investigate physical mechanisms that may

contribute to the apparent 'non-flamelet' behavior of turbulent flames. A simplified, one-dimensional formulation of the transient diffusion flame problem was used, and chemical reactions were treated by a 'skeletal' mechanism. Three factors affecting the structure of methane-air diffusion flames were considered: i) changes in the profile of scalar dissipation through the reaction zone, ii) temporal variation of the scalar dissipation rate, and iii) elimination of differential diffusion by setting all Lewis numbers to unity.

Results indicate that changes in the shape of the scalar dissipation profile and periodic variation of the scalar dissipation rate have relatively minor effects on species mass fractions. However, the mass fractions of OH and CO overshoot their steady state limits when a flamelet is subjected a sudden decrease in scalar dissipation. The predicted overshoot occurs without the laminar flame being first pushed to the brink of extinction, and recovery of the flame to steady-state conditions is relatively slow. This shows that details of the strain history can be important and that certain types of unsteady strain can contribute to the high OH and CO mass fractions measured in turbulent flames. Significant changes in species mass fractions also occur when all Lewis numbers are set to zero. In particular, the peak mass fractions of OH, CO, and H_2 all increase when differential diffusion is eliminated. This result shows the need to conduct further experimental work on the role of differential diffusion of species in turbulent flames.

New Measurement Capabilities: The Raman scattering collection optics have been redesigned to increase efficiency and improve the SNR of the major species measurements. These improvements we enhance our ability to quantify departures from equilibrium of specific reactions. We have also recently added the capability to measure NO as a second fluorescent species. The new optical configuration for the multi-species measurements is shown in Fig. 3. Because NO can exists over wide ranges in temperature and mixture fraction, quenching corrections to the fluorescence data will be more critical than for OH in converting fluorescence signals to quantitative concentrations. The laser system for NO pumping can also be used for two-photon excitation of CO.

Plans: The Raman/Rayleigh/OH/NO system will be applied initially in H_2-air jet flames, where high temperatures will generate substantial NO concentrations. Data from these flames will be used to evaluate the ability of turbulent combustion models to predict NO concentrations. Further experiments on lifted flames will be conducted to investigate the balance between premixed and diffusion flame structures in the stabilization region over a range of liftoff heights. Experiments are in progress to quantify the effects of the Halon CF_3Br on the extinction characteristics of piloted methane jet flames. Experiments are planned to quantify differential diffusion effects in flames of H_2/CO_2 in air.

Publications 1990-Present

R. S. Barlow, R. W. Dibble, J.-Y. Chen, and R. P. Lucht, "Effect of Damkohler Number on Superequilibrium OH Concentration in Turbulent Nonpremixed Jet Flames," *Combust. Flame,* **82**: 235-251 (1990)

R. S. Barlow, R. W. Dibble, S. H. Stårner, and R. W. Bilger, "Piloted Diffusion Flames of Nitrogen Diluted Methane Near Extinction: OH Measurements," *Twenty-Third Symposium (International) on Combustion* (The Combustion Institute, Pittsburgh, PA, 1991), pp. 583-589 (1990).

R. S. Barlow and C. Q. Morrison, "Two-Phase Velocity Measurements in Dense Particle-Laden Jets," *Expt. Fluids* **9**, 93-104 (1990).

R. S. Barlow, D. C. Fourguette, M. G. Mungal, and R. W. Dibble, "Experiments on the Structure of a Compressible Annular Reacting Shear Layer," *AIAA J.*, to appear.

R. S. Barlow and J.-Y. Chen, "On Transient Flamelets and Their Relationship to Turbulent Nonpremixed Flames," *Twenty-Fourth Symposium (International) on Combustion* (The Combustion Institute, Pittsburgh, PA), accepted, (1992).

R. W. Dibble, S. H. Stårner, A. R. Masri, and R. S. Barlow, "An Improved Method of Data Acquisition and Reduction of Laser Raman-Rayleigh Scattering from Multispecies," *Appl. Phys. B.* **51**, 39-43 (1990).

A. R. Masri, R. W. Dibble, R. S. Barlow, "Simultaneous Raman-Rayleigh-Fluorescence Measurements in Turbulent Nonpremixed Flames of H_2-CO_2 Near Extinction," *Combust. Flame*, to appear (1990).

A. R. Masri, R. W. Dibble, and R. S. Barlow, "Raman-Rayleigh Measurements in Bluff-Body Stabilized Flames of Hydrocarbon Fuels," *Twenty-Fourth Symposium (International) on Combustion* (The Combustion Institute, Pittsburgh, PA), submitted, (1992).

A. R. Masri, R. W. Dibble, and R. S. Barlow, "The Structure of Turbulent Nonpremixed Flames of Methanol Over a Range of Mixing Rates," *Combust. Flame*, in press (1992).

S. H. Stårner, R. W. Bilger, R. W. Dibble, and R. S. Barlow, "Piloted Diffusion Flames of Dilute Methane Near Extinction: Mean Structure from Raman/Rayleigh/Fluorescence Measurements," *Comb. Sci. Tech.* **70**: 111-133 (1990).

S. H. Stårner, R. W. Bilger, R. W. Dibble, and R. S. Barlow, "Piloted Diffusion Flames of Dilute Methane Near Extinction: Detailed Structure from Laser Measurements," *Comb. Sci. Tech.* **72**: 225 (1990).

S. H. Stårner, R. W. Bilger, R. W. Dibble, and R. S. Barlow, "Piloted Diffusion Flames of $CO/CH_4/N_2$ and $CO/H_2/N_2$ Near Extinction," *Combust. Flame*, in press (1991).

S. H. Stårner, R. W. Bilger, R. W. Dibble, and R. S. Barlow, "Some Raman/Rayleigh/LIF Measurements in Turbulent Propane Flames," *Twenty-Third Symposium (International) on Combustion*, (The Combustion Institute, Pittsburgh, PA), 645-651 (1990).

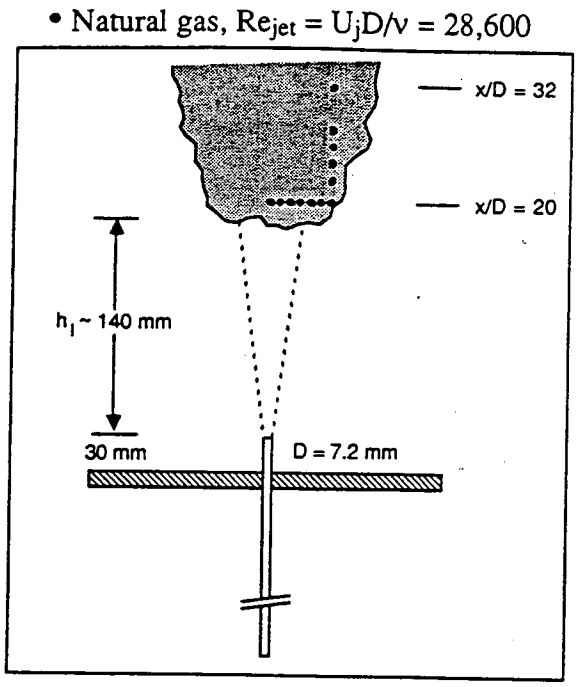

Fig. 1. Lifted flame configuration and measurement locations.

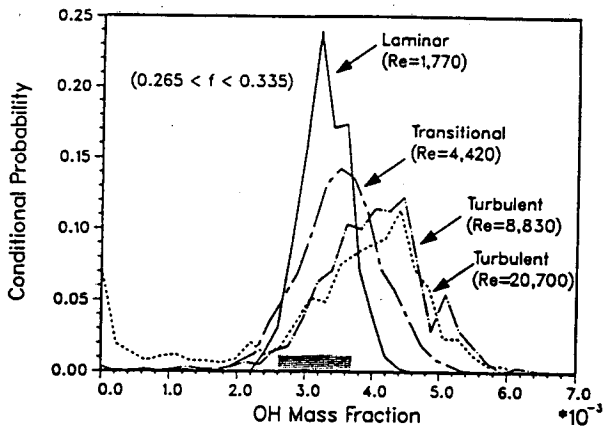

Fig. 2. Conditional pdfs of OH mass fraction in four methane jet flames. The range of maximum OH mass fractions for steady laminar flame calculations is shaded.

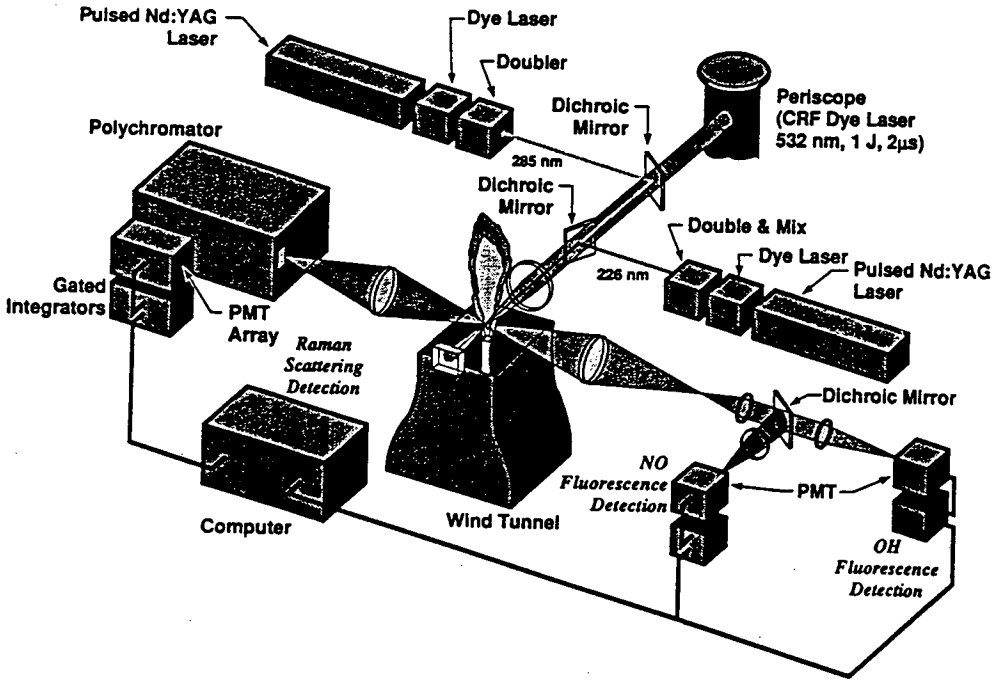

Fig. 3. Configuration for the Raman/Rayleigh/OH/NO point measurements system.

COMBUSTION-RELATED STUDIES USING WEAKLY-BONDED COMPLEXES

Robert A. Beaudet
Department of Chemistry
University of Southern California
Los Angeles, CA 90089-0482
Tel: (213) 743-2997
FAX: (213) 743-7757

PROGRAM SCOPE:

Binary van der Waals complexes involving species of interest to combustion research are prepared in supersonic free-jet expansions, and their photochemical and photophysical properties are probed by using IR tunable diode laser (TDL) spectroscopy. In the first phase, geometries and other molecular properties are being determined from vibration-rotational spectra. In the second phase, these complexes will be used as precursors to study photoinitiated reactions in precursor geometry limited environments. Two complementary classes of binary complexes are being investigated. The first involves molecular oxygen and hydrogen containing constituents (e.g. O_2-HCN, O_2-HF, O_2-HCl, O_2-HBr, O_2-HI and O_2-hydrocarbons). These species are interesting candidates for study since upon photodissociating the hydride portion, the reaction of H and O_2 via the vibrationally excited $HO_2^{\dagger}$ intermediate can conceivably be studied, {*e.g.* BrH-O_2 + hν(193 nm) → Br-H-O_2 → Br + $HO_2^{\dagger}$ → Br + OH + O}. High resolution IR spectroscopy of such complexes have not been obtained previously and the structural information deriving from IR spectra is certainly very useful for better designing and understanding photoinitiated reactions that occur in these complexes .

The second thrust area is the study of a set of novel species involving oxygen *atoms* and small molecules such as HF, HCl, HBr, HI, HCN and simple hydrocarbons. An expansion gas is seeded with a precursor such as SO_2 and a second constituent. $O(^3P)$ is prepared by precursor photolysis just before the start of the supersonic expansion. Since the reactions of $O(^3P)$ and the above mentioned small molecules have significant activation energies, the complexes will be able to form and survive in the free-jet expansions, *e.g.*, the $O(^3P)$ + HCl reaction has an activation energy of 22 kJ/mol., which is considerably higher than the thermal collisional energy. Hence, the complex can be stabilized in the shallow van der Waals potential well just outside the activation barrier. Our initial objective is to study structural properties of these clusters by using laser IR spectroscopy. Once that proves successful, we will exploit vibrational excitation of the HX to promote the hydrogen exchange reaction of O + HX → OH + X occurring in these complexes. The nascent state distribution of the OH product can be probed with LIF. Experiments are also under way in which the nascent product state distribution of a photodissociation can be probed by using IR spectroscopy.

PROGRESS:

We have now constructed a vacuum system and a satisfactory pulsed slit nozzle to prepare reasonable concentrations of radical species by the photolysis of an appropriate precursor. In principle, the pumping system can sustain a pulsed slit valve as large as 250 mm x 0.20 mm with 2-3 atmospheres stagnation pressure when the slit is opened for 2-4 milliseconds at 3 Hz. The vacuum system consists of a 17.2 L/s vane pump in combination with a Leybold Ruvac WA251 roots pump with a pumping speed of 85 L/s. In turn

this combination backs an Edwards vapor jet booster pump (Model 18B4A) with a pumping speed of 4000 L/s (air) or 6000 L/s (H_2). This pumping system evacuates a 24" x 24" x20" chamber. Due to its height, the vapor booster pump is connected to the chamber by a U-shaped 12" diameter SS pipe. This large total volume also acts as a buffer chamber for the pulsed expansion.

We have successfully constructed and operated two different types of pulsed nozzles. The first is a large pulsed slit valve with a 125 mm x.0.20 mm slit, which is mechanically opened by three modified General Valve solenoids. This valve is an extension of our first pulsed valve design,[1] and has been successfully tested and operated to study IR spectroscopy of van der Waals complexes. The longer optical pathlength affords greater sensitivity than our previous pulsed slits. The second nozzle has a 38 mm x 0.15 mm slit and is designed for use with photolysis. The length of the slit has been selected to match the size of the excimer laser beam. The nozzle has a secondary chamber after the valve, in which the photolysis occurs. This chamber and the slit is formed by two UV transmitting quartz plates. The highest yield is obtained when the photolysis laser is focussed about one millimeter upstream from the slit opening. In this way, the radicals formed have some drift time to thermalize before being further cooled by the supersonic expansion. We can also achieve satisfactory photolysis by directing the laser beam head-on into a regular slit nozzle along the translational axis.

We are now producing high yields of complexes of O2 with other species. At first, we tried to form O_2 complexes by expanding O_2/hydride mixtures in argon and in neon without much success. By varying the backing pressure and the composition of the expanding gas, cooling can be controlled over a limited range: *e.g.*, increasing the backing pressure lowers the temperature, thereby increasing condensation. We were unsuccessful with O_2 as the carrier gas; it was not an effective coolant and it seemed to promote the formation of dimers such as $(N_2O)_2$ and$(HCl)_2$. These experiments were tried with a 4 cm pulsed slit, and the results were marginal and not reproducible. Also, we did not have sufficient pumping speed to use helium as a carrier gas except at very low stagnation pressures. It was not until we sought oxygen complexes in the new apparatus with its 12 cm slit and high pumping throughput that we were successful. The key to success was using helium as a carrier, with backing pressures ~ 2 atm, high pumping speeds and good vacuum. Low temperatures were achieved without the competition of an efficient clustering gas such as argon. In fact, this is an excellent way to form high yields of these dimers without contaminants. We hypothesize that because argon and neon are such good clustering agents, they preferentially complex with, and deplete, other reagents. Helium does not cluster so well, but requires high pumping speeds to remove it from the chamber efficiently and achieve the low temperatures. Our best results are obtained with N_2O/O_2/He mixtures of 1/10/1500 and stagnation pressures of about 2 atmospheres.

N_2O has been chosen as the companion molecule for our first experiments because of its large absorption cross-section, and because we have an excellent diode in the 2220 cm^{-1} region. We have also collected the necessary computational tools to calculate and fit spectra of these open shell complexes. Consistent with our predictions, the spectrum of this complex is very dense. It appears that the large spin-spin contribution, $\lambda S_z \cdot S_z$ is quenched. While $\lambda = 2$ cm^{-1} in O_2, its value appears to be one or two orders of magnitude smaller in this complex. This is a sensitive measure of the electronic interactions between the two components even at these small van der Waals interactions. Our final goal is to work our way toward obtaining O_2-HCN and O_2-HX species for studying prealigned reactions. We are still awaiting an acceptable diode in the DCl region for the O_2-DCl cluster. It should be emphasized that high resolution spectroscopy on these open shell complexes is virgin territory. To our knowledge, this is the first observation of O_2 binary clusters. The analysis of

this spectrum is underway . This work represents the first open shell binary cluster studied by infrared rovibrational spectroscopy.

We have also obtained spectra of CH_4-N_2O. The spectrum is very dense, but regular. We believe that complexes of methane and its halides could also be interesting for photolysis experiments after their structures have been determined.

For the last year, our greatest effort has been directed at finding complexes of $O(^3P)$ with small molecules of interest in combustion. This was the most ambitious, but risky, segment of the work proposed originally. However, because it had the highest payoff, it received our concentrated effort. Our goal was to produce $O(^3P)$-HX complexes and to study reactions induced by essentially vibrational excitation. Satisfactory results have been obtained for the generation of $O(^3P)$ by photolysis of SO_2 at 193nm with a Lambda Physik EGM 201 excimer laser.

$$SO_2 \longrightarrow SO(^3\Sigma^-) + O(^3P) + 6300\ cm^{-1}$$

Because the $O(^3P)$ cannot be directly observed with our current experimental setup, we have inferred the production of the ground state oxygen atoms by detecting the vibrational spectrum of the co-produced transient species, $SO(^3\Sigma^-)$. We estimate that essentially all the SO_2 in the photolysis region is decomposed. We have attempted to cluster the oxygen with a large number of constituents, including CO_2, CO and N_2O, all of which have excellent IR absorption cross-sections. If clusters are present, we have not been able to detect them. We will make one last attempt to make a radical-molecule cluster observable by IR absorption. Dr. Yaomin Lin who obtained his Ph.D. with M. Heaven is attempting to produce and detect Ar-OD. We are awaiting a diode in the 2360 cm^{-1} region for this experiment. If successful we can bootstrap up from there. If not, this phase will be discontinued.

FUTURE WORK

Though our results with oxygen atom clusters have been disappointing, we are impressed with the capabilities of the new apparatus. We have enough pumping capacity to support *two* 12 cm pulsed slit nozzles operating at 3 Hz. This opens up intriguing new avenues of attack. Using a single nozzle has limitations. Since the two components must be premixed with the carrier gas in the single jet experiments, they must not react spontaneously with each other, and only one species must absorb energy and dissociate at the photolysis laser wavelength. Using 193 nm radiation, this seriously limits the possible combinations of molecules. Also, in reaction dynamics studies, LIF is often used to determine the vibration-rotation population distributions. Though LIF is sensitive, it is not very universal. However, *crossed* molecular beams emanating from two slit jets offers many new possibilities. These pulsed slits will form cold wedges, one of which contains a radical prepared by photolysis. The collision zone will be probed with the TDL to determine the rotation-vibration distributions of the products. Though reactants will be cooled by the expansion to low temperatures, they will have reasonable center-of-mass collision energies (e.g., ~ 2000 cm^{-1}). Thus, we must select reactions with proper entrance channel barriers. We choose reactions where radical production is efficient, and we also desire reaction products with large IR absorption cross-sections such as N_2O, CO_2 and CO, particularly for the first experiments. This approach will make many more reactions amenable to study than are now possible with LIF detection. We believe this can be an important new tool in studying combustion dynamics. Note that it would be too ambitious to form binary clusters in these experiments. We will investigate reactions between monomers and will set conditions to minimize cluster formation.

Numerous reactions of interest to combustion can be studied in this way. We select for the first experiments reactions that produce a strong vibrational absorber in frequency regions where we either own or can purchase acceptable diodes. Thus, we will concentrate first on the NH + NO reaction. This has two exothermic channels, only one of which has been extensively studied.[2-5]

$$NH + NO \rightarrow HNNO^{\dagger} \rightarrow N_2 + OH \qquad \Delta H_o^o = -34{,}100\ cm^{-1} \quad (1a)$$

$$\rightarrow N_2O + H \qquad \Delta H_o^o = -12{,}320\ cm^{-1} \quad (1b)$$

The first reaction is the most exothermic and the easiest to study: OH is detected by LIF. To study the second channel, either N_2O or H atoms must be detected. Fueno *et al.*[6] has determined the N_2O yield in a static cell with a mass spectrometer: the channel producing N_2O accounts for about 70% of the NH reacted. NH was prepared in high yield by various ways, photolysis of HNCO or $CHBr_3/NO/Ar$[7] at 193 nm, or of NH_3 at 193 or 248 nm.

---

1. S.W. Sharpe, R. Sheeks, C. Wittig, and R.A. Beaudet, *Chem. Phys. Lett.* **151**, 267 (1988).
2. W. Hack and K. Rathman, *J. Phys. Chem.* **94**, 4155 (1990).
3. W. Hack and A. Wilms, Z. Phys. Chem. **93**, 3540 (1989).
4. T. Fueno, M. Fukuda, and K. Yokoyama, Chem. Phys. **124**, 265 (1988),
5. J. A. Harrison, A. R. Whyte, and L. F. Phillips, Chem Phys. Lett. **129**,346 (1986).
6. Fueno, ibid.
7. K. Yamasaki, S. Okada, M. Koshi, and H. Matsui, J. Chem. Phys. **95**, 5087 (1991).

PUBLICATIONS RELATED TO COMBUSTION RESEARCH

1 Infrared Absorption Spectroscopy of the CO_2-Ar Complex in the 2376 cm^{-1} Combination Band Region: The Intermolecular Bend, S.W. Sharpe, D. Reifschneider, C. Wittig, and R.A. Beaudet, *J. Chem. Phys.* 94, 233 (1991).

2. Photoinitiated Reactions in Weakly-Bonded Complexes, S.K. Shin, Y. Chen, S. Nicholaisen, S.W. Sharpe, R.A. Beaudet, and C. Wittig *Adv. Photochem.*. Vol. 15.

3. Photoinitiated Reactions in Weakly-Bonded Complexes: Entrance Channel Specificity, Y. Chen, Y.P. Zeng, S.K. Shin, G. Hoffmann, D. Oh, S. Sharpe, R.A. Beaudet, and C. Wittig, Submitted: *Advance Molecular Vibrational and Collision Dynamics*. Vol 1B, J. M. Bowman and M. A. Ratner, ed., 1991.

4. Infrared Absorption Spectroscopy of the CO-Ar Complex, A. R. W. McKellar, Y. P. Zeng, S. W. Sharpe, C. Wittig, and R. A. Beaudet, J. Molec. Spectr. in press.

5. Infrared Spectroscopy of CO_2-D(H)Br and its molecular structure, Y. P. Zeng, S. W. Sharpe, S. K. Shin, C. Wittig, and R. A. Beaudet, *Journal of Chemical Physics.submitted.*

6. Infrared Absorption Spectroscopy of the Weakly Bonded CO-Cl_2 Complex. S. Bunte, J. B. Miller, Z. S. Huang, J. E. Verdasco, C. Wittig, and R. A. Beaudet. J. Phys. Chem.accepted

7. High Resolution Infrared Diode Laser Spectroscopy of the SO($^3\Sigma^-$) in a Secondary-Slit Supersonic Expansion., Z. S. Huang, J. E. Verdasco, C. Wittig, and R. A. Beaudet, Chem. Phys. Lett.accepted

Photoionization-Photoelectron Research

J. Berkowitz and B. Ruscic
Chemistry Division, Argonne National Laboratory (Bldg. 203)
9700 South Cass Avenue
Argonne, IL 60439-4843

The photoionization research program is aimed at understanding the basic processes of interaction of vacuum ultraviolet (VUV) light with atoms and molecules. This research provides valuable information on both thermochemistry and dynamics. Our recent studies cover the gamut from photoionization mass spectrometry (PIMS) of atoms to transient species to buckminsterfullerene.

Recent Progress

I. Recent VUV-PIMS Studies of Transient Species

A. The important combustion intermediates CH_3O and CH_2OH

Both of these species were prepared *in situ* by the reaction of F atoms with CH_3OH. Additional experiments were performed using CD_3OH, CH_3OD and CD_3OD. The adiabatic ionization potential of CH_2OH (CD_2OH) was found to be 7.549 ± 0.006 (7.540 ± 0.006) eV, in good agreement with earlier photoelectron spectroscopic (PES) values of 7.56 ± 0.01 (7.55 ± 0.01) eV. However, although CD_3O^+ was studied, CH_3O^+ could not be detected in the F + CH_3OH or F + CH_3OD experiments. The ionization potential of CD_3O was found to be 10.726 ± 0.008 eV, making the cation metastable with respect to CD_2OH^+ and $HCO^+ + D_2$. Apparently, the lifetime of CH_3O^+ is too short (< 3 x 10^{-6} s) to be detected, but CD_3O^+ survives longer. An earlier PES value for I.P. (CH_3O^+) of 7.37 ± 0.03 eV is clearly in error, due to misassignment of the species. The current value for I.P. (CD_3O) makes plausible a previous estimate for ΔH_f° (CH_3O^+), based on a rather involved argument.

B. The analogous thio intermediates CH_3S and CH_2SH

Both CH_3S and CH_2SH were prepared *in situ* by the reaction of F atoms with CH_3SH. Confirmatory experiments were performed with CD_3SH, where the CD_3S and CD_2SH species appear at different masses. The adiabatic ionization potentials obtained are 7.536 ± 0.003 (7.522 ± 0.003) eV for CH_2SH (CD_2SH) and 9.262 ± 0.005 (9.268 ± 0.005) eV for CH_3S (CD_3S). The latter value is slightly higher than a recently published one (9.225 ± 0.014 eV).[1] No prior value exists for IP (CH_2SH). A discrepancy in the difference of ΔH_{f0}° (CH_3S^+) and ΔH_{f0}° (CH_2SH^+) arising from recent theoretical[2] and experimental determinations is resolved in favor of the *ab initio* values. Also, we find that D_0° (H-CH_2SH) ≤ 93.95 ± 0.13 kcal/mol, and more probably 92.4 ± 2.0 kcal/mol, while D_0° (CH_3S-H) = 86.0 ± 0.6 kcal/mol. Unlike the CH_3O^+/CD_3O^+ case, both CH_3S^+ and CD_3S^+ are observed.

1. S. Nourbakhsh, K. Norwood, G.-Z. He and C. Y. Ng, J. Am. Chem. Soc. 113, 6311, (1991).
2. R. H. Nobes and L. Radom, Chem. Phys. Lett. (in press).

C. Thioformaldehyde and HCS

The reaction of F atoms with CH_3SH generates some free CH_2S and HCS by consecutive H abstraction. We are in the process of studying these species from this reaction, and also using other sources. We tentatively obtain IP(CH_2S) = 9.376 ± 0.003 eV, which enables one to select between two earlier PES values of 9.38 and 9.34 ± 0.01 eV. No direct determination of IP(HCS) exists. Our goal in this work is to establish ΔH_{f0}^{o} (CH_2S^+) and ΔH_{f0}^{o} (HCS^+), and through their respective ionization potentials, ΔH_{f0}^{o} (CH_2S) and ΔH_{f0}^{o} (HCS). If successful, we shall have established the successive bond energies in going from CH_3SH through the various intermediates to the elements.

D. The recently synthesized CH_3OF

The VUV-PIMS of CH_3OF displays a prominent parent ion peak, whose adiabatic onset is 11.340 ± 0.008 eV, although much lower energy fragmentation processes (CH_2O^+ + HF, 8.0 eV; CH_2OH^+ + F, 9.3 eV) are possible. These lower energy processes have very low intensity. Two higher energy processes, to CH_3^+ + OF and CH_2O^+ + H + F are observed. Their thresholds are used to determine ΔH_{f0}^{o} (CH_3OF) ≥ -23.0 ± 0.7 kcal/mol, or D_o (CH_3O-F) ≤ 47.4 ± 1.2 kcal/mol. CH_2OF^+ is a significant fragment, whose appearance energy leads to ΔH_{f0}^{o} (CH_2OF^+) ≈ 215.1 ± 0.8 kcal/mol.

II. VUV-PIMS Studies of Heavy Systems

A. Buckminsterfullerene

Gaseous C_{60} has been studied by photoionization mass spectrometry between the ionization threshold and 40.8 eV. An adiabatic threshold of 7.57 ± 0.01 eV is observed, which may be slightly low due to hot bands. The energy derivative of the photoion yield curve is in rough agreement with the He I photoelectron spectrum on the positions of some peaks, but others are weak or absent. The discrepancy is not attributed to autoionization, but rather to selection rules governing the ejection of low energy electrons into high angular momentum waves. C_{60}^{++} is observed at higher energies, and becomes ~ 0.6 as intense as C_{60}^{+} at 40.8 eV. The photoion yield curve of C_{60}^{++}, approximately linear well above threshold, appears to exhibit curvature near threshold, thwarting an attempt to make a distinction between two alternative values of the second ionization potential. Fragmentation to form C_{58}^{+} is only observed at the highest energy, 40.8 eV. The unimolecular decay is modelled by quasiequilibrium theory. In this model, the kinetic shift is of the order of 30 eV, and the minimum energy for dissociation into C_{58}^{+} + C_2 seems to be 6.0-6.5 eV.

B. Pnicogen clusters (As_n, Sb_n, Bi_n)

1. As_2, As_3 and As_4

Sublimation of arsenic yields (predominantly) As_4. Some autoionizing structure is observed in the photoion yield curve as of As_4^+(As_4). I.P. (As_4) ≤ 8.49 eV, and may be much lower, due to severe geometric changes upon ionization. A.P. As_3^+ (As_4) leads to ΔH_{f0}^{o} (As_3^+) ≤ 228.7 ± 1.3 kcal/mol. Sublimation of InAs yields mostly As_2, with some As_4 and no detectable As_3. From an upper limit to the As_3 intensity, and assuming equilibrium conditions, we deduce ΔH_{f0}^{o} (As_3) ≥ 60.0 kcal/mol, and probably ΔH_{f0}^{o} (As_3) ≅ 63 kcal/mol. Consequently, I.P. (As_3) < 7.32 eV, and probably 7.19 eV. The adiabatic IP of As_2 is 9.69 ± 0.02 eV. Two prominent autoionizing Rydberg series converge to

the $A^2\Sigma_g^+$ state of As_2^+, with an IP of 10.238 ± 0.002 eV. At higher energy, three members of a window resonance series are observed, converging to the $B^2\Sigma_u^+$ state of As_2^+, with an IP of 15.37 eV.

2. s-like window resonances in pnicogen atoms and diatomic molecules

Photoexcitation of electrons from the sub-valence s orbitals of atoms of groups V-VIII gives rise to asymmetric peak shapes ($|q| \approx 1$-2) for elements in the first row, and to window resonances ($|q|<1$) for the heavier analogs. An analogous pattern is now seen for related transitions emanating from $ns\sigma_u$ orbitals in the corresponding homonuclear diatomic molecules of the pnicogens and chalcogens. This correlation is at first glance surprising, since there is a change of symmetry, the molecular orbitals are not localized, and the excitation is to p-like Rydberg orbitals in the atoms, but restricted to gerade (s, d) Rydberg orbitals in the molecules. Rationalizations are offered for this systematics, and trends within the pattern. The relationship of this behavior to oscillator strengths and photoelectron spectra is discussed, and suggestions are made for future research.

3. Sb_n and Bi_n

Several laser photoionization and photodissociation studies of Sb_n, Bi_n and their cations have appeared recently, ostensibly motivated by the importance of these species in the plasmas used for chemical vapor deposition of semiconductor materials. When the species are generated by supersonic expansion, the relation between observed ions and their neutral progenitors is often obscured. The present studies utilize thermochemistry to generate essentially unique masses for study. In this way, we have studied Sb_2, Sb_3 and Sb_4, and also Bi, Bi_2, Bi_3 and Bi_4. We have already been able to correct some of the laser-supersonic expansion studies. Current evidence points to the trimers as being essentially triangular, unlike N_3, which is linear. We hope to be able to provide a complete picture of the energetics and photoionization dynamics of all the pnicogen clusters and their cations.

Future Plans

I. Short term

We plan to complete our studies of CH_2S and HCS. We intend to apply the chemical reaction method to the important combustion intermediates HCO and HO_2. We also plan to complete our high temperature-high mass range studies of Sb_n and Bi_n.

II. Longer Term

We are in the process of assembling a VUV laser system. This apparatus should enable us to achieve still higher resolution in selected wavelength regions, particularly in the 90-105nm region. Since the VUV laser is pulsed, it is well suited for the study of very short lived transient species, which are more readily generated by pulsed methods.

We also plan to use photoionization methods to prepare state-selected ions for the study of ion-molecule reactions of relevance in combustion and other chemical processes.

Work supported by the U.S. Department of Energy, Office of Basic Energy Sciences, Division of Chemical Sciences, under Contract W-31-109-ENG-38.

Publications of DOE Sponsored Research (1990-92)

Photoionization Studies of GeH_n (n = 2-4). B. Ruscic, M. Schwarz and J. Berkowitz, J. Chem. Phys. 92, 1865-1875 (1990)

Electric Field Effects in the Photoionization of N_2 Near Threshold. J. Berkowitz and B. Ruscic, J. Chem. Phys. 93, 1741-1746 (1990)

Photoionization of HBr and DBr near Threshold. B. Ruscic and J. Berkowitz, J. Chem. Phys. 93, 1747-1754 (1990)

Photoion-Pair Formation and Photoelectron-Induced Dissociative Attachment in C_2H_2: D_o (HCC-H). B. Ruscic and J. Berkowitz, J. Chem. Phys. 93, 5586-5593 (1990)

Partial Cross Sections in the Photoionization of Open-Shell Atoms: Photoelectron Spectroscopy of Te. G. L. Goodman and J. Berkowitz, J. Chem. Phys. 94, 321-330 (1991)

Photoionization Mass Spectrometric Studies of Free Radicals. J. Berkowitz and B. Ruscic, in "Vacuum Ultraviolet Photoionization and Photodissociation of Molecules and Clusters", C.-Y. Ng, Ed., World Scientific, New Jersey (1991), p. 1-41

Photoionization Mass Spectrometric Study of Si_2H_6. B. Ruscic and J. Berkowitz, J. Chem. Phys. 95, 2407-2415 (1991)

Photoionization Mass Spectrometric Studies of the Transient Species Si_2H_n (n= 2-5). B. Ruscic and J. Berkowitz, J. Chem. Phys. 95, 2416-2432 (1991)

Photoionization Mass Spectrometric Study of N_2H_2 and N_2H_3: N-H, N=N Bond Energies and Photon Affinity of N_2. B. Ruscic and J. Berkowitz, J. Chem. Phys. 95, 4378-4884 (1991)

Photoionization Mass Spectrometric Studies of the Isomeric Transient Species CD_2OH and CD_3O. B. Ruscic and J. Berkowitz, J. Chem. Phys. 95, 4033-4039 (1991)

Photoionization Mass Spectrometric Study of CH_3OF. B. Ruscic, E. H. Appelman and J. Berkowitz, J. Chem. Phys. 95, 7957-7961 (1991)

Vacuum Ultraviolet Photoionization Mass Spectrometric Study of C_{60}. R. K. Yoo, B. Ruscic and J. Berkowitz, J. Chem. Phys. 96, 911-918 (1992)

Photoionization of As_2 and As_4: Implications for Group V Clusters. R. K. Yoo, B. Ruscic and J. Berkowitz, J. Chem. Phys. (accepted).

On s-like Window Resonances in Some Atoms and Homonuclear Diatomic Molecules. J. Berkowitz, B. Ruscic and R. K. Yoo, Comments on Atomic and Molecular Physics (submitted).

Energy Partitioning in Elementary Chemical Processes

Richard Bersohn
Department of Chemistry
Columbia University
New York, NY 10027

VUV laser induced fluorescence is used to detect atoms which are the products of chemical reactions and photodissociation. The dynamics of photodissociation of molecular hydrides has been studied at 121.6 nm and an improved method for the detection of bromine and chlorine atoms in both spin orbit states has been developed.

Photodissociation of hydrides at 121.6 nm

121.6 nm is the wavelength emitted by hydrogen atoms in the 2p state. Half of all the solar VUV radiation is at this wavelength and it is therefore important both practically and theoretically to study photochemistry at this energy. One difficulty is that the existing pulsed VUV sources, synchrotrons or lasers are generally too weak to produce an adequate number of fragments for subsequent probing. Two photon resonant four wave frequency difference mixing does produce the strongest monochromatic pulses especially when two resonances are exploited. This can be done in Kr gas if, for example, one mixes two photons of 47046 cm^{-1} with one photon near 11830 cm^{-1}. The sum of the energies of the first two photons are resonant with the 5p[01/2] state of Kr and the VUV photon at 82235 cm^{-1} is near the Kr resonance line at 80906 cm^{-1}.

A special but highly important set of molecules are the hydrides whose hydrogen atoms can be dissociated by one VUV photon and then excited by another;

$RH + h\nu \rightarrow R + H$
$H + h\nu \rightarrow H^*(2p)$

By sweeping the IR frequency the vuv frequency is swept through the absorption spectrum of the H atom. The second moment of this spectrum yields the atom's average translational energy, $\langle E_T \rangle$. Hydrides dissociated this way include H_2O, CH_4, SiH_4, GeH_4, HCCH and their partially deuterated isotopomers. In all cases release of H is favored over D, typically by a factor of two. Methane releases H atoms with average kinetic energies near 50 kcal/mol which rules out the exit channel CH_2 + 2H. HCN produces H atoms with average kinetic energies of 75 kcal/mol, the fastest so far generated by photodissociation.

Halogen atom fine structure state population ratios

Cl and Br atoms are generated by chemical reactions or photodissociations in both J=3/2 and 1/2 states, separated by 881 and 3685 cm^{-1} respectively. The ratio of the populations in these two states depends on the overlap of absorption bands and on surface crossing between the excited states during the collision or half collision. Techniques for measuring this ratio involve VUV LIF(Br atoms)[1], IR emission (I and Br atoms)[2], diode laser absorption (Cl atoms)[3] and REMPI (Cl atoms).[4].

The VUV LIF and REMPI techniques are more sensitive than those based on IR. REMPI is the most sensitive but has the disadvantage that it requires very low pressures and strong focusing of the probing light on the reaction system. AS previously implemented, the VUV LIF technique required generation of VUV by mixing two laser beams in magnesium vapor. We have found that generation of VUV by frequency tripling in CO[5] is more convenient and produces good signals as shown in Fig. 1. The following transitions are utilized:

Atom	Lower State	Upper State	Energy(cm^{-1})	Wavelength (nm)
Cl	^2P	^2P	74861	133.58
Cl	$^2P_{3/2}$	$^2P_{1/2}$	73980	135.17
	$^2P_{1/2}$	$^2P_{1/2}$		
Br	^2P	^4P	64900	154.08
Br	$^2P_{3/2}$	$^2P_{3/2}$	65218	153.33
	$^2P_{1/2}$	$^2P_{1/2}$		

It is planned to apply this technique to reactions in which Cl or Br atoms are products.

Future research

The projects described above are being completed and we will begin a new, difficult three laser experiment on mode specific chemistry.[6] In particular, we plan to study the oxidation of vibrationally excited hydrocarbons. The first example will be the reaction of $O(^3P)$ atoms with HCCH. The two major reaction channels involve C-H and C-C bond cleavages producing H atoms or CO molecules. The symmetric C-H or C-C stretch will be excited by stimulated Raman scattering and the effect on the yields of the two channels will be measured. The fundamental question the experiment tries to answer is- does the transition state "remember" the specific mode of excitation or is energy simply randomized in the transition state? The state distribution of the CO product will be probed with and without vibrational excitation of the acetylene. Should this experiment succeed ethylene and methane would be the next targets.

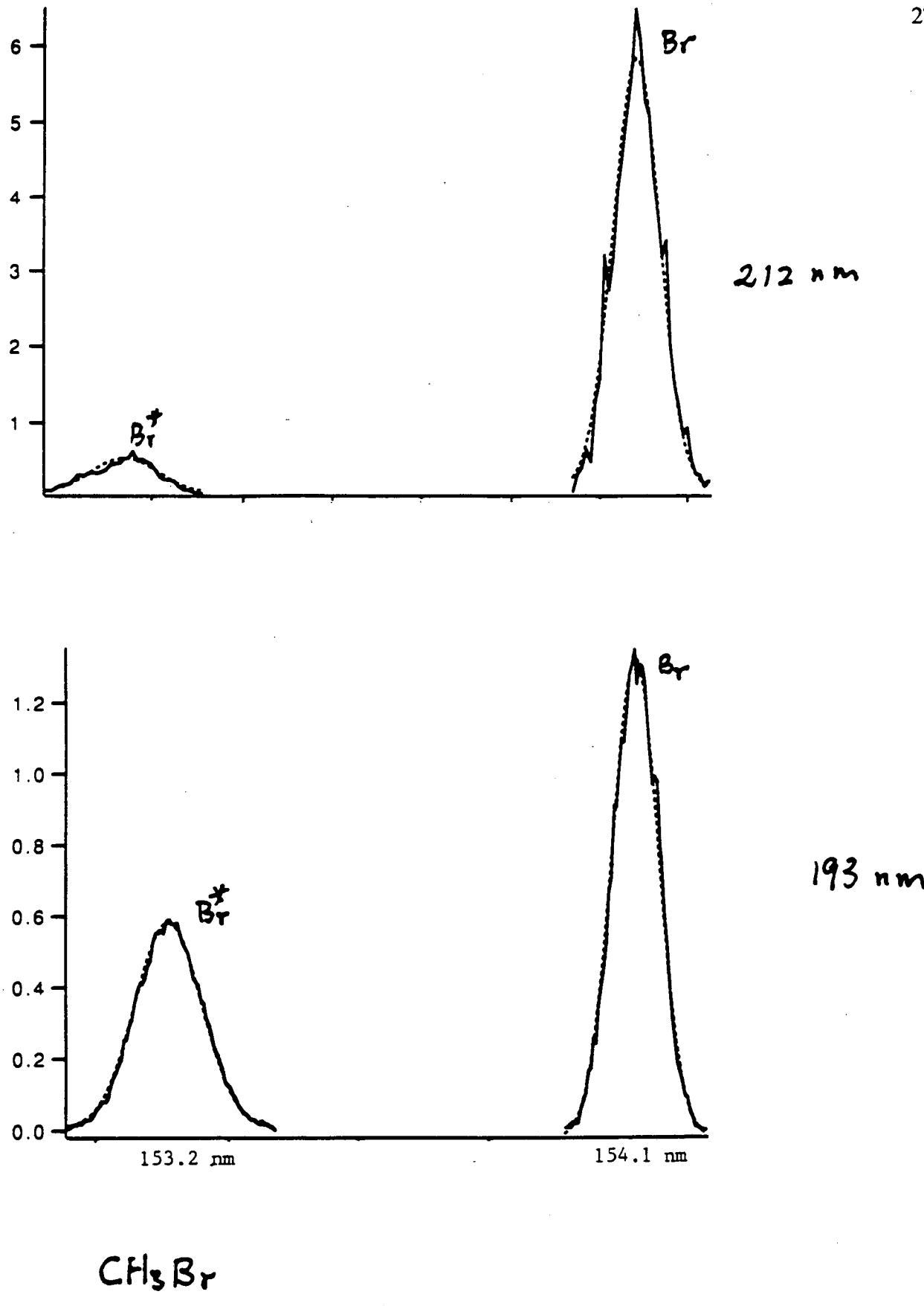

Fig. 1 LIF spectra of Br atoms photodissociated from CH_3Br. Abscissa scale is not linear.

References

1. J.W.Hepburn,K.Liu,R.G.Macdonald,F.J.Northrop, and J.C.Polanyi, J.Chem.Phys. 75,3353(1981)

2. W.H.Pence,S.L.Baughcum and S.R.Leone, J.Phys.Chem. 85,3844(1981)

3. J.Park,Y.Lee and G.W.Flynn, Chem.Phys.Lett.186,441(1991)

4. Y.Matsumi,K.Tonokura,M.Kawasaki,G.Inoue,S.Satyapal and R.Bersohn, J.Chem.Phys. 94,2669(1991)

5. J.H.Glownia and R.K.Sander in Laser Techniques for Extreme Ultraviolet Spectroscopy (Boulder,1982) AIP Conference Proceedings No.90, 1982

6. A.Sinha,M.C.Hsiao,F.F.Crim, J.Chem.Phys. 94,4928(1991)

Publications on Research Supported by the DOE 1990-92

1. The isotope exchange reaction of fast hydrogen atoms with deuterated alkenes and alkynes with G.W.Johnston and S.Satyapal, J.Chem.Phys. 92,206(1990)
2. Unimolecular decomposition of methyl substituted benzenes into benzyl radicals and hydrogen atoms with J.Park and I.Oref J.Chem.Phys. 93,5700(1990)
3. Properties of Hydrogen Atoms Newly Generated in Chemical Reactions with G.Johnston,J.Park,B.Katz, S.Satyapal,N.Shafer and K.Tsukiyama, Acc.Chem.Res. 23,232(1990)
4. The hydrogen atom channel in the photodissociation of ethylene, with S.Satyapal,G.Johnston and I.Oref, J.Chem.Phys. 93,6398(1990)
5. Unimolecular dissociation of cyclopentadiene and indene with W.Yi and A.Chattopadhyay, J.Chem.Phys. 94,5984(1991)
6. The photodissociation of acetylene with S.Satyapal, J.Phys.Chem. 95,8004(1991)
7. Temperatures of Fragments in Unimolecular Dissociations, chapter in Mode Selective Chemistry, J.Jortner et al. (eds.), Kluwer Academic Publishers, 1991

Theoretical Studies of Combustion Dynamics

Joel M. Bowman
Department of Chemistry
Emory University
Atlanta, GA 30322

The basic objectives of this program are to develop and apply theoretical techniques to fundamental dynamical processes of importance in gas phase combustion. There are two major areas currently supported by this grant. One is reactive scattering of diatom-diatom systems, and the other is the dynamics of complex formation and decay based on L^2 methods. In all of these studies we focus on systems which are of interest experimentally and for which potential energy surfaces based, at least in part, on *ab initio* calculations are available.

I. Reduced dimensionality theory of quantum reactive scattering

We applied our adiabatic/bend reduced dimensionality quantum theory to a study of mode selectivity in the reactions

$$H_2O(v_1,v_b,v_2) + H \rightarrow OH(v) + H_2(v')$$

$$HOD(v_1,v_b,v_2) + H \rightarrow OH(v) + HD(v'),\ OD(v)+H_2(v').$$

These reactions in the forward directions have been recently studied experimentally by two groups.[1,2] In the case of the reaction with HOD, striking mode specificity with respect to the product branching ratio was seen. We found similar specificity in our calculations, which are shown below for zero total angular momentum.

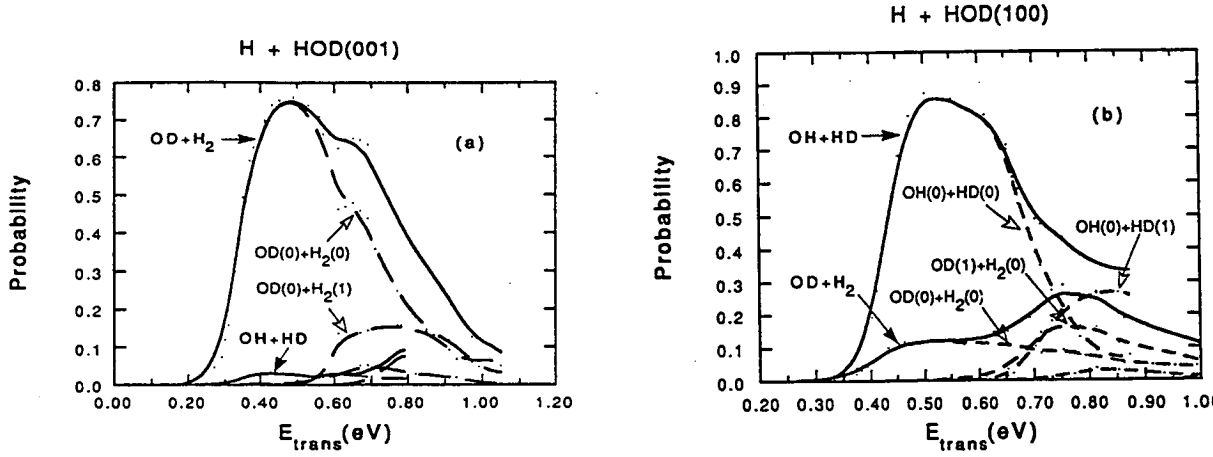

(a) Reaction probabilities H+HOD(001) [OH excitation] → H_2(v)+OD(v') and → HD(v)+OH(v'), as a function of the initial translational energy measured with respect to the energy of the HOD(001) vibrational state. Solid curve labeled "OH+HD" is the reaction probability summed over the vibrational states of OH and HD, and H_2+OD. Solid curve labeled "OD+H2" is the reaction probability summed over the vibrational states of OD and H_2. (b) Analogous to (a) but for H+HOD(100) [OD excitation] → H_2(v)+OD(v') and HD(v)+OH(v').

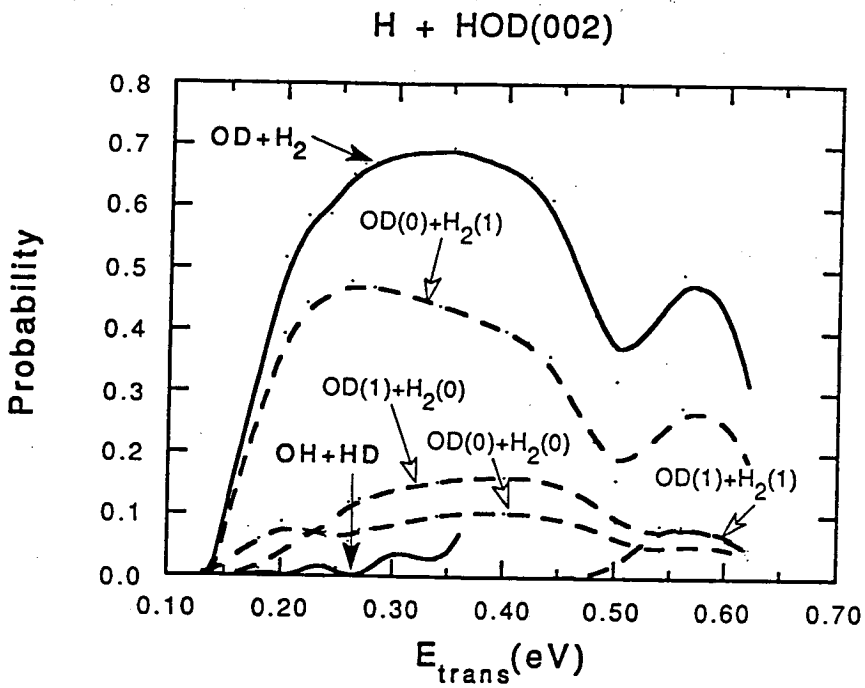

Reaction probabilities for H+HOD(002) [OH excitation] → H_2(v)+OD(v') and HD(v)+OH(v'), as a function of the initial translational energy measured with respect to the energy of the vibrational state HOD(002).

As seen excitation of the OH local mode in HOD leads predominantly to the H_2+OD products, whereas excitation of the OD local mode in HOD leads predominantly to the HD+OH products. These effects can be understood from the substantial OH (or OD) stretch character of the transition state normal mode corresponding to the imaginary reaction path frequency. Thus, excitation of the OH (or OD) stretch greatly excites motion along the reaction coordinate.

Future work will include calculations for non-zero total angular momentum, which will result in the calculation of rate constants and cross sections. Also, we hope to extend the calculations to higher translational energies so that the entire range of the "hot atom" experiments can be covered by the calculations. We also hope to begin calculations on the Cl+H_2O → HCl+OH reaction.

II. Resonances and highly excited states of HCO and HO_2

We are continuing our collaboration with Dr. Al Wagner in comparisons of L^2 and scattering resonances for H+CO. In our most recent work, we found very good agreement for the positions of resonances for J = 1. While we do not find substantial K-asymmetry, we do see significant centrifugal effects, especially for highly excited bend states.

A study of the time dependence of OH overtone excitation in non-rotating HO_2 below and slightly above dissociation has been completed, and reported. We also finished a complete calculation of the absorption spectrum of HO_2 up to dissociation. In the latter, we found a very interesting "gap" in the spectrum in the region of transitions with energies in the vicinity of the barrier height to isomerization.

Future calculations will include multichannel distorted wave calculations of the resonances in these systems.

References

1. (a) A. Sinha, M. C. Hsiao, and F. F. Crim, J. Chem. Phys. **94**, 4928 (1991); (b) A. Sinha, J. Phys. Chem. **94**, 4391 (1990); (c) A. Sinha, M. C. Hsiao, and F. F. Crim, J. Chem. Phys. **92**, 6334 (1990); (d) F. F. Crim, M. C. Hsiao, J. L. Scott, A. Sinha, and R. L. Vander Wal, Philos. Trans. R. Soc. London, Ser. A **332**, 259 (1990).

2. M. J. Bronikowski, W. R. Simpson, B. Girard, and R. N. Zare, J. Chem. Phys. **95**, 8647 (1991).

PUBLICATIONS SUPPORTED BY THE DOE (1990-present)

New reduced dimensionality rate constants for $D+H_2$ and $H+D_2$, J. M. Bowman and Q. Sun, J. Phys. Chem. **94**, 718 (1990).

A comparison of scattering and and L2 photodetachment Franck-Condon factors for reduced dimensionality $ClHCl^- \rightarrow Cl+HCl+e^-$, Q. Sun, B. Gazdy and J. M. Bowman,J. Chem Soc. Farad. Trans. **86**, 1737 (1990).

Reduced dimensionality diatom-diatom reactive scattering: Application to a model $H_2+A_2 \rightarrow H+HA_2$, Q. Sun and J.M. Bowman, J. Chem. Phys. **92**, 1021 (1990).

Reduced dimensionality quantum reactive scattering: $H_2+CN \rightarrow H+HCN$, Q. Sun and J.M. Bowman, J. Chem. Phys. **92**, 5201 (1990).

Experimental and reduced dimensionality quantum rate coefficients for $H_2(D_2)+CN \rightarrow H(D)CN+H(D)$, Q. Sun, D.L. Yang, N.S. Wang, J.M. Bowman, and M.C. Lin, J. Chem. Phys. **93**, 4730 (1990).

Theoretical to experimental rate constant comparisons for two isotopic modifications of the simplest chemical reaction, $H+H_2$, J.V. Michael, J.R. Fisher, J.M. Bowman, and Q. Sun, Science, **249**, 269 (1990).

Reduced dimensionality quantum calculations ... for the Cl+HCl reaction: Comparison with centrifugal-sudden distorted wave Born, coupled channel ..., and experimental results, Q. Sun, J.M. Bowman, G.C. Schatz, J.R. Sharp, and J.N.L. Connor, J. Chem. Phys. **92**, 1677 (1990).

A simple method to adjust potential energy surfaces: Application to HCO, J.M. Bowman and B. Gazdy, J. Chem. Phys. **94**, 816 (1991).

Comment on "Effect of Rotational Quantum States (J=0, 1) on the Tunneling Reaction $H_2+H \rightarrow H+H_2$ in Parahydrogen Solid at 4.2 K", J.M. Bowman, J. Phys. Chem. **95**, 4921 (1991).

Theoretical stabilization and scattering studies of resonances in the addition reaction H + CO $\rightleftharpoons$ HCO, B. Gazdy, J.M. Bowman, S-W. Cho, and A.F. Wagner, J. Chem. Phys. **94**, 4192 (1991).

An L^2 stabilization study of bound states and resonances in HCO, B. Gazdy and J.M. Bowman, in Adv. Molec. Vibs. and Coll. Dynamics, eds. J.M. Bowman and M.A. Ratner, (JAI, Greenwich, 1991), pp. 105-137.

"Feature Article": Reduced dimensionality theory of quantum reactive scattering, J.M. Bowman, J. Phys. Chem. **95**, 4960 (1991).

Vibrational energies and wavefunctions of high energy localized and floppy states of HO_2, J. M. Bowman, Chem. Phys. Lett. **180**, 249 (1991).

Time dependence of OH overtone relaxation in the hydroperoxyl radical, D. Chapman, J.M. Bowman, and B. Gazdy, J. Chem. Phys. **96**, 1919 (1992).

Theoretical studies of the reactivity and spectroscopy of H + CO $\rightleftharpoons$ HCO. I. Stabilization and scattering studies of resonances for J=0 on the Harding *ab initio* surface, B. Gazdy, J.M. Bowman, S-W. Cho, and A.F. Wagner, J. Chem. Phys. in press.

Isolated resonance decomposition of a multichannel S-matrix: A test from the scattering of H + CO $\rightleftharpoons$ HCO, S-W. Cho, A.F. Wagner, B. Gazdy, and J.M. Bowman, J. Chem. Phys. in press.

The addition and dissociation reaction H + CO $\rightleftharpoons$ HCO. 3. Implementation of isolated resonance RRKM theory with exact quantum studies for J=0, S-W. Cho, A.F. Wagner, B. Gazdy, and J.M. Bowman, J. Phys. Chem. in press.

Reduced dimensionality quantum calculations of mode specificity in the $OH+H_2 \rightarrow H_2O$ reaction, D-S. Wang, and J.M. Bowman, J. Chem. Phys. in press.

Mode selectivity in reactions of H with HOD(100), HOD(001) and HOD(002), J.M. Bowman and D-S. Wang, J. Chem. Phys. in press.

Nancy J. Brown

LAWRENCE BERKELEY LABORATORY, BERKELEY, CALIFORNIA 94720

Recent research has been concerned with the application of functional sensitivity analysis to determine the relationship between dynamic observables and the potential energy surface structure. This provides an understanding of how different regions of the potential play a part in controlling the dynamics, and thereby influence the eventual outcome of calculated observables. Functional sensitivity analysis has been applied to classical dynamics studies of energy transfer and to quantum mechanical studies of reactive scattering.

Research on quantum functional sensitivity analysis (QFSA) studies of reactive scattering research is being performed in collaboration with Dr.'s Johnny Chang and Mikael D'Mello and with Professors Herschel Rabitz and Robert Wyatt. One of the current objectives of this study is to address a fundamental question concerning the use of functional sensitivity analysis as a tool in improving potential energy surfaces. If a sensitivity analysis is performed during the construction of a potential energy surface when the fitted surface is based upon a modest number of ab initio points, will the results of sensitivity analysis reveal where the higher density of ab initio points should be calculated? Sensitivity analysis of quantum reactive scattering was performed for the collinear H + H_2 reaction on three potential energy surfaces: an "incorrect" potential, the PK-2 surface; the more correct Liu, Siegbahn, Truhlar, Horowitz[1] surface, LSTH; and the most correct Double Many Body Expansion surface, DMBE[2], of Varandas et al. We determined sensitivity maps as a function of energy in the regions of threshold, strong tunneling and resonance. The same sensitivity structure obtains on all surfaces in the same region but not at the identical energy. Functional sensitivity analysis can be used to direct quantum chemists to calculate ab initio points in the important regions of configuration space.

Two sensitivity analysis techniques have been used to demonstrate how one can predict observables on new or perturbed potential energy surfaces (PES) without doing any additional dynamics calculations on the new PESs. Both techniques require the computation of the observable (O) and its sensitivity to variations in the potential ($\delta O/\delta V$) on just one surface. The first approach uses a simple first order expansion of the observable with respect to δV. The second approach uses a nonlinear least-squares fit of particular features in the observable, and then uses the same functional form to predict the observable on a different PES but with a modified set of fitting parameters. The new fitting parameters are related to the old ones via a functional Taylor expansion. Both approaches work well when variations in the potential are small. When the potential difference is large, the second approach gives reasonable results even in cases where the first approach gives spurious predictions. These ideas have been tested for the collinear H +

H_2 reaction with the framework of quantum reactive scattering using the log-derivative version of the Kohn variational principle for the scattering calculations.

The effects of features in the potential energy surface on the collinear H + H_2 reaction rate coefficient have also been investigated by the method of QFSA. The calculations use QFSA to connect features in the microscopic realm, with their response upon macroscopic quantities of chemical interest, via the intermediary sensitivities of the reactive transition probabilities. While the sensitivities of the individual transition probabilities show considerable structure, there is an attendant loss of structure in the rate coefficient sensitivities because of thermal averaging. We considered temperatures in the range 200 to 2400 K and found that the most important region of the PES is the low energy shoulder of the barrier rather than the top of the barrier. We also found regions near the barrier where an increase in the potential surface actually increases the reaction rate. The effects of using different underlying potentials (the PK-2, LSTH, and DMBE surfaces) on the nature of the results were also determined. The absolute sensitivity magnitudes on the PK-2 surface vary considerably from the other two, but the relative change in the rate coefficient, $k^{-1}\delta k/\delta V$, is the same for all three potentials. Furthermore, the identified regions of importance on the potential surfaces remain essentially the same.

Work (in collaboration with Johnny Chang and Herschel Rabitz) on the functional sensitivity analysis of co-planar rotationally inelastic collisions continued. The collisions are studied with quasi-classical molecular dynamics. We investigated the effect of initial translational energy (5 and 10 kcal/mol) on the structure of the sensitivity coefficients and the full sensitivity maps. Sensitivity coefficients are proportional to the sensitivities to the various radial terms in the PES, which is expanded in a series of products of radial and angular terms. The behavior of the radial sensitivities with respect to initial translational energy shows some interesting characteristics. The magnitudes of the sensitivities do not change dramatically with initial translational energy. The sensitivities at 10 kcal/mol exhibit earlier (with respect to R) nonzero structure because the trajectories at the higher energy are able to penetrate further into the potential core as the classically accessible region is increased. The sensitivities at the two energies often have similar shapes, showing positive, then negative values, or the opposite, but the peaks and valleys appear at different values of R. Consequently, for a given R, regions of positive sensitivity at one energy become negative at the other. This implies that a perturbation of the potential at a fixed value of R will affect observables differently at the two energies. The full sensitivity maps are constructed by adding the Fourier components. Behavior found in the individual radial components manifests itself in the full sensitivity maps so that regions of positive sensitivity at one energy are negative at the other energy. We had anticipated that H_2 would behave more like a spherical atom as the initial kinetic energy was increased. This was not observed in the full sensitivity maps.

A modeling study of the reduction of NOx by HNCO, which is co-sponsored by the California Institute for Energy Efficiency, is nearly completed.

A chemical mechanism has been constructed for modeling NOx reduction by HNCO in exhaust mixtures typical of natural gas combustion. The reduction was modeled assuming plug flow and either isothermal or constant pressure adiabatic combustion. Model calculations were compared with experiments to establish model validity. Variables considered in the set of modeling experiments were the initial concentrations of NOx (NO and NO_2), CH_4, H_2, and HNCO and the initial exhaust gas temperature. Ignition of the post-combustion mixture is important in the reduction process. Additional fuel, which in these studies was H_2, must be added to the natural gas exhaust mixture to affect reduction in a 1 second residence time. Immediately before NO is reduced, the HNCO concentration declines, the NH_3 and OH concentrations are at a maximum, NO_2 to NO conversion occurs. The reduction of NO occurs concurrently with N_2O production. The temperature window for optimum reduction is very sharp (approximately 75 K) and is influenced by the exhaust gas "fuel" concentration and temperature. The window is shifted to lower temperatures with increased H_2 concentration. At the optimum reduction temperature for a given composition, the final N_2O concentration decreases, the final HNCO and NH_3 concentrations increase with increasing H_2 concentration. For an adiabatic system, when ignition occurs and final temperatures exceed 1200 K, NO is produced. Sensitivity analysis revealed that the reduction process was critically dependent on radical generation and ignition chemistry, and that NH_3 and NO chemistry are strongly coupled.

References

1. Liu, B., (1973), J. Chem. Phys. **58**, 1925.

Siegbahn, P. and Liu, B., (1978), J. Chem. Phys. **68**, 2457.

Truhlar, D.G. and Horowitz, C.J., (1978), J. Chem. Phys. **68**, 2466.

Truhlar, D.G. and Horowitz, C.J., (1979), J. Chem. Phys. **71**, 1514.

2. Varandas, A.J.C., Brown, F.B., Mead, C.A., Truhlar, D.G., and Blais, N.C., (1987), J. Chem. Phys. **86**, 6258.

Martin, R. J. and Brown, N. J. (1990), "Nitrous Oxide Formation and Destruction in Lean Premixed Combustion," Combustion and Flame 80, p 238-255. Also LBL Report No. 27127.

Martin, R. J. and Brown, N. J. (1990), "Analysis and Studies of Nitrous Oxide Chemistry in Lean Premixed Combustion," Combustion and Flame 82, p 312-333. Also LBL Report No. 27128.

Brown, N. J. (1990), "Rate Coefficient Calculations for Combustion Modeling," Progress in Astronautics and Aeronautics 135, p 37-56. Also LBL Report No. 27129.

Brown, N. J. and Longuemare, Maria (1990), "Calculation of Rotational Energy Transfer Rates for HD (v=1) in Collisions with Thermal HD," Journal of Chemical Physics 93, p 2413-2417. Also LBL Report No. 28697.

Martin, R. J., Lucas, D., and Brown, N. J. (1990), "Nitrogen Species Measurement in a Flash Ignited Combustion System." Extended Abstract for the Joint Meeting of the Canadian Combustion Section and the Western States Section of the Combustion Institute and also poster session at the Twenty-third Symposium (International) on Combustion. Also LBL Report No. 28735.

Chang, J., Brown, N. J., D'Mello, M., Wyatt, R. E., and Rabitz, H. (1992), "Quantum Functional Sensitivity Analysis for the Collinear $H+H_2$ Reaction Rate Coefficient," Journal of Chemical Physics 96, p 3523-3530.

Chang, J., Brown, N. J., and Rabitz, H., (1992), "Construction of Classical Functional Sensitivity Maps for Rotationally Inelastic Collisions of H_2 with HD," submitted to Journal of Physical Chemistry. Also LBL Report No. 31750.

Brown, N. J. (1992), "Statistical and Dynamical Calculations of the $H_2 + OH \rightarrow H_2O + H$ Rate Coefficient," submitted to Journal of Physical Chemistry. Also LBL Report No. 31388.

PHOTOFRAGMENT IMAGING

David W. Chandler
Sandia National Laboratories
Livermore, CA 94550

Over the past few years the photochemistry of small molecules has been investigated using the photofragment imaging technique[1,2]. Bond energies, spectroscopy of radicals, dissociation dynamics and branching ratios are examples of information obtained by this technique. Along with extending the technique to the study of bimolecular reactions, efforts to make the technique as quantitative as possible have been the focus of the research effort. To this end, we have measured the bond energy of the C-H bond in acetylene, the branching ratio of $I(^2P_{1/2})$ to $I(^2P_{3/2})$ in the dissociation of HI, the energetics of CH_3Br, CD_3Br, C_2H_5Br and C_2H_5OBr dissociation, and the alignment of the CD_3 fragment from CD_3I photolysis. In an effort to extend the technique to bimolecular reactions, we have studied the reaction of H with HI forming $H_2(v,j)$ + $I(^2P_{1/2}$ or $^2P_{3/2})$.

We have applied photofragment ion imaging to investigate the dissociation dynamics of low-lying, doubly excited states of molecular hydrogen. A doubly excited electronic state is one in which both of the hydrogen electrons reside in excited molecular orbitals. Two-step, two-color multiphoton excitation of H_2, first via 201.8 nm, two-photon excitation into the E, F $^1\Sigma_g^+$ (v_E=0, J=1) state, followed by ~563 nm, 1+m (m=1,2) excitation through the B" $^1\Sigma_u^+$ (v=0, J=0,2), D $^1\Pi_u$ (v=2, J=1,2), and B' $^1\Sigma_u^+$ (v=4, J=0,2) states provides a ready means of populating several low-lying doubly excited states of H_2 with increasing equilibrium internuclear separations. From these doubly excited repulsive states, both dissociation and autoionization processes are possible. Because the excitation energy remains relatively constant as each intermediate state is accessed, differences in the photodissociation dynamics via each state can be ascribed directly to the effects of changing internuclear separation and electronic symmetry of the intermediate and dissociative states. H^+ fragments detected from each photodissociation pathway are distinguished by their differing velocities, determined from an ion image.

One of the ultimate goals in the field of reaction dynamics is to be able to measure the angular distribution of products in a quantum-state-specific manner. As a step in this direction, we have reported the first application of ion imaging to a bimolecular reaction[3]. We study the H + HI $\rightarrow$ H_2 + I reaction in a neat supersonic molecular beam of HI. The supersonic expansion provides a reaction precursor possessing a very narrow thermal velocity distribution. By avoiding a thermally equilibrated HI source (eg. an effusive beam, or bulb), the center-of-mass collision energy spread has been substantially reduced. Fast H atoms are formed by laser photolysis of HI, and the H_2 (v=1, J=11,13) products are ionized by (2+1) resonance-enhanced multiphoton ionization (REMPI) before being imaged onto a position-sensitive detector. In this way we have measured the laboratory-frame velocity distribution of the state-selected reaction products. Early dynamical studies of the H + HI abstraction reaction attempted to measure the angular distribution of the molecular product but failed because of background problems. More recently, internal state distributions of the molecular product have been determined, but without angular information.

Collected images are the projection of the laboratory-frame product velocity distribution for the specific H_2 quantum states ionized. Fig. 1 shows the reconstructed velocity distribution for H_2 formed in the (v=1, J=11) quantum state, that is an intensity slice through the reconstructed 3-dimensional distribution of fragments. The inner region is attributable to low kinetic energy H_2 formed from laser-induced cluster chemistry within the molecular beam. The outer region corresponds to faster moving product from the abstraction reaction. Fig. 2 illustrates an intensity profile taken as a thin horizontal slice through the center of the image. Analysis of this profile shows that several reaction pathways are responsible for the production of H_2 in a particular quantum state.

UV photolysis of HI generates both fast (2.63 eV) and slow (1.70 eV) H atoms with a difference in kinetic energy corresponding to the concomitant photolytic production of ground state I ($^2P_{3/2}$) and excited state I* ($^2P_{1/2}$), respectively. Moreover, it is energetically possible to form both ground state and electronically excited iodine atoms as abstraction reaction products along with the H_2. Hence, a total of four possible reaction pathways may be active in this system. The fastest possible H_2 will be formed by a reaction of fast H atoms with HI, producing ground state I ($^2P_{3/2}$). Here, H_2 (v=1, J=11) possesses 2.69 eV of translational energy. The slowest possible H_2 will be formed by a reaction of slow H atoms with HI, producing I* ($^2P_{1/2}$). Here, H_2 (v=1, J=11) possesses 0.82 eV of translational energy. The two intermediate pathways (fast H/I* production and slow H/I production channels) cannot be distinguished energetically in this experiment. H_2 (v=1, J=11) produced via these pathways possesses 1.76 eV of translational energy. Markers in figure 2 indicate the onset of H_2 (v=1, J=11) formed via each of these reaction channels. All reaction channels are evident in the image. Analysis of the images shows that the branching ratio for the reaction producing I or I* is a strong function of the velocity of the collision. The faster collision energy 2.63 eV H atoms lead to a branching ratio of $0.5 \pm .1$ for I*/I+I* ratio. The slower (1.7 eV) H atoms produce I* with an I*/I+I* ratio of $\sim 0.9 \pm .1$. This is the first time this reaction channel has been observed and its presence could help explain some of the discrepancies noted between the measured product internal state distribution and the calculated distributions (which do not take this channel into account). This work was done in collaboration with Dr. R. N. Zare (Stanford), Mark Buntine (Stanford), and David Baldwin (SNL).

We (Dr. R. N. Zare (Stanford), Mark Buntine (Stanford) and Theo Kitsopoulos (SNL)) are presently extending the technique to study H + D_2 in a crossed beam arrangement. When successful this will allow us to measure the angular distribution of each quantum state of the HD product.

1. D.W. Chandler and P.L. Houston, J. Chem. Phys. **87**, 1445 (1987).

2. D.P. Baldwin, M.A. Buntine and D.W. Chandler, J. Chem. Phys. **93**, 6578 (1990); D.W. Chandler, J.W. Thoman, Jr., M.H.M. Janssen and D.H. Parker, Chem. Phys. Lett. **156**, 151 (1989); D.W. Chandler, M.H.M. Janssen, S. Stolte, R.N. Strickland, J.W. Thoman, Jr. and D.H. Parker, J. Phys. Chem. **94**, 4839 (1990); J.W. Thoman, Jr., D.W. Chandler, D.H. Parker and M.H.M. Janssen, Laser Chem. **9**, 27 (1988).

3. M. A. Buntine, David P. Baldwin, Richard N. Zare and David W. Chandler, J. Chem. Phys. 94, 4672 (1991).

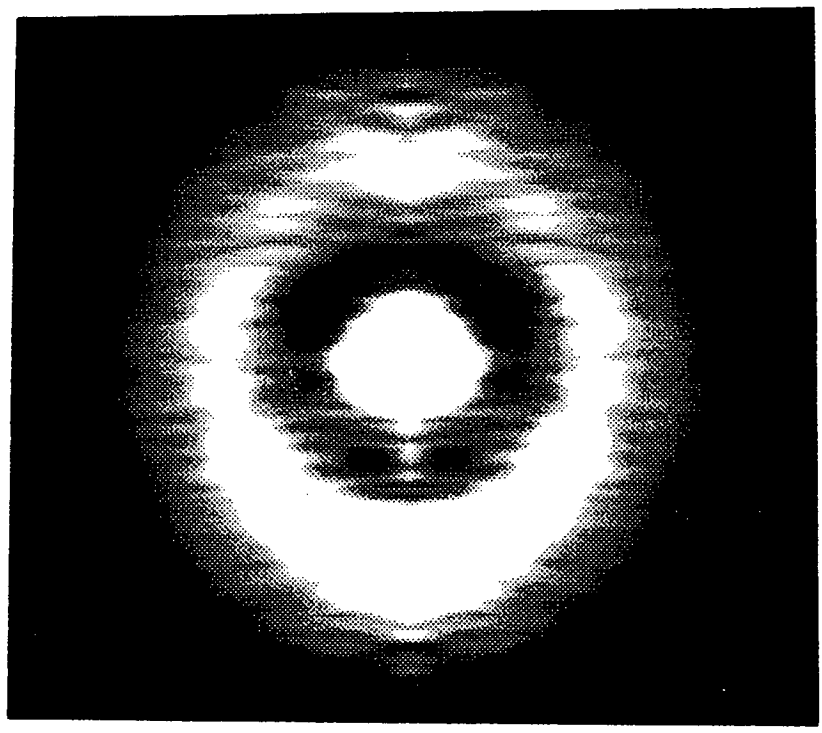

Fig. 1. Velocity distribution from ion image of H_2 (v=1, J=11) formed in the reaction H + HI → H_2 + I initiated in a beam of neat HI. Fast H atoms are formed by laser photolysis of HI, and the H_2 products are ionized before being projected onto a position-sensitive detector.

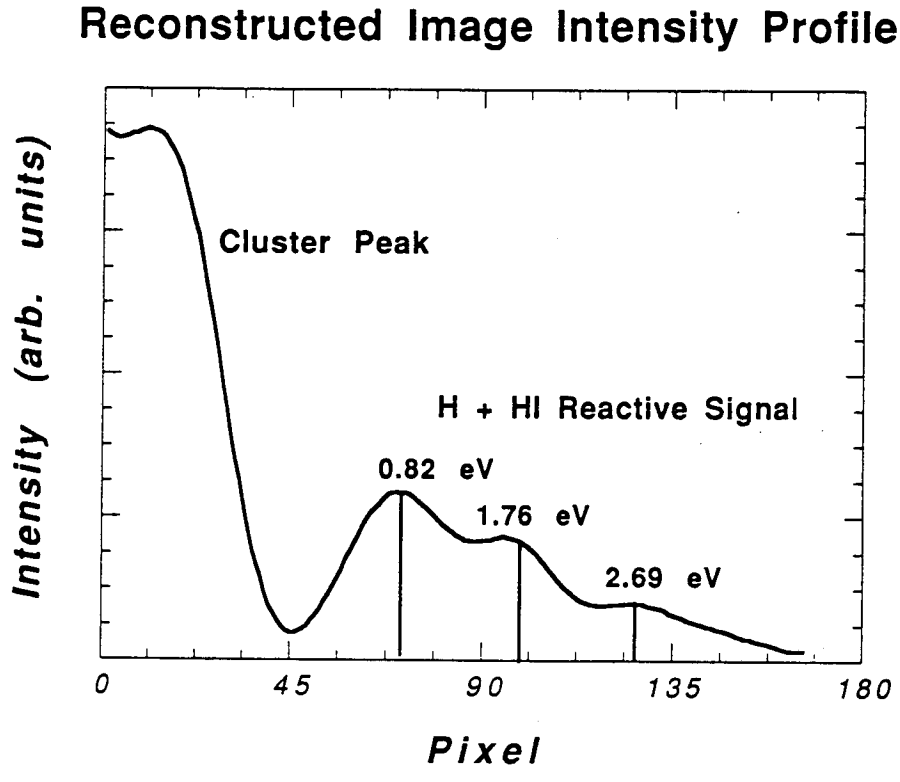

Fig 2. An intensity profile of the image, Fig.1, shows the onset of products from several competing reaction pathways.

Publication 1989-91

David W. Chandler, John W. Thoman Jr., David H. Parker, Maurice Janssen and Steven Stolte, "Ion Imaging: The 266-nm photolysis of CD_3I," J. Phys. Chem **94**, 4839 (1990).

David W. Chandler, John W. Thoman Jr. and Wayne P. Hess, "Photofragment Imaging: The Photodissociation of Bromomethane, Bromoethane and Bromoethanol" accepted for publication in Resonant Ionization Spectroscopy and its Applications, Proceedings to be published (1990).

Eric A. Rohlfing and David W. Chandler, "Two-color Pyrometric Imaging of Laser-Heated Carbon Particles in a Supersonic Flow",Chem. Phys. Lett., **170** 44 (1990).

David P. Baldwin, Mark A. Buntine, and David W. Chandler, "Photodissociation of Acetylene: Determination of D_0 (HCC-H) by photofragment imaging" J. Chem Phys. 93, 6578 (1990).

Robin N. Strickland and David W. Chandler, "Reconstruction of Axisymmetric Image from its Blurred and Noisy Projection" Applied Optics **30**,1811 (1991).

Maurice H. M. Janssen, David H. Parker, Greg O. Sitz, Steven Stolte and David W. Chandler, "Rotational Alignment of the CD3 Fragment From the 266-nm Photodissociation of CD3I". accepted for publication in J. Phys. Chem. **95**, 8007 (1991).

Mark A. Buntine, David P. Baldwin, R. N. Zare and David W. Chandler, " Application of Ion Imaging to Atom-Molecule Exchange Reactions: H + HI → H2 + I". J. Chem. Phys. **94**, 4672 (1991).

G. van den Hoek, J. W. Thoman Jr., D. W. Chandler and S. Stolte,"REMPI spectroscopy of CF3I in the Bulk and in a Molecular Beam". Chem. Phys. Lett. **188**, 412 (1992).

M. A. Buntine, David P. Baldwin and David W. Chandler "Photodissociation Dynamics of Doubly Excited Rydberg States of Molecular Hydrogen" J. Chem. Phys. Accepted (1992).

Mark A. Buntine, David W. Chandler and Carl C. Hayden " A Two-Color Laser-Induced Grating Technique for Gas-Phase Excited-State Spectroscopy" J. Chem. Phys. Submitted (1992).

Gerard Meijer and David W. Chandler "Degenerate Four Wave Mixing on Weak Transitions in the Gas Phase Using a Tunable Excimer Laser" Chem. Phys. Lett. accepted for publication (1992).

Gerard Meijer, Michel Versluis and David W. Chandler "Degenerate Four-Wave Mixing Using a Tunable Excimer Laser to Detect Combustion Gases" Accepted Twenty Fourth International Symposium on Combustion (1992).

Wayne P. Hess, David W. Chandler and John W. Thoman Jr. Photofragment Imaging:The 205 nm photodissociation of CH3Br and CD3 Br". Accepted for publication Chemical Physics (1992).

Direct Numerical Simulation of Turbulent Reacting Flows

Jacqueline H. Chen
Combustion Research Facility
Sandia National Laboratories
Livermore, California 94551-0969

Direct numerical simulations of turbulent reacting flows have been performed using the full compressible Navier-Stokes equations and a simplified chemistry model. The numerical formulation includes variable density, heat release, finite-rate chemical kinetics, non-unity Lewis numbers, and temperature dependent thermodynamic properties so that full coupling between chemistry and turbulence interactions can be considered. To date simulations have been performed to study the effect of compressibility on entrainment and mixing in a moderate convective Mach number mixing layer. Simulations are currently underway to study the structure of a nonpremixed flame in three-dimensional homogeneous turbulence subjected to transient effects, finite rate chemical kinetics, curvature, dilatation due to heat release, and differential molecular diffusion. Statistics on the nonpremixed flame will be computed and comparisons with flamelet and pdf models will be made.

Compressible Mixing Layer Simulations

Previous experiments and numerical simulations suggest that the flow structure changes significantly as the convective Mach number increases. Spanwise structures which are dominant at low convective Mach number are no longer present with any degree of regularity above a convective Mach number of 0.6. The structures appear to become much more three-dimensional. The role of organized structure at moderate convective Mach number on entrainment and subsequent mixing and chemical reaction was explored in this work using direct numerical simulation which provides detailed information concerning both the flow dynamics and the conserved scalar field.

Conserved scalar statistics and fast chemical reaction results derived from three-dimensional simulations at low and moderate convective Mach numbers were compared. It was found that the effect of compressibility is to produce highly three-dimensional turbulent flow structures which entrain and mix free stream fluid in several intermediate steps across the shear layer. The dynamics of these structures produces a conserved scalar whose histogram is marching across the layer. This is in contrast to the *non*marching probability density function corresponding to a low Mach number free shear layer which is dominated by spanwise flow structures. Product profiles and thicknesses were compared at low and moderate Mach numbers based on fast chemical reactions. Figure 1 shows the instantaneous conserved scalar field associated with a moderate convective Mach number mixing layer at several different streamwise locations and in a plan view slice through the center of the layer. Figure 2 shows a comparison of the histogram of the conserved scalar fields at low and moderate convective Mach number. Comparisons with future experiments involving pressure imaging in a high convective Mach number shear layer will be made.

Nonpremixed Flame Simulations

Simulations are currently underway to determine the effects of differential diffusion on the microstructure of a diffusion flame in isotropic decaying turbulence. A common

assumption made in modeling and in simulations is that all species have equal molecular diffusivities. This assumption leads to considerable simplification allowing the evolution of the species concentrations to be linearly related to a single mixture fraction. However, in practical hydrocarbon-air or hydrogen-air diffusion flames, the molecular diffusivities are far from being equal. An argument often made is that at high Reynolds numbers the small scale structure is washed out by molecular diffusion so that the lower order moments of the species concentrations are influenced primarily by the low wave number, large-scale motions. However, in flames with significant heat release, the Reynolds number may be reduced locally by as much as an order of magnitude , thereby reducing the separation between the energy containing and dissipative turbulence scales. In these regions differential diffusion effects may be significant. An important objective of this work is to quantify the differential diffusion effect and to use "numerical flow visualization" to identify the important physical mechanisms using data generated from direct numerical simulations.

Simulation results are being obtained in 1) constant density homogeneous turbulence with conserved scalars having Prandtl numbers differing by a factor of 4, and 2) variable density homogeneous turbulence with heat release and finite-rate kinetics and Schmidt numbers ranging from 0.2 - 1.0. The constant density simulation results suggest that the alignment of the differential scalar gradient conditioned on kinetic energy dissipation is in the most compressive principal strain direction, consistent with previous results for a single conserved scalar.

Future Plans

Three-dimensional simulations of diffusion flames in homogeneous turbulence with heat release are currently underway. The present simulations model the chemistry with a single-step irreversible Arrhenius reaction. Modifications have been made to include an intermediate step involving a species with a relatively high diffusivity compared to the reactant and product diffusivity. The amount of intermediate and product formation will depend upon the relative diffusivities, the ratio of reactant enthalpies, and the ratio of chemical reaction speeds. Comparisons will be made with upcoming differential diffusion experiments at the CRF including both single point measurements and PLIF imaging of conserved scalars in a coflowing jet.

Publications

J. H. Chen, B. J. Cantwell, and N. N. Mansour, "The Effect of Mach number on the Stability of a Plane Supersonic Wake," Physics of Fluids A 2, 984-1004 (1990).

J. H. Chen "The Effect of Compressibility on Conserved Scalar Entrainment in a Plane Free Shear Layer", *Eighth Symposium on Turbulent Shear Flows, Springer Verlag* (1992).

R. Sondergaard, J. H. Chen, J. Soria, B. J. Cantwell, "Local Topology of Small Scale Motions in Turbulent Shear Flows", *Eighth Symp. on Turbulent Shear Flows* (1991).

J. H. Chen, "The Effect of Compressibility on Conserved Scalar Mixing in a Plane Free Shear Layer", Paper no. WSS/CI 91-12, *Western States Section/ Combustion Inst., Spring Meeting, Boulder, CO (1991).*

J. H. Chen, "Differential Diffusion Statistics in Homogeneous Turbulence", *Fourth Intl. Conf. on Numerical Combustion, St. Petersburg, Fl.* (1991).

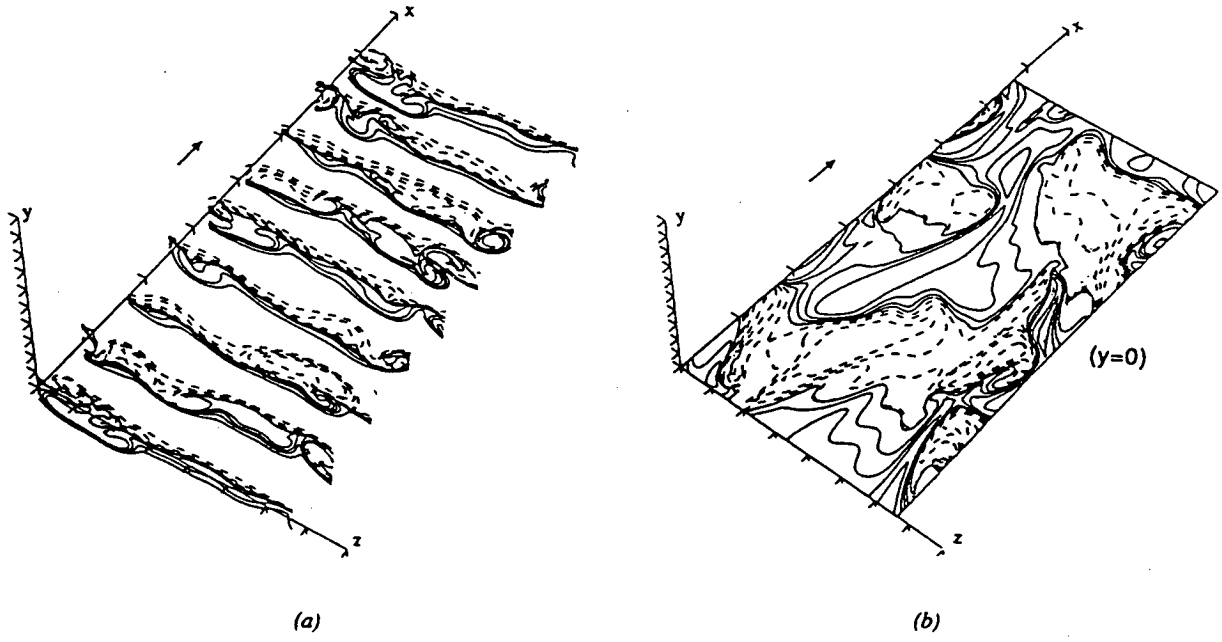

Figure 1. Contour plots of the conserved scalar at *Re=1600*, M_c=*0.8* for *a)* streamwise slices, *b)* plan view of midplane *(y=0)*.

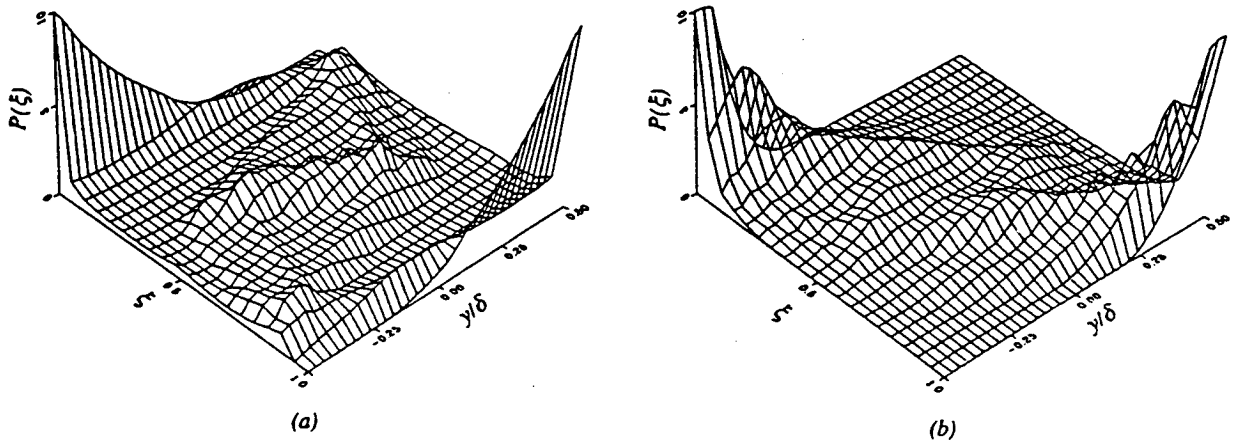

Figure 2. Histogram of the conserved scalar at *Re=1600*, *a)* M_c = *0.4* and *b)* M_c = *0.8*.

LASER SPECTROSCOPY OF HYDROCARBON RADICALS
DE-FG02-90ER14132

Peter Chen
Mallinckrodt Chemical Laboratory, Harvard University
Cambridge, Massachusetts 02138

We report the application of supersonic jet flash pyrolysis[1] to the clean, specific preparation of a wide range of hydrocarbon radicals, biradicals, and carbenes in a skimmed molecular beam. We have prepared ethynyl[2] (C_2H), vinyl[2,3] (C_2H_3), three isomers[4,5] of C_3H_2, propargyl[6] (C_3H_3), allyl[7] (C_3H_5), cyclobutadiene[8] (*c*-C_4H_4), and benzyne[9] (*o*-C_6H_4). Each species was produced cleanly and specifically, with little or no secondary reactions, by unimolecular thermal dissociation of appropriately designed and synthesized organic precursors.

Photoelectron spectra of the three isomeric C_3H_2 carbenes[4,5], and *ortho*-benzyne[9], were used to establish adiabatic ionization potentials for use in thermochemical determinations. The thermochemistry of carbenes and biradical-like species was found to follow a semiquantitative valence-bond picture in which the heat of formation of the carbene or biradical is reduced from an additivity estimate by the singlet-triplet splitting if the species has a singlet ground state. The triplet state is assigned to the "noninteracting biradical" of Benson additivity schemes.

Explicit modeling of the Franck-Condon envelope of the photoelectron spectra was used, along with chemical evidence, to identify the isomeric carbenes. We found, for cyclopropenylidene, that the simulated spectrum[10], using a geometry for $C_3H_2^{+\bullet}$ slightly adjusted from the optimized MP2/6-31G* structure, closely matched that obtained by experiment. Small variations in the bond lengths in the radical cation caused large, systematic changes in the simulated photoelectron spectrum. On this basis, we use the Franck-Condon modeling as a means to assign a geometry to this important ion.

We have recently obtained the only rotationally-resolved electronic spectrum of allyl and allyl-d_5 radical by 1+1 resonant multiphoton ionization. We identified the origin band of the $C^2B_1 \leftarrow X^2A_2$ transition by isotopic shifts, MPI photoelectron spectroscopy, and spectroscopic analysis. A partial rotational analysis yields geometric parameters for the excited state, which, by our photoelectron spectra, can be shown to resemble the ion in structure.

Future plans include further application of resonant MPI spectroscopy to the radicals that we have already found, as well as a continuing search for good precursors to new species. We plan to implement pulsed field ionization techniques in one of the existing instruments in order to obtain photoelectron spectra with one-to-two orders of magnitude better spectral resolution. Lastly, we plan to implement LIF detection in a new chamber to study isomerization in 2-butadienyl and α-styryl radicals.

1 D.W. Kohn, H. Clauberg, P. Chen, *Rev. Sci. Instr.* submitted.

2 J.A. Blush, J. Park, P. Chen, *J. Am. Chem. Soc.* **111**, 8951 (1989).

3 J.A. Blush, P. Chen, *J. Phys. Chem.* in press.

4 H. Clauberg, P. Chen, *J. Am. Chem. Soc.* **113**, 1445 (1991).

5 H. Clauberg, D.W. Minsek, P. Chen, *J. Am. Chem. Soc.* **114**, 99 (1992).

6 D.W. Minsek, P. Chen, *J. Phys. Chem.* **94**, 8399 (1990).

7 D.W. Minsek, J.A. Blush, P. Chen, *J. Phys. Chem.* **96**, 2025 (1992).

8 D.W. Kohn, P. Chen, in preparation.

9 X. Zhang, P. Chen, *J. Am. Chem. Soc.* in press.

10 H. Clauberg, P. Chen, *Int. J. Mass Spec. Ion Proc.* submitted.

Laser Spectroscopy and Dynamics of Transient Species Formed in Pyrolysis Reactions

Dennis J. Clouthier
Department of Chemistry
University of Kentucky
Lexington, KY 40506-0055

This research program is designed to study the spectroscopy and excited state dynamics of transient species produced primarily by pyrolysis techniques. Recent progress is summarized below.

1. Sub-Doppler Intracavity Dye Laser Spectroscopy

While on sabbatical leave in Anthony Merer's laboratory at UBC, I constructed a sub-Doppler intracavity dye laser spectrometer similar to that first reported in 1990 by Hill and Field.[1] By extending the cavity of a Coherent 599 scanning single mode dye laser, and modulating the laser frequency slightly while scanning, we were able to obtain very high resolution (linewidths as low as 10 MHz) sub-Doppler LIF spectra with very high sensitivity. We have applied this technique to the examining the sub-Doppler spectra of vanadium oxide (VO), cobalt oxide (CoO) and thioformaldehyde (H_2CS). In VO, the $B^4\Pi$-$X^4\Sigma^-$(1,0) band was studied and values of the principal hyperfine parameters were deduced from the spectra. These allowed the electron configuration of the excited state to definitely established as $(3d\delta)^2(3d\pi)^1$, rather than the alternative $(3d\delta)^1(3d\pi)^1(4s\sigma)^1$. Similar studies of CoO near 640 nm show that the ground state has the configuration $\sigma^2\pi^2\delta^3$. Extensive wavelength resolved fluorescence studies of intracavity excited CoO have also been carried out.

In the thioformaldehyde work we were most interested in examining the correlation between our earlier single rotational level photophysical measurements and the appearance of the spectrum when recorded at very high resolution and sensitivity. In the earlier work we found that about half the H_2CS excited state levels decay radiatively, with a lifetime of about 170 μs, and the other half have longer than radiative lifetimes, due to coupling with high rovibronic levels of the ground state. Some levels also show reduced relative yields of fluorescence. The sub-Doppler work now reveals that the upper state is riddled with small random perturbations, indicative of the first stages of the onset of quantum chaos in a small molecule. Examples of the types of structure observed are shown in Figures 1-4. The occurrence of extra lines and line shifts in these spectra correlate very well with the anomalous decay parameters, and show that the lifetime measurements are quite a sensitive probe of interactions with the ground state. S_1-S_0 interaction matrix elements of 0.001-0.006 cm^{-1} are found for levels involved in simple two level interactions. A few larger perturbations in the rotational structure are also observed, caused by additional local interactions with the nearby triplet state.

2. High Resolution FTIR Spectroscopy of Formyl Chloride

Formyl chloride is a transient species which readily decomposes to CO and HCl. Although the low resolution IR spectrum has been known for years,[2] high resolution studies have not been reported. The molecule is challenging because 5 of the 6 fundamentals are A/B hybrid bands and the $HCO^{35}Cl/HCO^{37}Cl$ isotopomers are both fairly abundant (3:1). Thus, the spectra are complex and congested. Despite these impediments, we have been able to get well-resolved spectra by using a Bomem DA3.002 instrument at a resolution of 0.004 cm^{-1} and deconvoluting the spectra to give a resolution of about 0.003 cm^{-1}. We have recorded several infrared bands of HCOCl and DCOCl and are analyzing the rotational structure. The analysis of the ν_3 band of HCOCl has been completed, including the A- and B-type structure of both chlorine isotopomers. The extensive infrared data has been combined with earlier microwave measurements[3] to provide a very precise set of ground state constants, and constants for the vibrationally excited state.

References

1. E. J. Hill and R. W. Field, J. Chem. Phys., **93**, 1 (1990).

2. I. C. Hisatsune and J. Heicklen, Can. J. Spectrosc., **18**, 77 (1973).

3. R. Wellington Davis and M. C. L. Gerry, J. Mol. Spectrosc., **97**, 117 (1983) and references therein.

Publications describing research supported under this grant (DE-FG05-86ER13544)

1. F. Ioannoni, D. C. Moule and D. J. Clouthier, "Laser Spectroscopic and Quantum Chemical Studies of the Lowest Excited States of Formic Acid", J. Phys. Chem., **94**, 2290 (1990).

2. D. J. Clouthier and J. Karolczak, "High Resolution Pulsed Dye Laser Calibration in the 500-350 nm Region Using Iodine Atlas Reference Lines", Rev. Sci. Instrum., **61**, 1607 (1990).

3. J. R. Dunlop and D. J. Clouthier, "Thioformaldehyde Single Rotational Level Photophysics: Longer Than Radiative Lifetimes and Reduced Fluorescence Yields in the Isolated Molecule", J. Chem. Phys., **93**, 6371 (1990).

4. D. J. Clouthier and J. Karolczak, "A Pyrolysis Jet Spectroscopic Study of the Rotationally Resolved Electronic Spectrum of Dichlorocarbene", J. Chem. Phys., **94**, 1 (1991).

5. J. R. Dunlop, J. Karolczak, D. J. Clouthier and S. C. Ross, "Pyrolysis Jet Spectroscopy: The S_1-S_0 Band System of Thioformaldehyde and the Excited State Bending Potential", J. Phys. Chem., **95**, 3045 (1991).

6. J. R. Dunlop, J. Karolczak, D. J. Clouthier and S. C. Ross, "Pyrolysis Jet Spectroscopy: Laser-Induced Phosphorescence of Thioformaldehyde and the Triplet Excited-State Bending Potential",

8. D. J. Clouthier, G. Huang and A. J. Merer, "A Spectroscopic View of Internal Conversion in a Small Polyatomic Molecule: Sub-Doppler Intracavity Dye Laser Spectroscopy of Thioformaldehyde", J. Chem. Phys., submitted.

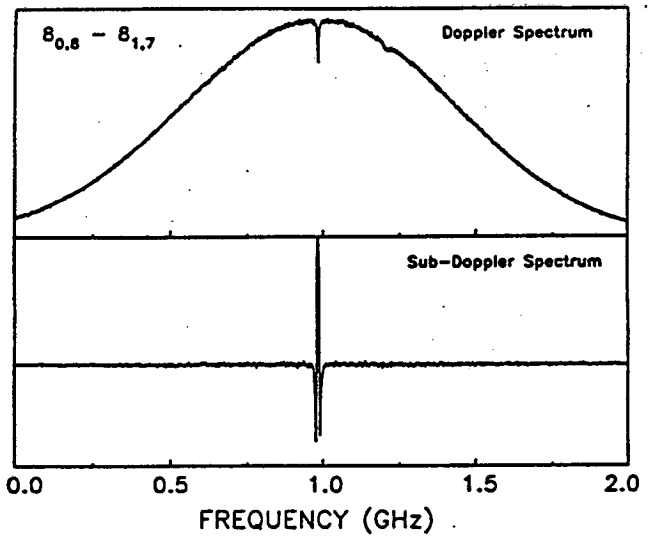

Fig. 1 Intracavity LIF spectra of H_2CS. The top panel is the DC PMT signal without laser frequency modulation, showing a prominent Lamb dip. The bottom panel shows the sub-Doppler spectrum. The upper state of this transition is unperturbed.

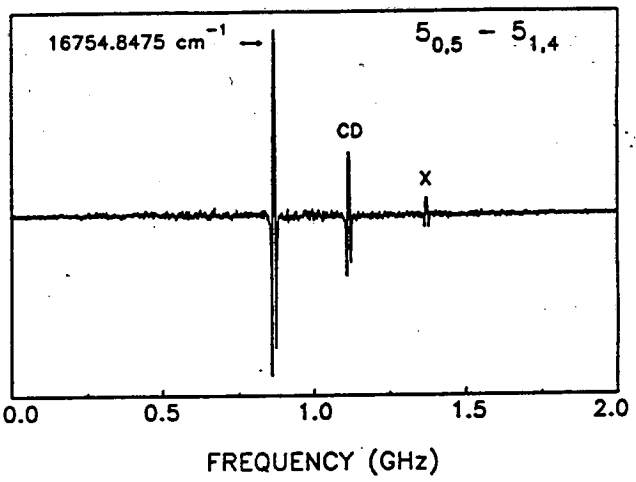

Fig. 2 Sub-Doppler spectrum of the $5_{0,5}$-$5_{1,4}$ transition, showing a perturbation by a single ground state level. "CD" denotes a center dip. "X" is an extra line due to direct absorption to a perturbing level.

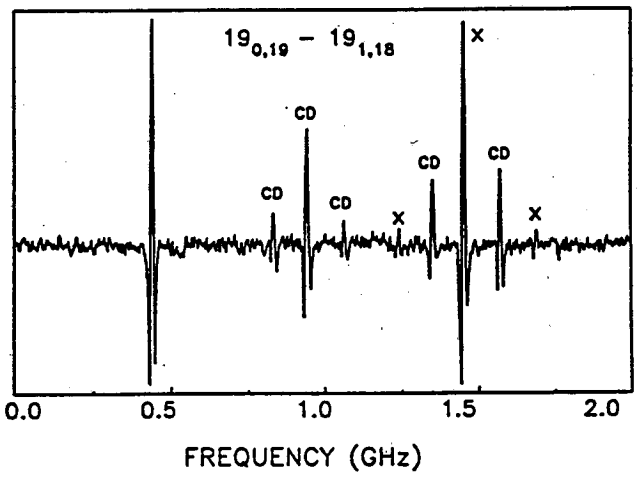

Fig. 3 Sub-Doppler spectrum of the $19_{0,19}$-$19_{1,18}$ transition. The upper state is perturbed by three ground state levels.

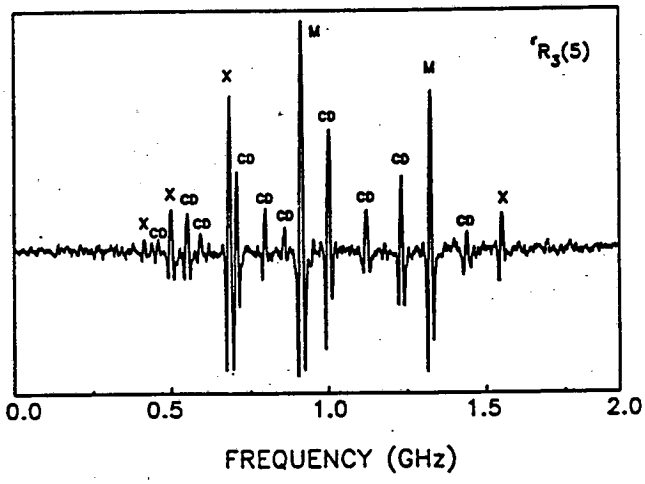

Fig. 4 Sub-Doppler spectrum of the $^rR_3(5)$ transition. "M" denotes a main line, which is a transition to a perturbed level of predominantly S_1 character. Ordinary and collision-induced center dips are observed.

A SHOCK TUBE STUDY OF THE REACTIONS OF THE HYDROXYL RADICAL WITH COMBUSTION SPECIES

N. Cohen
The Aerospace Corporation
El Segundo Calif.

DOE/SAN Grant DE-FG03-87ER13812

The reactions of OH radicals with hydrocarbons have received a great deal of attention in recent years because of these processes are principal steps in the oxidation of organic fuels--whether occuring in combustion/propulsion systems, in the atmosphere, or elsewhere. Of the various radicals capable of attacking hydrocarbons, OH radicals are generally the most reactive. In the atmosphere, the combined effects of the OH radical's reactivity and concentration make it the single species that determines the atmospheric lifetime of an organic substance.

The principal goals of the kineticist in the field of oxidation chemistry are (1) to measure as many elementary reaction rate coefficients as are conveniently studied in the laboratory; and (2) to develop theoretical and/or semiempirical tools for extrapolating from measured rate coefficients to unmeasured ones. The latter step is necessary because of the sheer number of reactions of possible interest. Ab initio theoretical studies provide the most refined nonexperimental procedures for the completion of part (2) of the above program, but again, the large number of reactions renders impractical detailed theoretical evaluation of every one. To this end, Benson and coworkers[1] developed the procedures of thermochemical kinetics: a collection of recipes and simple techniques for predicting reaction rate coefficients with reasonable accuracy. The method is most reliable when used simply to extrapolate rate coefficients from one temperature range to other temperatures, but a single temperature measurement can provide the basis for extrapolation. The procedure is further sharpened when applied to a family of homologous reactions for which a set of experimental measurements places more stringent constraints on the structural parameters of the activated complex that are required for the calculations. (It is assumed that the activated complexes for a homologous series of reactions are very similar to one another.) Studies of OH radicals with a series of alkanes have provided a wealth of experimental data that constitute an ideal test case for the application of thermochemical kinetics to predicting reaction rate coefficients.

To extend the semi-empirical techniques of Benson and coworkers, and to extend the database of reliable high temperature measurements of OH radicals with hydrocarbons and other fuels and their decomposition products, we undertook, with DOE support, a research program with both experimental and computational tasks.

In the experimental portion of this program we have carried out shock tube measurements of the reactions of OH radicals with several species. The experiments were performed behind reflected shock waves in a stainless steel shock tube. The tube has a 10-m-long, 16.2-cm-diameter test section with a 3-m-long-7.5 cm-diameter driver section. OH radicals were produced in most cases by shock-heating t-butyl hydroperoxide

(TBH) diluted in argon. TBH dissociates rapidly at our temperatures (near 1200 K) to produce t-butoxy and OH radicals. The t-butoxy radicals in turn rapidly pyrolyze to give CH_3 radicals and acetone; the acetone then decomposes to give CH_3 + CO. The overall process is thus

$$(CH_3)_3COOH \text{ --> } OH + 3CH_3 + CO \qquad (1)$$

Thin-film heat transfer gauges mounted in the tube wall signal the passage of the shock wave. The speed of the shock wave is calculated from the distance betweeen the gauges and the time between the heat transfer gauge signals. From the shock speed, the pressure and temperature behind the reflected shock are calculated.

The OH radicals then undergo several reactions in the absence of any other reagents, and have a characteristic half-life. When another reagent is present, it too can react with the OH. The disappearance rate of OH as a function of the concentration of the added reagent RH gives the reaction rate coefficient for the process, OH + RH --> products. The OH concentration behind the reflected shock wave was monitored by uv absorption using OH resonance radiation at 309 nm, produced by a microwave discharge through a mixture of helium and water vapor flowing at 70 torr.

To date we have completed and published[2,3,4]--shock tube measurements of the reactions of OH radicals with several species: H_2, CH_4, C_2H_6, c-C_5H_{10}, i-C_4H_{10}, i-C_8H_{18}, neo-C_8H_{18}, 2,3-dimethylbutane, C_2H_2, C_2H_4, C_3H_6, H_2CO, CH_3COCH_3, CH_3OH, and C_2H_5OH. The results, all near 1200 K and 1 atm, are summarized below.

Reagent	Rate Coefficient (10^9 L/mol-s)
H_2	2.7
CH_4	2.6
C_2H_6	9.0
c-C_5H_{10}	28.0
i-C_4H_{10}	12.6
neo-C_8H_{18}	18.0
i-C_8H_{18}	22.0
2,3-dimethylbutane	21.0
C_2H_2	0.28
C_2H_4	2.6
C_3H_6	9.6
H_2CO	12.0
CH_3COCH_3	5.3
CH_3OH	5.2
C_2H_5OH	5.3

In addition, in a separate set of experiments, the reaction rate of OH with CH_3 was measured.[5] This process is always occuring in our system because CH_3 radicals are produced in the decomposition of the TBH. As eq. (1) above shows, 3 CH_3 radicals are produced for every OH radical in the pyrolysis of TBH. In order to vary the ratio of [OH]:[CH_3], varying quantities of di-t-butyl-peroxide (TBP) were added to the TBH. Like TBH, TBP decomposes rapidly at the temperatures behind the reflected shock tube, but produces only CH_3 and CO:

$$(CH_3)_2COOC(CH_3)_3 \text{ --> } 4CH_3 + 2CO \qquad (2)$$

Extraction of the OH + CH_3 reaction rate coefficient of 1.1 x 10^{10} L/mol-s required the utilization of a detailed computer model. Although we did not directly measure the products of the reaction, we believe that the primary mechanism for OH removal by CH_3 near 1200 K and 1 atm is by their combination to form CH_3OH.

The work on the hydrocarbons provided the incentive for revising an earlier model[6] used to carry out thermochemical transition state theory (TST) calculations for the reaction rate coefficients of OH with alkanes. In a careful review of the application of TST to OH + alkane reactions, we concluded that there are good theoretical reasons for expecting different primary, secondary, or tertiary H atoms (distinguished on the basis of number of nearest neighboring C atoms) to have different rate parameters. If true, this invalidates the usual procedure of treating the total rate coefficient for OH + RH H abstraction processes as the sum of invariant primary, secondary, and tertiary rates multiplied by the respective number of such H atoms in the molecule. A separate question is whether there is really sufficient experimental evidence to justify distinguishing among different types of primary (or secondary, or tertiary) H atoms, or whether, given experimental and theoretical uncertainties, it is adequate to treat them all as equivalent. We concluded that there are measurable and unambiguous differences among various primary H atom abstractions, and possibly among secondary atoms, but the database cannot as yet distinguish among tertiary H atoms.

In our experimental work next year we intend to extend our measurements to other reagents. Additionally, we plan to incorporate the necessary analytical apparatus to permit measurements on some of the expected reaction products, thus allowing us to say more about the mechanisms of those reactions where more than one pathway is possible. We are currently reconstructing and improving the shock tube facility.

References

1. S. W. Benson, *Thermochemical Kinetics,* 2nd edn. (Wiley, 1976) and references cited therein.
2. J. F. Bott and N. Cohen, *Int. J. Chem. Kinet.* **16**, 1557 (1984).
3. J. F. Bott and N. Cohen, *Int. J. Chem. Kinet.* **21**, 485 (1989).
4. J. F. Bott and N. Cohen, *Int. J. Chem. Kinet.* **23**, 1075 (1991).
5. J. F. Bott and N. Cohen, *Int. J. Chem. Kinet.* **23**, 1017 (1991).
6. N. Cohen, *Int. J. Chem. Kinet.* **14**, 1339 (1982); **15**, 503 (1983).

Publications Related to this Grant (1990-92)

N. Cohen, "Are Reaction Rate Coefficients Additive? Revised Transition State Theory Calculations for OH + Alkane Reactions," *Int. J. Chem. Kinet.* **23**, 397 (1991).

N. Cohen and K. R. Westberg, "Chemical Kinetic Data Sheets For High-Temperature Chemical Reactions. Vol. II," *J. Phys. Chem. Ref. Data* **20**, 1211 (1991).

J. F. Bott and N. Cohen, "A Shock Tube Study of the Reactions of OH Radicals with Several Combustion Species," *Int. J. Chem. Kinet.* **23**, 1075 (1991).

J. F. Bott and N. Cohen, "A Shock Tube Study of the Reaction of Methyl Radicals with Hydroxyl Radicals," *Int. J. Chem. Kinet.* **23**, 1017 (1991).

RESONANCE IONIZATION DETECTION OF COMBUSTION RADICALS

Terrill A. Cool

School of Applied and Engineering Physics
Cornell University, Ithaca, New York 14853

Resonance enhanced multiphoton ionization (REMPI) spectroscopy, combined with molecular beam mass spectrometry, has an incomparable sensitivity for the detection of wide classes of organic molecules. The application of the REMPI technique to combustion diagnostics is acutely limited by a present lack of spectroscopic data for key flame radicals. In this program REMPI spectroscopic studies are undertaken of the electronic states of radical species of importance in the combustion of hydrocarbons and chlorinated hydrocarbons. Particular emphasis is placed on radical intermediates formed in the incineration of chlorinated organics present in hazardous wastes. Because many of these radicals are expected to be only weakly fluorescent, REMPI diagnostics may be the method of choice for laboratory flame studies directed toward the development and refinement of chemical kinetic flame models.

Recent Progress

Resonance Ionization Spectroscopy of HCO AND DCO, I: The $3p\ ^2\Pi$ Rydberg State

Resonance two-photon ionization (R2PI) spectroscopy has been used for medium resolution studies of HCO and DCO at wavelengths from 208 to 222 nm, made possible with the recent availability of the BBO (β-barium borate) frequency doubling crystal. Subband origins are measured for both symmetry components of the degenerate $3p\ ^2\Pi$ Rydberg states of HCO and DCO. A vibronic analysis, within the framework of perturbation theory, yields values of the Renner-Teller parameter ε, the quartic anharmonicity constant g_{22} and the dipolar vibronic parameter g_k. Harmonic frequencies ω_2 and bending vibrational anharmonicity constants x_{22} are determined for the $3p\ ^2\Pi$ and $X\ ^2\Sigma^+$ states of HCO and DCO. Observations of spin-orbit splitting of unique ($K=v_2+1$) levels of the $3p\ ^2\Pi$ vibronic manifold of HCO provide an estimate of the spin-orbit coupling constant A.

These studies permit the assignment of previously unidentified HCO subbands observed by (2+1) REMPI spectroscopy.[1] Unclassified bands with two-photon energies ranging from 45512 to 49200 cm^{-1}, tentatively associated with the nearby $3s\ ^2\Sigma^+$ Rydberg state, were tabulated in reference (1). These subbands, along with other R2PI subbands reported here, can now be assigned to the symmetric A′ component of the $3p\ ^2\Pi$ state. Accordingly all of the HCO subbands thus far observed belong to the $3p\ ^2\Pi$ Rydberg state; possible transitions to the $3p\sigma\ ^2\Sigma^+$ and $3s\ ^2\Sigma^+$ states remain undetected.

For DCO, of the 50 subbands observed with R2PI, 41 have also been assigned to A′ and A" components of the $3p\ ^2\Pi$ Rydberg state, while nine (K′,K") = (0,1) and (1,0) perpendicular subbands have yet to be identified.

The molecular parameters determined for HCO and DCO are given in Tables I and II.

Resonance Ionization Spectroscopy of HCO and DCO, II: The $\tilde{B}\ ^2A'$ Valence State

The importance of the formyl radical in hydrocarbon combustion mechanisms and atmospheric photochemistry has motivated two recent studies of laser-induced fluorescence (LIF) from HCO.[2,3] Spectroscopy of LIF from the $\tilde{B}$ state to 36 vibrational levels of the $\tilde{X}$ ground state[3] complements data from a recent photoelectron study[4] to provide a significantly improved description of the HCO $\tilde{X}\ ^2A'$ state.

Accurate *ab initio* calculations of the H + CO ground state potential energy surface[5] have been used for recent studies of reaction dynamics.[6,7] Vibrational energies calculated with this surface are in excellent agreement with the available data for the HCO $\tilde{X}$ state.

Table I: Measured Spectroscopic Constants of the 3p $^2\Pi$ State (cm^{-1})

	HCO	DCO
ω_2	799.9 (1.4)[a]	645.5 (1.6)
x_{22}	-3.30 (.12)	-2.70 (.17)
g_{22}	4.95 (.68)	4.36 (.47)
g_K	-2.11 (0.7)	-1.4 (.5)[b]
ϵ	0.071 (0.001)	0.069 (0.001)
T_0	45540.1 (3.3)	45444.0 (3.6)
A	0.9 (0.3)	0.9 (0.3)[c]

[a] Numbers in parentheses are the 2σ standard deviations.
[b] Estimated
[c] Measured for HCO

Table II: Measured Spectroscopic Constants of the Ground State $\tilde{X}\ ^2\Pi$ (A') (cm^{-1})

	HCO	DCO
ω_2	1103.6 (2.5)	861.4 (1.5)
ν_2[a]	1082.4 (2.7)	847.2 (1.6)
x_{22}	-10.6 (0.9)	-7.1 (0.2)

[a] The values of x_{12} and x_{23} are unknown. The fundamental frequency ν_2 is estimated by neglecting the contributions of x_{12} and x_{23} to the expression $\nu_2 = \omega_2 + 2x_{22} + (x_{12}+x_{23})/2$.

In the present program R2PI spectroscopy of the HCO $\tilde{B}\leftarrow\tilde{X}$ "hydrocarbon flame" band system has permitted the assignment of subband origins for seventeen vibronic bands of HCO and twenty of DCO. A major difficulty in previous flame emission studies[8,9] and the recent LIF analyses[2,3] of the HCO $\tilde{B}\leftarrow\tilde{X}$ transition has been the complexity associated with overlapping rotational structures of the numerous subbands of the $\tilde{B}\leftarrow\tilde{X}$ system. In the present work we have obtained medium resolution (0.4 cm^{-1}) resonance ionization spectra for $\tilde{B}\leftarrow\tilde{X}$ vibrational subbands of jet-cooled HCO and DCO at very low rotational temperatures (≈ 5 K).[9,10] This technique greatly facilitates subband origin determinations to yield vibrational level spacings of increased precision.

Term values, the three harmonic vibrational frequencies and six anharmonicity constants are measured for the $\tilde{B}\ ^2A'$ states of both molecules; see Table III. The observation of an increase in the effective asymmetric top rotational constant, A-(B+C)/2, with increasing vibrational quantum number identifies the $\tilde{B}$ state bending vibration with fundamental frequencies of 1382 cm^{-1} and 1213 cm^{-1} for HCO and DCO, respectively. The highest fundamental frequencies of 2597 cm^{-1} for HCO and 1944 cm^{-1}

for DCO correspond to CH(CD) stretching, while the lowest fundamental frequencies of 1066 cm^{-1} for HCO and 922 cm^{-1} for DCO correspond to the vibration of singly bonded C-O.

Research Plans

A flame sampling laser ionization mass spectrometer, constructed under this program, is in use for REMPI spectroscopy of several radical intermediates of importance in the combustion of chlorinated organics. A stoichiometric $CH_4/O_2/Ar$ base flame at a pressure of about 30 Torr is employed for these studies. Chlorinated organics, *e.g.*, methyl chloride, trichlorethylene, ethyl chloride, are added to the base in small concentrations (a few percent of the CH_4). Our initial objective is to simply identify the carriers of specific REMPI signatures without regard for precise measurements of spectroscopic constants. These spectral surveys will cover the range of laser wavelengths from 205 nm (BBO doubling cut-off) to 500 nm for the preheat and luminous zones of each flame system. Detailed spectroscopic studies, similar to those performed for HCO and DCO, of suitable candidates identified in these surveys will then be undertaken with use of the flame source, and/or with laser photolysis in a jet-cooled molecular beam apparatus of an appropriately chosen precursor.

1. P. J. H. Tjossem, D. A. Webb, T. A. Cool, and E. R. Grant, J. Chem. Phys. 88, 617 (1988).

2. X. Zhao, G. W. Adamson, and R. W. Field, "$\tilde{B}\ ^2A' \leftarrow \tilde{X}\ ^2A'$ Fluorescence Excitation Spectrum of the HCO Radical", unpublished (1990).

3. A. D. Sappey and D. R. Crosley, J. Chem. Phys. 93, 7601 (1990).

4. K. K. Murray, T. M. Miller, D. G. Leopold, and W. C. Lineberger, J. Chem. Phys. 84, 2520 (1986).

5. J. M. Bowman, J. S. Bittman, and L. B. Harding, J. Chem. Phys. 85, 911 (1986).

6. G. K. Chawla, G. C. McBane, P. L. Houston, and G. C. Schatz, J. Chem. Phys. 88, 5481 (1988).

Table III: Spectroscopic Constants of the $\tilde{B}$ (A') State (cm^{-1})

	HCO	DCO
ω_1	2798.4 (2.6)[a]	2068.8 (2.6)
ω_2	1411.9 (1.8)	1239.8 (2.2)
ω_3	1107.0 (2.6)	943.7 (1.4)
x_{11}	-76.4 (0.7)	-48.2 (0.7)
x_{22}	4.8 (0.4)	-7.2 (0.5)
x_{33}	-8.6 (0.4)	-3.5 (0.2)
x_{12}	-64.2 (0.9)	-26.1 (1.0)
x_{13}	-32.7 (1.5)	-30.2 (1.5)
x_{23}	-15.7 (0.7)	1.0 (0.1)
v_1	2597.1±2[b]	1944.2±2
v_2	1381.6±2	1212.9±2.5
v_3	1065.6±2.8	922.1±1.6
T_0	38694.5±2.4	38628.4±2

[a]The numbers in parentheses are the 2σ standard deviations (cm^{-1}).
[b]Estimated uncertanties are given for v_1, v_2, v_3 and T_0

7. G. C. McBane, S. H. Kable, P. L. Houston and G. C. Schatz, J. Chem. Phys. 94, 1141 (1991).

8. W. M. Vaidya, Proc. Roy. Soc. A 279, 572 (1964).

9. R. N. Dixon, Trans. Faraday Soc., 65, 3141 (1969).

Recent Research Publications of DOE Sponsored Research

T. A. Cool, "Combustion Species Detection by Resonance Enhanced Ionization," Lasers and Mass Spectrometry, ed. D. Lubman (Oxford, University Press, Oxford, 1990), 446.

T. A. Cool, P. M. Goodwin and C. E. Otis, H/D Isotope Effect in the Predissociation of C_2HD," J. Chem. Phys. 93, 3714 (1990).

T. A. Cool and P. M. Goodwin, "Observation of an Electronic State of C_2H Near 9 eV by Resonance Ionization Spectroscopy," J. Chem. Phys. 94, 6978 (1991).

X.-M. Song and T. A. Cool, "Resonance Ionization Spectroscopy of HCO and DCO. I. The $3p\ ^2\Pi$ Rydberg State", J. Chem. Phys. (in press).

T. A. Cool and X.-M. Song, "Resonance Ionization Spectroscopy of HCO and DCO. II. The $\tilde{B}\ ^2A'$ State", J. Chem. Phys. (in press).

UNIMOLECULAR REACTION DYNAMICS AND VIBRATIONAL OVERTONE SPECTROSCOPY OF HIGHLY VIBRATIONALLY EXCITED MOLECULES

F.F. Crim

Department of Chemistry
University of Wisconsin-Madison
Madison, Wisconsin 53706

This research determines the nature of highly vibrationally excited molecules, probes unimolecular reactions at the level of individual quantum states, and studies the dynamics of electronic photodissociation from highly vibrationally excited states. In our experiments, pulsed laser excitation of a vibrational overtone transition prepares a highly vibrationally excited molecule and time-resolved spectroscopic detection of products monitors their subsequent decomposition. We have used this scheme to follow unimolecular reactions of large[1,2] and small molecules[3,4,5] in both room temperature gases and supersonic expansions and to investigate the role that vibrational excitation plays in electronic photodissociation dynamics. Most recently we have used the localized nature of the highly vibrationally excited states we create to selectively break bonds in photodissociation and bimolecular reactions.

Vibrationally mediated photodissociation, in which a second photon dissociates molecules from a bound vibrationally excited state populated by vibrational overtone excitation, explores the nature of the initially excited state and its influence on the photodissociation dynamics. Our measurement on water excited in the region of the third overtone of the O-H stretching vibration, $H_2O(4\nu_{OH})$[6] shows the influence of the nature of the vibrationally excited intermediate state on the subsequent dynamics. By exciting two different vibrational states, corresponding either to four quanta of excitation in one bond $|04>^-$ or to three quanta in one bond and one quantum in the other $|13>^-$, we alter the dissociation dynamics significantly. In the former case, the photodissociation produces all of the OH fragments in $v=0$, but, in the latter case, more than half of them appear in $v=1$. A local mode model of the vibrational excitation describes this striking specificity in the dissociation dynamics. Because of the state specificity of the preparation and detection, we have also used vibrational overtone excitation to explore the role of initial rotation and bending vibration in the state-to-state photodissociation dynamics and to determine the relative photodissociation cross section for highly vibrationally excited water.[7] The detail of the experiments permits extensive comparison with *ab initio* theory that is becoming available, and we have compared our bond selective photodissociation of HOD and our observation of the influence of bending vibrations on the product state rotations with detailed calculations.[8,9]

The most recent extension of our work is to bond selected photodissociation and bimolecular reaction. Using the isolated nature of the O-H stretching vibration in water, we have selectively cleaved the O-H bond in HOD. In one experiment, we use vibrationally mediated photodissociation of $HOD(4\nu_{OH})$ to break only the O-H bond.[10] In another, we perform the first bond selected bimolecular reaction by reacting the H atom in $HOD(4\nu_{OH})$ preferentially with H atoms produced in a microwave discharge,

$$H + HOD(4\nu_{OH}) \rightarrow H_2 + OD.$$

The reaction probability to form OD is at least 100 times greater than that for the competing channel that produces OH by breaking the unexcited bond.[11] The nature of the initially excited state controls both the rate of the reaction of water with hydrogen atoms and the vibrational states of the products dramatically.[12] Reacting nearly isoenergetic states with different distribution of the excitation among stretches and bends shows that energy that is not in the most highly excited bond, which becomes the reaction coordinate, does not contribute to overcoming the barrier to reaction.

The disposal of energy into relative translation, rotation, and vibration of the products in the mode-selected reaction provides a view of the reaction dynamics and permits detailed comparison to classical trajectory and quantal scattering calculations. We directly determine the vibrational and rotational energy content of the OH fragment by laser induced fluorescence (LIF) and can infer limits to the relative translational energy from the widths of the transitions in the LIF excitation spectrum.[13] Only 4% of the available energy appears in rotations and vibrations of the OH product, and its Doppler width shows that *less than* 53% (5000 cm^{-1}) appears in relative translation. Detecting the heavier OH fragment limits the resolution of the translational energy release measurement. Our data show that there is *at least* 4000 cm^{-1} of internal energy in the H_2 formed in the reaction. Theoretical calculations suggest the energy is likely to be in vibration, and we are developing a vacuum ultraviolet detection capability that allows us to determine the H_2 internal energy content directly.

1. E.S. McGinley and F.F. Crim, J. Chem. Phys. **85**, 5741 (1986); J. Chem. Phys. **85**, 5754 (1986).

2. T.R. Rizzo and F.F. Crim, J. Chem. Phys. **76**, 2754 (1982).

3. (a) T.R. Rizzo, C.C. Hayden, and F.F. Crim, J. Chem. Phys. **81**, 4501 (1986). (b) H.R. Dübal and F.F. Crim, J. Chem. Phys. **83**, 3863 (1985). (c) T.M. Ticich, T.R. Rizzo, H.R. Dübal, and F.F. Crim, J. Chem. Phys. **84**, 1508 (1986).

4. L.J. Butler, T.M. Ticich, M.D. Likar, and F.F. Crim, J. Chem. Phys. **85**, 2331 (1986).

5. A. Sinha, R.L. Vander Wal, and F.F. Crim, J. Chem. Phys. **92**, 401 (1990).

6. R.L. Vander Wal and F.F. Crim, J. Phys. Chem. **93**, 5331 (1989).

7. F. F. Crim, M. C. Hsiao, J. L. Scott, A. Sinha, and R. L. Vander Wal. Phil. Trans. Roy. Soc. **332**, 259 (1990).

8. R. L. Vander Wal, J. L. Scott, F. F. Crim, K. Weide, and R. Schinke, J. Chem. Phys. **94**, (1991) (in press).

9. R. Schinke, R. L. Vander Wal, J. L. Scott, and F. F. Crim, J. Chem. Phys. **94**, 283 (1991).

10. R.L. Vander Wal, J.L. Scott, and F.F. Crim, J. Chem. Phys. **92**, 803 (1990).

11. A. Sinha, M. C. Hsiao, and F. F. Crim, J. Chem. Phys. **92**, 6333 (1990).

12. A. Sinha, M. C. Hsiao, and F. F. Crim, J. Chem. Phys. **94**, 4928 (1991).

13. M. C. Hsiao, A. Sinha, and F. F. Crim, J. Phys. Chem. **95**, 8263 (1991).

RECENT DOE SPONSORED PUBLICATIONS

Published 1990-92

Selectively Breaking the O-H Bond in HOD, R.L. Vander Wal, J.L. Scott, and F.F. Crim, J. Chem. Phys. **92**, 803 (1990).

Selectively Breaking the O-H Bond in HOD. R.L. Vander Wal, J.L. Scott, and F.F. Crim, J. Chem. Phys. **92**, 803 (1990).

Bond-Selected Bimolecular Chemistry: H + HOD($4v_{OH}$) → OD + H_2, A. Sinha, M. C. Hsiao, and F. F. Crim, J. Chem. Phys. **92**, 6333 (1990).

State- and Bond-Selected Photodissociation and Bimolecular Reaction of Water. F. F. Crim, M. C. Hsiao, J. L. Scott, A. Sinha, and R. L. Vander Wal. Phil. Trans. Roy. Soc. **332**, 259 (1990).

State and Bond Selected Unimolecular Reactions, F. F. Crim, Science **249**, 1387 (1990).

State Resolved Photodissociation of Vibrationally Excited Water: Rotations, Stretching Vibrations, and Relative Cross Sections, R. L. Vander Wal, J. L. Scott, and F. F. Crim, J. Chem. Phys. **94**, 1859 (1991).

The Effect of Bending Vibrations on Product Rotations in the Fully State-Resolved Photodissociation of the A-State of Water. R. Schinke, R. L. Vander Wal, J. L. Scott, and F. F. Crim, J. Chem. Phys. **94**, 283 (1991).

An Experimental and Theoretical Study of the Bond-Selected Photodissociation of HOD. R. L. Vander Wal, J. L. Scott, F. F. Crim, K. Weide, and R. Schinke, J. Chem. Phys. **94**, 3548 (1991).

Controlling Bimolecular Reactions: Mode and Bond Selected Reaction of Water with Hydrogen Atoms. A. Sinha, M. C. Hsiao, and F. F. Crim, J. Chem. Phys. **94**, 4928 (1991).

Energy Disposal in the Vibrational State- and Bond-Selected Reaction of Water with Hydrogen Atoms. M. C. Hsiao, A. Sinha, and F. F. Crim, J. Phys. Chem. **95**, 8263 (1991).

Mode- and Bond-Selected Bimolecular Reaction of Water. F. F. Crim, A. Sinha, M. C. Hsiao, and J. D. Thoemke, in Mode Selective Chemistry, J. Jortner, *et al.* editors, (1991), pp. 217-225.

In Press

The Photodissociation of Water in the First Absorption Band: A Prototype for Dissociation on a Repulsive Potential Energy Surface. V. Engel, V. Staemmler, R. L. Vander Wal, F. F. Crim, R. J. Sension, B. Hudson, P. Andresen, S. Hennig, K. Weide, and R. Schinke, J. Phys. Chem. **96**, (1992) (in press).

FLAME STUDIES, LASER DIAGNOSTICS, AND CHEMICAL KINETICS

David R. Crosley, David M. Golden, and Gregory P. Smith
Molecular Physics Laboratory
SRI International
Menlo Park, California 94025

The goal of this research is an understanding of flame chemistry, based on consistent, soundly based reaction rate constants and verified by sensitive measurements of reaction intermediates, generally using laser-induced fluorescence. The approach comprises spectroscopic investigations, measurements of the quantum state and temperature dependence of quenching of electronically excited states, reaction rate determinations at elevated temperature, and the estimation of reaction rate coefficients within a properly based theory. The problems addressed are the classic examples of those controlled by the chemical kinetics of combustion systems, viz., the formation of NO_x and soot pollutants. During the past year our efforts have concentrated on the quenching of highly rotationally excited NH, transition probabilities in emission from the v' = 3 level of OH, and the kinetic derivation of bond energies.

Quenching of highly rotationally excited NH The collisional quenching of first row diatomic hydrides is of interest in that, at least for simple collision partners, realistic potential surfaces are available and scattering computations can be performed. Tests of these surface and dynamic calculations can come from experiments that probe collisions on a state-specific basis. For OH and NH, excited state quenching cross sections σ_Q decrease with increasing rotation of the radical, for many colliders.[1] The quenching collisions result from a transitory complex formed on an anisotropic, attractive surface. When the hydride does not rotate, it an the collider find valleys in the surface to form the complex; as it rotates, the surface is averaged, reducing the effects of the especially attractive regions. For low N', σ_Q falls off exponentially with rotational energy. At fast enough rotation, however, one might expect that the averaging of the surface becomes complete, and σ_Q would decrease no further. This experiment is designed as a systematic investigation of that hypothesis.

Highly rotationally excited NH in the ground $X^3\Sigma^-$ state is formed by multiphoton photolysis of NH_3 by an ArF laser. Excitation scans showed that levels up to N" = 30 are produced in this process, having some 13,400 cm^{-1} or about 1/3 the available excess energy from two 103 nm photons. These NH molecules were then excited to the $A^3\Pi_i$ state with a tunable dye laser; the quenching was determined through the pressure dependence of the time decay of the fluorescence.

Five colliders were studied: NH_3, CH_4, CO, H_2, and D_2. Special attention was paid to determinations for low N', especially for CH_4 as the example. This was to ensure that the present results could be directly compared with previous results up to N' = 7, obtained using thermally populated NH in a room temperature discharge flow.[2] The agreement was very good. Results for NH_3 are shown in the figure; those for the other gases appear similar. Here, the

logarithm of σ_Q is plotted vs. N'(N'+1). Note the exponential decrease at low N' (seen even more definitively in the results of Ref. 2). However, at higher N', σ_Q levels off, in accord with the simple dynamic model.

From the intercepts of decay rate vs. pressure, one can also obtain the radiative lifetimes as a function of N'. Recent ab initio calculations of these lifetimes have been performed.[3] If they are scaled to match the well-determined low N' value 2 of 420 ns[2], the predictions of the N' variations are in excellent agreement with the present experimental results.

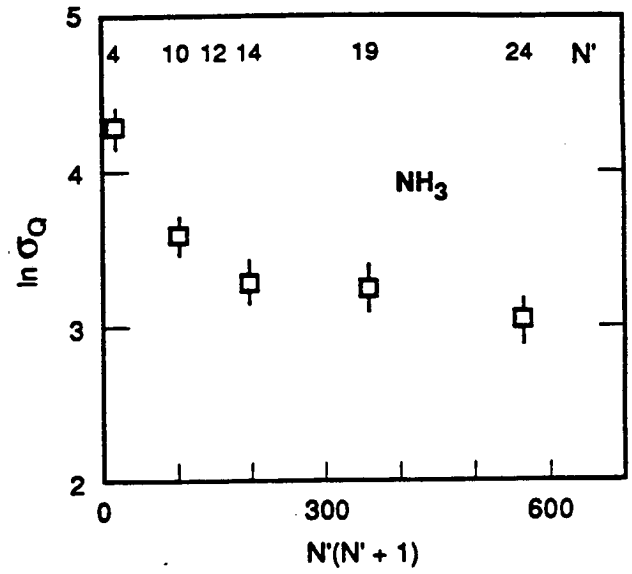

Plot of the logarithm of the quenching cross section σ_Q vs. N'(N'+1), for NH collider. The exponential decrease at low N' (more evident in the results for N'=1-7 in Ref. 2) and the leveling off at higher N' are seen. The change to a constant value occurs near N' = 14 for all colliders.

Transition probabilities in emission from v' = 3 The v' = 3 level of OH is of particular interest in combustion diagnostics, owing to the ability to excite it using a KrF laser near 248 nm.[4] We have made measurements of the vibrational band transition probabilities in emission from v' = 3, using fluorescence scans following excitation with a tunable laser. The OH is present in the burnt gases of a methane/oxygen flame at 10 Torr pressure. Operation at this low pressure avoids spectral congestion due to vibrational energy transfer, which occurs even for this predissociated v' = 3 level for pressures of 100 Torr and less.

Fluorescence from v' = 3 can be observed out to v" = 5 of the ground state. Therefore these bands can serve to monitor highly excited OH for example, in experiments on collision dynamics or studies of the nascent state distributions from chemical reactions. Although the absorption cross sections are weak, they are strong enough to excite with common dye lasers. In future experiments, v' = 2 and 4 will be studied. These will be combined with earlier results[5] for v' = 1 and 0 to formulate an improved electronic transition moment for OH, and calculate transition probabilities for a wide range of vibrational and rotational levels.

Kinetic derivations of bond energies Radical heats of formation and bond dissociation energies, vital to understanding hydrocarbon combustions, are often derived or inferred from kinetics measurements. (The reverse also applies.) The precise relationship between observed activation energies and thermodynamic bond energies depends upon the heat capacity terms in a proper transition state theory interpretation of the reaction mechanism involved. Thus we have examined two key methods: alkyl radical - hydrogen halide metathesis reactions, and bond scission pyrolysis.

A recently published RRKM theory calculation[6] suggests the negative activation energies reported by some investigators for the R + HX reactions (upon which many alkyl radical

thermodynamic discrepancies rest) may be accounted for by formation of a weakly bound complex. If experimentally confirmed, this would fix key bond energies and significantly alter conventional concepts about basic abstraction kinetics.

Most organometallic and many organic bond energies and radical heats of formation are derived from pyrolysis activation energies. A hindered rotation model of the transition state which becomes looser at low temperature is needed to fit most decomposition or radical recombination data. One consequence of this more refined treatment is to raise bond dissociation energy values by 1-2 kcal/mole above the values typically quoted from activation energy measurements.

This work was supported by the Basic Energy Sciences Division of the Department of Energy. We thank Jay Jeffries, Ellen Chappell, and Kristen Steffens for their participation in the experiments.

References

1. D. R. Crosley, J. Phys. Chem. **93**, 6273 (1989).
2. N. L. Garland and D. R. Crosley, J. Chem. Phys. **90**, 3566 (1989).
3. D. Patel-Misra, G. Parlant, D. G. Sauder, D. R. Yarkony, and P. J. Dagdigian, J. Chem. Phys. **94**, 1913 (1991).
4. P. Andresen, A. Bath, W. Gröger, H. W. Lülf, G. Meijer and J. J. ter Meulen, Appl. Opt. **27**, 365 (1988).
5. R. A. Copeland, J. B. Jeffries and D. R. Crosley, Chem. Phys. Lett. **138**, 425 (1987).
6. A. B. McEwen and D. M. Golden, J. Mol. Struct. **224**, 357 (1990).

Publications, 1990 TO 1992

1. J. P. Puttemans, G. P. Smith, and D. M. Golden, "Comments on Cyclopentadienyl Compound Thermochemistry," J. Phys. Chem. 94, 3227 (1990).
2. I. J. Wysong, J. B. Jeffries, and D. R. Crosley, "Rotational Level Dependence of Quenching of NH_2 $\tilde{A}$ by Helium," J. Chem. Phys. 93, 237 (1990).
3. A. B. McEwen and D. M. Golden, "Reaction of t-$C_4H_9^*$ with HI. Possible Negative Activation Energies," J. Mol. Struct. 224, 357 (1990).
4. D. R. Crosley and J. B. Jeffries, "Temperature Measurements by Laser-Induced Fluorescence of the Hydroxyl Radical," Seventh Symposium on Temperature, Its Measurement and Control in Science and Industry, in press, 1992.
5. G. P. Smith, J. A. Manion, M. J. Rossi, and D. M. Golden, "Relationship between Bond Dissociation Energies and Activation Energies for Bond Scission," Int. J. Chem. Kinetics, submitted, 1992.
6. E. L. Chappell, J. B. Jeffries, and D. R. Crosley, "Quenching of Highly Rotationally Excited NH $A^3\Pi_i$," J. Chem. Phys., submitted, 1992.

INFRARED ABSORPTION SPECTROSCOPY AND CHEMICAL KINETICS OF FREE RADICAL

Robert F. Curl and Graham P. Glass

Department of Chemistry and Rice Quantum Institute

Rice University, Houston, TX 77251

Infrared kinetic spectroscopy using excimer laser flash photolysis and either color-center or diode laser probing has been employed to study chemical kinetics and high resolution spectra of the ketenyl (HCCO) and the propargyl (C_3H_3) radicals, both of which are of importance in hydrocarbon combustion.

KINETICS OF KETENYL RADICAL

Ketenyl radicals were produced by 193 nm excimer laser photolysis of ketene

$$H_2CCO + h\nu\ (193\ nm) \rightarrow HCCO + H \qquad (1a)$$

$$\rightarrow {}^1CH_2 + CO \qquad (1b)$$

and probed with a tunable diode laser operating at 2014 cm^{-1}. Under these conditions, any singlet methylene which may be formed via reaction 1b should react with the precursor, ketene, at a rate fast enough[1] to ensure its total removal from the photolysis cell within 1 μs.

In the presence of 2 to 8 Torr of O_2, the ketenyl radical was observed to decay exponentially with time constants that ranged from 20 to 5 μs. A Stern-Volmer plot of the exponential decay rates is shown in figure 1. From this plot, the second order rate constant for the reaction of the ketenyl radical with O_2 at room temperature was determined as 6.5(6) x 10^{-13} cm^3 $molecule^{-1}$ s^{-1}. The rate constant thus obtained compares well with the value of 6.3 x 10^{-13} $cm^3 molecule^{-1} s^{-1}$ obtained by Peeters et. al.[2] but is more than an order of magnitude greater than the value of 3.7 x 10^{-14} $cm^3 molecule^{-1} s^{-1}$ obtained by Jones and Bayes[3].

Numerous experimental measurements indicate that, in lean hydrocarbon flames, the concentration of O_2 is at least 100 times greater than that of the various free radical species that are present.[4] In view of this, reaction with O_2 must be the major loss mechanism for HCCO in such flames.

The reaction of HCCO with molecular oxygen can occur in principal via any of the following channels:

$HCCO + O_2$	→	$CO_2 + HCO$	ΔH = -531 kJ/mol	(2a)
	→	$CO_2 + H + CO$	ΔH = -464 kJ/mol	(2b)
	→	$HCOO + CO$	ΔH = ?	(2c)
	→	$2CO + OH$	ΔH = -359 kJ/mol	(2d)
	→	$C_2O + HO_2$	ΔH = 205 kJ/mol	(2e)
	→	$O + HCO + CO$	ΔH = 0 kJ/mol	(2f)
+M	→	$HCO_2CO + M$	$\Delta H<0$	(2g)

An attempt was made to identify the most significant reaction pathway by determining the overall yield of CO. From such measurements the major reaction channel was tentatively identified as 2d, a channel which produces 2 molecules of CO for every molecule of HCCO consumed.

The observe decay of ketenyl was found to be largely unaltered by the addition of acetylene. By comparing the observed decay to that predicted in a number of computer simulations, an upper bound to the rate constant for the reaction between HCCO and acetylene of 1 x 10^{-13} cm^3 $molecule^{-1}s^{-1}$ could be estimated.

INFRARED KINETIC SPECTROSCOPY OF THE PROPARGYL RADICAL

The acetylenic CH stretch (ν_1) of the propargyl radical, H_2C-C≡C-H, has been observed by infrared kinetic spectroscopy. Propargyl is produced by the flash photolysis of either propargyl bromide or propargyl chloride at 193 nm,

$$CH_2XCCH + h\nu\ (193\ nm) \rightarrow CH_2CCH + X\ \ (X=Br,Cl)$$

and the acetylenic CH stretch observed using a color center laser probe. An overview of the spectrum is shown in Fig. 2. As can be seen, near the band center it very much resembles the spectrum of a diatomic molecule with a Q-branch. Only a-type ($\Delta K=0$) transitions are expected for this band. The spacing between the lines is in agreement with the value of B+C calculated from the *ab initio* structure[5] of propargyl. The simplicity of the observed spectrum implies that there are very small changes in the spectroscopic constants A, D_K, D_{NK} upon excitation of the CH stretch. The different K subbands overlap almost exactly and give a spectrum with little structure. However, near N=15 the spectrum becomes unexpectedly complex, the K subbands separating out rapidly with increasing N as can be seen in the high resolution portion of the P branch of the propargyl radical depicted in Fig. 3. We believe this is due to perturbation of the upper state by a combination or overtone state. For a short N region before the band breaks up near N=15, two satellite lines are seen place symmetrically about the intense components. These are identified as K=1 components split from the main line by asymmetry. If propargyl is effectively planar implying C_{2v} symmetry, even K levels will have a spin weight of three and odd K levels will have a spin weight of one for these vibrational states because the electronic wave function is expected to be of B_1 symmetry. The relative intensity of the K=1 satellites to the main line is in accord with prediction using these spin weights. The rotational constants, B', C', B", C" have been obtained by fitting this spectrum and agree quite closely with those calculated from the *ab initio* structure. There is no indication in the spectrum of spin-rotation splittings caused by the odd electron. However, a hot band spectrum can be seen as a set of lines with about 10-15% the intensity of the main series. The vibrational state which is the lower level for these satellite lines has not yet been assigned.

The decay of the propargyl signals with time follows second order kinetics. The magnetic dipole allowed fine structure transition of the bromine atom at 3685 cm^{-1} can also be observed with the same apparatus. This signal decays with first order kinetics. Under the same conditions, the propargyl decay is slower than that of the bromine atom. These observations show that propargyl does not react with the precursor C_3H_3Br nor with Br. Presumably, propargyl is reacting with itself.

---

[1]A. O. Langford, H. Petek, and C. B.Moore, J. Chem. Phys. 78 (1983) 6650.

[2]J. Peeters, M. Schaekers, and C. Vinckier, J. Phys. Chem. 90 (1986) 6552, and references therein.

[3]I. T. N. Jones and K. D. Bayes, Proc. R. Soc. Lond. A335 (1973) 547.

[4]J. Vandooren, and P. J. Van Tiggelen, Symp. (Int.) Combust., [Proc.] 16 (1977) 1133. K. H. Eberius, K. Hoyerman, and H. G. Wagner, Symp. (Int.) Combust., [Proc.] 14 (1973) 147.

[5]H. Honjou, M. Yoshimine, J. Pacansky, J. Phys. Chem. 91, 4455 (1987).

Publications 1990 to present

1. "Acetylene Combustion Reactions: Rate Constant Measurements of HCCO with O_2 and C_2H_2", K. K. Murray, K. G. Unfried, G. P. Glass, and R. F. Curl, Chem. Phys. Lett. (accepted).

2. "Infrared Flash Kinetic Spectroscopy of the Ketenyl Radical", K. G. Unfried, G. P. Glass, and R. F. Curl, *Chem. Phys. Lett.* **177**, 33-38 (1991).

3. "Thermal DeNOx: No HNO at Room Temperature", K. G. Unfried, G. P. Glass, and R. F. Curl, *Chem. Phys. Letters* **173**, 337-342 (1990).

4. "Rate Constant Measurements of C_2H with CH_4, C_2H_6, C_2H_4, D_2, and CO", D. R. Lander, K. G. Unfried, G. P. Glass, and R. F. Curl, *J. Phys. Chem.* **94**, 7759-63 (1990).

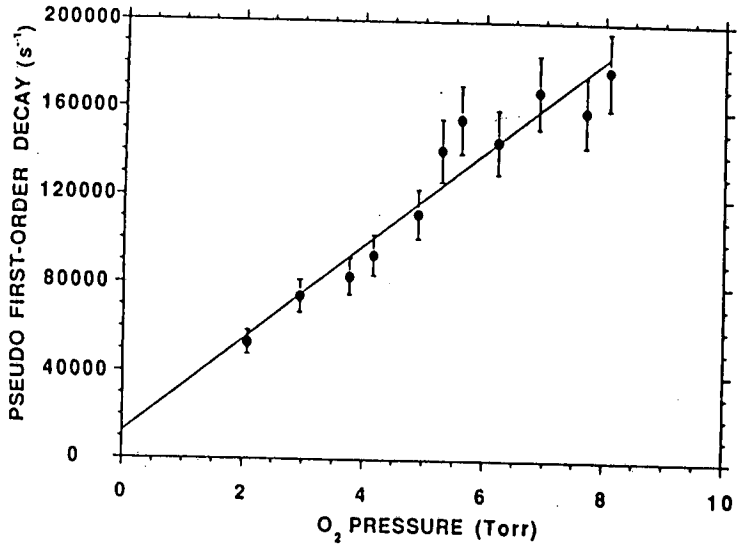

Fig. 1. Stern-Volmer plot for the reaction of HCCO with O_2.

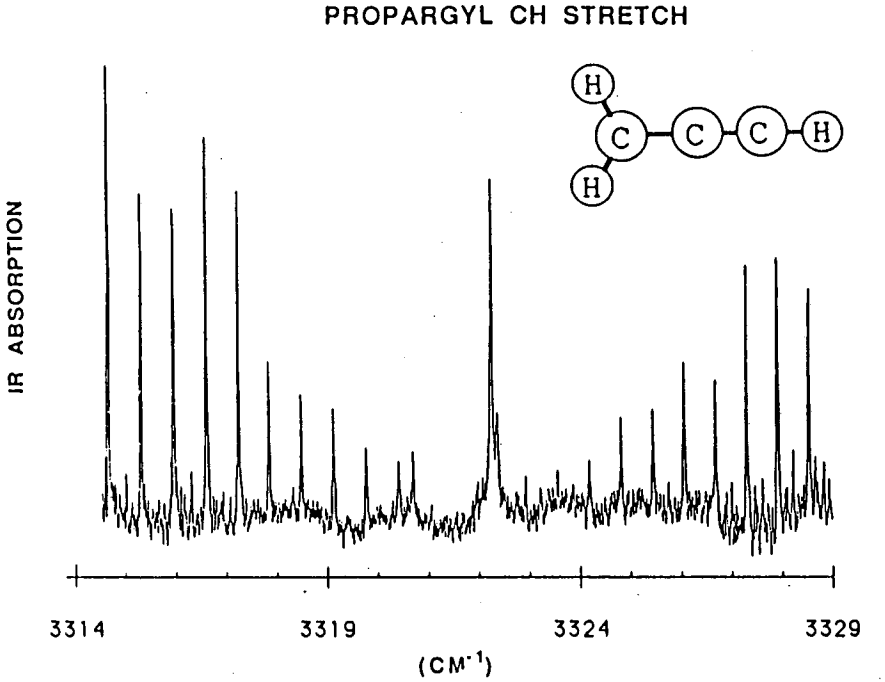

Fig. 2. Acetylenic CH stretching band of propargyl radical.

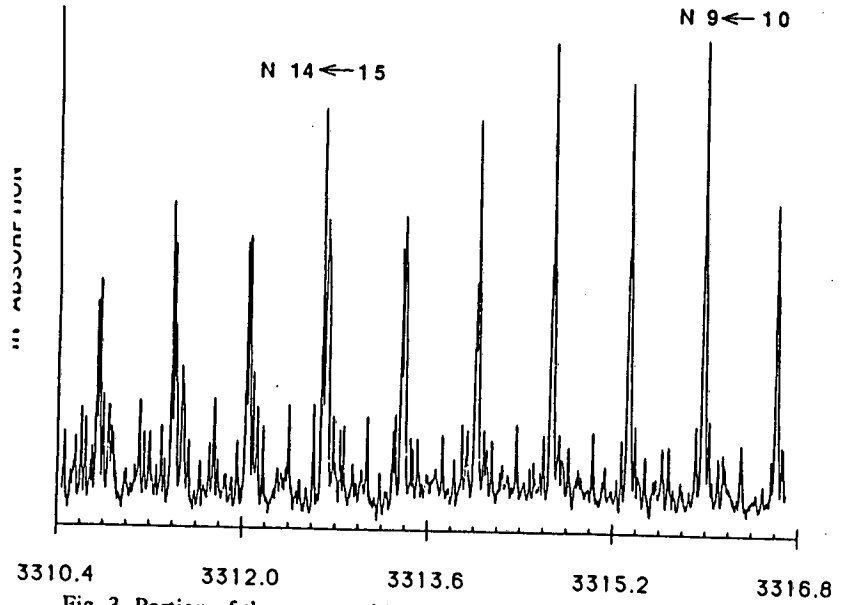

Fig. 3. Portion of the propargyl P-branch at high resolution showing onset of complex structure.

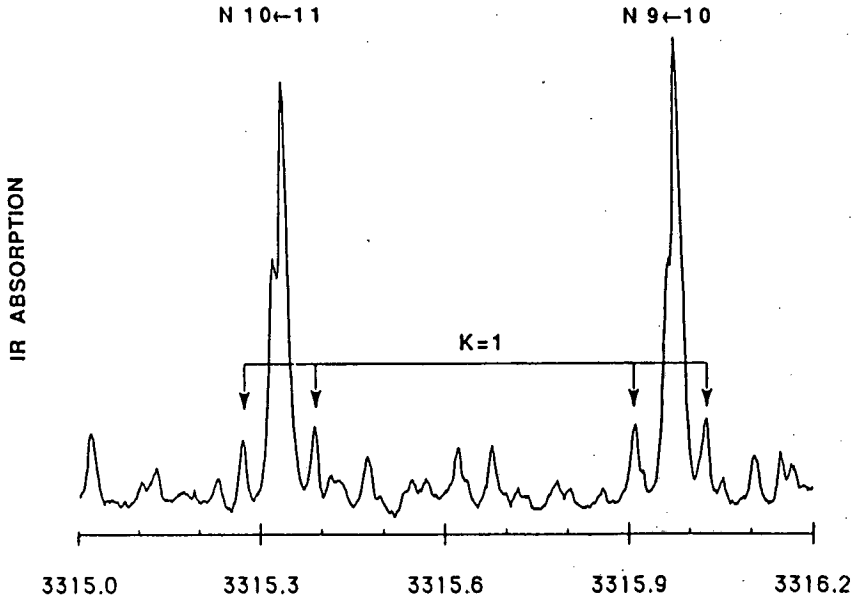

Fig. 4. K=1 satellites in propargyl spectrum.

Spectroscopy and Reactions of Transient Molecules by Time-Resolved Fourier Transform Emission Spectroscopy

Hai-Lung Dai
Department of Chemistry
University of Pennsylvania
Philadelphia, PA 19104-6323

I. Introduction

A time-resolved Fourier transform emission spectroscopic technique (TRFTES) with several tens of nanoseconds time- and 0.1 - 1 cm^{-1} spectral-resolution has been developed for detecting and resolving emission spectra in the IR, visible, and UV regions. This technique, in combination with the Stimulated Emission Pumping (SEP) technique, will greatly enhance our capability to study the vibrational spectroscopy and the reaction kinetics and dynamics of transient molecules.

II. Recent Progress

A. Time-Resolved Fourier Transform Emission Spectroscopy with 25 nsec Time- and 0.25 cm^{-1} Spectral-Resolution in the Visible

Stimulated Emission Pumping is a powerful technique for studying the high vibrational levels. Many of its advantages are derived from using a laser (the DUMP) to enhance a particular transition among the many in PUMP laser induced fluorescence (LIF). Dispersing the LIF can in principle provide the same information but in practice is unachievable in most experimental conditions. The dispersing instrument used allows only the photons within the selected bandwidth to be detected, while discarding all the rest of the photons in the LIF. This limits the detection S/N and reduces resolution and sensitivity.

In principle, the use of a Fourier Transform Spectrometer as the dispersion instrument can avoid these disadvantages since all the photons are involved in constructing the interferogram. However, this would require that the FT Spectrometer be used for pulsed-laser induced fluorescence with lifetimes that often are ~10^{-7} sec. A Brucker Instrument IFS-88 FTIR Spectrometer with visible and UV capability has been acquired for this purpose. This FT Spectrometer has the "step-scan" function that allows the transient fluorescence decay to be taken at a selected moving-minor position, I(t,x). Reconstruction of I(t,x) at fixed t allows the interferogram to be obtained with time-resolution. A transient digitizer (40 MHz), coupled with the FT Spectrometer, enables the recording of the LIF spectrum with 25 nsec time resolution. This can in principle be achieved in the wavelength range from IR to UV at 0.1-1 cm^{-1} resolution. The first test of this technique was done on I_2 LIF in the visible. It was shown that a time-resolved I_2 fluorescence spectrum covering a frequency range of 4,000 cm^{-1} recorded after the laser excitation of a single rovibronic level took only 90 minutes to achieve.

B. Observation of New Vibrational Levels in the $\tilde{a}^1A_1$ State of CH_2

There are many advantages in using the TRFTES technique to study the vibrational spectroscopy of a transient molecule. The improved sensitivity for detecting the dispersed fluorescence requires a minimum amount of the species. Time resolution in the spectrum

ensures proper assignment of observed features to the right species. The kinetics of the excited levels of the transient species can also be studied (see next subsection). Furthermore, the accuracy of the FT technique in frequency calibration reduces experimental complexity. Fig. 1 shows a segment of the dispersed fluorescence spectrum taken for a sample containing ~1 mTorr CH_2 after the pulse laser excitation of the $\tilde{b}^1A_2$, 2^{16}, 4_{04} level. A newly assigned vibrational level (1,2,0) is shown in the figure. The vibrational term value of this level is determined to be 5445.4 cm^{-1}, comparing well with the *ab initio* calculation value of 5452 cm^{-1} (Green et al., *J. Chem. Phys.* 94, 118 (1991)). The rotational constants have also been determined to be A = 22.5, B = 11.12, C = 6.72 cm^{-1}.

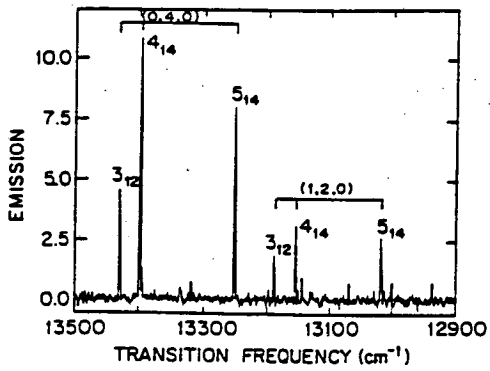

Fig. 1. Dispersed fluorescence spectrum from the $\tilde{b}$, 2^{16}, 4_{04} level of CH_2.

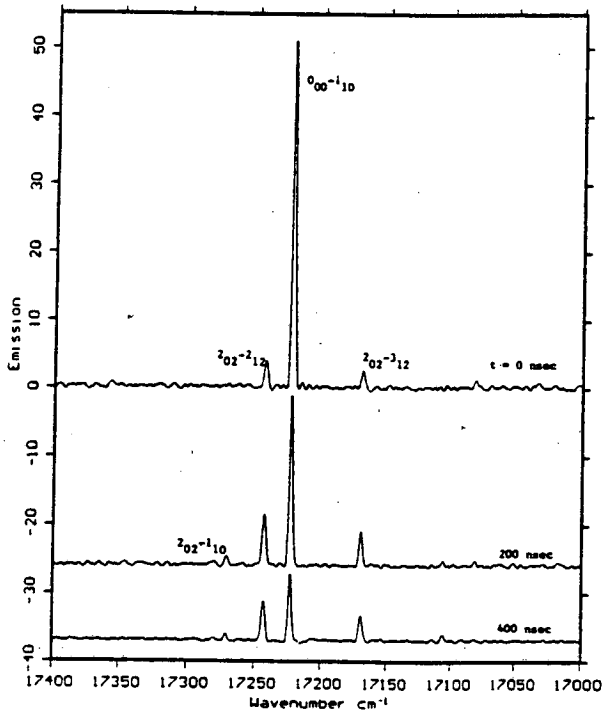

Fig. 2. Dispersed fluorescence spectra at different times after laser excitation of the $\tilde{b}$, 2^{16}, 0_{00} level of CH_2. Ketene pressure is maintained at 200 mTorr.

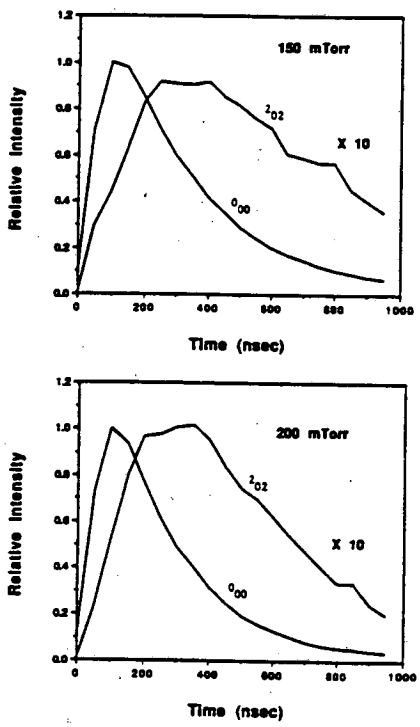

Fig. 3. Fluorescence intensities from the 0_{00} and 2_{02} levels as a function time after the initial excitation of the 0_{00} level.

C. Determination of the Reaction and Rotational Relaxation Cross Sections of $\tilde{b}^1A_2$ CH_2.

The evolution of the emission spectrum in time can be used to deduce the relaxation kinetics of the excited level. Fig. 2 shows the growth of collisional satellite transitions from the 2_{02} rotational level in the $\tilde{b}$, 2^{16} level after the initial excitation of the $\tilde{b}$, 2^{16}, 0_{00} level by a laser pulse. The 2_{02} population arises from collisionally induced rotational relaxation of the 0_{00} level. A plot of the rotational transition intensities shows the time-evolution of the 0_{00} and 2_{02} populations (Fig.3). Analysis of the time- and pressure-dependent spectra allowed us to determine the total extinction cross section for a single rotational level in the $\tilde{b}$, 2^{16} level to be 74 ± 1 Å^2. This value is about twice the size of the $\tilde{a}$ state reaction cross section (Langford, Petek, and Moore, *J. Chem. Phys.* **78**, 6650 (1983)), indicating a higher reactivity in the $\tilde{b}$ state. Of the total extinction cross section, ≤ 5 Å^2 is from rotational relaxation. We have also identified the propensity rules on the rotational quantum number changes in rotational relaxation collisions. They are consistent with those for a linear molecule like CH_2 in the $\tilde{b}$ state.

III. Future Plans

A. Difluoro-vinylidene (F_2CC) Identification and Characterization

The success of the SEP and the TRFTES methods in characterizing the vibration-rotation structure of CH_2 indicates that other transient radicals with optically accessible electronic transitions can be studied the same way. Preliminary studies on the difluoro-vinylidene (F_2CC) radical have been carried out.

The F_2CC radical is interesting for several reasons. It is a small but important freon radical. From *ab initio* calculations (Gallo and Schaefer, *J. Chem. Phys.* **93**, 865 (1990)), it assumes the same structure as vinylidene. But unlike vinylidene it is thermally stable. A previous study of emission from a fluorocarbon plasma has claimed the observation of F_2CC vibronic transitions associated with the CF_2 rocking motion (Khalturin et al., *J. Gen. Chem. USSR* **58**, 1203 (1988)).

To begin with, we have attempted to confirm these results. F_2CC is generated by photolysis of $F_2C_2 = CO$, which is synthesized by an organic group at Penn, with an excimer laser at 308 nm. Tunable laser pulses in the 470-480 nm region have been used to induce fluorescence. Several LIF features have been observed. Initial analysis of the rotational band structures generated rotational constants consistent with the calculated F_2CC structure.

B. The Acetylene-Vinylidene Isomerization Reaction

An *ab initio* calculation (Osamura, Schaefer, Gray, and Miller, *J. Am. Chem. Soc.* **103**, 1904 (1981)) showed that on the $\tilde{X}$ state potential surface the vinylidene isomer exists at 39.5 kcal/mole above the acetylene equilibrium potential energy. The zero-point energy corrected barrier for isomerization to vinylidene is 40.2 kcal/mole. There are only two IR active normal modes (with frequencies at 3,583 and 764 cm-1) in acetylene. On the other hand, all six normal vibrations are IR active in vinylidene.

We intend to use SEP to excite acetylene to a high vibrational level in the $\tilde{X}$ state and then use TRFTES to resolve the IR emission from this level. Since the intermediate $\tilde{A}$ state has a trans-bend structure, the Franck-Condon factor allows SEP excitation of vibrational levels containing large amplitude bending motion in the $\tilde{X}$ state. These are eigenstates that most likely would have their wavefunctions spread over to the vinylidene structure. The vibrational levels below the isomerization barrier should give only two peaks assignable to the two acetylene IR active modes. However, once the eigenstate energy is higher than ~14,000 cm^{-1}, these eigenstates containing vinylidene character should give fluorescence spectra showing new peaks. A study like this would confirm the existence of vinylidene, determine the barrier height, and even obtain all of the vinylidene vibrational frequencies.

IV. Publications from DOE-Sponsored Research

Bending Overtones and Barrier Height of the $\tilde{a}^1A_1$ State of CH_2 by Flash Photolysis Stimulated Emission Pumping, *J. Chem. Phys.* **93**, 4615 (1990), Wei Xie, Carmel Harkin, and Hai-Lung Dai.

Preventing Rapid Decomposition of Rhodamine Dyes in Excimer-Pumped Pulsed Dye Lasers, *Rev. Sci. Instr.* **61**, 191 (1990), Paul D. Arias and Hai-Lung Dai.

Laser Vibrational Spectroscopy of Transient, Weakly Bound and Reactive Molecules, *Applied Spectr.* **44**, 1595 (1990), Hai-Lung Dai.

Vibration-Rotation Spectroscopy with Dye Lasers: Higher Sensitivity and Extended Frequency Range via Stimulated Emission Pumping, *Lambda Physik Highlights* **23**, 1 (1990), Uwe Brinkmann and Hai-Lung Dai.

The Chemical and Physical Properties of Vibration-Rotation Eigenstates of H_2CO (S_0) at 28,300 cm^{-1}, in "Advances in Molecular Vibrations," ed. J. M. Bowman (JAI Press, Connecticut, 1991), pp. 305-327, H. L. Dai.

Vibrational Spectroscopy and Dynamics of Transient and Weakly Bound Molecules by Stimulated Emission Pumping, in "Advances in Multi-Photon Processes and Spectroscopy," ed. S. H. Lin (World Scientific, 1991), Vol. 7, pp. 159-230, H. L. Dai.

Time-resolved Fourier Transform Spectroscopy with $<10^{-7}$ Second Time- and 0.25 cm^{-1} Spectral-Resolution in the Visible Region, *Rev. Sci. Instr.* **00**, 0000 (1992), G. V. Hartland, W. Xie, H. L. Dai, A. Simon, and M. J. Anderson.

Observation of Strong $\Delta K_a=5$ Transitions in the $\tilde{b}^1B_1 \leftarrow \tilde{a}^1A_1$ LIF Spectrum of CH_2, *J. Mol. Spectr.*, submitted, W. Xie and H. L. Dai.

COMPREHENSIVE MECHANISMS FOR COMBUSTION CHEMISTRY: EXPERIMENT, MODELING, AND SENSITIVITY ANALYSIS

Frederick L. Dryer and Richard A. Yetter
Department of Mechanical and Aerospace Engineering
Princeton University, Princeton, New Jersey 08544-5263
Grant No. DE-FG02-86ER-13503

Program Scope

This research program is an integrated effort to determine reactions and reaction mechanisms responsible for the oxidation of small molecule hydrocarbons under conditions representative of combustion environments. The experimental aspects of the program are conducted in an atmospheric pressure flow reactor (APFR), as well as in a variable pressure flow reactor (VPFR) over pressures from 1 to 15 atmospheres, temperatures from 600 to 1100 K, and observation times from 100 to 2,000 milli-seconds. Insitu optical diagnostics, especially resonance absorption, as well as gas sampling methods are utilized to characterize chemical composition. Continuous, on-line, non-dispersive infrared analyses (CO_x), electrochemical techniques (O_2), selective thermal conductivity methods (H_2), and Fourier Transform Infrared (FTIR) analyses (CO_x, H_2O, $<C_4$ species) as well as off-line gas chromatographic and gas chromatographic/mass spectrometric analytical methods are applied to determine sampled chemical compositions.

The modeling aspects of the program emphasize the use of hierarchical mechanistic construction methods, along with path and elemental gradient sensitivity analyses, to develop and study the behavior of detailed kinetic mechanisms. Mechanistic studies are utilized for interpreting the experimental observations, for developing comprehensive kinetic models for use in general combustion modeling, and for identifying important elementary reactions which require improved definition (reaction products and absolute rates). Modeling and experiments under constrained reaction conditions produced for H_2/Oxidant and CO/H_2/Oxidant systems perturbed by small amounts of hydrocarbon additives are used to evaluate absolute reaction rates and to investigate the compatibility of published elementary kinetic data within the context of mechanistic observations.

Of present interest are: the CO/H_2/Oxidant system and its perturbation by small amounts of hydrocarbons or hydrocarbon oxygenates; the pyrolysis and oxidation of simple aldehydes; the pyrolysis and oxidation of simple alcohols; and the pyrolysis and oxidation of simple olefins. Of considerable significance to all of the above is the experimental and mechanistic extension of research on these systems to pressures as high as 15 atmospheres, and to temperatures as low as 700 K.

Recent Progress

A. Hydrogen and Carbon Monoxide Oxidations

During the past year, a number of publications[1-4] have appeared in the literature which summarize our work on the CO oxidation in the presence of moisture or hydrogen, at atmospheric pressure. Experimental data generated in the APFR[1], along with shock tube data, static reactor data, and published elementary reaction and thermochemical results, were utilized to develop a comprehensive reaction mechanism which reproduced experimental observations encompassing a combined temperature range of 823-2870 K, fuel oxidizer equivalence ratios from 0.0005 to 6.0, C/H ratios from between 0.005 and 128, and pressures from 0.3 to 2.2 atmospheres[2]. Subsequently, hydroxyl radical concentrations measured in fuel lean $CO/H_2/O_2$ experiments in the APFR[3,4] were found to be within +/- 30% (at worst) of those predicted by the model, over a range of temperatures from 990 - 1115 K.

Recently, we have initiated VPFR experiments on H_2/O_2 and $CO/H_2O/O_2$ to investigate the effects of higher pressure on their reaction characteristics. Stable species reaction profiles have been obtained at a number of pressures (one to nine atmospheres). The VPFR design is fundamentally different than that of the APFR in that the reaction zone is positioned relative to a fixed sampling location by moving the reactor fuel injection and mixing location, thus facilitating optical diagnostics. Relative laser induced fluorescence results at several radial positions in earlier APFR experiments[5] showed that line-of-sight

resonance absorption is an accurate means of determining hydroxyl radical concentrations at axial locations in these reactors. Addition of instrumentation to perform resonance absorption measurements in the VPFR is nearly complete.

Figure 1 shows an example of $CO/H_2O/O_2$ data (symbols) for a pressure of 3 atmospheres and an initial temperature of 1038 K. Note that for the first 50% consumption of CO, the maximum rate of reaction is slower than that observed during the latter half of the reaction. The solid lines are the predictions of the model published in reference 2. The slow reaction phase is predicted to be too slow, while the fast reaction phase is too fast. The transition between the two regimes corresponds to a change in the dominance of $H + O_2 + M = HO_2 + M$ versus $H + O_2 = OH + O$. Studies of the H_2/O_2 system crossing this same limit, but at lower temperature, have shown good agreement between model and experiment. Sensitivity analyses comparisons for increasing pressure from one to three atmospheres show that the discrepancies between the model and experiment of the $CO/H_2/O_2$ system may result from the increased importance of the reactions $CO + O + M = CO_2 + M$, $CO + HO_2 = CO_2 + OH$, $H + O_2 + M = HO_2 + M$, $H + HO_2 = OH + OH$, and $H + HO_2 = H_2 + O_2$. Each of these reactions have large uncertainties for temperatures near 1040 K and are reactions which require further experimental and theoretical study.

B. Ethanol Oxidation

Experimental and computational studies of ethanol oxidation at APFR conditions are reported in detail in a recent publication[6]. Ethanol oxidation experiments at atmospheric pressure near 1100 K and at equivalence ratios from 0.61-1.24 were compared with detailed kinetic computations which consider all three isomeric forms of the C_2H_5O radical (Figure 2). The agreement between the model and experiment at 1100 K was optimized by varying the branching ratio of the reactions of C_2H_5OH with OH and H, with the best comparisons obtained for the following: 30% C_2H_4OH + 50% CH_3CHOH + 20% CH_3CH_2O + XH. (The branching ratios of other reactions for ethanol with O and CH_3 were estimated from the literature and by analogy with methanol.) This result is consistent with the prediction of Hess and Tully[7] for intermediate temperature conditions. The primary source of ethene in ethanol oxidation is verified to be the decomposition of the C_2H_4OH radical.

Many features of ethanol oxidation are similar to those of methanol. For a major part of the reaction, chain branching is suppressed by fast straight chain reactions and chain termination reactions to the extent that the concentrations of the major radicals actually decrease during most of the latter half of the fuel decay. Because of the large amounts of aldehydes and HO_2 produced, H atoms react more quickly in straight chain reactions than with oxygen. An important difference, however, is increased chain termination through reactions involving CH_3. In addition, direct fuel dehydration (C_2H_4OH decomposition) is an additional and significant mechanism contributing to the production of OH. The reaction $CH_3 + HO_2$, was found to be critically important to the production of both OH and H via formation and further decomposition of CH_3O, as well as to termination (ie. formation of CH_4 and H_2). This reaction is also of substantial importance to hydrocarbon oxidation phenomena at high pressures[8], and further measurements of its rate and branching ratio are needed. The under-predictions of acetylene in the present model suggest that the extrapolation of the rate constant for $C_2H_3 + O_2$ of Slagel et al.[9] results in a rate constant which is too fast at 1100 K, although uncertainty in the rate of vinyl radical decomposition may also be a factor. Finally, if the reaction $C_2H_4OH + O_2 = CH_3CHO + HO_2$ is found to have a non-negligible rate, it will be of significance to both ethanol and ethene oxidations, particularly at higher pressures.

Future Plans

Experiments will continue on the pyrolysis and oxidation of simple oxygenates and olefins, particularly at higher pressures (and to a lesser extent, lower temperatures). In addition to studying the H_2/O_2, $CO/H_2/O_2$ systems and perturbation of these systems by trace amounts of hydrocarbons, at pressures to fifteen atmospheres, experiments are also planned on H_2O_2 decomposition over similar pressure ranges, A major emphasis of much of this work will be to extend experimental and computational studies to higher pressures and lower temperatures to emphasize the role of oxygenated intermediates and HO_2 reactions.

References

1. R.A. Yetter, F.L. Dryer, and H. Rabitz, "Flow Reaction Studies of Carbon Monoxide/Hydrogen/Oxygen Kinetics" , Comb. Sci. and Tech., 79, 129 (1991).

2. R.A. Yetter, F.L. Dryer, and H. Rabitz, "A Comprehensive Reaction Mechanism for Carbon Monoxide/Hydrogen/Oxygen Kinetics", Comb. Sci. and Tech., 79, 97 (1991).

3. G. T. Linteris, K. Brezinsky, and F.L. Dryer, "A High Temperature 180 Degree Laser Induced Fluorescence Probe for Remote Trace Radical Concentration Measurements", Applied Optics Letters, 30, 381 (1991).
4. G. T. Linteris, K. Brezinsky, and F.L. Dryer, "Hydroxyl Radical Concentration Measurements in Moist Carbon Monoxide Oxidation in a Chemical Kinetic Flow Reactor", Combust. and Flame, 86, 162 (1991).
5. G.T. Linteris, "Trace Radical Species Detection in a Turbulent Chemical Kinetic Flow Reactor Using a 180° Laser Induced Fluorescence Probe", Ph.D. Thesis, Department of Mechanical and Aerospace Engineering, Princeton University, Princeton, NJ, February, 1990. Report T-1878.
6. T.S. Norton and F.L. Dryer, "An Experimental and Modeling Study of Ethanol Oxidation Kinetics in an Atmospheric Pressure Flow Reactor", I.J. Chem. Kin., Accepted for Publication. In Galley form, January 1992.
7. W.P. Hess and F.P. Tully, Chem. Phys. Lett., 152, 183 (1983).
8. M.L. Vermeersch, T.J. Held, Y. Stein, and F.L. Dryer, " Autoignition Chemistry Studies of n-Butane in a Variable Pressure Flow Reactor", 1991 SAE Fuels and Lubricants Meeting, Toronto Ontario, October 5-8,. 1991. Paper No. 912316. Accepted for Publication in SAE Transactions.
9. I.R. Slagle, J.Y. Park, M.C. Heaven, and D. Gutman, J. Am. Chem. Soc. 106, 4356 (1984).

Publications and Theses, 1990 - Present

1. R.A. Yetter and F.L. Dryer, "Inhibition of Moist Carbon Monoxide by Trace Amounts of Hydrocarbons", Twenty-Fourth International Symposium on Combustion, Sydney, Australia, July 5-10, 1992. Accepted for Presentation.
2. T.S. Norton and F.L. Dryer, "An Experimental and Modeling Study of Ethanol Oxidation Kinetics in an Atmospheric Pressure Flow Reactor", I.J. Chem. Kin., Accepted for Publication. In Galley form, January 1992.
3. S.Hochgreb and F.L. Dryer, "Decomposition of 1,3,5-Trioxane at 700-800 K", J. Phys. Chem., 96, 295 (1992).
4. R.A. Yetter, F.L. Dryer, and D.M. Golden, "Combustion Kinetics for High Speed Chemically Reacting Flows", An invited Contribution to Major Research Topics in Combustion, ICASE/NASA Series, M.Y. Hussaini, A. Kumar and R.G. Voigt, eds., Springer-Verlag, NY, 1992. pp. 309.
5. S. Hochgreb, Ph.D. Thesis, Department of Mechanical and Aerospace Engineering, Princeton University, Princeton, NJ., April 1991. MAE 1910-T.
6. F.L. Dryer, "The Phenomenology of Modeling Combustion Chemistry", Part 1, Chapter 3, in Fossil Fuel Combustion - A Sourcebook, W. Bartok and A.F. Sarofim, eds., John Wiley and Sons Inc., NY, 1991.
7. G. T. Linteris, K. Brezinsky, and F.L. Dryer, "Hydroxyl Radical Concentration Measurements in Moist Carbon Monoxide Oxidation in a Chemical Kinetic Flow Reactor", Combust. and Flame, 86, 162 (1991).
8. R.A. Yetter, F.L. Dryer, and H. Rabitz, "A Comprehensive Reaction Mechanism for Carbon Monoxide/Hydrogen/Oxygen Kinetics", Comb. Sci. and Tech., 79, 97 (1991).
9. R.A. Yetter, F.L. Dryer, and H. Rabitz, "Flow Reaction Studies of Carbon Monoxide/Hydrogen/Oxygen Kinetics" , Comb. Sci. and Tech., 79, 129 (1991).
10. G. T. Linteris, K. Brezinsky, and F.L. Dryer, "A High Temperature 180 Degree Laser Induced Fluorescence Probe for Remote Trace Radical Concentration Measurements", Applied Optics Letters, 30, 381 (1991).
11. .S. Norton and F.L. Dryer, "The Flow Reactor Oxidation of C_1 - C_4 Alcohols", Twenty Third International Symposium on Combustion, The Combustion Institute, Pittsburgh, PA, 1990. p. 179.
12. S. Hochgreb, R.A. Yetter, and F.L. Dryer, "The Oxidation of CH_2O in the Intermediate Temperature Range (943-995 K)", Twenty Third International Symposium on Combustion, The Combustion Institute, Pittsburgh, PA, 1990. p.171.
13. G.T. Linteris, "Trace Radical Species Detection in a Turbulent Chemical Kinetic Flow Reactor Using a 180° Laser Induced Fluorescence Probe", Ph.D. Thesis, Department of Mechanical and Aerospace Engineering, Princeton University, Princeton, NJ, February, 1990. Report T-1878.
14. T.S. Norton, "The Combustion Chemistry of Simple Alcohol Fuels", Ph.D. Thesis, Department of Mechanical and Aerospace Engineering, Princeton University, Princeton, NJ, January, 1990. Report T-1877.
15. T.S. Norton and F.L. Dryer, "Toward a Comprehensive Mechanism for Methanol Pyrolysis", Int. J. Chem. Kinet., 22, 219 (1990).

Figures

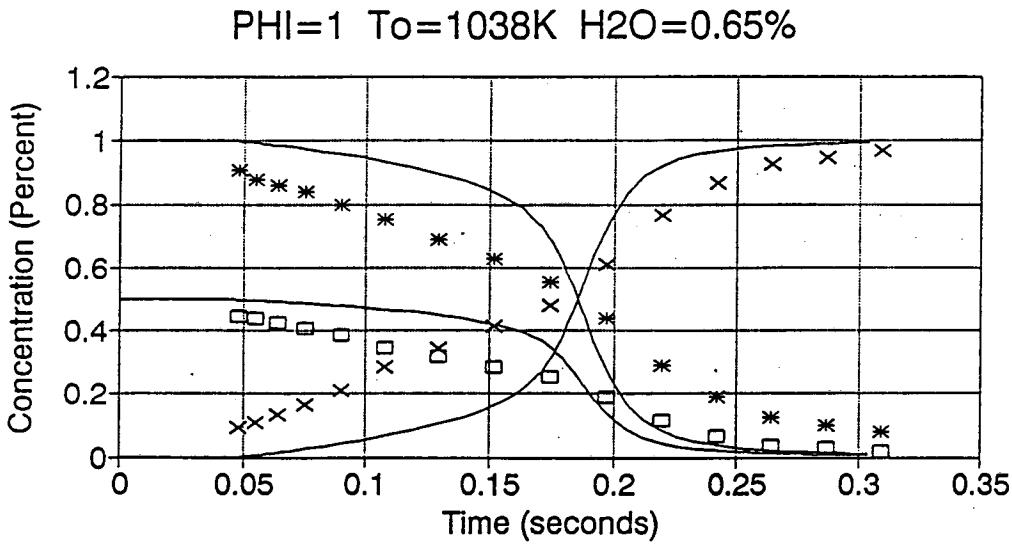

Figure 1. Experimental and numerical concentration profiles for a $CO/H_2O/O_2$ reaction in the VPFR at a pressure of 3 atmospheres and an initial temperature of 1038 K. Modeling and experimental results are matched at 50% CO depletion. Solid lines are predictions using the model of reference 2. Experimental data: squares - oxygen; crosses - carbon dioxide; stars- carbon monoxide.

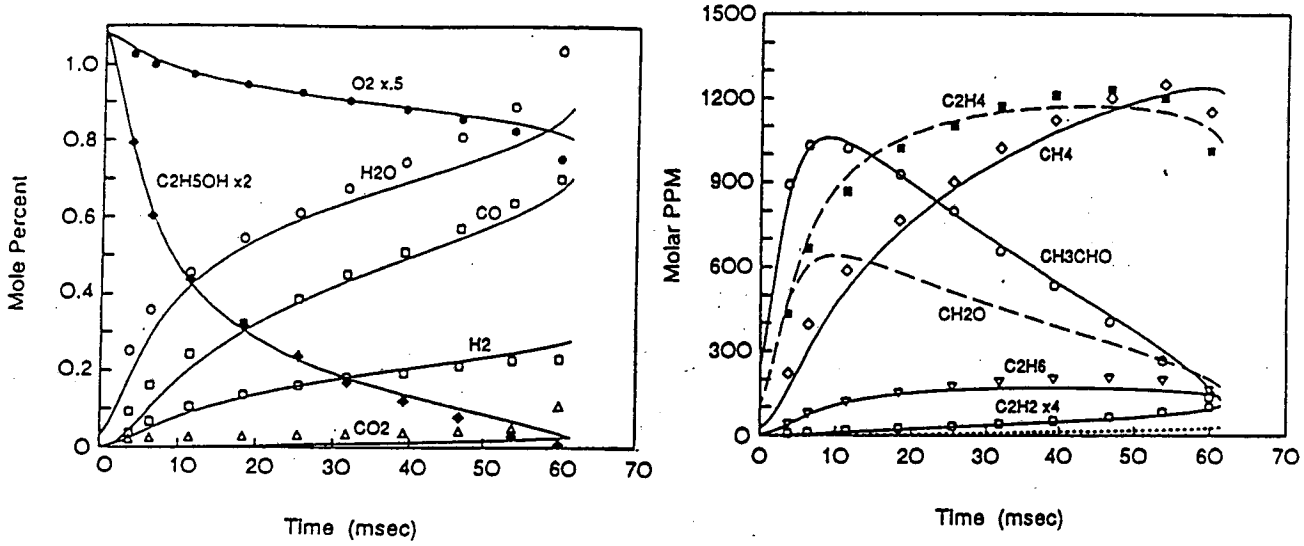

Figure 2..A comparison of the predictions for ethanol oxidation using the mechanism of Reference 6 with experimental data obtained in the APFR for a fuel lean condition (Equivalence Ratio = 0.81). The modeled profiles are offset by 4.6 milliseconds for alignment with the experimental data at the first experimental data point. The formaldehyde prediction from the model is shown for completeness (no experimental data). Two calculated profiles are shown for acetylene. The dotted line prediction is for the value of $C_2H_3 + O_2$ predicted from reference 9, and the solid line results are for a reduction of the rate by a factor of four.

Studies of Reaction Product Branching Fractions and Reaction Rate Coefficients for Elementary Chemical Reactions

Joseph L. Durant, Jr.
Combustion Research Facility
Sandia National Laboratories
Livermore, CA

The measurement of the reaction rate coefficient for an elementary chemical reaction is often only part of the complete characterization of the reaction. Many reactions can proceed through multiple channels, giving rise to different reaction products. For these reactions, measurement of the branching fraction for formation of specific products forms the second half of the complete study of the reaction. The discharge-flow technique has many advantages for the measurement of product branching fractions of elementary chemical reactions. Recognizing this, we constructed a discharge-flow apparatus to complement our use of the laser photolysis/cw-laser-induced-fluorescence (LP/cwLIF) technique used at Sandia. This allows us to undertake complete studies of gas-phase reactions with multiple product channels. Additionally, we have established a close theoretical collaboration that has served to enhance both our experimental effort and the theoretical effort.

Knowledge of the product branching fractions of several NH-radical reactions is of great importance to the understanding of NOx formation and destruction mechanisms in combustion processes. In particular, we are focusing on the reactions NH + NO $\rightarrow$ N_2 + OH/N_2O + H and NH + O_2 $\rightarrow$ H + NO_2/OH + NO. We have examined a cw NH source based on the successive reaction of F-atoms with NH_3 and NH_2. In preliminary experiments we observed production of NH and NH_2 radicals, as predicted. We found that use of $[NH_3]_0 > \sim 2 \times 10^{12}$ molecules/cm^3 leads to formation of species detected between m/e = 28 - 32 (presumably N_2H_x species). Lowering the initial $[NH_3]$ makes the source very sensitive to the rate of the wall-loss reactions of NH_2 and NH. We carried out experiments using uncoated quartz, Halocarbon wax coated and Teflon AF coated flow tubes, all of which had unacceptable wall-loss rates for NH and NH_2.

Work has continued using simultaneous mixing of NH_3 with F and $^{15}N^{18}O$. We detect signals at m/e = 47 ($^{14}N^{15}N^{18}O$) in these experiments; preliminary analysis suggests of branching fraction of 20% into the NH + NO $\rightarrow$ N_2O + H channel. Use of mass spectrometric detection and isotopically labeled reactants allows us to monitor $H_2{}^{18}O$, $^{14}N^{15}N$ and $^{14}N^{15}N^{18}O$ products from the simultaneous reactions of NH_2 and NH with NO. Of considerable interest is the effect of deuterium atom substitution on the branching fractions of the NH + NO $\rightarrow$ products and the NH_2 + NO $\rightarrow$ products reactions. One would expect deuterium substitution to favor production of products that do not require hydrogen-atom migration. The temperature dependence of this effect will provide information concerning the barriers to intramolecular hydrogen-atom migration.

To complement these product studies, we are also extending the capabilities of the highly precise LP/cwLIF technique to the measurement of reaction-rate coefficients for reactions of the NH radical. We have frequency doubled a cw ring-dye laser to obtain several milliwatts of laser light at 337 nm, enabling the cwLIF detection of the NH radical. Work is continuing towards measuring the reaction rate coefficients of NH and ND with NO and O_2.

Our laboratory has the demonstrated ability to carry out precise measurements of both reaction-rate coefficients and product-branching fractions. We are presently bringing both of these capabilities to bear on the important reactions of the NH radical. The ability to fully characterize these reactions will lead to an enhanced understanding of the mechanisms of elementary bimolecular reactions. Additionally, the characterization of the intramolecular hydrogen-atom migration in these reactions will provide benchmarks for evaluating newly developed path integral methods in quantum statistical mechanics.

Publications

J. A. Miller, J. V. Volponi, J. L. Durant, Jr., J. E. M. Goldsmith, G. A. Fisk and R. J. Kee, "The Structure and Reaction Mechanism of Rich, Non-Sooting $C_2H_2/O_2/Ar$ Flames," Twenty-Third Symposium (International) on Combustion, in press (1991).

J. L. Durant, Jr., "Anomalous Methoxy-Radical Yields in the Fluorine + Methanol → Products Reaction. I: Experimental," Journal of Physical Chemistry, **95**, 1070 (1991).

J. A. Gray, P. H. Paul and J. L. Durant, Jr. "Electronic Quenching Rates for $NO(A^2\Sigma^+)$ Measured in a Shock Tube," Chemical Physics Letters, **190**, 266 (1992)

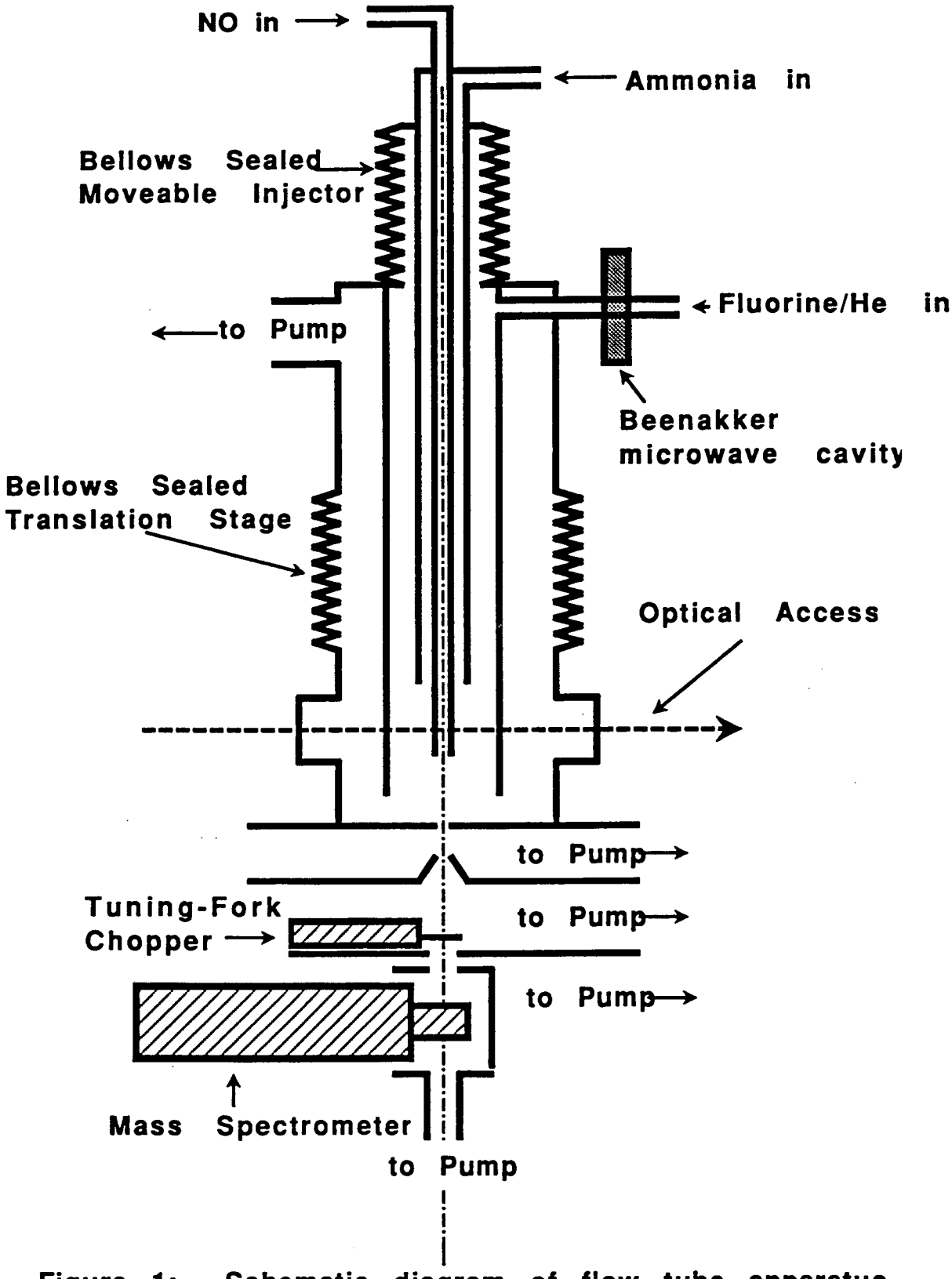

Figure 1: Schematic diagram of flow tube apparatus. Bellows sealed translation stages are used for the moveable injector and to move the entire flow tube to allow use of optical diagnostics.

LASER PHOTOELECTRON SPECTROSCOPY OF IONS

G. Barney Ellison
Department of Chemistry & Biochemistry
University of Colorado
Boulder, CO 80309-0215

Grant DE-FG02-87ER13695

This enterprise uses photoelectron spectroscopy to study the properties of negative ions and radicals. The essence of our experiment is to cross a 0.6 keV mass-selected ion beam (M^-) with the output of a CW laser, $\hbar\omega_o$. The resultant detached photoelectrons with kinetic energy, KE, are energy analyzed by means of a set of electrostatic hemispherical analyzers.

$$M^- + \hbar\omega_o \rightarrow M + e(KE)^-$$

Analysis of the photoelectron spectra enables us to extract molecular electron affinities, vibrational frequencies and electronic splittings of the final radical, M, as well as the relative molecular geometries of ions (M^-) and radicals (M).

We have scrutinized the two simplest nitrenes: methylnitrene (CH_3N) and phenylnitrene (C_6H_5N). By preparing the corresponding anions, CH_3N^- and $C_6H_5N^-$, we have studied these nitrene biradicals. Singlet methylnitrene is especially interesting since it is formally a "transition state."

$$^1[CH_3N] \rightarrow CH_2{=}NH \qquad (1)$$

We have measured the negative ion photoelectron spectra of CH_3N^- and find the electron affinity: $EA(CH_3N) = 0.024 \pm 0.010$ eV. All attempts to prepare the CD_3N^- ion failed so we cannot search for isotope shifts. This may be related to the fact that the $EA(CD_3N) \equiv kT$; our deuterated ions may be just collisionally detached before they can be extracted into an ion beam. Fig. 1 is an overview of the methylnitrene photodetachment spectra. We observe two states of the final CH_3N; the ground state $\tilde{X}\,^3A_2$ and the first

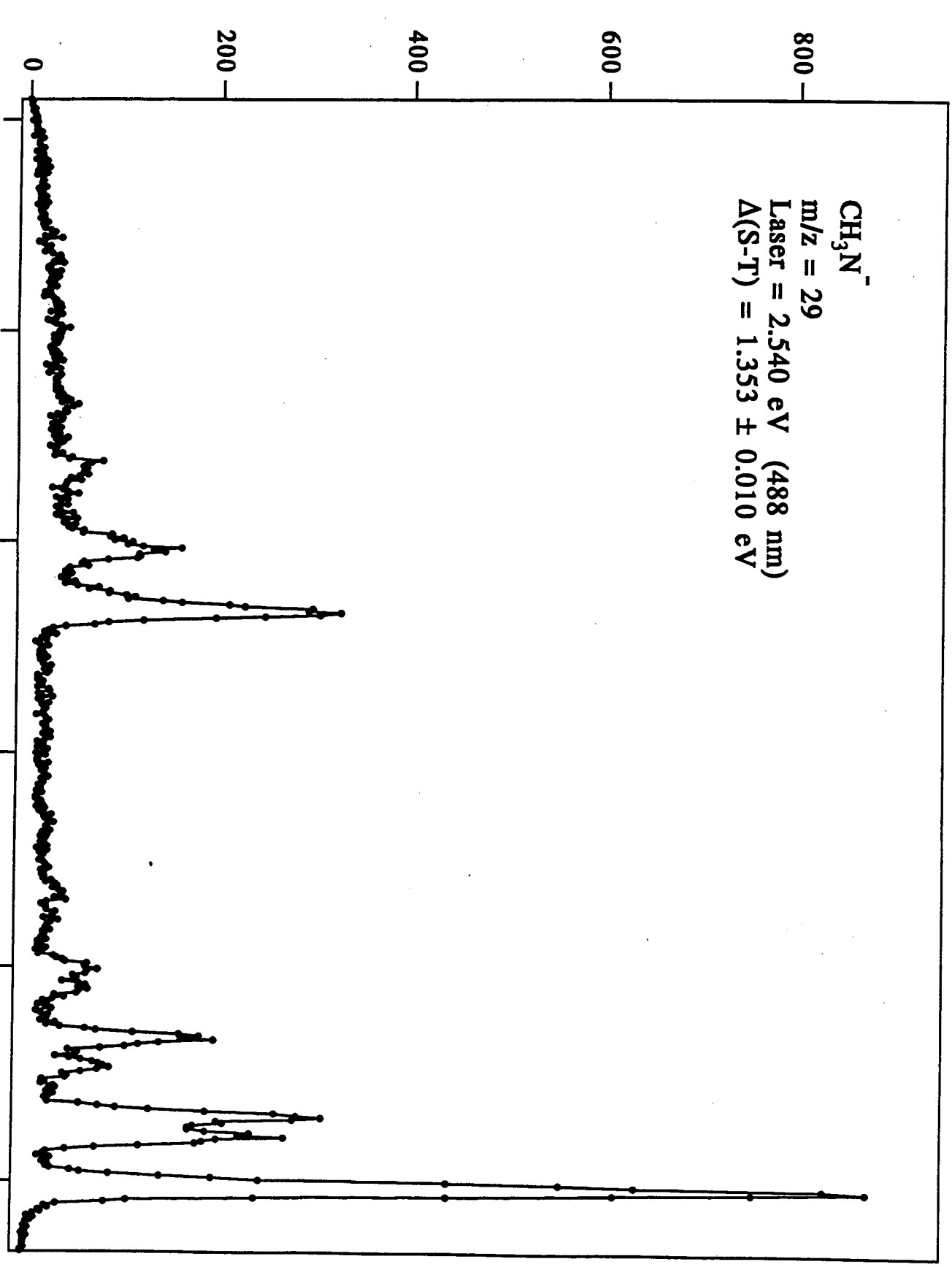
Photoelectron Counts
0
200
400
600
800
0.0
0.5
1.0
1.5
2.0
2.5
CM Photoelectron Kinetic Energy (eV)
CH_3N^-
m/z = 29
Laser = 2.540 eV (488 nm)
Δ(S-T) = 1.353 ± 0.010 eV

excited state, $\tilde{a}\ ^1E$. Our measured singlet-triplet splitting is $\Delta E_{ST} = 1.353 \pm 0.0110$ eV. Earlier ab initio calculations suggested that the $\tilde{a}\ ^1E$ CH_3N species was not bound with respect to the methyleneimine, CH_2=NH. Consequently there is believed to be no barrier to the rearrangement (1), yet we see structure in Fig. 1.

A more interesting nitrene is phenylnitrene, C_6H_5N. The chemistry of this reactive aromatic nitrene has been extensively studied and is very confusing. The ground states of several nitrenes have been studied by EPR spectroscopy and all but aminonitrenes are known to be a triplets. Phenylnitrene can be written as a species with a (p_x,p_y) pair of electrons triplet-coupled. The C_6H_5N radical is a symmetric, C_{2v} species and we employ the standard convention which adopts the C_2 axis as the *z*-axis and *x*-axis is perpendicular to the plane. Consequently the ground state of phenylnitrene is $\tilde{X}\ ^3A_2$ and we can represent our negative ion photodetachment experiment as:

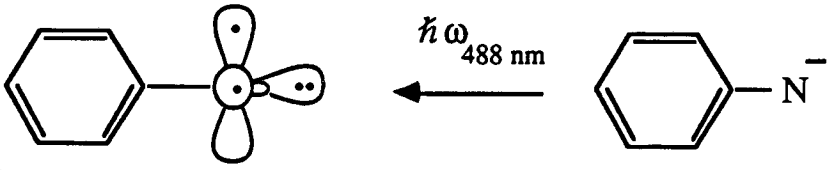

C_6H_5-N $\tilde{X}\ ^3A_2$ $\qquad$ C_6H_5-N$^-$ (2)

We have studied the photoelectron spectrum for the parent ion, $C_6H_5N^-$. We have also prepared intense ion beams of the deuterated species, $C_6D_5N^-$. We find EA(C_6H_5N) = 1.445 ± 0.015 eV and EA(C_6D_5N) = 1.448 ± 0.015 eV. Preliminary Franck-Condon factor analysis has been undertaken and we are refining our constants.

We have completed the move to a new laboratory and have a working spectrometer again. During the coming months a laser buildup cavity needs to be designed and fabricated. Right now a new afterglow ion source is being installed and optimized. We have begun preliminary studies of the CN_2 system. There are three interesting arrangements of these atoms:

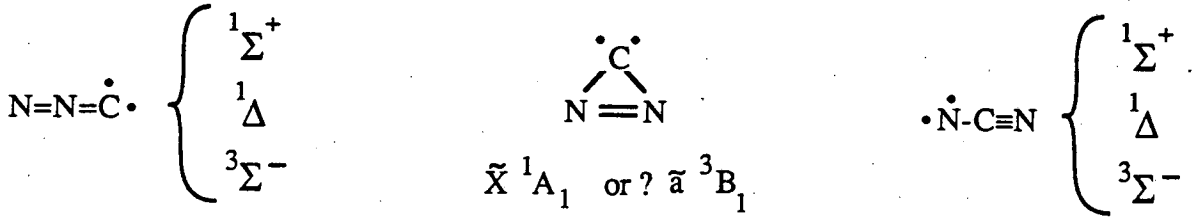

We are certain that we will be able to prepare beams of the [CNN]$^-$ isomer from ion

molecule reactions of O^- with CH_2N_2. It is likely that cyanamide may furnish us with the other linear isomer; $O^- + NH_2\text{-}CN \rightarrow [NCN]^- + H_2O$. Recent work in the laboratory of Dr. S.R. Kass at the University of Minnesota clearly indicates that diazirine will furnish clean ion beams of the cyclic, anti-aromatic ion *c*-$[CNN]^-$.

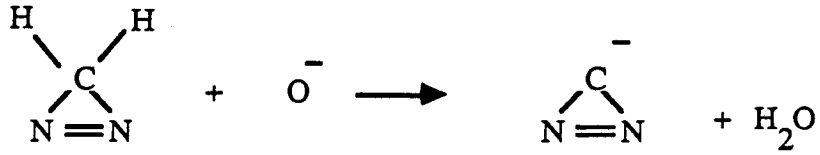

We know of no reports of the *c*-[CNN] radical; it might be a stable intermediate or perhaps it should be considered as the transition state, : N=N=C ⇌ *c*-[CNN] ⇌ N-C≡N, connecting the linear diradicals.

References

1. C. Tom Wickham-Jones, Sean Moran, and G. Barney Ellison, "Photoelectron Spectroscopy of BH_3^-," J. Chem. Phys. **90**, 795-806 (1989).

2. Mark R. Nimlos, J.R. Soderquist, and G. Barney Ellison, "The Spectroscopy of CH_3CO and CH_3CO^-," J. Amer. Chem. Soc. **111**, 7675-7681 (1989).

3. C. Tom Wickham-Jones, Kent M. Ervin, G. Barney Ellison, and W. Carl Lineberger, "NH_2 Electron Affinity," J. Chem. Phys. **91**, 2762-2763 (1989).

4. Michael J. Travers, Daniel C. Cowles, and G. Barney Ellison, "Reinvestigation of the Electron Affinities of O_2 and NO," Chem. Phys. Letts. **164**, 449-455 (1989).

5. Kent M. Ervin, Scott Gronert, S.E. Barlow, Mary K. Gilles, A.G. Harrison, Veronica M. Bierbaum, Charles H. DePuy, W.C. Lineberger, and G. Barney Ellison, "Bond Strengths of Ethylene and Acetylene," J. Amer. Chem. Soc. **112**, 5750-5759 (1990).

6. Daniel C. Cowles, Michael J. Travers, Jennifer L. Frueh, and G. Barney Ellison, "Photoelectron Spectroscopy of CH_2N^-," J. Chem. Phys. **94**, 3517-3528 (1991); J. Chem. Phys. **95**, 3864 (1991).

Low Energy Ion-Molecule Reactions

James M. Farrar

Department of Chemistry
University of Rochester
Rochester NY 14627

This project is concerned with elucidating the dynamics of elementary ion-molecule reactions at collision energies near and below 1 eV. From measurements of the angular and energy distributions of the reaction products, we infer intimate details about the nature of collisions leading to chemical reaction, the geometries and lifetimes of intermediate complexes that govern the reaction dynamics, and the collision energy dependence of these dynamical features. We employ the crossed beam low energy mass spectrometry technology that we have developed over the last several years, and the focus of our current research is on proton transfer and hydrogen atom transfer reactions of the ions O^-, OH^-, and OD^- with species such as H_2O, NH_3, and CH_4. We have completed extensive studies on the reactions of O^- with H_2O and NH_3 and will focus on those results in this report.

The reaction between O^- and H_2O,

$$O^- + H_2O \rightarrow OH^- + OH \qquad \Delta H^\circ = 0.34 \text{ eV} \qquad (1)$$

is an example of an endothermic reaction in which preliminary evidence for an intermediate collision complex comes from ion beam-collision cell measurements of total cross sections over the collision energy range from 0.17 to 3.5 eV.[1] We have studied the dynamics of collisions in this system over the relative kinetic energy range from 0.67 to 1.07 eV. Our work has shown that in order to gain a complete picture in this system, it is necessary to examine both reactive and nonreactive processes. In the case of reactive processes leading to OH^- products, we have found an interesting and surprisingly rapid variation in dynamics over a narrow collision energy range. In Figure 1, we show that at the lowest collision energy of 0.67 eV, the flux distribution has two clear peaks, with the dominant one in the backward direction. A detailed analysis of these fluxes shows that they are comprised of two dynamically distinct components. By applying the "osculating model" for chemical reactions proceeding through short-lived complexes,[2] we find that the $O^-{\cdot}H_2O$ species lives approximately half a rotational period. From moments of inertia taken from *ab initio* calculations[3], we estimate that the lifetime of the complex is approximately 250 fs, a result in excellent agreement with RRKM calculations carried out for this reaction.[1] The second component of the flux comes from a "rebound" collision process, in which O^- approaches H_2O along one of the O-H bonds, leading to a collision geometry with a near-collinear O···H···O configuration. In

this picture, we view the entering O^- as breaking an O-H bond in H_2O, with the new OH^- product recoiling in the backward direction. This mechanism is quite reasonable since the reaction is endothermic, and at threshold the cross section falls to zero, implying that low impact parameters lead to reaction.

Extensive phase space calculations of the OH^- product recoil distributions in this reaction recover the observed kinetic energy distributions quantitatively. In conjunction with the lifetimes we have extracted from angular distribution asymmetries, our picture of the dynamics at the lowest collision energies is that they are in excellent agreement with statistical theories.

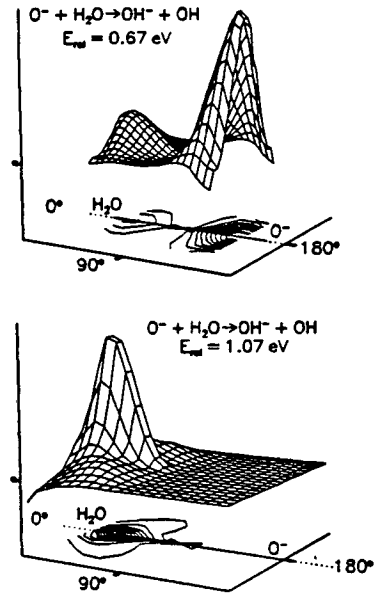

Figure 1 **Flux 3-D axonometric and contour projections for O^- + $H_2O \rightarrow OH^-$ + OH.**

This picture changes at the highest collision energies, exemplified by the data at 1.07 eV, where there is no longer evidence of complex formation, and the flux distribution has shifted strongly in the forward direction. Although a previous study of this reaction by Cross and Karnett[4] showed that the reaction is dominated by "Spectator Stripping" dynamics, such a process has a threshold of ~3 eV, a factor of three above our highest collision energy. In the lower energy range, the collision still involves significant interactions among all four atoms. Nevertheless, the rapid variation in reactive dynamics from backward scattering to transient complex behavior to forward scattering is an interesting phenomenon, a result that we attribute to the Heavy-Light-Heavy mass combination in this system.[5]

We have also studied the nonreactive scattering in this system. The data and Newton diagram for this process, shown in Figure 2 at a collision energy of 1.07 eV, indicate that the nonreactive scattering has two components. The higher energy component corresponds to direct nonreactive scattering of O^- from H_2O that is nearly elastic, or is only weakly inelastic. The second, lower energy component grows in with increasing lab scattering angle as the detector subtends angles near the centroid. This second component is essentially symmetric about the centroid and corresponds to O^- that has been ejected nonreactively from $O^-{\cdot}H_2O$ complexes formed by approaching reagents. The kinetic energy distributions we extract from these data are in good agreement with statistical phase space theory calculations, further supporting the notion that this reaction proceeds through a transient complex that partitions energy statistically.

The O^- + NH_3 system, producing OH^- + NH_2, is exothermic by 0.2 eV. The nonreactive scattering in this system is similar to that of the O^- + H_2O system, in that a significant fraction of O^- nonreactive events are highly inelastic and appear to proceed through an O^- ·NH_3 complex. However, the reactive scattering appears to be direct at all collision energies. While we would have expected the potential wells for the O^- ·H_2O and O^-·NH_3 complexes to be comparable in depth, leading to similar reactive dynamics, this difference suggests an underlying subtle difference in the potential surfaces. We hope to use *ab initio* calculations to explore the nature of barriers separating the intermediates O^-·NH_3/OH^-·NH_2 and O^-·H_2O/OH^-·OH and to provide insight into the reactive dynamics.

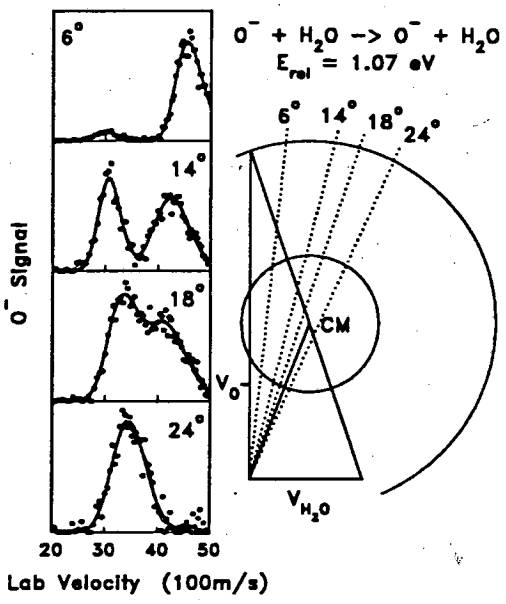

Figure 2 **Experimental data and Newton Diagram for O^- + H_2O nonreactive scattering.**

In addition to carrying out experiments using translational energy alone to promote these reactions, we are planning to use laser excitation in O-H and N-H internal degrees of freedom in the neutral reagents to explore the role of such selective excitation in promoting these reactions. The O^- + H_2O system appears to be the best candidate to date for such studies and will be our first target.

References

1. C. Lifshitz, J. Phys. Chem. **86**, 3634 (1981).
2. M. K. Bullitt, C. H. Fisher, and J. L. Kinsey, J. Chem. Phys. **60**, 478 (1974).
3. C. M. Roehl, J. T. Snodgrass, C. A. Deakyne, and M. T. Bowers, J. Chem. Phys. **94**, 6546 (1991).
4. M. P. Karnett and R. J. Cross, Chem. Phys. Lett. **82**, 277 (1981).
5. See, for example, A. Laganà, A. Aguilar, X. Gimenez, and J. M. Lucas, in *Advances in Molecular Vibrations and Collision Dynamics*, edited by J. M. Bowman (JAI Press, New York, 1992), to be published.

Publications

D. F. Varley, D. J. Levandier, and J. M. Farrar, "Dynamics of the Reaction of O^- with H_2O: Reactive and Nonreactive Decay of Collision Complexes," J. Chem. Phys. **96**, XXXX (1992).

Investigation of Degenerate Four-Wave Mixing for Quantitative Detection of Nitric Oxide

Roger L. Farrow, David J. Rakestraw, and Randall Vander Wal

Combustion Research Facility
Sandia National Laboratories
Livermore, CA 94550

Program Scope

Resonant degenerate four-wave mixing (DFWM) is currently the subject of intensive investigation as a sensitive diagnostic tool for molecular and atomic species.[1] In applications involving luminous or high-pressure reacting gases, DFWM has the advantage of generating a coherent (beam-like) signal, providing excellent immunity to background-light interference. Since multiple one-photon resonances are involved in the signal generation process, the DFWM technique can be very sensitive, approaching the sensitivity of laser-induced fluoresence (LIF) in some cases.

We are conducting fundamental and applied investigations of DFWM for quantitative measurements of trace species in reacting gases. In this abstract we will present results illustrating progress in: (1) high-resolution investigations of DFWM collisional line shapes and (2) measurements and modeling of DFWM spectral of NO in flames.

Recent Progress

Experiments were performed using a single-frequency laser based on a pulse-amplified ring-dye laser and using a grating-tuned pulsed laser with an intra-cavity etalon (Lambda-Physik 2002E). We amplified the former using three dye stages excited by an injection-seeded, frequency-doubled Nd:YAG laser. The frequency-doubled and mixed output radiation was tunable around 226 nm with pulse energies of 1-2 mJ and a bandwidth of ~0.004 cm^{-1}. The bandwidth of the grating-tuned laser was ~0.05 cm^{-1}. NO-He mixtures were contained in a static cell, using He pressures from 50 to 1100 Torr and NO pressures typically below 50 mTorr (maintaining beam absorption below 3%). We used a nearly phase-conjugate geometry in which the pump beams were counter-propagating and collinear and the probe beam was directed at a small (2.5 °) angle in the horizontal plane with respect to the pumps. All beams had vertical polarizations and were collimated and apertured to a diameter of 3.5 mm (cell measurements) or 1.5 mm (flame measurements). Pump-beam pulse energies ranged from 2-200 μJ. We also independently measured laser-induced fluorescence (LIF) generated primarily by the pump beams, detected through a color filter or a 0.25-m monochromator (both of which transmitted red-shifted LIF).

The flame measurements were conducted in an axi-symmetric diffusion flame sustained on a 6-mm diameter stainless-steel nozzle, surrounded by co-flowing gases from a 5-cm diameter honeycomb. We used gas flow rates of 0.8 slpm (standard liters per minute) of H_2 into the nozzle and 5.0 slpm of O_2 and 10.0 slpm of N_2 into the honeycomb. The estimated DFWM interaction length was on the order of 1 cm (comparable to the flame diameter).

The well-known sub-Doppler nature of DFWM line shapes in the phase-conjugate geometry is illustrated in Fig. 1. Shown is a comparison of a collision-free DFWM spectrum (connected symbols) and a fluorescence excitation spectrum (solid line) of three transitions at the O_{12} bandhead. The DFWM linewidths are limited primarily by the laser bandwidth and are

seen to be much narrower than the Doppler-broadened (0.1 cm^{-1}) fluorescence linewidths. The features seen at the tops of the fluorescence peaks are Lamb dips, arising from saturation induced by the counter-propagating pump beams.

We have further investigated DFWM line shapes over a wide range of foreign-gas pressures, from the Doppler regime to the collision-broadening regime. We find that the experimental line shapes are well described by a two-level, moving absorber model for DFWM, solved in the low-laser-intensity limit for collinear beams in the phase-conjugate geometry.[2] We measured the line shape of an isolated $O_{12}(2)$ transition at He pressures between 50 and 1100 Torr and fitted the data with the model line shape, varying the homogeneous broadening parameter γ_{12} for best fit at each pressure. Within experimental uncertainties of ±5% , the resulting values for γ_{12} were in good agreement with the homogeneous linewidths obtained by fitting LIF measurements of $O_{12}(2)$ with a Voigt profile. In addition, we found the experimental and model line shapes to be in excellent agreement over the entire He pressure range, as shown by the examples in Fig. 2.

In order to assess the sensitivity, potential interferences, and ability to interpret DFWM from NO in flames, we obtained DFWM, LIF and absorption spectra from thermally generated NO in an $H_2/O_2/N_2$ diffusion flame. The upper curve in Fig.3 is an example of a DFWM spectrum of the Q_1- and Q_{21}-branch bandhead region of NO, measured on the flame centerline approximately 8 mm above the burner nozzle. With the exception of features indicated by asterisks (which we attribute[3] to DFWM from molecular oxygen) all of the peaks can be assigned to branches of the NO $A^2\Sigma^+ \leftarrow X^2\Pi$ $(0 \leftarrow 0)$ band using published transition frequencies.[4] Despite the relatively low number density expected for thermal NO, we were able to obtain signal-to-noise ratios greater than 2000:1 (based on noise from stray light and from our detector electronics) using pump-pulse energies of only ~20 μJ [0.2 MW/(cm^2)].

A simulation of the DFWM flame spectrum was remarkably successful, considering the simplicity of the model and the fact that no adjusted parameters were employed. The simulation used a rotational temperature of 2300 K (estimated from LIF data), assumed γ_{12} = 0.15 cm^{-1} for all transitions (an approximation based on high-resolution measurements), and employed published transition frequencies[4] and line strengths.[5] The moving-absorber model was used to compute line shapes, and the laser bandwidth (equal to one-third of the observed linewidths) was included by convolving the spectrum with a Gaussian profile. Saturation was assumed to be absent. The result, shown by the lower curve in Fig. 3, is in excellent agreement with experiment for the dominant Q-branches transitions (the oxygen contributions were not modeled).

Future Plans

We are currently investigating the accuracy of relative line intensities predicted by the model by performing rotational temperature fits to DFWM spectra and evaluating the accuracy of results. We plan further investigations of high-temperature and high-pressure effects on DFWM by performing spectral measurements in an internally heated pressure vessel. We are concurrently developing a DFWM simulation and fitting code that incorporates current theoretical results and models and which will be made available to interested users.

A potentially important variation of DFWM uses infrared excitation to probe rotation-vibration transitions of molecules rather than electronic transitions. We are beginning new experiments using a single-mode, tunable optical-parametric oscillator/amplifier to generate radiation in the range of 1 to 4 μm in order to explore the feasibility of infrared DFWM.

We also plan to investigate the diagnostic applicability of another type of resonant four-wave mixing process that involves two laser frequencies.[6] This method uses pump beams of one frequency to generate a grating in the medium and a probe beam of another frequency to diffract from the grating, offering much greater selectivity and immunity to stray pump-beam radiation.

References

1. For example, see P. Ewart and S. V. O'Leary, Opt. Lett. **11**, 279 (1986), and D. J. Rakestraw, R. L. Farrow, and T. Dreier, Opt. Lett. **15**, 709 (1990).
2. R. L. Abrams, J. F. Lam, R. C. Lind, D. G. Steel, and P. F. Liao, "Phase Conjugation and High-Resolution Spectroscopy by Resonant Degenerate Four-Wave Mixing," in *Optical Phase Conjugation*, ed. R. A. Fisher (Academic Press, New York, 1983), p. 211.
3. I. J. Wysong, J. B. Jeffries, and D. R. Crosley, Opt. Lett. **14**, 767 (1989).
4. R. Engleman, Jr., P. E. Rouse , H. M. Peek, and V. D. Baiamonte, "Beta and Gamma Band Systems of Nitric Oxide," pp. 37, Los Alamos Scientific Lab. Report LA-4364, 1969.
5. M.-S. Chou, A. M. Dean, and D. Stern, J. Chem. Phys. **78**, 5962 (1983).
6. M. A. Buntine, D. W. Chandler, and C. C. Hayden, accepted by J. Chem. Phys; also, see abstracts by these authors in this volume.

BES-supported Publications, 1990-92

1. T. Dreier and D. J. Rakestraw, "Measurement of OH rotational temperatures in a flame using DFWM," Opt. Lett. **15**, 72 (1990).
2. T. Dreier and D. J. Rakestraw, "DFWM diagnostics on OH and NH radicals in flame," Appl. Phys. B **50**, 479 (1990).
3. D. J. Rakestraw, R. L. Farrow, and T. Dreier, "Two-dimensional imaging using degenerate four-wave mixing," Opt. Lett. **15**, 709 (1990).
4. G. O. Sitz and R. L. Farrow, "Pump-probe measurements of state-to-state rotational energy transfer rates in N_2 (n=1)," J. Chem. Phys. **93**, 7883 (1990).
5. L. A. Rahn, R. L. Farrow and G. J. Rosasco, "Measurement of the self-broadening of the H_2 Q(0-5) Raman transitions from 295 K to 1000 K," Phys. Rev. A **43**, 6075 (1991).
6. J. A. Gray and R. L. Farrow, "Predissociation lifetimes of OH $A\ ^2\Sigma^+$ ($\upsilon' = 3$) obtained from optical-optical double-resonance linewidth measurements," J. Chem. Phys. **95**, 7054 (1991).
7. D. J. Rakestraw, T. Dreier and L. R. Thorne, "Detection of NH radicals in flames using degenerate four-wave mixing", Proceedings of the *Twenty-Third International Symposium on Combustion*, 1901 (1991).
8. R. L. Vander Wal, B. E. Holmes, J. B Jeffries, P. M. Danehy, R. L. Farrow and D. J. Rakestraw, "Detection of HF using infrared degenerate four-wave mixing", in press, Chem. Phys. Lett.
9. R. L. Farrow, D. J. Rakestraw, and T. Dreier, "Investigation of the dependence of degenerate four-wave mixing line intensities on transition dipole moment," accepted by J. Opt. Soc. Am. B.
10. R. Vander Wal, R. L. Farrow, and D. J. Rakestraw, "High-resolution investigation of degenerate four-wave mixing in the γ(0,0) band of nitric oxide," accepted by the Twenty-Fourth International Combustion Symposium.

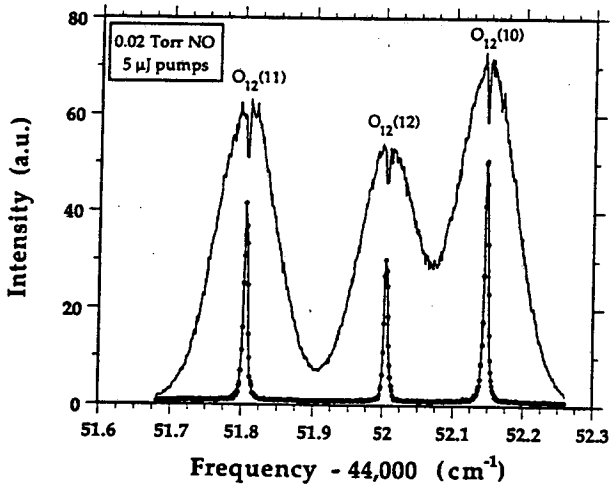

Fig. 1 Comparison between experimental DFWM spectral peaks forming the O_{12} bandhead of NO (connected symbols) and simultaneously measured fluorescence excitation spectra (solid curve). The sub-Doppler nature of the DFWM line shapes measured in the phase-conjugate geometry is clearly evident.

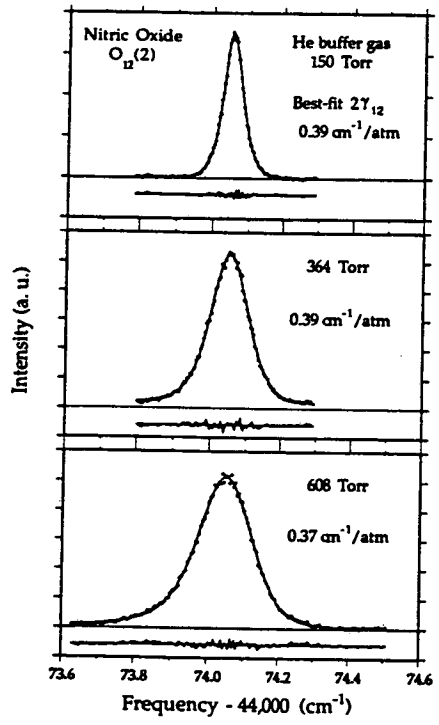

Fig. 2 Experimental O_{12} (2) line shapes (symbols) observed for 30-40 mTorr of NO in He gas at various pressures. The solid lines are theoretical profiles based on a two-level saturable absorber model for DFWM which includes absorber motion.[2] The value of $2\gamma_{12}$ obtained from fluorescence data is 0.38 cm^{-1}/atm, which agrees within experimental uncertainties with the best-fit values obtained with the model (given in the figure).

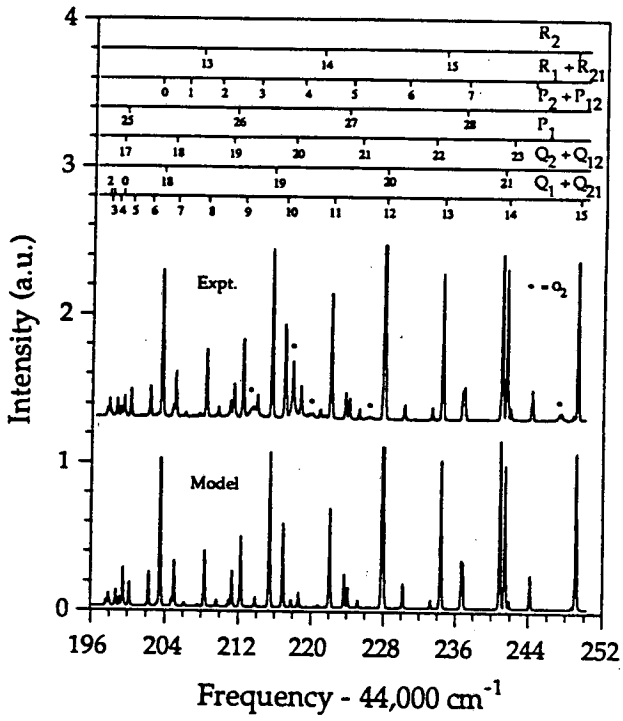

Fig. 3 Experimental (upper curve) and simulated spectra (lower curve) of the bandhead region of the $Q_1 + Q_{21}$ branches of NO measured in a $H_2/O_2/N_2$ diffusion flame. The experimental spectrum is offset for clarity. Branches of the NO $A^2\Sigma^+ \leftarrow X^2\Pi$ (0,0) band are indicated at the top of the figure. The peak near 44,228 cm^{-1} has been plotted offscale to enhance display of weaker lines. The experimental spectrum was obtained using a laser resolution of 0.055 cm^{-1} (FWHM).

High resolution Raman spectroscopy of complexes and clusters in molecular beams

P. M. Felker, G. V. Hartland, B. F. Henson, and V. A. Venturo
Department of Chemistry and Biochemistry
University of California, Los Angeles, CA 90024-1569

Program scope

The DoE-sponsored project in this laboratory has two facets. The first is the development of methods of nonlinear Raman spectroscopy for application in studies of sparse samples. The second is the application of such methods to structural and dynamical studies of molecules, complexes, and clusters in supersonic molecular beams. We have made progress in several areas, as described below. The first pertains to theoretical and experimental developments in Fourier transform stimulated emission spectroscopy (FT-SES) and Fourier transform hole-burning spectroscopy (FT-HBS). The second deals with progress in the development of ionization-detected stimulated Raman spectroscopies (IDSRS). The third involves the application of IDSRS methods to studies of jet-cooled benzene clusters. The fourth pertains to IDSRS results from studies of hydrogen-bonded complexes containing phenols. The fifth relates to IDSRS studies of carbazole-$(Ar)_n$ and benzene-$(Ar)_n$ clusters.

Developments in FT-SES and FT-HBS

As part of our development of Fourier transform versions of nonlinear Raman spectroscopies, we have invented and developed a Fourier transform version of stimulated emission spectroscopy. We have performed a detailed theoretical and experimental study of FT-SES as implemented with short-pulse lasers. This study indicates that the scheme has some advantages over frequency-domain SES in certain cases. The following summarizes the results.

1. The resolution of FT-SES is limited by the length of the measured interferogram. The bandwidths and pulsewidths of the excitation pulses do not play a role, nor does the delay between the pump and probe pulse trains. This means that the technique can be implemented at high resolution with short-pulse lasers, which are most effective at inducing depletions in species with short-lived excited states.
2. The Doppler broadening in FT-SES spectra is that which corresponds to the vibrational resonances that enter into such spectra, *not the vibronic resonances* associated with the pump and probe processes. This characteristic is different than frequency-domain SES, the Doppler broadening of which is essentially determined by the bandwidths of the pump and probe light sources.
3. The homogeneous broadening in FT-SES spectra is determined by the damping rates of ground-state density matrix elements. This means that the lifetimes of the pump-prepared excited states do not limit the resolution in the spectra. This same situation also obtains in frequency-domain SES.
4. Particularly simple rotational structure – namely, an overwhelmingly dominant Q-branch feature – often characterizes a vibrational resonance in a FT-SES spectrum. This feature facilitates the measurement of vibrational linewidths and vibrational frequencies in large species.
5. Finally, unpublished experimental results show that although the manifestations of rotational structure may not be apparent in a FT-SES spectrum (i.e., only a single peak is present per vibrational resonance), such manifestations *are apparent in the*

interferogram associated with that spectrum. The effect is analogous to the rotational coherence effects that enter into picosecond time-resolved results on isolated molecules. It could provide a means for the high resolution rotational spectroscopy of large species, just as rotational coherence spectroscopy does.

Fluorescence-detected hole-burning spectroscopy (HBS) is a double-resonance scheme that is an analog to SES in which excited-state vibrational frequencies are measured. We have demonstrated a Fourier transform version of HBS and analyzed it in a fashion similar to the way in which FT-SES was analyzed. The characteristics of the technique were found to be analogous to those of FT-SES.

Developments in IDSRS

Ionization-detected stimulated Raman spectroscopies are three-color (or four-color) double-resonance schemes in which the population shifts induced by stimulated Raman scattering processes are probed by resonantly enhanced multiphoton ionization (REMPI). Two variants of IDSRS exist. The first pertains to the measurement of the increase in population of the final state in the Raman process: ionization-gain stimulated Raman spectroscopy (IGSRS). The second involves the measurement of the population loss in the initial state of the Raman process: ionization-loss stimulated Raman spectroscopy (ILSRS). These methods have great potential in the ground-state vibrational spectroscopy of jet-cooled species. We have made several developments in IDSRS with this potential in mind. First, we have been the first to implement IDSRS with mass analysis. This development has been essential to the success of all our applications of IDSRS. Second, we have shown that IDSRS schemes can be implemented interferometrically as Fourier transform spectroscopies. These have the major advantage that the Raman resolution is limited by the interferometer, not by the bandwidths of the Raman excitation fields. Third, we are the first to have applied ILSRS in molecular beam studies. We have shown that it is a technique with wide applicability in species-specific, medium-to-high resolution vibrational spectroscopy of jet-cooled molecules and molecular clusters. Fourth, we have demonstrated that IDSRS methods can be implemented with two-color REMPI. In many cases, this scheme will allow better species-specificity in the measurement of Raman spectra.

IDSRS studies of benzene clusters

We have performed extensive mass-selective IDSRS studies on benzene dimer isotopomers. We have been particularly interested in characterizing the geometry of the species. Several important results bearing on this issue have been obtained. First, the IDSRS data are only consistent with a dimer in which the benzene moieties reside in inequivalent sites. Second, IDSRS evidence strongly indicates that one of the benzene sites ("site *b*") in the dimer is characterized by high symmetry (C_{3v} or higher) and the other ("site *a*") by lower symmetry. Third, the vibronic spectroscopy associated with the two sites is markedly different. The benzene in the site *b* exhibits marked van der Waals structure upon $S_1 \leftrightarrow S_0$ vibronic excitation. The site-*a* benzene moiety does not. Fourth, in the C–H stretch region the vibrational dynamics associated with site *a* is markedly different than that associated with site *b*. All of these results are consistent with a T-shaped dimer structure in which the stem of the T corresponds to site *a*, the top of the T corresponds to site *b*, and there is free internal rotation about the C_6 axis of the site-*b* moiety.

We have also obtained IDSRS results on benzene trimer isotopomers. Our results relating to geometry point to a symmetrical cyclic structure for the trimer. The evidence for this takes several forms: (a) the number of Raman resonances in the region of the ν_1 and

ν_2 fundamentals, (b) the shifts of those resonances as a function of isotopic substitution, and (c) the intensities of the resonances as a function of isotopic substitution. Results pertaining to the vibrational dynamics of the trimer have also been obtained. In particular, we find that the trimer lives for nanoseconds or longer upon vibrational excitation to the ν_1 region (992 cm^{-1}). In the region of the ν_2 fundamental (3070 cm^{-1}) the trimer lives for at least as long as 8 ps, as determined by linewidth measurements on the Raman resonances.

Mass-selective IDSRS experiments have also been performed on higher clusters of benzene. From these results one qualitative conclusion that emerges is that the tetramer, pentamer, and hexamer have benzene sites that are inequivalent. We also find dynamical behavior for the tetramer that is consistent with that of the dimer and trimer, namely that vibrational excitation to the ν_1 region gives rise to long-lived excited vibrational states. A prominent ν_1 resonance for the tetramer has a resolution-limited linewidth of 0.05 cm^{-1}, indicating a lifetime of greater than 100 ps.

IDSRS studies of phenol complexes

We have performed extensive frequency domain ILSRS experiments on jet-cooled, phenol-containing van der Waals complexes. Spectra were measured for phenol and mono-methyl- and monochloro-phenols in combination with water, methanol, ethanol, diethyl ether, ammonia, benzene, N_2, methane and argon. The spectra encompass four spectral regions: the C-C stretch region (800 to 1050 cm^{-1}), the phenolic C-O stretch region (near 1260 cm^{-1}), the aromatic C-H stetch region (near 3070 cm^{-1}) and the O-H stretch region ($\sim$ 3500 to 3700 cm^{-1}). The results are significant in several respects. First, they clearly show that mass-selective ILSRS is applicable in molecular beam vibrational spectroscopy at subwavenumber resolution throughout the vibrational fundamental region. Second, the spectra can be used to identify and characterize quantitatively "fingerprint" vibrational resonances for phenol – that is, phenolic resonances whose frequencies shift in a regular way upon H bonding. For example, the C-O and O-H stretch fundamentals shift blue and red, respectively upon H-bonding. These resonances have been used as probes of the local environment of phenols in condensed phases. Our molecular beam results provide previously unknown information as to the inherent H-bond induced shifts of the resonances. Third, with advances in the theoretical treatment of intermolecular interactions and the vibrational frequency shifts associated with them, the results may provide useful data with which to compare theoretical predictions. Fourth, in some cases the ILSRS results provide information in regard to the geometries of the complexes. For example, the phenol dimer results in the O-H stretch region strongly suggest that the species is such that one phenol is a proton donor and the other is a proton acceptor via its oxygen atom. We have used this information in conjunction with results from high resolution rotational spectroscopy to arrive at a geometry for the species. Fifth, we have observed behavior that is very suggestive of mode-selective dynamics in the O-H stretch region of phenol-H_2O and substituted phenol-H_2O complexes. Specifically, the linewidths of the water-localized O-H symmetric stretch fundamental in these species are about a factor of four narrower than the phenolic O-H stretch resonances in the same species, even though the latter occur at lower frequencies. In phenol-water, for example, the linewidth of the water-localized O-H stretch implies a lifetime longer than 17 ps, whereas that for the phenolic O-H stretch gives a lifetime longer than 4 ps. Sixth, spectra in the region of the C-O stretch of H-bonded and non-H-bonded complexes suggest that H-bonding produces an enhanced relaxation of the excited C-O stretch vibration in phenol.

Mass-selective ILSRS studies of doped rare gas clusters

Very recently we have begun a study of the vibrational spectroscopy of carbazole-

$(Ar)_n$ and benzene-$(Ar)_n$ clusters. These species have been studied in some detail both experimentally and theoretically by others. They are of interest because they represent a convenient model system for the study of the microscopic details of solvation. Our interest in them is two-fold. First, we wonder if the vibrational spectroscopy of the species is consistent with conclusions drawn from the results of vibronic spectroscopy. Second, we are interested in the vibrational dynamics of the dopant species and how the dynamics changes as a function of cluster size (i.e., degree of solvation). We have been successful in measuring size-selective Raman spectra from $n = 0$ to 14 for the carbazole-$(Ar)_n$ system and from $n = 0$ to 22 for the benzene-$(Ar)_n$ system. This work is on-going.

Future plans

The area of size-selective vibrational spectroscopy on clusters is wide-open. We plan to continue our ILSRS studies of solute-$(solvent)_n$ clusters. Studies of particular interest to us are ones in which the Raman spectra of the *solvent* species are measured as a function of cluster size. The second area we plan to explore in the future relates to picosecond time-domain measurements of ground-state dynamics in complexes and clusters. Such studies will be employ picosecond pump-probe IDSRS methods. Of interest are the dynamics of processes such as vibrational relaxation, intermolecular vibrational energy flow, and evaporation in molecluar clusters.

DoE-sponsored research from 1990-1992

1. G. V. Hartland, B. F. Henson, V. A. Venturo, R. A. Hertz, and P. M. Felker: "Applications of ionization-detected stimulated Raman spectroscopy in molecular beam studies," J. Opt. Soc. Am. B**7**, 1950-1959 (1990).
2. B. F. Henson, G. V. Hartland, V. A. Venturo, R. A. Hertz, and P. M. Felker: "Stimulated Raman spectroscopy in the ν_1 region of isotopically substituted benzene dimers: Evidence for symetrically inequivalent benzene moieties," Chem. Phys. Lett. **176**, 91-98 (1991).
3. G. V. Hartland, P. W. Joireman, L. L. Connell, and P. M. Felker: "High-resolution Fourier transform-stimulated emission and molecular beam hole-burning spectroscopy with picosecond excitation sources: Theoretical and experimental results," J. Chem. Phys. **96**, 179-197 (1992).
4. G. V. Hartland, B. F. Henson, V. A. Venturo, and P. M. Felker: "Ionization-loss stimulated Raman spectroscopy of jet-cooled hydrogen-bonded complexes containing phenols," J. Phys. Chem. **96**, 1164-1173 (1992).
5. V. A. Venturo, P. M. Maxton, B. F. Henson, and P. M. Felker: "Size-selective Raman spectroscopy of carbazole-$(Ar)_n$ clusters at subwavenumber resolution," J. Chem. Phys. **96**, in press, 15 May (1992).
6. B. F. Henson, G. V. Hartland, V. A. Venturo, P. M. Maxton, and P. M. Felker: "Stimulated Raman spectroscopy of complexes and clusters in supersonic molecular beams," Proc. Soc. Photo.-Opt. Instrum. Eng.**xxx**, in press (1992).
7. P. M. Felker, B. F. Henson, V. A. Venturo, and G. V. Hartland: "Applications of nonlinear Raman spectrosocpy to molecular beam studies," Proc. 13th Intl. Conf. on Raman Spectroscopy – in press.

Spectroscopic and Dynamical Studies of Highly Energized Small Polyatomic Molecules

Robert W. Field and Robert J. Silbey
Department of Chemistry
Massachusetts Institute of Technology
Cambridge, Massachusetts 02139

Spectroscopic studies of the acetylene $\tilde{X}\ ^1\Sigma_g^+$ potential energy surface at *chemically interesting* levels of vibrational excitation. The standard methods of extracting information from rotation-vibration spectra of polyatomic molecules invariably fail to provide intelligible information about unimolecular dynamics. The standard method [assignment of *eigenstates* → fit to set of Dunham type molecular constants → reduction to set of potential energy surface paremeters] typically fails because eigenstates encode long-time dynamics which are sensitive to subtle details of the entire potential surface. We have made significant progress toward the goal of extracting visualizable and interpretable "ball-and-spring" dynamics from spectra. Rather than replacing traditional spectroscopic spectrum-decoding methods by some new form of statistically-based pattern recognition (as we have proposed previously)[1-3], we have generalized the standard approach. The keys are (i) use of low resolution spectra to characterize short-time dynamics[4] and (ii) textbook harmonic oscillator scaling relationships [$\langle v|\, Q^n|\, v'\rangle \simeq v^{n/2}$] to extrapolate energy flow rates, observable at low energy as analyzable spectroscopic perturbations[5], from very slow and restrictive at low energy to very fast and global at high energy.

Our combined study of acetylene $\tilde{A}\,^1A_u \rightarrow \tilde{X}\ ^1\Sigma_g^+$ low resolution (30 cm^{-1}) Dispersed Fluorescence (DF) and high resolution (0.03 cm^{-1}) Stimulated Emission Pumping (SEP) spectra[4,6] allowed us to formulate and test a spectrum decoding procedure that should be generally applicable to molecules larger than C_2H_2. We have also made significant progress in identifying all of the factors which control the intensities of nominally forbidden rotation-vibration transitions, so that it will soon be possible to record the "pure and complete" sequences that are essential to the *valid* use of statistical measures[2,3] that will give rigorous and quantitative insights into the evolution from regular (localized) to chaotic (statistical) dynamics.

The $\tilde{A} \rightarrow \tilde{X}$ DF spectrum of HCCH contains long progressions in the two vibrational modes (CC stretch, *trans*-bend) expected to be Franck-Condon bright.[4] The members of these progressions evolve from a single vibrational eigenstate at low energy to many eigenstates at high energy. Each of these assignable feature states corresponds to the short-time localized dynamics of one Franck-Condon bright state. At this stage, two problems must be solved: (i) are the low resolution feature states *bona fide* consequences of the dynamics on the $\tilde{X}$ surface alone or some accidental consequence of the nodal structure of the $\tilde{A}$-state vibrational level from which the DF spectrum originates? (ii) Is the progression pattern-based assignment correct? The first question is answered by comparison of intensity patterns in DF spectra originating from two different $\tilde{A}$-state vibrational levels[4]. The second question is answered by detailed SEP examination of the rotational constant and vibrational fine structure of the lowest energy members of a progression.[6]

Almost half of the feature states in the HCCH $\tilde{A} \rightarrow \tilde{X}$ DF spectrum were members of CC stretch and *trans*-bend progressions built on some unknown Franck-Condon dark vibrational excitation[4]. Detailed SEP examination of one of the lowest members of such a progression proved that all of the extra progressions were built on excitation in the *cis*-bending vibration which obtains its intensity by a previously unknown $(v_4, v_5=0) \sim (v_4-2, v_5=2)$ Darling-Dennison (DD) interaction[6]. *This is the first (fastest) step in the vibrational*

energy flow out of SEP bright states. This interaction scales up predictably in both strength and number of interacting levels until $v_{bend} \approx 16$ where all members of the (16,0) ~ (14, 2) ~ ... (0,16) polyad become degenerate and the separation between *trans*-bend and *cis*-bend modes is obliterated.

Detailed examination of the bending DD resonance in the 7000 cm^{-1} region revealed the *second step* in the energy flow process, the "2345" Fermi resonance[7,8] in which one quantum each of CC stretch (v_2), *trans*-bend (v_4), and *cis*-bend (v_5) is exchanged for one quantum of the antisymmetric CH stretch (v_3). These bend-DD and 2345-Fermi resonances provide a quantitatively characterized energy flow path between the respective bright states in the SEP and high CH stretch overtone spectra[7].

In the process of examining the SEP spectrum near 7000 cm^{-1}, we discovered the importance of *axis-switching* transitions[9]. In fact, the axis switching mechanism causes some nominally forbidden rotation-vibration transitions to become more intense (quantitative predictions confirmed by experiment) than some of the allowed transitions![6] The unsuspected presence of axis switching transitions completely accounts for the puzzling discrepancy between the observed (ρ_{obs}) and anharmonic direct count calculated (ρ_{calc}) vibrational density of states.[10,11] The axis switching mechanism also permitted us to make definitive vibrational assignments of all previously unassigned levels observed by Wodtke et al in the SEP spectrum of HCN.[12,13]

We have shown that the transitions observable in the SEP spectrum of HCCH range in intensity over a factor of 1000![6] This gives us much greater sensitivity to weak anharmonic resonances than is available in high resolution infrared and Raman spectroscopy. Matrix element scaling permits us to use these spectroscopic observations to predict the rates and specific nature of sequential energy flow processes at chemically significant levels of vibrational excitation. This scaling procedure will also provide a useful way of recognizing the turning on of some new dynamical process (such as isomerization)[1] at an energy where the eigenstate spectra are genuinely uninterpretable.[14]

The lowest energy triplet state of acetylene. Last year we reported on SEP spectra which originated in DCCD $\tilde{A}\,^1A_u$ $v_3 = 5$ and terminated in vibrational levels near 25,800 cm^{-1}. We concluded that $T_0(\tilde{a}\,^3B_2) = 25{,}800\ cm^{-1}$, where the *cis*-bent $\tilde{a}$-state is the lowest energy isomeric minimum on the T_1 surface. The rotational selection rules were consistent only with a *cis*-bent $^3B_2$ state or highly excited *trans*-bending levels of $\tilde{X}\,^1\Sigma_g^+$ (the *trans*-bent and vinylidene triplet isomers could be ruled out). The pattern of vibrational intensities appeared to rule out the $\tilde{X}$-state assignment.[15] However, *ab initio* calculations indicated that the *cis*-bent $\tilde{a}\,^3B_2$ state lies at > 5000 cm^{-1} higher energy than the observed levels, thus ruling out the triplet assignment. We are left with the puzzling observation of strong transitions into several isolated and long-lived feature states at energies well above the high energy limit of the Franck-Condon accessible $\tilde{X}$-state vibrational quasi-continuum. The *intensity, isolation,* and *long lifetime* of these feature states require explanation.

Fluorescence excitation and SEP studies of the HCO $\tilde{B}^2A' - \tilde{X}^2A'$ system.

We have recorded SEP spectra of HCO. These spectra sample vibrational "levels" or "resonances" in the $\tilde{X}^2A'$ state at energies well above (~4000 cm^{-1}) the H—CO dissociation limit (D_0=5035 cm^{-1}). Our initial results show that the (v_{CH}, v_{CO}, v_{bend}) = (0, 5, 0) level (T_0 = 9091 cm^{-1}) has a longer lifetime (Γ = 0.8 cm^{-1}) than the lower lying (0, 4, 1) level
(Γ = 6 cm^{-1}) (T_0 = 8381 cm^{-1}). This mode specificity demonstrates the correctness of *ab initio* predictions of long-lived resonances and the relative effectiveness of C—H vs. C—O vs. bend vibrations in promoting dissociation[16]. We plan to extend our SEP studies to other vibrational levels of the $\tilde{X}^2A'$ state, especially

those predicted to lie close to the dissociation threshold, and to document the vibrational and rotational dependence of unimolecular dissociation rates.

REFERENCES

1. Y. Chen, D.M. Jonas, J.L. Kinsey, and R.W. Field, "High Resolution Spectroscopic Detection of Acetylene ↔ Vinylidene Isomerization by Spectral Cross-Correlation" J. Chem. Phys. 91, 3976-3987 (1989).

2. J.P. Pique, Y.M. Engel, R.D. Levine, Y.Chen, R.W. Field, and J.L. Kinsey, "Broad Spectral Features in the Stimulated Emission Pumping Spectrum of Acetylene", J. Chem. Phys. 88, 5972-5974 (1988).

3. J.P. Pique, Y. Chen, R.W. Field and J.L. Kinsey, "Chaos and Dynamics on 30fs-1ns Time Scales in Vibrationally Excited Acetylene: Fourier Transform of Stimulated Emission Pumping Spectrum", Phys. Rev. Letts. 58, 475-478 (1987).

4. K. Yamanouchi, N. Ikeda, S. Tsuchiya, D.M. Jonas, J.K. Lundberg, G.W. Adamson, and R.W. Field, "Vibrationally Highly Excited Acetylene as Studied by Dispersed Fluorescence and Stimulated Emission Pumping Spectroscopy: Vibrational Assignment of Feature States", J. Chem. Phys. 95, 6330-6342 (1991).

5. J. Pliva, J. Mol. Spectrosc. 44, 165 (1972).

6. D.M. Jonas, S.A.B. Solina, B. Rajaram, R.J. Silbey, R.W. Field, K. Yamanouchi, and S. Tsuchiya, "Intramolecular Vibrational Relaxation and Forbidden Transitions in the SEP Spectrum of Acetylene," J. Chem. Phys.

7. B.C. Smith and J.S. Winn, J. Chem. Phys. 94, 4120 (1991).

8. G. Strey and I.M. Mills, J. Mol. Spectrosc. 59, 103 (1976).

9. J.T. Hougen and J.K.G. Watson, Canad. J. Phys. 43, 298 (1965).

10. E. Abramson, R.W. Field, D. Imre, K.K. Innes, and J.L. Kinsey, "Fluorescence and Stimulated Emission $S_1 \rightarrow S_0$ Spectra of Acetylene: Regular and Ergodic Regions," J. Chem. Phys. 83, 453-465 (1985).

11. Y. Chen, S.D. Halle, D.M. Jonas, J.L. Kinsey, and R.W. Field, "Stimulated Emission Pumping Studies of Acetylene $\tilde{X}^1\Sigma_g^+$ in the 11,400-15,700 cm^{-1} Region: the Onset of Mixing", J. Opt. Soc. Am. B 7, 1805-1815 (1990).

12. X. Yang, C.A. Rogaski, and A.M. Wodtke, J. Opt. Soc. B 7, 1835 (1990).

13. D.M. Jonas, Xueming Yang, and A.M. Wodtke, "Axis-Switching Transitions and the Stimulated Emission Pumping Spectrum of HCN," J. Chem. Phys.

14. E. Abramson, R.W. Field, D. Imre, K.K. Innes, and J. L. Kinsey, "Stimulated Emission Pumping of Acetylene: Evidence for Quantum Chaotic Behavior near 27900 cm^{-1} of Excitation?," J. Chem. Phys. 80, 2298-2300 (1984).

15. J.K. Lundberg, R.W. Field, C.D. Sherrill, E.T. Seidl, Y. Xie, and H.F. Schaefer III, "Acetylene: Synergy Between Theory and Experiment," J. Chem. Phys.

16. B. Gazdy, J.M. Bowman, S.-W. Cho, and A.F. Wagner, J. Chem. Phys. 96, 2812 (1992) and S.-W. Cho, A.F. Wagner, B. Gazdy, and J.M. Bowman, J. Chem. Phys. 96, 2799 (1992).

Recent Publications (since 1990)

1. Y. Chen, S.D. Halle, D.M. Jonas, J.L. Kinsey, and R.W. Field, "Stimulated Emission Pumping Studies of Acetylene $\tilde{X}^1\Sigma_g^+$ in the 11,400-15,700 cm^{-1} Region: the Onset of Mixing", J. Opt. Soc. Am. B 7, 1805-1815 (1990).

2. P. Dupré, R. Jost, M. Lombardi, P.G. Green, E. Abramson, and R.W. Field, "Anomalous Behavior of the Anticrossing Density as a Function of Excitation Energy in the C_2H_2 Molecule", Chem. Phys. 152, 293-318 (1991).

3. K. Yamanouchi, N. Ikeda, S. Tsuchiya, D.M. Jonas, J.K. Lundberg, G.W. Adamson, and R.W. Field, "Vibrationally Highly Excited Acetylene as Studied by Dispersed Fluorescence and Stimulated Emission Pumping Spectroscopy: Vibrational Assignment of Feature States", J. Chem. Phys. 95, 6330-6342 (1991).

4. J.K. Lundberg, R.W. Field, C.D. Sherrill, E.T. Seidl, Y. Xie, and H.F. Schaefer III, "Acetylene: Synergy Between Theory and Experiment," J. Chem. Phys.

5. D.M. Jonas, S. Solina, B. Rajaram, R.J. Silbey, R.W. Field, K. Yamanouchi, and S. Tsuchiya, "Intramolecular Vibrational Relaxation and Forbidden Transitions in the SEP Spectrum of Acetylene," J. Chem. Phys.

6. D.M. Jonas, S.A.B. Solina, B. Rajaram, R.J. Silbey, R.W. Field, K. Yamanouchi, and S. Tsuchiya, "Intramolecular Vibrational Relaxation in the SEP Spectrum of Acetylene," J. Chem. Phys.

Laser Studies of Chemical Reaction and Collision Processes

George Flynn, Department of Chemistry, Columbia University
New York, New York 10027

Our work has concentrated on several interrelated projects in the area of laser photochemistry and photophysics which impinge on a variety of questions in combustion chemistry and general chemical kinetics: (1) Infrared diode laser probes of "hot" H atom collision processes involving the symmetric tops CD_3F and CF_3D in which reorientation of the top axis has been probed; (2) Infrared diode laser probes of the quenching of molecules with "chemically significant" amounts of energy in which the energy transfered to the quencher has, for the first time, been separated into its vibrational, rotational, and translational components; (3) Probes of quantum state distributions and velocity profiles for molecules produced by chemical reactions.

The Diode Laser Probe Technique

The application of infrared diode lasers to study time-dependent dynamic events was developed in our laboratory under DOE sponsorship. This technique provides exceptionally useful information about a wide variety of dynamic molecular processes. The essence of the diode absorption method is the realization that **any** vibrational-rotational level of a small polyatomic molecule can be monitored through an absorption transition of the type:

$$CD_3F(v_1,v_2,v_3,v_4,v_5,v_6;\ J,K,V) + h\nu(\lambda=4.5\ \mu m) \rightarrow CD_3F(v_1,v_2,v_3,v_4+1,v_5,v_6;\ J+1,K,V)$$

where v_i is the quantum number for mode i, J is the total rotational angular momentum quantum number, K is the projection of the total angular momentum on the molecular axis, and V the velocity. The source of infrared light is a continuously tunable, spectrally pure, cw, low power diode laser. Because of the extremely high spectral resolution of the infrared diode probe, the recoil velocity of molecules created by an encounter with a high energy atom or molecule can also be monitored by using a very stable interferometer to time resolve the infrared absorption profile through the Doppler effect. We have used this technique to monitor CO_2, OCS, N_2O, CS_2, DCl, CO, CD_3F, and CF_3D.

Hot Atom Excitation of Rotational States of Polyatomic Molecules

The basic experiment in these studies can be described by the equations

$H_2S+h\nu(193nm) \rightarrow H^*(HOT)+HS$ [HOT is *HOT*:~25,000K (53Kcal/mole)]

Collisional Excitation: $H^*(18{,}500\ cm^{-1})+CD_3F(0,0,0,0,0,0;J',K',V') \rightarrow CD_3F(0,0,0,0,0,0;J,K,V)+H$

Typical Probe: $CD_3F(0,0,0,0,0,0;J,K,V)+h\nu(4.5\ \mu) \rightarrow CD_3F(0,0,0,1,0,0;\ J+1,K,V)$

Upon collision of an H^* atom with methyl fluoride, a final rotational state J, K of the CD_3F molecule is produced. Rotational profiles and velocity recoil distributions have been determined for this collision process and compared to similar experiments with the molecule CF_3D as the collision partner with hot H atoms. The differences in the recoil linewidths observed for different K states for these two different molecules are extremely revealing. K measures the projection of the total angular momentum along the symmetric top axis. We find in the case of CD_3F that the magnitude of the velocity recoils decreases with increasing K quantum number while for CF_3D the velocity recoils increase with increasing K quantum number. These observations can be qualitatively explained by a simple model which takes into account the very different locations of the center of mass for these two molecules and the effectiveness of collisions in producing rotational excitation.

Quenching of Molecules with "Chemically Significant" Amounts of Energy

The simplest model for unimolecular decomposition is the Lindemann-Hinschelwood mechanism in which a substrate S is excited by collisions to a level S^* with energy sufficient to cause break up of the substrate. For large molecules the time scale for decomposition of S^* is sufficiently long that further collisions with the bath molecules can cause deactivation of the

excited substrate thus quenching the unimolecular decay process. While many studies of the quenching of such highly excited substrate molecules have been performed, until recently there was no technique which could be used to follow these processes with quantum state resolved detail on a single collision time scale. We have recently developed a technique for studying the deactivation of highly vibrationally excited donor molecules by small bath gas molecules on a single collision time scale using infrared diode laser probe techniques. By focussing on the bath states instead of the excited substrate S^*, we are able to completely resolve not only the vibrational excitation of the molecule but also, due to the extraordinary resolution of the diode probe method, the rotational excitation and translational recoil of these same vibrationally excited bath molecules.

In a typical experiment excited NO_2 molecules ($NO_2^{(E)}$) are produced at energy E=22,200 cm^{-1} by an excimer pumped dye laser,

$$NO_2 + h\nu\ (450.5\ nm) \rightarrow NO_2^{(E)}$$

Collisions with N_2O cause translational, rotational and vibrational excitation of the first ν_1 stretching (10^00, 1285 cm^{-1}) and ν_3 stretching (00^01, 2224 cm^{-1}) vibrational states, and rotational, translational excitation in the ground vibrationless (00^00) level,

$$NO_2^{(E)} + N_2O\ (00^00) \rightarrow NO_2^{(E-\Delta E)} + N_2O\ (00^01, J, V)$$
$$NO_2^{(E)} + N_2O\ (00^00) \rightarrow NO_2^{(E-\Delta E)} + N_2O\ (10^00, J', V')$$
$$NO_2^{(E)} + N_2O\ (00^00) \rightarrow NO_2^{(E-\Delta E)} + N_2O\ (00^00, J'', V'')$$

J, J', J'' represent rotational angular momentum quantum numbers, and V,V',V'', are the recoil velocities for the corresponding ro-vibrational states. A tunable diode laser operating cw at 4.5 μm is used to probe the P and/or R branch bands of the following transitions,

$$N_2O\ (00^01, J, V) + h\nu\ (4.5\ \mu m) \rightarrow N_2O\ (00^02, J\pm1, V)$$
$$N_2O\ (10^00, J', V') + h\nu\ (4.5\ \mu m) \rightarrow N_2O\ (10^01, J'\pm1, V')$$
$$N_2O\ (00^00, J'', V'') + h\nu\ (4.5\ \mu m) \rightarrow N_2O\ (00^01, J''\pm1, V'')$$

Velocity recoils are measured by probing the nascent Doppler profiles for different spectral lines. The initially excited NO_2 molecules can produce deexcited species, such as $NO_2^{(E-\Delta E)}$, which are also able to excite N_2O. In our experiments, however, the N_2O populations and Doppler velocity profiles are measured at such a short time after the initial dye laser excitation pump pulse and at such low sample pressures that these channels are minimized.

The interaction between excited $NO_2^{(E)}$ and N_2O leads to the excitation of translational, rotational and vibrational degrees of freedom of the N_2O molecules. The rotational distribution for the vibrationally excited states can be approximated by a Boltzmann distribution, and the increase in rotational temperature (ΔT^R) between the nascent rotational temperature and ambient temperature was ΔT^R_{100}=40±23K, and ΔT^R_{001}=37±18K.

The translational excitation of N_2O molecules scattered into the 10^00 and 00^01 states, as well as the recoil velocity of $N_2O(00^00,J'')$ rotationally excited ground state molecules produced by collisions with $NO_2^{(E)}$, were measured. The nascent absorption line shapes can be well fitted to a Gaussian function. The width of the fitted Doppler profile provides a measure of the translational temperature of the nascent N_2O molecules. The average increase in translational temperatures for the individual excited (00^01 and 10^00) ro-vibrational states derived from these line broadening measurements is 40±20K. The linewidth of the ground vibrationless state, which corresponds to a translational temperature of 900K for the J=62 level, is significantly broader than the room temperature ambient value, and substantially broader than the recoil linewidths for the two excited vibrational levels $N_2O(10^00)$ and $N_2O(00^01)$.

The translational excitation of the ground state is clearly much more efficient than that of the vibrationally excited states $N_2O(10^00)$ and $N_2O(00^01)$ in taking up energy from $NO_2^{(E)}$. The small rotational and translational energy increase accompanying vibrational excitation is

consistent with a long range, attractive force, vibrationally resonant energy transfer mechanism in which the gain of *vibrational* energy by the bath is closely matched by loss of *vibrational* energy by the donor $NO_2^{(E)}$. On the other hand, the large translational energy increase of the vibrationless ground state is consistent with a short range, repulsive force mechanism in which a small amount (~500-1000 cm^{-1}) of the internal vibrational energy of the $NO_2^{(E)}$ is transferred non-resonantly to the translational and rotational degrees of freedom of the bath states.

Chemical Dynamics of the Reaction between Chlorine Atoms and Hydrocarbons

In previous studies we have observed rotationally cold, but translationally hot DCl molecules produced by the reaction of chlorine atoms with deuterated cyclohexane. These results clearly represent nonstatistical partitioning of energy in this abstraction reaction. We are continuing these studies by investigating reactions of Cl atoms with other hydrocarbons to see if the unusual dynamics observed for Cl atom abstraction in the cyclohexane case are typical of such processes.

Present and Future Experimental Program

Present and future efforts using this high resolution infrared absorption probe technique are being concentrated on quantum state and recoil velocity resolved studies of chemical reactions; on the energy dependence of the quantum state resolved vibration/rotation excitation cross sections in collisional encounters between highly vibrationally excited molecules and cold bath gases; and on the determination of final vibrational, rotational, and translational energy profiles for collisions involving molecular reorientation.

DOE Publications

(1990-1992)

1. J. M. Hossenlopp, J. F. Hershberger, and G. W. Flynn, "Kinetics and Product Vibrational Energy Disposal Dynamics in the Reaction of Chlorine Atoms with D_2S," J. Phys. Chem. 94, 1346 (1990).
2. T. G. Kreutz, F. A. Khan, G. W. Flynn, "Inversion of Experimental Data to Generate State-to-State Cross Sections for Ro-Vibrationally Inelastic Scattering of CO_2 by Hot Hydrogen Atoms," J. Chem. Phys. 92, 347 (1990).
3. F. A. Khan, T. G. Kreutz, G. W. Flynn, and R. E. Weston, Jr., "State Resolved Vibrational, Rotational, and Translational Energy Deposition in $CO_2(00^01)$ Excited by Collisions with Hot Hydrogen Atoms," J. Chem. Phys. 92, 4876 (1990).
4. L. Zhu, T. G. Kreutz, A. S. Hewitt, and G. W. Flynn, "Diode Laser Probing of Vibrational, Rotational, and Translational Excitation of CO_2 Following Collisions with $O(^1D)$: Inelastic Scattering," J. Chem. Phys. 93, 3277 (1990)
5. T. G. Kreutz and G. W. Flynn, "Analysis of Translational, Rotational, and Vibrational Energy Transfer in Collisions between CO_2 and Hot Hydrogen Atoms: The Three Dimensional 'Breathing Ellipse' Model," J. Chem. Phys., 93,452(1990).
6. F. A. Khan, T. G. Kreutz, J. A. O'Neill, C. X. Wang, G. W. Flynn and R. E. Weston, Jr., "Collisional Excitation of $CO_2(01^11)$ by Hot Hydrogen Atoms: Alternating Intensities in State Resolved Vibrational, Rotational, and Translational Energy Transfer," J. Chem. Phys., 93,445(1990)
7. L. Zhu, J. Hershberger, and G. W. Flynn, "Quantum State Resolved Study of the Rovibrational Excitation of OCS by Hot Hydrogen Atoms," J. Chem. Phys. 92, 1687 (1990).
8. S. A. Hewitt, L. Zhu, and G. W. Flynn, "Diode Laser Probing of the Antisymmetric Stretch Mode of CO_2 Produced by Collisions with High Energy Electrons from 193 nm Excimer Laser Photolysis of Iodine," J. Chem. Phys. 92, 6974 (1990).

9. A. J. Sedlacek, R. E. Weston, Jr., and G. W. Flynn, "Br*+CO_2 Revisited: an Interrogation of E-V Energy Transfer with Time Resolved Diode Laser Spectroscopy," J. Chem. Phys. 93, 2812(1990)
10. James Z. Chou and George W. Flynn, "Energy Dependence of the Relaxation of Highly Excited NO_2 Donors Under Single Collision Conditions: Vibrational and Rotational State Dependence and Translational Recoil of CO_2 Quencher Molecules", J. Chem. Phys., 93, 6099(1990)
11. A. S. Hewitt, J. F. Hershberger, J. Z. Chou, G. W. Flynn, and R. E. Weston, Jr., "Rotationally and Translationally Resolved Hot Atom Collisional Excitation of the CO_2 Fermi Mixed Bend/Stretch Vibrational Levels By Time-Dependent Diode Laser Spectroscopy", J. Chem. Phys., 93,4922(1990)
12. James Z. Chou, Scott A. Hewitt, John F. Hershberger, and George W. Flynn, "Diode Laser Probing of the Low Frequency Vibrational Modes of Baths of CO_2 and N_2O Excited by Relaxation of Highly Excited NO_2", J. Chem. Phys. 93,8474(1990)
13. Lei Zhu, Scott A. Hewitt, and George W. Flynn, "Quantum Interference Effects in the Collisional Excitation of the Fermi Doublet States of CO_2 by Hot Electrons and Hot H(D) Atoms", J. Chem. Phys. 94,4088(1991)
14. A. J. Sedlacek, R. E. Weston, Jr., and G. W. Flynn, "Interrogating the Vibrational Relaxation of Higly Excited Polyatomics with Time-Resolved Diode Laser Spectroscopy: C_6H_6, C_6D_6, and C_6F_6+CO_2", J. Chem. Phys. 94, 6483 (1991)
15. Liedong Zheng, James Chou, and George Flynn, "Relaxation of Molecules with Chemically Significant Amounts of Energy: Vibrational, Rotational and Translational Energy Recoil of an N_2O Bath Due to Collisions with NO_2(E=63.5 KCAL/MOLE)", J. Phys. Chem. 95, 6759(1991)
16. Jeunghee Park, Yongsik Lee, and George Flynn, "Tunable Diode Laser Probe of Chlorine Atoms Produced from the Photodissociation of a Number of Molecular Precursors", Chem. Phys. Lett. 186,441(1991)
17. Jeunghee Park, Yongsik Lee, John F. Hershberger, Jeanne M. Hossenlopp, and George W. Flynn, "Chemical Dynamics of the Reaction between Chlorine Atoms and Deuterated Cyclohexane", J. Am. Chem. Soc. 114, 58(1992)
18. Ralph E. Weston, Jr. and George W. Flynn, "Relaxation of Molecules with Chemically Significant Amounts of Energy: The Dawn of the Quantum State Resolved Era", Ann. Rev. Phys. Chem., (1992) to be published.
19. C. K. Ni and G. W. Flynn, "Correlation between Molecular Recoil and Molecular Orientation in Collisions of Symmetric Top Molecules with Hot Hydrogen Atoms", Chem. Phys. Lett. (1992), to be published

March 1992

HTP KINETICS STUDIES ON ISOLATED ELEMENTARY COMBUSTION REACTIONS OVER WIDE TEMPERATURE RANGES

Arthur Fontijn

High-Temperature Reaction Kinetics Laboratory
The Isermann Department of Chemical Engineering
Rensselaer Polytechnic Institute
Troy, NY 12180-3590

Program Scope

The goals of this work are to provide accurate data on the temperature dependence of the kinetics of elementary combustion reactions, (i) for use by combustion modelers, and (ii) to gain a better fundamental understanding of, and hence predictive ability for, the chemistry involved. Experimental measurements are made mainly by using the pseudo-static HTP (high-temperature photochemistry) technique. This approach allows observations on single reactions in the 300 to 1800 K temperature range. Relative concentrations of atoms, produced by photolysis, are monitored by resonance fluorescence, pumped by a cw microwave-discharge flow-lamp. In the past year we have worked on the O-atom reactions with the four isomeric butenes, the H + HCl and the O + 1,3-butadiene reaction. Manuscripts on the former two are in preparation.

Recent Progress

The O-Atom Reactions with the Four Isomeric Butenes

Figure 1 summarizes our results on these reactions. The 1-butene study has already been published.[1] The following empirical best fit expressions have been obtained (all rate coefficients in this abstract are in cm^3 $molecule^{-1}$ s^{-1}):

$$O + 1\text{-}C_4H_8: k(340\text{-}1110\ K) = 2.7 \times 10^{-11} \exp(-624\ K/T) + 2.4 \times 10^{-9} \exp(-5657\ K/T) \quad (1)$$

$$O + iso\text{-}C_4H_8: k(284\text{-}886\ K) = 1.8 \times 10^{-11} \exp(-36\ K/T) \quad (2)$$

$$O + cis\text{-}2\text{-}C_4H_8: k(292\text{-}1086\ K) = 2.4 \times 10^{-17} (T/K)^{1.94} \exp(716\ K/T) \quad (3)$$

$$O + trans\text{-}2\text{-}C_4H_8: k(292\text{-}1022\ K) = 5.2 \times 10^{-16} (T/K)^{1.51} \exp(577\ K/T) \quad (4)$$

with accuracy limits of about ± 27%. These are in good agreement with previously reported low temperature (T < 500 K) data[2-5] as well as with the best fit expressions for the four reactions in the 260-860 K range given in an abstract by Perry.[6] In agreement with Perry, we find that the 1-butene reaction differs markedly from the other three, in that it has a much lower rate coefficient at low temperatures and shows a very strong upward curvature in its Arrhenius plot. In the following we suggest an explanation for these differences.

At low temperatures the reactions proceed by electrophilic addition of O atoms to the double bond.[3] However, H-atom abstraction leading to OH has been observed at higher temperatures, for reaction (1) by LIF[7] and for reactions (1) through (3) by mass spectrometry.[8] The transition state theory procedure of Singleton and Cvetanovic,[3] does not reproduce the strong curvature of reaction (1) at higher temperatures. However, addition of terms for H-abstraction results in good agreement with the experimental results. For the three other reactions, the higher rate coefficients for the addition channel obscure the small contribution of abstraction, hence the slighter curvature observed in their Arrhenius plots.

The difference in the values of the rate coefficients below 500 K requires an explanation based on the difference in the addition channels. Consideration of the electron donating effects[9] of the alkyl groups to the double bonds clarifies the observations in that the activation energy is influenced by the inductive and hyperconjugative effects of alkyl groups attached to the double bond.[10] In 1-butene one ethyl group is attached to that bond, while in the other butenes two methyl groups are attached there, resulting in an increase in the negative character of that bond, and a lower activation energies for reactions (2), (3), and (4). Since the four reactions have about the same pre-exponential factors, the rate coefficients for the 1-butene reaction are lower.

$H + HCl \rightarrow H_2 + Cl$

Baulch, et al. in their evaluation[11] considered the direct rate coefficient measurements on this reaction to be too scattered and unreliable to allow a recommendation. Instead they made a recommendation based on the reverse reaction. The data by Ambidge, et al.[12] for the forward reaction appeared[11] to be the most reliable. It may be seen in Fig. 2 that our results are in good agreement with both of these references. It is interesting to note, cf. Fig. 2, that the only previous measurements above 520 K on this reaction, i.e., those of Steiner and Rideal, as recalculated by Benson, et al.[13] are in good agreement with our measurements as well. The Baulch recommendation does not extend above 620 K, since that is the maximum temperature for which the reverse reaction has been measured. We thus have nearly doubled the temperature range for which k(T) for the forward reaction now may be considered to be reliably known. We also plan to study the reverse reaction and extend those measurements to higher temperatures.

The O-Atom 1,3-butadiene Reaction

The experiments on this reaction are nearing completion. The present results are best represented by $k(283\text{-}1016K) = 9.7 \times 10^{-16}(T/K)^{1.46}\exp(432\ K/T)$. These are in excellent agreement with earlier measurements[14] spanning the 297-574 K range and extend the temperature range by more than a factor of two.

Plans

We plan to study the O + methylacetylene and Cl + H_2, CH_4 reactions next. Methods for photolytic production of Cl atoms in use at lower temperatures suffer for our work from poor thermal stability of the precursors and fast secondary reactions. However, we have successfully studied a series of metal atom reactions by photolysis of their chlorides[15] and now plan to use these as high-temperature Cl sources.

Our work thus far has concentrated on rate coefficient measurements of reactions for which the rate-controlling step is unambiguous. To extend our scope we plan to do some preliminary product analysis work this coming year, in the hope of expanding such efforts in the future.

References

1. T. Ko, G.Y. Adusei and A. Fontijn, *J. Phys. Chem.*, 95, 9366 (1991).
2. R.E. Huie, J.T. Herron and D.D. Davis, *J. Phys. Chem.*, 76, 3311(1972).
3. D.L. Singleton and R.J. Cvetanovic,, *J. Am. Chem. Soc.*, 98, 6812(1976).
4. R. Atkinson and J.N. Pitts, Jr., *J. Chem. Phys.*, 67, 38(1977).
5. R. Browarzik and F. Stuhl, *J. Phys. Chem.*, 88, 6004(1984).
6. R.A. Perry, Abstracts of Papers, 188th A.C.S. National Meeting, August, 1984, Phys. 241.
7. K. Kleinermanns and A.C. Luntz, *J. Chem. Phys.*, 77, 3533(1982).
8. B. Blumenberg, K. Hoyermann and R. Sievert, Sixteenth Symposium(International) on Combustion, p.841, 1977.
9. P. Sykes, A Guidebook to Mechanism in Organic Chemistry, 3rd. ed., John Wiley, New York, 1970, pp. 20, 24, and 159.
10. C.A. Arrington and D.J. Cox, *J. Phys. Chem.*, 79, 2584 (1975).
11. D.L. Baulch, J. Duxbury, S.J. Grant, and D.C. Montague, *J. Phys. Chem. Ref. Data*, 10 (1981), Suppl. 1, p. 161-1 ff.
12. P.F. Ambidge, J.N. Bradley and D.A. Whytock, *J.C.S. Faraday I*, 72, 2143 (1976).
13. S.W. Benson, F.R. Cruickshank and R. Shaw, *Int. J. Chem. Kin.*, 1, 29 (1969).
14. W.S. Nip, D.L. Singleton and R.J. Cvetanovic, *Can. J. Chem.*, 57, 949 (1979).
15. A. Fontijn and P.M. Futerko, in Gas-Phase Metal Reactions, A. Fontijn, Ed., Elsevier, Amsterdam, in press, Chap. 6.

Research Publications Resulting From This Grant, 1990-1992

K. Mahmud, J-S. Kim and A. Fontijn, "An HTP Kinetics Study of the O + HCl Reaction from 350 to 1480 K", *J. Phys. Chem.*, 94, 2994-2998 (1990).

T. Ko, G.Y. Adusei and A. Fontijn, "Kinetics of the $O(^3P)$ + C_6H_6 Reaction over a Wide Temperature Range", *J. Phys. Chem.*, 95, 8745-8748 (1991).

T. Ko, G.Y. Adusei and A. Fontijn, "Kinetics of the Reactions between $O(^3P)$ and 1-Butene from 335 to 1110 K", *J. Phys. Chem.*, 95, 9366-9370 (1991).

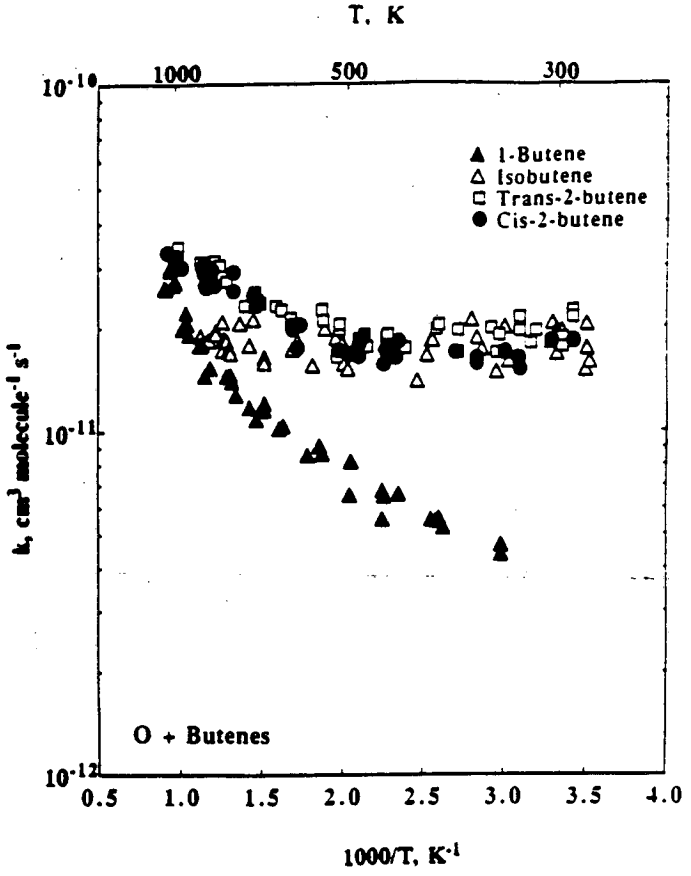

Figure 1. The Present Measurements on the O-Atom Reactions with the Four Isomeric Butenes.

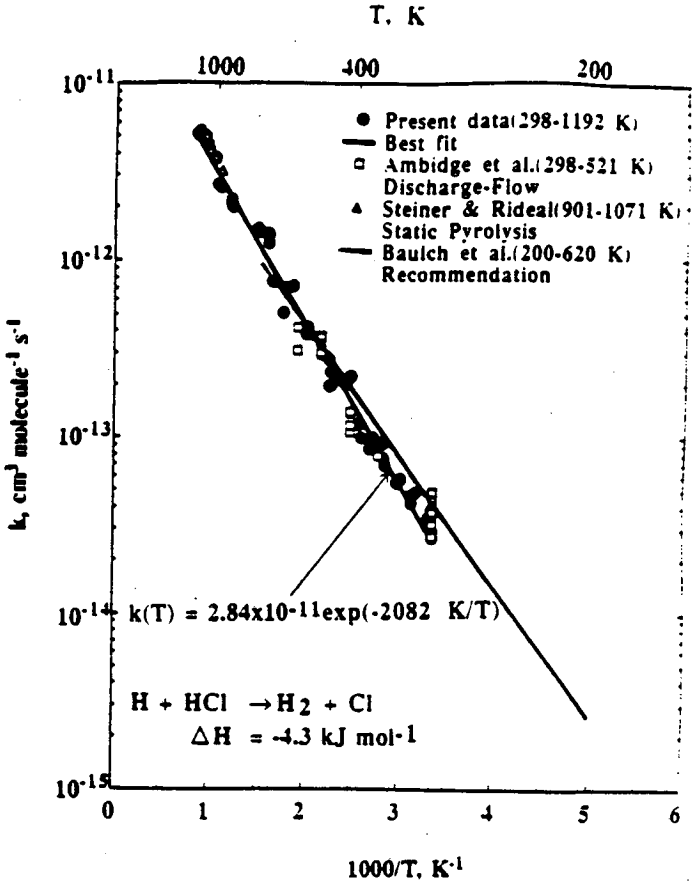

Figure 2. Summary of Observations on the H + HCl Reaction.

STATE-TO-STATE DYNAMICS OF MOLECULAR ENERGY TRANSFER

W. Ronald Gentry and Clayton F. Giese
Chemical Dynamics Laboratory
University of Minnesota
207 Pleasant St. SE
Minneapolis, MN 55455

PROGRAM SCOPE

This research program is meant to elucidate the elementary dynamical mechanisms of vibrational and rotational energy transfer between molecules, at a quantum-state resolved level of detail. Molecular beam techniques are used to isolate individual molecular collisions, and to control the kinetic energy of collision. Lasers are used both to prepare specific quantum states prior to collision by stimulated-emission pumping (SEP), and to measure the distribution of quantum states in the collision products by laser-induced fluorescence (LIF). The results are interpreted in terms of dynamical models, which may be cast in a classical, semiclassical or quantum mechanical framework, as appropriate.

RECENT PROGRESS

Under this DOE project to date, we have studied (1) state- and mode-selective vibrational excitation of iodine, aniline, para-difluorobenzene (pDFB) and trans-glyoxal in collisions with various species, and (2) rotationally-resolved inelastic scattering of iodine, para-difluorobenzene and trans-glyoxal in collisions with helium, and (3) energy transfer from highly excited vibrational levels of $I_2(X^1\Sigma_g^+)$ prepared by SEP.[1-9] Experiments of types (1) and (2) were carried out with molecules initially in the ground vibrational state, with a rotational temperature of about 1 K, prepared in a pulsed supersonic expansion.[10] Our recent investigations of type (3) represent the first crossed-beam experiments to employ SEP for the preparation of highly excited vibrational levels of the ground electronic state of a molecule.

One of the most significant results of our experiments with initially excited vibrational states is that we were able to verify the predictions of a new vibrational quantum number scaling law, based on the correspondence between the classical and quantal dynamics of forced harmonic oscillators. This correspondence[11] permits the probability $P_{m,n}$ for the quantum transition $m \rightarrow n$ to be written in the form

$$P_{m,n} = m!n!e^{-\varepsilon}\varepsilon^{m+n}S_{m,n}^2$$

where

$$S_{m,n} = \sum_{k=0}^{\min(m,n)} \frac{(-1)^k \varepsilon^{-k}}{(n-k)!k!(m-k)!}$$

and where

$$\varepsilon = \frac{\Delta E}{\hbar\omega}$$

is the classical energy transfer in units of the quantum level spacing. Thus, the quantum dynamics may be expressed in terms of the dynamics of the equivalent classical forced oscillator. In practical terms, this means that the cross section for a quantum state-to-state transition can be calculated from purely classical trajectories which yield a value of ε, and therefore $P_{m,n}$, for each set of initial conditions.

In the limits of small ε and/or large m, one can derive the scaling relation

$$P_{m,m+\Delta v}(\xi) = P_{0,\Delta v}(\varepsilon)$$

where the quantum number scaling for transitions $m \rightarrow m+\Delta v$ is all contained in the scaling of the classical energy transfer parameter. For excitation channels, the result is

$$\xi = \varepsilon\left[\frac{m!\Delta v!}{(m+\Delta v)!}\right]^{\frac{1}{\Delta v}}$$

and for relaxation channels, we have

$$\xi = \varepsilon\left[\frac{(m-\Delta v)!\Delta v!}{m!}\right]^{\frac{1}{\Delta v}}.$$

The experimental results obtained so far[8,9] for $\Delta v = \pm 1$ transitions in I_2 confirm the scaling prediction that the cross sections scale linearly with vibrational quantum number. This is in sharp contrast to the concept of an

"energy gap law," which would predict a constant cross section for single-quantum transitions of a harmonic oscillator.

FUTURE PLANS

We are presently engaged in measuring differential cross sections for rotational excitation of NO in collisions with Ar. Although a second detector for differential measurements was incorporated into the apparatus from the beginning,[10] this is the first experiment of that type we have attempted. We are extremely pleased with the excellent S/N ratios obtained so far, which can be attributed to the very high NO beam intensity and the reduction in background due to having the detector in a separate, differentially-pumped chamber.

In our first experiments, we are concentrating on measuring the final rotational state distribution at fixed scattering angle, as a function of the kinetic energy of collision. As of this writing, the data are still being analyzed. In future experiments, we hope to measure angle dependences and to observe vibrational as well as rotational excitation.

---

1. G. Hall, K Liu, M.J. McAuliffe, C.F. Giese, and W.R. Gentry, *J. Chem. Phys.* **78**, 5260 (1983).
2. K Liu, G. Hall, M.J. McAuliffe, C.F. Giese, and W.R. Gentry, *J. Chem. Phys.* **80**, 3494 (1984).
3. G. Hall, K Liu, M.J. McAuliffe, C.F. Giese, and W.R. Gentry, *J. Chem. Phys.* **81**, 5577 (1984).
4. G. Hall, C.F. Giese, and W.R. Gentry, *J. Chem. Phys.* **83**, 5343 (1985).
5. W.R. Gentry, in *Electronic and Atomic Collisions*, ed. by D.C. Lorents, W.E. Meyerhof and J.R. Peterson (Elsevier, Amsterdam, 1986), pp. 13-22.
6. G. Hall, K Liu, M.J. McAuliffe, C.F. Giese, and W.R. Gentry, *J. Chem. Phys.* **84**, 2624 (1986).
7. V.A. Shamamian, D.L. Catlett, Z. Ma, S. Jons, C.F. Giese and W.R. Gentry (unpublished).
8. Z. Ma, S. Jons, C. F. Giese and W. R. Gentry, *J. Chem. Phys.* **94**, 8608 (1991).
9. Z. Ma, S. Jons, C.F. Giese and W.R. Gentry (unpublished).
10. W. R. Gentry, Ch. 3 in *Atomic and Molecular Beam Methods*, ed. by G. Scoles (Oxford, New York, 1988).
11. W. R. Gentry, Ch. 12 in *Atom-Molecule Collision Theory—a Guide for the Experimentalist*, ed. by R. B. Bernstein (Plenum, New York, 1979).

AROMATIC-RADICAL OXIDATION KINETICS

I. Glassman and K. Brezinsky
Princeton University
Department of Mechanical and Aerospace Engineering
Princeton, N.J. 08544
Grant # DE-FG02-86ER13554

Research progress has been achieved in three areas of an ongoing program to understand the details of the combustion chemistry of aromatic species. These three experimental and modelling efforts are described below as are the implications of recent progress for future research.

I) Cyclopentadiene Oxidation

The oxidation of 1,3-cyclopentadiene was studied at approximately 1060K over an equivalence ratio range of 0.38 to 2.16 and at 950K with an equivalence ratio of 0.32. These oxidation studies are the first reported studies at high temperatures. At these high temperatures considerable quantities of CO and CO_2 were observed early in the reaction sequence. Carbon dioxide is usually formed, during the oxidation of hydrocarbons, from the oxidation of carbon monoxide. However, the early CO_2 formed during the oxidation of cyclopentadiene did not appear to entirely follow this well established pattern. Similarly, the acetylene concentration did not follow the well established pattern of increasing with increasing equivalence ratio; instead it decreased.

The anomalous production of early CO and CO_2 cannot be explained in terms of the conventional aromatic oxidation mechanisms. There are a number of routes to CO and CO_2 production that are possible in the cyclopentadiene sub-system. However, a great majority of them have been eliminated as implausible. The eliminated pathways are reactions involving:

low temperatures and meso-oxide intermediates
^{3}Cyclopentadiene and O_2 ($^3\Sigma g^-$)
^{2}Cyclopentadienyl and O_2 ($^3\Sigma g^-$)
formyl radical
$:CH_2$ ($^3B_1$) and O (^3P)
$:CH_2$ ($^3B_1$) and O_2 ($^3\Sigma g^-$)
acetylene to form CO_2 directly
ethynyl

Instead, a simple mechanism consistent with the flow reactor data and with known chemistry has been postulated and will be the subject of future research.

II) Benzene and Toluene Detailed Kinetic Modelling.

By constructing a kinetic model for the oxidation of toluene based on mechanistic and kinetic information from the literature and from thermochemical estimates, it was possible to reasonably model flow reactor oxidation experiments of benzene and toluene. The consumption rate of toluene and benzene for both lean and rich oxidation conditions is predicted quite well by the model as are many of the intermediates. The predictive capability of the model is a significant improvement over previously reported results and could be of great value in combustion modelling.

The inhibitory effect of two major toluene consumption reactions

$$C_6H_5CH_3 + OH \rightarrow C_6H_5CH_2 + H_2O$$

$$C_6H_5CH_3 + H \rightarrow C_6H_5CH_2 + H_2$$

was clearly indicated by a linear sensitivity analysis. Furthermore, the high sensitivity of the model results to the abstraction reaction:

$$C_6H_5CH_3 + O_2 \rightarrow C_6H_5CH_2 + HO_2$$

has allowed for an estimate of this reaction rate constant with reasonable confidence.

The major shortcomings of the model were found to be the over prediction of acetylene and the under-prediction of phenol compounds. The acetylene profiles were not predicted correctly for the higher temperature toluene oxidation even though the lower temperature benzene sub-model predicted reasonable levels. With regard to the phenol formation, the temperature dependence of the decomposition rate of phenoxy was expected to be the source of error since phenol was predicted reasonably well in the lower temperature benzene sub-model.

III. Modelling Laminar Flame Speeds

In order to model flame speed data available from the literature, the toluene mechanism derived from flow reactor experiments was coupled to the PREMIX code available from Sandia National Laboratories. The calculated flame speeds for stoichiometric toluene/air and benzene/air mixtures were approximately 23 cm/sec - well below the literature values of 39 and 48 cm/sec respectively. The low calculated flame speeds implied that the aromatics combustion process was not proceeding fast enough to the energy releasing, small molecule oxidation steps. The toluene model contained only a very basic sub-mechanism for the oxidation of species containing two or less carbon atoms in order to keep the number of reactions and species small. Therefore, the first attempt at altering the mechanism to obtain a higher flame speed consisted of replacing the abbreviated C_2 oxidation scheme with a more complete, validated one. The substitution of this C_2 scheme led to a marginal increase of only 4 cm/sec.

A sensitivity analysis of the flame speed to each rate constant in the toluene model indicated that there was little sensitivity (less than 2%) to the alkyl side chain oxidation steps. Greater sensitivity (2% or more) was found for a subset of nine rate constants directly related to the oxidation of the aromatic ring and its fragments. The benzene flame calculations revealed a sensitivity to these same reactions. Of course, the greatest sensitivity of the flame speed was found to be for the $CO + OH \rightarrow CO_2 + H$ reaction (11%) and for $H + O_2 \rightarrow OH + H$ (21%). Since these latter two reactions have been extensively studied no further consideration was given to changing their rate constants. In view of the greater availability of benzene flame speed data and the sensitivity of both the toluene and benzene flame speeds to the same rate constants, the toluene mechanism was reduced, for ease of calculation and analysis, to a benzene mechanism by the removal of all the toluene related steps.

Among the rate constants having the most effect on the flame speed a number are uncertain either because they are estimated rather than measured, measured over a narrow range of temperature, or have been determined in only one set of experiments. Therefore, sequentially for each uncertain rate constant, the value of A in the three parameter representation of the rate constant was increased or decreased as indicated by the sensitivity analysis in order to "walk" the flame speed up into the 40 cm/sec range.

The result of the changes was a calculated flame speed of 41.6 cm/sec. A

sensitivity analysis of this calculated flame speed indicated that changes in the rate constants of the three reactions of C_5 species would have a significant effect (2% or more) on the flame speed. A ten fold increase in the forward and reverse A values of

$$C_5H_4O \rightarrow CO + 2C_2H_2$$

was sufficient to raise the stoichiometric flame speed to 43.8 cm/sec, a value lower than that measured but within the range seemingly appropriate for benzene. The calculated flame speeds at other equivalence ratios were 31.2, 38.2, 48.7, and 50.1 cm/sec at Φ = 0.8, 0.9, 1.1 and 1.2 respectively.

Species profiles calculated with the altered rate constants for flow reactor conditions were significantly different from those obtained with the original model. The changes were not surprising since the altered rate constants were the same ones shown by sensitivity analysis of the benzene decay profile to be significant during the flow reactor modelling efforts. In particular, the altered rate constants led to an order of magnitude decrease in initial benzene concentration within 60 msec, maximization of the phenol concentration within 30 msec and, CO production and almost complete consumption within 120 msec. These latter observations suggest how the toluene/benzene model might be made more comprehensive in order to predict both flow reactor and flame speed results.

The altered model in its ability to approximately match the measured benzene flame speeds has required a much more rapid production and oxidation of the energy releasing, small molecule hydrocarbon fragments. However, the flow reactor profiles indicate that alteration of the rate constants in the above extent and manner is not fully justified. It appears that a subset of toluene/benzene reactions is needed that would not drastically affect the calculated species profiles at flow reactor temperatures but would lead to an accelerated production of small hydrocarbons at flame temperatures. This conclusion has two implications; the temperature dependent parameters of the above mentioned altered rate constants reactions may require re-adjustment in a way already suggested by some of the inadequacies revealed during flow reactor modelling and, the addition of high activation energy reactions, not currently in the toluene/benzene mechanism may be necessary in order to provide H atoms to drive the overall reaction progress. Given the inability of the models to adequately predict the details of the oxidation of cyclopentadiene, reactions of C_5 species may be the logical ones to investigate for inclusion in the model.

The inability of the present chemical kinetic models to predict the details of cyclopentadiene oxidation, some details of benzene and toluene oxidation and, laminar flame speeds has motivated a number of research directions.

IV. Future Research

1) An experimental and modelling examination of the perturbation of the oxidation of cyclopentadiene by the addition of NO_2 and CO in order to test some steps of the postulated mechanism of CO_2 formation.

2) A flow reactor investigation of the oxidation of phenol since this species links attack on the aromatic ring with the formation of cyclopentadiene.

3) Measurements of the stretch-free laminar flame speed of cyclopentadiene as a function of stoichiometry in order to develop an accurate data base for comparison with improved models.

V. Publications Resulting from Program Since 1990

Refereed

1) "The Oxidation of Toluene Perturbed by NO_2", Comb. Sci. Tech. 70, 33 (1990).

2) "Oxidation of O-Xylene", Twenty Third Symposium (Int'l) on Combustion, p.77 (1990).

3) "A High Temperature 180 Degree Laser Induced Fluorescence Probe for Remote Trace Radical Concentration Measurements", Applied Optics 30, 381 (1991).

4) "High Temperature Oxidation Mechanics of Meta and Para Xylene", J. Phys. Chem. 95, 1626 (1991).

5) "A Kinetic Model for the Oxidation of Toluene Near 1200K", J. Phys. Chem. 96, 2151 (1992).

6) "A Flow Reactor Study of the Oxidation of 1,3-Cyclopentadiene", MSE Thesis, Robert Butler, 1992.

Other Publications

1) "The High Temperature Oxidation of Toluene: Experiment and Model Compared", Eastern States Section/Combustion Institute Meeting, Extended Abstract #4, 1990.

2) "Oxidation of Cyclopentadiene at 1070K", Eastern States Section/Combustion Institute Meeting, Extended Abstract #2, 1990.

3) "Benzene/Toluene Oxidation Models: Studies Based on Flow Reactor and Laminar Flame Speed Data", Division of Fuel Chemistry, Preprint, ACS Symposium on Combustion Chemistry, National Meeting of the American Chemical Society, 1991.

KINETICS OF ELEMENTARY ATOMIC AND RADICAL REACTIONS

Robert J. Gordon

Department of Chemistry (m/c 111)
University of Illinois at Chicago
Box 4348, Chicago, IL 60680

During the past year we have continued to study the photodissociation of oxygen containing molecules and also the quenching of the $B^1\Sigma^+$ state of CO by various gases. In the following sections we review our progress in both projects.

A. ASE Effects in LIF Measurements of $O(^3P_j)$

We have measured the fine structure populations of $O(^3P)$ produced in the UV photodissociation of O_2, SO_2, SO_2, and NO_2, using laser-induced fluorescence to detect the fragment oxygen atoms. In the course of this work we discovered that the apparent populations observed when detecting the 3p→3s transition at 845 nm are much hotter than when detecting the 3s→2p transition at 130 nm. This effect is illustrated in Table I for several systems including a 300K Boltzmann distribution produced with a microwave discharge. We proposed that this effect is caused by amplified spontaneous emission (ASE) between the 3p and the 3s levels of $O(^3P)$, which we could observe along the axis of the probe laser beam.

To test this hypothesis we developed a kinetic model which includes both isotropic and amplified emission at 845 nm, isotropic emission at 130 nm, and multiphoton ionization. The results of this model are summarized in Figures 1 and 2. In Figure 1 is shown the time-averaged concentration of the 3p level as a function of ground state $O(^3P)$ concentration for a laser flux of 3×10^{26} photons cm^{-2} s^{-1}, both with and without the ASE effect. We find that ASE reduces the isotropic fluorescence at 845 nm by an amount which increases monotonically with number density. The effect that this has on the apparent populations is illustrated in Figure 2, using O_2 as an example. At low total concentrations the number density of the most populated state (generally j=2) is depleted the most, resulting in a hotter distribution, while at high concentrations all three levels are comparably depleted. We have observed both effects experimentally. In comparison, population measurements at 130 nm should be valid at all concentrations since ASE for the 3s→2p transition is negligible, and its oscillator strength is independent of j.

In another study we have observed collisionally induced energy transfer between different multiplet states of $O(^3P)$; e.g.

$$O(^3P_{j''}) + Ar \rightarrow O(^3P_{j'}) + Ar.$$

In initial experiments we have observed the pressure dependence of the relaxation rates of all three levels. For Ar as a collision partner the rate constants are approximately 10^{-11} cm^3 $molecule^{-1}$ s^{-1}.

B. Quenching of Electronically Excited CO

The $B^1\Sigma^+$ state of CO is the highest excited state of CO which dissociates to two ground state atoms. Since this is a Rydberg state, it might be expected to behave dynamically like a CO^+ ion with the outer electron carried along as a spectator. The Rydberg electron is easily detached and can interact strongly with a colliding atom or molecule. The dynamics of this electron depends very much on the properties of the collision partner.

In an ongoing study we used a tunable vuv (110-115 nm) laser to excite different vibrational (v=0 and 1) and rotational levels of the B state of CO in the presence of various quenching gases, including H_2, D_2, He, Ne, Ar, Kr, Xe, N_2, O_2, HF, and HCl. The decay rate of the excited state was determined both from real time measurements and from the pressure dependence of the fluorescence intensity.

During the past year we have focused our attention on collisions with argon. Our earlier work showed that Ar is unique inasmuch as it increases the non-resonant fluorescence emission from CO. What makes Ar unusual is that its lowest excited state is too high to remove energy from CO but lies low enough to interact strongly with it. Our current hypothesis is that a long-lived Ar-CO complex is formed which redistributes the electronic energy within the CO moiety.

To test our hypothesis we have rebuilt our apparatus to allow us to disperse the fluorescence with a 1 m VUV monochromator. Preliminary experiments show that the enhanced fluorescence comes from the $A^1\Pi$ valence state of CO. Vibrationally resolved spectra indicate that the population of the emitting A state differs from the state distribution that is normally obtained radiatively from the B→A transition.

Table I. The Effect of ASE on O(^{3}P) Population Measurements

System	Wavelength (nm)	Population (±2σ) j=2	j=1	j=0
SO_2 + 193 nm	130	58.7±3.6	30.7±3.0	10.6±2.0
	845	45.7±2.0	46.2±1.0	8.2±1.0
	Model	47.	37.	15.
O_2 + 157 nm	130	92.5±1.2	6.5±0.9	1.0±0.5
	845	73.4±2.7	22.2±2.9	4.6±1.2
	Model	74.0	21.3	4.7
NO_2 + 226 nm	130	54.0±5.0	32.0±5.0	14.0±2.0
	845	34.0±4.0	39.0±4.0	27.0±3.0
	Model	41.1	33.7	25.2
298 K Boltzmann Distribution	130	74.1±1.2	20.5±0.9	5.4±1.4
	845	61.6±0.7	34.0±0.4	4.4±0.4
	Actual	74.3	20.7	5.0
	Model	61.	31.	8.

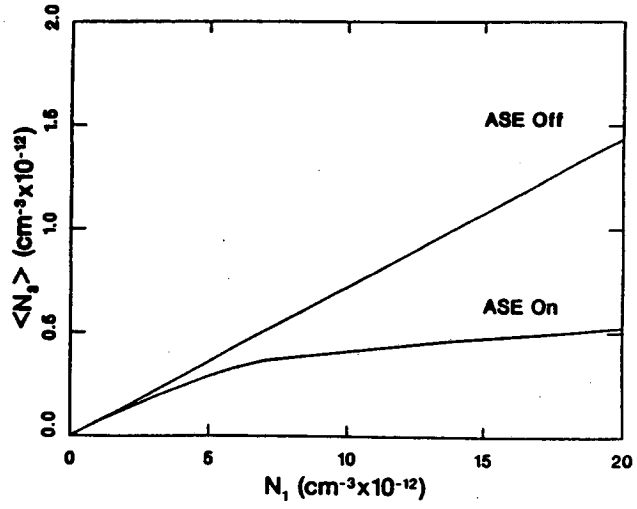

Figure 1. The effect of ASE on isotropic emission at 845 nm, as a function of the ground state population of a single multiplet level.

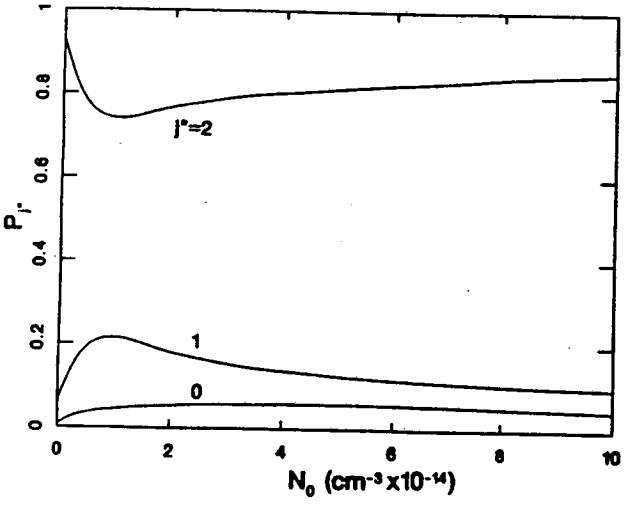

Figure 2. The effect of ASE on the observed fine structure population of O_2, as a function of total atom concentration.

DOE-Sponsored Publications from 1990 to 1992

1. Y.-F. Zhu, Y.-L. Huang, S. Arepalli, and R.J. Gordon, "Production of Vibrationally Excited Hydrogen Molecules," J. Appl. Phys. **67,** 604 (1990).

2. Y.-F. and R.J. Gordon, "The Production of $O(^3P)$ in the 157 nm Photodissociation of CO_2," J. Chem. Phys. **92,** 2897 (1990).

3. R.J. Gordon, "The Origin of Small and Large Molecule Behavior in the Vibrational Relaxation of Highly Excited Molecules," J. Chem. Phys. **92,** 4632 (1990).

4. K.M. Beck and R.J. Gordon, "Vibrational Relaxation of Highly Excited SiF_4 and C_6F_5H by Ar," J. Chem. Phys. **92,** 6011 (1990).

5. D.C. Robie, S. Arepalli, N. Presser, T. Kitsopoulis, and R.J. Gordon, "The Intramolecular Kinetic Isotope Effect for the Reaction $O(^3P)$ + HD," J. Chem. Phys. **92,** 7382 (1990).

6. Y.-L. Huang and R.J. Gordon, "The Multiplet State Distribution of $O(^3P)$ Produced in the 193 nm Photodissociation of SO_2," J. Chem. Phys. **93,** 868 (1990).

7. Y.-L. Huang and R.J. Gordon, "The Multiplet State Distribution of $O(^3P_j)$ Produced in the Photodissociation of O_2 at 157 nm," J. Chem. Phys. **94,** 2640 (1991).

8. Y. Matsumi, N. Shafer, K. Tonokura, M. Kawasaki, Y.-L. Huang and R.J. Gordon, "Doppler Profiles and Fine-Structure Branching Ratios from Photodissociation of Carbon Dioxide at 157 nm," J. Chem. Phys. **95,** 7311 (1991).

9. Y.-L. Huang and R.J. Gordon, "The Effect of Amplified Spontaneous Emission on the Measurement of the Multiplet State Distribution of Ground State Oxygen Atoms," (submitted).

Fundamental Spectroscopic Studies of Carbenes and Hydrocarbon Radicals

Carl A. Gottlieb and Patrick Thaddeus
Division of Applied Sciences
Harvard University
Cambridge, MA 02138

Highly reactive carbenes and carbon-chain radicals produced in low-pressure discharges through flowing mixtures of combustion gases are studied at millimeter wavelengths by observing their rotational spectra. The purpose is to provide definitive spectroscopic identification, accurate spectroscopic constants in the lowest vibrational states, and reliable structures of the key intermediates in reactions leading to aromatic hydrocarbons and soot particles in combustion.

The HCCCO and DCCCO Radicals

The propynonyl radical HCCCO may be an important intermediate in combustion processes and in the photodissociation of stable molecules. Lander *et al.* (*J. Chem. Phys.*, **94**, 7759 (1990)) found that CCH, a key radical in combustion chemistry, reacts with CO in a three-body addition reaction with the HCCCO radical as the product, and Tomašić and Scuseria (*J. Phys. Chem.*, **95**, 6905 (1991)) have studied this reaction theoretically and undertaken an extensive *ab initio* calculation of the structure of HCCCO. Haas *et al.* (*J. Phys. Chem.*, **95**, 5149 (1991)) determined by mass spectrometry that the HCCCO radical is a product of one of three dissociation pathways of HCCCHO and observed evidence for the secondary decay of hot HCCCO into CCH and CO.

Last year we reported the detection of an unidentified radical with measured rotational constants that were within 2% of those calculated *ab initio* for HCCCO and were in even closer agreement with rotational constants for the known molecule H_2CCCO with one H atom removed (Fig. 1). Isotopic substitution of the hydrogen, carbon, and oxygen established the presence of each of these elements, providing further evidence that we had detected HCCCO. Assignment of the HCCCO spectrum was initially hindered by a perturbation between the $K_a = 0$ and upper $K_a = 1$ stacks (Fig. 2) that produces anomalous spin splittings in the frequency range where HCCCO was first detected. The perturbed lines have now been identified among the many unknown lines in the C_2H_2, CO, and He discharge and analysis of the rotational spectra of HCCCO and DCCCO has been completed.

With rotational constants known for only two isotopic species, only a partial structure could be determined. From the experimental data, it was determined that the H-atom coordinates agree with the *ab initio* coordinates, whereas the moments of inertia of the CCCO chain agree best with "clipped" H_2CCCO. The HCH angle is probably less than the *ab initio* value of 139.1°, and is closer to the value of 117.2° found in H_2CCCO which is similar to the angle of 125° in HCO. If the odd electron is localized on the terminal C atom, as shown in Fig. 1, by analogy with HCO a large proton Fermi contact interaction is predicted, however, preliminary analysis of the proton hyperfine structure in one of the carbon-13 isotopic species indicates that the density of the odd electron is distributed

along the CCCO chain. We are continuing to work on isotopically substituted HCCCO to determine more parameters of the geometry and, by measuring hyperfine constants for the carbon nuclei, to determine the electron density along the CCC chain.

Our work constitutes the first spectroscopic identification of the HCCCO radical and provides a foundation for further spectroscopic investigation at other wavelengths. Specifically, our measurements establish the combination differences that will be observed in the vibrational spectrum of the free HCCCO radical, allowing this molecule to be identified in the IR in the presence of other molecules.

Vibrationally Excited CCH and CCD

We measured rotational transitions in the ν_3 ($^2\Sigma$), $\nu_1 + \nu_2$ ($^2\Pi$), and $\nu_2 + \nu_3$ ($^2\Pi$) vibronic states of CCH seen previously in the IR and observed, for the first time, the $2\nu_2$ ($^2\Sigma$) and $2\nu_2$ ($^2\Delta$) bending states. The millimeter-wave measurements yield improved rotational and fine structure constants for the ν_3, $\nu_1 + \nu_2$, and $\nu_2 + \nu_3$ states and accurate hyperfine constants which can be compared with the *ab initio* calculations by S. Peyerimhoff and coworkers (*J. Mol. Spectrosc.*, **150**, 56 (1991); **150**, 70 (1991)). In spite of the extensive IR work on CCH, the ν_1 band, arising from the C–H stretch, has not been conclusively identified because it: (1) lies close to the strong $A^2\Pi \leftarrow X^2\Sigma$ electronic transition, (2) is predicted to be weak, and (3) is masked by the C–H stretch in C_2H_2 in experiments in which CCH is generated from C_2H_2. It is believed that a band at 3299 cm^{-1} may be due to the C–H stretch (Stephens *et al.*, *J. Mol. Struct.*, **190**, 41 (1988)), however, its counterpart has not been observed in CCD. We observed the rotational spectrum for the upper state of the 3299 cm^{-1} band and then detected a spectrum in CCD which we believe arises from the same vibrational state. These constants may aid the identification in the IR of the ν_1 mode and hot bands involving the bending states.

New Vibrationally Excited States of Cyclopropenylidene

Recently Hirahara *et al.* (*J. Chem. Phys.*, **95**, 3975 (1991)) measured the ν_3 transition of cyclopropenylidene — the three-membered carbene ring we detected in 1985. Guided by the rotational and centrifugal constants of Hirahara *et al.* we observed strong rotational transitions in the ν_3 state in an allene discharge, detected rotational transitions in three new vibrational states (two with A and one with B symmetry), and determined an accurate set of spectroscopic constants for all four vibrational states. Tentative assignment of these states is made by comparing the measured inertial defects with those derived from harmonic force constants calculated *ab initio* (A. D. McLean, personal communication). Conclusive assignment awaits either calculation of the vibration-rotation constants or IR measurements. Our millimeter-wave spectroscopic constants should help guide further IR investigations of cyclopropenylidene.

Hyperfine Structure of the SiC Radical

Following our detection of SiC in its $X^3\Pi$ ground state we measured the rotational spectra of the $Si^{13}C$ and ^{29}SiC radicals. Well-resolved hyperfine splittings in the three fine-structure ladders allowed determination of the magnetic hyperfine constants to 2% or better. Of the seven open shell diatomic SiC molecules observed by high resolution spectroscopy, hyperfine structure of ^{29}Si has been completely analyzed only in SiC. Estimates of the electron density derived from our measurements are in qualitative agreement

with an *ab initio* calculation (S. R. Langhoff, personal communication), however, definitive determination of the electron density in SiC awaits a calculation that reproduces our hyperfine constants.

Search for New Sulfur Bearing Radicals

Although the HCO, HCCO, and HCCCO radicals are now well characterized spectroscopically, remarkably little is known about the analogous sulfur bearing radicals HCS, HCCS, and HCCCS. We therefore undertook a wide frequency survey in a discharge through CS_2 and C_2H_2 and identified over 3000 lines from sulfur bearing molecules including 300 magnetic lines from new radicals. We anticipate that several new sulfur bearing molecules will be identified in the next few months.

Future Plans

Our major effort during the next year will continue to be devoted to searches for new carbenes and radicals with a strong emphasis on three and five membered carbene rings, vinylidene (H_2CC) in the $^3B_2$ state, and propargylene (HCCCH). We plan to measure the structures of these species once the spectra of the normal species are characterized, and, in parallel with our continuing work with discharges, to explore new methods for producing hydrocarbon radicals and carbenes.

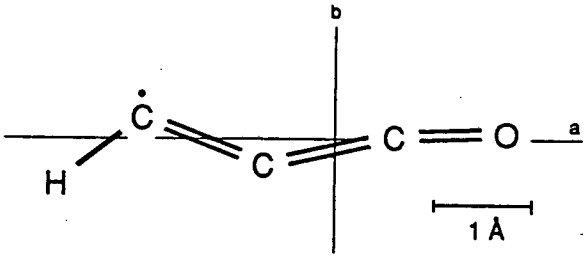

Figure 1

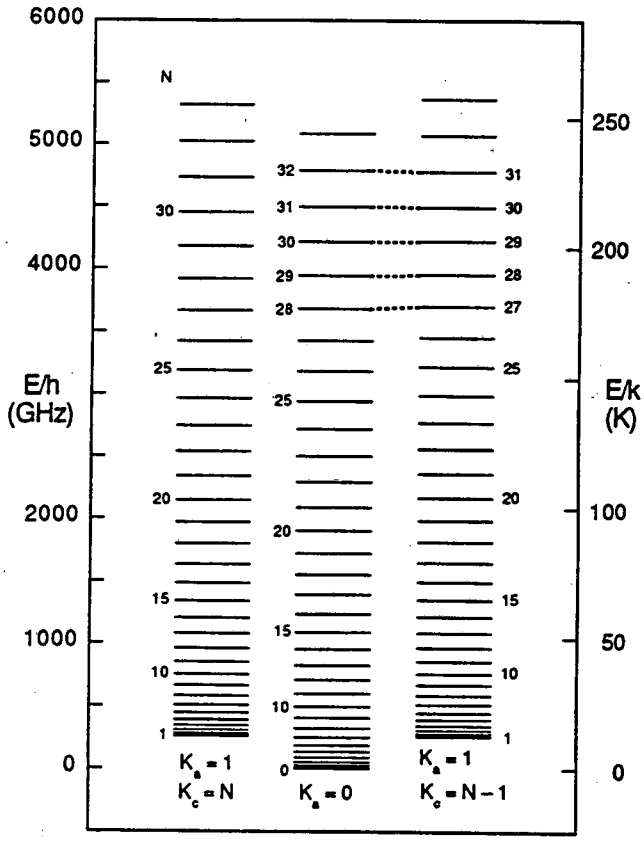

Figure 2

Figure Captions

Figure 1. Geometry of HCCCO obtained by removing an H atom from the known molecule H_2CCCO (Brown *et al.*, *J. Am. Chem. Soc.*, **107**, 4109 (1985)). The dot on the first carbon denotes the approximate location of the unpaired electron on the assumption that the CC and CO bonds are essentially double bonds, as drawn.

Figure 2. $K_a = 0$ and $K_a = 1$ ladders of HCCCO, spin doubling omitted. Dashed lines indicate the near-degeneracy responsible for perturbations in the spin doublets near $N = 30$.

Publications

1. R. Mollaaghababa, C. A. Gottlieb, J. M. Vrtilek, and P. Thaddeus, "Rotational Spectra of Carbon 13 and Vibrationally Excited SiC", *Astrophys. J. (Letters)*, **352**, L21 (1990).
2. J. M. Vrtilek, C. A. Gottlieb, E. W. Gottlieb, T. C. Killian, and P. Thaddeus, "Laboratory Detection of Propadienylidene, H_2CCC", *Astrophys. J. (Letters)*, **364**, L53 (1990).
3. T. C. Killian, J. M. Vrtilek, C. A. Gottlieb, E. W. Gottlieb, and P. Thaddeus, "Laboratory Detection of a Second Carbon Chain Carbene: Butatrienylidene, H_2C_4", *Astrophys. J. (Letters)*, **365**, L89 (1990).
4. R. Mollaaghababa, C. A. Gottlieb, J. M. Vrtilek, and P. Thaddeus, "The Millimeter-Wave Spectrum of Highly Vibrationally Excited SiO", *Astrophys. J. (Letters)*, **368**, L19 (1991).
5. A. L. Cooksy, S. Drucker, J. Faeder, C. A. Gottlieb, and W. Klemperer, "High Resolution Spectrum of the $v = 1$ state of ArHCN," *J. Chem. Phys.*, **95**, 3017 (1991).
6. R. Mollaagababa, C. A. Gottlieb, and P. Thaddeus, "Hyperfine Structure of the SiC Radical," *J. Chem. Phys.*, in press.
7. A. L. Cooksy, J. K. G. Watson, C. A. Gottlieb, and P. Thaddeus, "The Rotational Spectrum of the Carbon Chain Radical HCCCO," *Astrophys. J.*, **386**, L27 (1992).
8. A. L. Cooksy, J. K. G. Watson, C. A. Gottlieb, and P. Thaddeus, "The Millimeter-Wave Spectra of the HCCCO and DCCCO Radicals," *J. Mol. Spectrosc.*, **153**, in press.

Quantitative LIF diagnostics at high temperature

Jeffrey A. Gray, Joseph L. Durant, Jr. and Philip H. Paul
Combustion Research Facility
Sandia National Laboratories
Livermore, CA 94551-0969

and

John W. Thoman, Jr.
Chemistry Department
Williams College
Williamstown, MA 01267-2692

Program Scope

Because of the importance of free-radical species such as hydroxyl (OH) and nitric oxide (NO) in understanding combustion chemistry and turbulence/chemistry interactions, the development of laser-induced fluorescence (LIF) diagnostics has been widespread. LIF techniques are very sensitive and relatively simple to implement, but collisional quenching corrections in combustion applications have limited the accuracy of concentration and temperature measurements. The goal of this program is to use spectroscopic and kinetic measurements to quantify radiative and collisional effects on LIF signals. For example, we have measured the natural linewidth of several OH A-X (3,0) rotational transitions to determine predissociation lifetimes in the upper state,[1] which were presumed to be short compared to quenching lifetimes,[2] and, as a result, we make quantitative predictions about the applicability of predissociation fluorescence methods at high pressures. In other cases quenching corrections can be applied directly: NO A-state quenching rates for several collision partners have been measured at room temperature and in heated flow tubes;[3-7] however, very few measurements have been done at flame temperatures and extrapolations of lower-temperature data have not been aided by convincing, general models of the quenching process.

Recent Results

We have developed a shock-tube apparatus to measure collisional de-excitation rates for NO by a variety of combustion-related species.[8,9] NO is excited near the origin of the γ-band system (A-X (0,0) ~226 nm) using a Nd:YAG-pumped dye laser with UV wavelength extension. Red-shifted fluorescence (0,3) is detected to avoid radiation trapping by hot NO behind the incident shock waves and recorded at 2.5-ns intervals following a single laser pulse. Temperatures are carefully controlled using a double-diaphragm to initiate shock waves through gas mixtures containing more than 99% argon,

which is a very inefficient quencher. The number densities of NO and individual other species are chosen such that the observed decay lifetime of the LIF intensity is optimized between the natural radiative lifetime (206 ns) and the laser pulse width (8 ns). We repeat several (5-10) shock experiments for each set of initial conditions to reduce random errors in the measurements.

We have determined quenching rate coefficients (k_m) for N_2, O_2, CO_2, CO, NO, H_2O, CH_4 and Ar at temperatures including 295 K, 860 - 2260 K (incident shock), and 3450 & 4520 K (reflected shock); these measurements involved more than 500 shock-tube runs. Values for k_m at specific temperatures were then normalized by the relative collision velocity to derive quenching cross sections ($\sigma_m \equiv k_m/\langle v \rangle$). Cross sections for the most efficient quencher species studied are shown in Fig 1. Together, these species are responsible for more than 80% of the total quenching under typical flame conditions. All of these quenching cross sections are probably now known more accurately than the respective species concentrations. In addition, the temperature dependence of quenching by various collision partners is clearly quite different.

Several models of the quenching process have been investigated to understand and predict the temperature variations of cross sections. A charge-transfer (harpoon) model, which has frequently been applied to describe atomic collisions, appears to be most successful in comparison with our measurements. Crossing radii (r_c) for covalent and ion-pair potential surfaces are calculated using the known ionization potential of NO $A^2\Sigma^+$, electron affinities for each collision partner, and standard Lennard-Jones coefficients. The predicted hard-sphere cross sections using these radii ($\sigma=\pi r_c^2$) are shown by the arrows to the right side of Fig. 1. This model also predicts a large temperature variation for the N_2 quenching cross section due to an energy barrier for curve crossing at the entrance channel. An Ahhrenius plot of our data and the model results for N_2 quenching is shown in Fig. 2. The predicted activation energy is in good agreement with the observations, and the curvature at high temperature represents collisions with vibrationally excited N_2 which has a curve crossing at larger radius.

<u>Future Work</u>

Free radicals such as OH, O and H now contribute the largest uncertainty to LIF measurements of NO concentration in reacting flows. Our charge-transfer model predicts large quenching cross sections for these species. In addition, H-NO* and O-NO* collision studies may be useful tests of potential surfaces derived from photodissociation experiments or *ab initio* calculations. We initially plan to produce radicals by thermal mechanisms behind shock waves. For example, thermal dissociation of N_2O at temperatures above ~1500 K should provide a high enough O-atom density to measure its quenching rate. Slightly more complicated schemes involving H_2/O_2 mixtures at different equivalence ratios should provide variable, yet well

modeled amounts of H and OH whose quenching contributions will then be the only unknowns in the H_2/O_2 combustion mechanism (H_2 is predicted to have a negligible cross section). Excimer-laser photolysis is also being considered as a sources of radicals. Finally, measurements of OH $A^2\Sigma^+$ quenching by numerous flame species could be made for the first time at high temperature using our shock tube. OH quenching involves a strong interdependence on excited-state rotational level and temperature which seriously affects quantitative imaging of OH in flames.

References

1. J. A. Gray and R. L. Farrow, J. Chem. Phys. **95**, 7054 (1991).

2. P. Andresen, A. Bath, W. Groger, H. W. Lulf, G. Meijer and J. J. ter Meulen, Appl. Opt. **27**, 365 (1988).

3. I. S. McDermid and J. B. Laudenslager, J. Quant. Spectrosc. Radiat. Transfer **27**, 483 (1982).

4. R. J. Cattolica, T. G. Mataga, and J. A. Cavolowsky, J. Quant. Spectrosc. Radiat. Transfer **42**, 499 (1989).

5. M. Asscher and Y. Haas, J. Chem. Phys. **76**, 2115 (1982).

6. M. C. Drake and J. W. Ratcliffe, report GMR-7426, General Motors Research Laboratory (1991).

7. G. A. Raiche and D. R. Crosley, J. Chem. Phys. **92**, 5211 (1990).

8. J. A. Gray, Rev. Sci. Instrum. **61**, 1825 (1990).

9. J. A. Gray, P. H. Paul and J. L. Durant, Chem. Phys. Lett. **190**, 266 (1992).

BES-Supported Publications

1. J. A. Gray and R. L. Farrow, "Predissociation lifetimes of OH $A^2\Sigma^+$ (v'=3) obtained from optical-optical double resonance linewidth measurements", J. Chem. Phys. **95**, 7054 (1991).

2. J. A. Gray, P. H. Paul and J. L. Durant, "Electronic quenching rates for NO ($A^2\Sigma^+$) measured in a shock tube", Chem. Phys. Lett. **190**, 266 (1992).

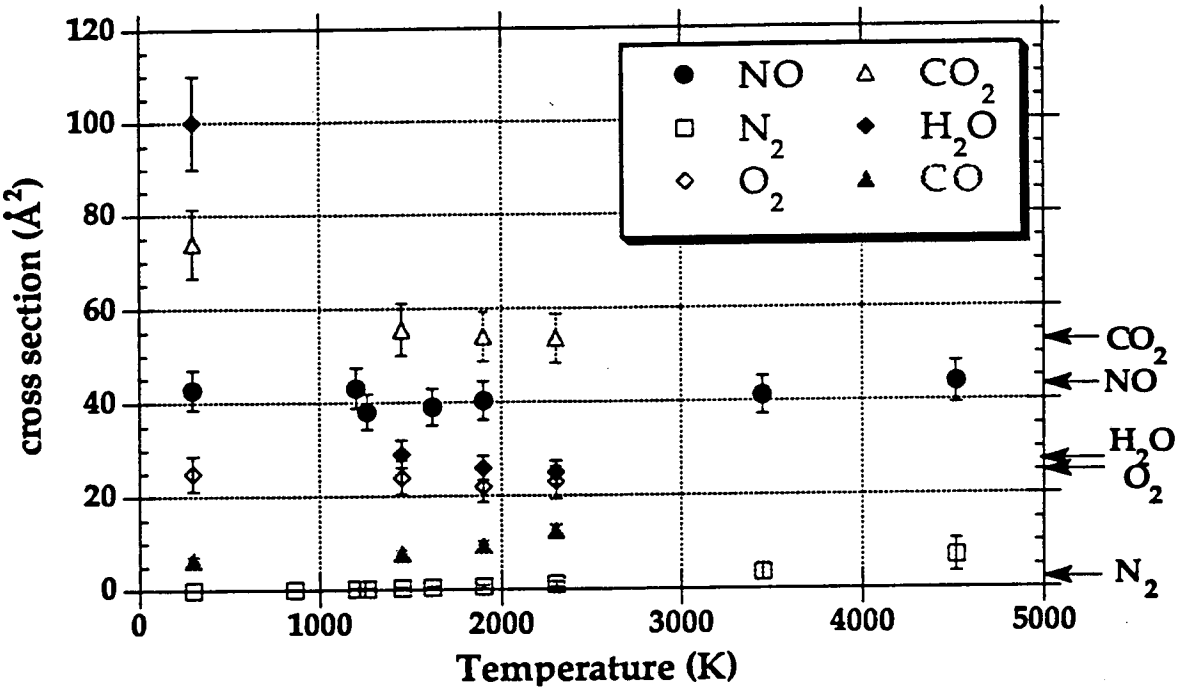

Fig. 1: Observed cross-sections for collisional quenching of NO $A^2\Sigma^+$ by several combustion-related species (M) were obtained from LIF decay rates measured in shock-heated mixtures of Ar, M and NO. Arrows indicate the values predicted using a charge-transfer (harpoon) model.

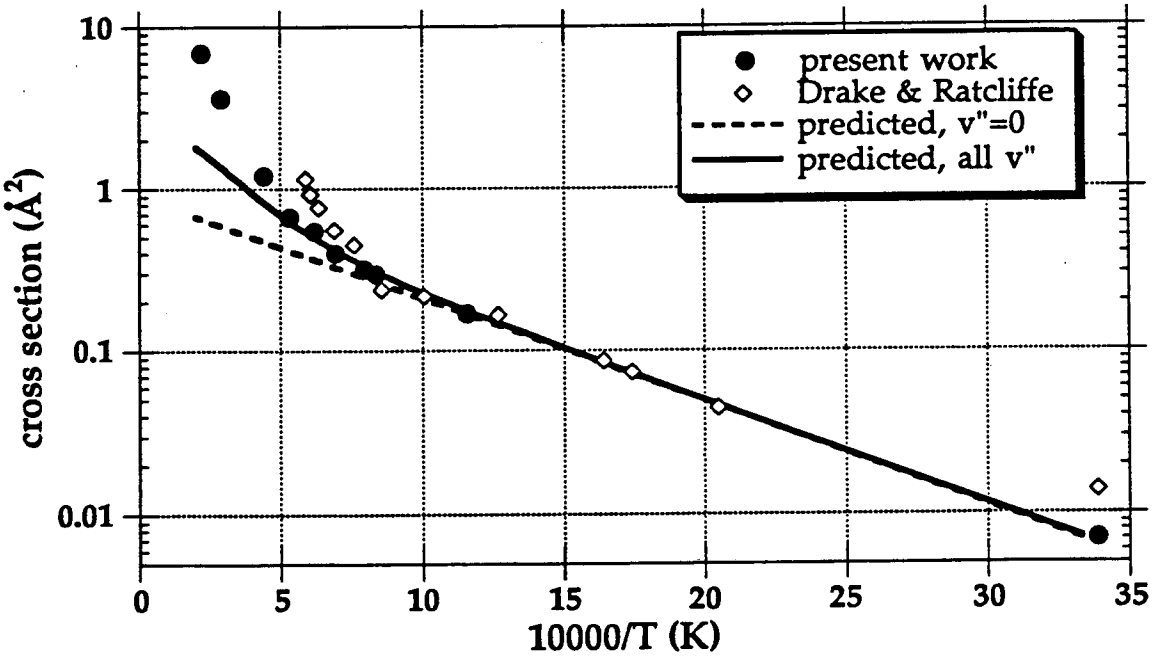

Fig. 2: Observed and predicted cross-sections for NO (A) quenching by N_2 both indicate that the process requires an activation energy. The super-exponential rise observed at the highest temperatures is partly described by collisions with vibrationally excited N_2 which has a larger effective cross-section.

STUDIES OF COMBUSTION KINETICS AND MECHANISMS

David Gutman, Department of Chemistry
Catholic University of America, Washington, D. C. 20064

RESEARCH OBJECTIVES

The objective of the current research is to gain new quantitative knowledge of the kinetics and mechanisms of the reactions of polyatomic free radicals which are important in hydrocarbon combustion processses. The special facility designed and built for these studies (which includes a heatable tubular reactor coupled to a photoionization mass spectrometer) is continually being improved. Where possible, these experimental studies are coupled with theoretical ones, sometimes conducted in collaboration with others, to obtain an improved understanding of the factors determining reactivity.

COMPLETED STUDIES

A. KINETICS OF THE UNIMOLECULAR DECOMPOSITION OF C_2H_5 with Y. Feng, J. T. Niiranen, A. Bencsura, V. D. Knyazev, and W. Tsang; J. Phys. Chem., Submitted for Publication, 1992

The unimolecular decomposition of C_2H_5 in helium has been studied in a tubular reactor coupled to a photoionization mass spectrometer. The conditions covered were $877 \leq T/K \leq 1094$ and $0.71 \leq [He]/10^{16} cm^{-3} \leq 15.8$. The rate constants, which lie close to the low-pressure limit, were analyzed using both RRKM theory and a Master Equation analysis. The high precision and accuracy of the measured rate constants (see Fig. 1) and knowledge of the high-pressure limit rate constant made it possible to determine the magnitude and temperature dependence of the step size down. RRKM and Master Equation data-fitting procedures provide different values of $<\Delta E>_{down}$ and different indications of its temperature dependence (See Fig. 2). The source of these differences is understood and explained. The results of the Master Equation analysis yield the expression $<\Delta E>_{down} = 0.255 T^{1.0} / cm^{-1}$ which, when extrapolated to lower temperatures (as low as 285 K) represents well the weak collision effects of this reaction observed by others.

B. KINETICS OF THE THERMAL DECOMPOSITION OF THE n-PROPYL RADICAL. A. Bencsura, V. D. Knyazev, S.-B. Xing, I. R. Slagle, and D. Gutman; Symp. Internat. Combust, 1992, (Accepted for presentation and publication)

The kinetics of the unimolecular decomposition of the n-propyl radical has been investigated. The decomposition was monitored in time-resolved experiments by using a heatable tubular reactor coupled to a photoionization mass spectrometer. The radicals were produced by pulsed excimer photolysis of 4-heptanone. Unimolecular rate constants were determined as a function of bath gas (He, Ar, and N_2), temperature (12 temperatures between 620 and 730K) and bath gas density (6 densities between 3 and $30x10^{16}$ molecule cm^{-3} for He and 3 densities between 3 and $12x10^{16}$ molecule cm^{-3} for Ar and N_2). The rate constants are in the fall-off region under the conditions of these experiments. The data were fit using a Master Equation analysis. The average step-size down (the adjusted parameter in the analysis) is 220(He), 261(N_2), and 267(Ar) - all cm^{-1}. The unimolecular rate constants were parameterized for the temperature range 300-1000K and 0.001 to 10 atmospheres using a modified Lindemann-Hinshelwood expression. The energy transfer parameter, the step-size down, was assumed to be directly proportional to temperature in this temperature range.

C. KINETICS OF THE UNIMOLECULAR DECOMPOSITION OF CH_3CO I. R. Slagle, A. Bencsura, V. D. Knyazev, S.-B. Xing: Study in Progress

Because of the success in determinining the temperature dependence of the step-size down in the unimolecular decomposition of C_2H_5 (near 1000 K), we are remeasureing more accurately the unimolecular rate constants for the decomposition of CH_3CO, which is also essentially at the low pressure limit under our experimental conditions. Experiments are being conducted in the temperature range, 412-512 K. The bath gases used are He, Ar, and N_2. This study, combined with the other investigations of unimolecular decompositions of free radicals studied to date, is providing a coherent picture of energy transfer behavior in these reactions which extends from ≈400 K to ≈1100 K. This information complements the energy-transfer information being obtained from shock tube experiments conducted above 1000 K.

FUTURE STUDIES

During the next year the studies of the unimolecular decomposition of free radicals will continue. Additional investigations of the kinetics and mechanisms of the reactions of unsaturated polyatomic free radicals with molecular oxygen will be initiated. Finally, we shall begin a new set of experiments designed to investigate the chemical kinetics of cross combination reactions involving methyl radicals, CH_3 + R.

PUBLICATIONS (1990-Present)

1. A. F. Wagner, I. R. Slagle, D. Sarzynski, and D. Gutman, J. Phys. Chem. 1990, 94, 1853, "Experimental and Theoretical Studies of the $C_2H_5 + O_2$ Reaction Kinetics".
2. I. R. Slagle, J. R. Bernhardt, D. Gutman, M. A. Hanning-Lee, and D. Gutman, J. Phys. Chem. 1990, 94, 3652, "Kinetics of the Reaction between O Atoms and Allyl Radicals".
3. I. R. Slagle, G. W. Gmurczyk, L. Batt, and D. Gutman, 23rd Symposium (International) on Combustion; The Combustion Institute, 1991, 23, 115, "Kinetics of the Reaction between Oxygen Atoms and Propargyl Radicals".
4. I. R. Slagle, L. Batt, G. W. Gmurczyk, D. Gutman, and W. Tsang, J. Phys. Chem. 1991, 95, 7732. "The Unimolecular Decomposition of the Neopentyl Radical".
5. P. W. Seakins, I. R. Slagle, D. Gutman, M. J. Pilling, W. Tsang, and S. H. Robertson, 1992, Study completed, Manuscript in final preparation, "Time Resolved Studies of the i-C_3H_7 Decomposition using Laser-Flash Photolysis/Photoionization Mass Spectrometry".
6. Y. Feng, J. T. Niiranen, A. Bencsura, V. D. Knyasev, and W. Tsang; J. Phys. Chem., 1992, J. Phys. Chem., Submitted for Publication, Kinetics of the Unimolecular Decomposition of C_2H_5.
7. A. Bencsura, V. D. Knyazev, S.-B. Xing, I. R. Slagle, and D. Gutman; Symposium (International) on Combustion, 1992, (Accepted for presentation and publication), "Kinetics of the Thermal Decompositon of the n-Propyl Radical".
8. I. R. Slagle, A. Bencsura, S.-B. Xing, and D. Gutman; Symposium (International) on Combustion, 1992, (Accepted for presentation and publication). "Kinetics and Thermochemistry of the Oxidation of Unsaturated Radicals: $C_4H_5 + O_2$".

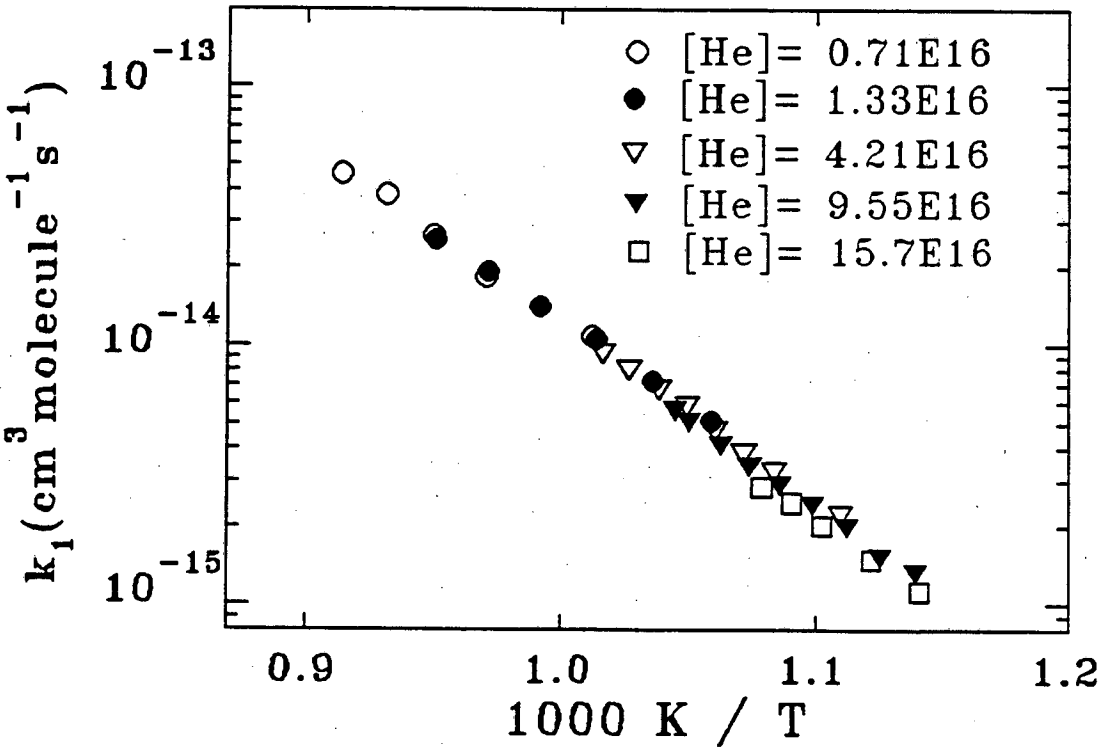

FIGURE 1 - Plot of Measured Second-Order C_2H_5 Decomposition Rate Constants.

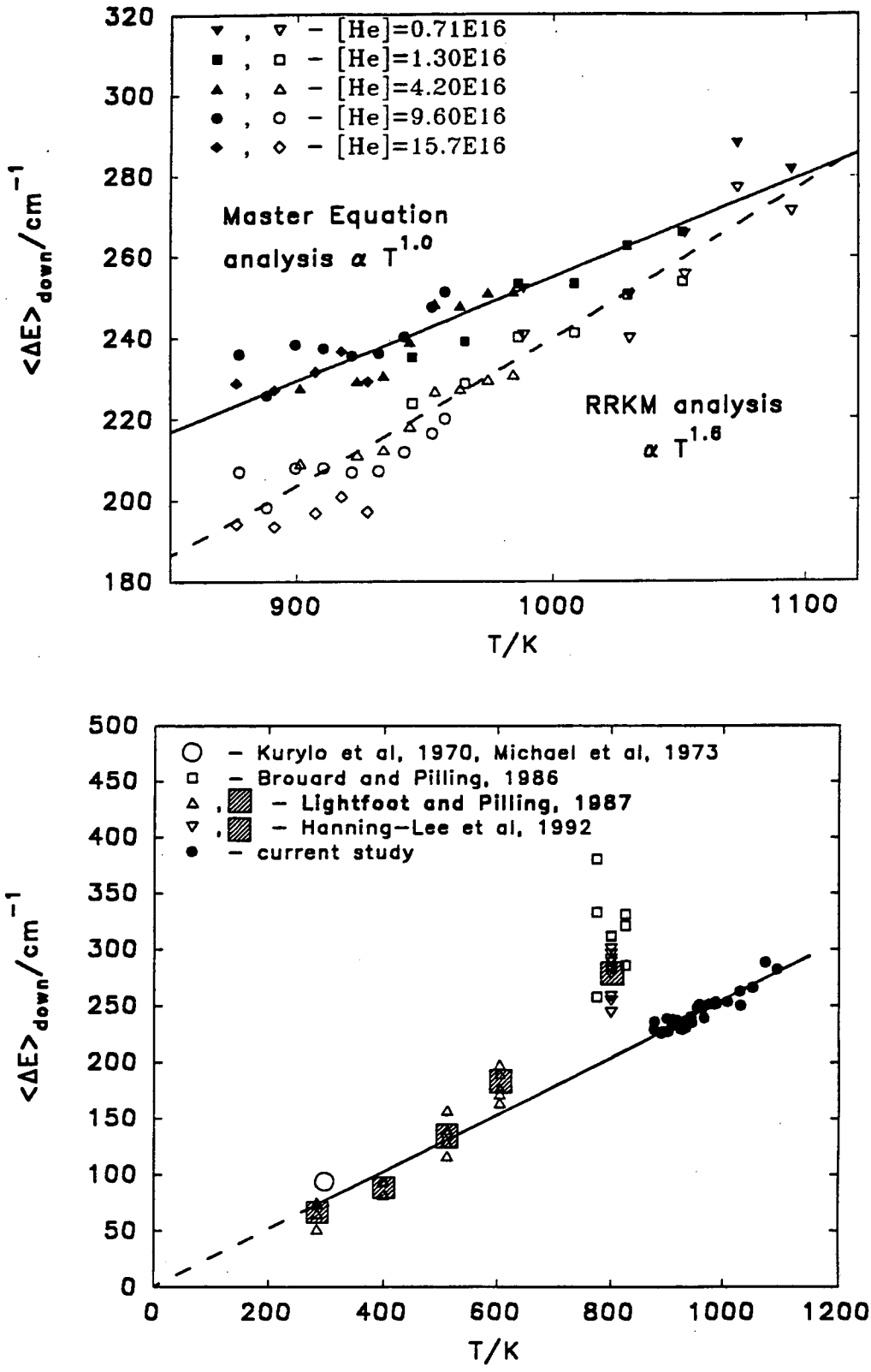

FIGURE 2 - Display of temperature dependence of $<\Delta E>_{down}$ for C_2H_5 decomposition. Above: from measured rate constants in Fig. 1 using both Master Equation and RRKM analyses of the data. Below: Master Equation values displayed with those derived from the results of other studies conducted at lower temperatures. Line is extrapolated temperature dependence observed near 1000 K.

SPECTROSCOPY AND KINETICS OF COMBUSTION GASES AT HIGH TEMPERATURES

Ronald K. Hanson and C. T. Bowman
High Temperature Gasdynamics Laboratory
Department of Mechanical Engineering
Stanford University
Stanford, CA 94305-3032

Program Scope

This program involves two complementary activities: (1) development and application of cw ring dye laser absorption methods for sensitive detection of radical species and measurement of fundamental spectroscopic parameters at high temperatures; and (2) shock tube studies of radical-molecule and radical-radical reactions relevant to combustion. Species currently under investigation in the spectroscopic portion of the research include NO and CH_3; this has necessitated the development of a unique intracavity frequency-doubling system for our cw laser which operates at wavelengths in the range 210-230 nm. Shock tube studies of reaction kinetics currently are focussed on reactions of CH_3 radicals.

Recent Progress

Work during the current reporting period has been focussed on the following activities:

UV Ring Dye Laser Development Over the past three years we have been working to extend the wavelength operating envelope of our cw ring dye laser further into the UV. In our initial effort we were able to implement a custom-built BBO frequency-doubler which provided access to wavelengths in the range 220-230 nm. This system provided output power levels up to 1 mW when pumped with 6 W of all-lines UV from an argon ion laser. More recently, we have been able to extend the laser to 209 nm using a new BBO crystal cut with a different phase-matching angle. In addition, refinements in other cavity elements and in our system alignment procedures have led to a modest improvement in laser power, to a maximum of about 1.5 mW. To our knowledge, this laser system is unique, and it provides important new capability both for fundamental spectroscopic studies and for sensitive detection of several important combustion species in shock tube kinetics experiments.

High-Resolution Spectroscopy We have begun to use this new UV laser capability for detailed study of absorption lineshapes of NO in the (0,0) band of the A←X system near 225 nm. Thus far, measurements have been made over a temperature range from 300-3000 K, with either nitrogen or argon as collision partners, thereby allowing determination of the temperature dependence of the collision-broadening coefficients. The absorption lineshapes are usually fit with Voigt profiles, although Galatry fitting routines have also been used. An example high temperature absorption record obtained with shock wave heating to 1584 K is shown in Fig. 1 for a 0.5% NO/Ar mixture. The important observations in this work have been that NO collision-broadening coefficients are quite large (about 5 times those observed in similar studies of OH lineshapes) and they exhibit very little dependence on rotational quantum number (again, in contrast with similar measurements of OH lines). We also measured collision shifts for several NO transitions, with the unexpected result that shift coefficients are typically 1/3 as large as the broadening coefficients for NO. Typical results for the broadening and shift coefficients versus

temperature are shown in Fig. 2. Finally, we should mention that strong collision-induced lineshape asymmetries were observed, especially at the low temperature end of the data set. Details of this initial work on NO spectroscopy may be found in paper 5 cited in the following Publications section. Future work will include expansion of the temperature range studied, and extension of collision partners to include H_2O and O_2.

Methyl Diagnostics and Kinetics During the past year we have used the UV ring dye laser to map out the absorption coefficient of CH_3 between 215 and 225 nm. The spectrum is relatively smooth, with two broad peaks near 216 nm. In order to put the measured wavelength and temperature dependences of the absorption coefficient on an absolute basis, as needed for subsequent shock tube kinetics studies, we measured the absorption at known levels of CH_3; several candidate sources of CH_3 were used, including tetramethyl tin, azomethane, tetramethyl silane, methyl iodide, and ethane. All of these species are highly reactive at high temperatures, and hence we found it necessary to combine the measurements with detailed kinetic modeling in order to find the optimum chemical mixtures for the temperatures of interest. The result of these measurements has been: (1) determination of the optimum detection wavelength for CH_3 absorption measurements, 216.6 nm; and (2) accurate determination of the absolute absorption coefficient at 216.6 nm as a function of temperature. It is important to note that we find an absorption coefficient which is about twice that inferred in earlier studies by other workers using a broadband arc source. A description of this work appears in papers 4 and 6 cited in the Publications section which follows.

With the sensitive laser absorption diagnostic now characterized, we are beginning study of methyl reactions. Recent activity has involved assessment of candidate sources of CH_3, including azomethane, methyl iodide, tetramethyl tin and ethane. A detailed mechanism for hydrocarbon reactions has been compiled for use in analyzing the CH_3 data, and preliminary experiments have been conducted of ethane and methane pyrolysis and oxidation reactions. In future work we plan to measure rate coefficients for reactions of CH_3 with O_2, NO, H_2 and OH.

Future Plans

Research during the coming year will include the following activities:

1. Continued work to improve the power level, wavelength operating range and stability of the UV ring dye laser.

2. Continued study of absorption lineshapes of NO, including determination of collision-broadening and collision-shift coefficients for H_2O, O_2, N_2 and Ar collision partners. This will include experimental measurements in static cell, flame and shock tube environments, and evaluation of available theories for NO lineshapes.

3. Continue study of ethane decomposition and initiate studies of CH_3 reactions with O_2, NO, H_2 and OH.

Publications (1990 - 1992)

1. D. F. Davidson and R. K. Hanson, "High Temperature Reaction Rate Coefficients Derived from N-Atom ARAS Measurements and Excimer Photolysis of NO," Int. J. of Chemical Kinetics **22**, 843-861 (1990).

2. D. A. Masten, R. K. Hanson and C. T. Bowman, "Shock Tube Study of the Reaction H + O_2 → OH + O Using OH Laser Absorption," J. Phys. Chem. **94**, 7119-7128 (1990).

3. D. F. Davidson and R. K. Hanson, "A Direct Comparison of Shock Tube Photolysis and Pyrolysis Methods in the Determination of the Rate Coefficient for O + H_2 → OH + H," Combustion and Flame **82**, 445-447 (1990).

4. D. F. Davidson, A. Y. Chang, M. D. DiRosa and R. K. Hanson, "Development of a CW Laser Absorption Diagnostics for CH_3," paper WSS/CI 91-20 at WSS/CI Spring Meeting, Boulder, CO, March 18-19, 1991.

5. A. Y. Chang, M. D. DiRosa and R. K. Hanson, "Temperature Dependence of Collision Broadening and Shift in the NO A←X (0,0) Band in the Presence of Argon and Nitrogen," J. Quant. Spectrosc. Radiat. Transfer, in press.

6. D. F. Davidson, A. I. Chang, M. D. DiRosa and R. K. Hanson, "A CW Laser Absorption Diagnostic for Methyl Radicals, J. Quant. Spectrosc. and Radiat. Transfer, submitted 3/92.

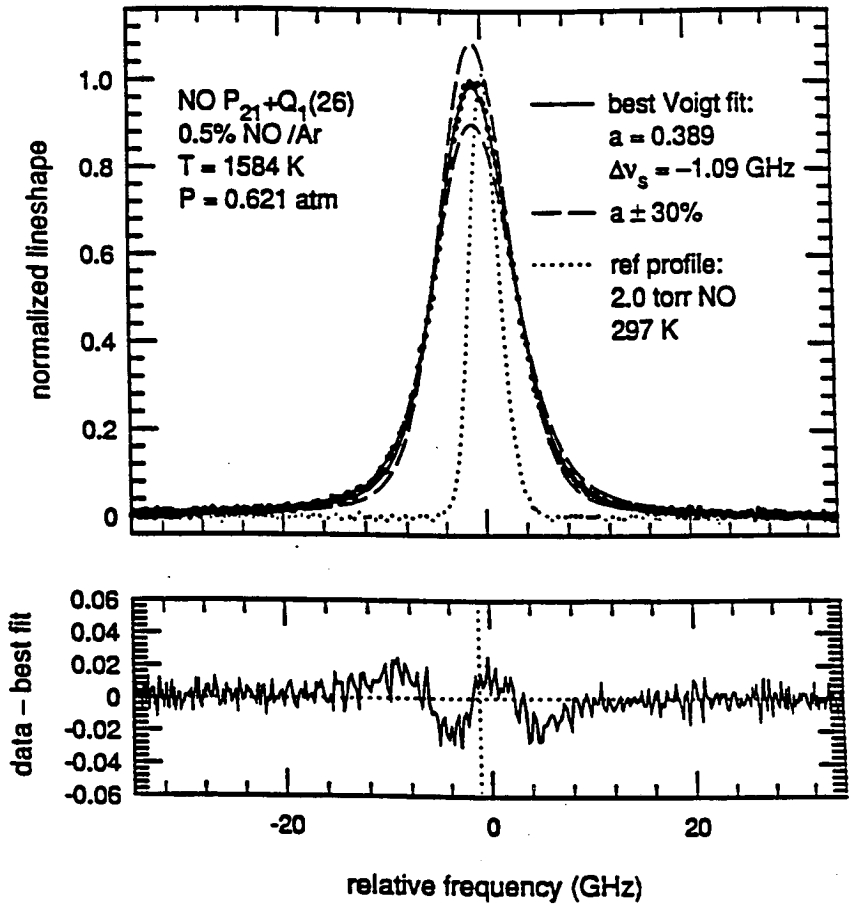

Fig. 1. Absorption lineshape and shift data for NO in Ar.

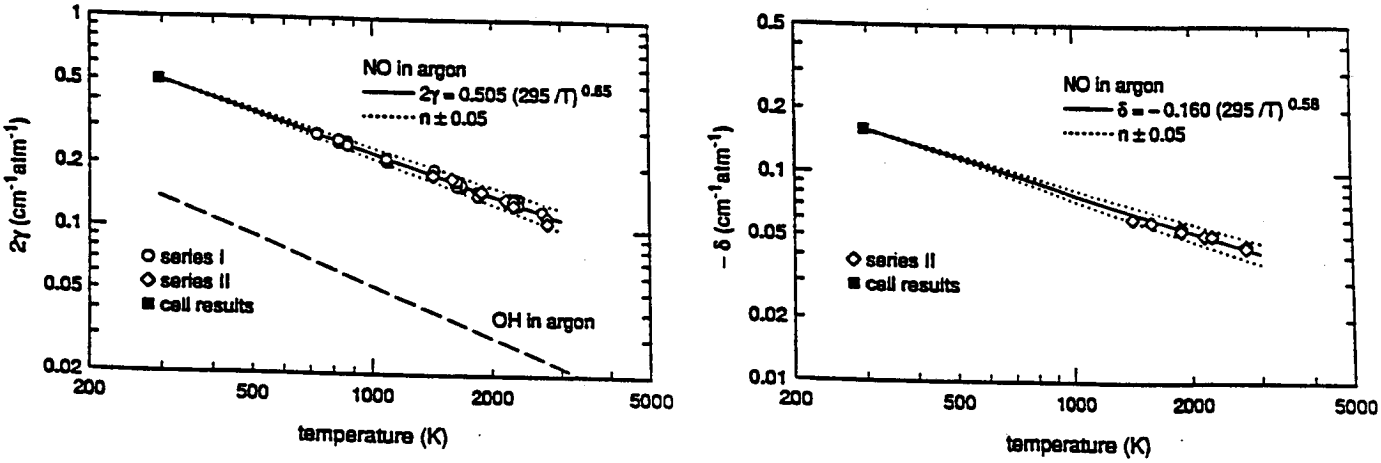

Fig. 2. Collision-broadening and shift coefficients for NO in Ar as a function of temperature.

Theoretical Studies of Potential Energy Surfaces and Computational Methods*

Lawrence B. Harding, Robert J. Harrison and Ron Shepard

Chemistry Division
Argonne National Laboratory
Argonne, IL 60439

The goal of this program is to calculate accurate potential energy surfaces (PES) for both reactive and nonreactive systems. To do this the electronic Schrödinger equation must be solved. Our approach to this problem starts with multiconfiguration self-consistent field (MCSCF) reference wave functions. These reference wavefunctions are designed to be sufficiently flexible to accurately describe changes in the electronic structure over a broad range of geometries. Electron correlation effects are included via multireference, singles and doubles configuration interaction (CI) calculations. With this approach, we are able to provide useful predictions of the energetics for a broad range of systems. Complementary to this theoretical effort, a new initiative in the group aims to harness the cost-effectiveness and high peak-performance offered by parallel computers. We are following a dual strategy of porting existing production codes to few processor machines as well as developing tools and algorithms suitable for highly parallel computers. The following is a summary of recent progress and future plans in this program.

Global Ground State Methylene Potential Surface. This year a global, ground state potential surface for CH_2 has been constructed. The surface is based on large (polarized triple-zeta) basis set, MRSDCI calculations employing a full valence, CAS reference wavefunction. These calculations are expected to be accurate to within a few kcal/mole. The calculations indicate the presence of three low energy surface crossings, two for linear geometries and one for C_{2v} geometries. The C_{2v} crossing between the $^3B_1$ and $^3A_2$ surfaces provides a zero barrier route for the $C+H_2$ insertion reaction. Linear surfaces crossings between $^3\Pi$ and $^3\Sigma^-$ surfaces were also located for both the CH + H addition and abstraction reactions.

A modified many-body expansion was used to fit the complex topology of this surface. The potential is constructed from a qualitatively accurate, globally defined, inverse power series expansion and a number of more accurate locally defined potentials. The local potentials are switched on and off with polynomial switching functions of finite range. The local potentials in the vicinity of the surface crossings are constructed from a diabatic representation to describe the conical intersections that result from these crossings. It is planned that this surface will be used both in dynamical studies on the effect of the $^3B_1$-$^3A_2$ conical intersection on the $C+H_2$ insertion reaction and as a building block in the planned construction of a global CH_3 surface.

Electronic Structure Code Maintenance and Development. During the past year, the COLUMBUS Program System of electronic structure codes has been maintained on the various machines used by the Theoretical Chemistry Group, including the Sun workstations, the Stardent Titans, the Argonne Cray X-MP, and the Cray Y-MP at SCRI at Florida State University. Additionally, the codes have been ported to the group's new Alliant FX/2812 and to the Cray-2 at NERSC at Livermore National Laboratory. The COLUMBUS Program System is maintained and developed collaboratively with several researchers including Isaiah Shavitt and Russell M. Pitzer (Ohio State University), Hans Lischka (University of Vienna, Austria), and Reinhart Ahlrichs (University of Karlsruhe, Federal Republic of Germany).

A general multireference configuration interaction energy gradient code, CIGRD, has been developed. In addition to allowing frozen core orbitals, the program also includes density matrix and fock matrix resolution of invariant active orbital subspaces and fock matrix resolution of the virtual orbitals. Analytic energy gradients may also be computed for multireference coupled-pair-functional energies. In addition to the computation of analytic energy gradients, the new formalism lends itself to the computation of other general energy response properties. These are properties that may be written in the form $dE^{ci}/d\lambda$ where λ is a measure of a perturbation to the standard electronic hamiltonian operator. These properties include the dipole moment and the dipole moment derivatives. Examples of both of these properties have been demonstrated with the new method. Calculations of analytic energy gradients for large-scale MRSDCI wave functions using program CIGRD demonstrate, for the first time, that the effort required for the energy gradient is a small fraction of that required for the energy, even for larger molecules with many degrees of freedom. This property is due to a new formulation of the energy gradient, based on successive orbital transformations, and to a strict adherence to the principle of eliminating any displacement dependence from the intermediate computations. The method also exploits the natural advantage of variational energies, such as MRSDCI and MR-ACPF, over nonvariational energy methods such as perturbation theory or coupled-cluster expansions.

Public Distribution of the COLUMBUS Program System. The COLUMBUS Program System is now available using the *anonymous ftp* facility of internet from the server `ftp.tcg.anl.gov`. In addition to the source code, the complete online documentation, installation scripts, example calculations, and numerous other utilities are included in the distribution.

Electronic Structure Method Development. A new method of MCSCF wave function optimization has been developed. This method, called Trigonometric Interpolation, is based on a nonlinear transformation of the wave function variation coordinates along with the construction of a global interpolating function. This interpolating function is constructed for each MCSCF iteration in such a way that it reproduces certain known behavior of the exact energy function. The optimization of the wave function correction parameters on this interpolating function does not require integral transformations or density matrix constructions, although one-index transformation and transition density matrix techniques may be used if desired. The nonlinear coordinate transformations, along with the necessary derivatives, are computed with simple matrix operations, and require only $O(N_{orb}^3)$ effort. The new method may be implemented as a simple extension to essentially any existing second-order MCSCF code, the required changes being localized within a rather small part of the overall iterative procedure.

Full CI calculations. A new full-CI program is being developed for massively parallel machines. The new program is fully spin-adapted and uses an algorithm up to an order of magnitude faster than the previous most efficient implementation. It is anticipated that running on the Touchstone Delta this code will make routine benchmark-quality FCI calculations with $O(10^8–10^9)$ configurations that have up to now required substantial effort and resources. A prototype version is running in parallel on our Alliant FX/2800, computing vibrational frequencies for CH_3 at the FCI level of theory in a cc-pVDZ basis. On the Alliant this new code runs this problem as fast as the our determinant code on a single processor of a CRAY-2.

Parallel programming. Our portable message-passing toolkit is now in use at over 50 sites, including universities, and both national and industrial laboratories (e.g. Ford, GM, Boeing). It has been ported to many new UNIX machines and has been extensively optimized on the Touchstone Delta. A model (no I/O) four-index transformation code realized over 13 GFLOPS on the Touchstone Delta. A realistic benchmark including I/O would achieve approximately 4 GFLOPS. This toolkit has been used to implement many portable parallel programs, including the

parallel version of the COLUMBUS MRSDCI program, in collaboration with the group of H. Lischka at the University of Vienna. This code has been benchmarked on many parallel machines, including CRAY-YMP, iPSC-i860, Alliant and a network of SUNs. Poor scaling of I/O with the number of processes currently limits performance; but this bottleneck is being addressed with an AO integral driven algorithm.

A three day international workshop with 40 invited participants was held in July, 1991. This was funded jointly by ANL discretionary funds and the Molecular Science research Center, Battelle Memorial Pacific Northwest Laboratories. The research subjects represented included: the simulation of condensed phases and biological systems with molecular dynamics, ab initio electronic structure, classical and quantum reaction dynamics, quantum monte carlo methods, parallel programming languages and performance modeling. The proceedings of the workshop will be published in a special double issue of Theoretica Chimica Acta.

Greens Function Monte Carlo. Work is in progress on a new exact Green's Function Monte Carlo (GFMC) algorithm. A standard approximation to the importance-sampled short-time Greens's function is related via an integral equation to the exact importance-sampled Green's function. The resulting algorithm is a simple modification to existing short-time Diffusion Quantum Monte Carlo codes, and requires computation of no new information. This work is still within the fixed-node approximation for fermions.

*Work performed under the auspices of the Office of Basic Energy Sciences, Division of Chemical Sciences, U.S. Department of Energy, under Contract W-31-109-Eng-38.

PUBLICATIONS:

A Data Compression Method Applicable to First-Order Convergent Iterative Procedures
R. Shepard, *J. Comp. Chem.* **11**, 45-57 (1990)

Ab Initio Theoretical Studies of the CH_2+H $\rightleftharpoons$ CH_3 $\rightleftharpoons$ CH+H_2 Reactions
M. Aoyagi, R. Shepard, A. F. Wagner, T. H. Dunning, and F. B. Brown
J. Phys.Chem. **94**, 3236-3241 (1990)

Ab Initio Examination of the Electronic Excitation Spectrum of CCH
A.G. Koures and L.B. Harding, *J. Phys. Chem.* **95**, 1035-1040 (1991)

Approximating Full-CI with Selected CI and Perturbation Theory
R.J. Harrison, *J. Chem. Phys.* **94**, 5021-5031 (1991)

Analytical Calculation of Full CI Response Properties Application to Be
H. Koch and R.J. Harrison, *J. Chem. Phys.* **95**, 7479-7485 (1991)

Portable Tools and Applications for Parallel Computers
R.J. Harrison, *Int. J. Quant. Chem.* **40**, 847-863 (1991)

A Parallel Version of ARGOS. A Distributed Memory Model for Shared Memory Computers
R.J. Harrison and R.A. Kendall, *Theor. Chim. Acta* **79**, 337-347 (1991)

Proceedings of the Argonne Integral Evaluation Workshop
Edited by J. Almlöf, R. Shepard, and R. J. Harrison, *Int. J. Quantum Chem.* **40** (1991)

Theoretical Studies of the Hydrogen Peroxide Potential Surface. 2. An Ab Initio, Long-Range, $OH(^2\Pi) + OH(^2\Pi)$ Potential
L. B. Harding, *J. Phys. Chem.* **95**, 8653-8660 (1991)

REMPI Mass Spectrum of the OH Radical in the Gas Phase
R. Forster, H. Hippler, K. Hoyermann, G. Rhode and L.B. Harding
Chem. Phys. Letts. **183**, 465-470 (1991)

An Ab Initio Theoretical Study of the $CH_2+H \rightleftharpoons CH_3 \rightleftharpoons CH+H_2$ Reactions
M. Aoyagi, R. Shepard and A. F. Wagner
International Journal of Supercomputing Applications **5**, 72-89 (1991)

The COLUMBUS Standard Integral File Structure: A Proposed Interchange Format
R. Shepard, *Int. J. Quantum Chem.* **40**, 865-887 (1991)

A General MRCI Gradient Program
R. Shepard, H. Lischka, P. G. Szalay, T. Kovar, and M. Ernzerhof
J. Chem. Phys. **96**, 2085-2098 (1992)

Isotope Effects in Addition Reactions of Importance in Combustion: Theoretical Studies of the Reactions $CH+H_2 \rightleftharpoons CH_3^* \rightleftharpoons CH_2+H$
A.F. Wagner and L.B. Harding, *ACS Symposium Series* (in press)

The Homogeneous Pyrolysis of Acetylene II: The High Temperature Radical Chain Mechanism
J.H. Kiefer, S.S. Sidhu, R.D. Kern, K. Xie, H. Chen, and L.B. Harding
Comb. Science Tech. (in press)

On the Global Convergence of MCSCF Wave Function Optimization: The Method of Trigonometric Interpolation
R. Shepard, *Theoretica Chim. Acta* (in press)

Elimination of the Diagonalization Bottleneck in Parallel Direct-SCF Calculations
R. Shepard, *Theoretica Chim.Acta* (in press)

A Quasiclassical Trajectory Study of OH Rotational Excitation in OH+CO Collisions using Ab Initio Potential Surfaces
K. Kudla, A.G. Koures, L.B. Harding, and G.C. Schatz, *J. Chem. Phys.* (in press)

A Portable, Parallel Four-Index Transformation: A Distributed-Memory Approach
L.A. Covick, K.M. Sando and R.J. Harrison, *J. Comp. Chem.* (in press)

Moving Beyond Message Passing. Experiments with A distributed-Data Model
R.J. Harrison, *Theoretica Chim. Acta* (in press)

Electron Affinities of the First Row Atoms Revisited: Systematic Basis Sets and Wavefunctions
R.A. Kendall, T.H. Dunning, Jr. and R.J. Harrison, *J. Chem. Phys.* (in press)

Laser Induced Grating Spectroscopy

Carl C. Hayden and David W. Chandler
Combustion Research Facility
Sandia National Laboratory
Livermore, CA 94551

Highly vibrationally excited molecules play an important role in many chemical processes and are often intermediates in chemical reactions. Characterizing these highly vibrationally excited molecules spectroscopically can be difficult because they are usually only present in low concentrations. This abstract describes our progress at developing a technique to detect absorptions of laser-excited molecules. We have shown that it is sufficiently sensitive to use with very weak optical transitions such as vibrational overtones.

The sensitivity of this method results from the use of the transient-grating technique[1] to detect laser-induced absorption. The transient grating is produced by the interference of two light beams of the same frequency, derived from a single laser, that cross at a small angle in the sample. When these excitation beams are tuned to an absorption of the gas sample, their interference creates a periodically varying spatial distribution of excited molecules. Absorption by the excited molecules is probed with a separate laser beam at a different frequency. For a probe laser frequency that is absorbed by the excited molecules, the spatial modulation of their number density acts as a transmission diffraction grating, and a small fraction of the probe beam is diffracted into a new direction. The experimental apparatus is shown schematically in Fig. 1.

A primary advantage of the laser-induced grating technique is that it can detect absorption of excited molecules directly. The technique is very sensitive because the measurements are background free, in contrast to usual absorption methods that require detecting minute intensity changes in light beams. Another sensitive approach to monitoring excited state absorption, laser detection of dissociation fragments, requires that the absorption result in dissociation and that there are appropriate techniques for detecting the fragments. However, since the grating technique directly monitors the induced absorption at the probe wavelength it is applicable to the study of a much wider range of excited state absorptions.

For optimum diffraction efficiency the probe beam must satisfy the Bragg condition for the grating. This determines the necessary incidence angle of the probe relative to the excitation beams. Focussing the laser beams relaxes this phase-matching condition somewhat, allowing the excitation or probe beam wavelength to be scanned over a fairly wide range.

In initial experiments, the $\Delta v=4$ overtone of the OH stretch in water was excited and the absorption of the excited water molecules was probed at 266 nm. This system was chosen to test the sensitivity of the technique because the overtone absorption is extremely weak and the absorption of the vibrationally excited molecules has been previously observed[2]. The water absorption at 266 nm is due to a dissociative electronic transition that occurs at wavelengths below 200 nm for ground-state water but is shifted far to the red upon vibrational excitation. The overtone excitation was performed using the output of a Nd:YAG-pumped dye laser operating in the 720 nm region. Approximately 30 mJ of the dye laser output was split equally between the two excitation beams. Fig. 2 shows the spectrum obtained when the excitation-laser wavelength is scanned through a region of the $\Delta v=4$ overtone absorption in water. The spectrum is detected by monitoring diffracted 266 nm probe light. Spectra were taken at water pressures from 20 torr down to about 3 torr to ensure that collisional processes within the 7 ns laser pulse widths did not dominate the spectrum. This spectrum shows that, using the transient grating method, it is possible to detect induced absorptions in small concentrations of laser excited molecules thus allowing

us to study excited states that are accessed only by very weak optical transitions such as vibrational overtones.

As the pressure in the sample is increased so that collisions remove energy from the initially excited molecules thermal gratings are produced which will diffract the probe laser beam independent of its wavelength. We have taken 4-0 and 5-0 O-H stretching overtone spectra of methanol using this effect with an experimental apparatus identical to that used to detect the population grating produced in water (Fig.1). We distinguish population gratings from thermal gratings by the time signature of the signal intensity as a function of time delay between the pump and probe laser beams as well as the pressure dependence of the signal.

We have also performed experiments in which the excitation beams excite an electronic transition in gas-phase iodine and the probe beam, at a longer wavelength, is tuned over transitions that de-excite the molecules by stimulated emission to highly vibrationally excited ground-state levels. In this case the probe beam is diffracted by a grating of spatially modulated gain instead of absorption. The difference between the excitation and probe-beam frequencies corresponds to the energy of high vibrational levels of the ground electronic state of iodine. Figure 3 shows a spectrum obtained using iodine at its room temperature vapor pressure. The excitation wavelength at 532 nm is obtained by frequency doubling a single-mode, injection-seeded Nd:YAG laser. The probe beam is obtained from a dye laser pumped by the same Nd:YAG laser. Although the probe-beam wavelength scans over a great number of iodine absorption lines, diffraction signal appears only when the probe laser is tuned to a transition involving a state selected by the excitation laser.

Two types of transitions cause diffracted signal from the probe beam. In one case, the probe causes stimulated emission from a grating composed of excited-state molecules and the spectrum observed corresponds to the fluorescence spectrum from the excited state. In the other case, the grating consists of ground electronic state molecules in the particular state depleted by the excitation beams and the resulting spectrum is the absorption spectrum of that state. The dispersed fluorescence spectrum in Fig. 3 shows that some of the lines in the induced-grating spectrum do not correspond to fluorescence wavelengths and therefore must result from ground state absorptions. All of the observed transitions have been assigned.

In related experiments, an tunable ArF excimer laser beam (~193 nm) was used to generate three parallel beams of intense UV light (about 1 mj/pulse each) arranged at three corners of a rectangle. This is the experimental arrangement used to perform Degenerate Four Wave Mixing in a forward geometry. In this manner we are able to detect H_2 via the two-photon allowed E,F $^1\Sigma_g^+ \leftarrow X^1\Sigma_g^+$ transition, CO via the spin-forbidden $a^3\Pi \leftarrow X^1\Sigma^+$ transition and O_2 via the B $^3\Sigma^-_u \leftarrow X\ ^3\Sigma^-_g$ (Schumann-Runge band) transition. The tunable KrF excimer laser (~248 nm) was used to monitor H_2O via the C $^1B_1 \leftarrow X\ ^1A_1$ transition. The signal comes out of the sample as a light beam at the fourth corner of the rectangle. In all cases the molecules are detected state-selectively. Success of these initial experiments indicates that this technique may have wide application in combustion systems. It is not possible at this time to state with certainty the origin of the gratings that are being formed in these gas-phase sample but from the almost linear power dependences we observe in these experiments it is clear that we are in a highly saturated regime.

These initial experiments demonstrate that this technique is a very promising approach to measuring absorptions of excited state molecules in the gas phase. It is applicable to a wide range of molecules, and can give information about states that do not fluoresce. An additional example of such a system is gas phase nitric acid in which we have recently detected induced absorptions following overtone excitation. One important consideration in interpreting results from the grating technique is that it is sensitive to both absorption and refractive-index modulations induced in the sample. This can create signals

that are not related to the absorptions of interest. Further work is needed to understand these additional signal sources. Additional work will also be directed toward measuring absorption spectra of molecules in vibrational overtone states and extending the technique to other molecules.

References:

1. See, for example, H.J. Eichler, P. Gunter, and D.W. Pohl, *Laser-Induced Dynamic Gratings*, (Springer-Verlag, Berlin, Heidelberg, 1986).

2. R.L. Vander Wal and F.F. Crim, J. Phys. Chem. **93**, 5331 (1989).

Publications:

Mark A. Buntine, David W. Chandler and Carl C. Hayden " A Two-Color Laser-Induced Grating Technique for Gas-Phase Excited-State Spectroscopy" J. Chem. Phys. Submitted (1992).

Gerard Meijer and David W. Chandler "Degenerate Four Wave Mixing on Weak Transitions in the Gas Phase Using a Tunable Excimer Laser" Chem. Phys. Lett. accepted for publication (1992).

Gerard Meijer, Michel Versluis and David W. Chandler "Degenerate Four-Wave Mixing Using a Tunable Excimer Laser to Detect Combustion Gases" Accepted Twenty Fourth International Symposium on Combustion (1992).

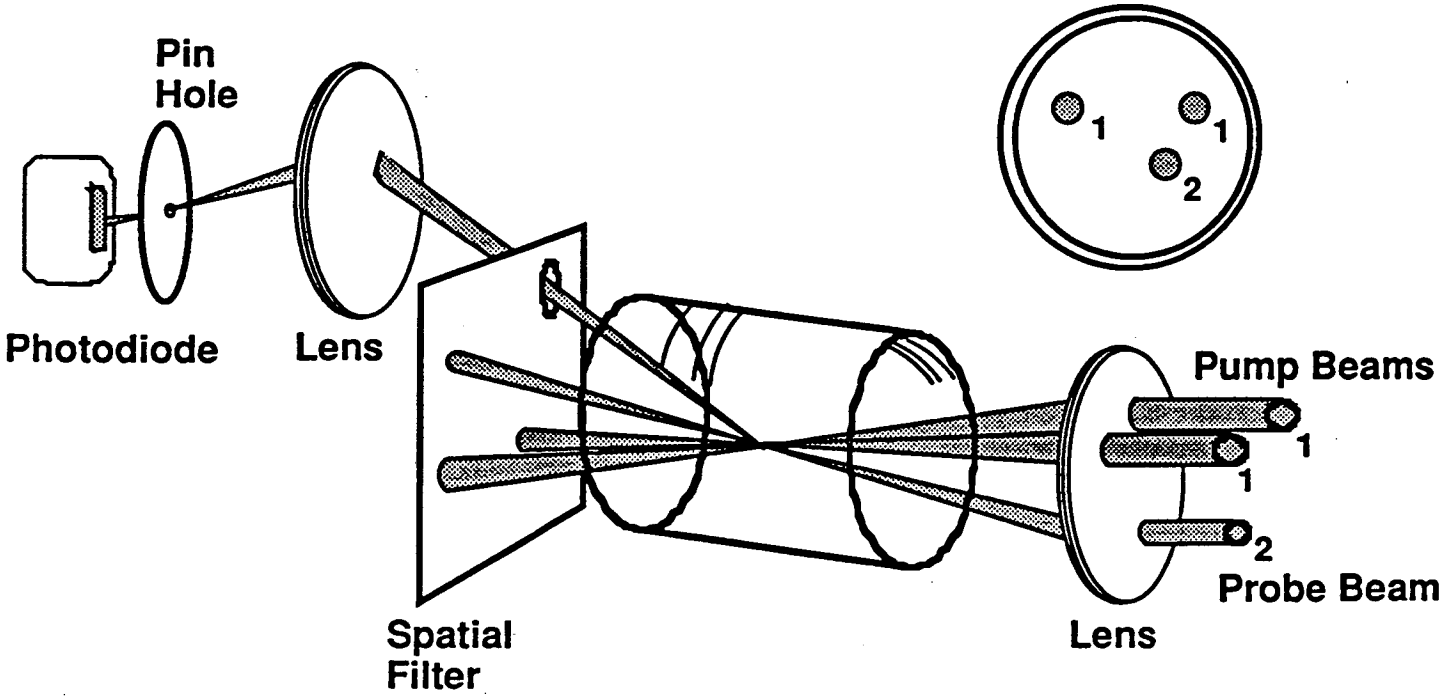

Figure 1. Schematic diagram of the experimental setup for two-color, laser-induced grating (TCLIG) excited-state spectroscopy experiments.

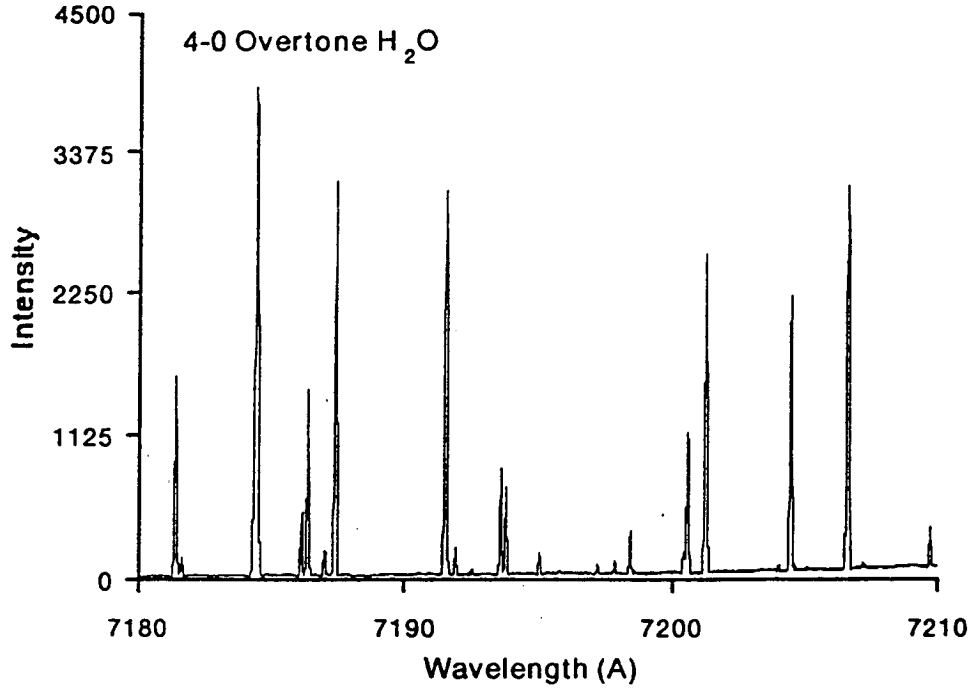

Figure 2. A portion of the 4-0 overtone spectrum of the OH stretch in water. The spectrum was obtained from an 18 torr sample of water vapor by monitoring the diffraction of a 266 nm probe beam as the excitation laser was scanned through the wavelength range shown.

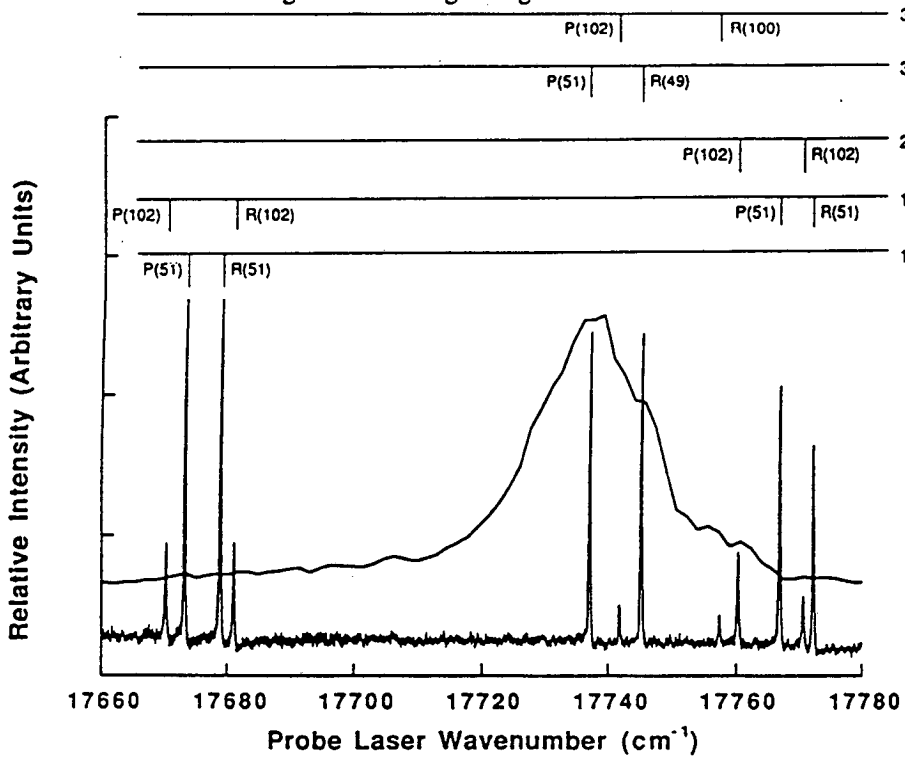

Figure3. Transient grating spectrum of I_2 recorded via TwoColor-LIGS detection. Resonances are evident from both stimulated emission and diffraction from ground state rotational levels depleted by *pump*-laser photons. The *pump* laser was tuned to the near-degenerate I_2 ($B\ ^3\Pi_{0u}^+ - X\ ^1\Sigma_g^+$) 32-0 P(51) and 34-0 P(102) transitions. Stimulated emission resonances in the spectrum are labelled by the rotational quantum number of the X (v=5) vibronic state. Ground state absorption features are labelled by the vibronic transition into the B electronic state. Also shown by the upper curve is the corresponding dispersed emission spectrum following excitation by the *pump* laser.

Femtosecond Laser Studies of Ultrafast Intramolecular Processes

Carl Hayden and Rick Trebino
Combustion Research Facility
Sandia National Laboratories
Livermore, CA 94551-0969

Program Scope

The goal of this research is to better understand the detailed mechanisms of chemical reactions by measuring the rates of fundamental chemical processes. In this work femtosecond laser pulses are used to initiate chemical processes and to follow the progress of these processes in time. We are currently studying the predissociation of NO_2 in the UV as a function of excitation wavelength. In addition, we are developing techniques to measure the time evolution of large-amplitude vibrations in ground-electronic-state molecules.

Recent Progress

In recent experiments we have directly observed transient absorption from the excited state in the near-UV predissociation of NO_2. Studies of the absorption and photofragment-excitation spectra of NO_2[1-3] have found spectral structure indicating that near the dissociation threshold at 398 nm, the initially excited state must have a lifetime on the order of several picoseconds. The spectral features become much broader at higher excitation energies, implying a shorter lifetime, but some structure persists for excitation energies more than 5000 cm^{-1} above the dissociation threshold. The product state distributions also show evidence for a change in the dissociation dynamics with increasing energy. At an excitation wavelength of 337 nm, about 4500 cm^{-1} above threshold, the dissociation produces a highly nonstatistical product state distribution.[4] However, for 347 nm dissociation, the product state distribution appears to be statistical.[5] Femtosecond transient-absorption measurements allow us to study these changes in the dissociation dynamics directly by following the NO_2 dissociation process in real time.

The femtosecond pulses needed for these experiments are produced by a laser system that we have developed over the past two years. Low power pulses are generated initially by a colliding-pulse mode-locked dye laser operating at 628 nm. These 300 pJ pulses are amplified to 100 μJ in a multi-pass dye amplifier. A portion of the amplified pulse is focussed into a thin quartz window to generate a broad-band continuum. The desired bandwidth filtered from this continuum is further amplified to produce a high energy, tunable output. For the current experiments, this laser system generates 300 μJ pulses tunable around 750 nm with a pulse length of about 60 fsec. Doubling into the UV yields 180 fsec pulses with pulse energies of about 25 μJ. Recently we have added an additional continuum source and amplifier chain for experiments that require precisely synchronized, independently tunable excitation and probe pulses.

Our experiments on NO_2 predissociation were performed by directly measuring the change in transmission of a probe pulse as a function of its time delay relative to the excitation pulse. The output from the femtosecond dye amplifier system is first frequency doubled with low efficiency to produce the probe pulse and then the remaining near IR is also doubled but with higher efficiency to generate the excitation pulse. The two pulses are weakly focussed through a cell containing the flowing NO_2 sample. The probe pulse intensity is monitored before and after passing through the sample cell and the change in sample transmission is calculated on each shot by a computer. The computer also controls the scanning of a precision translation stage that determines the relative delay between the excitation and probe pulses.

The initial results of these transient-absorption experiments are shown in Figure 1. The total change in transmission displayed is about one percent. All of the plots have a positive going coherence spike at zero delay, which is due to the windows and remains even when NO_2 is removed from the cell . The NO_2 absorption transient is negative going, starting at zero delay and continuing for positive delays, where the probe follows the excitation pulse. The negative sign of the transmission change indicates that the dominant effect observed is excited-state absorption, as opposed to stimulated emission back to the ground state. The final transmission level is higher than the initial transmission due to the depletion of ground state molecules by the photodissociation. The observed decays place a lower limit on the predissociation lifetime, but the dissociation lifetime may exceed the observed decay time if the excited state absorption evolves out of the bandwidth of the probe before the molecule dissociates. Compared to the results at longer wavelengths, the data at 370 nm appear to show a significant change in the excited state dynamics. The decay at this wavelength is faster, consistent with the spectral data, and also shows some structure. This could result from the excitation of more than one resonant intermediate state, or perhaps from interference between exit channels. Further data are needed to determine in detail the dynamics that give rise to these results.

Future Plans

The initial results obtained with NO_2 indicate that transient-absorption techniques will make it possible to follow the predissociation process in time. More sensitive transient absorption probes, such as transient grating methods or the use of the antiresonant ring,[6] can be used to improve the signal-to-noise ratio in the experiments so that more detailed comparisons can be made among results at different wavelengths. It would also simplify interpretation of the results if the probe absorption were to a single, well-defined state for all excitation wavelengths. The ability of our laser system to provide independently tunable excitation and probe wavelengths makes this possible.

Another important objective of our research program is to study the time evolution of large amplitude motions on the *ground* electronic potential surface, where most chemical reactions occur. Initially we plan to use vibrational overtone excitation on a femtosecond time scale to excite hydrogen-atom stretching vibrations. The time evolution of this excitation throughout the molecule will be followed by monitoring changes in the UV absorption with femtosecond probe pulses. Our laser system is designed to produce high

energy pulses in the 750 nm region for the purpose of exciting the third overtone of OH stretching vibrations.

References

1. T. C. Hall, Jr. and F. E. Blacet, J. Chem. Phys. **20**, 1745 (1952).
2. U. Robra, H. Zacharias and K. H. Welge, Z. Physik D **16**, 175 (1990).
3. J. Miyawaki, K. Yamanouchi and S. Tsuchiya, Chem. Phys. Lett. **180**, 287 (1991).
4. H. Zacharias, M. Geilhaupt, K. Meier and K. H. Welge, J. Chem. Phys. **74**, 218 (1981).
5. M. Quack and J. Troe, Ber. Bunseges. Phys. Chem. **79**, 469 (1975).
6. R. Trebino and C. C. Hayden, Opt. Lett. **16**, 493 (1991).

Publications, 1990-Present

C.C. Hayden and R. Trebino, "Coherent Interactions in Two-Beam Excite-Probe Absorption Measurements: Phase Gratings in Flowing Samples," Appl. Phys. B **51**, 350 (1990).

R. Trebino and C.C. Hayden, "The Anti-Resonant Ring in Ultrafast Excite-Probe Spectroscopy," in *Ultrafast Phenomena VII*, eds. C.B. Harris, E.P Ippen, G.A. Mourou, and A.H. Zewail, (Springer-Verlag, Berlin, Heidelberg, 1990), p. 157.

R. Trebino, C.C. Hayden, A.M. Johnson, W.M. Simpson, and A.M. Levine, "Chirp and Self-Phase Modulation in Induced-Grating Autocorrelation Measurements of Ultrashort Pulses," Opt. Lett. **15**, 1079 (1990).

R. Trebino and C.C. Hayden, "Velocity Measurement Using the Phase of a Laser-Induced Grating," Opt. Lett. **15**, 1397 (1990).

R. Trebino and C.C. Hayden, "Anti-Resonant-Ring Transient Spectroscopy," Opt. Lett. **16**, 493 (1991).

A.M. Levine, E. Ozizmir, R. Trebino, and C.C. Hayden, "New Developments in Autocorrelation Measurements of Ultrashort Pulses," *Laser Spectroscopy X*, eds. M. Ducloy, E. Giacobino, and G. Camy (1991) in press.

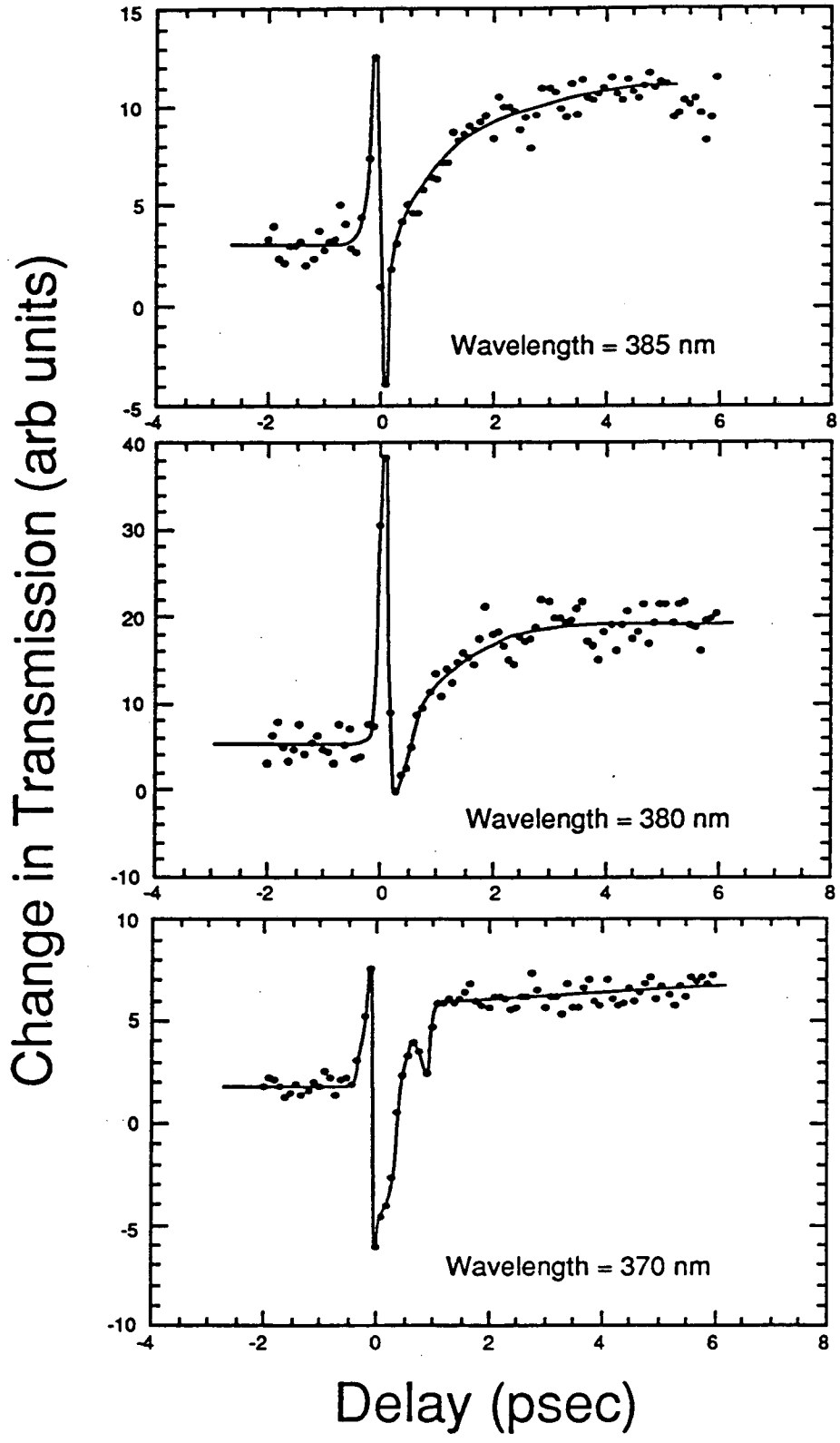

Figure 1. NO_2 transient absorption at three wavelengths. The probe and excitation pulses have the same wavelength. The line through the points is added for clarity and is not a fit to the data.

Elementary Reaction Rate Measurements at High Temperatures by Tunable-Laser Flash-Absorption

Jan P. Hessler

Gas Phase Chemical Dynamics Group
Chemistry Division
Argonne National Laboratory
9700 South Cass Avenue
Argonne, Illinois 60439

The major objective of this program is to measure thermal rate coefficients and branching ratios of elementary reactions. To perform these measurements, we have constructed an ultrahigh-purity shock tube to generate temperatures between 1000 and 5500 K. The tunable-laser flash-absorption technique is used to measure the rate of change of the concentration of species which absorb below 50,000 cm^{-1} *e.g.*: OH, CH, and CH_3. This technique is being extended into the vacuum-ultraviolet spectral region where we can measure atomic species *e.g.*: H, D, C, O, and N; and diatomic species *e.g.*: O_2, CO, and OH.

Correlation Analysis While evaluating our high-temperature measurements of the kinetic behavior of hydroxyl to determine the rate coefficient for $H + O_2 \rightarrow O + OH$ we noticed that sensitivity coefficients did not quantitatively predict the relative importance of different reactions nor did they provide any information about the correlation between the rates of the reactions. Rates of reactions are correlated if a change in one rate coefficient may be accompanied by a correlated change in another rate coefficient such that a calculation of an experimental observation would remain essentially the same. To establish a new quantitative scheme for utilizing sensitivity coefficients we have combined concepts from non-linear least-squares analysis with the definition of sensitivity coefficients to devise a scheme which determines (1) the relative importance of reactions for predicting the behavior of a specific observable over a given interval, and (2) the degree to which the reactions are correlated. This scheme may be used to design experiments, to calculate the propagation of uncertainties when rate coefficients have been determined, and to compare the relative accuracy of different experiments. This scheme uses a standard code for evaluating sensitivity coefficients[1] and represents a relatively simple addition to any sensitivity analysis.

Methyl Chemistry Since the reaction of methyl with molecular oxygen is the main branching process in any hydrocarbon oxidation system and because methyl is the simplest alkyl radical, we begin with methyl chemistry. We have used the correlation analysis scheme discussed above to shown why azomethane is the best pyrolytic source of methyl radicals for chemical studies at high temperatures. At combustion temperatures there are two main channels for the reaction of methyl radicals with molecular oxygen

$$CH_3 + O_2 \rightarrow CH_3O_2^* \rightarrow CH_3O + O \rightarrow CH_2O + O + H \quad \text{(Rxn. 51 + 156)}$$

$$CH_3 + O_2 \rightarrow CH_3O_2^* \rightarrow CH_2OOH \rightarrow CH_2O + OH \quad \text{(Rxn. 52)}$$

Reactions 51 and 156 are endothermic whereas reaction 52 is exothermic. The energy difference between these two channels is just the dissociation energy

of hydroxyl, D_0^0/k = 50970 K. Because of this large energy difference, the branching ratio between these channels will control the ignition rate of hydrocarbon/oxygen mixtures.

We have used the above correlation analysis to show that in very lean mixtures, $[O_2]_0/[C_2H_6N_2]_0 > 4000$, the hydroxyl radical may be monitored to measure the rate of reaction 52 without any significant interference from other hydrocarbon reactions. To illustrate this we show, in figure 1, the fractional sensitivity for the measurement of hydroxyl with initial mole fractions of azomethane, oxygen, and argon at 0.01%, 42%, and 58% respectively and at a temperature of 1544 K and a pressure of 151.4 kPa.

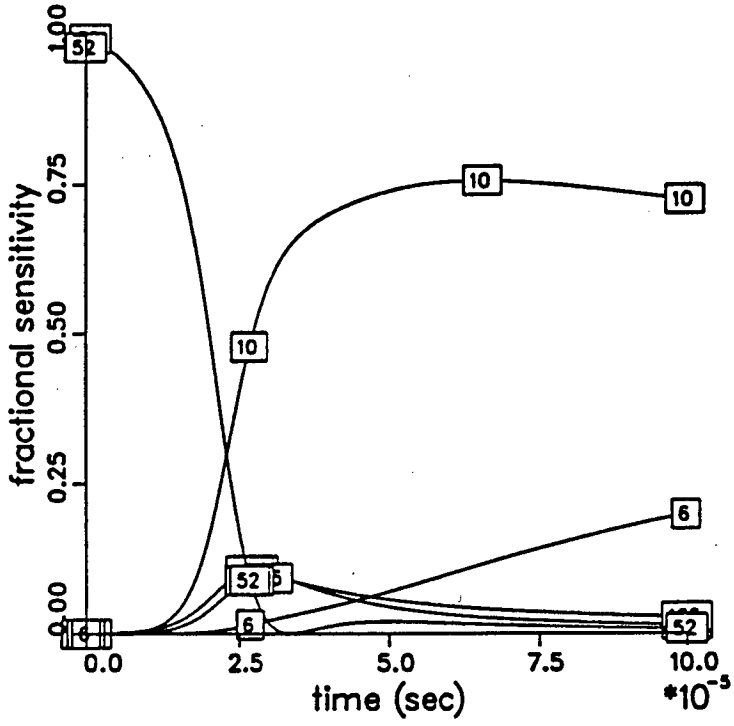

6 O+H2<=>OH+H
10 2OH<=>H2O+O
52 CH3+O2<=>CH2O+OH
165 CH2O+M<=>CO+H2+M
169 CH2O+OH<=>HCO+H2O

Figure 1. Fractional sensitivities for measurement of hydroxyl.

In figure 2, we show the measured absorption profile for hydroxyl and the results of the non-linear least-squares analysis used to determine the rate coefficient of reaction 52. A preliminary analysis of our results gives

$$k(CH_3 + O_2 \rightarrow CH_2O + OH) = 5.1 \times 10^{-12} \exp\{-8700/T(K)\} \quad cm^3s^{-1}.$$

The above activation energy is significantly higher than the most recent measurement[2] and calculation.[3]

Parallel Computations for Least-Squares Analysis The complete reaction mechanism used to describe the oxidation of methyl contains over one-hundred-fifty reactions. Even a "core" mechanism, which may be used to describe shock tube experiments at very early times is relatively large. To perform a multi-dimensional least-squares analysis of experimental data with large mechanisms we employ parallel processing at the time consuming step of numerically evaluating derivatives. We have implemented a code for such processing on our

Alliant Concentrix 2800. The CPU time and, more importantly, the human time required for data analysis is significantly reduced by the use of a parallel computer architecture.

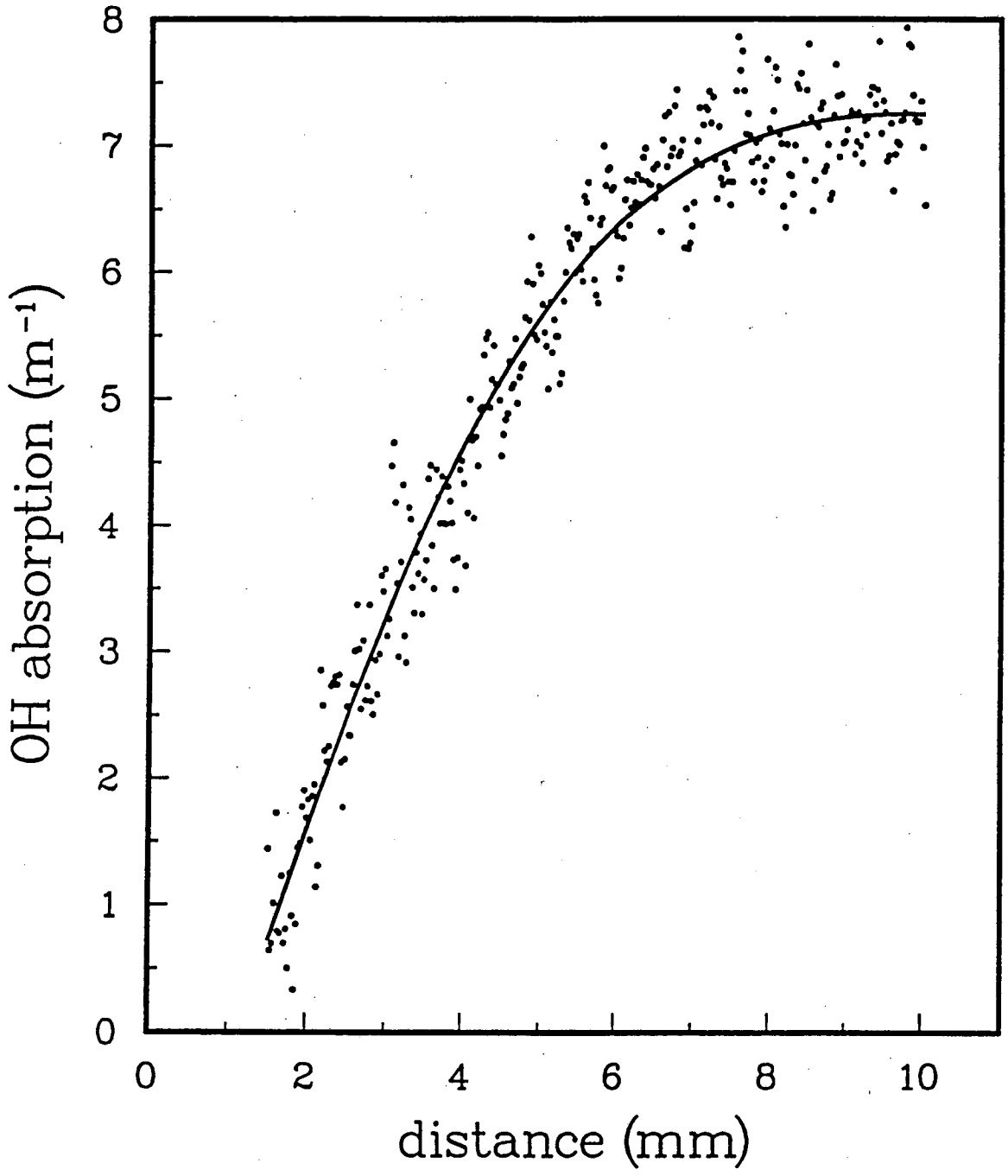

Figure 2. Hydroxyl absorption profile obtained with initial mole fractions given in the text. Shock parameters: Mach No. 4.354, T_2(K) 1544, and P_2(kPa) 151.4.

This work is supported by the United States Department of Energy, Office of Basic Energy Sciences, under contract W-31-109-ENG-38.

Publications Supported by this Program, 1990-92

"Ionization and Dissociation of H_2 in a Static Electric Field: Levels Near the Ionization Threshold," W. L. Glab and J. P. Hessler, *Phys. Rev. A.* 42, 5486-99 (1990).

"Tunable-Laser Flash-Absorption, A New Technique for Measuring Rates and Yields of Chemical Reactions at High Temperatures," W. A. VonDrasek, S. Okajima, J. H. Kiefer, P. J. Ogren, and J. P. Hessler, *Appl. Opt.* 29, 4899-4906 (1990).

"Rate coefficient for the reaction $H + O_2 \rightarrow OH + O$; Results at high temperatures, 2000 TO 5300 K," H. Du and J. P. Hessler, *J. Chem. Phys.* 96, 1077-92 (1992).

References

1. A. E. Lutz, R. J. Kee, and J. A. Miller, *SENKIN: A Fortran Program for Predicting Homogeneous Gas Phase Chemical Kinetics With Sensitivity Analysis*, Sandia Report No. SAND87-8248.UC-4, 1988.

2. K. Saito, R. Ito, T. Kakumoto, and A. Imamura, *J. Phys. Chem.* 90, 1422 (1986).

3. R. Zellner and F. Ewig, *J. Phys. Chem.* 92, 2971 (1988).

Spectroscopic Investigation of the Vibrational Quasi-Continuum Arising from Internal Rotation of a Methyl Group

Jon T. Hougen, Molecular Physics Division, NIST, Gaithersburg, MD 20899

The goal of this project is to use spectroscopic techniques to investigate in detail phenomena involving the vibrational quasi-continuum in a simple physical system. Acetaldehyde was chosen for the study because: (i) methyl groups are known to be important promotors of intramolecular vibrational relaxation[1-3], (ii) the internal rotation of a methyl group is an easily describable large-amplitude motion, which should retain its simple character even at high levels of excitation, and (iii) the aldehyde carbonyl group offers the possibility of both vibrational and electronic probing.

The present investigation of the ground electronic state has three parts: **(1)** understanding the "isolated" internal-rotation motion below, at, and above the top of the torsional barrier, **(2)** understanding in detail traditional (bond stretching and bending) vibrational fundamental and overtone states, and **(3)** understanding interactions involving states with multiquantum excitations of at least one of these two kinds of motion. Activities during the first year and one-half of this project will be grouped under the three headings of this paragraph.

(1) The internal-rotor manifold

We have shown[4], by making new microwave measurements at NIST, that previous problems[5,6] in understanding energy levels in the ground torsional state (v_t=0) of acetaldehyde arose from an incorrect data set rather than incorrect theory (as was sometimes conjectured). Similarly, by making new microwave measurements at NIST and extending the theoretical model somewhat, we have achieved[7] a global fit to essentially experimental accuracy of existing microwave and infrared data for v_t = 0 and 1.

The next step in trying to understand the internal-rotor manifold involves investigating the torsional levels just below (v_t=2) and just above (v_t=3) the top of the barrier. These next two torsional levels are still not high enough in energy to interact strongly with ordinary vibrations, so that we will again look for understanding on the basis of the torsion-rotation Hamiltonian alone. As experimental data we have obtained a broad-band submillimeter pure rotation spectrum of acetaldehyde recorded at room temperature by S. Belov and M. Tretyakov in Nizhnii Novgorod, Russia. All of the v_t=0 lines and about half of the v_t=1 lines in this beautiful spectrum have been identified and added to our previous global fit. Based on this fit, a number of lines from the v_t=2 torsional level have been predicted and tentatively identified by I. Kleiner. Work in the immediate future will concentrate on identifying and fitting more of these v_t=2 submillimeter lines. Should this be successful, and all indications are that it will be, we hope to identify v_t=3 transitions in this same submillimeter spectrum.

It was originally planned that a Fourier transform spectrum of the $v_t = 2 \leftarrow 0$ band would be recorded by this time, in order to study the v_t=2 torsion-rotation levels. The recording of the submillimeter pure

rotation spectrum has removed some of the urgency for recording this far infrared vibrational band. This, coupled with the temporary unavailability of a suitable Bruker FTIR instrument, has led to a one-year postponement of this far infrared study.

A theoretical paper is in preparation with Dr. I. Kleiner which discusses intensity questions associated with the K_a,K_c rotational quantum numbers, forbidden "c-type" transitions, and matrix elements of the dipole moment operator in a molecule exhibiting internal rotation. In this paper, an attempt is made to clarify some of the existing confusion by discussing these intensity questions in terms of the competition between internal rotation effects and asymmetric-rotor K-type doubling effects for control of the the "good quantum numbers" in the final eigenfunctions, and by using extended group theory[8]. The possibility of writing a new version of the Brussels global fit program, which includes intensity predictions incorporating these theoretical results, and which possibly also uses banded matrices to permit treating higher J values, is under discussion with I. Kleiner (University of Paris) and M. Godefroid (University of Brussels).

(2) The traditional vibrational manifold

Excellent room-temperature Bruker FTIR spectra have been recorded in Brussels (M. Herman) for three low-lying ordinary vibrational fundamental modes[9]: ν_{14}, the CH bend at 763 cm^{-1}, and ν_9, ν_{13} the in-plane and out-of-plane components of the CH_3 rock at 919 and 867 cm^{-1}. Analysis of the 763 cm^{-1} band is in progress (I. Kleiner), but hampered by congestion near the band center. Dr. S. Belov is exploring the possibility of using G. Fraser's slit-nozzle diode laser set-up at NIST to examine the band centers of some or all of these bands. In principle we expect these cold slit-nozzle spectra to be simple enough to permit unambiguous analysis, even with the mode gap problems always encountered with diode spectra.

However, in a related study G. Fraser, B. Pate and M. Tretyakov have recorded at NIST a jet-cooled CO_2 side-band laser spectrum of the 919 cm^{-1} band. As mentioned above, it was expected that this jet-cooled spectrum of a low-lying vibration would be quite simple. Nevertheless, at present over 400 lines have been recorded but only 60 or so have been assigned (mainly by using the microwave-infrared double resonance capability of the NIST CO_2 sideband spectrometer). More work is needed to determine if the explanation for this unexpectedly complicated spectrum is: (1) stronger than expected vibrational hot bands in the cold jet, (2) stronger than expected forbidden c-type transitions, or (3) stronger than expected interactions of this methyl rock fundamental with the very sparse density of bath states in the vicinity. We are now leaning to the third of these explanations because of the large perturbations apparently present in the band. This would imply that strong methyl-top internal rotation interactions of the type responsible for enhanced energy transfer rates may set in at much lower vibrational energies than previously expected.

Drs. S. Urban and P. Pracna (Phys. Chem. Institute in Prague) are planning to record, in collaboration with Dr. K. Yamada in Cologne, another (not yet decided) low-lying vibration-rotation band using the Giessen Bruker FTIR instrument. The precise band to be chosen and the schedule for recording and analyzing the band will become clearer by summer.

(3) Interactions between internal rotation and ordinary vibrations

Dr. J. Ortigoso will begin a three-month stay at NIST in April 1992. It is probable that he will begin at that time to develop the theoretical model needed to treat the perturbations observed in the CO_2 sideband spectrum at 919 cm^{-1}. We believe at present that this model must take into account interactions between the angular momentum of internal rotation and the angular momentum generated by the nearly degenerate in-plane and out-of-plane methyl rocking vibrations.

---

[1]M. Noble and E. K. C. Lee, J. Chem. Phys. **81**, 1632-1642 (1984).
[2]V. A. Walters, S. T. colson, D. L. Snavely, K. B. Wiberg and B. M. Jamison, J. Phys. Chem. **89**, 3857-3861 (1985).
[3]C. S. Parmenter and B. M. Stone, J. Chem. Phys. **84**, 4710-4711 (1986).
[4]I. Kleiner, J. T. Hougen, R. D. Suenram, F. J. Lovas and M. Godefroid, J. Mol. Spectrosc. **148** 38-49 (1991).
[5]W. Liang, J. G. Baker, E. Herbst, R. A. Booker and F. C. DeLucia, J. Mol. Spectrosc. **120**, 298-310 (1986).
[6]I. Kleiner, M. Godefroid, M. Herman and A. R. W. McKellar, J. Mol. Spectrosc. **142**, 238-253 (1990).
[7]I. Kleiner, J. T. Hougen, R. D. Suenram, F. J. Lovas and M. Godefroid, J. Mol. Spectrosc. **153** (1992) in press.
[8]J. T. Hougen and B. J. DeKoven, J. Mol. Spectrosc. **98**, 375-391 (1983).
[9]T. Shimanouchi, "Tables of Molecular Vibrational Frequencies, Consolidated Volume I," NSRDS-NBS 39, 1972.

Publication of DoE sponsored research:

"The Ground Torsional State of Acetaldehyde"
I. Kleiner, J. T. Hougen, R. D. Suenram, F. J. Lovas and M. Godefroid, J. Mol. Spectrosc. **148**, 38-49 (1991).

"The Ground and First Torsional States of Acetaldehyde"
I. Kleiner, J. T. Hougen, R. D. Suenram, F. J. Lovas and M. Godefroid, J. Mol. Spectrosc. **153**, (1992) (in press).

"Selection Rules and Intensity Calculations for a C_s Asymmetric Top Molecule Containing a Methyl Group Internal Rotor"
I. Kleiner and J. T. Hougen. In preparation.

DOE/ER/13934-1

STUDIES OF COMBUSTION REACTIONS AT THE STATE-RESOLVED DIFFERENTIAL CROSS SECTION LEVEL

P. L. Houston, A. G. Suits, L. S. Bontuyan, and B. J. Whitaker

Department of Chemistry
Cornell University
Ithaca, NY 14853-1301

Program Scope

State-resolved differential reaction cross sections provide perhaps the most detailed information about the mechanism of a chemical reaction, but heretofore they have been extremely difficult to measure. This program explores a new technique for obtaining differential cross sections with product state resolution. The three-dimensional velocity distribution of state-selected reaction products is determined by ionizing the appropriate product, waiting for a delay while it recoils along the trajectory imparted by the reaction, and finally projecting the spatial distribution of ions onto a two dimensional screen using a pulsed electric field. Knowledge of the arrival time allows the ion position to be converted to a velocity, and the density of velocity projections can be inverted mathematically to provide the three-dimensional velocity distribution for the selected product. The main apparatus has been constructed and tested using photodissociations. We report here the first test results using crossed beams to investigate collisions between Ar and NO. Future research will both develop further the new technique and employ it to investigate methyl radical, formyl radical, and hydrogen atom reactions which are important in combustion processes. We intend specifically to characterize the reactions of CH_3 with H_2 and H_2CO; of HCO with O_2; and of H with CH_4, CO_2, and O_2.

Recent Progress

State-resolved differential cross sections provide detailed information about the mechanism and potential energy surface governing a chemical reaction, but they have heretofore been difficult to measure. This abstract describes a new technique for obtaining differential cross sections with both product state resolution and simultaneous detection of all scattering angles. The three-dimensional velocity distribution of state-selected reaction products is determined by ionizing the appropriate product and accelerating the ions onto a detector using a pulsed electric field. The resulting image is a two-dimensional projection of the three-dimensional velocity distribution. Visual inspection provides immediate qualitative information about the reaction, while mathematical analysis can provide detailed differential cross sections. We have used the technique to investigate the inelastic collision process Ar + NO($^2\Pi_{1/2}$,v=0,J=0.5) → Ar + NO($^2\Pi_{1/2}$,v=0,J') at a collision energy of 0.21 eV. Rotational rainbows in the product angular distribution are directly observed to change in position as a function of the final rotational state; the peak of the angular distribution moves toward the backward hemisphere and the angular distribution broadens with an increase in final rotational quantum number.

The collision dynamics of Ar + NO have been investigated previously at the total cross section level.[1-3] Using laser-induced fluorescence and two crossed beams, Joswig *et al.* found interference effects in the scattering of NO(v=0,J=0.5) by He, Ar, and Ne; the total cross section for scattering to

NO product states displayed oscillations as a function of the final rotational quantum number. The oscillations also appeared in coupled-states calculations using the electron gas potential of Nielson *et al.*[4] The interference is due to scattering from the two different ends of the nearly homonuclear diatomic molecule.[5] Two potential surfaces are important, one in which the orbital of the unpaired electron is in the plane containing the three atoms (A'), and one in which it is perpendicular to this plane (A''). As shown by Alexander,[6] multiplet changing collisions provide information about the difference between these two potentials, while multiplet conserving collisions provide information about the sum. Thus, state-resolved differential cross sections such as those made possible by the new method described here will be important in determining these two potential energy surfaces.

The new method for making these measurements is similar to that already used to determine the angular distribution of state-selected photofragments.[7-12] A variant of the method has also been used to investigate the H + HI → H_2 + I reaction,[13] although not in crossed molecular beams. In our configuration, a doubly differentially pumped primary beam is formed by expanding 7% NO in He from a total pressure of 1100 torr through a pulsed nozzle 85 cm from the interaction region. The expansion yields a rotational distribution in the beam given by $N_{J=0.5}=1$, $N_{J=1.5}=0.037$, $N_{J=2.5}=0.006$. The secondary Ar beam is formed by expansion of 1040 torr through a pulsed nozzle 15 cm from the interaction region. A pulsed laser beam at a wavelength near 226 nm was propagated counter to the Ar beam and used to ionize state-selected NO products on the axis of a Wiley-McLaren[14] time-of-flight mass spectrometer. The ions were accelerated in a direction perpendicular to the plane of the molecular beams by fields of ~800 volts/cm. After ~6 μs, the ions struck the first of two, 2"-diameter channelplate detectors, causing emission secondary electrons with a gain of ~10^7. Electrons from the channelplates were accelerated to a fast phosphor coated onto one end of a fiber-optic bundle mounted through a vacuum flange. A CID Camera (Xybion), gated according to the flight time for the mass of interest and equipped with a 480x512 pixel array, captured each image for averaging and analysis. A real-time video averager (Poynting RA-512) summed 256 images with 16 bit resolution. The most significant 8-bit slice of the resulting sum was normalized for laser power and stored in a computer. Alternate sets of images obtained with the Ar beam off were subtracted from those with both beams on. Roughly 300,000 laser shots were averaged for Figure 2 and Figure 3 shown below.

Figure 1 displays a superposition of two images obtained when a trace of NO is also seeded in the secondary Ar beam. In one of the two superimposed images the ionization laser propagates counter to the primary beam, while in the second it propagates counter to the secondary beam. The laser is tuned to ionize NO($^2\Pi_{1/2}$,v=0,J=0.5), the principal component of each beam, so the illuminated section of each of the molecular beams is visible in the figure. The intersection of the two beams is the collision region. The dark spots below and to the left of this intersection represent NO molecules that were ionized at the intersection of the beams and that traversed the intervening distance in the time between ionization and detection, ~6 μs. Measurement of distances and the delay time provides the velocity, dispersion, and size for each molecular beam. A "Newton" diagram for the collision can be easily constructed for elastic collisions; it is superimposed on Figure 1.

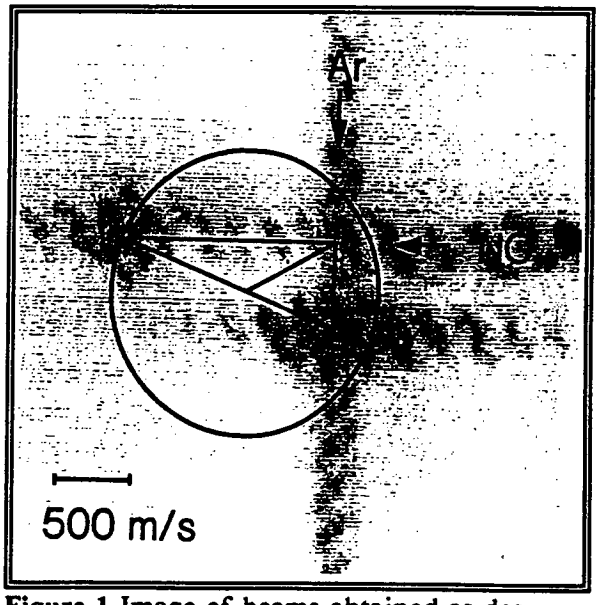

Figure 1 Image of beams obtained as described in the text, shown superimposed with a Newton diagram for elastic scattering.

Figure 2 gives the image obtained when the probe laser (now propagating only counter to the pure Ar beam) is tuned to ionize

$NO(^2\Pi_{1/2},v=0,J=11.5)$. Despite some ionization of background room-temperature NO along the laser beam, the projection of the Newton sphere for the scattering is clearly visible. The scattering is actually symmetric about the relative velocity vector, but the detection sensitivity depends both on the velocity component perpendicular to the laser beam and on a center-of-mass to laboratory Jacobian. Qualitative analysis shows that the angular distribution is peaked at 30° with a FWHM of about 20°. This rotational rainbow in the scattering angular distribution is expected for atom-diatom collisions, even at the level of classical mechanics and hard ellipse scattering.[15]

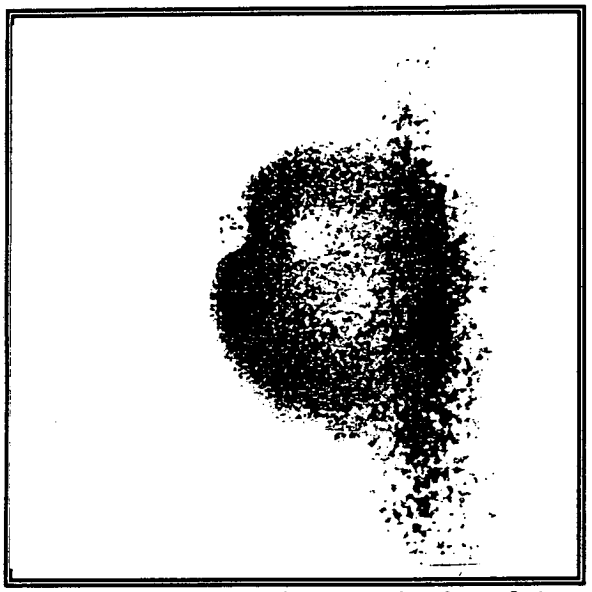

Figure 2 Two-dimensional projection of the scattering distribution for $NO(^2\Pi_{1/2},v=0,J=11.5)$.

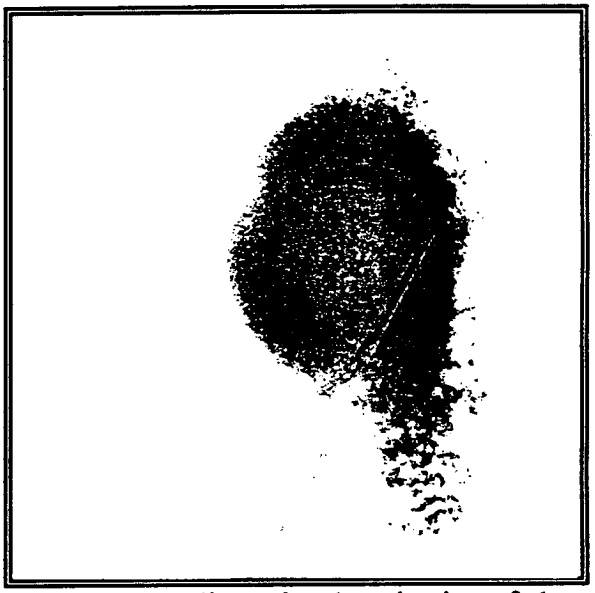

Figure 3 Two-dimensional projection of the scattering distribution for $NO(^2\pi_{1/2},v=0,J=18.5)$.

Figure 3 displays the image obtained when $NO(^2\Pi_{1/2},v=0,J=18.5)$ is ionized. The product scattering is more diffuse and is centered much further toward the backward hemisphere; qualitative analysis places the peak at 60° with a FWHM of 30°. In addition, the Newton sphere is measurably smaller, in accord with the lesser available energy for translation. Images were also recorded for J=9.5 (0±10°, FWHM=20°) and J=15.5 (40°, FWHM=30°).

The figures show that the imaging technique can provide direct qualitative information about the collision dynamics. Although a quantitative analysis of the images is not yet complete, it is clear to us that the detailed differential cross section can be obtained by a forward convolution technique which includes the density to flux transformation and the center-of-mass to laboratory Jacobian. The advantages of the technique are: *1)* that the state-resolution is limited only by the spectral resolution of the laser and the energy separation between molecular eigenstates, and *2)* that the entire angular distribution is recorded for each laser pulse. Potential disadvantages of the technique are that the molecule to be probed must be able to undergo state-selected multiphoton ionization. The data thus far provide encouragement that the state-selected differential cross sections needed to determine the two potential energy surfaces involved in the Ar+NO system can be obtained.

Our future plans are to extend this technique to reactive collisions, particularly to those in combustion. We intend specifically to characterize the reactions of CH_3 with H_2 and H_2CO; of HCO with O_2; and of H with CH_4, CO_2, and O_2.

References

[1] A. S. Sudbo and M. M. T. Loy, Chem. Phys. Lett. **82**, 135 (1981).
[2] P. Andresen, H. Joswig, H. Pauly, and R. Schinke, J. Chem. Phys. 77, 2204 (1982).
[3] H. Joswig, P. Andresen, and R. Schinke, J. Chem. Phys. **85**, 1904 (1986).
[4] G. C. Nielson, S. A. Parker, and R. T Pack, J. Chem. Phys. **66**, 1396 (1977).
[5] C. W. McCurdy and W. H. Miller, J. Chem. Phys. **67**, 463 (1977).
[6] M. H. Alexander, J. Chem. Phys. **76**, 5974 (1982).
[7] D. W. Chandler and P. L. Houston, J. Chem. Phys. **87** 1445 (1987).
[8] D. W. Chandler, J. W. Thoman, Jr., M. H. M. Janssen, and D. H. Parker, Chem. Phys. Lett. **156** 151 (1989).
[9] D. W. Chandler, M. H. M. Janssen, S. Stolte, R. N. Strickland, J. W. Thoman, Jr., and D. H. Parker, J. Phys. Chem. **94** 4839 (1990).
[10] J. W. Thoman, D. W. Chandler, D. H. Parker, M. H. M. Janssen, Laser Chem. **9** 27 (1988).
[11] D. P. Baldwin, M. A. Buntine, and D. W. Chandler, J. Chem. Phys. **93** 6578 (1990).
[12] T. Suzuki, V. P. Hradil, S. A. Hewitt, P. L. Houston, and B. J. Whitaker, Chem. Phys. Lett. **187**, 257 (1991).
[13] M. A. Buntine, D. P. Baldwin, R. N. Zare, and D. W. Chandler, J. Chem. Phys. **94** 4672 (1991).
[14] W. C. Wiley and I. H. McLaren, Rev. Sci. Instrum. **26** (1955) 1150.
[15] R. Schinke and J. M. Bowman, "Rotational Rainbows in Atom-Diatom Scattering," in *Molecular Collision Dynamics*, Chapter 4, J. M. Bowman, ed., (Springer-Verlag, Berlin, 1983), p. 61.

Publications Acknowledging DOE Support

[1] R. Ogorzalek Loo, H.-P. Haerri, G. E. Hall, and P. L. Houston, "Methyl Vibration, Rotation, and Alignment from a Multiphoton Ionization Study of the 266-nm Photodissociation of Methyl Iodide," J. Chem. Phys. **90**, 4222-4236 (1989).

[2] K. A. Trentelman, S. H. Kable, D. B. Moss, and P. L. Houston, "Photodissociation Dynamics of Acetone at 193 nm: Photofragment Internal and Translational Energy Distributions," J. Chem. Phys. **91**, 7498-7513 (1989).

[3] D. B. Moss, K. A. Trentelman, and P. L. Houston, "193 Photodissociation Dynamics of Nitromethane," J. Chem. Phys. **96**, 237-247 (1992).

[4] A. G. Suits, L. S. Bontuyan, P. L. Houston, and B. J. Whitaker, "Differential Cross Sections for State-Selected Products by Direct Imaging: Ar + NO," J. Chem. Phys., accepted.

AROMATICS OXIDATION AND SOOT FORMATION IN FLAMES

Jack B. Howard

SCOPE

This project is concerned with the kinetics and mechanisms of aromatics oxidation and soot formation in flames. After the recent discovery of fullerenes in the flames being studied, the focus was expanded to include kinetics and mechanisms of fullerenes formation. The scope includes detailed measurements of profiles of stable and radical species concentrations in low-pressure one-dimensional premixed flames. Intermediate species identifications and mole fraction, flux, and net reaction rates calculated from the profile measurements are used to test postulated reaction mechanisms. Particular objectives are to identify and to determine or confirm rate constants for the main benzene oxidation reactions in flames, and to characterize fullerenes and their formation mechanisms and kinetics.

In the benzene oxidation study, trace amounts of benzene are added to a low pressure premixed one-dimensional H_2-O_2 flame to ensure that oxidative destruction products are at sufficiently low concentrations so as not to compete with the oxidants. Detailed profiles of stable and radical species concentrations are measured through the reaction zone using molecular beam sampling with on-line mass spectrometry. The formation of fullerenes is studied in benzene-oxygen flames using probe sampling with spectroscopic analysis of collected samples. The experimental data are employed in a numberical analysis that accounts for species diffusion and convection and produces profiles of flux and net reaction rate for each species. All the profiles - mole fraction, flux and net reaction rate - are systematically studied to obtain partial equilibrium relationships, rate constants, and other information pertinent to kinetics and mechanisms.

RECENT PROGRESS

Benzene Oxidation

Measurements were begun in a rich hydrogen flame (fuel equivalence ratio = 1.79, cold gas velocity at burner = 101 cm/sec, 31.3% Ar) spiked with 1/2% benzene. Flames with lower cold gas velocities were planned, but proved to be unstable with the sampling probe near the burner. The maximum temperature reached by the flame is expected to be significantly greater than the 1650 K previously planned, an advantage of the greater flow rate. The reaction zone of the chosen flame was found to be sufficiently wide (about 8.5 mm) for good spatial resolution.

Qualitative probing has revealed the presence of significant quantities of C_5H_5, C_5H_6, C_6H_5, C_6H_7, C_6H_6O (or C_6H_5OH), and C_6H_7O (or C_6H_6OH). Present in trace quantities is phenoxy radical, C_6H_5O. Cyclopentadiene is present in much greater amounts than cyclopentadienyl radical. This is consistent with previous measurements in this laboratory in a nearly sooting benzene flame. It has not yet been determined if the hydrogenated benzene and phenol (or oxycyclohexadienyl) are present in amounts above the isotopic contribution from the parent species.

The mass 16 signal has been found to be overwhelmingly CH_4 in the preheat and reaction regions of the flame, and the implied concentration of O-atom is too low for this species to be an important oxidant in the flame. Therefore, the predominant oxidants under these conditions are OH and O_2. The lack of an important O-atom pathway will simplify analysis of the relative importance of the two main oxidants. Relative signal profiles for H_2, O_2, and CO have been measured.

Mass discrimination factors (MDFs) are required to make these profiles quantitative. Our experiments have shown that MDF measurements for rich hydrogen flames are much more difficult than for hydrocarbon flames. The MDF for H_2, while varying somewhat less with density in the hydrogen flame, must be more accurately know if H-atom balances are to be closed. Furthermore, we have found that the MDFs for the other species have greater variation and much more composition sensitivity in this flame.

Fullerenes Formation

Fullerenes C_{60} and C_{70} were produced in varying amounts in premixed laminar benzene/oxygen/argon flames operated under ranges of conditions including pressures 12 to 100 torr and C/O ratios from 0.717 to 1.072, the critical value for soot formation being 0.760. The fullerenes were identified in toluene extracts of condenses flame material including soot, using high performance liquid chromatography (HPLC) with diode-array spectrophotometric detection, mass spectrometry and infrared spectrophotometry.

The yields of C_{60} and C_{70} and the C_{70}/C_{60} ratio depend on temperature, pressure, carbon/oxygen ratio and residence time in the flame. In the sooting flames, C_{60} and C_{70} first appear well after the onset of soot formation. The mass of $C_{60}+C_{70}$ produced is in the range 0.0026%-9.2% of the soot, compared to 1-14% from the conventional graphite vaporization method, and the largest $C_{60}+C_{70}$ yield is 0.26% of the fuel carbon, observed at a pressure of 20 torr. A $C_{60}+C_{70}$ yield of $2x10^{-4}$% of the fuel carbon was found in a nonsooting flame. The largest rate of production of $C_{60}+C_{70}$ was observed in a sooting flame at a pressure of 100 torr. The C_{70}/C_{60} molar ratio varied over the range 0.26-5.7, compared to 0.02-0.18 for the graphite vaporization method, and can be controlled by selection of flame conditions.

Depending on flame conditions, the $C_{60}+C_{70}$ fullerenes were produced with varying amounts of polycyclic aromatic hydrocarbons (PAH). The mass ratio of PAH to $C_{60}+C_{70}$ varies roughly from 0.01 to 100 over the range of conditions studied. Also, the $C_{60}+C_{70}$ fullerenes are accompanied by 3-6 smaller satellite peaks whose spectral and chromatographic properties strongly suggest fullerene-like structures, the identification of which has been achieved with liquid chromatography/mass spectrometry.

One of the objectives of the research is to understand the mechanisms and kinetics of the formation of fullerenes and soot in flames. Although the topic of fullerenes is new and soot formation in flames has been studied for more than 150 years, intercomparison of the two processes is helpful to the understanding of each. The largest yeilds of fullerenes do not occur in the most heavily sooting flames. Also, the fullerene yield increases with increasing temperature or decreasing pressure under conditions where the same changes result in lower soot yields. These trends in the data reflect substantial differences between the formation mechanisms of fullerenes as compared to those of soot. Both formation processes involve many of the same generic reactions, but to different extents of involvement as required by the very different structures being formed. Soot formation does not involve the development of curved or bowl-shaped structures as required for fullerenes, nor would these curved structures permit the rapid stacking required in the reactive coagulation of the relatively flat sheet-like soot precursors. That the very special fullerene structures are formed in flames and that the formation occurs in the presence or absence of soot formation, provide new insight into the generic reactions important to both processes.

A preliminary kinetic mechanism has been constructed for the formation of fullerenes C_{60} and C_{70} in flames, based on types of reactions used in describing growth of polycyclic aromatic hydrocarbons (PAH), and including additional chemical processes needed to describe evolution of the unique structural features of fullerenes. The resulting detailed kinetic mechanism consists of classes of reactions, each characterized with an approximate rate coefficient, including processes for ring formation (via H-atom abstraction, C_2H2 addition, and cyclization leading to ring closing), dimerization of aromatic molecules, and cage closing via H_2 elimination and ring closing, but also allowing for additional processes such as intramolecular rearrangements. The types of rearrangements considered and their relevance to curved PAH and fullerene formation chemistry has been explored.

Curved PAH, including benzo[ghil]fluoranthene ($C_{18}H_{10}$) and dibenzo[ghi,mno] fluoranthene (corannulene) $C_{20}H_{10}$, are likely fullerene precursors. Corannulene is considered a key intermediate in the fullerene formation mechanism, and its possible formation routes are described. Alternatives to corannulene as an intermediate have been discussed and will be assessed later if interesting. The mechanism now being studied is based on corannulene and other related PAH of C_{5v} symmetry.

Preliminary kinetic testing of the mechanism, using approximate rate coefficients based on analogous planar PAH reactions, shows the mechanism to be plausible within the uncertainties of the rate coefficients and the experimental data on fullerenes formation rate. The mechanism is also qualitatively consistent with reported trends in fullerene yields in flames with respect to temperature and pressure.

FUTURE PLANS

The benzene oxidation studies will include completion of mole fraction profile measurements for all of the important species in a rich H_2/O_2 flame. Mole fraction profiles of selected species in the flame will be measured with different amounts of benzene added. Intermediates and products of benzene destruction in a lean H_2/O_2 flame will be measured under conditions where the $O+C_6H_6$ reaction is dominant. A previously studied stoichiometric benzene/oxygen flame will be re-examined to assess, through modeling calculations, the extent to which the rates, intermediates and products of benzene destruction observed in the benzene flame can be predicted using current information including the results of this study.

In the work on fullerenes formation, one of the objectives will be to identify the structure of different isomers of fullerenes C_{60} and C_{70} which are observed in flames. This effort will require production and separation of sufficient quantities of the isomers to permit molecular characterization by NMR, ir, vis and uv spectroscopy, and possibly other techniques. Also, the work will include measurement of concentration profiles of fullerenes under different flame conditions, and use of the data to study kinetics and mechanisms of fullerene formation and destruction reactions.

PUBLICATIONS (1990, 1991 and 1992)

McKinnon, J.T. and Howard, J.B., "Application of Formation Model: Effects of Chlorine", Combustion Science and Technology, **74**, 175-197 (1990).

Howard, J.B., "Radical Sites as Active Sites in Carbon Addition and Oxidation Reactions at High Temperatures", in Fundamental Issues in Control of Carbon Gasification Reactivity, J. Lahaye and P. Ehrburger, Eds. pp. 377-382, Kluwer Academic Publishers, 1991.

Howard, J.B., McKinnon, J.T., Makarovsky, Y., Lafleur, A.L. and Johnson, M.E., "Fullerenes C_{60} and C_{70} in Flames", Nature, **352**, 139-141 (1991).

Howard, J.B., McKinnon, J.T., Makarovsky, Y., Lafleur, A.L., and Johnson, M.E., "Production and Characterization of Fullerenes in Flames", A.C.S. Fuel Chem. Div. Preprints, **36(3)**, 1022-1025 (1991).

Pope, C.J. and Howard, J.B., "Fluxes and Net Reaction Rates of Flame Species Pertinent to Fullerenes", A.C.S. Fuel Chem. Div. Preprints, **36(4)**, 1541-1546 (1991).

Howard, J.B., "Carbon Addition and Oxidation Reactions in Heterogeneous Combustion and Soot Formation", Twenty-Third Symposium (International) on Combustion, The Combustion Institute, Pittsburgh, 1107-1127 (1991).

Shandross, R.A., Longwell, J.P., and Howard, J.B., "Noncatalytic Thermocouple Coating for Low-Pressure Flames", Combust. Flame, **85**, 282-284 (1991).

Anacleto, J.F., Perreault, H., Boyd, R.K., Pleasance, S., Quilliam, M.A., Sim, P.G., Howard, J.B., Makarovsky, Y., Lafleur, A.L., "C_{60} and C_{70} Fullerene Isomers Generated in Flames", Rapid Communications in Mass Spectrometry (March, 1992).

Howard, J.B., "Fullerenes Formation in Flames", Twenty-Fourth Symposium (International) on Combustion, The Combustion Institute, Pittsburgh. (accepted for publication).

McKinnon, J.T. and Howard, J.B., Twenty-Fourth Symposium (International) on Combustion, The Combustion Institute, Pittsburgh (accepted for publication).

IONIZATION PROBES OF MOLECULAR STRUCTURE AND CHEMISTRY

Philip M. Johnson
Department of Chemistry
State University of New York, Stony Brook, NY 11794

INTRODUCTION

We have continued the development of laser ionization tools toward the study of the spectroscopy and dynamics of molecules relevant to combustion processes. When high intensity laser beams interact with any physical system composed of electrons and nuclei, an almost inevitable result of the high electric field strengths in the light beam is that electrons are separated from the nuclei. This ionization, when carried out in a controlled way, can provide a great deal of information about the molecular system, including energies and dynamics of electronic states, and can provide a fingerprint for the detection of an atom or molecule.

IONIZATION VERSUS DISSOCIATION IN CO_2

One of the molecules we have spent considerable effort on is carbon dioxide. Besides its obvious relevance in combustion, it presents a great challenge to spectroscopy because of its propensity toward dissociation in all of its excited states. Multiphoton ionization spectroscopy is usually not applicable to the study of dissociating molecules because the dissociation competes effectively with ionization, resulting in no signal. However, with high enough laser fluence, ionization can compete with dissociation in the longer lived states, exposing them for study from the continuous spectral background resulting from rapidly dissociating states. The intense laser field produces effects not seen in ordinary spectroscopy, and we have been studying the various spectroscopic and photophysical effects found through the multiphoton ionization and multiphoton photoelectron spectra.

Photoelectron spectroscopy is a very useful technique for finding out about properties of both neutral molecules and ions. For carbon dioxide it provides a means of determining photoionization and photodissociation mechanisms. Our previous studies on carbon dioxide have elucidated some of its multiphoton spectroscopy and discovered several fascinating photophysical processes. One of the more intriguing of these in terms of its possibilities concerning the detailed understanding of photodissociation is the appearance of long non-Franck-Condon progressions in the multiphoton photoelectron spectra. These appear to be indicative of some sort of ionization during the process of dissociation, and there is a potential to be able to learn about the details of dissociation. In the three-photon resonant four-photon ionization process, ionization could be competing with dissociation at either the three-photon or the four-photon level. For the former, a bound state would be predissociating, creating a wave packet which could be ionized at various points along the reaction coordinate. The photoelectron spectrum

would be intensity dependent because higher laser fields would promote ionization before the wave packet has a chance to travel very far. At the four-photon level, excitation can be directly to a neutral dissociation continuum where the molecule can autoionize while in the process of dissociation. The photoelectron spectrum would not be intensity dependent. We have measured the intensity dependence of the vibrational structure seen in the photoelectron spectra over almost a factor of two in laser intensity and found no changes, providing evidence that the multiphoton ionization of CO_2 through its Rydberg states proceeds through autoionization of bound, neutral dissociative states. This may be explained by a propensity toward excitation of core electrons to antibonding orbitals in preference to excitation of a Rydberg electron which is decoupled from the core.

HIGH RESOLUTION VIBRATIONAL SPECTROSCOPY OF CATIONS

Threshold ionization spectroscopy provides similar information to photoelectron spectroscopy in that it locates the energy levels of an ion but it does so by means of scanning a tunable photon source over the ionization continuum looking for ionization thresholds. A recently developed variant of threshold ionization spectroscopy, usually called ZEKE, has shown to be as useful as traditional photoelectron spectroscopy (where the kinetic energy of ejected electrons are measured) but with higher resolution and much better signal-to-noise when using standard laboratory lasers. It has recently been realized that the ZEKE or pulsed field ionization (PFI) method of measuring threshold ionization spectra is exploiting the field ionization of very high Rydberg states which exist just before each ionization threshold.

Aromatic molecules are of great importance in combustion research since they constitute a significant fraction of unleaded gasoline. We chose to develop our capabilities in threshold ionization spectroscopy using aromatic molecules because of their importance and because their electronic structure allows a pump-probe type of excitation scheme which avoids the use of vacuum ultraviolet laser beams. Among aromatics, the diazines are noted for their small S_1-T_1 energy gap which gives them unique and interesting photophysical properties. Their electronic structure is also interesting because lone-pair electrons in almost non-interacting orbitals produce an effect called "spontaneous symmetry breaking" in SCF calculations and may have implications in the structure of the molecule itself, particularly in the ion. We have studied the basic threshold ionization spectroscopy of diazines pyrazine and pyrimidine, acquiring high resolution vibrational spectra of the ground state ion while resonant with various vibrational levels of S_1. We are therefore able to determine 11 out of 24 of the vibrations of pyrazine ion and compare them to vibrational frequencies calculated from an SCF force field. Most of the frequencies agree quite well, but two out-of-plane vibrations, 5 and 10a, have considerably reduced frequencies which indicate a distortion of the potential along those normal coordinates. In pyrimidine, where the lone-pair interaction is much stronger, all the vibrations agree well with the SCF results.

In the course of this work we have developed a new technique of detecting

ionization thresholds which depends only upon measuring the ions produced by field ionization of high Rydberg states and therefore retains mass information. This mass analyzed threshold ionization spectroscopy (MATI) is done by exploiting the narrow kinetic energy distribution of the molecules in a supersonic beam and the fact that near a threshold ions can be separated from Rydbergs by a small electric field. With a series of grids in the beam path, field ionized Rydbergs are made to arrive at the detector before any directly produced ions and gating on the earlier arriving species while scanning ionization wavelengths produces a threshold ionization spectrum of only the mass of interest. The viability of the scheme was demonstrated by producing the same spectrum for pyrazine by electron and ion detection. More recently we have recorded the MATI spectrum of the benzene-argon van der Waals complex in the presence of many other clusters, and have continued to explore alternative methods of separating ions and Rydberg states in order to improve the mass resolution and sensitivity of the method. It is anticipated that this method will also enable the production of state selected ion beams for use in reactivity studies.

IN PROGRESS

Currently we are recording the fluorescence spectra of the ions and photoproducts produced in the multiphoton ionization and dissociation of carbon dioxide in order to determine the nature of the exit channels of the multiphoton dynamics. We are also looking at the photochemistry of benzene clusters and benzene-oxygen clusters using multiphoton mass spectrometry and MATI.

DOE PUBLICATIONS

P. M. Johnson and M. Wu, "Autoionization structure and rotational contours in the multiphoton ionization spectrum of carbon dioxide," J. Chem. Phys. **94**, 868 (1991).

P. M. Johnson, "Resonance ionization spectra as a reflection of excited state dynamics," Inst. Phys. Conf. Ser. No. 114: Section 4 [RIS 90], IOP Publishing Ltd, 145 (1991).

L. Zhu and P. M. Johnson, "Mass analyzed threshold ionization spectroscopy," J. Chem. Phys. **94**, 5769 (1991).

M. Wu, D. P. Taylor and P. M. Johnson, "Resonance enhanced multiphoton ionization-photoelectron spectra of CO_2 (I): Photoabsorption above the ionization potential," J. Chem. Phys. **94**, 7596 (1991).

M. Wu, D. P. Taylor and P. M. Johnson, "Resonance enhanced multiphoton ionization-photoelectron spectra of CO_2 (II): Competition between photoionization and dissociation," J. Chem. Phys. **95**, 761 (1991).

S. Hillenbrand, L. Zhu, and P. M. Johnson, "The pulsed field ionization spectrum and lifetimes of the states at the S_1 origin of pyrazine," J. Chem. Phys. **95**, 2237 (1991).

PHOTOCHEMISTRY OF MATERIALS IN THE STRATOSPHERE

Principal Investigator: Harold S. Johnston
Chemical Sciences Division
Lawrence Berkeley

Mailing address: Department of Chemistry
University of California
Berkeley, CA 94720

Program scope

This research is concerned with global change in the chemistry of the atmosphere, including theoretical and experimental gas-phase and heterogeneous photochemistry.

Recent Progress

Five graduate students completed their work on this project during the last 1.5 years and prepared 13 draft articles based on their theses. These draft articles were between 10% and 90% ready for submission to journals. Since retiring from teaching and experimental research at the University of California on July 1, 1991, the principal investigator on this project has put major effort into revising these draft papers for submission to the journals. Also, the principal investigator has studied the problem of stratospheric sulfate aerosols and their possible role in activating chlorine chemistry in the global lower stratosphere and has proposed a new mechanism involving nitrosyl sulfuric acid, $(ONO)(HO)SO_2$ or $NOHSO_4$, in converting inactive HCl to photochemically active ClNO. The thermodynamic and kinetic, necessary and sufficient conditions are worked out for the occurrence of this heterogeneous catalytic process.

Future Plans

The $NOHSO_4$ mechanism calls for new laboratory studies, new atmospheric observations, and new atmospheric modeling. To carry out some of these needed studies, this project is collaborating with CSD investigators at Berkeley and with others at Livermore and at Boulder, Colorado.

Acknowledgement

This work was supported by the Director, Office of Energy Research, Office of Basic Energy Sciences, Chemical Sciences Division of the U. S. Department of Energy under Contract No. DE-AC03-76SF00098.

References to Publications of DOE Sponsored Research

1. Harold S. Johnston, "M. J. Prather, and R. T. Watson, "The Atmospheric Effects of Stratospheric Aircraft," NASA Reference Publication 1250, January 1991, 28 pages, LBL-31860.

2. Harold S. Johnston, Chair of Panel of 20 members and author of text, Chapter 5, 56 pages, "Trends in Ozone Profile Measurements," Report of the International Ozone Trends Panel 1988 World Meteorological Organization Global Ozone Research and Monitoring Project-Report No. 18, written 1988, published 1991.

3. K. O. Patten, Jr., J. D. Burley, and H. S. Johnston, "Radiative Lifetimes of Nitrogen Dioxide for Excitation Wavelengths from 400 to 750 nm," J. Phys. Chem. **94**, 7960 (1990); LBL-28435.

4. Bongsoo Kim, B. L. Hammond, W. A. Lester, Jr., and H. S. Johnston, "Ab Initio Study of the Vibrational Spectra of NO_3," Chem. Phys. Lett. **168**, 131 (1990); LBL-28434.

5. Joel D. Burley, "Part I. Kinetic Energy Dependencies of Selected Ion-Molecule Reactions. Part II. Photochemistry of (FSO3)2, FSO3, and FNO." Ph. D. Dissertation, University of California, Berkeley, California, July 1991, LBL-31027.

6. Kenneth O. Patten, "Collisional Energy Transfer from Excited Nitrogen Dioxide," Ph. D. Dissertation, University of California, Berkeley, California, 244 pages, May 1991, LBL-30599.

7. Charles E. Miller, "The Photodissociation of R-NO_2 Molecules" Ph. D. Dissertation, University of California, Berkeley, California, April 1991, LBL-30540.

8.Bongsoo Kim, "NO_3, the Study of Molecular Properties and Photodissociation by ab initio Method, Spectroscopy, and Translational Spectroscopy," Ph.D. Dissertation, University of California, Berkeley, California, September 1990, LBL 29688.

9. Wade N. Sisk, "Nitrogen Dioxide Fluorescence Following Photolysis in a Supersonic Jet", Ph.D. Dissertation, University of California, Berkeley, California, May 1990; LBL-29112.

10. Wade N. Sisk, Charles E. Miller and Harold S. Johnston "Spectroscopy of Nitrogen Dioxide Fluorescence III. Internal Energy Distributions of fluorescent NO_2 after Photolysis of Jet-Cooled N_2O_4," accepted for publication in Journal of Physical Chemistry, January 1992, LBL-31551.

11. Charles E. Miller and Harold S. Johnston, "Spectroscopy of Nitrogen Dioxide Fluorescence IV. Variable Wavelength Photo-dissociation of $ClNO_2$ and $HONO_2$, accepted for publication in Journal of Physical Chemistry, January 1992, LBL-31552.

12. Bongsoo Kim, Philip L. Hunter, and H. S. Johnston, "NO_3 Radical Studied by Laser Induced Fluorescence," accepted for publication in Journal of Chemical Physics, October 1991.LBL-30869.

13. Joel D. Burley and H. S. Johnston, "Photoabsorption Cross Sections of $(FSO_3)_2$ and FSO_3," accepted for publication in J. Photochem. Photobiol. A: Chem., August 1991, LBL-31547.

Dynamical Analysis of Highly Excited Molecular Spectra. Michael E. Kellman, Department of Chemistry, University of Oregon, Eugene, OR 97403.

Program Scope:

The goal of this program is new methods for the analysis of highly excited vibrational states of molecules where usual normal modes analysis is rendered inadequate by strong nonlinear resonances and classically chaotic dynamics. New methods of spectral analysis, pattern recognition, and assignment are sought using techniques of nonlinear dynamics including bifurcation theory, phase space classification, and quantization of phase space structures.

Recent Progress and Future Plans:

This is a new DOE project which investigates crucial advances beyond our earlier attempts to analyze highly excited spectra. The key new developments expected are methods for classification of multidimensional systems and systems with a high degree of classical chaos. Where appropriate, principal references are given to earlier work sponsored under separate auspices.

The central problem underlying our work is the fact that the usual normal modes analysis and assignments based on this analysis are seriously inadequate or misleading in the high energy regime of highly anharmonic vibrations with strong coupling. Roughly speaking, in the low-energy, normal mode regime there is regular dynamics described in phase space by quasiperiodic motion on a single set of invariant tori. In the strongly coupled, highly anharmonic regime, the phase space bifurcates or becomes divided into regions with distinct types of motion. (The simplest example in molecules is probably the distinction between normal and local modes.) When, in addition, the motion is chaotic, the invariant tori no longer exist. Our goals are the classification of the phase space structure in the highly anharmonic regime, the assignment of new quantum numbers based on this phase space structure, and the recognition of patterns signifying the phase space structure and classified by the new quantum number assignments.

An early paper [1] proposed a "bootstrap" method for fitting spectra of chaotic systems which are unassignable in terms of normal modes quantum numbers. A second paper [2] described a vector method to deduce new quantum numbers from a multiple resonance fit of a spectrum. (This latter method is now being applied by R.W. Field and coworkers to C_2H_2.) The bootstrap method of [1] is useful for fitting spectra of chaotic systems and obtaining potential surfaces [3]. However, it does not yield any quantum numbers for spectral pattern elucidation and assignment. The "vector" method of [2] does yield a partial set of quantum numbers. However, this set becomes smaller the higher the degree of chaos and the greater the detail of spectral resolution. A new development in our group aims to combine the bootstrap fitting method, the "vector" assignment method, and a new phenomenological approach, to obtain a complete set of quantum numbers. This new approach is based on correlation diagrams. The new assignment is made by taking account of diabatic energy level curves (near avoided crossings) in a correlation diagram from the zero-order to strongly coupled limits of the fit of an experimental spectrum. The fitting is strongly based on the "bootstrap" procedure. In this case, the bootstrap Hamiltonian uses effective resonance couplings, as opposed to potential surfaces used in other applications [3]. We have tested this correlation diagram approach on relatively weakly coupled systems such as H_2O, with good results. We are now testing it on model triatomic systems with a strong degree of chaos. If this succeeds, we plan to apply the method to C_2H_2, using data provided by the MIT group. The bootstrap fitting should be especially useful here because there are large gaps in the energy ranges currently covered by the MIT experiments.

The second area of work is bifurcation theory analysis of phase space structure derived from experimental spectra. In early work [4] we showed how to give an exhaustive phase space classification of two-mode systems coupled by a strong Fermi resonance, resulting in a new dynamically based quantum number scheme [5]. The goal now is extension of this approach to the much harder problem of multidimensional systems. A primary goal is again to obtain new assignment schemes. One object of the research is to relate these to the spectral patterns and phenomenological assignments from the correlation diagram approach described above. It is expected that the bifurcation analysis will result in a much better understanding of the patterns we find with the correlation approach, which will probably be easier to implement in practice. Under DOE auspices, we are performing *analytical* analysis of standard fitting Hamiltonians for three-mode systems (triatomics). This makes use of and extends some recent results in celestial mechanics. The relevance of that work is that it is based on normal form Hamiltonians, which are closely related to the phenomenological fitting Hamiltonians with nonlinear resonance terms used in spectroscopy and in much of our work. In the future, we hope to scale up this bifurcation approach to tetratomics, in particular, C_2H_2.

The final problem is the quantization of the phase space structure elucidated by the bifurcation analysis. This is necessary to achieve a truly rigorous quantum number assignment based on phase space structure. Our earlier work on assignment of systems such as the normal-local modes transition, or a single Fermi resonance in C-H bend-stretch spectra [4,5], made use of the fact that a good fit can be obtained with a single resonance coupling. This is implicitly based on the notion that the true dynamics in these systems, which sometimes undoubtedly contains a degree of chaos, is well-approximated by the remnants of invariant tori. In the present project, we are trying to put this idea on a rigorous basis and apply it to more complicated systems. We are doing this on the basis of mathematical work of Mather and others which shows that the remnants of tori are Cantor sets ("cantori"). We are attempting to apply this work to the assignment problem by semiclassically quantizing cantori, including the determination of wave functions. This approach is distinct from that of many others using periodic orbit sums, in which progress has been slow, and which does not take advantage in any explicit way of the phase space structure represented by the cantori.

1. J.M. Standard, E.D. Lynch, and M.E. Kellman, "Bootstrap Approach to Fitting Spectra of Molecules with Classically Chaotic Dynamics", J. Chem. Phys. 93, 159 (1990).

2. M.E. Kellman, "Approximate Constants of Motion for Vibrational Spectra of Many-Oscillator Systems with Multiple Anharmonic Resonances", J. Chem. Phys. 93, 6630 (1990).

3. J.M. Standard and M.E. Kellman, "Potential Energy Surfaces From Highly Excited Spectra Using the Bootstrap Method: Two-Dimensional Surfaces for Water and Ozone", J. Chem. Phys. 94, 4714 (1991).

4. L. Xiao and M.E. Kellman, "Catastrophe Map Classification of the Generalized Normal-Local Transition in Fermi Resonance Spectra", J. Chem. Phys. 93, 5805 (1990).

5. L. Xiao and M.E. Kellman, "New Assignment of Fermi Resonance Spectra", J. Chem. Phys. 93, 5821 (1990).

SHOCK TUBE STUDIES OF FUEL PYROLYSES

R.D. Kern, K. Xie and H. Chen
Department of Chemistry
University of New Orleans
New Orleans, Louisiana 70148

Program Scope

The formation of benzene from acyclic compounds, the decomposition pathways of aromatic ring compounds, and their relation to the pre-particle soot formation process define the major interests of our research program. Time-of-flight mass spectrometry (TOF) is used to analyze the species present during the observation time available in the reflected shock zone. Reaction time histories of the reactants, products, and intermediates are constructed and mechanisms are formulated to model the experimental data. Our work is often performed in collaboration with Professor John Kiefer and his use of laser schlieren densitometry (LS) to measure density gradients resulting from the heats of the various reactions involved in a particular pyrolytic system. The two techniques, TOF and LS, provide independent and complementary information about ring formation and ring rupture reactions.

Recent Progress

The efficiency with which propargyl radicals form benzene has been generally accepted. We were invited to speak at a recent Fuel Chemistry Symposium on combustion chemistry dealing with aromatic precursors and benzene formation at the American Chemical Society Meeting. Our experiments involved the production of C_3H_3 radicals from the high temperature pyrolysis of propargyl chloride. To our initial surprise, profiles due to m/e 78 (C_6H_6) were not observed although the decomposition of C_3H_3Cl occurred readily. It was subsequently deduced that the initial decomposition consisted of two channels:

$$C_3H_3Cl + M \text{ ------> } C_3H_2 + HCl \quad (1)$$

$$\text{------> } C_3H_3 + Cl \quad (2)$$

The former was shown to be dominant and there appears to be lacking effective pathways for the conversion of C_3H_2 to C_6H_6. However, experiments with mixtures containing C_3H_3Cl and H_2

exhibited C_6H_6 profiles. We proposed that an energized C_3H_4 adduct was formed.

$$C_3H_2 + H_2 \text{ ------> } [C_3H_4]^* \quad (3)$$

which had sufficient energy to isomerize to either allene or propyne. The decomposition of allene (A) or propyne (P) yields C_3H_3 + H.

$$C_3H_4 \text{ (A or P)} + M \text{ ------> } C_3H_3 + H \quad (4)$$

Additional support for this argument was acquired by investigating mixtures of $C_3H_3C\ell$ with either allene or propyne. In both cases, C_6H_6 is formed readily and at temperatures significantly lower (~ 1500 K) than those required for either A or P (~ 1770 K) reacting in the absence of $C_3H_3C\ell$. Although a reaction mechanism was proposed to model six different mixtures successfully, there are several key rate constants that are not well established, particularly for allene and propyne decomposing in the fall-off region.

In order to remedy these uncertainties, we commenced a collaborative effort with Professor John Kiefer to measure the dissociation rates of allene and propyne at high temperatures in our pressure regime (~ 0.4 atm) and to measure rates of benzene formation. The LS experiments were quite successful in determining the initial rates of allene and propyne decomposition to C_3H_3 + H. Evidence was presented for the direct formation of benzene from C_3H_3 radicals in a 4% allene mixture.

$$2\ C_3H_3 \text{ ------> } C_6H_6 \quad (5)$$

A 49 step mechanism was proposed to model the LS and TOF profiles. The results for a TOF experiment on a 3% allene-neon mixture at 1761 K are shown in Figures 1-4. The rate constant for allene decomposition measured for the first time by LS is employed in the calculation. The apparent discrepancy between the solid model line and the benzene data is readily explained by the carbon atom imbalance due to soot formation and the LS observation of beam attenuation due to solid formation at late observation times.

Work on the decomposition of aromatic rings continued with reports on chlorobenzene[2] and toluene.[3] Progress on our efforts regarding acetylene[4] and diacetylene[5] continued.

Future Plans

We are preparing a manuscript on shock tube studies of toluene pyrolysis for submission to the International Journal of Chemical Kinetics. We continue to model our data on propargyl chloride decomposition and the reactions of C_3H_3 to form benzene; a manuscript is planned for

FIGURE 1

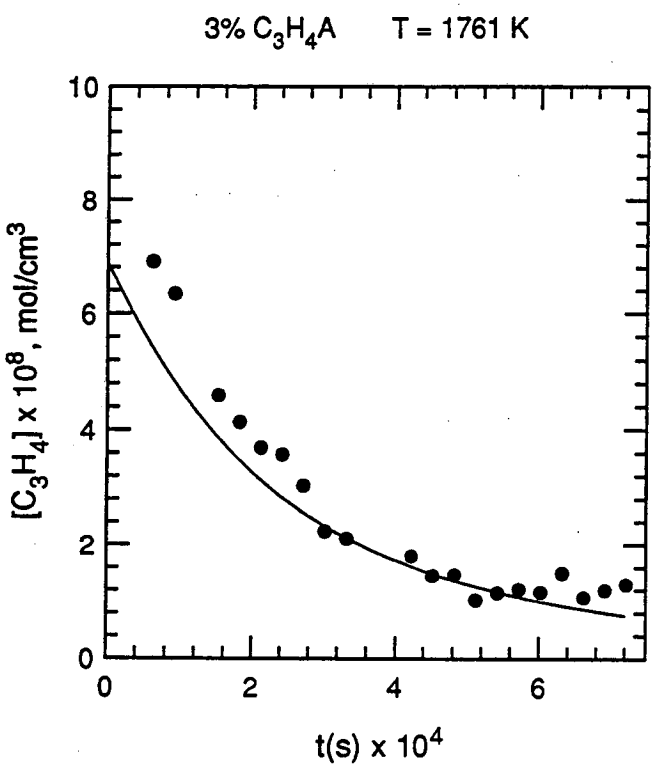

FIGURE 2

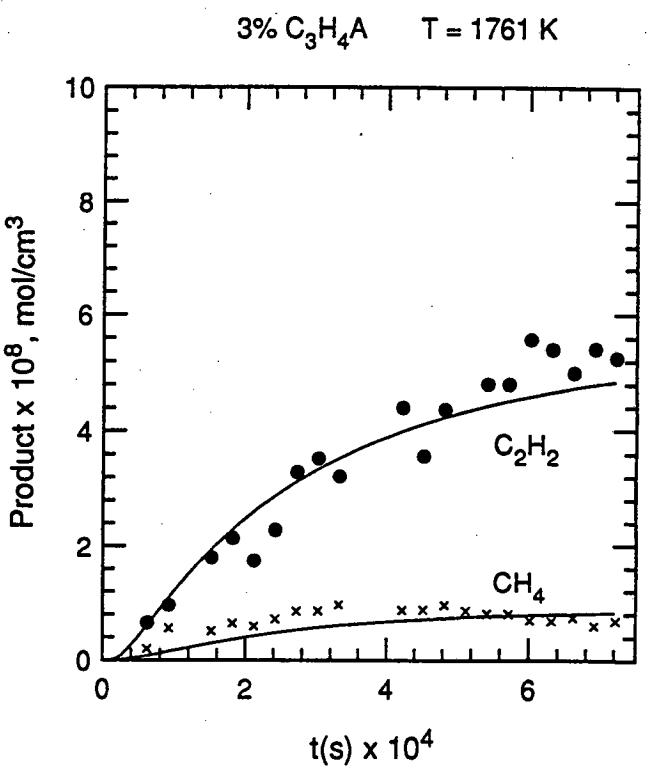

FIGURE 3

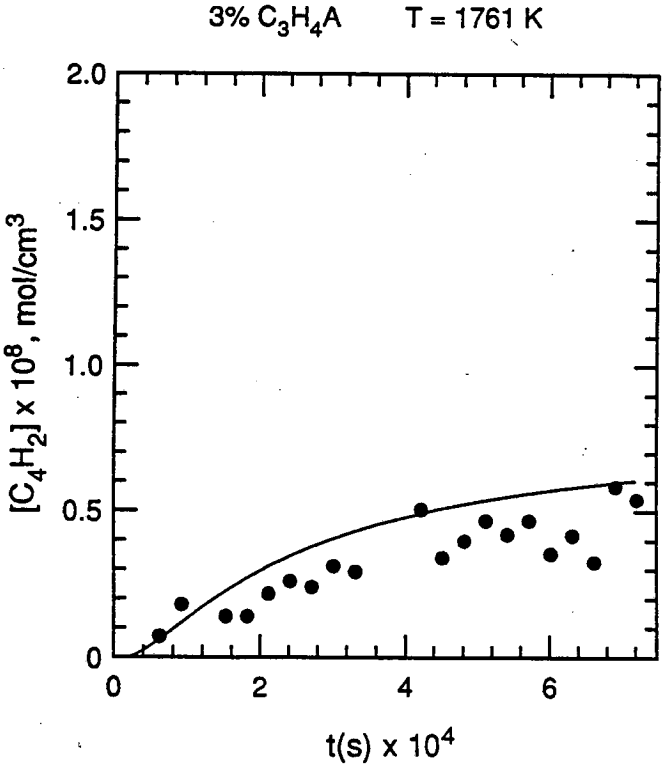

FIGURE 4

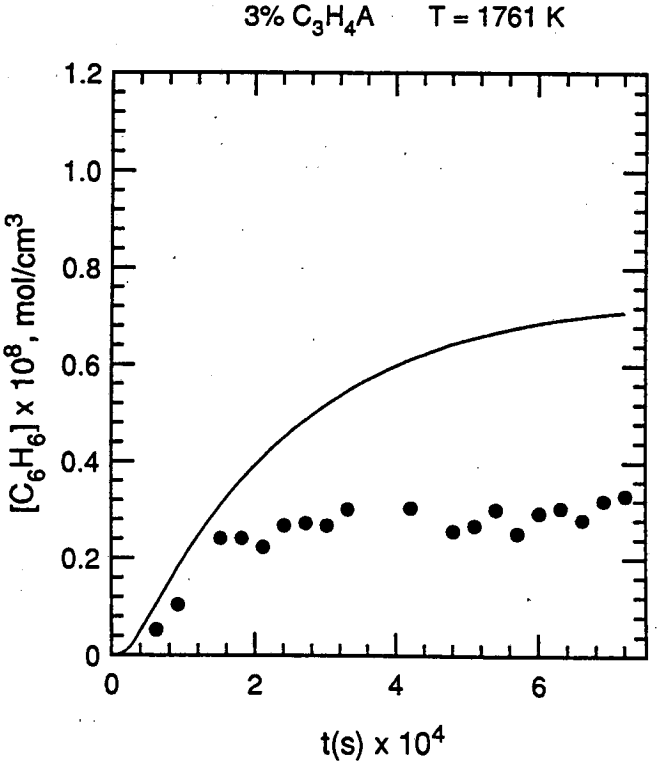

the Journal of Physical Chemistry. We plan to complete work on the decomposition of C_6H_2 in the presence of H_2 for presentation at the 19th Shock Tube Symposium.

References

1. R.D. Kern, K. Xie and H. Chen, "The Reactions of Propargyl Chloride and 1,5 Hexadiyne Behind Reflected Shock Waves", Symposium on Combustion Chemistry, Fuel Chemistry Division, 202nd American Chemical Society National Meeting, 1991, New York City, New York. Abstract published in Preprints of Div. of Fuel Chemistry 36, No. 4, p. 1423, American Chemical Society, 1991.

2. R.D. Kern, K. Xie and H. Chen, "A Shock Tube Study of Chlorobenzene Pyrolysis", Second International Congress on Toxic Combustion By-Products, 1991, Salt Lake City, Utah.

3. R.D. Kern, H.J. Singh, K. Xie and J.H. Kiefer, "Shock Tube Studies of Toluene Pyrolysis", Fall Technical Meeting of the Eastern Section of the Combustion Institute, 1991, Ithaca, New York.

4. R.D. Kern, K. Xie, H. Chen, J.H. Kiefer and S.S. Sidhu, "The Importance of Thermochemistry in the Pyrolysis of Acetylene at High Temperatures", International Seminar on High Temperature Chemistry, 1991, The University of Tokyo (Hongo Campus), Tokyo, Japan.

5. R.D. Kern, K. Xie, H. Chen and J.H. Kiefer, "The Reaction of C_4H_2 and H_2 Behind Reflected Shock Waves", 18th International Symposium on Shock Waves, 1991, Sendai, Japan.

Publications During 1990-92

1. R.D. Kern, H.J. Singh and K. Xie, "Shock Tube Study of the Thermal Decomposition of Acetaldehyde and Ethylene Oxide", 17th Symposium (International) on Shock Tubes and Waves, AIP Conference Proceedings 280: Current Topics in Shock Waves, Lehigh, Pennsylvania, 1990, p. 487-92.

2. R.D. Kern, H.J. Singh and K. Xie, "Identification of Chemi-ions Formed by Reactions of Deuterated Fuels in the Reflected Shock Zone", J. Phys. Chem. 94, 3333-35 (1990).

3. R.D. Kern, and K. Xie, "Shock Tube Studies of Gas Phase Reactions Preceding the Pre-Particle Soot Formation Process", Prog. in Energy and Combust. Sci., 17, 191-210 (1991).

4. R.D. Kern, K. Xie, H. Chen and J.H. Kiefer, "High Temperature Pyrolyses of Acetylene and Diacetylene Behind Reflected Shock Waves", Twenty Third Symposium (International) on Combustion, The Combustion Institute, Pittsburgh, PA, 1991, p. 69-75.

5. J.H. Kiefer, S.S. Sidhu, R.D. Kern, K. Xie, H. Chen and L.B. Harding, "The Homogeneous Pyrolysis of Acetylene II: The High Temperature Radical Chain Mechanism", Combustion Science and Technology, in press.

6. R.D. Kern, K. Xie, H. Chen, S.S. Sidhu and J.H. Kiefer, "The Reaction of C_4H_2 and H_2 Behind Reflected Shock Waves", 18th Symposium (International) on Shock Waves, in press.

7. R.D. Kern, K. Xie, and H. Chen, "A Shock Tube Study of Chlorobenzene Pyrolysis", Combustion Science and Technology, in press.

KINETICS OF COMBUSTION RELATED PROCESSES AT HIGH TEMPERATURES

J. H. Kiefer
Department of Chemical Engineering
University of Illinois at Chicago
Chicago, Illinois 60680

During this past year we have performed several pyrolysis studies which make use of unique features of the laser-schlieren (LS) technique, and, using a modification of our shock tube which permits the generation of well-formed but very weak shock waves, have made some surprising observations of vibrational relaxation in very large molecules.

Allene/propyne pyrolysis.

Measurements of decomposition in allene or propyne are always complicated by their mutual isomerization[1-4]. For one thing, this obstructs the measurement of separate dissociation rates for the two isomers. However, the LS technique can make precise measurements of endothermic rate within 1-2μs after shock heating, and the available isomerization rates[1-3] confirm that isomerization is negligible for such a small interval over a wide range of conditions. Also, the isomerization is near thermoneutral (ΔH°_{298} = 1.2 kcal/mol for propyne → allene) so its occurence in parallel with the slower dissociation does not interfere with the determination of dissociation rate.

Derived rate constants for both allene and propyne dissociation are shown in Figure 1 assuming the reaction is $C_3H_4 \rightarrow C_3H_3 + H$ in both, forming the resonance-stabilized propargyl radical. At the lower temperatures, the propyne rates lie slightly below those of allene, and this slight difference very closely mimics the greater stability of propyne, so that the reverse recombination rates are the same within experimental scatter. These rate constants seem to be close to their low-pressure limit, so this observation is consistent with there being no discernable barrier to H-atom addition at either end of the propargyl radical.

At our lowest temperatures (1700-1800K), with higher concentrations (4% in Kr) and higher pressures (@ 1atm), secondary processes are evident in the LS gradient profiles. In allene, below 1750K, the initial positive dissociation gradient quickly (in 1-4μs) becomes strongly negative. An interpretation of this result is suggested by the TOF product profiles for similar conditions generated by R.D. Kern and coworkers[4]. Here the only significant product whose formation is strongly exothermic is benzene. We have modeled these gradient profiles, including reactions which correctly generate the endothermic products of the TOF profiles (C_2H_2 and C_4H_2), and which incorporate various kinetic schemes for benzene formation. The only process having the correct kinetic behavior is the popular[4-6] $2C_3H_3 \rightarrow C_6H_6$. All paths which involve allene itself cause a too early transition to negative gradient.

We have very recently obtained measurements in propyne for the same conditions and find that the negative gradients are now absent. This certainly confirms our assumption that isomerization is unimportant here, but it places a severe strain on the notion of benzene formation by propargyl dimerization, since this same radical is readily formed in propyne decomposition. It is just possible, however, that the difference lies in the formation of substantial CH_3 in propyne pyrolysis (observed as methane) which can drive $CH_3 + C_3H_3 \rightarrow$ (various products) thereby both removing C_3H_3 and generating endothermicity. The modeling of this complex pyrolysis may well present too many problems, but, in collaboration with R.D. Kern, we are continuing this effort.

Methane Dissociation

The LS technique is well-suited to the measurement of dissociation rates in CH_4 because the fast

interfering secondary process $CH_4 + H \rightarrow CH_3 + H_2$ is again nearly thermoneutral (ΔH^o (2300K) = -1.2 kcal/mol). LS measurements of dissociation have already been reported[7], but these used very large CH_4 concentrations and did not explore the highest accessible temperatures.

Rate constants derived from the LS experiments done thus far are shown in Figure 2. Also shown is a "routine" RRKM fit to these low-pressure rates ($-\langle\Delta E\rangle_{all}$ = 145cm^{-1}) which allows an extrapolation to the lower temperatures of previous data. Evidently this study also favors the higher values summarized by Warnatz[8].

Relaxation and Dissociation in large Molecules

We have recently modified our shock tube with the insertion of various converging/diverging nozzles immediately after the diaphragm. With these we are able to produce clean, perfectly formed, but extremely weak shock waves. For example, with an 3/8" throat nozzle in the 2 1/2" tube we can generate shocks with T_2 = 600K, P_2 = 50 torr in krypton.

Our original intent was to use this facility for the study of unimolecular falloff in large molecules, but our initial study, the retro-Diels-Alder dissociation of norbornene ($C_7H_{10} \rightarrow C_5H_6 + C_2H_4$), immediately showed unusual features. Figures 3 and 4 show semi-log plots of density gradient in norbornene-krypton. Here several points are evident: i) The fast process is definitely vibrational relaxation; the predicted total density change ($u_1 \int (d\rho/dx)\, dt$) is correct at all temperatures. ii.) The relaxation is actually very fast, $P\tau \sim 1.7 \times 10^{-7}$ atm-s at 563K, iii.) The temperature dependence of $p\tau$ is very weak ($\sim T^{-1/2}$) so that relaxation can be seen at temperatures where decomposition also occurs, as in Figure 4, allowing an estimate of the unimolecular induction time ($P\tau$ (ind) ~ 0.7 μs-atm at 1262K). Remarkably, norbornene seems to be the largest molecule whose relaxation has been seen by any method. We have now also seen relaxation in methane and norbornadiene at dissociation temperatures. Norbornadiene relaxation (Figure 5) shows a surprising local maximum.

References

1. A. Lifshitz, M.Frenklach, and A. Burcat, J.Phys. Chem. 79, 1148 (1975); ibid. 80, 2437 (1976).
2. Y. Hidaka, et al., Int. J. Chem. Kinet. 21, 643 (1989); Chem. Phys. Lett. 119, 435 (1985).
3. T. Kakumoto, T. Ushirogouchi, K. Saito, and A. Imamura, J. Phys. Chem. 91, 183 (1987).
4. C.H. Wu and R.D. Kern, J. Phys. Chem. 91, 6291 (1987).
5. S.E. Stein, J.A. Walker, M.M. Suryan, and A. Fahr, 23rd Symposium on Combustion, The Combustion Institute, Pittsburgh, 1990/pg. 85.
6. U. Alkemade and K.H. Homann, Z. Phys. Chem 161, 19 (1989).
7. K. Tabayashi and S.H. Bauer, Combust. Flame 34, 63 (1979).
8. J. Warnatz in Combustion Chemistry, W.C. Gardiner, Jr., Ed., Springer, New York, 1984, pg. 239.
9. R.B. Klemm, J.W. Sutherland, M.J. Rabinowitz, P.M. Patterson, J.M. Quartemont, and W. Tao., J. Phys. Chem. 96, 1786 (1992).

Publications, 1990-present

1. The Mechanism of the Homogeneous Pyrolysis of Acetylene, J.H. Kiefer and W.A. Von Drasek, Int. J. Chem. Kinet. 22, 747 (1990).
2. The Decomposition of 1,3,5-Trioxane at Very High Temperatures, E.A. Irdam and J.H. Kiefer, Chem. Phys. Lett. 166, 491 (1990).
3. Tunable-Laser Flash-Absorption, A New Technique for Measuring Rates and Yields of Chemical

Reactions at High Temperatures, W.A. Von Drasek, S. Okajima, J.H. Kiefer, P.J. Ogren, and J.P. Hessler, Appl. Optics 29, 4899 (1990).
4. High Temperature Pyrolysis of Acetylene and Diacetylene Behind Reflected Shock Waves, R.D. Kern, K. Xie, H. Chen, and J.H. Kiefer, 23rd Symp. on Combustion, The Combustion Institute, Pittsburgh, 1990, pg. 69.
5. Rate of the Retro-Diels-Alder Dissociation of 1,2,3,6-Tetrahydropyridine over a Wide Temperature Range, S.S. Sidhu, J.H. Kiefer, A. Lifshitz, C. Tamburu, J.A. Walker, and W. Tsang, Int. J. Chem. Kinet. 23, 215 (1991).
6. The Reaction of C_2H_2 and H_2 Behind Reflected Shock Waves, R.D. Kern, K. Xie, K. Xie, H. Chen, and J.H. Kiefer, 18th Symposium on Shock Waves and Shock Tubes, Sendai 1991; in press.
7. Thermal Isomerization of Cyclopropanecarbonitrile. The Use of Multiple Chemical Thermometers in Single Pulse Shock Tube Experiments, A. Lifshitz, I. Shweiky, J.H. Kiefer, and S.S. Sidhu, 18th Symposium on Shock Waves and Shock Tubes, Sendai 1991; in press.
8. The Homogeneous Pyrolysis of Acetylene II: The High Temperature Radical Chain Mechanism, J.H. Kiefer, S.S. Sidhu, and R.D. Kern, K. Xie, H. Chen, and L.B. Harding, Combust. Sci. and Tech.; in press.
9. The Importance of Hindered Rotations and Other Anharmonic Effects in the Thermal Dissociation of Small Unsaturated Molecules: Application to HCN: A.F. Wagner, J.H. Kiefer and S.S. Kumaran, 24th Symposium on Combustion; accepted.
10. The Formaldehyde Decomposition Chain Mechanism: E.A. Irdam, J.H. Kiefer, L.B. Harding and A.F. Wagner, submitted to Int. J. Chem. Kinet.

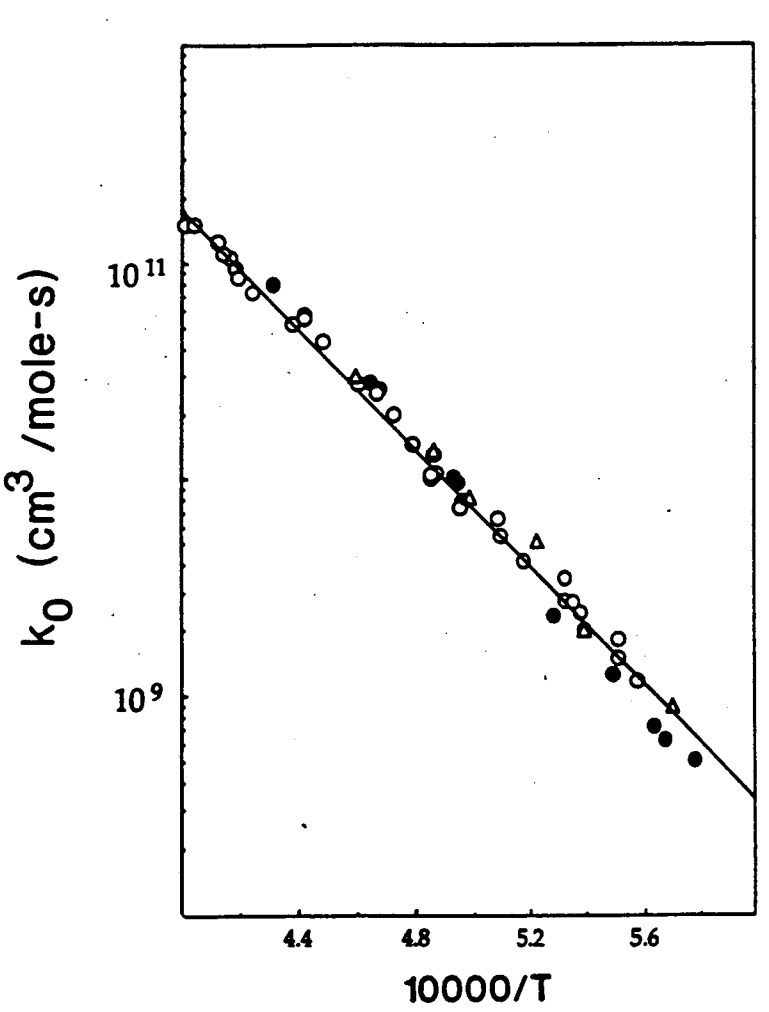

Figure 1: LS rate constants for allene (O, 2% in Kr; Δ, 4% in Kr) and propyne (●, 2% in Kr). The solid line merely indicates the linearity of the allene data.

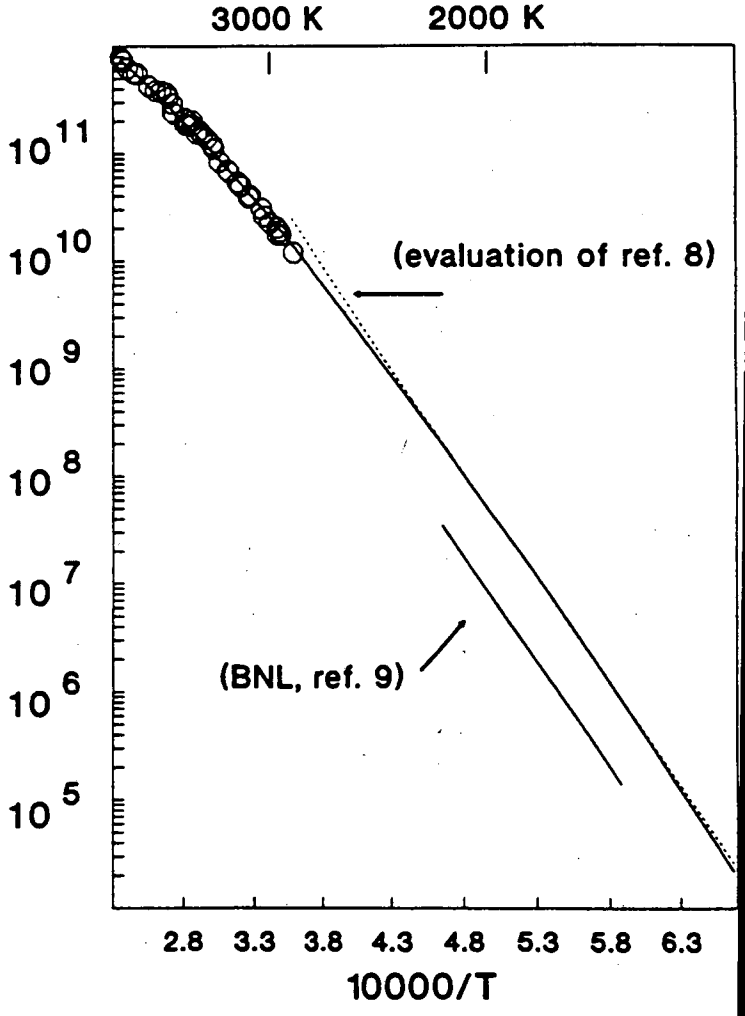

Figure 2: LS dissociation rate constants in 2% CH_4-Kr (○). The upper, curved solid line shows an RRKM fit to these data.

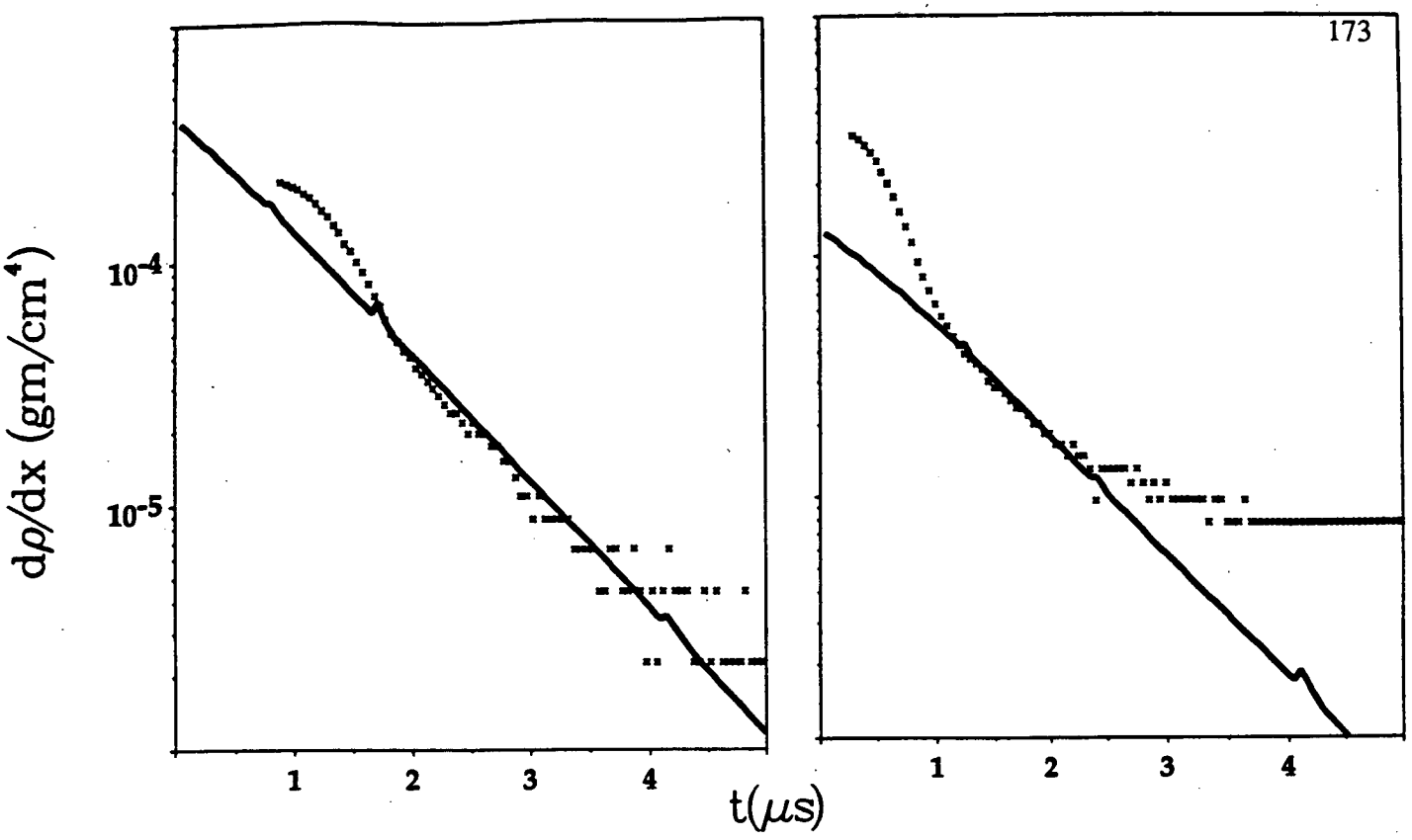

Figures 3 and 4: Relaxation (and dissociation) gradients in 2% Norbornene-Kr; 563K, 70torr; 1262K, 49torr. The lines are a simulation of the relaxation process.

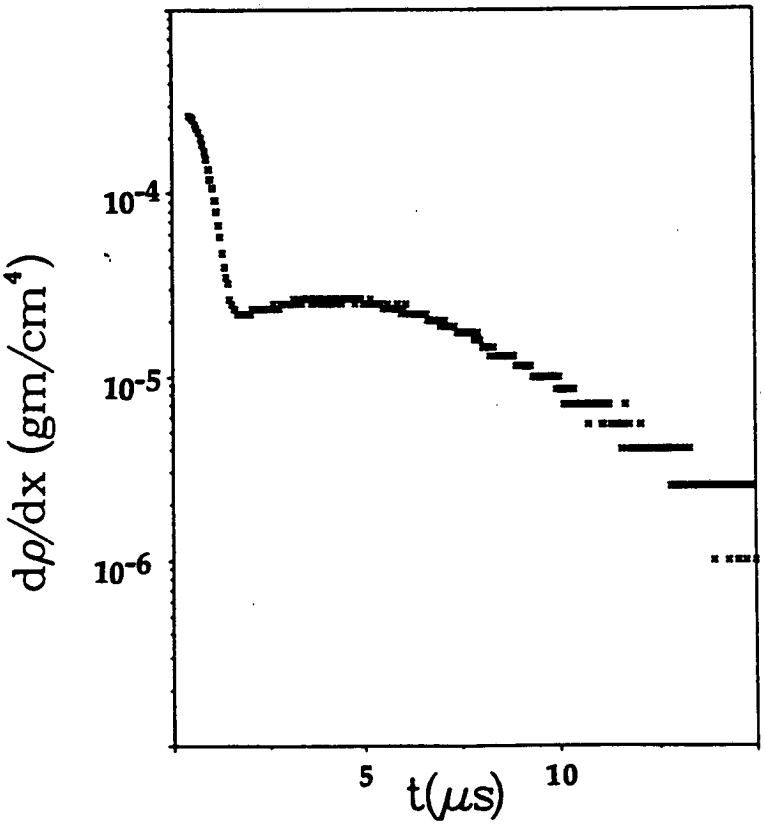

Figure 5: Relaxation gradients in 4% Norbornadiene-Kr; 680K, 29torr.

COMBUSTION KINETICS AND REACTION PATHWAYS

R. Bruce Klemm and James W. Sutherland
Combustion Kinetics Group/Bldg. 815
Department of Applied Science
Brookhaven National Laboratory
Upton, NY 11973

PROGRAM SCOPE

The scientific objectives of this project are (1) the measurement of absolute rate constants for combustion-related reactions of fuel compounds and intermediate species and (2) the determination of pathways for multichannel reactions. The focus of the research, in both cases, is on fundamental aspects of combustion chemistry. This experimentally based project features three independent methods in a multi-technique approach that provides unique capabilities in performing reliable kinetic measurements over an exceptionally wide range in temperature, 300K to 2500K. A discharge flow-photoionization mass spectrometer (DF-PIMS) experiment is used to identify primary products from multichannel reactions, to determine photoionization spectra for reactants and products, and to measure ionization energies of free radicals. The DF-PIMS apparatus was designed to be operated on the U-11 beam line at the National Synchrotron Light Source (NSLS) and thus take advantage of tunable vacuum ultraviolet light to achieve improved detection sensitivity and selectivity in monitoring free radicals.

RECENT PROGRESS

Further Study of the $H+CH_4 \leftrightarrow CH_3+H_2$ Reaction and CH_4 Dissociation.

The thermal dissociation of methane is of fundamental interest and the kinetics of this reaction have a direct bearing on CH_4 pyrolysis and combustion. Recent work reported from this laboratory (publications #5 and #10) provided direct kinetic measurements of the dissociation of methane and the reaction of atomic hydrogen with methane,

$$CH_4 + Ar \rightarrow CH_3 + H + Ar \quad (1)$$
$$H + CH_4 \rightarrow CH_3 + H_2. \quad (2)$$

The rate constant expressions derived in these studies, over the indicated temperature ranges, are given below:

reaction (1), 1700 - 2150K:

$$k_1^\circ = 6.8\times10^{-8} \exp(-44900/T) \text{cm}^3 \text{ molecule}^{-1} \text{ s}^{-1} \quad (I)$$

reaction (2), 400 - 1800K:

$$k_2 = 6.4\times10^{-18} T^{2.11} \exp(-3900/T) \text{ cm}^3 \text{ molecule}^{-1} \text{ s}^{-1} \quad (II)$$

RRKM and master equation calculations indicate that k_1 was measured very near the low pressure limit for methane dissociation in argon (thus the designation as k_1°).

These results come at a time of renewed interest in methane dissociation kinetics; and it is therefore particularly noteworthy that our new kinetic measurements differ substantially (by factors of about 5) from those reported in numerous indirect studies (1975-1990) for reaction (1) and from those of Roth and Just (1975) for both reaction (1) and reaction (2). A re-investigation of reaction (2) in Just's laboratory (in which H atoms are produced rapidly via dissociation of ethyl iodide: $C_2H_5I \rightarrow C_2H_5 + I$; $C_2H_5 \rightarrow C_2H_4 + H$) provides

preliminary results that are only slightly lower (≈30%) than the reported results of Roth and Just, (1975). In addition, further experiments in Just's laboratory (1992–private communication) to determine k_1^o show only a small difference with that reported by Roth and Just (1975). Since part of our study of methane dissociation (1992) depended on the rate constant for reaction (2) (1991), we have performed additional experiments to further investigate the kinetics of reaction (2). In this study, the rate constant for the reverse reaction,

$$CH_3 + H_2 \rightarrow CH_4 + H \qquad (-2)$$

was determined by generating CH_3 radicals via thermal dissociation of acetone or ethane and by following the subsequent formation of H using the atomic resonance absorption technique. Values of k_{-2} determined in this study may thus be compared to those derived by conversion of k_2 using the equilibrium constant,

$$k_{-2} = k_2 / K_2 \qquad (III)$$

In addition, some further experiments were carried out to measure k_1^o and RRKM/master equation calculations were performed to investigate the fall–off behavior of both CH_4 and CD_4. The detection limit for the [H] was about $3x10^{10}$ atoms cm^{-3}. Rate constants for both reactions were obtained under pseudo–first–order conditions. In addition, computer simulations verified that kinetic complications were avoided.

For the reaction of CH_3+H_2, either acetone or ethane was used to generate CH_3 radicals rapidly by thermal dissociation in argon. Twenty–four experiments were performed over the temperature range 1346K to 1793K and a rate constant expression derived using linear least–squares analysis:

$$k_{-2}(T) = (6.0\pm0.7)x10^{-12} \exp(-5920\pm190K/T) \text{ cm}^3 \text{ molecule}^{-1} \text{ s}^{-1}.$$

Values from this expression agree well with those computed using $k_{-2} = k_2/K_2$ (where k_2 is the rate constant for the $H+CH_4 \rightarrow CH_3+H_2$ reaction and K_2 is the equilbrium constant) as reported in an earlier study (1991) from this laboratory. The discrepancy between these results and those (for k_2) reported by Roth and Just therefore remains.

For the methane dissociation study, experiments were performed with both CH_4/Ar mixtures and CH_4/H_2/Ar mixtures over the limited temperature range, 1756K to 1947K. In the CH_4/Ar experiments, a steady state analysis was employed wherein k_1^o (the low pressure limit rate constant for dissociation of CH_4 in argon) is equated to $[H]_{ss}xk_2/[Ar]$. This analysis therefore relies directly on the absolute [H] calibration and the value for k_2. In the CH_4/H_2Ar experiments, it was necessary to use computer simulations to fit the [H] build–ups since the reaction of CH_3 with H_2 converted a significant fraction of the CH_3 radicals to H–atoms (and CH_4). These new results for k_1^o are also in good agreement with previous results (1992) reported from this laboratory. RRKM/master equation calculations were performed for both CH_4 dissociation and CD_4 dissociation to evaluate the fall–off behavior of k_1^{uni} and to allow comparison of the present results with those of previous studies in other laboratories.

Within the framework of these calculations, the present results for the low pressure limit CH_4 dissociation rate constant, k_1^o, are not only consistent with those reported earlier but they agree as well with the re–evaluated rate data of Roth and Just (as reported in publication #5) and with those of Skinner and co–workers (1980) (for CD_4 dissociation as related through RRKM/master equation calculations). On the other hand, the results reported in indirect CH_4 dissociation studies (1975–1990) (notably those of Cobos and Troe (1990)) are all

much larger than the present values of k_1^o and k_1^{uni} (as determined by RRKM/master equation calculations). This work clearly delineates a major discrepancy in the kinetics of the low pressure, thermal dissociation of methane (and the kinetics of the $H+CH_4 \leftrightarrow CH_3+H_2$ reaction) and thus may have implications regarding: (i) energy transfer efficiency; (ii) rate constants measured relative to reactions (1) and (2) (e.g. derived via simulations); (iii) modeling studies of methane pyrolysis and combustion; and (iv) the importance of a second channel to products (e.g. CH_2+H_2). Due to the fundamental importance of reaction (1) in particular, further experimental and theoretical studies are needed.

$O(^3P) + C_2H_6 \rightarrow C_2H_5 + OH$ (400K to 1500K)

The reactions of atomic oxygen with hydrocarbons are among the most important in the ignition process and the initial phases of combustion. It is essential, therefore, that rate constants for these reactions be known accurately over the widest possible temperature ranges. In the present study, rate constants for the $O + C_2H_6$ reaction were measured using three independent methods: (i) discharge flow-resonance fluorescence ($453<T<1048K$); (ii) flash photolysis-resonance fluorescence ($416<T<520K$); (iii) flash photolysis-shock tube ($728<T<1489K$). There is excellent agreement between the individual data sets obtained by these three independent techniques in the overlapping ranges of temperature. The data were well fit by the Arrhenius equation ($416K \leq T \leq 1489K$):

$$k(T) = 2.2\times10^{-10} \exp(-4030\ K/T)\ cm^3\ molecule^{-1}\ s^{-1}.$$

The mean deviation of the experimental points from this fit is ±11.1% at the one sigma level. However, slight curvature in the plot was evident at the highest temperatures; and thus an improved fit was obtained by using a three parameter expression:

$$k(T) = 1.45\times10^{-13}T^{0.857} \exp(-3340\ K/T)\ cm^3\ molecule^{-1}\ s^{-1}$$

The mean deviation of the experimental points from this fit is ±9.6%.

Reaction Pathways Studies Using PIMS

The reaction of N-atoms with ethyl radicals, which has several exothermic product channels, may be important in "prompt" NO_x mechanisms and it has been implicated as a complicating feature in flow tube studies of "active nitrogen."

$$\begin{aligned} N + C_2H_5 &\rightarrow HCNH + \underline{CH_3} \quad (-31) \\ &\rightarrow H_2CN + \underline{CH_3} \quad (-45) \\ &\rightarrow HCN + CH_4 \quad (-125) \\ &\rightarrow NH + \underline{C_2H_4} \quad (-47) \end{aligned}$$

Numbers in parentheses indicate the enthalpy of reaction in kcal mol^{-1} units. This study is part of the ongoing collaboration between BNL and NASA/GSFC (Stief and Nesbitt). By using perdeuterated ethane to generate C_2D_5, via F atom abstraction, it is possible to isolate the underlined products by mass. In a preliminary study, the $H_2CN + CH_3$ channel and the $NH + C_2H_4$ channel were indicated, qualitatively, to be major product pathways.

The photoionization spectrum of H_2COH was measured over the wavelength range 140 nm to 170 nm using DF-PIMS at the NSLS. Hydroxymethyl radicals (H_2COH and H_2COD) were generated in a flow tube by the reaction of F atoms with $CH_3OH(D)$. Ionization energies (IE) were determined directly from photoion thresholds. The IE values, 7.56±0.02 eV and 7.55±0.02 eV for H_2COH and H_2COD, respectively, are consistent with the recent PIMS results of Ruscic and Berkowitz (1991). The good

agreement between these two independent PIMS studies thus serves as an important confirmation of Dyke's (1984) photoelectron spectroscopic measurements.

FUTURE PLANS

Shock tube studies of hydrocarbon thermal dissociation in argon will be pursued for molecules that undergo predominantly C-H bond fission or whose radical fragments react rapidly with H_2 to generate H-atoms. Multitechnique kinetic studies of O-atom reactions with olefins will continue and be augumented by reaction pathways studies using DF-PIMS. Further work on the $N+C_2H_5$ reaction will attempt to determine a semi-quantitative measurement for the $C_2H_4(+NH)$ branching fraction. Photoionization spectra for D_2COH, D_2COD, CD_3O and CH_3O will be determined to measure ionization energies for these important radicals.

RECENT PUBLICATIONS

1. Sutherland, J. W., Patterson, P. M., and Klemm, R. B. A flash photolysis-shock tube kinetic investigation of the reaction of $O(^3P)$ atoms with ammonia. J. Phys. Chem. 94, 2471-75 (1990).

2. Patterson, P. M., Sutherland, J. W., and Klemm, R. B. High temperature study of the reaction of $O(^3P) + NH_3$. Proc. Seventeenth Int'l. Sympos. on Shock Tubes and Waves, American Institute of Physics, New York, 1990, pp. 444-49.

3. Klemm, R. B., Sutherland, J. W., Wickramaaratchi, M. W., and Yarwood, G. A flash photolysis-shock tube kinetic study of the reaction of $O(^3P)$ with ethylene: $1052K<T<2248K$. J. Phys. Chem. 94, 3354-57 (1990).

4. Smalley, J. F. and Klemm, R. B. Calculation of rate constants for the reactions of $O(^3P)$ with olefins using a non-adiabatic electronic tunneling model. J. Phys. Chem. 94, 3358-61 (1990).

5. Rabinowitz, M. J., Sutherland, J. W., Patterson, P. M., and Klemm, R. B. Direct rate constant measurements for $H+CH_4 \rightarrow CH_3+H_2$, 897-1792K, using the FP-ST technique. J. Phys. Chem. 95, 675-81 (1991).

6. Sutherland, J. W., Patterson, P. M., and Klemm, R. B. Rate constants for the reaction $O(^3P) + H_2O \leftrightarrow OH+OH$, over the temperature range 1053K to 2033K using two direct techniques. Proc. Twenty-third Int'l. Sympos. on Combustion, The Combustion Institute, Pittsburgh, 1990, pp. 51-57.

7. Nesbitt, F. L., Marston, G., Stief, L. J., Wickramaaratchi, M. A., Tao, W., and Klemm, R. B. Measurement of the photoionization spectra and ionization threshold of the H_2CN and D_2CN radicals. J. Phys. Chem. 95, 7613 (1991).

8. Yarwood, G., Sutherland, J. W., Wickramaaratchi, M. A., and Klemm, R. B. Direct rate constant measurement for the reaction $O+NO+Ar \rightarrow NO_2+Ar$, 300K to 1341K. J. Phys. Chem. 95, 8771 (1991).

9. Tao, W., Klemm, R. B., Nesbitt, F. L., and Stief, L. J. A discharge-flow photoionization mass spectrometric study of hydroxymethyl radicals (H_2COH and H_2COD): photoionization spectrum and ionization energy. J. Phys. Chem., in press.

10. Klemm, R. B., Sutherland, J. W., Rabinowitz, M. J., Patterson, P. M., Quartemont, J. M., and Tao, W. Shock tube kinetic study of methane dissociation: $1726K \leq T \leq 2134K$. J. Phys. Chem. 96, 1786 (1992).

Theoretical Investigations in Kinetics and Dynamics

Principal Investigator: Michael L. Koszykowski, Combustion Research Facility, Sandia National Laboratories, Livermore CA 94551-0969

Program Scope: These research activities consist of the utilization of state-of-the-art theoretical methods to investigate chemical-physics phenomina in support of combustion chemistry, diagnostics and modeling. Of particular interest is our continual attempt to expand the range of systems which can be addressed by the utilizational of cutting edge computer technology, specifically massively parallel computers.

Recent progress:

Investigations in Kinetics, Dynamics and Combustion Modeling

M. L. Koszykowski, R. Armstrong, and R. E. Cline, Jr.

We have carried out ab initio calculations using Møller-Plesset perturbation theory and several basis sets for the F + methanol hydrogen abstraction reaction in order to understand the theoretical basis for the anomalous large methoxy (product resulting from hydroxyl-side attack) vs hydroxymethyl (product resulting from methyl-side attack) yields observed experimentally. Of the three unique abstraction sites on methanol, we have located a saddle-point for the *syn* methyl channel, a hilltop for the *anti* methyl channel, and a minimum (hydrogen-bonded complex) for the hydroxyl channel. The classical barrier height was 1.89 kcal/mole for the methyl-side attack and negligible for the hydroxyl-side attack. Using conventional transition state theory, the rate coefficients (in units of cm^3 $molecule^{-1}$ s^{-1}) for methoxy production vary from 2.83×10^{-11} at 298 K to 1.30×10^{-10} at 1333 K. We have further validated this results by utilizing both multideterminate wave function calculations, as well as variational transition state theory. The calculated methoxy branching fractions for both calculations are consistent with the observations in the experiments of this series and vary from 0.70 at 298 K to 0.55 at 1333 K. Our analysis of these results provides a qualitative explanation for the anomalous large methoxy yields.

Another focus of our efforts has been to develop theoretical techniques to study vibrations of floppy systems. In our the area of investigation of vibrationally floppy systems, we have applied the correlation function quantum Monte Carlo (CFQMC) technique. CFQMC employs a guided random walk in nuclear configuration space to

simultaneously sample a manifold of excited vibrational states. At specified intervals during the walk, imaginary-time correlations are constructed for the matrix elements $\mathbf{H_{ij}}$ and $\mathbf{S_{ij}}$. After sufficient sampling to reduce statistical noise, a diagonalization is performed to project out each state onto its respective eigenstate. In terms of accuracy, CFQMC is not limited by the quality of the basis set and is a zero-variance technique. Because the random walks occur independently, QMC techniques are ideally suited to parallelization, and our results on the Ncube-2 show that we gain a factor of 80 in speed over a Cray X/MP24.. We are presently using the CFQMC technique to the study of highly coupled and anharmonic system C_3.

We have developed a classical simulation code for dense water and are investigating the effects of nonadditive polarizabilty interactions based on extensions of work done by E. Clementi, P. Kollman and others. After testing is completed we will simulate the vibrational spectrum of supercritical water at a variety of densities, and compare simulated spectra with diagnostics results. This is also a good test of the detail nonlocal interactions of the H_2O potential. We might expect good agreement with experiment at low density, where many-body effects are less important, and significant deviations at higher densities. The details of the experiment-theory comparison will give us insight as to how to improve the intermolecular water potentials.

Combustion modeling of turbulent flames with full chemistry is important in an attempt to understand pollutant formation in realistic combustion systems. The complexity of these calculations requires a tremendous amount of computation and the models are currently limited by conventional supercomputer resources. Since integration of the stiff chemical kinetics accounts for over 99% of the total CPU time, these models have been limited to reduced chemical mechanisms and simple systems. Parallel computing circumvents some of these limitations by allowing independent chemical kinetic calculations for each statistical sample of the pdf Monte Carlo method under study here.

The strategy for developing massively parallel computational codes for this and other models is the use of the new Parallel Object-oriented Environment & Toolkit (POET).

Existing tools for parallel software development generally fall into two categories: 1) high-level tools and compilers that hide the parallelization details, making them easy to use but also hiding the pitfalls that lead to bottlenecks; or, 2) low-level tools for message passing that create scalable code, but require such detailed knowledge of algorithms and software that they are difficult for the non-systems programmer to use. through the use of a well-defined, object-oriented interface, similar to the X toolkit approach. An important point: POET is written in C++ in an extensible manner that guarantees scalable code (for example, if we have twice as many processors available the code will finish in half the time).

The results of interfacing the PDF model with POET will yield the first investigation of a turbulent nonpremixed flame with a full chemical mechanism. This benchmark calculation will useful immediately for examining the limitations of various reduced chemical mechanisms. Because the toolkit is object oriented and handles only the grid, chemistry, and communications aspects of the model, we will be able to readily incorporate other fluid mechanics and chemistry models and codes as they are developed.

Publications:

W. A. Glauser and M. L. Koszykowski, "Quantum Monte Carlo Study of Excited Vibrational States of Water using a Parallel Algorithm," J. Comp. Chem., (submitted).

W. A. Glauser, M. L. Koszykowski, W. A. Lester, and Brian L. Hammond, "Random Walk Approach to Mapping Nodal Regions of N-Body Wavefunctions. I. Ground State Hartree-Folk Wavefunctions for First Row Atoms," J. Chem. Phys., (submitted).

W. A. Glauser and M. L. Koszykowski, "Anomalous Methoxy Yields In the Fluorine + Methanol Reaction. 2. Theory," J. Phys. Chem., **95**, 10705, 1991.

W. A. Glauser and M. L. Koszykowski, "Vibrational Dispersion Interactions in Van der Waals Complexes: Effect upon Stability and Infrared Spectra," J. Phys. Chem., **95**, 8507 (1991).

B. C. Garrett, M. L. Koszykowski, C. F. Melius, and M. Page, "Theoretical Calculations of the Thermal Rate Constants for Gas-Phase Chemical Reactions of $H+NH_3$, H_2+NH_2, $D+ND_3$, and D_2+ND_2," J. Phys. Chem. **94**, 7096 (1990).

B. M. Rice, B. C. Garrett, M. L. Koszykowski, S. M. Foiles, M. S. Daw, Kinetic Isotope Effects for Hydrogen Diffusion in Bulk Nickel and on Nickel Surfaces, J. Chem. Phys., **92**, 775, 1990.

LASER SOURCES AND TECHNIQUES FOR SPECTROSCOPY AND DYNAMICS

Andrew H. Kung

Chemical Sciences Division
Lawrence Berkeley Laboratory
Berkeley, California, 94720

Project Scope

This project focusses on developing and demonstrating novel laser and spectroscopic techniques in the IR, UV and VUV regions to study combustion related molecular dynamical processes at the microscopic level. The approach is to develop ultrahigh resolution laser sources to obtain and analyze photoionization, florescence, and photoelectron spectra of jet-cooled transient free radicals and of reaction products resulting from unimolecular or bimolecular dissociation. This work is in close collaboration with Y.T.Lee's group and C.B.Moore's group.

Recent Progress

1. Development of Ultranarrow Bandwidth VUV-XUV Laser System. An ultrahigh brightness laser system was developed a few years ago for applications in spectroscopy and dynamics in the VUV-XUV region. The laser utilizes pulse amplification of a single-mode ring dye laser, together with frequency multiplication in non-linear crystals and a pulsed jet to get to the short wavelength region. The utility of this laser system was demonstrated in an ultrahigh resolution (1+1) photoionization study of krypton where the hyperfine structure and isotope shift of several Rydberg states of Kr were measured with very high precision, and in state-selected ionization of nitrogen where selectively vibrationally excited N_2 ions were produced in large quantities. More recently the laser system has been used in product state distribution mapping in H_2 elimination from cyclohexadiene (see below) and from ethylene (Y.T.Lee group).

2. Dynamics of H_2 Elimination from Cyclohexadiene. A comprehensive study of the dynamics of H_2 elimination from 1,4- and 1,3-cyclohexadiene has been completed. Rotational and vibrational quantum state distributions for the H_2 product were measured that complement translational energy distribution studies. State specific detection of H_2 was accomplished via (1+1) REMPI. The vibrational and rotational energy distributions indicate a tight and symmetric transition state which is supported by theoretical calculations. The distribution of H_2 translational energy both over a given ro-vibrational state and over all the populated quantum states confirms the concerted and synchronous nature of the dissociation process and the dominance of the potential barrier to the release of the translational energy of the H_2 product. A (v,J) correlation for H_2 with $v \parallel J$ primarily is observed from anisotropy in the Doppler profiles. This correlation between the velocity and rotational angular momentum vectors indicates that the H_2 moves away

from the transition state complex with a helicopter type motion. The study shows the significant utility of the high resolution laser system in understanding the dynamics of primary photodissociation of polyatomic molecules.

3. Lawrence Berkeley Laboratory Advanced Light Source Chemical Physics Beamline. Technical support was provided to the development of the Chemical Dynamics Initiative jointly proposed by the Sandia National Laboratories and the Lawrence Berkeley Laboratory. The initiative includes the construction of a bend magnet beamline and a U10 undulator beamline at the Chemical Dynamics Research Laboratory adjacent to the ALS. The initial beamline design by the LBL ALS team that have been proposed for the bending magnet and the U10 undulator were reexamined to meet design conditions which were revised in user workshops held in 1991. In the new design, the width of the ALS beam spot in the horizontal direction at the molecular beam sample is kept at less than 10 microns. The height of the beam from the floor is reduced to match that of the ALS at approximately 1.5 meters. It was discovered that by reducing the deviation angle at the monochromator grating from 15 degrees to 10 degrees the astigmatism of the beam at the sample location can be improved, ranging from 20% at 125 nm to a factor of 2.2 at 200 nm and 2.7 at 50 nm. Most of the calculations on the beamline design were performed by Masato Koike of the Center of X-Ray Optics, LBL, who is collaborating with us on this project. The new results have been incorporated in the Conceptual Design Report for the CDRL.

Future Plans

The primary focus will be on developing a high power mid-infrared laser for multiphoton dissociation studies. Another focus will be to complete the construction of a picosecond tunable VUV source and to demonstrate its utility in reaction dynamics applications. Both of these lasers will play a very important role in the emphasis to understand the chemical reactivity of polyatomic radicals.

1. High Resolution High Power Tunable Infrared Laser. Recent workshops and reviews have identified that fundamental studies in the primary dissociation and spectroscopy of free radicals of hydrocarbons are essential for the understanding the processes that underlie combustion of fossil fuels. These studies can best be performed using infrared sources both to produce the free-radicals by multiphoton excitation and to probe the reactive intermediates. The vibrational infrared region from 3 to 10 microns would he most interesting region to study. However sufficiently powerful sources do not exist today. We propose to investigate methods to generate modestly high power infrared that would permit demonstration of the feasibility of multiphoton excitation in an isolated molecular setting and allow some of the critical experiments to be performed. The focus will be on evaluating the use of nonlinear optical techniques such as high order Raman shifting of high power visible tunable lasers to produce high resolution nanosecond infrared pulses. The goal is to obtain a high repetition rate infrared source tunable from 3 to 10 microns, with pulse energy of greater than 25 mJ, and with near-transform-limited resolution.

2. Investigation of the High Lying Electronic State of Polyatomic Radicals. High lying electronic states of polyatomic radicals are relatively unknown. Some of them are expected to have a fast dissociation lifetime. With our unique high resolution VUV laser, it is now possible to investigate these high lying electronically excited states through (1+1) photoionization. The successful investigation of high lying electronically excited states will both enrich our knowledge and allow us to assess whether infrared vibrational spectroscopy for polyatomic radicals can be obtained by the ion-dip approach.

3. Vibrational Spectroscopy of Polyatomic Radicals. Although there have been some progress made in the small radicals, the vibrational spectra of larger polyatomic molecules are still largely unknown. With the development of a high power tunable laser, it will be possible to investigate vibrational motion of polyatomic radicals either using the flop-in technique by selectively ionizing vibrationally excited radicals or by using the ion-dip technique.

4. Development of a Picosecond Tunable UV/VUV Laser. A picosecond UV/VUV laser system has been developed for the study of unimolecular dynamics. The system provides two independently tunable picosecond pulses for UV excitation and time delayed VUV ionization. Over the last year, greater than 40 microjoules near 266nm and greater than 10^8 photons near 119nm (measured after a VUV monochromator) with a cross correlation of the precursor pulses of less than 4 picoseconds have been achieved.

Work is in progress to obtain the instrument response function by studying the photodissociation of methyl iodide. The molecule is pumped near 266 nm, and after a variable delay, all species present are ionized by a 119nm 1 photon process. The ions are separated by Time Of Flight Mass Spectrometry and the appearance rate of I^+ and CH_{3+} ions is measured. Preliminary results yield a response of ~5 ps.

Further work will focus on the photodissociation of halobenzenes using the same technique. These molecules are expected to have lifetimes of several picoseconds. We are also developing a picosecond photoelectron spectrometer to directly observe the decay of electronic excitation in isolated molecules through internal conversion or intersystem crossing.

Recent Publications:

E.F. Cromwell, D.J. Liu, M.J.J. Vrakking, A.H. Kung, and Y.T. Lee, Dynamics of H_2 Elimination from 1,4-Cyclohexadiene, J. Chem. Phys. **92**, 3230-3231 (1990).

E.F. Cromwell, D.J. Liu, M.J.J. Vrakking, A.H. Kung, and Y.T. Lee, Dynamics of H_2 Elimination from Cyclohexadiene, J. Chem. Phys. **95**, 297-307 (1991).

A.H. Kung and Y.T. Lee, Spectroscopy and Reaction Dynamics Using Ultrahigh Resolution VUV Lasers, in **Vacuum Ultraviolet Photoionization and Photodissociation of Molecules and Clusters**, C.Y. Ng, editor, World Scientific Publishing Company, Singapore (1991), pp.487-502.

Molecular Beam Studies of Reaction Dynamics

Yuan T. Lee
Chemical Sciences Division
Lawrence Berkeley Laboratory
Berkeley, California 94720

Scope of Project

The major thrust of this research project is to elucidate detailed dynamics of simple elementary reactions that are theoretically important and to unravel the mechanism of complex chemical reactions or photochemical processes that play important roles in many macroscopic processes. Molecular beams of reactants are used to study individual reactive encounters between molecules or to monitor photodissociation events in a collision-free environment. Most of the information is derived from measurement of the product fragment energy, angular, and state distributions. Recent activities are centered on the mechanisms of elementary chemical reactions involving oxygen atoms with unsaturated hydrocarbons, the dynamics of endothermic substitution reactions, the dependence of the chemical reactivity of electronically excited atoms on the alignment of excited orbitals, the primary photochemical processes of polyatomic molecules, intramolecular energy transfer of chemically activated and locally excited molecules, the energetics of free radicals that are important to combustion processes, the infrared-absorption spectra of carbonium ions and hydrated hydronium ions, and bond-selective photodissociation through electric excitation.

Current Research and Recent Results

A. Primary Dissociation Processes

1. Infrared Spectroscopy of Ionic Clusters Containing CH_5^+. Ionic clusters containing CH_5^+ have been investigated using infrared laser spectroscopy based upon vibrational predissociation. In this technique, mass-selected parent ions are exposed to tunable IR laser radiation while they are trapped in an octapole ion trap. The number of daughter ions formed by vibrational predissociation of the trapped parent ions is measured with a quadrupole mass spectrometer. This technique has higher sensitivity than direct absorption IR techniques, which is very important for the study of weakly bound clusters which can not be generated in large numbers in the cold ion form.

Last year we studied three solvated CH_5^+ dimers: $CH_5^+(H_2)$, $CH_5^+(CH_4)$, and $CH_5^+(H_2O)$ in the frequency region from 2650 cm^{-1} to 4150 cm^{-1} with 0.2 cm^{-1} resolution. In their spectra, it was found that each band has a splitted feature which may originate from tunneling motion of these clusters. Usually, for weakly bound clusters, there has been observed such a tunneling splitting in their spectra.

2. The Photochemistry of Methyl Acetylene at 193 nm. The investigation of reactions, thermochemistry and photochemistry of small hydrocarbon molecules and radicals with high carbon atoms to hydrogen atoms ratio are very important in combustion chemistry. In our recent investigation of the photodissociation of allene at 193 nm, a question arises on the possible facile isomerization of the excited molecule. The question can be answered if we compare the results of the allene experiment with those of another C_3H_4 isomer, namely methylacetylene (propyne). If the H atom migration is facile in the electronically excited state, many common features will be detected between these two systems.

3. Photodissociation of CH_3 Radical at 193 nm. There has been recent interest in whether or not the dissociation of methyl radical proceeds via the loss of atomic or molecular hydrogen. Although both channels are thermodynamically accessible at 193 nm, calculations have shown that the "least motion" pathway to H_2 elimination (symmetry forbidden dissociation along the C_{2v} axis) involves a barrier of ~75 kcal/mol. H_2 elimination was therefore thought to be unlikely. More recent calculations have shown that if the H_2 takes a

symmetry allowed "non-least motion" pathway the barrier may be less than 4 kcal/mol. Because there are many such low barrier pathways it is important to study the dissociation of CH_3 and determine the relative importance of both channels.

Preliminary results indicate that at 193 nm CH_3 dissociates to predominately CH_2 + H. The high degree of energy release into product translation is suggestive of dissociation from an electronically excited state. Further work is needed to fully characterize the energetics of the dissociation and understand why elimination of H_2 is not an important process.

4. Molecular Beam Studies of the Retro-Diels-Alder Decomposition of Tetralin. Tetralin (1,2,3,4-tetrahydronaphthalene, $C_{10}H_{12}$) has a hydroaromatic structure typically found in coal and serves as a model coal compound. It has further importance in coal chemistry since it is used as a solvent and a hydrogen donor in coal liquefaction. In these contexts, the decomposition mechanism of this compound is of central importance. Since one its major decomposition pathways involves the retro-Diels-Alder reaction, tetralin also provides an opportunity to investigate the nature of the transition state in this reaction, which has been a source of considerable controversy. The argument has focused on whether the reaction proceeds in a concerted fashion or step-wise, through a biradical transition state. By measuring the distribution of the energy released into translation of the products, one can distinguish these two mechanisms.

Tetralin decomposition was studied using crossed laser-molecular beams techniques. Both ultraviolet (193 nm) and infrared multiphoton excitation were used in conjunction with photofragmentation translational spectroscopy. After 193 nm excitation, tetralin decomposed via the retro-Diels-Alder reaction ($C_{10}H_{12} \rightarrow C_8H_8 + C_2H_4$) and through molecular elimination of H_2. The secondary decomposition of the C_8H_8 product of the retro-Diels-Alder reaction formed C_6H_4 and C_2H_4. The infrared multiphoton dissociation of tetralin also led to decomposition via the retro-diels-Alder reaction. For the retro-Diels-Alder decomposition of tetralin, the measured translational energy distribution of the products was peaked away from zero, indicative of a concerted mechanism. This indication was supported by using impulsive models of the partitioning of energy into the translational degrees of freedom.

B. Reaction Dynamics

1. $D + H_2 \text{ --> } DH + H$ High Resolution Reactive Scattering Experiment. We have recently completed constructing and optimizing a new crossed molecular beam apparatus for measurement of rotational-state-resolved angular distributions. A beam of D atoms is generated by laser photolysis of DI and crossed with a pulsed beam of H_2. The DH reaction products are state-specifically ionized downstream from the crossing region using a doppler-free 2+1 REMPI scheme and the resulting ions are imaged onto a position sensitive detector. By varying the delay between the D-atom generation and the detection, we can map out the angular distribution of a specific rovibrational DH product state.

2. Ozone Reactions with Br, Cl Atoms. BrO and ClO radical species play a very important role in catalytic destruction cycles of ozone in Stratosphere. Two elementary reactions Br + O_3 and Cl + O_3 have been studied by crossed molecular beams technique.

(a) $Br + O_3 \text{ ---> } BrO + O_2$ (ΔH° = -30.8 kcal/mole) has been investigated at five different collision energies from 5 kcal/mole to 26 kcal/mole. BrO product angular distribution and TOF distribution have been measured at each collision energy. BrO_3 collision long-lived complex is evident from BrO angular distribution, even at the highest collision energy. Some forward scattered product BrO (with respect to Br beam) is also observed. Preliminary analysis of the experimental results shows that average translational energy release in the products is about 30% of total available energy.

(b) $Cl + O_3 \text{ ---> } ClO + O_2$ (ΔH° = -39.0 kcal/mole) has been studied at four different collision energies from 6 kcal/mole to 30 kcal/mole. The results are quite similar to those of Br + O_3, except that there is more forward scattered product ClO, average translational energy release in the products is about 40% of total energy.

Future Plans

A. Primary Dissociation Processes

1. Photodissociation of Propane and Butane. Experiments dating back to the early 1960's have involved probing the dissociation pathways of saturated hydrocarbons. However, to date no agreement has been reached among experimentalists as to the primary processes involved in the dissociation of these simple molecules. During the past year, the primary and secondary processes involved in the 157 nm photodissociation of cyclopropane, propane, butane, and isobutane have been determined. This work was accomplished due in part to the recent availability of a 157 nm high power pulsed vacuum ultraviolet laser. We find H and H_2 loss to be the dominant elimination channels for the straight chain hydrocarbons, butane and propane. In contrast, for the branched hydrocarbon system isobutane, carbon-carbon cleavage is the dominant channel. In the cyclic hydrocarbon, cyclopropane, molecular elimination to form methylene and ethylene is the dominant dissociation pathway.

2. Primary and Secondary Photodissociation of Aromatic and Heterocyclic Compounds. As part of a continuing effort to understand combustion related chemistry, especially the initiation processes in pyrolysis of coal, photodissociation of naphthalene, and S- and N- containing heterocyclic compounds will be investigated using the technique of photofragmentation translational spectroscopy.

The information on the primary and secondary processes involved in the pyrolysis of S- and N- containing molecules in coal are very important in the abatement of NO_x and SO_2 in the combustion of coals.

3. VUV Photochemistry of Small Molecules. Using a new high power VUV excimer laser operating at 157 nm, the photochemistry of CO_2, SO_2, SiH_4, CH_3Cl, CH_3Br and CH_2BrCl was studied via the photofragmentation translational spectroscopy technique.

In CO_2 photolysis an interesting spin-forbidden process was observed, leading to CO + $O(^3P)$ products. The electronic branching ratio $O(^3P)/O(^1D)$ was found to be 0.06. The vibrational branching ratio for the CO(v) + $O(^1D)$ was found to be $[CO(v=0)]/[CO(v=1)]$ = 1.3. In the photolysis of SO_2, a channel leading to S + O_2 products was observed, as well as the expected SO + O channel. The molecules CH_3X (X= Br, Cl) were shown to eliminate H, X and HX upon irradiation at 157nm. In addition, the molecule CH_2BrCl was found to eliminate molecular BrCl.

The photochemistry of SiH_4 is interesting and relevant to the microelectronics industry (i.e. laser chemical vapor deposition of silicon thin films). It was previously thought that SiH_4 decomposes through H atom elimination to form the SiH_3 radical. We have shown, however, that molecular H_2 elimination, forming the $SiH_2(^1A_1)$ diradical is a major channel, thus altering our view of silane photochemistry.

4. Photodissociation Dynamics of ClO_2. The photochemical decomposition of the symmetric chlorine dioxide radical (ClO_2) in the atmosphere is of potential importance in the balance of global ozone. However, there has been considerable uncertainty regarding the excited state dynamics of this molecule. Two chemically distinct photodissociation pathways are thermodynamically possible upon electronic excitation at wavelengths shorter than 496nm:

$$OClO \rightarrow ClO(^2\Pi) + O(^3P) \quad (1)$$

$$\rightarrow Cl(^2P) + O_2(^3\Sigma_g, ^1\Delta_g) \quad (2)$$

Although it has generally been believed that channel (1) dominates, there has been considerable controversy regarding the possible existence of channel (2) since it leads to catalytic decomposition of ozone in the atmosphere. Although a number of groups have attempted to determine Cl atom quantum yields and identify the electronic state(s) of the O_2 molecule, the results have been largely inconclusive. We have studied the

dynamics of these processes using photofragment translational energy spectroscopy with a tunable excitation laser and have clearly observed both fragment partners for both channels.

5. Primary Dissociation Processes of Fulvene. In the primary dissociation of benzene, one of the most surprising observations is the existence of a dissociation channel which involves the elimination of CH_3. Since only one H atom is attached to each of the C atoms in a benzene molecule, extensive isomerization and H-migration must take place in the isolated hot benzene. One of the isomers of benzene which might be the precurser of CH_3 elimination is fulvene, $CH_2=C_5H_4$. It is speculated that when a H atom migrates from cyclic C_5H_4 to CH_2, then the C-C bond will become a single bond and the excitation energy is sufficient to break a single C-C bond. Whether this conclusion is correct or not depends on the nature of the C_5H_3 radical formed. So far, none of the linear or cyclic structure of conventional structure suggests C_5H_3 stability is sufficient to drive $C_6H_6 \rightarrow CH_3 + C_5H_3$. Direct dissociation studies of fulvene will be very illuminating. If the above mentioned mechanism is correct, CH_3 elimination from fulvene should be a very important channel.

B. Reaction Dynamics

1. Reactions of Vinyl Radicals with O_2 and OH. In acetylene polymerization, H atoms are known to play an important role, and the vinyl radicals formed by the addition of H to C_2H_2 are important intermediates.

Reaction mechanism of vinyl radicals with O_2 and OH are two important topics which need to be investigated further. Our recent studies of the photodissociation of vinyl bromide has shown that vinyl radicals can be produced efficiently by using 193 nm photons to dissociate vinylbromide in the supersonic expansion.

The reactions involving two radicals are challenging experiments for crossed molecular beam studies. Further improvement of the crossed molecular beam technique will be needed to advance combustion related chemistry involving polyatomic radicals.

2. Crossed Beam Chemistry of Transition Metals with Simple Molecules. The recent development of an apparatus capable of generating seeded supersonic beams of transition metals will open the door to the study of a broad spectrum of reactions of importance in combustion, catalysis, and corrosion. An exciting prospect, for example, is the reaction of transition metals with hydrocarbons. But during the first year of the investigation of the transition metal atoms we will focus our attention to simple molecules such as oxygen and halogen molecules. By studying the actual molecular events under precisely defined conditions, a microscopic understanding of these important catalytic reactions may be obtained.

3. The Reaction of $Li + H_2 \rightarrow LiH + H$ $\Delta E = 192.6$ kj/mol. $Li + H_2$ is a relatively simple system that accurate theoretical prediction of its dynamic behavior might be feasible. With our crossed molecular beam apparatus, this reaction can be studied under single collision condition and the detailed reaction dynamics can be probed. However, in our experiment the ground state lithium atom does not have enough energy to initiate the reaction. Laser excitation of lithium to 2P or 3D states would provide the energy required. The hyperfine structures of lithium electronic state post considerable difficulties in the laser excitation practice. Recently, an optical pumping scheme has been designed, which utilizes two dye lasers to pump lithium to the high-lying states. Experimental results will be compared with theoretical calculations to achieve a better understanding of the reaction dynamics.

4. Reaction of O_3 with unsaturated hydrocarbons. Adducts formed by the addition of O atoms with unsaturated hydrocarbons are important reaction intermediates in the reaction of oxygen atoms with unsaturated hydrocarbons. Just like other radical species, the heat of formation of the adducts is not well determined because of obvious experimental difficulties.

One possible way of obtaining this information is the investigation of the threshold energies required for the formation of adducts in the endothermic reactions between unsaturated hydrocarbons with O_3

$$C_2H_4 + O_3 \text{ --> } C_2H_4O\bullet + O_2$$

$$C_6H_6 + O_3 \text{ --> } C_6H_6O\bullet + O_2$$

Molecule-molecule reactions under single collision conditions have only been observed in the reactions of F_2 molecules with iodine containing molecules and benzene. The transfer of an oxygen atom from O_3 to a stable molecules is a very interesting and challenging reaction which is worth pursuing in earnest.

5. Cl Atom Reaction with NO_2 Molecule. Endothermic reaction $Cl + NO_2 \rightarrow ClO + NO$ ($\Delta H^\circ \approx 9$ kcal/mole) is the reaction to connect NO_x and ClO_x groups in atmospheric chemistry. Because $ClNO_2$ is a stable molecule, collision long-lived complex is expected to form in this reaction. By the unique feature of crossed molecular beam experiment, collision energies could be adjusted to probe the energy dependence of reaction probability in this endothermic reaction. Threshold region could be well studied by lowing collision energy.

6. Reaction of Oxygen Atom with Halogen Containing Olefins. Combustion of halogen containing organic molecules, especially the identity of halogen containing products, has been of great interest due to environmental concerns. Reaction of oxygen atoms and halogen containing unsaturated hydrocarbons will be investigated systematically.

For carrying our these investigations, as well as other reactions which are of importance to combustion, a hydrocarbon free molecular beam apparatus is needed. The recent advances of turbomolecular pumps, especially the magnetically suspended turbomolecular pump will make it possible to do so.

Publications

1. J.M. Price, M.W. Crofton, and Y. T. Lee, Vibrational Spectroscopy of the Ammoniated Ammonium Ions, $NH_4^+(NH_3)_n$ (n=1-10). J. Phys. Chem. **95**, 2182-2195 (1991). LBL-29016
2. P.S. Weiss, J.M. Mestdagh, H. Schmidt, M.H. Covinsky, and Y.T. Lee, The Reactions of Ground State and Electronically Excited Sodium Atoms with Methyl Bromide and Molecular Chlorine. J. Phys. Chem. **95**, 3005-3011 (1991). LBL-29811
3. Eric J. Hintsa, Xinsheng Zhao, William M. Jackson, Walter B. Miller, Alec M. Wodtke, and Yuan T. Lee, Production and Photodissociation of CCl_3 Radicals in a Molecular Beam. J. Phys. Chem. **95**, 2799-2801 (1991). LBL-29640
4. B.A. Balko, J. Zhang, and Y.T. Lee, 193 nm Photodissociation of Acetylene. J. Chem. Phys. **94**, 7958-7966 (1991). LBL-30184
5. E.F. Cromwell, D.-J. Liu, M.J.J. Vrakking, A.H. Kung, and Y.T. Lee, Dynamics of H_2 Elimination from Cyclohexadiene. J. Chem. Phys. **95**, 297-307 (1991). LBL-30198
6. A.H. Kung and Yuan T. Lee, Spectroscopy and Reaction Dynamics Using Ultrahigh Resolution VUV Lasers. In **Vacuum Ultraviolet Photoionization and Photodissociation of Molecules and Clusters**, C.Y. Ng, editor, World Scientific Publishing Company, Singapore (1991), pp.487-502. LBL-30075
7. Deon S. Anex, John C. Allman, and Yuan T. Lee, Initial Dissociation Processes in 1,3,5-trinitroazetidine, in **Chemistry of Energetic Materials**, George A. Olah and David R. Squire, eds., Academic Press, San Diego, California (1991), pp.27-54. ONR 432-819/12/90.
8. R.E. Continetti, B.A. Balko, and Y.T. Lee, Photodissociation of H_2S and the HS Radical at 193.3 nm. Chem. Phys. Lett. **184**, 400-405 (1991). LBL-30778
9. W.M. Jackson, Deon S. Anex, R.E. Continetti, B.A. Balko, and Y.T. Lee, Molecular Beam Studies of the Photolysis of Allene and the Secondary Dissociation of the C_3H_x Fragments. J. Chem. Phys. **95**, 7327-7336 (1991). LBL-31171
10. Arthur G. Suits, Hongtao Hou, H. Floyd Davis, Yuan T. Lee, and Jean-Michel Mestdagh, Reaction Geometry from Orbital Alignment Dependence of Ion Pair Production in Crossed Beams $Ba(^1P_1)$-Br_2 Reactions. J. Chem. Phys. **95**, 8178-8187 (1991). LBL-31064
11. Arthur G. Suits, Hongtao Hou, H. Floyd Davis, and Yuan T. Lee, Dynamics of Ba-Br_2 Chemi-Ionization Reactions. J. Phys. Chem. **95**, 8207-8211 (1991). LBL-30364
12. M.W. Crofton, J.M. Price, and Y.T. Lee, IR Spectroscopy 2of Hydrogen Bonded Charged Clusters. In **Clusters of Atoms and Molecules**, H. Haberland, editor, Springer-Verlag, Berlin (1991) pp.. LBL-29681

SUBMITTED ONLY

1. R.E. Continetti and Yuan T. Lee, Molecular Beam Studies and Hot Atom Chemistry. Handbook of Hot Atom Chemistry, eds., J.P. Adloff, P.O. Gaspar, A.G. Maddock, M. Immamura, T. Matsuura, H. Sano, and K. Yoshihara, Kodansha Ltd. Publishers, Tokyo, Japan (1992). LBL-29314
2. Michael H. Covinsky, Arthur G. Suits, H. Floyd Davis, and Yuan T. Lee, The Reaction Dynamics of Sodium with Ozone. J. Chem. Phys. (submitted) (1991). LBL-30555
3. Anne-Marie Schmoltner, Deon S. Anex, and Yuan T. Lee, IR Multiphoton Dissociation of Anisole: Production and Dissociation of Phenoxy Radical. J. Phys. Chem. (in press) (1991). LBL-30788
4. A.G. Suits, P. de Pujo, O. Sublemontier, J.-P. Visticot, J. Berlande, T. Gustravsson, J.-M. Mestdagh, P. Meynadier, and Y.T. Lee, The Dynamics of Electronically Inelastic Collisions from 3-Dimensional Doppler Measurements. Phys. Rev. Lett. (in press) (1991). LBL-30900
5. Albert Stolow, Barbara A. Balko, Evan F. Cromwell, Jingsong Zhang, and Yuan T. Lee, The Dynamics of H_2 Elimination from Ethylene. J. Photochem. Photobiol. (in press) (1991). LBL-31009
6. B.A. Balko, J. Zhang, and Y.T. Lee, Photodissociation of Ethylene at 193 nm. J. Chem. Phys. (submitted) (1991). LBL-31102
7. Arthur G. Suits, Hongtao Hou, H. Floyd Davis, and Yuan T. Lee, Reaction Dynamics from Orbital Alignment Dependence and Angular Distributions of Ions Produced in Collision of $Ba(^1P)$ with NO_2 and O_3. J. Chem. Phys. (submitted) (1991). LBL-31260
8. Marcus J.J. Vrakking, Allan Bracker, and Yuan T. Lee, Comment on Two-Photon Spectroscopy of N_2: Multiphoton Ionization, Laser-Induced Fluorescence, and Direct Absorption via the $a''^1\Sigma_{g+}$ State. J. Chem. Phys. (submitted) (1991). LBL-31486
9. H. Floyd Davis, Arthur G. Suits, and Yuan T. Lee, Reactions of Barium Atoms with Triatomic Oxidants. 1: Ba + NO_2. J. Chem. Phys. (submitted) (1991). LBL-31492

TIME-RESOLVED FTIR EMISSION STUDIES OF LASER PHOTOFRAGMENTATION AND RADICAL REACTIONS

Stephen R. Leone
Joint Institute for Laboratory Astrophysics and
Department of Chemistry and Biochemistry
University of Colorado
Boulder, Colorado 80309-0440

Time-resolved Fourier transform infrared emission experiments are used to study photofragmentation processes, single collision reactions, energy transfer events, and laser-initiated radical-radical reactions. The apparatus unites a commercial FTIR spectrometer with a high repetition rate excimer laser. Fringes of the He:Ne reference laser are used for the time synchronization of the FTIR as the mirror sweeps. The zero crossings of these fringes are also used to trigger the variable repetition rate laser with a chosen delay time. Following a short delay after the laser pulse, the analog-to-digital converter samples the signal on the infrared detector. Thus emissions from the excited fragments of the photolysis event are recorded with the FTIR at specific time delays after the laser pulse. We also utilize the capability to multiplex time delays after the laser pulse to obtain several sequential time-resolved spectra at once.

Through the use of improved background-limited detectors and multipass collection optics, spectra from a number of diatomic molecules and polyatomic radicals have been obtained in various processes. The method has been applied to study numerous photofragmentation events in order to obtain vibrational and rotational populations, e.g. vinyl chloride (HCl[v] product), dichloroethylene (HCl[v]), fluorochloroethylene (HF[v,J]), acetylene (C_2H[v,J]), acetone (CH_3[v], CO[v,J]), ammonia (NH_2[v,J]). The dynamics of the photofragmentation processes have been considered in detail as potential sources of well-characterized radicals for reactive studies.

The dissociation of ammonia revealed our first results of alignment details in a fragmentation process. The NH_2 fragment is highly excited rotationally in the $^2A_1$ electronically excited state. This rotational motion is almost exclusively around the K_a inertial axis of the NH_2. This axis lies in the plane of the molecule, passing almost through the N atom and parallel to a line joining the two H atoms. The rotational motion indicates that the dissociation is highly aligned. However, no polarization experiments are required to obtain this information. The intensities of the rotational lines in the asymmetric top molecule contain the necessary information to determine the alignment dynamics directly. This study was carried out in collaboration with visiting Prof. M. N. R. Ashfold.

The new studies have focused more specifically on collision processes, such as single collision energy transfer and radical-radical reactions. We employ the FTIR technique in the study of single collision energy transfer from translationally fast H atoms, electronically excited $Br^*(^2P_{1/2})$ and $I^*(^2P_{1/2})$, as well as radical-radical reactions, e.g. $CH_3 + O$, $CF_3 + H(D)$, and $Cl + C_2H_5$. A few examples of these new collision studies are given below.

We probed vibrational and rotational excitation and alignment dynamics in a single collision experiment of 2.2 eV H atoms colliding with H_2O. The fast H atoms are produced by photolysis of H_2S and these atoms collide with H_2O in a jet. The water molecules are excited in many vibrational modes by the 2.2 eV H atom, including the symmetric and antisymmetric stretch and two quanta of the bend. In the antisymmetric stretch, there is a dramatic propensity to produce primarily motion about the K_c inertial axis, which is the axis perpendicular to the plane of the water molecule. This K_c motion strictly defines the collision geometry that leads to the antisymmetric stretch excitation. From the observed direction of the rotational angular momentum, the collision that produces the excitation must be constrained to occur approximately in the plane of the water molecule. It is important to point out, again, that alignment information is obtained in this case without any external polarization equipment, solely through the rotational substructure of the excited states.

The study of the reaction of methyl radical with oxygen atoms revealed an important new pathway for product formation at room temperature. Methyl radicals and O atoms are produced simultaneously with the pulsed 193 nm excimer laser using a variety of precursors, including acetone, methyl iodide, and SO_2. The reaction is known to produce formaldehyde and H atoms, $CH_3 + O \rightarrow H_2CO + H$. However, with the FTIR emission technique, a major pathway that produces vibrationally excited CO(v) was detected, $CH_3 + O \rightarrow CO(v) + H_2 + H$. This pathway has an estimated branching fraction of 0.4±0.1. The vibrational distribution in CO v=1-8 has an approximate temperature of 12,700±1400 K. The significance of the result is that reaction bypasses the formaldehyde product a substantial fraction of the time, generating the more fully oxidized CO product.

Experiments have also been carried out on other reaction systems and radical-radical reactions. The excimer laser is used to form an initial density of Cl atoms from Cl_2, and hydrocarbon emission signals from the chain chlorination of cyclohexane have been observed. Studies have also been carried out to form Cl atoms and ethyl radicals simultaneously at high densities and to study the time evolution of the HCl product from the addition-elimination process: $Cl + C_2H_5 \rightarrow [C_2H_5Cl] \rightarrow C_2H_4 + HCl(v)$. By using two lasers and suitable time delays, we are able to demonstrate that the vibrationally excited HCl is formed by the interaction of Cl with ethyl radicals. Sequences of time-resolved FTIR emission spectra have been acquired, and the risetime of the v=4 state was analyzed to determine the reaction rate constant of the radical-radical process. Rotationally resolved studies on $CF_3 + H(D) \rightarrow HF(v) + CF_2$ and fast atom collisions of H(D) + HF(DF) are also underway.

List of Publications Supported by this Contract

S. R. Leone, 1990-1992

S. R. Leone, "Novel laser gain and time-resolved FTIR studies of photochemistry," in Proceedings, First International Conference on Laboratory Research for Planetary Atmospheres," ed. by K. Fox, J. E. Allen, Jr., L. J. Stief, and D. T. Quillen (NASA, 1990), p. 129.

E. L. Woodbridge, M. N. R. Ashfold, and S. R. Leone, "Photodissociation of ammonia at 193.3 nm: Rovibrational state distribution of the $NH_2(A^2A_1)$ fragment," J. Chem. Phys. 94, 4195 (1991).

C. M. Lovejoy, L. Goldfarb, and S. R. Leone, "Preferential in-plane rotational excitation of H_2O (001) by translational-to-vibrational transfer from 2.2 eV H atoms," J. Chem. Phys. (in press).

P. W. Seakins and S. R. Leone, "A laser flash photolysis/time resolved FTIR emission study of a new channel in the reaction of CH_3 + O: The production of CO(v)," J. Phys. Chem. (in press).

SPECTROSCOPY AND REACTION DYNAMICS OF COLLISION COMPLEXES CONTAINING HYDROXYL RADICALS

Marsha I. Lester
Department of Chemistry
University of Pennsylvania
Philadelphia, PA 19104-6323

The goal of this program is to provide a detailed picture of the intermolecular potential between the open-shell hydroxyl radical and various collision partners. Our work has focused on the spectroscopic characterization of the interaction potential between an argon atom and a hydroxyl radical in the ground X $^2\Pi$ and excited A $^2\Sigma^+$ electronic states. Experimental identification of the bound states supported by the Ar + OH($^2\Pi$) and Ar + OH($^2\Sigma^+$) potentials makes it feasible to derive realistic potential energy surfaces for these systems.[1] The experimentally derived intermolecular potentials provide a rigorous test of *ab initio* theory[2] and a basis for understanding the dramatically different collision dynamics taking place on the ground and excited electronic state surfaces.[3,4]

Mapping the OH (X $^2\Pi$) + Ar Potential via Stimulated Emission Pumping

Most of the previous experimental work on OH-Ar has utilized electronic spectroscopy to probe the intermolecular potentials in the ground and excited electronic states. These measurements give limited information on the ground state potential in the vicinity of the potential minimum. More global information on the OH (X $^2\Pi$) + Ar potential can be obtained by accessing excited intermolecular vibrations, which sample regions of the potential energy surface which lie far from the equilibrium position. Recently, we have demonstrated that stimulated emission pumping (SEP) can be used to directly access virtually all of the intermolecular stretching and bending vibrational levels supported by the ground state surface from the zero-point level through the dissociation limit.[5,6]

In our application of the SEP technique, OH-Ar complexes are first prepared by a PUMP laser in an excited intermolecular vibrational level of the A electronic state with zero quanta of OH stretch. Prior to radiative decay of the OH-Ar complexes from the excited electronic state, a DUMP laser is introduced to stimulate transitions down to excited intermolecular levels in the ground electronic state. As the DUMP laser is scanned, a fluorescence "dip" occurs each time the DUMP laser induces a rovibronic transition from the prepared level to a bound state, predissociative resonance, or continuum region of the ground state potential. The large change in the OH-Ar potential upon electronic excitation enables SEP to access excited intermolecular vibrations that sample a wide range of orientations and distances.

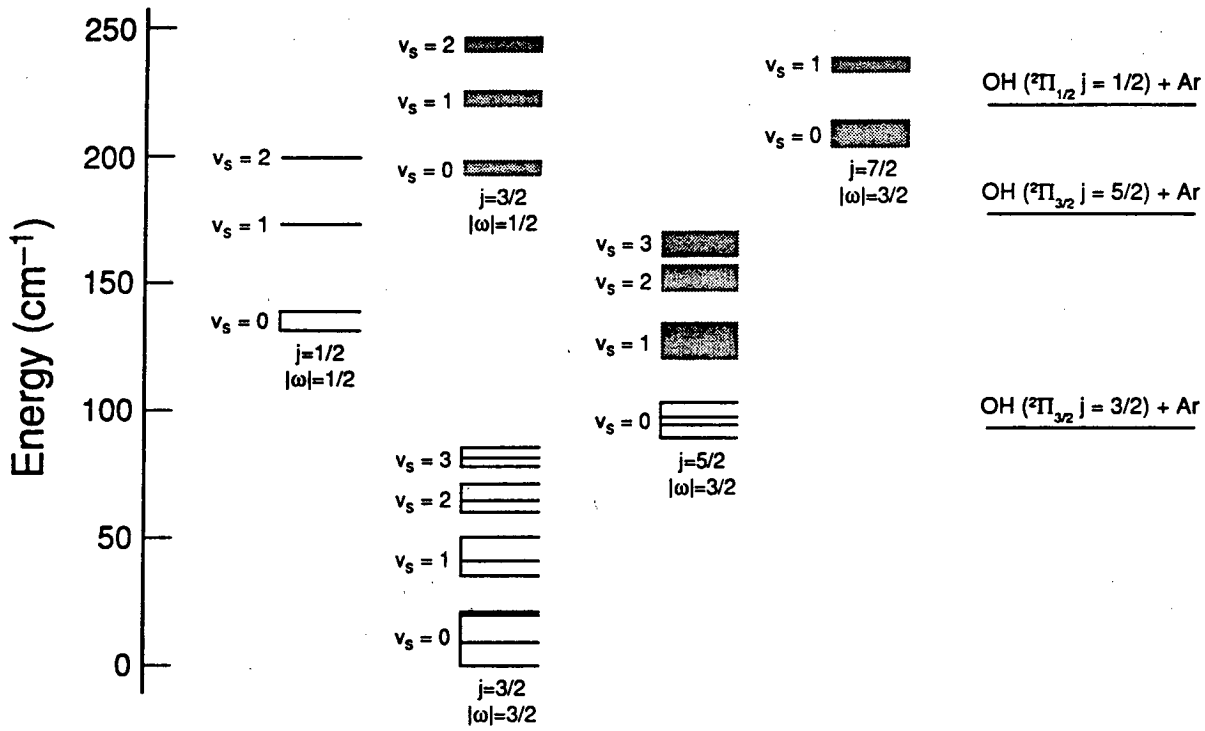

Fig. 1 Intermolecular energy levels supported by the OH (X $^2\Pi$) + Ar ($^1S_0$) potential.

The intermolecular vibrational energy levels of OH-Ar (X $^2\Pi$) which have been observed by SEP are shown above in Fig. 1. Theoretical calculations predict a manifold of $2j+1$ bending levels associated with each j,ω rotational level of OH (X $^2\Pi$) arising from a Stark-type splitting of the orientational degeneracy of each OH rotational level in the presence of the argon atom.[7,8] This bending level pattern is unique to open-shell complexes which have non-zero electronic angular momentum along the diatom axis. The lowest four levels observed are assigned as the manifold of bending levels derived from the lowest rotational level of OH ($j=3/2$, $\omega=3/2$). The energy spread across the manifold of bending levels reflects the anisotropy of the intermolecular potential. At higher energies the bending level pattern is repeated with one, two, and three quanta of intermolecular stretching excitation (v_s). The energy spread across the bending levels decreases with intermolecular stretching excitation, showing that the intermolecular potential becomes more isotropic as the average OH-Ar separation distance is increased. Another group of bending levels has been identified near 96 cm^{-1}, correlating to the rotationally excited $j=5/2$, $\omega=3/2$ level of OH. The first dissociation limit of OH-Ar to OH ($^2\Pi_{3/2}$) $v=0$, $j=3/2$ + Ar ($^1S_0$) occurs between 93 and 103 cm^{-1} above the zero-point level as evidenced by the onset of bound-free transitions. We are currently deriving a global potential energy surface for the OH (X $^2\Pi$) + Ar system based on the experimentally observed intermolecular energy levels from 0 - 89 cm^{-1}.

Using SEP, we have also accessed many metastable levels which lie as much as 200 cm^{-1} beyond the first dissociation limit.[5,6] Manifolds of OH-Ar bending levels have been identified correlating with the excited $j=5/2$ and $j=7/2$ rotational levels of OH ($^2\Pi_{3/2}$). Complexes prepared in these levels undergo rapid rotational predissociation by using OH rotational excitation to break the OH-Ar intermolecular bond. In addition, OH-Ar

complexes have been prepared in intermolecular vibrational levels of the spin-orbit excited state correlating with OH ($^2\Pi_{1/2}$), all of which lie beyond the first dissociation limit. These complexes may predissociate by spin-orbit relaxation, yielding OH fragments in the lower $^2\Pi_{3/2}$ spin-orbit state. Spin-orbit predissociation occurs on the time-scale of the 6 ns laser pulse, as deduced from the $\geq$ 50% depletion of the fluorescence signal when the DUMP laser stimulates emission to the $j=1/2$, $\omega=1/2$ level at 139 cm^{-1}.

Perturbation Theory Calculations

We have implemented perturbation theory in order to understand the physical origin of various features in the stimulated emission spectra of OH-Ar ($X\ ^2\Pi$).[9] For example, we experimentally observed a large splitting between pairs of rotational levels with the same total angular momentum but opposite parity in the first excited bending level at 9.7 cm^{-1}. Using perturbation theory, we showed that the magnitude of the parity splitting is directly proportional to the change in the intermolecular potential when the odd electron in the free radical lies in or out of the O-H-Ar plane, the A′ and A″ surfaces. In chemically bound species, this perturbative term is known as Renner-Teller coupling. The measured splitting was then used to infer the magnitude of the difference between the A′ and A″ potential energy surfaces ($\sim$12 cm^{-1}) in the region sampled by the first excited bend. We also used perturbation theory to elucidate the couplings which induce rotational and spin-orbit predissociation in OH-Ar. The rate of rotational predissociation is dependent on off-diagonal (anisotropic) terms in the interaction potential, while the rate of spin-orbit predissociation depends on the difference between the A′ and A″ potentials at short-range.

References

1. J. M. Bowman, B. Gazdy, P. Schafer, and M. C. Heaven, *J. Phys. Chem.* **94**, 2226 (1990); **94**, 8858E (1990).

2. A. Degli-Esposti and H.-J. Werner, *J. Chem. Phys.* **93**, 3351 (1990).

3. K. J. Rensberger, J. B. Jeffries, and D. R. Crosley, *J. Chem. Phys.* **90**, 2174 (1989).

4. M. T. Berry, M. R. Brustein, and M. I. Lester, *J. Chem. Phys.* **90**, 5878 (1989).

5. M. T. Berry, M. R. Brustein, M. I. Lester, C. Chakravarty, and D. C. Clary, *Chem. Phys. Lett.* **178**, 301 (1991).

6. M. T. Berry, R. A. Loomis, L. C. Giancarlo, and M. I. Lester, *J. Chem. Phys.*, in press.

7. C. Chakravarty and D. C. Clary, *J. Chem. Phys.* **94**, 4149 (1991).

8. M.-L. Dubernet, D. Flower, and J. M. Hutson, *J. Chem. Phys.* **94**, 7602 (1991).

9. W. H. Green, Jr. and M. I. Lester, *J. Chem. Phys.* **96**, 2573 (1992).

DOE Supported Publications, 1990 - 92

1. M. I. Lester, "1988-89: The Year of OH-Ar", in *Dynamics of Polyatomic van der Waals Complexes*, N. Halberstadt and K. C. Janda, Eds., (Plenum Press, New York, 1990) 143-155.

2. M. T. Berry, M. R. Brustein, and M. I. Lester, "Van der Waals Vibrational Dependence in the Vibrational Predissociation of OH-Ar", *J. Chem. Phys.* **92**, 6469-6479 (1990).

3. M. T. Berry, M. R. Brustein, M. I. Lester, C. Chakravarty, and D. C. Clary, "Stimulated Emission Pumping of van der Waals Vibrations in the Ground Electronic State of OH-Ar", *Chem. Phys. Lett.* **78**, 301-310 (1991).

4. W. H. Green, Jr. and M. I. Lester, "A Perturbation Theory Guide to Open-Shell Complexes: OH-Ar ($X\ ^2\Pi$)", *J. Chem. Phys.* **96**, 2573-2584 (1992).

5. M. T. Berry, R. A. Loomis, L. C. Giancarlo, and M. I. Lester, "Stimulated Emission Pumping of Intermolecular Vibrations in OH-Ar ($X\ ^2\Pi$)", *J. Chem. Phys.*, in press.

Theoretical Studies of Molecular Interactions

William A. Lester, Jr.

Chemical Sciences Division, Lawrence Berkeley
Laboratory and Department of Chemistry,
University of California, Berkeley, California 94720

Scope of the Project

This research program is directed at extending fundamental knowledge of atoms and molecules including their electronic structure, mutual interaction, collision dynamics, and interaction with radiation. The approach combines the use of *ab initio* methods--Hartree-Fock (HF), multiconfiguration HF, configuration interaction, and the recently developed quantum Monte Carlo (QMC)--to describe electronic structure, intermolecular interactions, and other properties, with various methods of characterizing inelastic and reactive collision processes, and photodissociation dynamics. Present activity is focused on the development and application of the QMC method.

Recent Progress

Trial Function Optimization with Quantum Monte Carlo

We have developed algorithms for optimizing trial functions, i.e., the functions that guide the random walk in QMC, based on variational random walks and on fixed samples. Although both energy and variance minimization were carried out with the former approach, the consistently best result were obtained with the latter method, i.e., minimizing the variance over a fixed sample. In either approach, the correlation energy recovered typically exceeds sophisticated *ab initio* basis set methods and, for the fixed sample method, achieves 95-100%.

CO Interaction with 3d-Metal Surfaces (with C.A. Taft)

Ab initio unrestricted Hartree-Fock calculations were carried out on the M-CO systems (M = Sc to Cu) and the results rationalized in terms of Pauling's resonating valence-bond theory. The findings are that CO absorption on Sc, Ti, V, Cr, Mn, and Fe surfaces will be dissociative, and nondissociative on Co, Ni, and Cu surfaces in agreement with experimental evidence. The CO dissociation arises primarily from a charge-transfer process with bonds resonating among the metal, C, and O atoms. The electron transfer covers a complete cycle in which the CO bond is broken and electroneutrality of the catalytic surface is maintained. The tilted precursor state of dissociation involves strong M → CO charge transfer. The main

The tilted precursor state of dissociation involves strong M → CO charge transfer. The main goal of this effort was to describe general trends of CO adsorption on 3d-transition metal surfaces as a step towards understanding catalytic behavior.

CO Interaction with the Fe (100) Surface (with C.A. Taft)

Fe → CO charge transfer in the systems FeCO and Fe_5CO has been calculated using *ab initio* unrestricted Hartree-Fock, effective-core-potential, and multiple-scattering $X\alpha$ molecular cluster methods and shown to correlate to the observed stretching frequencies on Fe(100). The increasing values of the Fe → CO charge transfer obtained as CO inclines toward the surface are consistent with the assignment of the low stretching frequency (1210 cm^{-1}) to the precursor state of CO dissociation on the Fe surface.

Future Plans

Quantum Monte Carlo Study of the Energetics of CH-Containing Systems

Hydrocarbons provide a plethora of interesting chemical questions. To make possible QMC studies of the most interesting issues, the subject effort has been initiated that draws on the broad range of recently developed QMC methodologies. Systems planned for the present effort are CH, C_2H, and C_2H_2, as well as C_2. The primary effort will use the fixed-node short-time approximation QMC approach with optimized trial functions.

Quantum Monte Carlo Gradients and Second-Derivatives

Although approaches for analytical evaluation of 1st and 2nd derivatives with respect to nuclear position are routinely obtainable with *ab initio* basis set methods, QMC has lacked the capability to accurately evaluate these quantities because of the magnitude of the statistical errors. An approach similar to the QMC correlated sampling method, but for systems with nodes, is being tested and appears promising for direct QMC computation of derivatives and would make possible the calculation of optimized QMC geometries. This capability is essential for extracting maximal accuracy from QMC estimates of energy properties (binding energies, barriers to reaction, IPs and EAs).

DOE Supported Publications 1990 - 92

1. B. L. Hammond, S.-Y. Huang, W. A. Lester, Jr., and M. Dupuis, "Theoretical Study of the $O(^3P)$ + Allene Reaction," J. Phys. Chem. 94, 7969, (1990).

2. Z. Z. Yang, L. S. Wang, Y. T. Lee, D.A. Shirley, S.-Y. Huang, and W. A. Lester, Jr., "Molecular Beam Photoelectron Spectroscopy of Allene," Chem. Phys. Letters 171, 9 (1990).

3. B. Bernu, D. M. Ceperley, and W. A. Lester, Jr., "The Calculation of Excited States with Quantum Monte Carlo. II. Vibrational Excited States," J. Chem. Phys. 93, 552 (1990).

4. B. Kim, B. L. Hammond, W. A. Lester, Jr., and H. S. Johnston, "*Ab Initio* Study of the Vibrational Spectra of NO_3," Chem. Phys. Letters 168, 131 (1990).

5. B. L. Hammond, W. A. Lester, Jr., M. Braga, and C. A. Taft, "Theoretical Study of the Interaction of Ionized Transition Metals (Cr, Mn, Fe, Co, Ni, Cu) with Argon," Phys. Rev. B 41, 10 447 (1990).

6. P. R. Seidl, K. Z. Leal, J. W. Carneiro, J. G. R. Tostes, C. A. Taft, B.L. Hammond, and W. A. Lester, Jr., "*Ab Initio* Charge Distributions in Half-Cage Compounds," J. Mol. Struct. (Theochem) 204, 183 (1990).

7. W. A. Lester, Jr. and B. L. Hammond, "Quantum Monte Carlo for the Electronic Structure of Atoms and Molecules," Annu. Rev. Phys. Chem. 41, 283 (1990).

8. W. A. Lester, Jr., "Supercomputing and Research in Theoretical Chemistry," in *Energy Sciences Supercumputing 1990*, 34 (1990).

9. B. N. Barnett, "Quantum Monte Carlo for Atoms and Molecules," Ph.D. Dissertation, University of California, Berkeley.

10. A. C. Pavao, M. Braga, C. A. Taft, B. L. Hammond, and W. A. Lester, Jr., "Theoretical Study of the CO Interaction with 3d-Metal Surfaces," Phys. Rev. B. 43, 6962 (1991).

11. P. Pernot and W. A. Lester, Jr., "Quantum Time-Dependent Treatment of Molecular Collisions: Scattering of He by $H_2(B\ ^1\Sigma_u^+)$," Comp. Phys. Commu. 63, 259 (1991).

12. P. Pernot and W. A. Lester, Jr., "Multidimensional Wave-Packet Analysis: Splitting Method for Time-Resolved Property Determination," Int. J. Quant. Chem. 40, 577 (1991).

13. A. C. Pavao, M. Braga, C. A. Taft, B. L. Hammond, and W. A. Lester, Jr., "Theoretical Study of the CO Interaction with the Fe (100) Surface," Phys. Rev. B. 44, 1910 (1991).

14. B. L. Hammond, M. M. Soto, R.N. Barnett, and W. A. Lester, Jr., "On Quantum Monte Carlo for the Electronic Structure of Molecules," J. Mol. Struc. (Theochem) 234, 525 (1991).

15. Z. Sun, R. N. Barnett, and W. A. Lester, Jr., "Optimization of a Multideterminent Wave Function for Quantum Monte Carlo," J. Chem. Phys. 96, 2422 (1992).

16. J. S. Francisco, Y. Zhao, W. A. Lester, Jr., and I. H. Williams, "Theoretical Studies for the Structure and Thermochemistry of FO_2 Radical: Comparison of Moller-Plesset Perturbation, Complete-Active-Space Self-Consistent Field, and Quadratic Configuration Interaction Methods, "J. Chem. Phys. 96, 2861 (1992).

17. R. N. Barnett, P. J. Reynolds, and W. A. Lester, Jr., "Monte Carlo Determination of the Oscillator Strength and Excited State Lifetime for the Li $2^2S \rightarrow 2^2P$ Transition," accepted by Int. J. Quant. Chem.

PREMIXED TURBULENT COMBUSTION

Paul A. Libby

Department of Applied Mechannics and Engineering Sciences
University of California San Diego
La Jolla, California 92093

PROGRAM SCOPE

This research sponsored by the Office of Basic Energy Sciences, Division of Chemical Sciences under Contract No. DE-FG03-86ER13527 involves theoretical studies of premixed turbulent combustion. Roughly two distinct areas are considered. One relates to laminar flames in various geometric configurations, the study of which is relevant to premixed turbulent combustion since under conditions of applied interest chemical reaction within turbulent flames occurs on molecularly dominated surfaces, laminar flamelets. We study the structure and extinction characteristics of these flamelets in opposed jets with and without swirl and in other configurations, e.g., cylindrical flames. The results of such studies provide the reacting microstructures of turbulent flames. The second area of current research relates to premixed flames in stagnating turbulence. Because of their attractive features, experiments on such flames are known to be underway at one laboratory in the United States and at five others in Western Europe. Our theoretical studies are intended to complement these efforts.

RECENT PROGRESS

We review briefly current efforts on the two topics of our research noted earlier.

Laminar Flames

The experiments of Chen *et al** on the influence of swirl on back-to-back laminar flames in counterflowing reactant streams stimulate interest in the theory for such flames. Particularly challenging from the theoretical point of view is their finding that the initial influence of swirl, i.e., of small rotation, is to make the flames more robust, i.e., more resistant to extinction due to rate of strain, a result consistent with the wide use of swirl to stabilize flames, but that at a critical rotation rate, the flames are less robust. The separation of the range of swirl into two regimes, one for moderate rotation and a second for strong rotation, is suggested by these observations.

The flow considered by Libby *et al*[1] involves two identical laminar reactant streams flowing counter to one another with either corotating or counterrotating swirl in each. Under the assumption that a Reynolds number $\mathrm{Re} \equiv W\, d/\nu_0$, where W is the exit velocity from the jets, d is the half spacing between the jets and ν_0 is the kinematic viscosity of the reactants, is large, it is possible to divide the flow into inviscid zones separated by one or two thin flames. Reference 1 introduces a swirl parameter $\tilde{\Omega}$ which is a dimensionless measure of the relative importance of the swirl and the axial velocity. Moderate swirl, the situation treated therein, is defined by $\tilde{\Omega} < \pi$. In this case the plane containing the stagnation point, termed the stagnation plane, and the plane of symmetry are coincident. Moreover, conventional Reynold number scaling applies, i.e., the appropriate similarity parameter for desribing the structure of

* Z.H.Chen, G.E.Liu and S.H.Sohrab, Combust.Sci.Tech. 51, 39 (1987).

the flame is proportional to $Re^{1/2}$, and the although there is a tendency for the radial velocity near the plane of symmetry to diminish as $\bar{\Omega}$ increases, there is radial outflow everywhere. Application of activation energy asymptotics to describe the chemical kinetic behaviour of the system leads to a prediction of an increase in the robustness of the flame under these conditions of moderate swirl, a prediction as noted earlier in accord with the observations of Chen *et al.*

This theory fails when the stagnation plane separates from the plane of symmetry and radial inflow arises, behavior associated with $\bar{\Omega} = \pi$. To describe the flow as $\bar{\Omega}$ approaches and exceeds π an entirely new scaling, one involving multiplication by $Re^{1/3}$, is called for. The extended theory is given in Kim *et al* [2] and involves careful attention to the interaction of the viscous region centered on the plane of symmetry, the radial pressure distribution and the position of the stagnation plane. Three small parameters must be taken into account: the reciprocal of the Reynolds number, the location of the stagnation plane expressed as z_s/d and the rotation parameter $\pi - \bar{\Omega}$. Although the analysis is developed on the basis of asymptotically small values of each of these quantities, it is found that only the large magnitude of the Reynolds number is critical, i.e., the results apply for arbitrarily large values of $\bar{\Omega} - \pi$ and arbitrary separation of the stagnation plane from the plane of symmetry. The same description of chemical behavior used earlier is applied.

The most important finding from this study is that rotation at rates corresponding to $\bar{\Omega} > \pi$ makes the flames less robust, more prone to extinction, again in accord with the observations of Chen *et al.* A second finding is that for all degrees of rotation beyond $\bar{\Omega} = \pi$ there is only one stagnation plane between the plane of symmetry and the exit plane of the jets, a finding which removes the multiple stagnation planes found by Sivishinsky and Sohrab* on the basis of an inviscid analysis.

Premixed Flames in Stagnating Turbulence

It is generally recognized that the greatest advances in combustion research both with respect to understanding and predictive capability are achieved when experimental, theoretical and computational efforts are brought to bear in a coordinated fashion. However, this ideal is seldom realized for a variety of reasons. It is therefore important to identify flows which facilitate the desireable close coordination of these efforts. One such flow represents an extension to the turbulent case of that widely used in laminar studies, namely flames in counterflowing configurations. Within this term we refer both to opposed streams and to single streams impinging on surfaces.

A wide variety of laminar flames in such configurations have been studied in the laboratory. In premixed systems two identical reactant streams flowing counter to one another result in one or two flames depending on the aerothermochemical situtation. The attractiveness of these flows insofar as experiments are concerned relates to the ease with which they can be established in the laboratory, the accessibility they provide for instrumentation, the absence of contaminating surfaces resulting in either heat losses or hetereogeneous reactions and the possibility of readily covering the entire range of chemical behavior from chemical equilibrium to extinction. But these flows have attractive characteristics for theory and computation as well. In particular by restricting attention to the neighborhood of the axis the partial differential equations describing the applicable conservation laws are reduced to ordinary differential equations with the consequence that both theory and computation are greatly facilitated. Thus the desired coordinate among the three areaas of combustion research is encouraged by consideration of these flows. As a result there is an extensive literature relating to the theory, computation and experiment of these laminar flames.

If it is considered that a grid or baffle can be installed so that the gas exiting from each jet is turbulent, every laminar flame in counterflowing streams has its counterpart as a turbulent flame with the

* G.I.Sivishinsky and S.H.Sohrab. Combust.Sci.Tech. 53,67 (1987).

corresponding theoretical, computational and experimental attractiveness. Especially important with respect to turbulent combustion is the possibility of readily studying in these flows extinction. At present there exists a general notion of the acrothermochemical mechanisms involved in the extinction of premixed turbulent flames but additional theoretical and experimental attention is required to provide validation.

The first experiments on these flames are due to Cho *et al* * who study a single reactant stream impinging on a solid surface. These same authors report further experiments in 1988.** Following these publications and the wide recognition of the importance of these flows for fundamental studies in turbulent combustion, a number of other investigators have carried out experiments involving other configurations: a single reactant stream impinging on a surface, two opposed reactant streams and opposed streams of fuel and oxidizer corresponding to the nonpremixed case. It seems clear that in due course the entire range of laminar flames studied in the laboratory will in due course be replicated in turbulent flows.

The first theoretical treatment of premixed flames in opposed reactant streams is due to Bray *et al* [3] Two different gradient models for turbulent transport are employed in this initial study, a simple algebraic model and that associated with the the $k-\varepsilon$ theory. The mean rate of creation of product, the quantity which in turbulent flows describes the chemical kinetic behaviour of the system, is represented in terms of a frequency factor multiplied by the ratio of a turbulence time and a chemical time, a ratio which provisionally is taken to be constant. Despite this severe idealization the theory is able to predict extinction and although comparison of theory and experiment in this regard is at present only qualitative, the possibility of studying an important aspect of premixed turbulent combustion is clearly established.

Recent extension of this work is described in Bray *et al* * which considers the flow arising from a single reactant stream impinging on a solid surface, the case corresponding roughly to the experiments of Cho *et al* referenced earlier. The significant feature making the analysis of this flow different from that of two opposed reatant streams is the viscous sublayer existing immediately adjacent to the wall. The description of the mean velocity components adopted in this work is such that the flame is restricted to the neighborhood of the wall. Unfortunately, presently available experimental data relate to mean rates of strain sufficiently low so that the flame is relatively remote from the wall. However, in due course experiments at higher rates of strain and thus flames close to the wall are expected so that the present theory will be available for comparison.

Related to the study of premixed flames in stagnating turbulence is the analysis of such turbulence in constant density flows. Such turbulence involves several processes quite distinct from the usual free and wall bounded flows treated extensively by a variety of methods. In particular turbulence production is due to compressive and extensive rates of strain rather than mean shear. As a consequence these flows provide a test of the universality of current predictive methods. Champion and Libby [4,5] * apply to the description of these flows asymptotic methods which expose in a clear fashion the important processes in the various regions, at the wall, close to the wall and between the jet exit and the wall.

---

* P.Cho, C.K.Law, J.R.Hertzberg and R.Cheng. Twenty-first Symposium (Interantional) on Combustion, The Combustion Institute, 1493 (1986)
P.Cho, C.K.Law, J.R.Hertzberg and R.Cheng. Twenty-second Symposium (Interantional) on Combustion, The Combustion Institute, 739 (1988)

* Bray,K.N.C., Champion,M. and Libby,P.A., Premixed flames in stagnating turbulence. Part III. The $k-\varepsilon$ theory for reactants impinging on a wall. Combustion and Flame (Submitted)

* Champion,M. and Libby,P.A., Reynolds stress description of opposed and impinging turbulent jets. Part I. Opposed jets. Phys.Fluids A (Submitted)

FUTURE PLANS

We intend to take up several additional studies of laminar flames in the near future. One concerns the propogation of flames within the core of a vortex. There is experimental evidence that such propogation is extraordinarily rapid but there appears to be no applicable theory accounting for this behavior. A second topic in this area relates to the influence of curvature on the rate of propogation of laminar flames. Studies to date of this influence are restricted to small curvature but experimental evidence seems to suggest that curvature can alter laminar flames to a greater extent than is indicated by previous analyses.

The major thrust of our future work will be confined to premixed flames in stagnating turbulence. At the present time we have underway two extensions of our previous analyses. One concerns application to opposed reactant streams of the Bray-Moss-Libby (BML) model of premixed turbulent combustion, a model which avoids the gradient assumption. In this case a closed set of equations has been obtained but their numerical analysis involves significant difficulties which arise for poorly understood reasons. A second relates to the free-standing flames, i.e., to the case which corresponds to the experimental data presently available, namely when the flame is sufficiently remote from the wall in the case of impinging jets or from the plane of symmetry in the case of opposed jets so that the mean concentration of product is always unity on the downstream edge of the flame. In order to include the possibility of the countergradient diffusion observed experimentally it is essential to use the BML-model for the study of these flames so clearly these two efforts are related. There are a variety of further problems to be examined in connection with these flames including the important matter of their extinction characteristics.

PUBLICATIONS FROM DOE RESEARCH

[1] Libby,P.A., Williams,F.A. and Sivishinsky,G.I., Influences of swirl on the structure and extinction of strained premixed flames. Part I: Moderate rates of rotation. Phys.Fluids A. 2:1213 (1990).

[2] Kim,J.S., Libby,P.A. and Williams,F.A., Influences of swirl on the structure and extinction of strained premixed flames. Part II: Strong rates of rotation. Phys.Fluids A. (To appear).

[3] Bray,K.N.C., Champion,M. and Libby,P.A., Premixed flames in stagnating turbulence: Part I. The general formulation for counterflowing streams and gradient models for turbulent transport. Combustion and Flame 84:391 (1991).

[4] Champion,M. and Libby,P.A., Stagnation streamline turbulence revisited. AIAA J. 28:1515 (1990).

[5] Champion,M. and Libby,P.A.,Asymptotic analysis of stagnating turbulence. AIAA J. 29:16 (1991).

ABSTRACT

Quantum Dynamics of Fast Chemical Reactions
DE-FG02-87ER13679

John C. Light, James Franck Institute
University of Chicago, Chicago, IL 60637

During the past year the initial goals of this research were accomplished, namely the development and application of direct quantum methods for the calculation of thermal rate constants for bimolecular exchange reactions.[1,2] In addition the dissociation of H_3^* (in a Rydberg state) was examined[3] and the incorporation of optical potentials into the reactive scattering calculations was begun.

For the thermal rate constants, we used the quantum flux-flux autocorrelation function formalism of Miller[4] in the hyperspherical coordinates of Pack[5] with the symmetry adapted discrete variable representation (DVR) developed earlier[6] under this grant. This was implemented by diagonalizing the Hamiltonian in the large (~ 15,000) DVR basis and projecting the eigenvectors of the thermal flux operators onto this basis. For $D+H_2$[1] and $H+D_2$[2], total angular momenta up to J = 25 were required for convergence. Although Coriolis coupling was neglected, asymmetric top coupling was included to second order perturbation theory for these calculations. Because of the increased mass of the $H+D_2$ system, some 600 accurate eigenstates of the Hamiltonian were required for each symmetry, J, and K block in order to converge the calculations.

Our results for the $H+D_2$ reactions are compared with the CEQB calculations of Sun and Bowman,[7] the VTST calculations of Garrett and Truhlar,[8] and the recent experiments of Michael and Fisher.[9] Agreement is very good over some five orders of magnitude in the rate constant.

Table I

k(T) for $H+D_2 \rightarrow HD+D$

T	VTST[8] CVT/MCPVAG	CEQB[7]	This Work[2]	Expt[9] (cm^3/molecule-sec)
300	1.8	1.7	1.7	2.1 (-17)*
500	-	6.2	5.6	6.8 (-15)
700	-	9.6	7.8	10.0 (-14)
900	-	4.9	3.7	5.4 (-13)
1100	-	-	1.1	1.7 (-12)
1300	-	-	2.4	3.9 (-12)
1500	5.6	-	4.6	7.5 (-12)

*(-17) = 10^{-17} and applies across the table

The H_3^* Rydberg molecule has an equilateral triangular configuration in the v = 0, n = 3 metastable state (like the H_3^+ molecular ion). On transition to the ground state, the $H+H_2(v,J)$ and H+H+H channels are open via the $^2A_1$ and $^2B_2$ electronic surfaces (in C_{2v} symmetry) In collaboration with the TAMP group at Lawrence Livermore National Laboratory we developed the initial wave packet, DVR, and find state projections for this problem.[3] The time evolution of the wave packet was calculated in 3-dimensions for J = 0 at total energies up to 6 eV. The wave packet was propagated to the asymptotic region where energy and H_2 internal state analysis was done. Figure 1 shows the vibrational and

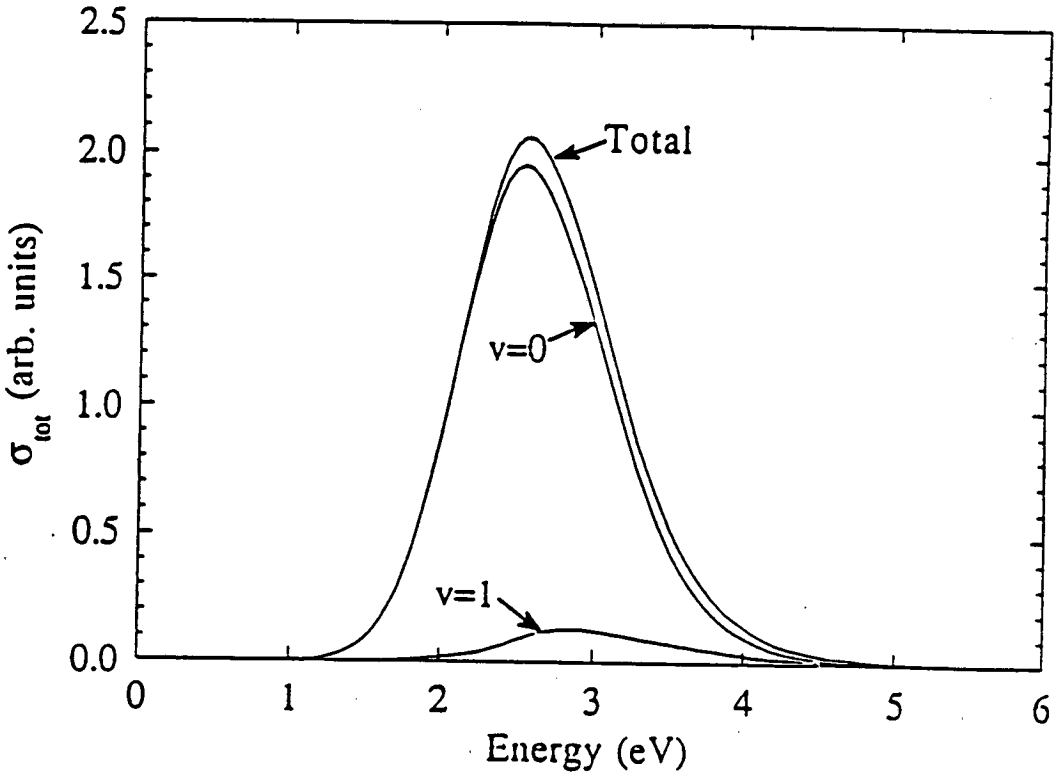

translational energy distributions of the H_2, summed over rotational states. Since the three body dissociation threshold is 4.74 eV, only projections onto the bound H_2 states were done. The dissociation is largely vibrationally adiabatic. In Figure 2 the rotational distributions for v = 0 and v = 1 are shown at the energy of the 2p $^2A_2$" Rydberg state, 5.6 eV. The increase in rotational excitation with v is observed experimentally.

Finally we are investigating the use of optical potentials (negative imaginary potentials) in conjunction with three types of scattering processes. For pre-dissociation (and photodissociation) of van der Waal's molecules, diagonalization of the Hamiltonian with V_{opt} included should yield reasonable (± 20%) estimates of the resonance lifetimes. Inclusion of an optical potential in H for reactive scattering permits evaluation of the

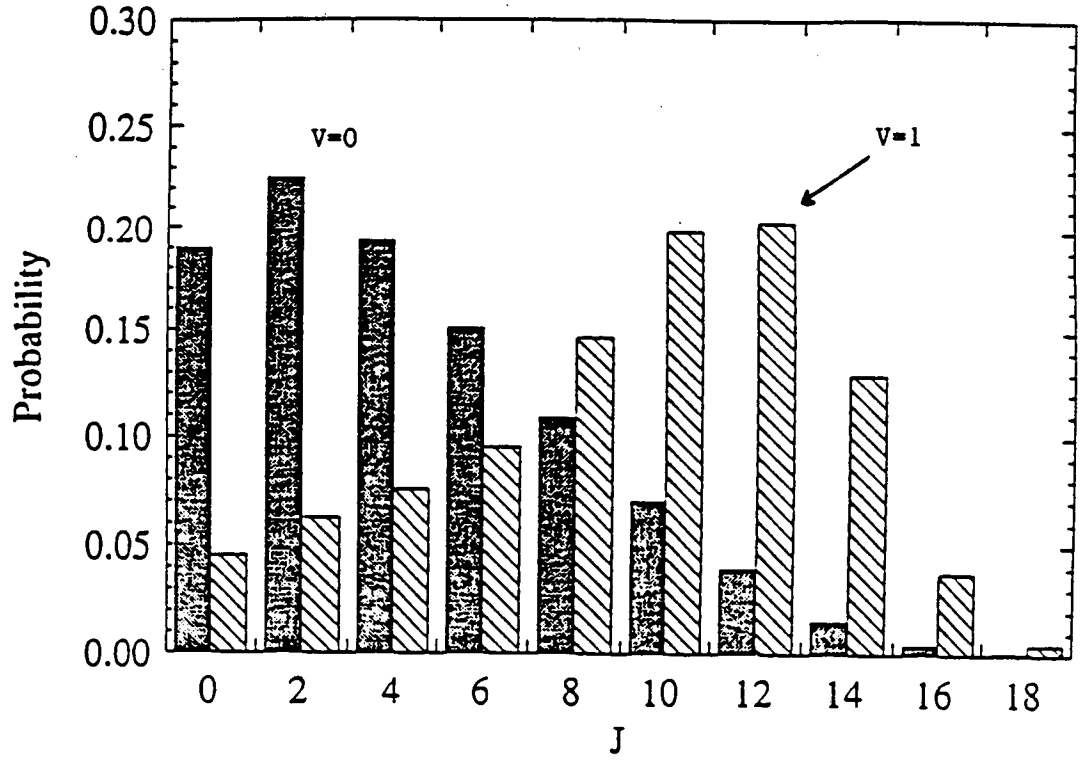

thermal rate constants with the flux-flux correlation function integrated analytically to $t \rightarrow \infty$. Finally diagonalization of H with an optical potential yields an L^2 approximation to $G^+(E)$, the out-going Green's function, and somewhat simplified evaluation of the T matrix as suggested by Neuhauser[11] and by Seideman and Miller.[12] In the latter two cases the use of the optical potential should reduce the coordinate range required for the L^2 calculation.

References

(1) T.J. Park and J.C. Light, J. Chem. Phys. 94, 2946 (1991).

(2) T.J. Park and J.C. Light, J. Chem. Phys. (in press).

(3) J.L. Krause, A.E. Orel, K.C. Kulander, and J.C. Light, J. Chem. Phys. (in press).

(4) W.H. Miller, J. Chem. Phys. 61, 1823 (1974).

(5) R.T. Pad, Chem. Phys. Lett. 108, 333 (1984).

(6) T.J. Park and J.C. Light, J. Chem. Phys. 911, 974 (1989).

(7) Q. Sun and J. Bowman, J. Phys. Chem. 94, 718 (1990).

(8) B.C. Garrett and D.G. Truhlar, J. Chem. Phys. 72, 3460 (1980).

(9) J.V. Michael and J.R. Fisher, J. Chem. Phys. 92, 3394 (1990).

(10) P.C. Cosby and H. Helm, Phys. Rev. Lett. 61, 298 (1988).

(11) D. Neuhauser, private communication.

(12) T. Seideman and W.H. Miller, preprint (private communication).

Kinetics and Mechanisms of Reactions Involving Small Aromatic Reactive Intermediates

M. C. Lin (P.I.)
Department of Chemistry
Emory University
Atlanta, GA 30322

Introduction

Small aromatic reactive intermediates such as C_6H_5, C_6H_5O and C_6H_4 are important prototype species of their respective homologs. Both C_6H_5 and its oxidation product, C_6H_5O, are believed to be important reactive intermediates which may play a pivotal role in hydrocarbon combustion chemistry, particularly with respect to soot formation under fuel-rich conditions.

Despite their fundamental and practical importance, experimental data on their reactivities towards combustion species are quite limited. There have been no reports of reliable absolute reaction rate measurements on C_6H_5 to date. Almost all rate constants currently existing in the literature are based on relative product concentration measurements, assuming a certain value for the rate constant of the phenyl recombination process. The situation with C_6H_5O and C_6H_4 is not much better. The crux of the problem lies in the lack of convenient and reliable techniques for the detection of these reactive species.

In this newly funded DOE project, we have attempted to utilize two different diagnostic methods to monitor the formation and reaction of these small aromatic radicals. In the first method, we will develop the REMPI/MS (resonance-enhanced multiphoton ionization/mass spectrometry) technique, using different ionization schemes, such as (1+1), (2+1) and (1+2) REMPI, which stand for resonant one-photon + an additional photon to ionize, etc. for radical detection. Our initial studies center on the generation and spectroscopy of these three aromatic species by the pulsed photolysis of their aromatic precursor molecules (such nitiosobenzene and phenyl iodide for C_6H_5) on cold single crystal surfaces, followed by REMPI/MS-TOF measurements inside a quadruple mass spectrometer. Kinetic measurements will be carried out after the completion of spectroscopic studies.

The second diagnostic method centers on LRA (laser resonance absorption). Both extra- and intra-cavity absorption techniques are being explored currently. With the conventional extra-cavity absorption method, a reproducible ratioing technique is being developed for small absorptions ($I_a/I_o \approx 1\%$). With the intra-cavity absorption measurement, the technique developed recently by O'Keefe and Deacon [Rev. Sci. Instrum. 59, 2544, 1988] has been utilized. This technique can be applied to study the spectroscopy of weak transitions.

The results of our preliminary studies for C_6H_5 using REMPI/MS and LRA are briefly discussed below.

Recent Progress

A. Photofragmentation and REMPI/MS Product Detection

The photochemistry of adsorbed nitrosobenzene on a single crystal of Al_2O_3 (1120) has been studied at 193 and 248 nm using both electron impact ionization and REMPI/MS to measure the flight times of the fragmentation products. REMPI/MS spectra of C_6H_5 and NO were measured. The time-of-flight of NO measured by REMPI/MS in the 225-230 nm region revealed three different peaks, with the first two of which derived from the NO directly desorbed from the surface and the third peak from the photofragmentation of the desorbed parent molecules. These molecules were further photofragmented by the REMPI laser. The rotational temperatures of the NO in the first two peaks are about 400 and 200 K, respectively.

The EI/MS and REMPI/MS results of the arometic fragments suggests that both 193 and 248 nm photolyses of C_6H_5NO produced a fair amount of C_6H_6 and a small yield of $C_{12}H_{10}$. This indicates that the C_6H_5 fragment might have undergone extensive surface reactions. The wavelength (REMPI) scan for both m/z 77 and m/z 78 revealed either that the phenyl radical and benzene have very similar REMPI/MS spectra or that the m/z 77 signal derived extensively from benzene REMPI. A detailed analysis of these results is currently underway.

B. LRA Measurement of C_6H_5 Kinetics

The cavity-ring-down method has been employed to measure the kinetics of C_6H_5 reactions, initially with O_2:

$$C_6H_5 + O_2 \leftrightarrow C_6H_5OO^{\dagger} \rightarrow C_6H_5O + O$$

The reaction has been reported by Priedl and Zellner [Ber. Bensenges. Phys. Chem. 93, 1417, 1989] to be unmeasurably slow, with k (298-400 K) $\leq 2 \times 10^{-17}$ cm^3/s. This surprisingly slow rate has been confirmed by our measurement, $k_{O_2} = 4.2 \times 10^{-17}$ cm^3/s. at 297 K. The slow rate suggests that the energy barrier for the entrance addition reaction, $C_6H_5 + O_2 \rightarrow C_6H_5O_2$ may be as high as 2 - 3 kcal/mole.

A similar study for the addition-elimination reaction:

$$C_6H_5 + C_2H_2 \leftrightarrow C_6H_5C_2H_2^{\dagger} \rightarrow C_6H_5C_2H + H$$

also indicates that the reaction is very slow. At 297 K, we measured the rate constant to be $k_{C_2H_2} = 1.4 \times 10^{-17}$ cm^3/s. This value is consistent with the upper limit reported by Priedl and Zellner, $k_{C_2H_2} \leq 2 \times 10^{-17}$ cm^3/s at 298 K.

In our experiment, the $n \leftarrow \pi$ transition at 505 nm previously reported by Porter and Ward [Proc. Roy. Soc. 287, 457, 1965] was used in the intra-cavity absorption measurements.

Experiments are underway to study the effects of temperature and pressure on the above two and many other reactions of interest to the soot-formation chemistry.

Publications Resulted from Previous DOE Support:

About 20 articles have been published from a previous grant to the Catholic University of America under contract no: DE-FG05-85ER-13373 (Jun. 1985 - May 1987, with extension to Aug. 1989). The following four papers appeared between FY-90 and 92:

1. "CO Formation in Thermal Decomposition of CH_3ONO at High Temperatures: Kinetic Modeling of the CH_3O Decomposition Rate" T. K. Choudhury, Y. He, W. A. Sanders and M. C. Lin, J. Phys. Chem., 94, 2394 (1990).

2. "Homogeneous Pyrolysis of Acetylacetone at High Temperatures in Shock Waves" T. K. CHoudhurry and M. C. Lin, Int. J. Chem. Kinet., 22, 491 (1990).

3. "Thermal Decomposition of t-Butyl Alcohol in Shock Waves", T. K. Choudhury, M. C. Lin, C.-Y. Lin and W. A. Sanders, Combust. Sci. Technol., 71, 219 (1990).

4. "Effects of Nitric Oxide on the Thermal Decomposition of CH_3ONO: Rate Constants for the HNO + HNO and HNO + 2NO Reactions" Y. He and M. C. Lin, Int. J. Chem. Kinet., (in press).

Crossed-Beam Studies of the Dynamics of Radical Reactions

K. Liu and R.G. Macdonald
Chemistry Division
Argonne National Laboratory
Argonne IL 60439

Scope

The objective of this program is to characterize the detailed dynamics of elementary radical reactions in a comprehensive manner and to better understand radical reactivity in general. The radical beam is typically generated by a laser photolysis method. After colliding with the reacting molecule in a crossed-beam apparatus, the reaction product state distribution is interrogated by laser spectroscopic techniques. Several radicals of combustion significance, such as O, CH, OH, CN and NCO have been successfully generated and their collisional behavior has been studied or is being investigated in this manner.

Recent Results

(A) Inelastic Scattering of NCO($\tilde{X}\,^2\Pi$) +He: Rotational Energy Transfer

Over the past decade considerable progress has been made in understanding the collision dynamics of systems were multiple potential energy surfaces are involved. Much of this work, including that conducted in this laboratory on CH and OH radicals, has focussed on the accurate description of the dynamics of diatomic radicals with symmetric collision partners; however, there has been little work, both experimental or theoretical, on the collision dynamics of polyatomic radicals. The simplest extension into this new realm of polyatomic radical dynamics is to study a linear $^2\Pi$ radical. To this end, a crossed molecular beam investigation involving the linear NCO($\tilde{X}\,^2\Pi$) radical and He has been initiated. The NCO radical is a prototypical Hund's case (a) radical and as such its collision dynamics should be contrasted to previous studies involving the Hund's case (b) CH and intermediate case OH radical. State-to-state integral cross sections for the process:

$$NCO(\tilde{X}\,^2\Pi_{3/2}, 00^10) + He \rightarrow NCO(\tilde{X}^2\Pi_{3/2,1/2}, 00^10,J,e/f) + He \qquad (1)$$

have been made over the collision energy range of 0.8 to 4.0 kcal/mole. Two types of measurements were performed: (1) the product state distribution at fixed initial translational energy and (2) the translational energy dependence of individual product quantum states. At fixed collision energy, the NCO rotational state distribution from process (1) is different for scattering into each spin-orbit manifold. For spin-orbit conserving collisions the rotational state distribution is generally monotonically decreasing with increasing J'; while for spin-orbit changing collisions the product rotational state distribution is bell shaped with a maximum between J'=12 and 25 depending on the initial translational energy. Within experimental uncertainty, the rotational state distributions do not show any oscillations with J'. Excitation functions were measured for many fine-structure states, (K-doublet resolved). The general shape of these excitation functions were similar for scattering into either spin-orbit manifold: there is an increase from a threshold value until a maximum is reached and then a slow decrease with increasing collision energy. As ΔJ increases, a dynamical threshold is clearly established and the increase in the cross section

from threshold decreases markedly with increasing collision energy. All of the features of Process (1) that have been observed in this investigation can be understood from theoretical considerations of the inelastic scattering of $^2\Pi$ diatomic radicals and simple models for rotational energy transfer. These features are a dynamical consequence of the Renner-Teller effect.

(B) Inelastic Scattering of NCO($\tilde{X}\ ^2\Pi$) + He: Inter Renner-Teller Component Energy Transfer.

As a linear triatomic radical in an electronic state with $\Lambda \neq 0$ bends, the vibrationally excited levels are split as a result of vibronic interactions. This is the well known Renner-Teller effect. To date, there is no information at all on the collision dynamics of processes involving these vibronic levels. As a further advance into the study of collision dynamics of polyatomic radicals, preliminary experiments have been initiated to study the energy transfer pathways between vibronic levels of the the first excited bending level, (01^K0), of NCO in collisions with He. The total integral cross section for processes such as

$$NCO(01^00;\mu^2\Sigma) + He \rightarrow NCO(01^20;^2\Delta_{3/2}) + He \qquad (2a)$$

$$\rightarrow NCO(01^20;^2\Delta_{5/2}) + He \qquad (2b)$$

have been measured under single collision conditions. At a translational energy of 3.8 kcal mol^{-1}, it was found that the cross section for the inter Renner-Teller process (2a) was 6.3 times larger than for (2b) even though production of the ($01^20;^2\Delta_{5/2}$) vibronic level is energetically favoured by 0.27 kcal mol^{-1}. Such results can be understood from a conceptual model based on the same theoretical foundation used to understanding the inelastic scattering of $^2\Pi$ diatomic radicals. Currently, these concepts are being placed on a firmer and more rigorus theoretical basis.

Publications 1990-1992

1. Fine-Structure selectivity in polyatomic reaction products: CN($X^2\Sigma^+$, v=0, N=0,1) + $O_2 \rightarrow NCO(\tilde{X}^2\Pi_{3/2,1/2}, 00^10,J,e/f) + O$
   D.M. Sonnenfroh, R. G. Macdonald and K. Liu, J. Chem. Phys. 93, 1478-79 (1990).

2. A crossed-beam study of the state-resolved dynamics of CH($X^2\Pi$) + D_2. I. The inelastic scattering channel.
   R. G. Macdonald and K. Liu, J. Chem. Phys. 93, 2431-2442 (1990).

3. A crossed-beam study of the state-resolved dynamics of CH($X^2\Pi$) + D_2. II. The isotopic exchange channel.
   R. G. Macdonald and K. Liu, J. Chem. Phys. 93, 2443-2459 (1990).

4. Crossed-beam investigations of the state-resolved collision dynamics of simple radicals.
   K. Liu, R. G. Macdonald and A.F. Wagner, Int. Rev. Phys. Chem. 9, 187-225 (1990).

5. Number density to-flux transformation revisited: Kinematic effects in the use of laser-induced fluorescence for scattering experiments.
D. M. Sonnenfroh and K. Liu, Chem. Phys. Lett. 176, 183-190 (1990).

6. A crossed-beam study of the state-resolved integral cross sections for the inelastic scattering of $OH(X^2\Pi)$ with CO and N_2.
D. M. Sonnenfroh, R. G. Macdonald and K. Liu, J. Chem. Phys. 94, 6508-6518 (1991).

7. Inelastic scattering of $NCO(X^2\Pi)$ + He: Prototypical rotational state distributions for Hund's case (a) radicals.
R. G. Macdonald and K. Liu, J. Phys. Chem. 95, 9630-9633 (1991).

8. State-to-state collision dynamics of molecular free radicals.
R. G. Macdonald and K. Liu, SPIE Proc. (accepted) (1992).

NONPERTURBATIVE CALCULATIONS OF HIGH-LASER-INTENSITY EFFECTS IN RESONANT WAVE-MIXING SPECTROSCOPY

Robert P. Lucht
Combustion Research Facility
Sandia National Laboratories
Livermore, California 94551

Introduction

Resonant wave-mixing processes show great promise for sensitive, coherent detection of intermediate species in chemically reacting systems. However, many aspects of the fundamental physics of these techniques are currently not well understood, and predictive models for line shapes and signal intensities are at a very early stage of development. These research activities focus on the effect of high (saturation) laser intensities on line shapes and signal intensities in resonant wave-mixing processes.

Recent Progress

Multiwave (Higher-Order Wave) Mixing in Sodium (with R. Trebino and L. A. Rahn)

To investigate the diagnostic potential and the fundamental physics of nearly degenerate, resonant four-wave mixing (4WM), Trebino and Rahn[1] performed experiments on the sodium atom in flames. Two pulsed, nearly Fourier-transform-limited, nearly frequency-degenerate laser beams were tuned 1-2 cm^{-1} below the $3^2S_{1/2}$-$3^2P_{1/2}$ electronic resonance. At low laser intensities 4WM resonances were observed at $\omega_1-\omega_2 = 0$, corresponding to the Zeeman coherence, and at $\omega_1-\omega_2 = .059$ cm^{-1}, corresponding to the hyperfine splitting ω_{hfs}. As the laser intensities were increased, the 4WM resonances at ω_{hfs} broadened and spectral features appeared at $\omega_{hfs}/2$. Hypothesizing that the spectral features at $\omega_{hfs}/2$ were the result of higher-order wave-mixing processes, they used higher-order phase matching schemes to selectively detect signals strong subharmonic resonances at $\omega_{hfs}/2$ and $\omega_{hfs}/3$; weaker subharmonic resonances are also apparent at $\omega_{hfs}/4$ and $\omega_{hfs}/5$. Trebino and Rahn[2] developed a perturbative diagrammatic approach for the calculation of higher-order wave-mixing spectra, and were able to obtain good agreement between theory and experiment for spectra measured at low laser intensity.

In this section a nonperturbative (high laser intensity) theoretical approach is described that gives good agreement between theory and experiment over the entire range of laser intensities used in the experiments. The density matrix equations are directly integrated during the time duration of the laser pulses to give time-dependent density matrix elements for population [$\rho_{jj}(t)$] and coherence [$\rho_{kj}(t)$]; the medium polarization P(t) is then calculated from the density matrix elements $\rho_{kj}(t)$. The medium polarization is Fourier-analyzed to give the 4WM signal at $2\omega_1-\omega_2$, the 6WM signal at $3\omega_1-2\omega_2$, the 8WM signal at $4\omega_1-3\omega_2$, etc.The Zeeman sublevels in the hyperfine states in both the upper and lower electronic levels are included in a sixteen-level model of the sodium $3^2S_{1/2}$-$3^2P_{1/2}$ electronic resonance. The polarization properties of the laser radiation are accounted for by incorporating the direction cosines of the transition dipole matrix elements in the calculation.

In Fig. 1, calculated multiwave mixing spectra are compared with the experimental results of Trebino and Rahn.[1] As laser intensity increases, the peaks of the spectral features shift to greater frequency difference, the subharmonics at 0.015 and 0.012 cm^{-1} appear, and a spectral feature appears at approximately 0.04 cm^{-1}. All of the spectral features discussed above are present in the calculated as well as the experimental spectra. For both the high and low intensity spectra theoretical and experimentally measured laser intensities agree to within a factor of four, which is excellent agreement considering the difficulties of measuring absolute intensities.

Future work will involve examining the density matrix solutions in detail to elucidate the role of population-polarization coupling in determining the intensities of the subharmonic resonances.

Saturation and Pressure Effects in Degenerate Four-Wave Mixing (with R.L. Farrow and D. J. Rakestraw)

Degenerate four-wave mixing (DFWM) is a technique that shows great promise for sensitive measurements of transient gas-phase species. Applications of DFWM are being pursued actively at laboratories thorughout the world. However, much research is required on some fundamental aspects of the physics of the technique, such as collisional and laser intensity effects, before DFWM can be applied quantitatively in a wide range of chemically reacting media such as flames and plasmas. One of the most important questions is the effect of saturation on DFWM signal

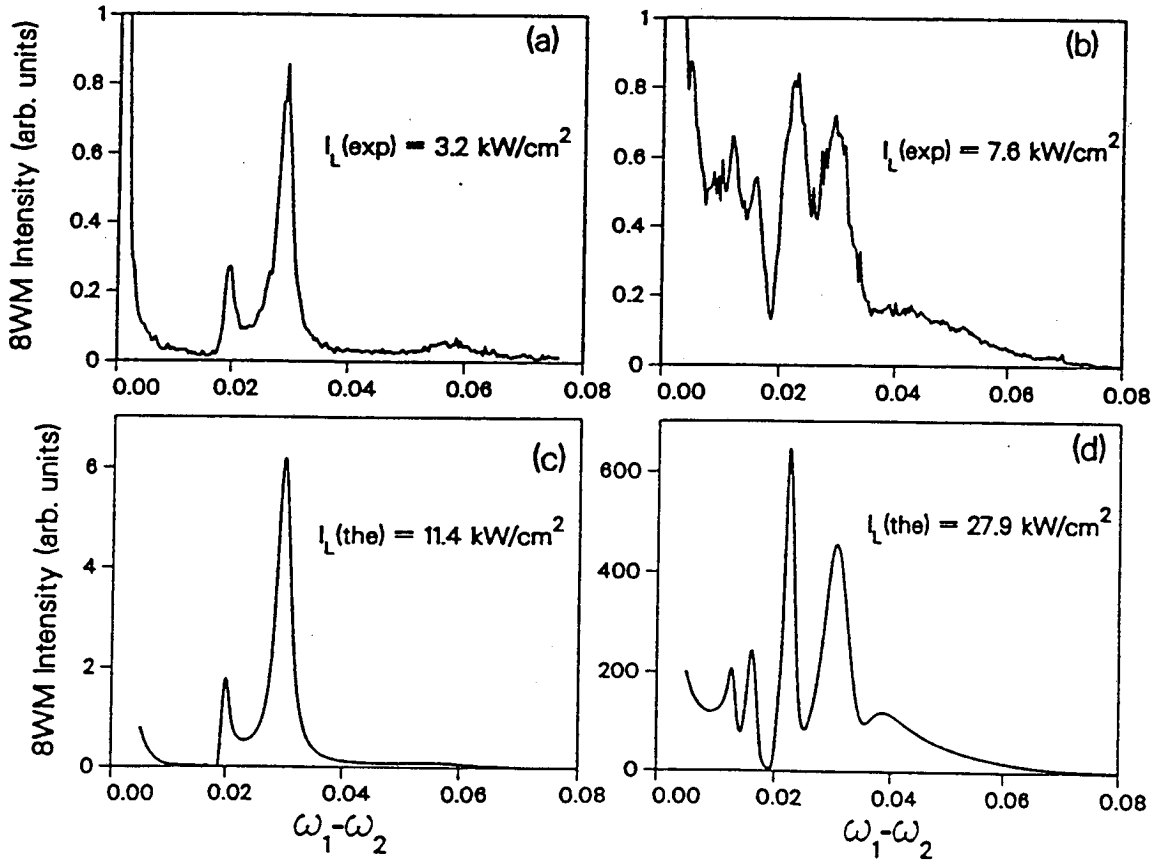

Figure 1. Experimental (a,b) and calculated (c,d) 8WM spectra at two different laser intensities.

intensities at conditions of interest for flames and plasmas. The temperature measurements of Dreier and Rakestraw[3] suggested that collisional effects on the signal intensity are minimized or eliminated by using saturation intensity laser beams. Farrow et al.[4] solved the two-level model equations of Abrams and Lind[5] in the limit of small absorption and showed that the DFWM peak signal intensity scaled as p^{-6} at low laser intensity, but at pump laser intensities significantly above the saturation intensity the peak signal intensity is independent of laser intensity. However, the model of Abrams and Lind assumes that the resonance line is homogeneously broadened and that that the probe laser intensity is weak (non-saturating); these assumptions will not hold for many conditions of interest for DFWM applications.

In this study the time- and space-dependent density matrix equations are integrated directly for a two-level system. Doppler effects are included by solving the equations for numerous velocity groups, removing the assumption of a homogeneously broadened line. For species such as OH and NO in flames, the Doppler width and collisional width are often comparable; DFWM saturation calculations for this case have not, to our knowledge, been performed previously. The restriction of the Abrams and Lind model on probe laser intensity is removed by this approach; both pump and probe intensities can be saturating.

The calculations are compared with single-mode laser measurements of NO DFWM in a cell filled with helium at various pressures. A comparison of measured and calculated NO DFWM line shapes for constant laser pulse energy at He pressures of 100, 300, and 520 Torr is shown in Fig. 2. At 100 Torr, the laser intensity is significantly above the saturation intensity for the line. The agreement between theory and experiment is excellent, although the experimental line shapes exhibit an asymmetry at high pressure that is not predicted by the model. The pressure dependence of the DFWM signal intensity is shown in Fig. 3. Excellent agreement between theory and experiment is obtained for a peak laser Rabi frequency of 0.030 cm^{-1}. The other curves shown serve to illustrate the reduced dependence of the peak DFWM signal intensity as laser power increases, even for lines that are predominantly Doppler-broadened.

These nonperturbative calculations are a powerful tool for assessing the utility of DFWM as a diagnostic for chemically reacting systems. Future modeling work will include the effects of multiple levels and multi-mode laser radiation, and the interaction of neighboring transitions.

References

1. R. Trebino and L. A. Rahn, Opt. Lett. **12**, 912-914 (1987).
2. R. Trebino and L. A. Rahn, Opt. Lett. **15**, 354-356 (1990).
3. T. Dreier and D. J. Rakestraw, Opt. Lett. **15**, 72 (1990).
4. R. L. Farrow, D. J. Rakestraw, and T. Dreier, "Investigation of the Dependence of Degenerate Four-Wave Mixing Line Intensities on Transition Dipole Moment," J. Opt. Soc. Am. B, accepted for publication.
5. R. L. Abrams and R. C. Lind, Opt. Lett. **2**, 94 (1978); Opt. Lett. **3**, 205 (1978).

6. R. L. Vander Wal, R. L. Farrow, and D. J. Rakestraw, "High-Resolution Investigation of Degenerate Four-Wave Mixing in the γ(0,0) Band of Nitric Oxide," *Twenty-Fourth Symposium (International) on Combustion*, accepted for publication.

BES-Supported Publications: 1990-1992

1. R. P. Lucht, R. Trebino, and L. A. Rahn, "Resonant Multiwave Mixing Spectra of Gas-Phase Sodium: Nonperturbative Calculations," Physical Review A, in press (1992).
2. R. P. Lucht, R. L. Farrow, R. Trebino, and L. A. Rahn, "Nonperturbative Calculations of High-Intensity Effects in Nonlinear Wave-Mixing Processes," *Laser Spectroscopy X*, (Eds. M. Ducloy, E. Giacbino, and G. Camy, World Scientific, 1992), in press.

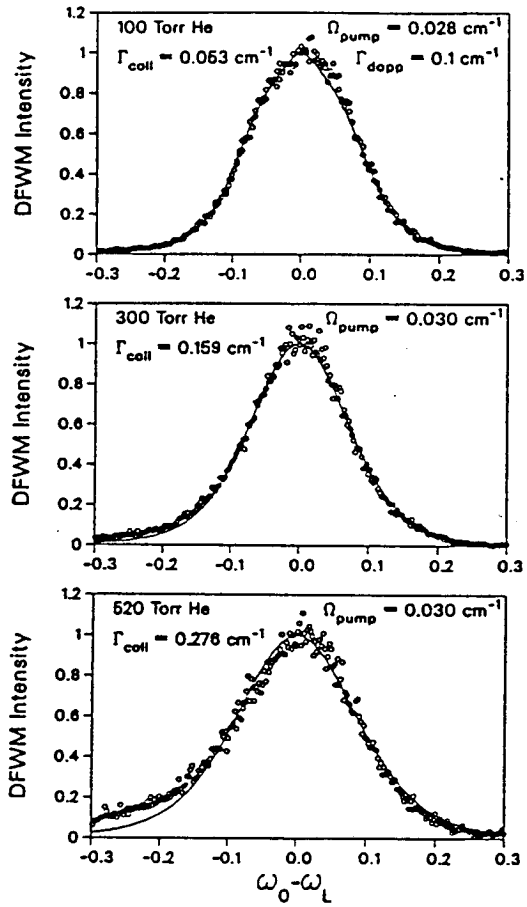

Figure 1. Comparison of predicted and measured DFWM lineshapes for the NO $O_{12}(2)$ transition in a He-filled cell. The Rabi frequency $\Omega_{pump} = \mu_{21}A_{pump}/4\pi\hbar c$, where μ_{21} is the dipole moment matrix element and A_{pump} is the peak electric field amplitude. The peak Ω_{pump} for a 5-nsec Gaussian laser pulse, and Doppler and collisional FWHMs are listed in the figures.

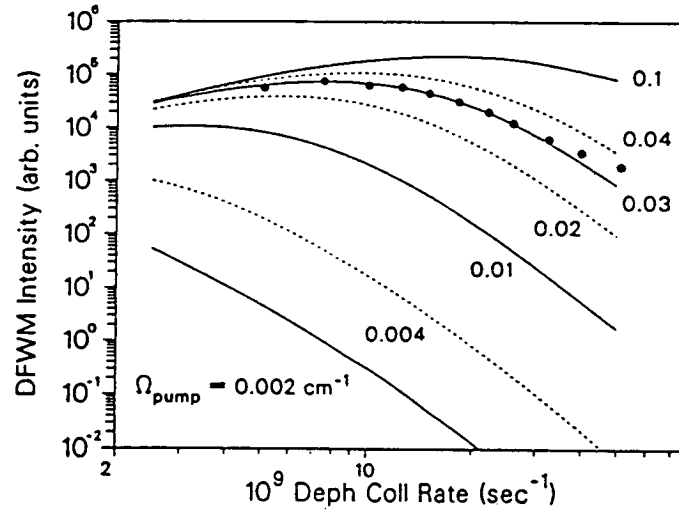

Figure 2. Pressure dependence of the peak DFWM signal intensity at various laser intensities. The solid cirlces are the experimental data of Vander Wal et al.[6] The dephasing rate is 5.0×10^9 sec^{-1} for a He pressure of 100 Torr. The pressure of NO in the cell is 30 mTorr.

FLASH PHOTOLYSIS-SHOCK TUBE STUDIES OF BIMOLECULAR REACTIONS

Joe V. Michael

Gas Phase Chemical Dynamics Group
Chemistry Division
Argonne National Laboratory
Argonne, IL 60439

Since its inception,[1] this project has concentrated on the measurement of thermal bimolecular reactions of atomic species with stable molecules. The flash or laser photolysis-shock tube (FP- or LP-ST) method involves first creating the atomic species by photolysis and then monitoring the atomic concentration with atomic resonance absorption spectrometry (ARAS) as a function of the reactant molecular concentration. Studies on H-, O-, and D-atoms have already been carried out with this apparatus. During the past year, two additional studies of this type have been completed. This first is with O-atoms, and the second is with N-atoms. Additionally, experiments designed to measure the curve of growth for Cl-atoms and studies on the thermal decomposition of CH_3Cl have been completed. Lastly, a new type of experiment is described in which radicals are first pyrolytically created and then react with a photolytically produced concentration of an atomic species. The method is called the pyrolysis photolysis-shock tube (PP-ST) technique and has been applied to the $O + CH_3$ reaction between 1609-1972 K.

In the first study, rate constants for the reaction,

$$O + CH_3Cl \rightarrow OH + CH_2Cl, \qquad (1)$$

have been measured over the temperature range, 556-1485 K.[2] Two different techniques have been used, (1) the LP-ST technique at Argonne (Lim and Michael) over the temperature range, 916-1485 K, and (2) the HTP technique at Rensselaer Polytechnic Institute (Ko and Fontijn) over the temperature range, 556-1291 K. Over the range of common temperature overlap, the rate constants are in excellent agreement. Therefore, the entire database has been analyzed together, and the results can be described by the three parameter expression,

$$k_1 = 2.57 \times 10^{-11}\, T^{0.31} \exp(-5633\ K/T)\ cm^3\ molecule^{-1}\ s^{-1}, \qquad (2)$$

for $556 \leq T \leq 1485$ K.

In the second study, rate constants for the reaction,

$$N + NO \rightarrow N_2 + O, \qquad (3)$$

have been measured over the temperature range, 1251-3152 K, with the LP-ST technique. N-atoms have been monitored by the ARAS technique. The data do not show T-dependence over this range and can be represented by,

$$k_3 = (3.7 \pm 0.9) \times 10^{-11}\ cm^3\ molecule^{-1}\ s^{-1}, \qquad (4)$$

This result is in satisfactory agreement with recent shock tube results by Davidson and Hanson[3] and Koshi et al.[4] who have used a similar technique It also agrees with results obtained between 196-400 K.[5] This wide invariance with temperature shows that this reaction is one of the simplest addition-elimination reactions of second row elements.

The thermal decomposition of CH_3Cl has been studied by observing the buildup of Cl-atoms with the ARAS technique. The results are shown in Fig. 1 and can be represented by the Arrhenius expression,

$$k_5 = 9.6 \times 10^9 \exp(-27449\ K/T)\ s^{-1}. \qquad (5)$$

Kondo, et al.[6] have previously studied this reaction, and the present results do not agree with their conclusions. k_5 has been used along with literature rate constants for the $CH_3 + CH_3$ reactions to provide profiles of $[CH_3]$. Subsequently, SO_2 has been introduced into the system, and the reactions of Cl-, H-, and O-atoms with it have been experimentally checked for importance. It appears that SO_2 is a spectator molecule at the concentrations, temperatures, and densities that are used. After CH_3Cl has had time to significantly decompose, the delayed photolysis of SO_2 then provides a pulse of O-atoms which are then subsequently monitored by the ARAS technique. The only process of sufficient rate to remove O-atoms under the present conditions is the reaction,

$$O + CH_3 \rightarrow H_2CO + H \text{ or } H_2 + CO + H. \qquad (6)$$

Fits to O-atom profiles under a variety of conditions gives the T-independent rate constant value,

$$k_6 = (1.4 \pm 0.3) \times 10^{-10}\ cm^3\ molecule^{-1}\ s^{-1}. \qquad (7)$$

This value agrees well with lower temperature determinations between 294-900 K.[7]

Additional atom with molecule reaction studies and, also thermal decomposition investigations, are in the planning stage at the present time. The reactions that will be studied will either be of theoretical interest to chemical kinetics or be of practical interest in hydrocarbon combustion.

This work was supported by the U. S. Department of Energy, Office of Basic Energy Sciences, Division of Chemical Sciences, under Contract No. W-31-109-ENG-38.

References

1. J. V. Michael, J. Chem. Phys. **90**, 189 (1989).
2. T. Ko, A. Fontijn, K. P. Lim, and J. V. Michael, Symp. (Int.) Combust., [Proc.] **24**, accepted.
3. D. F. Davidson and R. K. Hanson, Int. J. Chem. Kinet. **22**, 843 (1990).
4. M. Koshi, M. Yoshimura, K. Fukuda, H. Matsui, K. Saito, M. Watanabe, A. Imamura, and C. Chen. J. Chem. Phys. **93**, 8703 (1990).
5. J. H. Lee, J. V. Michael, W. A. Payne, and L. J. Stief, J. Chem. Phys. **69**, 3069 (1978).
6. O. Kondo, K. Saito, and I. Murakami, Bull. Chem. Soc. Jpn. **53**, 2133 (1980).
7. I. R. Slagle, D. Sarzynski, and D. Gutman, J. Phys. Chem. **91**, 4375 (1987).

Publications from DOE Sponsored Work from 1990-92.

Corrections for Non-Ideal Effects in Reflected Shock Waves at Low Mach Numbers, J. V. Michael and J. R. Fisher, *Current Topics in Shock Waves, Seventeenth International Symposium on Shock Waves and Shock Tubes*, Y. W. Kim, Ed., American Institute of Physics, New York, 1990, p. 210.

Rate Constants for the Reaction, O + C_2H_2 and O + C_2D_2 → Products, over the Temperature Range, ~850-1950K, by the Flash Photolysis- Shock Tube Technique. Determination of the Branching Ratio and a Further Theoretical Analysis, J. V. Michael and A. F. Wagner, J. Phys. Chem. **94**, 2453 (1990).

Rate Constants for the Reaction, D + D_2O → D_2 + OD, by the Flash Photolysis-Shock Tube Technique over the Temperature Range, 1285-2261 K: Results for the Back Reaction and a Comparison to the Protonated Case, J. R. Fisher and J. V. Michael, J. Phys. Chem. **94**, 2465 (1990).

Rate Constants for the Reaction, D + H_2 → HD + H, over the Temperature Range, 655-1979 K, by the Flash Photolysis-Shock Tube Technique, J. V. Michael and J. R. Fisher, J. Phys. Chem. **94**, 3318 (1990).

Rate Constants for the Reaction, H + D_2 → HD + D, over the Temperature Range, 724-2061 K, by the Flash Photolysis-Shock Tube Technique, J. V. Michael, J. Chem. Phys. **92**, 3394 (1990).

Theoretical and Experimental Rate Constants for Two Isotopic Modifications of the Reaction, H + H_2, Joe V. Michael, J. Robert Fisher, Joel M. Bowman, and Qiyan Sun, Science **249**, 269 (1990).

Rate Constants for the Reaction, O + H_2O → OH + OH, over the Temperature Range, 1500-2400 K, by the Flash Photolysis-Shock Tube Technique: A Further Consideration of the Back Reaction, Assa Lifshitz and J. V. Michael, Symp. (Int.) Combust., [Proc.] **23**, 59 (1990).

Rate Constants (296 to 1700 K) for the Reactions, C_2H + C_2H_2 → C_4H_2 + H and C_2D + C_2D_2 → C_4D_2 + D, K. S. Shin and J. V. Michael, J. Phys. Chem. **95**, 5864 (1991).

Rate Constants for the Reactions, H + O_2 → OH + O and D + O_2 → OD + O, over the Temperature Range, 1085 to 2278 K by the Laser Photolysis-Shock Tube Technique, K. S. Shin and J. V. Michael, J. Chem. Phys. **95**, 262 (1991).

Thermal Rate Constant Measurements by the Flash or Laser Photolysis-Shock Tube Method: Results for the Oxidations of H_2 and D_2, J. V. Michael, Preprint, 202nd American Chemical Society, Symposium on Combustion Chemisty, Fuel Chemistry Division **36**, 1563 (1991).

The Measurement of Thermal Bimolecular Rate Constants by the Flash Photolysis-Shock Tube (FP-ST) Technique: Comparison of Experiment to Theory, J. V. Michael, Advances in Chemical Kinetics and Dynamics, in press.

Measurement of Thermal Rate Constants by Flash or Laser Photolysis in Shock Tubes Oxidations of H_2 and D_2, J. V. Michael, Prog. Energy Combust. Sci., in press.

Isotope Effect Studies at High Temperatures by the Flash or Laser Photolysis-Shock Tube (FP-ST) Technique, J. V. Michael, in *Isotope Effects in Chemical Reactions and Photodecomposition Processes*, J. A. Kaye, editor, American Chemical Society, in press.

A Kinetics Study of the $O(^3P)$ + CH_3Cl Reaction over the 556-1485 K Range by the HTP and LP-ST Techniques, T. Ko, A. Fontijn, K. P. Lim, and J. V. Michael, Twenty-Fourth International Symposium on Combustion, accepted.

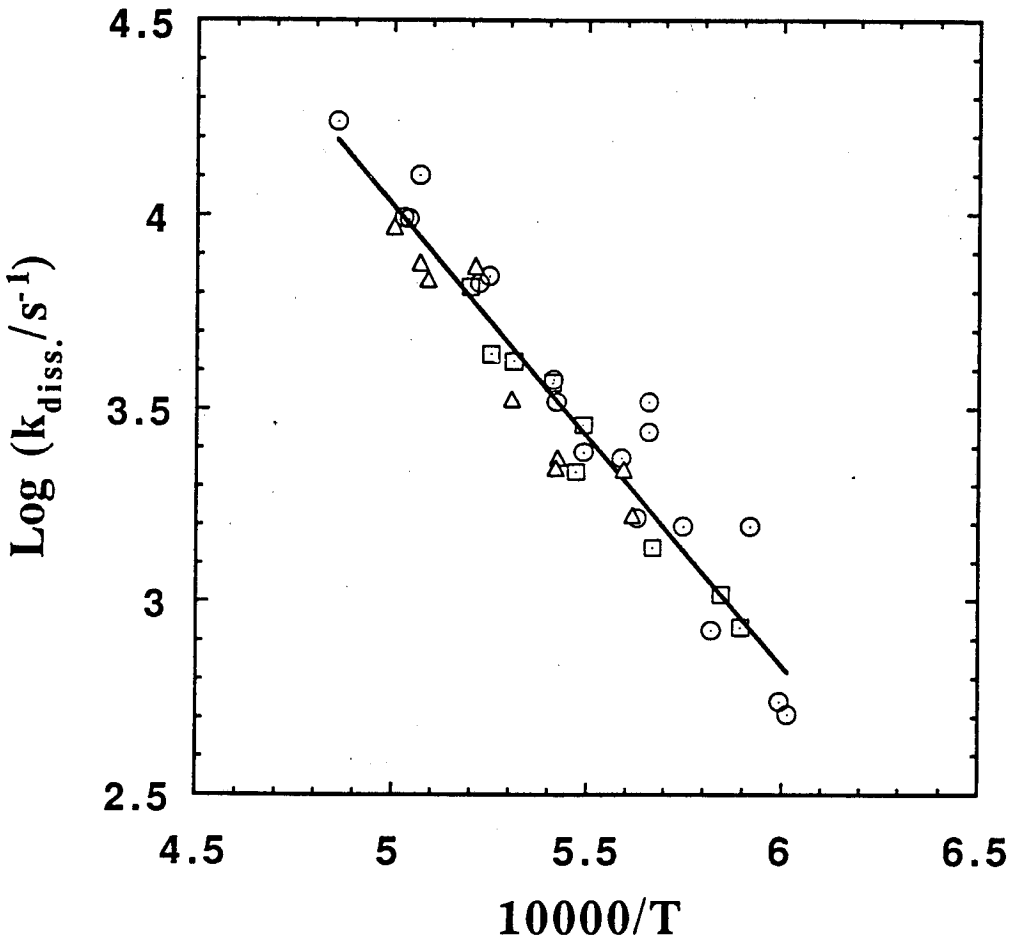

Figure 1: Rate data for $CH_3Cl \rightarrow CH_3$ + Cl. Circles are with P_1 = 15 torr, squares are with P_1 = 10 torr, and triangles are with P_1 = 6 torr. The line is calculated from eq (5).

CHEMICAL KINETICS AND COMBUSTION MODELING

James A. Miller
Combustion Research Facility
Sandia National Laboratories
Livermore, CA 94551-0969

The goal of this program is to gain qualitative insight into how pollutants are formed in combustion systems and to develop quantitative mathematical models to predict their formation rates. This necessarily involves combining several activities: low-pressure flame experiments, chemical kinetics modeling, theory, and kinetics experiments (in some instances). Our efforts are focused on problems involved with the nitrogen chemistry of combustion systems and on the formation of soot and PAH in flames.

The Reactions of Imidogen with Nitric Oxide and Molecular Oxygen (with C. F. Melius, Sandia National Laboratories):

Using potential energy surface information from BAC-MP4 calculations and statistical-dynamical methods, we have calculated the branching fraction for the NH + NO reaction,

$$\begin{aligned} NH + NO &\rightarrow N_2 + OH \qquad (1) \\ &\rightarrow N_2O + H. \qquad (2) \end{aligned}$$

We find that reaction (2) dominates over the entire temperature range considered, 300 K < T < 3500 K, with $f=k_1/(k_1+k_2)$ varying from about 0.19 at room temperature to about 0.30 at 3500 K. The branching fraction f can be expressed as $f=7.36\times10^{-2}T^{0.17}$. In addition, we have calculated rate coefficients for the two-channel process,

$$\begin{aligned} NH + O_2 &\rightarrow HNO + O \qquad (3) \\ &\rightarrow NO + OH. \qquad (4) \end{aligned}$$

In this case we find that reaction (4) dominates at low temperature, reaction (3) at high temperature. Between 300 K and 3300 K these rate coefficients can be expressed as (cm^3/mole-sec) $k_3=4.61\times10^5T^{2.0}\exp(-6500/RT)$ and $k_4=1.28\times10^6T^{1.5}\exp(-100/RT)$. All these results are in good agreement with available experimental data.

Unimolecular Reaction Mechanisms Involving C_3H_4, C_4H_4, and C_6H_6 Hydrocarbon Species (with C. F. Melius, Sandia National Laboratories, and E. M. Evleth, Université de Pierre et Marie Curie):

We have investigated unimolecular rearrangement processes of unsaturated aliphatic hydrocarbons representative of intermediates in rich hydrocarbon flames using the quantum chemical BAC-MP4 method. In particular, we have investigated the unimolecular reaction mechanisms involving (1) allene-cyclopropene-propyne rearrangement, (2) vinylacetylene pyrolysis leading to acetylene and diacetylene, and

(3) various C_6H_6 compounds, including 1,5-hexadiyne, 1,2,4,5-hexatetraene, and 1,2-hexadien-5-yne leading to 3,4-dimethylenecyclobutene, fulvene, benzene, 2-ethynyl-1,3-butadiene, and other C_6H_6 species. Rate constants for various reaction steps give good agreement with available experimental measurements. The reaction mechanisms are also consistent with various deuterium isotope labeling experiments. The results indicate that many different types of reaction mechanisms occur, including concerted pathways involving carbene and vinylidene intermediates and insertion reactions of vinylidenes into C-H bonds and C-C multiple bonds. New decomposition pathways for vinylacetylene pyrolysis, for conversion of 1,2-hexadien-5-yne to fulvene, and for conversion of fulvene to benzene arise from our investigation.

Modeling the Thermal DeNo$_x$ Process in Flow Reactors: Nitrous Oxide Formation and Surface Effects (with P. Glarborg and K. Dam-Johansen, Technical University of Denmark, and Robert J. Kee, Sandia National Laboratories):

We have investigated the impact of surface reactions such as NH_3 decomposition and radical adsorption on quartz reactor data for Thermal DeNO using a model that accounts for surface chemistry as well as molecular transport. Our calculations indicate that surface reactions under some conditions may cause a slight shift of the temperature window towards higher temperatures by inhibiting the gas phase chemistry.

The reaction mechanism for Thermal $DeNO_x$ has been revised in order to reflect recent experimental results. Among the important changes are a smaller chain branching ratio for the NH_2 + NO-reaction and a shorter NNH lifetime than previously used in modeling. The revised mechanism has been tested against a range of experimental flow reactor data for Thermal $DeNO_x$ with satisfactory results.

We have also modeled the formation of N_2O in Thermal $DeNO_x$ and calculations show good agreement with experimental data. The important reactions in formation and destruction of N_2O are indentified.

Future Directions (with J. V. Volponi, Sandia National Laboratories, and J. -F. Pauwels, CNRS, Lille, France):

We shall continue to pursue research problems that will allow us to gain more insight into the formation and growth of aromatic compounds in flames of aliphatic fuels. Currently we are investigating $H_2/O_2/Ar$ and $C_2H_2/O_2/Ar$ flames to which we add small amounts of allene (C_3H_4). We expect to develop a better understanding of the reaction paths followed by C_3H_3 and C_3H_2 by studying these flames in detail. We also anticipate that several elementary reactions requiring theoretical treatment will emerge from this work.

Publications (1990-92)

J. A. Miller, J. V. Volponi, J. L. Durant, J. E. M. Goldsmith, G. A. Fisk, and R. J. Kee, "The Structure and Reaction Mechanism of Rich, Non-Sooting $C_2H_2/O_2/Ar$ Flames," *Twenty-Third Symposium (International) on Combustion*, pp. 187-194 (1991)

J. E. M. Goldsmith, J. A. Miller, R. J. M. Anderson, and L. R. Williams, "Multiphoton-Excited Fluorescence Measurements of Absolute Concentration Profiles of Atomic Hydrogen in Low-Pressure Flames" *Twenty-Third Symposium (International) on Combustion*, pp. 1821-1827 (1991)

J. A. Miller and C. F. Melius, "Kinetic and Thermodynamic Issues in the Formation of Aromatic Compounds in Flames of Aliphatic Fuels", *Combustion and Flame,* in press (1992)

J. A. Miller, R. J. Kee, and C. K. Westbrook, "Chemical Kinetics and Combustion Modeling," *Annual Review of Physical Chemistry* **41**, 345-87 (1990)

J. A. Miller and C. T. Bowman, "Kinetic Modeling of the Reduction of Nitric Oxide in Combustion Products by Isocyanic Acid," *International Journal of Chemical Kinetics* **23**, 289-313 (1991)

J. A. Miller and C. F. Melius,"A Theoretical Analysis of the Reaction Between Hydrogen Atoms and Isocyanic Acid," *International Journal of Chemical Kinetics,* in press (1992)

G. Dixon-Lewis, V. Giovangigli, R. J. Kee, J. A. Miller, B. Rogg, M. D. Smooke, G. Stahl, and J. Warnatz,"Numerical Modelling of the Structure and Properties of Tubular Strained Laminar Premixed Flames," *Progress in Aeronautics and Astronautics,* Vol. 131, pp. 125-144 (1991)

H. K. Moffatt, P. Glarborg, R. J. Kee, J. F. Grcar, and J. A. Miller, "Surface PSR: A Fortran Program for Modeling Well-Stirred Reactors with Gas and Surface Reactions," SAND 91-8001 (1991)

J. A. Miller and C. F. Melius, "The Reactions of Imidogen with Nitric Oxide and Molecular Oxygen," *Twenty-Fourth Symposium (International) on Combustion* (accepted)

P. Glarborg, K. Dam-Johansen, J. A. Miller, and R. J. Kee, "Modeling the Thermal De-NO_x Process in Flow Reactors: Nitrous Oxide Formation and Surface Effects," submitted to *International Journal of Chemical Kinetics*

C. F. Melius, J. A. Miller, and E. M. Evleth, "Unimolecular Reaction Mechanisms Involving C_3H_4, C_4H_4, and C_6H_6 Hydrocarbon Species," *Twenty-Fourth Symposium (International) on Combustion* (accepted)

Reaction Dynamics in Polyatomic Molecular Systems

William H. Miller

Department of Chemistry, University of California, and
Chemical Sciences Division, Lawrence Berkeley Laboratory
Berkeley, California 94720

Recent Progress

The most dramatic progress we have made over the last year is in the area of developing a rigorous "quantum mechanical transition state theory (QMTST)" for chemical reactions, i.e., a direct (and correct) calculation of the rate constant for a reaction that avoids having to solve explicitly the complete state-to-state reactive scattering problem. The thermal rate constant for a bimolecular reaction, for example, can be expressed compactly as the Boltzmann average of the cumulative reaction probability[1] (CRP),

$$k(T) = [2\pi\hbar Q_r(T)]^{-1} \int_{-\infty}^{\infty} dE\, e^{-E/kT}\, N(E)\,, \tag{1}$$

which itself is the sum of state-to-state reaction probabilities (i.e., square moduli of S-matrix elements) over all states of reactants and products,

$$N(E) = \sum_{n_r,n_p} |S_{n_r,n_p}(E)|^2\,. \tag{2}$$

The goal of a QMTST is to be able to evaluate N(E) without having to resort to Eq. (2) (which involves the S-matrix and thus requires a complete solution of the reactive scattering problem).

There does exist a "direct" expression[2] for N(E),

$$N(E) = \frac{1}{2}(2\pi\hbar)^2\, \mathrm{tr}[F\delta(E-H)F\delta(E-H)]\,, \tag{3}$$

where F is a flux operator and H the total Hamiltonian of the system. Eq. (3) is completely equivalent to Eq. (2) but is free of any explicit reference to asymptotic quantum states of reactants and products. Progress in evaluating N(E) via Eq. (3) has been made[3] by using a discrete variable representation (DVR) for the Hamiltonian and flux operators, and by use of an absorbing potential $-i\Gamma(\mathbf{q})/2$ which is added to the Hamiltonian to enforce outgoing wave boundary conditions for the Green's function (here in a DVR),

$$\mathbf{G}(E) = (E\mathbf{1}-\mathbf{H}+i\Gamma/2)^{-1}\,, \tag{4}$$

from which the microcanonical density operator is obtained in the usual way,

$$\delta(E-\mathbf{H}) = -\frac{1}{\pi}\mathrm{Im}\mathbf{G}(E)\,. \tag{5}$$

Straight-forward algebra then leads to the following result[3,4] for N(E),

$$N(E) = \mathrm{tr}[\mathbf{G}(E)^{*}\bullet\Gamma_r\bullet\mathbf{G}(E)\bullet\Gamma_p]\,, \tag{6}$$

where all bold-face quantities are matrices in the DVR (Γ being diagonal since it is a potential

energy), and Γ_r and Γ_p are the parts of the absorbing potential in the reactant and product valleys, respectively (See Figure). Initial tests for the collinear and three-dimensional versions of the $H+H_2$ reaction indicate that Eq. (6) provides an efficient means for the rigorous, direct calculation of the CRP.

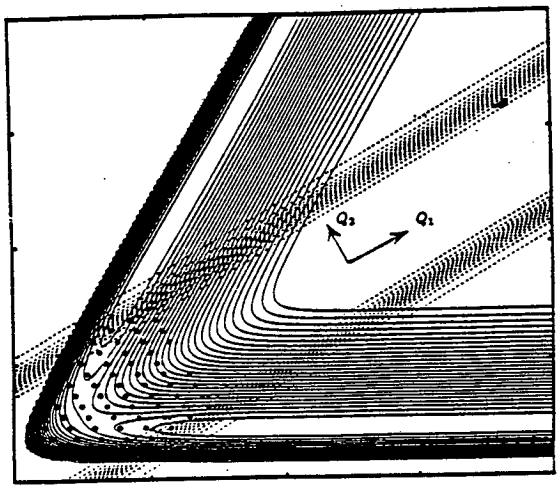

Contours (solid lines) of the potential energy surface for the $H+H_2 \rightarrow H_2+H$ reaction. The points are the DVR grid, and the dashed lines are the contours of the absorbing potential Γ.

Future Plans

There are a number of avenues for formal development as well as practical application that the above work opens up. This same discrete variable/absorbing potential Green's function, Eq. (4), for example, can also be used[4] to obtain state-to-state scattering information, i.e., the S-matrix

$$S_{n_p,n_r} = -\frac{i}{\hbar} \Phi^T_{n_p} \cdot \varepsilon_p \cdot G(E) \cdot \varepsilon_r \cdot \Phi_{n_r} , \qquad (7)$$

where $\varepsilon \equiv \Gamma/2$ and Φ_n is an incoming radial wave (free or distorted) in channel n. Whether Eq. (7) has any advantages over variational methods[5] for computing S-matrix remains to be seen, but one immediate advantage is that it is applicable even when dissociative channels are open, or even if the final state itself is dissociative. All of these issues remain to be explored.

References

1. W. H. Miller, J. Chem. Phys. **62**, 1899 (1975).
2. W. H. Miller, S. D. Schwartz, J. W. Tromp, J. Chem. Phys. **79**, 4889 (1983).
3. T. Seideman and W. H. Miller, Calculation of the Cummulative Reaction Probability via a Discrete Variable Representation with Absorbing Boundary Conditions, J. Chem. Phys. accepted.
4. T. Seideman and W. H. Miller, Quantum Mechanical Reaction Probabilities via a Discrete Variable Representation - Absorbing Boundary Condition Green's Function, J. Chem. Phys., submitted.
5. W. H. Miller, Ann. Rev. Phys. Chem. **41**, 245 (1990).

William H. Miller
1990 - 1992 (to date) DOE Publications

1. J. Z. H. Zhang and W. H. Miller, Photodissociation and Continuum Resonance Raman Cross Sections, and General Franck-Condon Intensities, from S-Matrix Kohn Scattering Calculations, with Application to the Photoelectron Spectrum of $H_2F^- + h\nu \rightarrow H_2 + F$, HF + H + e^-, J. Chem. Phys. **92**, 1811 (1990), LBL-27936.

2. G. A. Voth, D. Chandler, and W. H. Miller, A New Perspective on Quantum Mechanical Transition State Theory, in Quantum Simulations of Condensed Matter Phenomena, eds. J. J. D. Dolland and J. E. Gubernatis, World Scientific Press, 1990, pp. 391-400, LBL-28355.

3. W. H. Miller, Quantum Mechanical Reactive Scattering Theory for Simple Chemical Reactions: Recent Developments in Methodology and Applications, AIP Conference Proceedings 205, The Physics of Electronic and Atomic Collisions, 1990, pp. 442-450, LBL-27937.

4. Y.-T. Chang and W. H. Miller, An Empirical Valence Bond Model for Constructing Global Potential Energy Surfaces for Chemical Reactions of Polyatomic Molecular Systems, J. Phys. Chem. **94**, 5884 (1990), LBL-28774.

5. W. H. Miller, Recent Advances in Quantum Mechanical Reactive Scattering Theory, Including Comparison of Recent Experiments with Rigorous Calculations of State-to-State Cross Section for the H/D + $H_2 \rightarrow H_2$/HD + H Reaction, Ann. Rev. Phys. Chem. **41**, 245 (1990), LBL-28356.

6. R. E. Continetti, J. Z. H. Zhang and W.H. Miller, Resonance Structure in the Energy-Dependence of State-to-State Differential Scattering Cross Section for the D + H_2(v,j) $\rightarrow$ HD(v',j') + H Reaction, J. Chem. Phys. **93**, 5356 (1990), LBL-29162.

7. W. H. Miller, R. Hernandez, N. C. Handy, D. Jayatilaka, and A. Willetts, *Ab Initio* Calculation of Anharmonic Constants for a Transition State, with Application to Semiclassical Transition State Tunneling Probabilities," Chem. Phys. Lett. **172**, 62 (1990), LBL-29161.

8. W. H. Miller, R. Hernandez, C. B. Moore, and W. F. Polik, A Transition State Theory-Based Statistical Distribution of Unimolecular Decay Rates, with Application to Unimolecular Decomposition of Formaldehyde, J. Chem. Phys. **93**, 5657 (1990), LBL-29163.

9. W. H. Miller and J. Z. H. Zhang, How to Observe the Elusive Resonances in H or D + $H_2 \rightarrow$ H_2 or HD + H Reactive Scattering, J. Phys. Chem. **95**, 12 (1991), LBL-29939.

10. W. H. Miller, Some New Approaches to Semiclassical and Quantum Transition State Theory, Ber. Bunsenges Phys. Chem. **95**, 389 (1991), LBL-29938.

11. W. H. Miller and T. Seideman, Transition State Theory , Siegert Eigenstates, and Quantum Mechanical Reaction Rates, J. Chem. Phys. **95**, 1768 (1991), LBL-30639.

12. W. H. Miller, Quantum Mechanical Reactive Scattering for Chemical Reactions, NATO ASI Bad Windsheim, LBL-31627.

13. Y. T. Chang, C. Minichino, and W. H. Miller, Classical Trajectory Studies of the Molecular Dissociation Dynamics of Formaldehyde: $H_2CO \rightarrow H_2$ + CO, J. Chem. Phys., accepted, LBL-31623.

William H. Miller
1990-1992 Publications

14. W. H. Miller, Reaction Dynamics in Polyatomic Molecular Systems: Some Approaches for Constructing Potential Energy Surfaces and Incorporating Quantum Effects in Classical Trajectory Simulations, NATO Advanced Research Workshop on Computation Methods in Bio-Technology, LBL-31626.

15. W. H. Miller, S-Matrix Version of the Kohn Variational Principle for Quantum Scattering Theory of Chemical Reactions, JAI Press, LBL-31625.

16. T. Seideman and W. H. Miller, Calculation of the Cumulative Reaction Probability via a Discrete Variable Representation with Absorbing Boundary Conditions, J. Chem. Phys., accepted, LBL-31624.

Photochemical Reaction Dynamics

C. Bradley Moore

Materials and Chemical Sciences Division of the Lawrence Berkeley Laboratory and Department of Chemistry, University of California, Berkeley, California 94720

The purpose of the program is to develop a fundamental understanding of unimolecular and bimolecular reaction dynamics with applications in combustion and energy systems. Recently completed and on-going work is abstracted below.

I. Experimental Observation of Transition State Vibrational Structure in the Dissociation of Ketene

Edward R. Lovejoy, Sang Kyu Kim, and C. Bradley Moore

Rate constants for the dissociation of highly vibrationally excited ketene (CH_2CO) have been measured at the threshold for the production of $CH_2(^3B_1)$ and $CO(^1\Sigma^+)$. The rate constant increases in a step-wise manner with increasing energy, consistent with the longstanding premise that the rate of a unimolecular reaction is controlled by flux through quantized transition state thresholds, Fig. 1. The data provide a vibrational spectrum of the transition state in which torsional and C-C-O bending vibrations are identified.

II. Kinetics of intramolecular carbon atom exchange in ketene

Edward R. Lovejoy, Sang Kyu Kim, Ramón A. Alvarez and C. Bradley Moore

Intramolecular carbon atom exchange in highly vibrationally excited ketene was studied by monitoring the carbon monoxide fragments (^{12}CO and ^{13}CO) from the photodissociation of $^{12}CH_2{}^{13}CO$ and $^{13}CH_2{}^{12}CO$. Two experimental techniques were employed. In one set of experiments the IR transient absorptions of ^{12}CO and ^{13}CO were measured following pulsed excimer excitation of ketene ^{13}C isotopomers, giving carbon atom exchange yields at 351 and 308 nm in a low pressure gas cell. In the other set of experiments, jet-cooled ketene ^{13}C isotopomers were excited with tunable near-UV radiation, and the CO products were detected by monitoring their VUV laser-induced fluorescence. Carbon atom exchange yields were measured for energies extending from below the triplet decomposition threshold ($CH_2CO \rightarrow CH_2(X^3B_1) + CO(X^1\Sigma^+)$) to about 4000 cm^{-1} above the singlet threshold ($CH_2CO \rightarrow CH_2(a^1A_1) + CO(X^1\Sigma^+)$). The exchange yields range from 4 to 19 %, and the energy dependence of the yield exhibits pronounced structure, with maxima at the triplet and singlet decomposition thresholds. Kinetic measurements of the appearance of the CO products were also performed. The time constant for the appearance of the exchanged CO (e.g. ^{13}CO from $^{13}CH_2{}^{12}CO$) is significantly longer than that for the direct CO fragment (e.g. ^{12}CO from $^{13}CH_2{}^{12}CO$). All the experimental observations are consistent with a simple reaction mechanism involving ketene isomerization, $^{13}CH_2{}^{12}CO \rightleftarrows {}^{12}CH_2{}^{13}CO$, and dissociation, $^{13}CH_2{}^{12}CO \rightarrow {}^{13}CH_2 + {}^{12}CO$ and $^{12}CH_2{}^{13}CO \rightarrow {}^{12}CH_2 + {}^{13}CO$. The isomerization rate constant was determined by analyzing the CO kinetics and the carbon atom exchange yields in terms of the simple isomerization mechanism. A fit of the energy dependence of the isomerization rate constant to the results of tunneling-corrected RRKM calculations gave the threshold (28360 ± 60 cm^{-1}) for the isomerization process.

III. Gas-Phase Rates of Alkane C-H Oxidative Addition to a Transient CpRh(CO) Complex

E.P. Wasserman, C.B. Moore and R.G. Bergman

The gas-phase irradiation of $CpRh(CO)_2$($Cp = \eta^5$-C_5H_5) was examined in order to study the rates of reaction of the 16-electron intermediates presumed to be involved in the C-H oxidative addition of alkanes. "Naked" (unsolvated) CpRh(CO) was detected, and direct measurements of the rates of reaction of this very short-lived complex with alkane C-H bonds were made. Activation of C-H bonds occurs on almost every collision for alkanes of moderate size, and intermediates in which the alkanes are bound to the metal centers, without their C-H bonds being fully broken, are implicated as intermediates in the overall reaction.

IV. Work in Progress

Energy transfer and chemical reaction rates are being studied for triplet CH_2 radicals. A diode laser infrared flash kinetic spectrometer is being used to study the reaction with O_2 in order to identify product states and intermediates. Reaction rates for radical-radical reactions are being measured. Spectroscopy of radical-radical and radical-molecule reaction complexes is planned.

Unimolecular reaction dynamics are being studied by photofragment spectroscopy. The yield and rates for carbon atom exchange are studied by photolysis of $^{13}CH_2CO$ and CH_2 ^{13}CO in a molecular beam. Rates are measured as a function of photolysis energy with cm^{-1} resolution. UV-IR two-step excitation experiments are proposed for the future to resolve rotational quantum states in transition state spectroscopy and to record vibrational spectra of molecules with sufficient energy to dissociate.

Infrared and ultraviolet spectra of intermediates in organometallic photochemistry in gas and liquid phase are being studied jointly with R.G. Bergman. Emphasis is on CH activation chemistry. Studies of CH activation systems in liquid Kr and Xe are proceeding well.

IV. Publications

1. I-C. Chen and C.B. Moore, "Photofragmentation of Ketene to $CH_2(\tilde{X}^3B_1)$ + CO : I. Barrier Height And Dissociation Rate Constant," J. Chem. Phys. **94**, 263 (1990).

2. I-C. Chen and C.B. Moore, "Photofragmentation of Ketene to $CH_2(\tilde{X}^3B_1)$ + CO: II. Rotational State Distributions of Product CO," J. Chem. Phys. **94**, 269 (1990).

3. T.J. Butenhoff, R.S. Chuck, H.-H. Limbach and C.B. Moore, "The Near-Infrared Photochemistry of Porphine Imbedded in a n-Hexane Matrix." Spectrochim. Acta A, **46A**, 519 (1990).

4. T.J. Butenhoff, R.S. Chuck, H.-H. Limbach and C.B. Moore, "Vibrational Photochemistry of Porphine Imbedded in a n-Hexane-d_{14} Shpol'skii Matrix," J. Phys. Chem. K.S. Pitzer 75th Birthday issue **94**, 7847 (1990).

5. C.B. Moore, Q.-K. Zheng, Y.S. Choi, W.H. Green, S.K. Kim, A.J. Mahoney, W.H. Miller, C.D. Pibel, W.F. Polik and P. Teal, "The High Resolution Spectroscopy of Dissociating Molecules," Phil. Trans. R. Soc. Lond. A **332**, 109 (1990).

6. E.R. Lovejoy, R.A. Alvarez and C.B. Moore, "The Yield of CO in the Reaction: $CH_2(\tilde{a}^1A_1) + CH_2CO$," Chem. Phys. Lett. **174**, 151 (1990).

7. S.K. Kim, Y.S. Choi, C.D. Pibel, Q.-K. Zheng and C.B. Moore, "Determination of the Singlet/Triplet Branching Ratio in the Photodissociation of Ketene," J. Chem. Phys. **94**, 1954 (1991).

8. E.R. Lovejoy, S.K. Kim, R.A. Alvarez and C. B. Moore, "Kinetics of Intramolecular Carbon Atom Exchange in Ketene," J. Chem. Phys. **95**, 4081 (1991).

9. E.P. Wasserman, C.B. Moore and R.G. Bergman, "Gas-Phase Rates of Alkane C-H Oxidative Addition to a Transient CpRh(CO) Complex," Science **255**, 315 (1992).

10. W.H. Green, C.B. Moore and W.F. Polik, "Transition States and Rate Constants for Unimolecular Reactions," Ann. Rev. Phy. Chem. (in press) (1992).

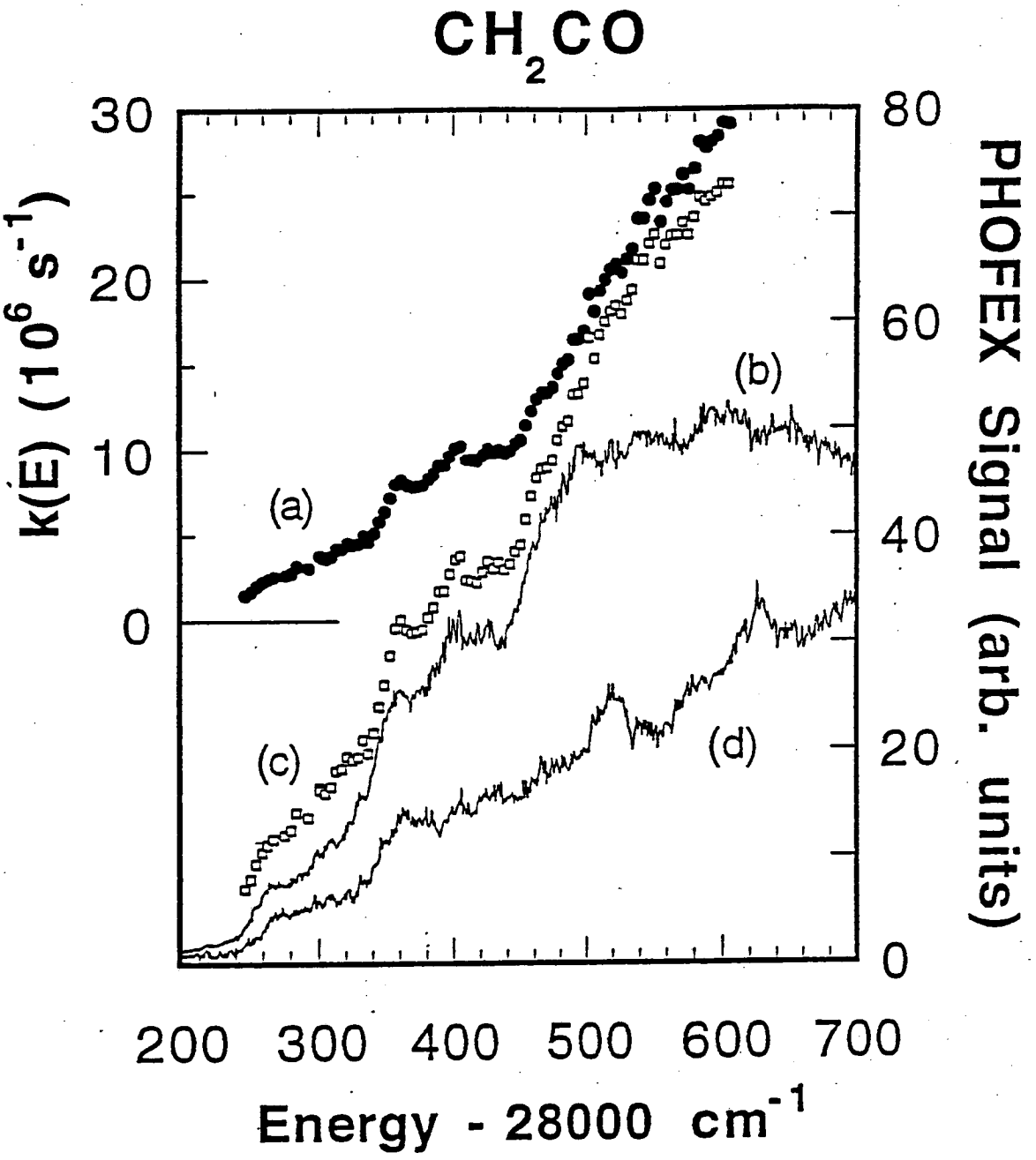

Figure 1. Triplet CH_2CO rate constant and PHOFEX data. (a) Experimental rate constants for the unimolecular decay of ketene. (b) CO($v=0,J_p=12$) PHOFEX signal. (c) PHOFEX spectrum calculated with the experimental rate constant data. (d) CO($v=0,J_p=2$) PHOFEX signal. The actual ratio of the yields of CO($v=0,J_p=12$) to C0($v=0,J_p=2$) is about 20:1 at 28500 cm^{-1} for CH_2CO.

Gas-Phase Chemical Dynamics

James T. Muckerman, Trevor J. Sears, and Gregory E. Hall
Chemistry Department, Brookhaven National Laboratory, Upton, NY 11973

Program Scope

Research in this program is directed toward the spectroscopy of small free radicals and the state-to-state dynamics of gas phase collision, energy transfer, and photodissociation phenomena. Two projects from this group are highlighted in this year's abstracts by Jack Preses and Ralph Weston; other work is summarized here.

Infrared spectroscopy of HOCO

A new infrared diode laser spectrometer has been used to record extensive regions of the C=O stretching band of the hydroxyformyl, HOCO, radical. The high-resolution spectrum provides both accurate data to characterize this region of the OH + CO → HOCO → H + CO_2 potential energy surface, and a convenient spectroscopic method for monitoring the HOCO radical in reaction systems. Last year, we reported the observation of vibration-rotation transitions in HOCO by kinetic spectroscopy using absorption of a tunable diode laser. The radical was formed by photolysis of acetic or acrylic acids at 193 nm. The spectrum has now been assigned for both HOCO and DOCO. Analysis of the spectrum enabled part of the rotational spectrum of the radical, previously detected at the Center for Astrophysics, Harvard University and attributed to HOCO on chemical grounds, to be assigned. Subsequently many more rotational transitions in both HOCO and DOCO have been detected and assigned. The rotational constants for the two isotopomers HOCO and DOCO demonstrate conclusively that we have detected the *trans* isomer, in agreement with all recent quantum mechanical calculations. Perturbations are observed in the v_2=1 excited state that may arise *via* interactions with levels of the *cis* isomer or through anharmonic mixing with combinations of some lower energy vibrations of the molecule. Further analysis will be required to explain our observations, which may yield the energy of the *cis* isomer.

Spectroscopy of NCO and NCNH

Extensive laser induced fluorescence (LIF) measurements of NCO formed in the reaction CN + O_2 → NCO + O in a supersonic free jet expansion have been made. The rotational temperature achieved in our source was typically 10–15 K, and absorption from vibrationally excited levels was found to be very weak. In the A ↔ X system of the radical, the (v_1, v_2, v_3) = (200) ↔ (000) and (120) ↔ (000) bands have been rotationally analyzed for the first time, and wavelength resolved fluorescence measurements have been made to characterize many ground state levels for the first time. Stimulated emission pumping (SEP) experiments were carried out on vibronic states associated with levels involving excitation in all three vibrational modes with energies of up to 6000 cm^{-1} above the vibrationless level.

The characteristics of the vibronic states for which SEP measurements were made can be conveniently divided into two types: those containing excitation in only the v_3 mode, and all others.

The rotational energy levels in the former case can, to a very good approximation, be considered in isolation even at the highest energies accessed in our work. In contrast, vibronic levels associated with excitation in the ν_1 and ν_2 vibrations are extensively mixed by a combination of Renner-Teller, spin-orbit and Fermi-resonance interactions. Modeling of their rotational structure to the precision of our measurements requires a fairly complicated effective Hamiltonian. The stimulated emission pumping spectra of NCO in its (ν_1,ν_2,ν_3) = (040), (120), and (200) sets of interacting Π symmetry levels represent the most complete data set on such levels for any molecule exhibiting a Renner-Teller effect. An effective Hamiltonian based on perturbation theory operating only within the manifold of this set of levels has been used in order to fit the experimental data and to extract effective parameters describing the various interactions present in the molecule.

The isoelectronic species, HNCN, has been the subject of rather little spectroscopic study since its detection nearly 30 years ago. It is of interest because the presence of the off-axis hydrogen atom lifts the electronic degeneracy of the state of NCO and leads to a ground $^2A''$ state with a low lying $^2A'$ state which was not detected in the original work. The two states can be thought of as the result of a very large Renner-Teller effect in the linear molecule. We have generated this radical in a free jet expansion by 193 nm photolysis of a mixture of cyanogen and ammonia in a nitrogen carrier gas. The radical has been identified by its LIF spectrum, and we have also made some dispersed fluorescence measurements. We see no evidence for activity in the out-of-plane torsional mode that can couple the ground and low lying electronic states; however, much additional work remains to be done.

Doppler spectroscopy of velocity-aligned reactions

We have developed a new approach to the detailed study of reactive and inelastic molecular collisions that relies on the precise measurement of Doppler line shapes of single rotational lines in the laser-induced-fluorescence (LIF) spectra of nascent reaction products. The technique has been applied to the reaction $H + O_2 \rightarrow OH + O$, a chain-branching reaction of crucial importance to most combustion systems. Hydrogen atoms are generated with an aligned, anisotropic velocity distribution by photodissociation of HX precursors (X = SH, Br, Cl, I) with a polarized ultraviolet laser pulse. After a short delay to allow reactive collisions of fast H atoms with thermal O_2, the nascent OH radicals are detected by high resolution LIF. The Doppler line shapes observed depend on the laboratory velocity distribution, which in turn carry a detailed memory of the angular correlations between the reactants and products for each spectroscopically selected final state. These techniques are a conceptually simple extension of conventional pump-probe laser experiments, exploiting the time and frequency resolution of polarized lasers, and revealing qualitatively significant features of the reactive scattering.

For the $H + O_2 \rightarrow OH + O$ reaction at 2.3 eV collision energy, the most populated nascent OH rotational states at N=17 have Doppler line shapes consistent with the sharply peaked forward and backward angular distributions predicted by Schinke (Göttingen, Germany). Remarkably, however, the line shapes are qualitatively different for the two lambda doublet states of the same rotational levels. The less-populated $\Pi(A'')$ component (probed by Q branch transitions) is accurately fit by Schinke's quasi-classical trajectory calculations, although the more populated $\Pi(A')$ component (probed by R and P branch transitions) cannot be described by the same differential cross section. Explaining these results seems to require the participation of more than the single potential energy surface commonly assumed for this reaction. Recent reinvestigation of the thermal kinetics of this

reaction (Hessler, Argonne) has also suggested that the low-lying $^2A'$ excited state of HO_2 may need to be considered for an accurate understanding of this crucial combustion reaction.

A numerical approach to the direct inversion of observed Doppler line shapes to give estimates of the state-resolved differential cross-sections is proving successful. It provides a systematic means of identifying how much information is contained in the line shapes, and gives the angular distribution in terms of a small number of orthogonal terms, similar to the Legendre polynomials. The first term is nearly isotropic; a bias in the reaction toward forward or backward scattering shows up in the second term; preferential sideways or front and back scattering shows up in the third term, and so on. The application to the $H + O_2 \rightarrow OH + O$ Doppler line shape data is leading to a more quantitative understanding of the method.

The reaction of $H + H_2O \rightarrow OH + H_2$ is becoming one of the best-studied reactions involving four atoms. Crim (Wisconsin) has demonstrated bond-selective reactions following selective vibrational excitation of HOD, and Clary (Cambridge) has been extending serious quantum reactive scattering calculations to this relatively simple four atom system. The state-resolved differential cross section methods developed here for the $H + O_2 \rightarrow OH + O$ reaction can be applied to this reaction as well. This kind of detailed measurement can provide stringent tests of the methods being developed to treat these more complex systems. Preliminary results here contradict the previous work of Kleinermanns and Wolfrum (Heidelburg) on the reaction of fast, photochemically generated H atoms with H_2O: the 193 nm excimer laser light used to generate H atoms also generates OH from the dissociation of water. Despite the small absorption cross section of water at 193 nm, the direct photoproduction of OH far exceeds the prompt yield of OH from the reaction of H with H_2O. The reaction needs to be studied with a longer photolysis wavelength, to avoid water dissociation.

Theoretical aspects of molecular dynamics

The experimental efforts in this program benefit from augmentation by theoretical investigations of molecular dynamics. The primary focus of this work is the development and application of time-dependent methods for treating inelastic and molecular encounters in systems, especially those with more than a few degrees of freedom. The general thrust involves partitioning the system's degrees of freedom into classical and quantal subspaces in a reasonable and consistent manner. For sufficiently small systems, all degrees of freedom may be treated quantally.

The quantal aspects of this work involve propagation of wavepackets, either as direct solutions of the Schrödinger equation or in the context of a combined classical/quantal treatment. An original method has been developed for propagating wavepackets which is not subject to some of the limitations of the FFT (Fast Fourier Transform) technique. The method is based on the construction of analytic discrete variable representations (DVRs) using projection operators expressed in terms of appropriate basis sets, and a corresponding set of Gaussian quadrature points and weights. This method has been applied to one- and multi-dimensional quantal problems having either time-dependent or time-independent Hamiltonians. An example of a time-independent application is our recent study of the vibrational levels of the electronically excited van der Waals radical complex Ar–OH($A\ ^2\Sigma^+$). A time-dependent example, currently being studied is the time evolution of HF vibrational state populations in the field of one or two lasers of various frequencies, pulse duration and electric field strengths.

Predesorption of vibrationally excited CO from NaCl(100). The predesorption of vibrationally excited CO adsorbed on a NaCl(100) surface has been examined in a fully quantal treatment using the analytic discrete variable wavepacket method mentioned above. A three-dimensional model for the CO–NaCl system was developed which treats the CO stretching, bending (frustrated rotational, or librational), and translational coordinates as dynamical variables. Our previous combined quantal/classical studies of collinear models involving surface motion, which allowed energy transfer from the excited adsorbate to the surface in addition to desorption, indicated that the low-frequency surface motion in NaCl is essentially uncoupled from the dynamics of the excited adsorbate. Consequently, in this study we have employed the potential energy surface of Moiseyev *et al.*, which neglects both surface motion and surface corrugation. Initial conditions for the wavepacket calculations, representing a variety of predesorptive resonances in which energy is distributed differently between the stretching and bending modes of the adsorbate–surface complex, were determined by time-independent quantum mechanical calculations using an analytic DVR basis in the bending and translational coordinates, with a single "eigenfunction" in the stretching coordinate.

Our wavepacket calculations indicate that the excited CO stretching mode alone does not induce any detectable desorption. Exciting the bending mode in conjunction with the stretching mode appears to mediate the coupling between the stretching and translational degrees of freedom, but the desorption is still quite slow, occuring on a microsecond time scale. Exciting the bending mode alone to a (resonance) state comparable in energy to the excited stretching state produces more rapid desorption. The computed lifetime for this type of predesorption (*i.e.*, bending, or rotational) is in the nanosecond range. The results of parallel classical trajectory calculations are qualitatively consistent with many aspects of the quantum calculation, but for the case of pure rotational predesorption the classical lifetime is orders of magnitude shorter than the quantal value.

Recent Publications

Electronic Spectroscopy of the ArOH and ArOD Complexes
W. M. Fawzy and M. C. Heaven
J. Chem. Phys. 92, 909-916 (1990)

Photodissociation of RNCS and RSCN (R = H, CH_3, C_2H_5): Evidence for an Excited State Isomerization and Energy Deposition in the NCS Product
F. J. Northrup and T. J. Sears
J. Chem. Phys. 93, 2337-2345 (1990)

Photodissociation of RNCS and RSCN (R = H, CH_3, C_2H_5) at 248 and 193 nm: CN Product Energy Distributions
F. J. Northrup and T. J. Sears
J. Chem. Phys. 93, 2346-2356 (1990)

Infrared Diode Laser Spectroscopy of the ν_3 Fundamental of the CD_3 Radical
W. M. Fawzy, T. Sears and P. B. Davies
J. Chem. Phys. 92, 7021-7026 (1990)

Desorption of Vibrationally Excited Adsorbates in Competition with Relaxation: A Classical Picture
Y. Guan, J. T. Muckerman and T. Uzer
J. Chem. Phys. 93, 4383-4399 (1990)

Stimulated Emission Pumping Spectroscopy Study of Jet-Cooled C_3: Pure Bending Levels and Bend-Symmetric Stretch Combination Levels of $X\ ^1\Sigma_g^+$
F. J. Northrup and T. J. Sears
J. Opt. Soc. Amer. B7, 1924-1934 (1990)

P-Type Doubling in the Infrared Spectrum of NO-HF
W. M. Fawzy, G. T. Frazer, J. T. Hougen and A. P. Pine
J. Chem. Phys. 93, 2992-3004 (1990)

Desorption of Vibrationally Excited Adsorbates in Competition with Relaxation: A Quantal Picture
Y. Guan, J. T. Muckerman and T. Uzer
J. Chem. Phys. 93, 4400-4412 (1990)

Renner-Teller, Spin-Orbit and Fermi-Resonance Interactions in $X\ ^2\Pi$ NCS Investigated by LIF Spectroscopy
F. J. Northrup and T. J. Sears
Molec. Phys. 71, 45-64 (1990)

Some Useful Discrete Variable Representations for Problems in Time-Dependent and Time-Independent Quantum Mechanics
J. T. Muckerman
Chem. Phys. Lett. 173, 200-205 (1990)

Solution of Time-Dependent Schrödinger Equation Employing a Basis of Explicit Discrete Coordinate of Eigenfunctions: Spherical and Azimuthal Symmetry, Adiabaticity, and Multiphoton Excitation of a Rotating Morse Oscillator
F. J. Lin and J. T. Muckerman
Comput. Phys. Commun. 63, 538-568 (1991)

On the Use of Grid Methods for the Solution of Reactive Scattering Problems in Hyperspherical Coordinates
N. Markovic, G. D. Billing and J. T. Muckerman
Chem. Phys. Lett. 172, 509-514 (1990)

A Semi-Rigid Bender Analysis of an Extensive Set of Rotation-Vibration Levels in $X\ ^1\Sigma_g^+ C_3$
F. J. Northrup, T. J. Sears and E. A. Rohlfing
J. Molec. Spectrosc. 145, 74-88 (1991)

Photodissociation of Acetone at 193 nm: Rotational- and Vibrational-State Distributions of Methyl Fragments by Diode Laser Absorption/Gain Spectroscopy
G. E. Hall, D. Vanden Bout and T. J. Sears
J. Chem. Phys. 94, 4182-4188 (1991)

The FIR LMR Spectrum of FO_2: Some Classic Examples of Level Anticrossing Resonances
U. Bley, P. B. Davies, M. Grantz, T. J. Sears and F. Temps
Chem. Phys. 152, 281-292 (1991)

Calculation of the Vibrational Levels of the Electronically Excited Ar-OH($A\ ^2\Sigma^+$) Using a Proposed Potential Energy Surface and Analytic Discrete Variable Representations
Y. Guan and J. T. Muckerman
J. Phys. Chem. **95**, 8293-8299 (1991)

Avoided Crossings in the FIR LMR Spectrum of HCO
J. M. Brown, H. E. Radford and T. J. Sears
J. Molec. Spectrosc. **148**, 20-37 (1991)

Far Infrared Laser Frequencies of CH_3OD and N_2H_4
H. E. Radford, K. M. Evenson, F. Matushima, L. R. Zink, G. P. Galvao and T. J. Sears
J. Infrared & Millimeter Waves **12**, 1161-1166 (1991)

The $S(^1D)$ + N_2 Quenching Process: Determination of the Branching Ratios of Triplet Fine Structure Products
G. C. McBane, I. Burak, G. E. Hall and P. L. Houston
J. Phys. Chem. (in press)

Measurement of ($00v_3$) Levels in $X\ ^2\Pi$ NCO by Stimulated Emission Pumping Spectroscopy
F. J. Northrup, M. Wu and T. J. Sears
J. Chem. Phys. (in press)

Stimulated Emission Pumping: Applications to Highly Vibrationally Excited Transient Molecules
F. J. Northrup and T. J. Sears
In *Annual Review of Physical Chemistry*, Strauss, H. L., ed.; Annual Reviews, Inc., Palo Alto, CA (submitted)

High Resolution Fourier Transfer Spectroscopy Using Infrared Synchrotron Radiation. I. Instrumentation
K. D. Moller, D. Scardino, T. Sears, D. Carlson, C. J. Hirschmugl, G. P. Williams, E. Chang and H. T. Liu
Int. J. Infrared & Millimeter Waves (submitted)

Time-Resolved FTIR Studies of the Photodissociation of Pyruvic Acid at 193 nm
G. E. Hall, J. T. Muckerman, J. M. Preses, R. E. Weston Jr. and G. W. Flynn
Chem. Phys. Lett. (submitted)

FAST BEAM PHOTODISSOCIATION OF FREE RADICALS

Daniel M. Neumark
Chemical Sciences Division
Lawrence Berkeley Laboratory
University of California
Berkeley, CA 94720

While many photodissociation studies of stable molecules have been performed in recent years, it has proved difficult to extend these experiments to studies of reactive free radicals. This is largely due to the difficulty of implementing a clean, well-characterized source of free radicals. We have developed a novel approach to this problem by setting up an experiment in which free radicals are generated by photodetachment of a mass-selected anion beam,[1] rather than the more conventional strategies in which radicals are formed by photolysis of a stable precursor or by a chemical reaction. Since nearly all radicals have a positive electron affinity, this approach should be quite general.

In the experiment, an 8 keV beam of cold, mass-selected anions is photodetached with a pulsed laser. The resulting neutral radicals are photodissociated with a second pulsed laser, and the photofragments are detected with high (~50%) efficiency using a microchannel plate detector which lies about 100 cm downstream from the photodissociation laser. The center of the detector is blocked so that the undissociated radicals do not impinge on it, but the photofragments move off the beam axis and strike the detector. The experiment can be operated in several modes. We can measure the total photofragment signal as a function of dissociation laser wavelength, thereby mapping out the dissociative electronic transitions of the radical. We can measure the time-of-flight distribution of the photofragments, thereby obtaining an approximated kinetic energy distribution at a fixed photodissociation wavelength. Finally, using a two-particle position and time sensing detector, we can determine detailed photofragment energy and angular distributions.

Thus far, we have performed dissociation cross section and time-of-flight measurements on the N_3, NCO, and CH_2NO_2 radicals. We found that the $A(^2\Sigma^+) \leftarrow X\ (^2\Pi)$ transition in N_3 near 270 nm results in predissociation to the spin-allowed $N(^2D) + N_2$ channel. In contrast, in NCO, the $B(^2\Pi) \leftarrow X(^2\Sigma)$ transition leads to predissociation to the spin-forbidden $N(^4S)$ + CO channel for dissociation wavelengths above 260 nm; at lower wavelengths, the spin-allowed $N(^2D)$ + CO channel opens and is the dominant channel. From these results, we obtain $\Delta H_f(NCO) = 30.5$ kcal/mol, about 5 kcal/mol lower than the literature value. Our experiments on CH_2NO_2 photodissociation at several wavelengths indicate that the primary products are $CH_2 + NO_2$, and that the NO_2 is most likely electronically excited.

---

[1] R. E. Continetti, D. R. Cyr, R. B. Metz, and D. M. Neumark, Chem. Phys. Lett. **182**, 406 (1991).

We have recently begun experiments with our two-particle position and time-sensing detector in which O_2 is photodissociated via the Schumann-Runge band. We form vibrationally excited O_2 by photodetachment of O_2^- and excite rotationally predissociating transitions of the $v'=7 \leftarrow v''=4$ band near 210 nm. This work has shown that the current energy resolution of the detector is 50 meV. Preliminary studies of N_3 dissociation with this detector yield resolved peaks in the photofragment kinetic energy distribution due to the N_2 vibrational state distributions associated with the various N atom electronic states. We find that a small amount of $N(^4S) + N_2$ is produced when the (000) vibrational level of the N_3 $A(^2\Sigma^+)$ state dissociates, but this spin-forbidden channel is quenched when the (010) level dissociates. A new anode design for this detector which should yield considerably improved energy resolution is now being tested.

Daniel M. Neumark
1990 - 1992 (to date) DOE Publications

1. R. E. Continetti, D. R. Cyr, R. B. Metz, and D. M. Neumark, "Fast Beam Studies of N_3 Photodissociation," Chem. Phys. Lett. 182, 406 (1991); LBL-31879.

2. R. B. Metz and D. M. Neumark, "Adiabatic Three-Dimensional Simulations of the IHI-, BrHI- and BrHBr- Photoelectron Spectra," J. Chem. Phys. (accepted); LBL-31880.

3. D. R. Cyr, R. E. Continetti, R. B. Metz, D. L. Osborn, and D. M. Neumark, "Fast Beam Studies of NCO Free Radical Photodissociation," J. Chem. Phys. (submitted); LBL-32365.

Vacuum Ultraviolet Photoionization and Photodissociation of Molecules, Clusters, and Radicals.

C. Y. Ng
Ames Laboratory, USDOE and Department of Chemistry,
Iowa State University, Ames, Iowa 50011

The goals of this program are: (1) to obtain accurate thermochemical data, such as ionization energies (IE) and bond dissociation energies, for neutral polyatomic molecules, radicals, and their ions; (2) to study the photoionization (PI) and photodissociation (PD) dynamics of molecules, radicals, and clusters induced by the absorption of ultraviolet (UV) and vacuum ultraviolet (VUV) photons; (3) to investigate the detailed reaction dynamics and mechanisms of fast radical-molecule and radical-radical reactions.

Our current interest in PI and photoelectron (PE) spectroscopic studies has been centered on radicals. Many radicals can be produced readily in electrical discharge, PD, and thermal pyrolysis sources, coexisting with their precursors and secondary reaction products. We have been the first to demonstrate that, using a pulsed photoelectron-photoion coincidence (PEPICO) scheme, the PE spectrum of a radical in a mixture of other species can be measured with high sensitivity. Using a discharge source and the pulsed PEPICO method, we have obtained PEPICO spectra for SO, S_2, S_2O, and S_2O_2.[1] When radicals, especially polyatomic radicals, are prepared by conventional methods under effusion beam conditions, their internal excitations are often difficult to assess, making it difficult to estimate the hot band effects on the measured IEs. Progress in the PI study of polyatomic radicals may require the use of a supersonically cooled radical source. Most recently, we have developed a versatile polyatomic radical source by combining the excimer laser PD and supersonic beam methods. Preliminary experiments using this source indicate that vibrational excitation up to 40 kcal/mol can be relaxed efficiently in the supersonic expansion. Ionization energies for CH_3S,[2] CH_2Br, CS,[3] and CH_3SS have been measured. In the coming years, we plan to perform PI and PE spectroscopic measurements of a series of hydrocarbon and organosulfur radicals. By incorporating a high repetition rate (500 Hz) excimer laser and pulsed valve, we hope to produce a pseudocontinuous cold radical beam for PEPICO measurements.

In principle, the dissociation energy of the ABC-D bond can be calculated by combining the measured appearance energy (AE) for the dissociative PI process of a stable molecule ABCD ($ABCD + h\nu \rightarrow ABC^+ + D + e^-$) and the IE of the radical ABC measured in PI. However, as a result of the kinetic shift effect and the finite instrumental sensitivity, experimental AEs are the upper bound of the true threshold. The kinetic shift and vibrational hot band effects are counteracting effects. A quantitative assessment of the extent of influence by each of these effects is a complicated task. Nevertheless, the value for the ABC-D bond dissociation energy can be measured directly in a VUV and/or UV laser PD experiment by examining the kinetic energy release of the process, $ABCD + h\nu \rightarrow ABC + D$. A rotating beam source laser photofragmentation TOF mass

spectrometric apparatus has been built and used to measure the energetics of product channels involved in the 193nm photodissociation of a series of organosulfur molecules.[4-9]

The combination of VUV PI and PD experiments completes the thermochemical cycle and allows the proper assessment of the accuracy of the experimental onsets and the values for the bond dissociation energies.

Detailed understanding of molecular PD processes requires information about the rovibronic distributions of the photofragments. In conformity with our recent focus on the energetics and dynamics of VUV photoionzation processes of radicals, effort has been made to develop an experimental scheme to measure absolute state-to-state PD cross sections of radicals. Absolute cross sections for $S(^3P,^1D)$ resulting from the 193nm photodissociation of SCH_3 and HS have been measured.[10]

References:

(1) K. Norwood and C. Y. Ng, *Chem. Phys. Lett.* **156**, 145 (1989).
(2) S. Nourbakhsh, K. Norwood, G.-Z. He,[a] and C. Y. Ng, *J. Am. Chem. Soc.* **113**, 6311 (1991).
(3) K. Norwood, S Nourbakhsh, G.-Z. He, and C. Y. Ng, *Chem. Phys. Lett.* **184**, 147 (1991).
(4) W.-B. Tzeng, H.-M. Yin, W.-Y. Leung, J.-Y. Luo, S. Nourbakhsh, G. D. Flesch and C. Y. Ng, *J. Chem. Phys.* **88**, 1658 (1988).
(5) S. Nourbakhsh, C.-L. Liao, and C. Y. Ng, *J. Chem. Phys.* **92**, 6587 (1990).
(6) S. Nourbakhsh, K. Norwood, H.-M. Yin, C.-L. Liao, and C. Y. Ng, *J. Chem. Phys.* **95**, 5014 (1991).
(7) S. Nourbakhsh, K. Norwood, H.-M. Yin, C.-L. Liao, and C.Y. Ng, *J. Chem. Phys.* **95**, 946 (1991).
(8) S. Nourbakhsh, H.-M. Yin, C.-L. Liao, and C. Y. Ng, *Chem. Phys. Lett.* **183**, 348-352 (1991).
(9) S. Nourbakhsh, H.-M. Yin, C.-L. Liao, and C. Y. Ng, *Chem. Phys. Lett.* in press.
(10) C.-W. Hsu, C. L. Liao, P. Tjossom, and C. Y. Ng, to be published.

Publications During the Past Two years in this field:

1. K. Norwood and C. Y. Ng, "Observation of a SO_2^+ Threshold Photoelectron Band in the Energy Range 14.4-15.5 eV", *J. Chem. Phys.* 92, 1513 (1990).
2. K. Norwood and C. Y. Ng, "Photoionization of Hydrogen Atom Near the Ionization Threshold", *J. Chem. Phys.* 93, 1480-81 (1990).
3. S. Nourbakhsh, C.-L. Liao, and C. Y. Ng, "A 193nm Laser Photofragmentation Time-of-Flight Mass Spectrometric Study of CH_3SSCH_3, $SSCH_3$, and SCH_3 ", *J. Chem. Phys.* 92, 6587-93 (1990).
4. K. Norwood, A. Ali, G. D. Flesch, and C. Y. Ng, "A Photoelectron-Photoion Coincidence Study of $Fe(CO)_5$ ", *J. Am. Chem. Soc.* 112, 7502-08 (1990).

5. K. Norwood and C. Y. Ng, "A Study of the Unimolecular Dissociation of SO_2^+(C,D,E) Using the Photoelectron-Photoion Coincidence Method", *J. Chem. Phys.* 93, 6440-47 (1990).
6. C. Y. Ng, Review Article: "Molecular Beam Photoionization and Photoelctron-Photoion Coincidence Studies of High Temperature Molecules, Clusters, and Radicals", in *VUV photoionization and Photodissociation of Molecules and Clusters*, edited by C. Y. Ng (World Scientific, Singapore, 1991).
7. S. Nourbakhsh, K. Norwood, H.-M. Yin, C.-L. Liao, and C. Y. Ng, "Vacuum Ultraviolet Photodissociation and Photoionization Studies of CH_3SCH_3 and SCH_3", *J. Chem. Phys.* **95**, 5014-5023 (1991).
8. S. Nourbakhsh, K. Norwood, H.-M. Yin, C.-L. Liao, and C.Y. Ng, "Vacuum Ultraviolet Photodissociation and Photoionization Studies of CH_3SH and SH", *J. Chem. Phys.* **95**, 946 (1991).
9. S. Nourbakhsh, H.-M. Yin, C.-L. Liao, and C. Y. Ng, "A 193 nm Laser Photofragmentation Time-of-Flight Mass Spectrometric Study of CH_3CH_2SH", *Chem. Phys. Lett.* **183**, 348-352 (1991).
10. S. Nourbakhsh, K. Norwood, G.-Z. He,[a] and C. Y. Ng, "Photoionization Study of Supersonically Cooled Polyatomic Radicals: Heat of Formation of CH_3S^+", *J. Am. Chem. Soc.* (Communication) **113**, 6311 (1991).
11. K. Norwood, S Nourbakhsh, G.-Z. He, and C. Y. Ng, "Photoionization Study of Supersonically Cooled CS Formed in the Excimer Laser Photodissociation of CS_2". *Chem. Phys. Lett.* **184**, 147 (1991).
12. K. Norwood and C. Y. Ng, "Observation of Autoionizing Rydberg Series Converging to $SO_3^+(^2E',^2A_1')$", *J. Chem. Phys.* **95**, 5553 (1991).
13. K. Norwood, A Ali, and C. Y. Ng, "A Photoelectron-Photoion Study of H_2O and $(H_2O)_2$, *J. Chem. Phys.* **95**, 8029 (1991).
14. S. Nourbakhsh, H.-M. Yin, C.-L. Liao, and C. Y. Ng, "A 193 nm Laser Photofragmentation Time-of-Flight Mass Spectrometric Study of C_6H_5SH and $C_6H_5SCH_3$", *Chem. Phys. Lett.*, in press.
15. C.-L. Liao, C.-W. Hsu, and C. Y. Ng, "Dynamics of S production in the 193nm Photodissociation of CH_3SSCH_3, CH_3SCH_3, CH_3SH, and H_2S", Invited Paper, *SPIE Conference* on "Optical Methods for Time- and State-Resolved Selective Chemistry", edited by C. Y. Ng, Los Angeles, Jan. 23-25, 1992, in press.
16. C. Y. Ng, editor, *Vacuum Ultraviolet Photoionization and Photodissociation of Molecules and Clusters* (World Scientific, Singapore, 1991), 572 pages.
17. C. Y. Ng and M. Baer, editors, *State-Selected and State-to-State Ion-Molecule Reaction Dynamics I: Experiment* (Wiley, New York, 1992), *Adv. Chem. Phys.* Vol. **82**, 686 pages.
18. M. Baer and C. Y. Ng, editors, *State-Selected and State-to-State Ion-Molecule Reaction Dynamics II: Theory* (Wiley, New York, 1992), *Adv. Chem. Phys.* Vol. 82, 561 pages.
19. C. Y. Ng, editor, *Optical Methods for Time- and State-Selected Chemistry*, Conference Proceeding, SPIE Laser Symposium, Los Angeles, Jan. 23-25, 1992, in press.
20. C. Y. Ng, S.-W. Chiu, and W.-K. Li, "An *ab initio* Molecular Orbital Study of the Methylthio and Mercaptomethy Radicals", *J. Chem. Res.*, submitted.

Quantitative Imaging of Turbulent and Reacting Flows

Phillip H. Paul and Noel T. Clemens
Combustion Research Facility
Sandia National Laboratories
Livermore, CA 94551-0969

Background

Quantitative digital imaging, using planar laser light scattering techniques is being developed for the analysis of turbulent and reacting flows. Quantitative image data, implying both a direct relation to flowfield variables as well as sufficient signal and spatial dynamic range, can be readily processed to yield two-dimensional distributions of flowfield scalars and in turn two-dimensional images of gradients and turbulence scales. Much of the development of imaging techniques to date has concentrated on understanding the requisite molecular spectroscopy and collision dynamics to be able to determine how flowfield variable information is encoded into the measured signal. From this standpoint the image is seen as a collection of single point measurements. Our present effort is aimed at realizing necessary improvements in signal and spatial dynamic range, signal-to-noise ratio and spatial resolution in the imaging system as well as developing excitation/detection strategies which provide for a quantitative measure of particular flowfield scalars.

We have completed the development of an advanced intensified camera system. The design of the system was based on detailed modeling of signal and image transfer properties of fast UV imaging lenses, image intensifiers and CCD detector arrays. While this system is suitable for direct scalar imaging, derived quantities (e.g. temperature or velocity images) require an exceptionally wide dynamic range imaging detector. To apply these diagnostics to reacting flows also requires a very fast shuttered camera. We have developed and successfully tested a new type of gated low-light level detector. This system relies on fast switching of a proximity focused image-diode which is direct fiber-optic coupled to a cooled CCD array. Tests on this new detector show significant improvements in detection limit, dynamic range and spatial resolution as compared to microchannel plate intensified arrays. This represents an important advance in quantitative PLIF imaging.

For applications in reacting flows we have chosen planar laser-induced fluorescence (PLIF) imaging as our primary diagnostic tool. PLIF is a species specific diagnostic which provides relatively high signal levels and access to most radical species of interest. To be able to develop experimental strategies which provide PLIF images of particular flowfield scalars requires a consideration of collisional quenching effects. We have completed an effort to model collisional quenching of OH $A^2\Sigma$ and NO $A^2\Sigma$. The purpose of this work is to provide a physical framework to consolidate experimental quenching cross-section measurements and then provide sets of correlations which can be used to design experiments or extrapolate to typical flowfield conditions. The model for the hydroxyl radical is an extension of a collisional-complex formalism which has been adapted to include the effects of molecular orientation to describe the known J-dependent quenching of OH. The model for NO quenching is based on a curve-crossing or 'harpoon' mechanism with the crossing probability based on a Landua-Zener formalism. The later model has been used successfully to match quenching measurements made in our laboratory (see abstract by J. A. Gray et al.).

Recent Results

We have completed an imaging study of the structure of OH in a highly turbulent non-premixed H_2-air flame. Large scale image data sets have been recorded which span the full length of the flame. We have studied both pure H_2 and 50% Ar and He diluted H_2 flames

having nozzle Reynolds numbers ranging from 30,000 to 120,000. Fully resolved fine scale measurements have also been made for several axial stations in these flows. Processing and interpretation of these data is presently being undertaken.

A detailed study has also been undertaken of the flow in the near-field non-reacting round jet. In the near field this flow displays a very 2-D shear-layer like character which makes it of particular interest as a basis for comparison to direct numerical simulation results. Here we have used PLIF imaging of NO $A^2\Sigma$ to obtain very high quality images of the conserved scalar fields. Image data sets have been recorded over the range of $800 < Re_\delta < 80{,}000$ (a Reynolds number based on the mixing layer thickness at mid image). At the highest Reynolds number, it is no longer possible to fully resolve the finest flowfield structure. There is then an ambiguity in the meaning of the measured signal: for a resolution element containing equal portions of jet and ambient fluid, the same signal will be recorded if the two fluids are fully segregated or if they are fully mixed at a molecular scale. To provide some insight into the process of mixing in these highly turbulent flows we have developed the 'cold-chemistry' approach. We take advantage of the low cross-section for quenching of NO by N_2 and the high cross-section for quenching by O_2, 0.006 and 25 Å respectively. By using PLIF of NO $A^2\Sigma$ to image an NO seeded N_2 jet mixing into ambient air, the weighting imposed by the quenching provides a signal which can be directly interpreted as that fraction of the resolution element which contains pure unmixed fluid. This approach provides a powerful tool for studying the degree of mixing in a highly turbulent flow at a subresolution scale. Processing and interpretation of the conserved scalar and 'cold-chemistry' data is presently being undertaken. Initial results will be in the form of conserved scalar PDF's. A parallel effort has been initiated to compare these results to that obtained from simulations.

Future Work

We plan to test a new excitation/detection scheme for PLIF imaging of the CH radical. In hydrocarbon flames CH provides a unique means to study flame-front topology. Previous methods have provided relatively poor signal levels forcing a sacrifice in spatial resolution which has then limited the use of CH imaging to only sightly turbulent flows. Test of alternate excitation strategies for PLIF imaging of NO, O_2 and for formaldehyde are also planned. The flow facility used for the jet near-field experiments has been modified to allow imaging studies of differential diffusion in a geometry which can be readily compared to simulation results. We also plan to use the same flow cell to study transition to turbulence of a reacting flow.

Publications related to this work

1 D. B. Makel, P. H. Paul and N. T. Clemens, 'PLIF imaging of a subscale rocket exhaust,' (1992) paper WSS/CI 92-5.

2 P. H. Paul, 'The application of intensified array detectors to quantitative PLIF imaging,' (1991) paper AIAA 91-2315.

3 P. H. Paul, U. E. Meier and R. K. Hanson 'Single-shot, multiple-camera PLIF imaging of gaseous flows,' (1991) paper AIAA 91-0459.

4 N. T. Clemens, P. H. Paul, M. G. Mungal and R. K. Hanson, 'Scalar mixing in the supersonic shear layer,' (1991) paper AIAA 91-1720

5 R. K. Hanson, J. M. Seitzman and P. H. Paul, 'PLIF imaging of combustion gases,' Ap. Phys. B. **50** 441-454 (1990).

6 P. H. Paul, I. van Cruyningen, R. K. Hanson and G. Kychakoff, 'High resolution digital flowfield imaging of jets,' Exp. in Fluids **9** 241-251 (1990).

A High Resolution Infrared Double Resonance Technique for Molecular Eigenstate Spectroscopy in a Free Jet

D. S. Perry, Jungsug Go, and G. A. Bethardy
University of Akron, Akron OH 44325-3601

I. Introduction

Intramolecular vibrational redistribution (IVR) appears to be a universal property of polyatomic molecules in energy regions where the vibrational density of states is greater than about 5 to 30 states per cm^{-1}. Interest in IVR stems from its central importance to the spectroscopy, photochemistry, and reaction kinetics of these molecules.

An energy level scheme for IVR is shown in Fig. 1. The bright state, φ_s, which in our case may be a C-H stretching vibration, carries the oscillator strength from the ground state. This bright state may mix with bath rotational-vibrational levels to form a clump of molecular eigenstates, each of which carries a portion of the oscillator strength from the ground state. In our work we explicitly resolve transitions to each of these molecular eigenstates. Detailed information about the nature of IVR is contained in the frequencies and intensities of the observed discrete transitions. Our measurements are strictly in the frequency domain but information is obtained about the decay of the zero order state, φ_s, which could be prepared in a hypothetical experiment as a coherent excitation of the clump of molecular eigenstates.

The goal of this research is to probe the coupling mechanisms by which IVR takes place. The most fundamental distinction to be made is between anharmonic coupling which is independent of molecular rotation and rotationally-mediated coupling. Of the rotationally-mediated mechanisms, Coriolis coupling is generally assumed to be stronger than centrifugal coupling. Coriolis interactions may be further classified as x, y, or z according to the axis about which the coupling rotation occurs. Each of these mechanisms obeys different symmetry restrictions and therefore each leaves its characteristic signature on fully resolved molecular spectra.

High resolution single resonance techniques such as slit jet absorption and optothermal detection have been successful in resolving clumps of molecular eigenstates and providing detailed insights into the nature of IVR for some polyatomics in the energy range 3000 cm^{-1} to 7000 cm^{-1}. The success of these methods is attributable to (i) sub-Doppler experimental resolution and (ii) the spectral simplification achieved by supercooling the molecules in a nozzle expansion. However even under the above conditions real molecular spectra contain overlapping pure sequences requiring the tedious application of ground state combination differences to assign hundreds of lines. Even after the necessary time is spent, significant ambiguities in the assignments remain.

The ethanol spectra in Fig. 2 exemplify some of these difficulties. Even at high

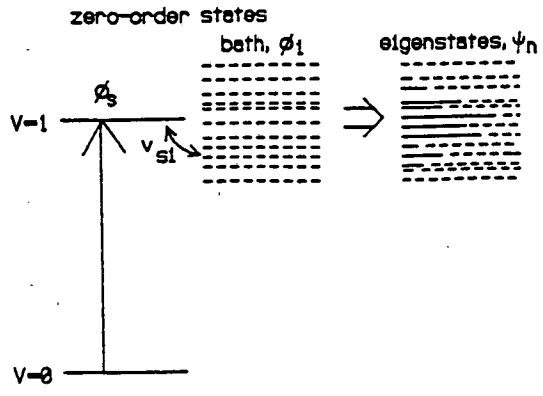

Figure 1. Energy level scheme for IVR.

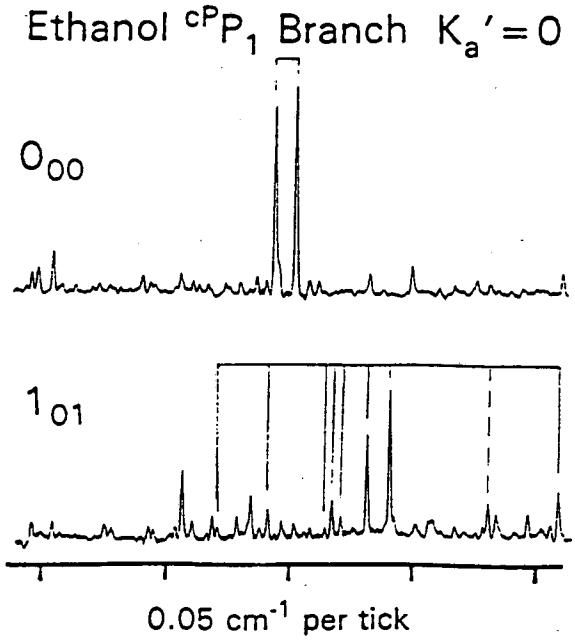

Figure 2. Sample ethanol spectra from the c-type band at 2990 cm-1 recorded using a slit jet. Upper state rotational assignments are indicated.

experimental resolution, the presence of multiple pure sequences results in congested spectra and the loss or miss-assignment of many small peaks. In the worst cases such spectra may be rendered completely unassignable. Because of tunneling between the three equivalent positions of the methyl group, the spectra in Fig. 2 are the superposition of spectra from two non-interacting nuclear spin species. Assignment of the nuclear spin species by combination differences is not possible because the tunneling splitting in the ground state is extremely small. While some insight can be obtained from approximate separations, the most rigorous analysis of the spectra requires a confident assignment of all good quantum numbers. Since there is only one route to the upper state 0_{00} clump, assignment of these levels by combination differences is not possible. These missing assignments would carry the information about the coupling strength of the zero-order 0_{00} state which would most clearly distinguish anharmonic and Coriolis coupling mechanisms.

By going to an infrared double resonance technique, we add to the single resonance methodology the power of a second high resolution infrared dimension. The method which we shall describe below has the following features:

(i) applicable in a free-jet environment,

(ii) intrinsically high resolution (5 - 30 MHz),

(iii) a single pure sequence per spectrum which implies an even greater effective resolution,

(iv) high sensitivity, sometimes better than the corresponding single resonance spectrum,

(v) assignment of all good quantum numbers, and

(vi) ability to reach vibrations not accessible to single resonance studies.

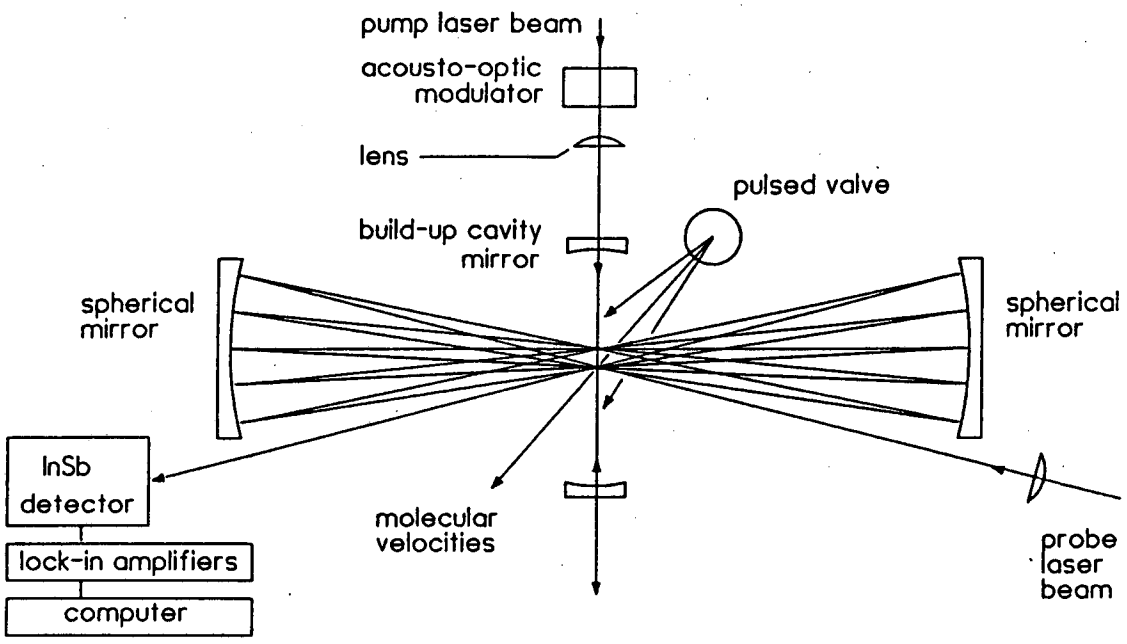

Figure 3. Experimental setup for free-jet infrared double resonance experiments.

II. Experimental

Infrared beams from two F-center lasers intersect in a free jet such that both laser beams lie in a plane normal to the molecular velocities in the intersection volume (Fig. 3). This arrangement ensures that both laser beams interact with molecules having zero Doppler shift and therefore guarantees sub-Doppler resolution. The pump laser beam passes through a resonant Fabry-Perot etalon which enhances the pump laser intensity in the crossing volume by 60 times. Absorption of the probe laser beam is enhanced by nine passes through the active volume. The pump beam is acousto-optically modulated at 400 kHz and the absorption of the probe beam is monitored with phase sensitive detection tuned to this frequency. The detection scheme takes advantage of the 1/f noise characteristic of the probe laser and allows recovery of much of the sensitivity loss normally associated with double resonance experiments.

III. Double Resonance Results

The pump laser was tuned to specific J, K lines in the propyne ν_1 band ($v=1\leftarrow0$). The probe laser was then scanned through the ν_1 ($v=2\leftarrow1$) region. The resulting spectra (Fig. 4) probe vibrational levels in the 6500 cm^{-1} with a signal-to-noise of up to 600:1. About twice as many lines are identified and assigned in each pure sequence as in the corresponding optothermal single resonance spectra of the same region[1]. It is of particular interest that non-resonantly coupled states are directly observed. We intend to apply this technique to other bands and to ethanol and 1-butyne.

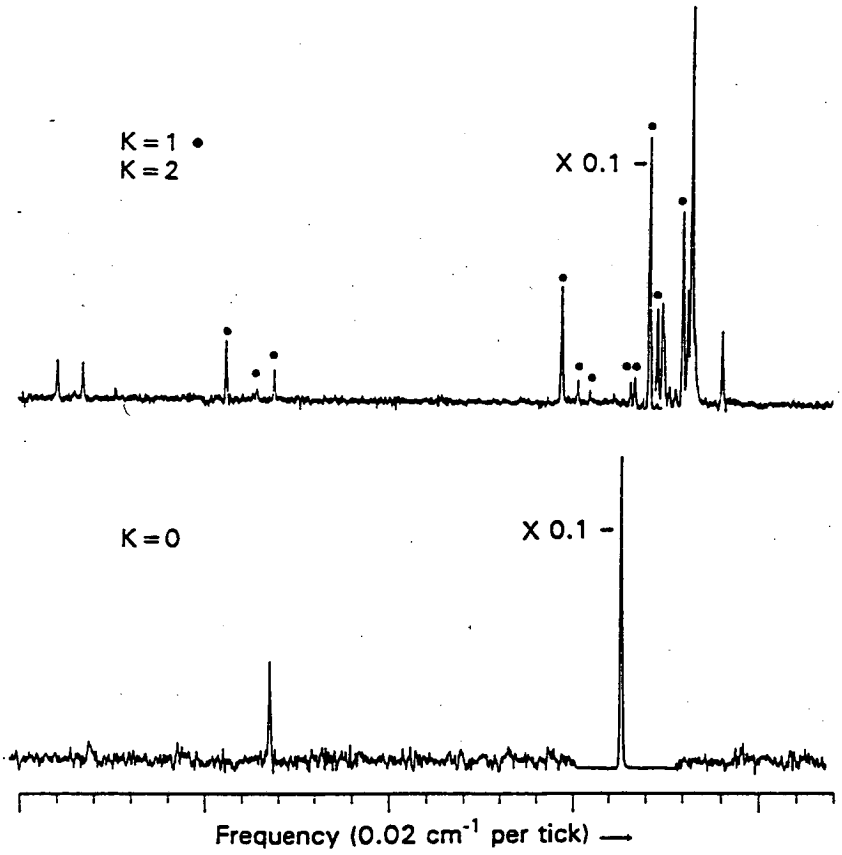

Figure 4. Infrared double resonance spectra of propyne showing transitions preparing J=5 levels in the $2\nu_1$ region near 6570 cm^{-1}. In order to present the large and small peaks in the same plot, the single largest peak in each spectrum is shown with the gain reduced by 10 times.

IV. Single Resonance Results

Spectra of the asymmetric (c-type) C-H stretch of ethanol and of 1-butyne have been recorded in the 2990 cm^{-1} region. Analysis by ground state combination differences reveals IVR ranging from sparse to intermediate case but with contrasting mechanisms for the two similar bands. In 1-butyne the coupling mechanism is dominantly anharmonic with only an indication of weak z-type Coriolis coupling. In ethanol (Fig. 2), the anharmonic coupling remains but is dominated by x/y and z-type Coriolis coupling. It is our objective to understand and generalize the reasons for these qualitatively different coupling mechanisms.

V. Random Matrix Simulations of IVR

We have developed a random matrix methodology capable of implementing rather general models of IVR including, for example, anharmonic coupling and the 3 types of Coriolis interactions. The mechanism for coupling among the bath states as well as coupling of the bright state to the bath is addressed. The method allows the simulation of experimental spectra in which competing IVR mechanisms are present and therefore enables us to extract the strength of each mechanism from the experimental data.

---

1. We are grateful to K. K. Lehmann for providing the optothermal results in advance of publication.

REACTION AND DIFFUSION IN TURBULENT COMBUSTION

Principal Investigator: S.B. Pope
Cornell University, Ithaca, NY 14853

INTRODUCTION

The object of the research is to use Direct Numerical Simulations (DNS) to study the coupled processes of reaction and molecular mixing in turbulent combustion. Because of inevitable computational limitations, it is impossible to simulate turbulent combustion in the parameter range of practical interest. Instead, our approach is to study very simple turbulent reactive flows that contain qualitatively the same pheonomena as real flames. Based on the insights and information gained, statistical models will be developed that are applicable to practical combustion devices.

Recent progress has been made in two areas, although the results are still preliminary.

NON-PREMIXED REACTION IN ISOTROPIC TURBULENCE

Our approach is to perform DNS for the simplest possible flow and reaction scheme that retains the essence of the problem being addressed. The flow is constant-density, homogeneous, isotropic, turbulence, with forcing at the large scales to produce statistical stationarity.

The thermochemistry is characterized by a mixture fraction ξ and a reaction progress variable Y. In the high Damkohler number limit, Y adopts its equilibrium value, denoted by $Y_e(\xi)$: and, in genral, we define the perturbation

$$y \equiv Y_e(\xi) - Y.$$

Deterministic forcing is added to the evolution equations for $\xi(\mathbf{x}, t)$ and $y(\mathbf{x}, t)$ so that these fields too are statistically stationary.

We have developed a simple reaction scheme that is representative of non-premixed combustion. To a first approximation, the reaction rate of y,

$S(\xi, y)$, is characterized by: the stoichiometric mixture fraction, ξ_s; the width (in mixture fraction space) of the reaction zone, $\Delta\xi_r$; and a time scale τ_r.

Extensive testing has been performed to determine the resolution requirements in the direct numerical simulations. In addition to the Reynolds number R_λ, the resolution required depends strongly on $\xi'/\Delta\xi_r$, where ξ' is the r.m.s. mixture fraction. Broad reaction zones (i.e. small $\xi'/\Delta\xi_r$) are, of course, more easily resolved.

Figures 1 and 2 illustrate preliminary results. They show scatter plots of y and ξ for two cases. In both cases the Reynolds number $R_\lambda \approx 20$ and the Damkohler number (based on the Kolmogorov scales) $Da \approx 9$ are the same. But Fig. 1 pertains to much broader reaction zones ($\xi'/\Delta\xi_r = 0.0625$) than does Fig. 2 ($\xi'/\Delta\xi_r = 0.6$).

These simulations are continuing. Different parameters are being considered, and the results obtained related to prevailing theories and models.

MOLECULAR MOTION IN TURBULENCE

Ultimately, molecular mixing is due to the motion of molecules relative to each other. We have used DNS to study the motion of molecules in homogeneous turbulence.

Direct numerical simulations have been used previously (Yeung & Pope 1989) to determine Lagrangian statistics by following an ensemble of N fluid particles. Let $\mathbf{X}(t)$ denote the position of one such particle. We now also track an ensemble of N molecules, with position denoted by $\mathbf{Y}(t)$, from coincident initial conditions (i.e. $\mathbf{Y}(0) = \mathbf{X}(0)$). This is achieved by numerically integrating the stochastic differential equation for $\mathbf{Y}(t)$, which involves the molecular diffusion coefficient $D = \nu/Sc$ (where ν is the kinematic viscosity and Sc is the Schmidt number).

From the N time series of $\mathbf{X}(t)$ and $\mathbf{Y}(t)$ we have extracted many statistics on the dispersion of molecules (e.g. $\langle \mathbf{Y}(t) \cdot \mathbf{Y}(t) \rangle$) and on the relative dispersion between molecules and fluid particles (e.g. $\langle (\mathbf{Y} - \mathbf{X}) \cdot (\mathbf{Y} - \mathbf{X}) \rangle$). It is found that these statistics are in good agreement with the theory of Saffman (1961). For example, the theory predicts (to order t^3)

$$\langle Y(t)^2 \rangle = \langle X(t)^2 \rangle + 2Dt - \frac{1}{9} D t^3 / \tau_\eta^2,$$

where τ_η is the Kolmogorov time scale. The term that is linear in t gives the

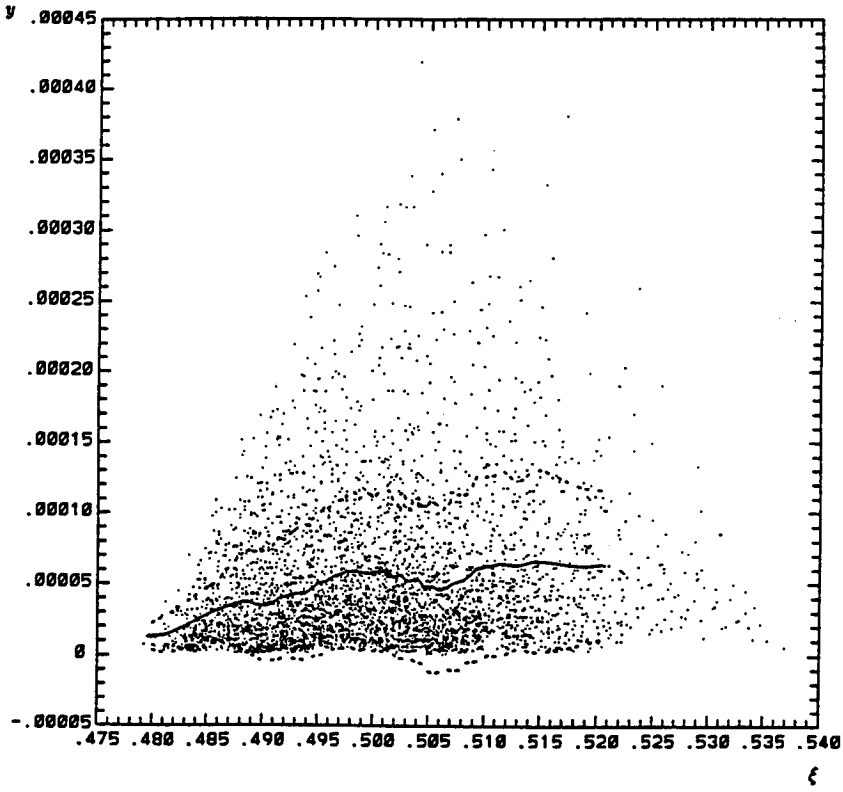

Fig. 1: Scatter plot of y and ξ from DNS of non-premixed reaction in isotropic turbulence. $R_\lambda \approx 20$, $Da \approx 9$, $\xi'/\Delta\xi_r = 0.0625$. Lines show conditional mean $\langle y|\xi \rangle$ plus and minus one standard deviation.

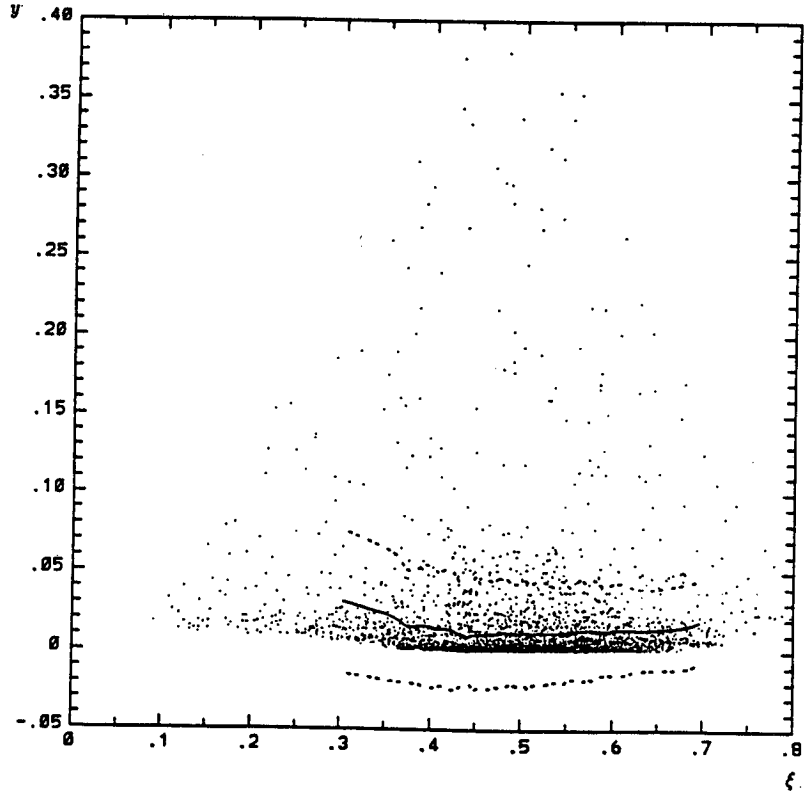

Fig. 2: Same as Fig. 1, but $\xi'/\Delta\xi_r = 0.6$.

direct additive contribution of molecular diffusion. The term that is cubic in t gives, interestingly, a decrease in molecular dispersion with an increase in the molecular diffusivity, which is due to a decorrelation of the fluid velocity following a molecule. Figure 3 shows $\langle Y(t)^2 \rangle$ plotted in such a way as to reveal terms higher than linear in t. Excellent agreement with Saffman's theory is evident for all Schmidt numbers investigated.

Higher-order statistics are also being investgated. Figure 4 shows the flatness factor of the relative displacement $Y(t) - X(t)$. For low Schmidt number ($Sc = 0.1$) this is close to the Gaussian value of 3 for all time; whereas for $Sc = 10$, it rises above 10 before decreasing. For this case it is found that (to a good approximation) the pdf of $|\mathbf{Y} - \mathbf{X}|$ is log-normal.

REFERENCES

Saffman, P.G. (1961) J. Fluid Mech. **8**, 273.

Yeung, P.K. & Pope, S.B. (1989) J. Fluid Mech. **207**, 531.

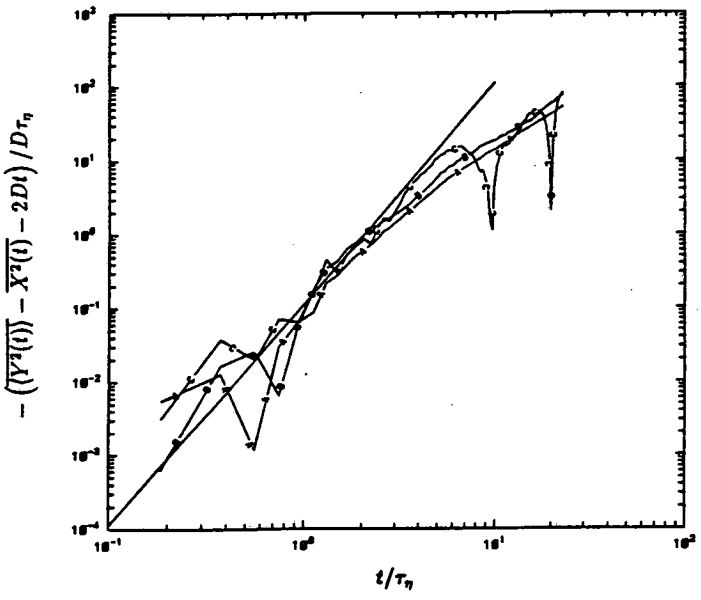

Fig. 3: Difference between molecular and fluid-particle dispersion in isotropic turbulence. A, $Sc = 0.1$; B, $Sc = 1.0$; C, $Sc = 10.0$. Solid line, Saffman's theory $\frac{1}{9}(t/\tau_\eta)^3$.

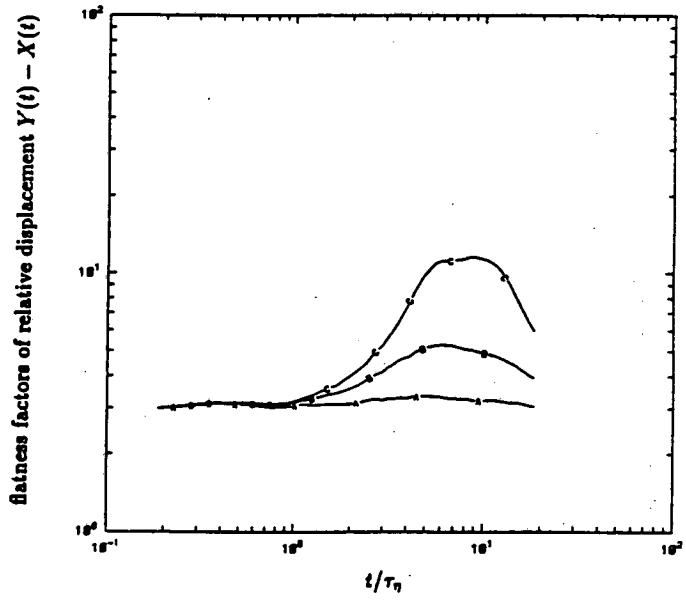

Fig. 4: Flatness factor of relative distance between molecules and fluid particles for the simulations of Fig. 3.

Time-Resolved Fourier-Transform IR Fluorescence Spectroscopy

Jack M. Preses
Chemistry Department
Brookhaven National Laboratory
Upton, NY 11973

Program Scope

In this research program we have constructed and begun to use a time-resolved Fourier-transform infrared emission spectrophotometer. This technique is uniquely able to obtain detailed, yet global information about the dynamics of chemical reactions following photodissociation by ultraviolet radiation from an excimer laser. It can serve as an independent tool for elucidating energy flow during chemical reactions, and as a useful "road map" for high-resolution studies using diode lasers.

Recent Progress

The construction of the instrument has recently been completed. It is based on a BOMEM DA-3 cw absorption FTIR spectrophotometer. The conceptual design of the time-resolving part of the instrument is descended from those of J.J. Sloan[1] and S.R. Leone[2] . While the moving mirror smoothly traverses its path through the interferometer, its progress is marked by equally spaced fringes generated by a stable, single-frequency He:Ne laser. At each fringe, the photolysis laser is fired, and one point of an infrared emission interferogram is recorded at one hundred two-microsecond time intervals following the laser pulse. Multiple mirror scans are added to improve signal to noise. Following data acquisition, the data are reassembled into individual "time slice" interferograms. Where the two-microsecond time resolution is not essential, time slices may be summed to further improve signal to noise. Fourier transforms are performed by numerical integration of the Fourier integrals on a fast RISC processor using our own software, which is tailored to meet the the particular requirements for transformation of weak emission signals.

The vibrational distribution of the CO_2 generated by the UV-induced photofragmentation of pyruvic acid (2-oxo-propanoic acid) has been investigated previously.[3,4,5] Several publications have appeared in the literature describing possible mechanisms for pyruvic acid decomposition after 193 nm excimer laser irradiation or IRMPD (Infrared Multiple Photon Dissociation) of pyruvic acid in the gas phase.[6] There are two likely mechanisms for the photodecarboxylation of pyruvic acid. In one possible mechanism, excited pyruvic acid ejects CO_2, leaving behind a hydroxycarbene, which subsequently rearranges to acetaldehyde. In the second mechanism, excited pyruvic acid ejects CO_2 and forms acetaldehyde in a concerted process. Since the two possible reaction pathways proceed *via* different primary products, the energy available to the CO_2 vibrations differs as well. A detailed examination of the near-nascent CO_2 vibrational distribution can, therefore, help to clarify which of the possible mechanisms is correct. Previous investigations have used either low-resolution IR emission from the ν_3 vibrational manifold of the product CO_2 (at $\sim$4.3 μm), or diode laser absorption spectroscopy in the same region. The IR fluorescence experiments of Rosenfeld and Weiner indicated that the CO_2 was produced in vibrational states higher than the 00^01 state. This was confirmed by the more quantitative measurements of G. Flynn's group at Columbia University, who determined populations of several levels in the 00^0p and $0n^l0$ manifolds, from which they derived vibrational temperatures of 3700$\pm$1000 K and 1800$\pm$150 K, respectively.

The unresolved emission spectrum, with a maximum at ~2200 cm^{-1}, that we observe at ~10 μs after the photolysis pulse is strongly red-shifted from the room-temperature absorption spectrum of CO_2. The peak gradually shifts to the blue at longer times, and after 150 μs the spectrum has clearly identifiable vibrational-rotational lines from the CO_2 00^01 state. At earlier times, even the highest resolution spectra obtainable would not be able to resolve rovibrational line structure, due to the very high densities of states at the energies involved. A statistical model for the population distributions using a linear surprisal gives reasonable agreement with our observations and with the vibrational temperatures found by the Flynn group. This agreement is obtained only if the available energy is set equal to the 150 kcal/mol released if acetaldehyde is formed directly. Production of the hydroxycarbene ($CH_3\ddot{C}OH$) as an intermediate releases only 98 kcal/mol, and with this energy the linear surprisal model cannot be made to agree with the experimental observations.

The production of CO from acetone has been studied using time-resolved FTIR by the group of S.R. Leone (JILA, U. of Colorado).[7] We have observed essentially the same vibrationally excited CO product. In Leone's experiments, vibrationally excited CH_3 radicals, which are known to be produced along with the vibrationally excited CO, were not observed. In our latest experiments with 1 cm^{-1} resolution, we observe an emission band in the 3000 cm^{-1} region which can be attributed to vibrationally excited CH_3. However, if we degrade the resolution of our spectra by transforming fewer interferogram points than were collected, the CH_3 emission becomes more distinct. The important lesson here is that the population in polyatomic radicals can be distributed over a vastly larger number of levels than in diatomic radicals. Therefore, each emission line from a polyatomic radical may carry too little intensity to stand out above the noise in a high-resolution spectrum collected near the limit of signal to noise. When lines are effectively "binned" by lowering resolution, the resulting signals are visible above the noise.

Preliminary experiments have been conducted to observe CO and ethyl radical emission from the photodecomposition of diethyl ketone. CO emission is clearly observed. Further experiments will be necessary to pin down the ethyl radical emission which also may be produced. Here, the lesson of CH_3 from acetone must be considered, and the even greater number of degrees of freedom accessible to ethyl radicals will only exacerbate the difficulty of determining distributions from our observations. It may be necessary to improve the efficiency of our collection optics to produce good signals from ethyl radicals. However, a determination of the vibrational (and possibly rotational) population distribution of CO will provide information about the photodissociation dynamics.

Future Plans

The promising experiments on the excimer laser-induced decomposition of diethyl ketone, will continue. This molecule can be a source of CO, ethyl and, perhaps, propanoyl (CH_3CH_2CO) radicals. Much more work needs to be done in order to sort out the dynamics of the photodissociation and the relaxation of the excited products. The first order of business is to confirm the apparent ethyl signals. This may entail construction of "Welsh cell" (multipass) optics in order to collect infrared emission more efficiently. Next, the task of inverting the observed spectra into a vibrational distribution is considerably more daunting than that encountered in the assignment of CO_2 emission from pyruvic acid. The source of the emission is an unstable radical, so that the spectroscopic constants are less well-determined. Second, the signals themselves are intrinsically much weaker than those obtained from CO_2. Third, there are many more internal degrees of freedom available to ethyl than to CO_2, so that it may be hopeless to infer unique vibrational distributions from the observations.

Other systems which may be studied include strongly exothermic reactions that may produce vibrationally excited radicals, such as the photodecomposition of acetic acid, where the $CH_3 + HOCO$ channel has recently been confirmed by diode laser absorption measurements. Reactions of the ubiquitous combustion radical methylidyne, CH, with O_2 proceed with nearly gas kinetic rate constants, producing at least three sets of products. Branching ratios for these reactions have not been determined, and time-resolved FTIR can be used to observe CO, CO_2, and OH products.

Reactions which are weakly exothermic or endothermic will not produce highly vibrationally excited products, so that these systems will not be suitable for study by IR fluorescence methods. With some comparatively minor modification, our instrument can be used for time-dependent absorption studies. These experiments are complementary to *both* fluorescence experiments and to diode-laser studies. Here, the signal-to-noise ratios obtainable depend not only on the intrinsic properties of the molecules or radicals being investigated, but also on whether an external IR source can produce sufficient photons per unit time to generate good signals with short time resolution. In any case, a White cell will be necessary to produce long absorption path lengths. A good example of a reaction to be studied by this method is

$$CH + CH_4 \longrightarrow CH_3 + CH_2 \quad \Delta H^0 = -3.3 \text{ kcal/mol} \quad .$$

Absorption experiments in the C-H stretch region near 3000 cm^{-1} may be able to characterize the products of this reaction. This experiment will probably require a flow system for the gas sample.

Finally, many radicals have transitions among excited states in the visible and near-IR regions of the spectrum. Operation of the interferometer in the visible region of the spectrum can produce entire time-resolved spectra with spectral resolution comparable to that currently available from the SEP experiments performed in our group. Optics for visible interferometry are available from the manufacturer of our interferometer, so that conversion of the interferometer is straightforward. A commercially available dye laser will also be necessary for laser-induced fluorescence experiments. With this experimental arrangement, it should be possible to measure rovibronic energy levels in the ground state of many free radicals at near laser-limited resolution and at a rate orders of magnitude faster than is currently possible. A good example of a visible/near-IR experiment involves an examination of the 800-1600 nm emission from $(HO_2)^*$ produced in the reaction of H atoms with O_2. FTIR experiments can help to decide between various direct and indirect production mechanisms for the HO_2 *A* state.

REFERENCES

1. J.J. Sloan, and E.J. Kruus in: *Time Resolved Spectroscopy (Advances in Spectroscopy)* eds. R.J.H. Clark and R.E. Hester, (Wiley, New York, 1989).

2. S.R. Leone, *Acc. Chem. Res.* **22** 139 (1989), and references therein.

3. P.A. Leermakers and G.F. Vesley, *J. Am. Chem. Soc.* **85** 3776 (1963); G.F. Vesley and P.A. Leermakers, *J. Phys. Chem.* **68** 2364 (1964); R.N. Rosenfeld and B. Weiner, *J. Am. Chem. Soc.* **95** 3485 (1983); R.N. Rosenfeld, and B. Weiner, *J. Am. Chem. Soc.* **105** 3485 (1983).

4. C.F. Wood, J.A. O'Neill, and G.W. Flynn, *Chem. Phys. Lett.* **109** 317 (1984).

5. J.A. O'Neill, T.G. Kreutz, and G.W. Flynn, *J. Chem. Phys.* **87** 4598 (1987).

6. J.L. Buechele, E. Weitz, and F.D. Lewis, *Chem. Phys. Lett.* **77** 280 (1981).

7. E.L. Woodbridge, T.R. Fletcher, and S.R. Leone, *J. Phys. Chem.* **92** 5387 (1988).

Publications 1990–92

J.M. Preses and R.A. Holroyd, Temperature Dependence of Fluorescence from Liquid Butane, Pentane, and Hexane: Lifetimes and Quantum Yields, *J. Chem Phys.* **92** 2938-2942 (1990).

J.M. Preses, J.R. Grover, Å Kvick and M.G. White, Chemistry with Synchrotron Radiation. *Amer Sci.* **78** 424-437 (1990).

G.E. Hall, J.T. Muckerman, J.M. Preses, R.E. Weston, Jr., and G.W. Flynn, Time-Resolved Studies of the Photodissociation of Pyruvic Acid at 193 nm. *Chem. Phys. Lett.* in press.

Analysis of Forward and Inverse Problems in Chemical Dynamics and Spectroscopy

by

Herschel Rabitz
Department of Chemistry
Princeton University
Princeton, NJ 08544

I. Program Scope. The goal of this research is to provide a better understanding of the relationship between structure in potential surfaces, and the behavior of resultant dynamical observables. This problem is being pursued from both the forward and inverse perspectives. In the case of forward analysis, one starts with a potential surface and proceeds to compute dynamical observables. In this case, the objective is to discern those parts of the potential surface that control significant dynamical events. In the case of inversion, the objective is to ultimately provide an algorithm for the stable inversion of quality laboratory data, to yield the underlying fundamental potential surfaces. The forward and inverse problems are intimately related, physically as well as operationally, through their common use of functional sensitivity analysis to map the forward and inverse observable $\Leftrightarrow$ potential relationships.

II. Recent Progress.

A. Forward Analysis. An overall objective of this research is the goal for mapping out how detailed structure in intermolecular potentials is carried from level to level in the dynamical hierarchy, proceeding from detailed differential cross sections up through macroscopic kinetic observables. The various components of this research are outlined below, according to the type of dynamical observables involved.

1. Inelastic Dynamics. The largest body of information on relating potential structure to dynamics exists for inelastic molecular collisions. Of special concern to us has been the family of physical observables associated with what are called generalized cross sections. These include traditional inelastic state-to-state transitions, as well as transport cross sections, and cross sections arising for collisions in the presence of electric and magnetic fields, etc. In general, each observable cross section σ_i of type i will have a distinct mapping from the potential surface $V(\underset{\sim}{r})$ and this quantitative relationship is revealed through the functional sensitivity coefficients $\delta\sigma_i/\delta V(\underset{\sim}{r})$. Thus, for example, a sensitivity coefficient $\delta\sigma_i/\delta V(\underset{\sim}{r})$ contour map may be directly superimposed on the potential surface $V(\underset{\sim}{r})$, and the significance of any given region may be directly read from the map. Of special interest is the overall information content of these maps $\delta\sigma_i/\delta V(\underset{\sim}{r})$ for an entire collection of observables. This type of question may be addressed by computing the left- and right-hand eigenvectors of the sensitivity coefficient matrix by use of a singular value decomposition. By an examination of the eigenvectors, the potential surface may be decomposed into variant (important) and invariant subspaces. In a corresponding fashion, the important and unimportant types of experimental data σ_i, i = 1, 2,...may be identified. An analysis of this type has been performed on the He + H_2 rotationally inelastic system, and the techniques involved have a close bearing on the tools being employed in the inversion work of section B. below.

2. Reactive Dynamics. Naturally, many of the same questions arising in inelastic dynamics above once again occur when considering chemical reactivity. A specific issue of concern is the identification of the significant regions at and around the reactive barrier. Other than performing a functional sensitivity analysis, the only other means of addressing this matter has been the tedious performance of repeated dynamics on a large family of distinct potential surfaces. Recent progress utilizing functional sensitivity analysis has focused on two systems. First, the collinear $H + H_2$ exchange reaction was studied to explore how sensitivity information from one potential surface may be used to predict observables from a second surface. The observables included threshold behavior, the location and width of energy resonances, etc. By characterizing how these key features draw on the potential surface, it is possible to more readily transfer information from one surface to another. The sensitivity of the rate constant for the $H + H_2$ system was also studied as a function of temperature. In a second illustration, the three-dimensional $F + H_2$ reaction was studied involving the total angular momenta $J = 5$ and $J = 10$. One identified region of importance was the saddle point and approaching slope. In addition, the inner wall of the exit valley was also found to be significant. It is planned to carry out further computations with converged cross sections, and the implications of results of this type are expected to be significant for further refinements of the potential surface. Much of this work is being carried out in collaboration with Nancy Brown, Berkeley, and Robert Wyatt, Austin.

3. Chemical Kinetics. This work is concerned with identifying how chemical species profiles are controlled by the underlying kinetic and transport processes in the reaction mechanism. A detailed study of this type was carried out for the laminar $CO - H_2 - O_2$ flame under steady state conditions. The reactions of the hydroperoxy radical with hydrogen, oxygen, and hydroxy radicals were found to be extremely important at all temperatures in the fuel lean (40 torr) flame studied. The diffusive mixing of chemical species from the low and the high temperature portions of the flame, and the large heats of reaction associated with the hydroperoxy radicals were found to be responsible for the increased importance of these reactions. In this study, as well as other combustion sensitivity analysis computations, it has been found that a striking degree of self-similarity or related structure appears amongst the sensitivity coefficients. The appearance of this behavior has potentially important significance for the ability to simplify complex models by lumping their chemical species or eliminating sets of reactions. It has been argued that the presence of a dominant coupling dependent variable, principally the temperature in combustion or explosive systems, can entrain the remaining species to follow its own lead in terms of response to system disturbances and identification of the important steps in the mechanism. The further implications of this behavior continue to be explored.

B. Inverse Algorithm Development. The ability to compute forward mapping functional sensitivity coefficients discussed in item A. above provides a basis for constructing an inversion algorithm. The objective here is to produce a stable and reliable algorithm which may be coupled with quality laboratory studies to ultimately extract valuable potential surface information from the data. The traditional route to stabilizing chemical dynamics inversions has been through the introduction of constrained potential forms, with as few parameters as possible for fitting. Although such a procedure can, in fact, stabilize an inversion, it is dangerous as all real potentials do not correspond to constrained forms. Thus, the inverse approach taken here has been based on the logic of introducing the mildest possible constraint to achieve stabilization. It has been found that merely requiring that the inverted potentials be

smooth (i.e., differentiable to low order) can produce a stable inversion procedure. The inversion algorithm makes explicit use of the forward sensitivity coefficients $\delta O_i/\delta V(\underset{\sim}{r})$ associated with the i-th observable as the kernel of an iterative inversion algorithm. This procedure is closely connected with the singular value decomposition mentioned in item A.1. above. Summarized below are recent results based on this methodology.

1. Molecular Collision Dynamics. Until now, the algorithm has been exclusively applied to gas-phase elastic scattering as a testing ground for the techniques. An important goal is to extend this methodology into the realm of inelastic scattering, where for even the simplest systems, there is still much controversy about the details of the potential surfaces. The key characteristic of inelastic scattering is its multichannel nature when performing the iterative inversion computations. A convenient analog of such problems arises when considering gas-surface elastic scattering. In this case, the various momentum transfer channels produce a mathematical problem analogous to gas-phase inelastic scattering. As a first effort in this direction, a simulation of the full three-dimensional inversion for the He-Xe/C(0001) system was studied. Here, helium is being scattered from a xenon overlayer on graphite. The inversion procedure was found to be capable of extracting the full interaction potential from simulated low energy diffraction data. Studies of this type are continuing for more corrugated surfaces to gain further experience. Ultimately, these studies will revert again to the gas-phase to treat inelastic dynamics, including the presence of realistic noise and true laboratory data as it becomes available.

2. Spectral Inversion. As a complement to dynamical laboratory data, high resolution spectroscopy is a rich source of physical information, especially for accessible bound state regions of potential surfaces. For diatomic systems, the well known RKR method is often capable of producing reliable inversions, but the case of triatomic or larger molecules remains a challenge. Once again, computational issues are important here, including the stability of the algorithm. As an initial step into this new class of inversion problems, the simulated inversion of ground state H_2 vibration-rotation spectral data was undertaken. The potential was recovered to high accuracy. Of particular note here was the introduction of noise into the simulated data, with the encouraging result that the procedure did not attempt to overfit the data. The requirement of achieving a smooth potential has the dual affect of simultaneously filtering out the high frequency components associated with noise in the data. Current studies are continuing on more complex diatomic inversions, and preparations are underway to move on to triatomic systems.

Publication List

1. Determination of Constrained Lumping Schemes for a Catalytic Reforming Model, G. Li and H. Rabitz, Chem. Eng. Sci., in press.

2. A method for inverting curvilinear transformations of relevance in the quantum mechanical Hamiltonian describing n-body systems, J.P. Leroy, R. Wallace, and H. Rabitz, J. Math. Chem., in press.

3. How do Different Regions of the Potential Surface Affect the Collision Dynamics of H_2 with HD?, J. Chang, N.J. Brown, and H. Rabitz. J. Chem. Phys., in press.

4. Inversion of gas-surface scattering data for potential determination using functional sensitivity analysis: II. Extraction of the full interaction potential from low energy diffraction data, T-S Ho and H. Rabitz, J. Chem. Phys., in press.

5. Regularized Inversion of Diatomic Vibration-rotation Spectral Data: A Functional Sensitivity Analysis Approach, H. Heo, T-S Ho, K.K. Lehmann, and H. Rabitz, J. Chem. Phys., in press.

6. Parametric Sensitivity Analysis and Self-Similarity in Thermal Explosion Theory, S. Vajda and H. Rabitz, Chem. Eng. Sci., in press.

7. Sensitivity Analysis of a Steady-state Premixed Laminar $CO+H_2+O_2$ Flame, M. Mishra, R. Yetter, Y. Reuven, and H. Rabitz, Int. J. Chem. Kinetics, in press.

8. Quantum Functional Sensitivity Analysis for the Collinear H + H_2 Reaction Rate Coefficient, J. Chang, N.J. Brown, M. D'Mello, R.E. Wyatt, and H. Rabitz, J. Chem. Phys., in press.

9. The rotation-vibration potential of He-H_2 and its connection with physical phenomena, M.J. Smith and H. Rabitz, J. Chem. Phys., **94**, 7114 (1991).

10. Inversion of gas-surface scattering data for potential determination using functional sensitivity analysis. I. A case study for the He-XE/C(0001) potential, T-S Ho and H. Rabitz, J. Chem. Phys., **94**, 2305 (1991).

11. Factorization of Certain Evolution Operators Using Lie Algebra: Formulation of the Method, M. Demiralp and H. Rabitz, J. Math. Chem., **6**, 165 (1991).

12. Factorization of Certain Evolution Operators Using Lie Algebra: Convergence Theorems, M. Demiralp and H. Rabitz, J. Math. Chem., **6**, 193 (1991).

13. Convergence Properties of a Class of Boundary Element Approximations to Linear Diffusion Problems with Localized Nonlinear Reactions, A.P. Peirce, A. Askar, and H. Rabitz, Numerical Methods for Partial Differential Equations, **6**, 75 (1990).

High-Resolution Inverse Raman and Resonant-Wave-Mixing Spectroscopy

Principal Investigator: Larry A. Rahn, Combustion Research Facility, Sandia National Laboratories, Livermore, CA 94551-0969

Program Scope: These research activities consist of high-resolution inverse Raman spectroscopy (IRS) and resonant wave-mixing spectroscopy to support the development of nonlinear-optical techniques for temperature and concentration measurements in combustion experiments. Objectives of this work include development of spectral models of important molecular species needed to perform coherent anti-Stokes Raman spectroscopy (CARS) measurements and the investigation of new nonlinear-optical processes as potential diagnostic techniques. Some of the techniques being investigated include frequency-degenerate and nearly frequency-degenerate resonant four-wave-mixing (DFWM and NDFWM), and resonant multi-wave mixing (RMWM).

Recent progress:

High-Resolution Resonant-Wave-Mixing Spectroscopy of Flame OH

Larry A. Rahn and Michael S. Brown*

In this abstract we report high-resolution degenerate (DFWM) and nearly-degenerate (NDFWM) four-wave mixing spectra of the $R_1(9)$ $A^2\Sigma^+ \rightarrow X^2\Pi(0,0)$ transition of OH measured in a hydrogen/oxygen flame. These spectra were recorded in the post-flame gases of a hydrogen/oxygen flame with a resolution of ≤ 0.006 cm^{-1} near 307 nm using the frequency-doubled outputs from two pulse-amplified cw dye lasers. Two different phase-matching geometries were used. In the phase-conjugate geometry the forward and backward pump beams were counter propagating while the probe laser beam nearly copropagated with the forward pump, forming an angle of $< 3°$ in the horizontal plane. In the forward geometry, all three beams were nearly copropagating in a three-dimensionally phase-matched configuration. Each beam was linearly polarized, collimated and apertured to a diameter between ~0.6 and 2.0 mm. Linear absorption of the beams amounted to 5% or less. The flame was produced above a flat-flame burner 60 mm in diameter using gas flows of 4.8 l/min of H_2 and 3.0 l/min of O_2. The spectra were recorded at a height of 5 mm above the burner which corresponds to an OH temperature and concentration of ~1450 K and ~2×10^{15} cm^{-3}, respectively. For the spectra reported here, beam intensities were held to $I < 70$ kW/cm^2 or about one-tenth the saturation intensity (I_s) for the $R_1(9)$ transition.

The $R_1(9)$ OH line consists of two strong transitions spaced ~ 0.013 cm^{-1} apart between hyperfine sublevels of the $J'' = 9.5$ and $J' = 10.5$ states where J denotes the total angular momentum excluding the hyperfine structure. Each of these hyperfine states has degenerate Zeeman levels that can contribute to the amplitude of the DFWM signal. Due to inelastic collisional broadening, the hyperfine transitions are not spectrally resolved in our experiment. The spectrum from the phase-conjugate geometry[1] is shown in Fig. 1. The fit to the experimental line shape (solid line) in Fig. 1 is calculated from an analytical solution for the collinear DFWM signal for a two-level system including the effects of atomic velocity in a full perturbative treatment.[2] As seen, this model accurately predicts the measured spectra both near line center and out into the wings. The fit shown in Fig. 1 yields a homogeneous dephasing rate, $\Gamma = 0.062 \pm 0.006$ cm^{-1}. The halfwidth is expected to be sensitive to the angle between the forward pump and probe, but the contribution is negligible for the < 3

degree angle used in these measurements. We obtained good agreement between the DFWM-fit value of Γ and independent measures of the homogeneous broadening of the related (Λ-doublet) even-parity transition by Doppler-free two-photon-excited fluorescence measurements and by comparisons to previous broadening and lifetime measurements.

The perturbative solution for the third order DFWM polarization used to analyze our phase-conjugate-geometry data produces a line shape with two interesting limits. In the limit of extreme homogeneous broadening, $\Gamma / k_o v_p >> 1$, the predicted spectral line shape becomes a Lorentzian-cubed profile having an actual halfwidth of $\Gamma\,(2^{1/3} - 1)^{1/2}$. This limiting form agrees with the stationary atom result of Abrams and Lind.[2] In the limit of extreme Doppler broadening, $\Gamma / k_o v_p << 1$, the spectral line shape reduces to a simple Lorentzian with a halfwidth of Γ. Both of these line shapes have been drawn with the value of $\Gamma = 0.062$ cm^{-1} in Fig. 1 for comparison.

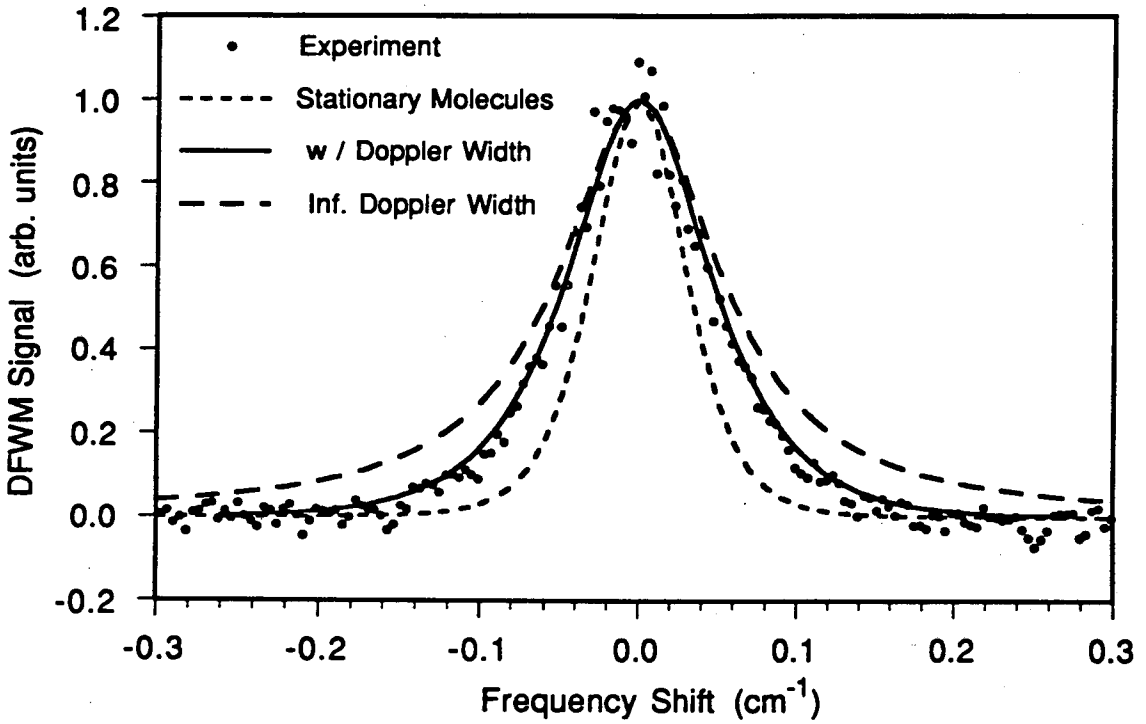

Fig. 1. The DFWM spectral profile of the $R_1(9)$ $A^2\Sigma^+ \rightarrow X^2\Pi(0,0)$ transition of OH measured in a hydrogen/oxygen flame. The measured data (symbols) are shown with three predictions of the two-level model: 1) for stationary molecules (short dashes), 2) for nonstationary molecules (solid line) and 3) in the infinite Doppler limit (long dashes).

In more recent experiments, we have measured the NDFWM spectral profiles of a number of OH transitions. NDFWM spectra are acquired by tuning the probe laser while the pump lasers are held fixed and reveal the lifetimes (T_1) of the processes that contribute to the DFWM spectra. The NDFWM spectrum of the $R_1(9)$ transition is shown in Fig. 2 for the case in which all of the lasers were parallel polarized. The narrow feature at line center is not observed when the probe-laser polarization is rotated by 90 degrees. This feature provides strong evidence for a long-lived contribution to the signal and only appears when the pump and probe laser fields produce an intensity grating at their intersection. We

conclude that this contribution is a direct consequence of collisional quenching of excited-state OH molecules to long-lived vibrationally-excited ground states. These molecules are thus removed from the probed rotational manifold and form a depletion grating that can be relaxed only by vibrational relaxation or diffusion. The fit shown in Fig. 2 is derived from perturbation theory calculations and includes a separate contribution to account for the long-lived component. This line shape is similar to that developed for NDFWM in atomic sodium vapor[3,4] in which long-lived population gratings are also observed.

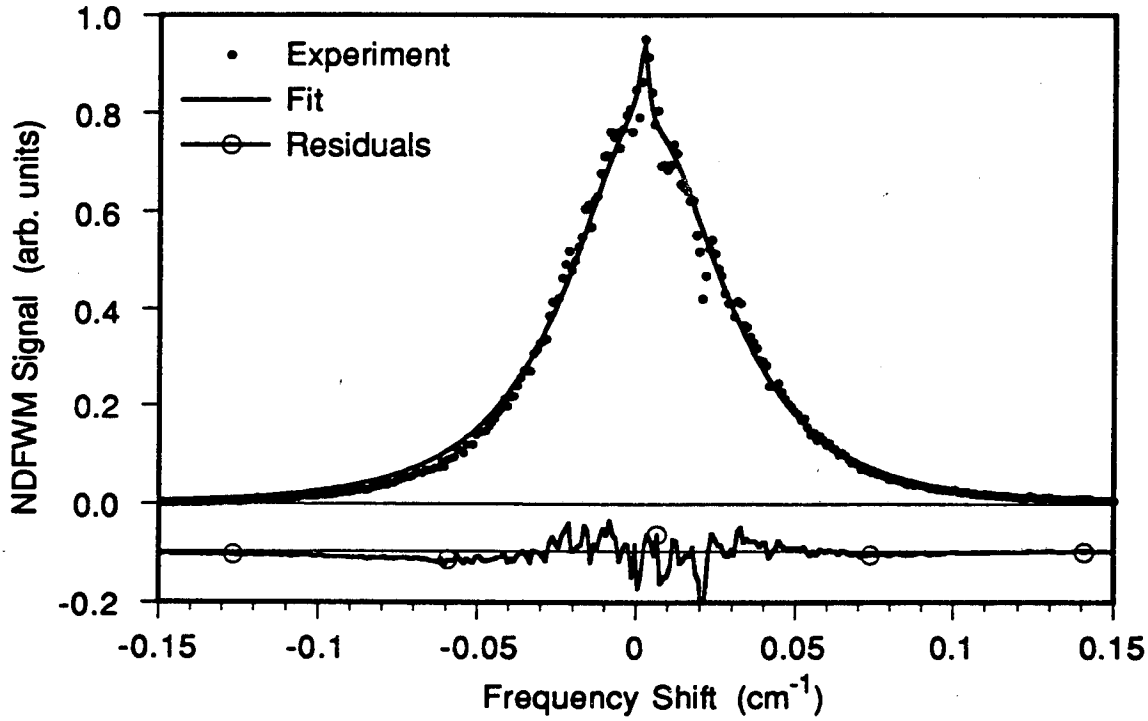

Fig. 2. The NDFWM spectral profile of the $R_1(9)$ $A^2\Sigma^+ \rightarrow X^2\Pi(0,0)$ transition of OH measured in a hydrogen/oxygen flame. All laser polarizations are parallel. The measured data (filled symbols) are shown with the perturbation-theory fit for nonstationary molecules (solid line) with the difference between theory and experiment (solid line with open symbols) plotted at the bottom. The narrow feature at line center is evidence for a long-lived population-grating contribution to the signal

*Molecular Physics Lab., PS 061, SRI International, 333 Ravenswood Ave., Palo Alto, CA 94025.

REFERENCES

1) Michael S. Brown , Larry A. Rahn and Thomas Dreier, Opt. Lett. **17**, 76 (1992).
2) R. L. Abrams, J. F. Lam, R. C. Lind, D. G. Steel and P. F. Liao, in *Optical Phase Conjugation*, R. A. Fisher ed. (Academic Press Inc., New York, 1983).
3) L. J. Rothberg and N. Bloembergen, Phys. Rev. A **30**, 2327 (1984).
4) P. R. Berman, D. G. Steel, Galina Khitrova and Jing Liu, Phys. Rev. A **38**, 252 (1988).

Future Plans

The NDFWM experiments on OH will continue in the a variable-pressure flame. Pressure and collision-partner studies in this flame will help elucidate the nature of the population grating effects and will allow the development of a complete model for the mechanisms and line shapes for DFWM. Studies on other states and or molecules with a predissociative excited state will be performed. Also, cross-population (one pump beam at a different resonance frequency) studies will be made in an attempt to separate excited and ground-state lifetime measurements.

Inverse Raman (IRS) experiments will continue with emphasis on H_2 and O_2 line-broadening studies. The effort to develop a comprehensive description of H_2 line profiles in combustion gases will continue, with further measurements on speed-dependent profiles and foreign-gas broadening of H_2. IRS studies of collisional broadening of the O_2 Q will be initiated in a new internally-heated pressure vessel. We will also initiate a program to measure pure-rotational S-branch broadening coefficients for H_2 and O_2. Some of the O_2 studies will be performed in a planned collaboration with G. Millot and B. Lavorel (Dijon, France). We will also pursue semiclassical line-broadening calculations in collaboration with J. P. Looney (NIST) using the theory of J. Bonamy and D. Robert.

L. A. Rahn: BES-Supported Research Publications 1990-92

Robert P. Lucht, Rick Trebino, and L. A. Rahn, "Resonant Multiwave Mixing Spectra of Gas-Phase Sodium: Nonperturbative Calculations,"Phys. Rev. A., accepted.

L. A. Rahn, Michael S. Brown and Thomas Dreier, "High-Resolution Degenerate Four-Wave-Mixing Spectral Profiles of OH," Opt. Lett. **17**, 76 (1992).

L. A. Rahn, R. L. Farrow, and G. J. Rosasco, "Measurement of the Self-Broadening of the H_2 Q(0-5) Transitions from 295 to 1000 K," Phys. Rev. A **43**, 6075 (1991).

J. E. M. Goldsmith and L. A. Rahn, "Doppler-Free Two-Photon-Excited Fluorescence Spectroscopy of Atomic Hydrogen in Flames," Opt. Lett. **15**, 814 (1990).

L. A. Rahn and G. J. Rosasco, "Measurement of the Density Shift of the H_2 Q(0-5) Transitions from 295 K to 1000 K," Phys. Rev. A, **41**, 3698 (1990).

R. Trebino and L. A. Rahn, "Calculation of Higher-Order Wave-Mixing Spectra," Opt. Lett. **15**, 354 (1990).

D. A. Greenhalgh and L. A. Rahn, " Temperature and pressure Dependence of the ν_1 Band of Water Vapour by High-Resolution Inverse Raman Spectroscopy," J. Raman Spectros. **21**, 847-855 (1990).

REACTIONS OF CARBON ATOMS USING PULSED MOLECULAR BEAMS

Hanna Reisler
Department of Chemistry, University of Southern California,
Los Angeles, CA 90089-0482

The objective of this research program is to elucidate the dynamics of the reactions of carbon atoms with simple molecules. Detailed studies of carbon atom reactions have been hindered by the absence of good, clean sources of $C(^3P)$ and $C(^1D)$. In contrast to the corresponding reactions of ground-state $O(^3P)$, relatively few studies have examined reactions of $C(^3P)$, due mainly to difficulties in source preparation. Therefore, prerequisite to dynamical investigations is the development of adequate sources and their characterization. Laser ablation of graphite promises to be an efficient and relatively clean source of $C(^3P)$. The reaction of $C(^3P)$ with N_2O is studied at a collision energy of 0.9 ± 0.4 eV in a crossed, pulsed molecular beam arrangement using laser ablation for carbon atom production. Nascent $CN(X^2\Sigma^+)$ and $NO(X^2\Pi)$ products are detected by laser induced fluorescence (LIF).

Assuming the validity of spin conservation and symmetry correlation rules and an intermediate of C_S symmetry, the reaction of ground state atomic carbon with nitrous oxide may proceed through the following allowed pathways:

$$C(^3P_J) + N_2O(\tilde{X}^1\Sigma^+) \rightarrow CO(a^3\Pi) + N_2(X^1\Sigma^+) \quad \Delta H = -3.41 \text{ eV} \quad (1)$$
$$\rightarrow CO(X^1\Sigma^+) + N_2(B^3\Pi) \quad \Delta H = -2.07 \text{ eV} \quad (2)$$
$$\rightarrow CN(X^2\Sigma^+) + NO(X^2\Pi) \quad \Delta H = -2.88 \text{ eV} \quad (3)$$
$$\rightarrow CN(A^2\Pi) + NO(X^2\Pi) \quad \Delta H = -1.47 \text{ eV} \quad (4)$$

Chemiluminescence from the electronically excited products of reactions (1) and (2) has not been observed, while $CN(A \rightarrow X)$ chemiluminescence from reaction (4) remains a source of controversy.

The crossed molecular-beam apparatus employed in these studies consists of an octagonal stainless steel reaction chamber and an ablation chamber containing the carbon source, each separately pumped by a liquid-nitrogen trapped diffusion pump, giving average background pressures with both beams on of $\leq 3 \times 10^{-5}$ Torr and $\leq 8 \times 10^{-5}$ Torr for the source and main chambers, respectively. The atomic beam is generated by free laser ablation of a spectroscopic-grade graphite rod. The free ablation produces a pulsed beam of short temporal duration (10-20 μs FWHM) at the interaction region, which is translationally 'hot' compared to beams produced by atom entrainment in the expansion of a carrier gas from a pulsed nozzle. In this work, approximately 20 mJ of 355 nm radiation from a Nd:YAG laser (14 ns FWHM) is focused to a 1-mm spot at the graphite rod surface with a 50-cm fused silica lens. To ensure good shot-to-shot stability the rod is maintained in constant helical motion. The neutral beam is generated by expansion of a 10% mixture of N_2O in He through the 0.5-mm orifice of a pulsed nozzle (150 μs) at a typical stagnation pressure of 10 psig (0.7 atm). The nozzle is oriented perpendicular to the atomic beam centerline. The experimental timing sequence is controlled by a master pulse/delay generator with 10-ns resolution. Pulses from this generator trigger the pulsed nozzle and the ablation laser so that the carbon and N_2O beams overlap temporally at the center of the

chamber. The probe laser pulse is delayed by 15 μs with respect to the ablation pulse. In the current experimental geometry, the probe laser beam propagates in a direction orthogonal to the photomultiplier tube (PMT) axis and oriented at 45° to the axis of the atomic beam and 90° to the molecular beam.

LIF signals were obtained for both $CN(X^2\Sigma^+)$ and $NO(X^2\Pi)$. A typical $CN(B^2\Sigma^+ - X^2\Sigma^+)$ LIF spectrum, corrected for probe power variations, showing the $\Delta v = -2$ sequence is displayed in Fig. 1. The CN product is rotationally and vibrationally 'hot' with bandheads of $v \leq 7$ clearly identified and the maximum population is in $v = 3$. The observed rovibrational excitation is in good agreement with the work of Costes *et al.* [1] who, using the $\Delta v = -1$ sequence, reported rotational temperatures up to 11,000 K (based on mean energies) and an inverted vibrational distribution which peaked at $v = 3$ and extended to $v = 6$. The $\Delta v = -2$ progression allows the detection of higher vibrational levels due to reduced spectral conjestion. We find that rotational levels ≤ 60 are significantly populated and easily identified for $v = 0$ and 1.

In this work, state-resolved detection of $NO(X^2\Pi)$ is reported for the first time. In analogy to CN, a high degree of rotational excitation is observed with levels in excess of $J = 60.5$ being detected. The rotational distribution for the $v = 0$ level of $NO(^2\Pi_{1/2})$ is displayed in Fig. 2, and a similar distribution is obtained for $NO(^2\Pi_{3/2})$. The distribution is inverted with a maximum population in $J = 49.5$. The vibrational population in $v = 0{:}1{:}2$ was found to be 1:0.45:0.12. These ratios have been corrected for the Franck-Condon factors associated with both excitation and emission to $v'' = 0$-7 convoluted with the wavelength response of the filter/PMT combination.

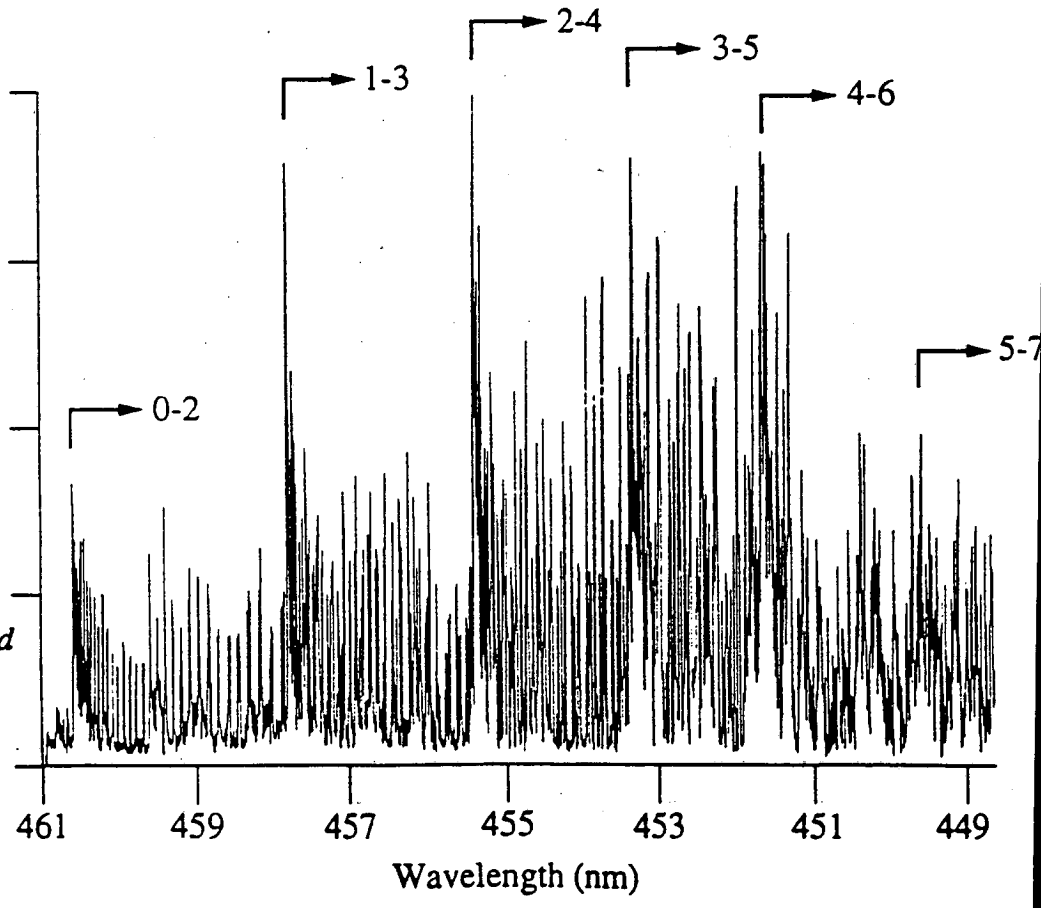

Fig. 1. Nascent $CN(B^2\Sigma^+ - X^2\Sigma^+)$ LIF spectrum observed from the reaction of $C(^3P)$ with N_2O. The $\Delta v = -2$ sequence was excited.

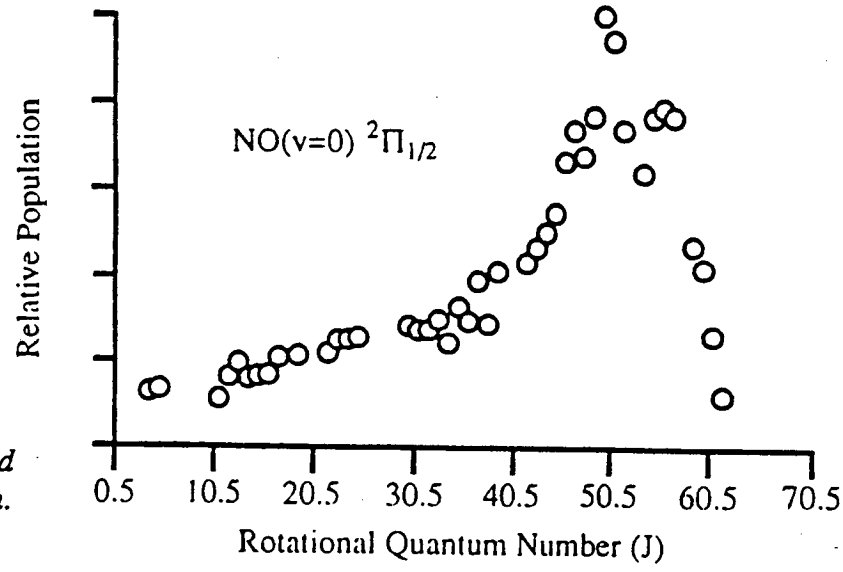

Fig. 2. Nascent rotational distribution of the v = 0 level of NO($^2\Pi_{1/2}$) produced in the C(^{3}P) + N_2O reaction.

The velocity of the molecular beam is taken to be ~ 1500 m s^{-1} (10% N_2O/He) and that of the C(^{3}P) is estimated in the range 3000-5000 m s^{-1} from the appearance time of the signal and the translational distributions determined by time-of-flight following 351 nm graphite ablation [2]. E_{trans} is thus estimated to be 0.9 ± 0.4 eV. Since N_2O is cooled to ~ 10 K in the supersonic expansion, E_{int} is negligible and we estimate that E_{avail} = 3.9 ± 0.4 eV.

The CN excitation limit observed by Costes *et al.* and ourselves suggests that nearly half of E_{avail} is deposited as internal energy of CN. Of the remaining ≥ 50%, significantly less appears as internal excitation of the NO fragment, which is formed vibrationally cool; $\langle f_v \rangle \approx 5\%$ while $\langle f_R(NO) \rangle \approx \langle f_R(CN) \rangle$, where f_i is the fraction of energy deposited in the ith degree of freedom. Such nonstatistical energy partitioning with one vibrationally 'hot' and one vibrationally 'cold' product is indicative of a reaction mechanism with substantial 'direct' character. However, in the C(^{3}P) + N_2O reaction the NO species is not a true spectator, since some level of energy flow into the N-O bond occurs. This suggests an attractive interaction between the CN and NO and the formation of a short lived intermediate which falls apart before complete energy randomization over all internal degrees of freedom. At the large collision energies employed in this work we suggest that the C(^{3}P) + N_2O reaction is predominantly direct and attractive in nature although exhibiting some indirect character. An interaction between CN and NO, induced by the presence of the well corresponding with the CNNO complex intermediate, allows some transfer of energy into the NO bond before the fragments separate permanently. Such compex effects are well known on attractive surfaces.

For this reaction, the large reduced mass, high collision energy, and large range of reactive impact parameters (evidenced by the large reaction cross section) suggest that fragment rotational excitation is not restricted by reactant orbital angular momentum, $L=\mu vb$. Rather, the fraction of angular momentum appearing as product rotation is determined by details of the PES, namely the anisotropy in the potential or the geometry of the reactive path. The 'hot' rotational distributions observed suggest a non-linear intermediate such that forces acting towards fragmentation impart a torque on the departing radicals.

The reaction of $C(^3P)$ with N_2O can yield $NO(X^2\Pi)$ via two pathways corresponding to CN in its ground ($X^2\Sigma^+$) and first excited ($A^2\Pi$) states. The NO rotational excitations obtained in this work show no evidence for the involvement of two reaction channels. For example, no bimodality in the rotational distributions is observed, which might be expected if reaction (4), with 1.41 eV less available energy, was important.

Future Plans

Although this work has gone some way in elucidating the reaction dynamics, it is apparent that many questions still remain. Investigation of the effect of translational energy on intermediate lifetime and thus relative energy deposition in the reaction fragments is the first on our list. Therefore, we have implemented a second configuration for graphite ablation where the carbon vapor is entrained by He from a second pulsed nozzle. In order to obtain high intensities of the atomic constituent, we found it necessary to use He pulses of short duration (< 40 μs). Analysis of product fine-structure components and determination of vector correlations are presently in progress in our laboratory. Our future plans also include studying endothermic reactions of $C(^3P)$ with vibrationally excited reactants. An optical parametric oscillatore (OPO) which uses $LiNbO_3$ crystals has been constructed and yields 3-15 mJ at 2700-6800 cm^{-1}. An OPO based on BBO crystals is now under construction and is expected to yield higher conversion efficiencies and damage thresholds in the wavelength range 410-2700 nm.

References:

[8] M. Costes, C. Naulin, G. Dorthe and Z. Moudden, Laser Chem. 10 (1990) 367.

[14] R.W. Dreyfus, R. Kelly and R.E. Walkup, Nucl. Inst. and Meth. B23 (1987) 557.

DOE Supported Publications 1990-1992:

[1] *Identification of the 278.2 nm peak of the CCl $A^2\Delta$-$X^2\Pi$ system as the O-O P_1 bandhead*, D.C. Robie, J. de Juan and H. Reisler, J. Molec. Spectrosc., **150**, 296 (1991).

[2] *A crossed beam study of the reaction $C(^3P)+N_2O$: Energy partitioning between the NO and CN products* , S.A. Reid, F. Winterbottom, D.C. Scott, J. de Juan and H. Reisler, Chem. Phys. Lett. **189**,430 (1992).

[3] *The reactions of $C(^1D)$ with H_2 and HCl: Product state excitations, Λ-doublet propensities and branching ratios*, D.C. Scott, J. de Juan, D.C. Robie, D.M. Schwarz-Lavi and H. Reisler, J. Phys. Chem., in press (1992)

Spectroscopic Probes of Vibrationally Excited Molecules at Chemically Significant Energies

Thomas R. Rizzo

Department of Chemistry
University of Rochester
Rochester, NY 14627

This project involves the development and application of new spectroscopic techniques for investigating small polyatomic molecules with chemically significant amounts of vibrational energy. Highly excited species produced by exothermic reactions in combustion processes sample high energy regions of their potential energy surface, and a better understanding of the surface topology and bond dissociation energies will allow more accurate models of their dissociation dynamics.

Double Resonance Overtone Spectroscopy and State-to-State Dynamics of H_2O_2

We have in the last year completed our analysis of the rotationally resolved overtone transitions to states above the unimolecular dissociation threshold.[7,8] The dependence of the spectra on the rotational quantum numbers J, and K help determine the nature of the couplings that cause redistribution of the initial excitation energy prior to dissociation. Highly resolved overtone transitions to predissociative levels also indicate that near threshold, the relative timescales of IVR and unimolecular dissociation do not differ as much as statistical theories of unimolecular dissociation assume.

We have also completed analysis of product energy partitioning data from 36 different H_2O_2 rovibrational states ranging in energy from 3–2000 cm^{-1} above the unimolecular dissociation threshold.[9] These results indicate that while the predictions of Phase Space Theory are in reasonable agreement with our measured product distributions, clear deviations from statistical behavior do exist. This result suggests that for molecules as small as H_2O_2, the density of states is sufficiently small that statistical theories may not apply as well as to larger systems. The state-specific data that we have obtained provides a stringent test of calculated potential energy surfaces of H_2O_2 as well as dynamical calculations carried out on such surfaces.

Double Resonance Overtone Spectroscopy of HN_3

We have recently begun to apply our infrared-optical double resonance technique to investigate the unimolecular dissociation dynamics of hydrazoic acid (HN_3). The dissociation dynamics of this molecule are expected to be fundamentally different from that of H_2O_2 insofar as a curve crossing between the ground state and a low lying dissociative excited state can lead to dissociation via a spin forbidden channel to produce NH ($^3\Sigma$) + N_2. At sufficiently high energies on the ground potential surface, there is a competition between dissociation on the spin allowed singlet surface and spin forbidden triplet surface which is sharply dependent upon the reactant energy. Moreover, the topology of the exit channel on the singlet surface is not well characterized. There appears to be a barrier along the coordinate to produce NH($^1\Delta$) + N_2, however estimates of this barrier range from 450 to 1740 cm^{-1}.

We have begun to perform both infrared-optical and optical-infrared double resonance studies of this molecule to investigate its dissociation dynamics on both the singlet and triplet surface. Figure 1 shows

the simplification achieved in the $6v_{NH}$ overtone spectrum using the former approach.

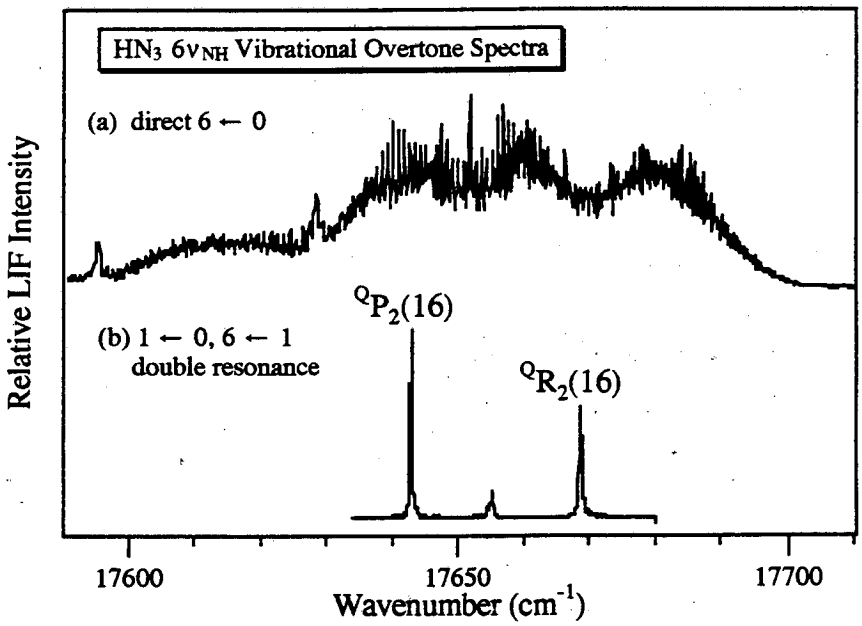

Figure 1
$6v_{NH}$ vibrational overtone excitation spectra of HN_3 recorded by (a) direct overtone excitation; (b) infrared-optical double resonance

To date we have obtained simplified vibrational overtone spectra of both the $5v_{NH}$ and $6v_{NH}$ vibrational overtone bands and are in the process of assigning these spectra. We are also attempting to access combination bands containing $6v_{NH}$ and one quantum of low frequency vibration which will put HN_3 molecules right at the energy of the barrier on the singlet surface. Observing which reactant states are actually above the barrier and measuring the product state distributions will help us determine the barrier height.

Vibrational Overtone Spectroscopy of Jet-Cooled Molecules

We have recently developed a technique that allows the detection of vibrational overtone transitions to non-dissociative levels in low pressure environments where spectral simplification methods are applicable.[10] This approach uses infrared multiphoton dissociation (IRMPD) of the vibrationally excited molecules produced after overtone excitation. Spectroscopic detection (of the overtone absorption) is achieved by monitoring dissociation products *via* LIF. This method relies on our ability to selectively dissociate vibrationally excited molecules *via* IRMPD without dissociating the large excess of ground state molecules. We have demonstrated such selectivity in preliminary experiments on CH_3OH cooled in a supersonic free jet. Our initial results show that the Δv_{OH}=4 and Δv_{OH}=5 vibrational overtone transitions, which have widths of 100-150 cm^{-1} when recorded by room temperature photoacoustic spectroscopy, are broadened primarily by thermal inhomogeneous spectral congestion. While initial applications of this approach have been to measure direct overtone spectra in a supersonic free jet, it should also lend itself to detecting infrared-optical double resonance overtone excitation.

Future Plans

In the coming year we plan to apply infrared-optical double resonance to examine the dissociation dynamics of HOCl and HONO. The former is a small enough system that is should be amenable to *ab initio* potential energy surface calculations as well as high level dynamical calculations on such a surface. Our studies will be aimed at precisely determining the bond dissociation energy and probing the potential surface topology along the dissociation coordinate.

The HONO molecule can exist in cis- and trans- forms and is a prototype system for isomerization reactions. We plan to use infrared optical double resonance to probe the dynamics of unimolecular isomerization at the v=1 and v=2 levels of the OH stretch.

Publications from DOE Supported Work 1990-92

1. X. Luo and T. R. Rizzo. "Rotationally Resolved Vibrational Overtone Spectroscopy of Hydrogen Peroxide at Chemically Significant Energies." J. Chem. Phys. **93**, 8620 (1990).

2. X. Luo, P. R. Fleming, T. A. Seckel and T. R. Rizzo. "Broad Vibrational Overtone Linewidths in the $7\nu_{OH}$ Band of Rotationally Selected NH_2OH." J. Chem. Phys. **93**, 9194 (1990).

3. X. Luo and T. R. Rizzo. "Unimolecular Dissociation of Hydrogen Peroxide from Single Rovibrational States Near Threshold." J. Chem. Phys. **94**, 889 (1991).

4. P. R. Fleming, M. Li and T. R. Rizzo. "Infrared Spectroscopy of Vibrationally Excited $HONO_2$: Shedding Light on the Dark States of IVR." J. Chem. Phys. **94**, 2425 (1991).

5. P. R. Fleming, M. Li and T. R. Rizzo. "Local Modes of HOOH Probed by Optical-Infrared Double Resonance." J. Chem. Phys. (in press) (1991).

6. P. R. Fleming and T. R. Rizzo. "Infrared spectrum of t-butyl hydroperoxide excited to the $4\nu_{OH}$ vibrational overtone level." J. Chem. Phys. **95**, 1461 (1991).

7. P. R. Fleming, X. Luo, and T. R. Rizzo,"Multiple Laser Probes of Intramolecular Dynamics at Chemically Significant Energies", in *Mode Selective Chemistry*, B. Pullman and J. Jortner, eds., (Kluwer, Dordrecht, 1991).

8. X. Luo and T. R. Rizzo, "Vibrational overtone spectroscopy of the $4\nu_{OH}+\nu_{OH'}$ combination band of HOOH via sequential local mode-local mode excitation." J. Chem. Phys. **96**, (in press) (1992).

9. X. Luo and T. R. Rizzo, "Product Energy Partitioning from the Unimolecular Decomposition of Vibrationally and Rotationally State Selected Hydrogen Peroxide." J. Chem. Phys. **96**, (in press) (1992).

Submitted:

10. R. D. F. Settle and T. R. Rizzo, "A new approach to vibrational overtone spectroscopy of jet-cooled molecules: Application to CH3OH.", J. Chem. Phys. , (submitted) (1992).

Spectroscopy and Reactivity of Carbonaceous Clusters

Eric A. Rohlfing
Combustion Research Facility
Sandia National Laboratories
Livermore, CA 94551

This program emphasizes two different areas of research on carbon (C_n) and carbonaceous (C_nX_m , X=H or Si) clusters that are differentiated both by the size of the clusters ($n \leq 3$ versus $n \geq 6$) and the focus of the research (molecular spectroscopy versus chemical reactivity). We create the clusters by laser vaporization of a substrate into an inert-gas atmosphere in the throat of a pulsed nozzle. Subsequent free-jet expansion then provides an ideal environment for spectroscopic studies of small transient molecules and for the formation of molecular beams of clusters that can be probed with photoionization/mass spectrometry. Our spectroscopic studies focus on molecules that show unusual intramolecular dynamics on the ground-state potential energy surface. The emphasis of our cluster reactivity studies is on the chemistry of species that may be precursors to fullerenes or soot in combustion.

(1) Molecular Spectroscopy

We have completed a spectroscopic study of the somewhat elusive SiC radical. We generate SiC by adjusting the conditions in the laser-vaporization source so that the laser-generated plasma is less well constrained by the carrier gas. This enhances production of SiC relative to the more stable SiC_2. The SiC radical produced under these nonequilibrium conditions is vibrationally hot because it undergoes fewer collisions with helium in the flow channel but is rotationally cool (~40 K) due to the free-jet expansion. We use vibrational-band selected laser-induced fluorescence to measure the first nine cold rovibronic bands of the SiC C $^3\Pi$-X $^3\Pi$ system (v'=0-8; v"=0) and the (2,1), (0,2), (2,3), (2,4), and (2,5) hot bands. Each spectrum is assigned using the method of combination differences and least-squares fit to a $^3\Pi$–$^3\Pi$ Hamiltonian. Vibrational term energies and rotational constants are determined for v'=0-8 of the C state and for v"=0-5 of the X state.

Resonant four-wave mixing (RFWM) spectroscopy has recently been applied to a variety of chemically interesting problems in the gas phase. Vaccaro and co-workers (J. Chem. Phys.**96**, 1640 (1992)) used a degenerate four-wave mixing (DFWM) detection method to obtain background-free stimulated-emission pumping (SEP) spectra of CS_2 in a static cell. In a similar vein, Hayden and co-workers used two-color laser-induced grating spectroscopy (LIGS) to generate SEP spectra of room-temperature I_2 (see abstract by Hayden and Chandler). We have successfully applied DFWM to obtain excitation spectra of C_3 and SiC_2 and two-color LIGS to produce background-free SEP spectra of SiC_2. These transient molecules are produced with a laser-vaporization source and are probed in a free jet where $N \sim 10^{12}$ cm^{-3} per rotational state. SiC_2 is of current interest to us because it should display large-amplitude pseudorotation that samples the nearly isoenergetic cyclic and linear isomers in the ground state.

Two-color LIGS is an example of RFWM in which two pump beams at ω_1, resonant with one transition, interact with a probe beam at ω_2, resonant with another transition, to generate a signal beam at ω_2. In induced-grating terminology, the two pump beams interfere to form a modulated intensity pattern that leads to a spatial modulation of the complex index of refraction. The strength of the induced grating is dominated by the change in absorption coefficient due to the transfer of population from the ground to the excited state. The probe beam may scatter off of either of two such population gratings: one in the excited state and one in the depleted ground state. When the probe laser is scanned across a transition from the excited state down to another level in the ground state, the two-color LIGS spectrum maps an SEP spectrum. Fig. 1 shows a comparison of SEP spectra taken for SiC_2 using two-color LIGS and the conventional technique, in which dump transitions are detected as dips in the pump-laser-induced fluorescence. These spectra illustrate the tremendous advantage of background-free two-color LIGS for SEP spectroscopy on SiC_2. The fluorescence-dip spectrum is heavily saturated; the strong lines are significantly broadened and weak rotational lines are observed. The two-color LIGS spectrum was obtained with only ~5μJ/pulse in the probe beam and shows no saturation. Two-color LIGS is constrained by phase matching, i.e. for a given probe-beam angle there is only probe frequency at which perfect phase matching occurs. However, the effect of phase mismatch is small in our experiments because of the shallow crossing angles (~1°) and the short interaction length (~1 cm) in the free jet. We observe LIGS signals at probe frequencies separated by ~900 cm^{-1} without adjustment of the probe-beam angle. Our results for C_3 and SiC_2 demonstrate that RFWM has the potential to be a valuable spectroscopic tool for the study of jet-cooled transient molecules.

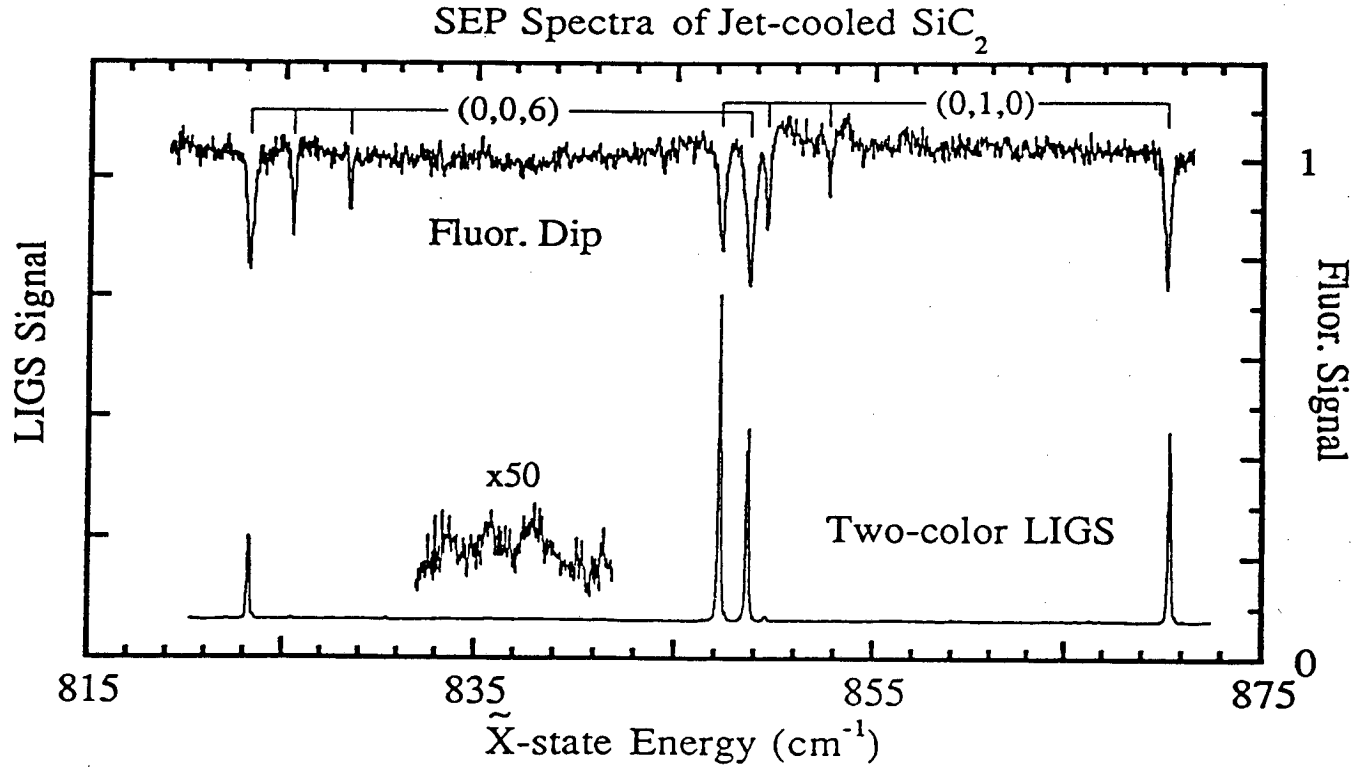

FIG. 1 A comparison of SEP spectra of the $\tilde{A}\,^1B_2$ - $\tilde{X}\,^1A_1$ band system of SiC_2 in a free jet obtained by fluorescence dip and two-color LIGS. The fluorescence-dip spectrum is an average of 10 laser shots per frequency increment and the LIGS spectrum is a 5-shot average. The pump excites the $^rR_2(2)_{e,o}$ rotational line. Ground-state vibrational assignments are shown; the rotational lines terminate on the $2_{21,20}$, $3_{22,21}$, $4_{23,22}$, and $4_{41,40}$ levels, in order of increasing energy.

(2) Chemical Reactivity

We have completed a study of the hydrogenation reactions of neutral carbon clusters, C_n+D_2, over a wide range of cluster sizes, n=6-75. Clusters are created by pulsed laser vaporization of graphite and react with D_2 in a pulsed, fast-flow reactor. After supersonic expansion and collimation the cluster reactants and products are photoionized by 118.2-nm light that is generated by frequency tripling the Nd:YAG third harmonic at 355 nm in a static xenon cell. The photoions are mass analyzed via high-resolution time-of-flight mass spectrometry using an angular reflectron. The observed ion signals provide information both on the decay of the C_n reactants and on the formation of the C_nD_m products. Fig. 2 shows examples of the kinetics of C_n decay and C_nD_m appearance for n=25 and 26. From the product appearance kinetics, we conclude that C_nD_m are formed via sequential D-atom addition and that, in some cases, loss of carbon may accompany hydrogenation. For example, more products appear in the n=25 channel than can be accounted for by the decay of C_{25}. The C_{2n} for $n\leq20$ show a preference for formation of C_nD_2, consistent with production of long-chain polyacetylenes. From fits to the decay of C_n signals, we determine the relative rate for the overall reaction as a function of cluster size; these are shown in Fig. 3. The observed drop in reactivity for C_{2n} near n=18 correlates well with the onset of the closed-shell fullerenes. The clusters produced in our laser-vaporization source are quite hot; optical pyrometry on the soot emanating from the source gives $T\leq2800$ K. At this temperature the differences in rate constants between C_n isomers (chains, rings, fullerenes) may be washed out due to the large amount of internal energy available to surmount activation barriers.

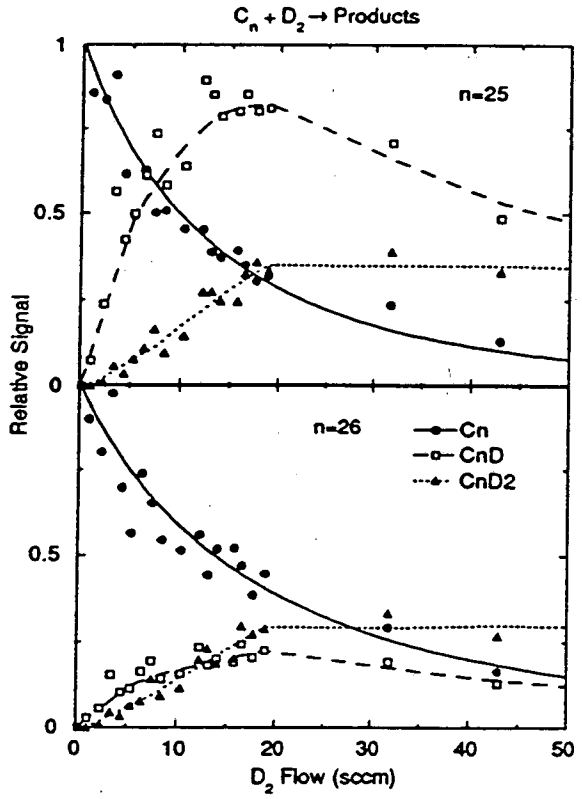

FIG. 2 Plots of the ion signals of C_n reactants and C_nD and C_nD_2 products as a function of D_2 flow rate for n=25 and n=26. The solid lines are fits to the decays of C_n (solid points); the dashed and dotted lines are not fits, but are drawn to aid in following the C_nD and C_nD_2 signals, respectively.

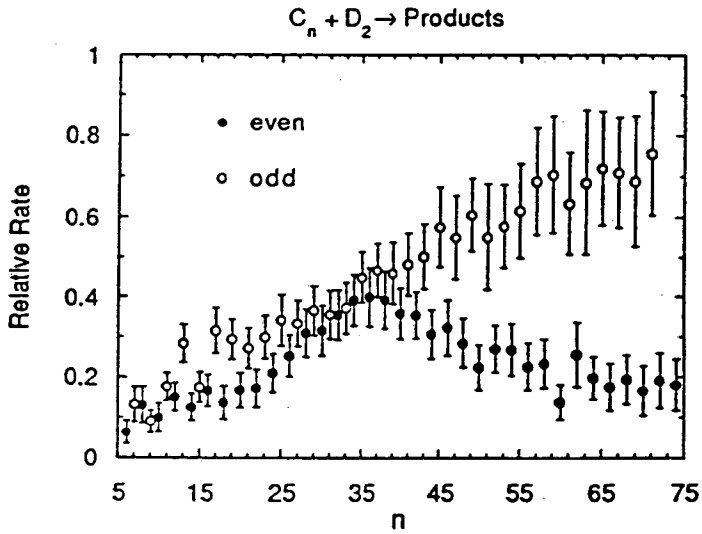

FIG. 3 The relative reaction rate for C_n+D_2 versus cluster size, n, obtained by exponential fits to the decays of the C_n signals. A relative rate of 1.0 corresponds to a bimolecular rate constant of 1×10^{-12} cm^3s^{-1} at an estimated temperature of $T\leq2800$ K.

(3) Future Work

Future work in this program will emphasize a more detailed understanding of the large-amplitude vibrational motion of SiC_2 through the use of SEP to levels near and above the barrier to pseudorotation. Two-color LIGS will be the method of choice for this work and we shall devote effort to the full development of this technique. We shall also continue our spectroscopic studies of other small C_n and C_nH_m transient molecules. The chemical reactions of carbon and carbonaceous clusters will be pursued using the fast flow reactor/TOF MS apparatus; greater control of the cluster temperature in the flow tube will be a high priority. We shall emphasize reactions of carbonaceous clusters with hydrocarbons since these might be prototypes for reactions that lead to fullerenes or soot in combustion.

Publications: 1990-present

T. J. Butenhoff and E. A. Rohlfing, "Resonant Four-Wave Mixing Spectroscopy of Transient Molecules in Free Jets," J. Chem. Phys., submitted (1992).

T. J. Butenhoff and E. A. Rohlfing, "Hydrogenation Reactions of Neutral Carbon Clusters: C_n (n=6-75) + D_2," Twenty-Fourth International Symposium on Combustion, accepted (1992).

T. J. Butenhoff and E. A. Rohlfing, "The C $^3\Pi$ - X $^3\Pi$ Band System of the SiC Radical," J. Chem. Phys. **95**, 3939(1991).

T. J. Butenhoff and E. A. Rohlfing, "Laser-Induced Fluorescence Spectroscopy of Jet-Cooled SiC_2," J. Chem. Phys. **95**, 1(1991).

F. J. Northrup, T. J. Sears, and E. A. Rohlfing, "A Semirigid Bender Analysis of an Extensive Set of Rotation-Vibration Levels in $\tilde{X}\,^1\Sigma_g^+$ C_3," J. Mol. Spectrosc. **145**, 74 (1991).

E. A. Rohlfing, "High-Resolution Time-of-Flight Mass Spectrometry of Carbon and Carbonaceous Clusters," J. Chem. Phys. **93**, 7851 (1990).

E. A. Rohlfing, "Stimulated Emission Pumping Spectroscopy of Jet-Cooled C_3: Antisymmetric Stretch-Bend Levels," J. Opt. Soc. Am. B **7**, 1915 (1990).

E. A. Rohlfing and D. W. Chandler, "Two-Color Pyrometric Imaging of Laser-Heated Carbon Particles in a Supersonic Flow," Chem. Phys. Lett. **170**, 44 (1990).

ELECTRONIC STRUCTURE, MOLECULAR BONDING, AND MOLECULAR POTENTIAL ENERGY SURFACES

Klaus Ruedenberg

Ames Laboratory-USDOE, Iowa State University, Ames, Iowa 50011

Program Scope

Accurate potential energy surfaces of ground and excited states, governing reactions between carbon, oxygen, nitrogen and hydrogen, are determined by ab-initio calculations. Global and critical features of such surfaces are elucidated. Energy changes are explained in terms of interactions between atoms.

Recent Progress

THE ELECTRONIC STATES OF OZONE

Because of the relevance of ozone for the life of our environment in general and for human health in particular, a knowledge of its energy states is of basic interest. Since experimental information is limited, the theoretical elucidation of its energy states can make useful contributions. An ab-initio study of its potential energy surfaces had been initiated by this research group in the past reporting period and has been continued in the present period.

Figure 1 shows the $^1A_1$ groundstate surface we established for O_3 in C_{2v} symmetry with the steepest descent path connecting the minima and saddle points. We extended this surface into the three-dimensional C_s region and established the transition states between the three equivalent minima. No transition state was found to exist for the abstraction of the central oxygen from the ring structure. Figure 2 contains contours of the $1^1A'$ and the $2^1A'$ surfaces in C_s in terms of coordinates explained below. Along the steepest descent path shown in Figure 1, we established the thirteen lowest singlet states so as to obtain an idea about this manifold. Figure 3 shows the correlation diagram of these states along this path. Noteworthy is that only the groundstate has a minimum for the ring structure; all excited singlet states are highly repulsive in this region. To produce the ground state experimentally in its ring structure by trickling down from excited states seems therefore difficult, an inference confirmed by past lack of success in such efforts. For the lowest five of these states (1^1A_1, 2^1A_1, $^1B_1$ $^1B_2$, $^1A_2$), the potential energy surfaces were determined in the entire relevant C_{2v} region and their minima found. We established that these C_{2v} minima are global minima in C_s only for 1^1A_1, 2^1A_1, $^1B_1$. They are transition states in C_s for $^1B_2$ and $^1A_2$. For the latter, we followed the steepest descent paths from these transition states into C_s in order to find minima in C_s, if any. However, all of them went directly towards the dissociation $O_3 \rightarrow O_2 +$

O. We conclude that no equilibrium structures exist for these states. Analogous investigations were initiated for the lowest triplet states, viz. $^3A_1$, $^3B_1$, $^3B_2$ and $^3A_2$.

Between the 1^1A_1 and 2^1A_1 states, an intersection point had been found in C_{2v} symmetry, as reported previously. We investigated the reason for this crossing of two states of like symmetry, a relatively rare occurrence to date, and showed it to be related to the fact that not only are the *adiabatic* states Ψ_1, Ψ_2 expressible as mixtures of two *diabatic* states Φ_1, Φ_2 which exchange dominance near the crossing but, *in addition, each of the diabatic states by itself suffers a change in the relative dominance between two constituent component configurations.*

Furthermore, since Teller's general theory implies that the intersection *point* found in C_{2v} symmetry must be a point on an intersection *seam* (i.e. a one-dimensional curve) in C_s symmetry, we determined this seam in its full length. It is a closed curve which is displayed in Figure 4, the first such curve ever determined. The coordinates used were $\xi_1 = X_1/X_3$, $\xi_2 = X_2/X_3$ and X_3, where

$$X_1 = (R_{23} - R_{13})/\sqrt{2}, \qquad X_2 = R_{23} + R_{13} - 2R_{12})/\sqrt{6}, \qquad X_3 = (R_{12} + R_{23} + R_{13})/2\sqrt{3}$$

with R_{ij} being the internuclear distances. The coordinates ξ_1, ξ_2 determine the angular shape of the molecule whereas X_3 determines its scale. The domain of possible (ξ_1,ξ_2) value covers the equilateral triangle shown in Figure 4. Since the intersection seam is a closed loop, it is seen to have a second point in C_{2v}. But at this point, the 2^1A_1 state, which becomes $2^1A'$ in C_s turns into $^1B_1$ in C_{2v}. It seems conceivable that an excitation to the $2^1A'$ state by a two-photon absorption might populate the groundstate ring structure by radiationless deexcitation through the intersection.

Future Plans

The study of the triplet state potential energy surfaces of ozone will be completed. The critical points, minima and transition states etc., on the various surfaces will be elucidated through an analysis of their electronic structures. The energy changes will be analysed in terms of interactions between the three atoms.

Publications Supported by this Program, 1990, 1991, 1992

Nonspherical Atom Densities and Chemical Deformation Densities from X-Ray Scattering. K. Ruedenberg and W. H. E. Schwarz, J. Chem. Phys., 92, 4956 (1990).

The Potential Energy Surface of the Ground State of Carbon Dioxide. S. S. Xantheas, S. T. Elbert and K. Ruedenberg, Chem. Phys. Letters, 166, 39 (1990).

An Intersection Seam between the Ground State of Ozone and an Excited State of Like Symmetry. K. Ruedenberg, S. Xantheas, S. T. Elbert, J. Chem. Phys., 93, 7519 (1990).

The Ring Opening of Cyclopropylidene to Allene: Global Features of the Reaction Surface. P. Valtazanos, S. T. Elbert, S. Xantheas, K. Ruedenberg, Theor. Chim. Acta, 78, 287 (1991).

The Ring Opening of Cyclopropylidene to Allene and the Isomerization of Allene: Ab-Initio Interpretation of the Electronic Rearrangements in terms of Quasiatomic Orbitals. S. Xantheas, P. Valtazanos, K. Ruedenberg, Theor. Chim. Acta, 78, 327 (1991).

The Ring Opening of Cyclopropylidene to Allene: Key Features of the Accurate Reaction Surface. P. Valtazanos, S. Xantheas, S. T. Elbert, K. Ruedenberg, Theor. Chim. Acta, 78, 365 (1991).

The Ring Opening of Substituted Cyclopropylidene to Substituted Allene: The Effect of Steric and Long Range Electrostatic Interactions. P. Valtazanos and K. Ruedenberg, Theor. Chim. Acta, 78, 397 (1991).

Potential Energy Surfaces of Ozone. S. Xantheas, G. J. Atchity, S. T. Elbert, K. Ruedenberg, J. Chem. Phys., 94 8054 (1991).

Potential Energy Surfaces Near Intersections. G. Atchity, S. Xantheas, and K. Ruedenberg, J. Chem. Phys. 95, 1862 (1991).

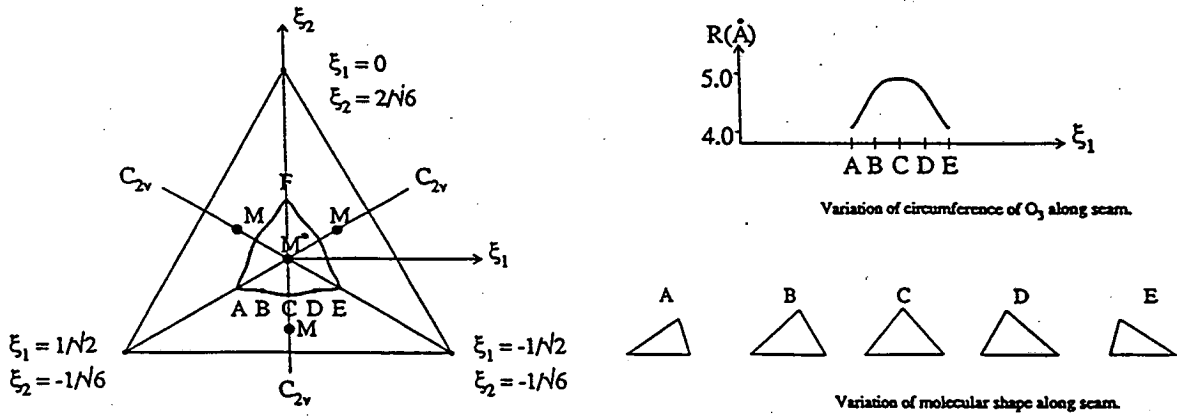

Figure 4. Intersection seam ABCDEFA between 1^1A_1 and 2^1A_1 states of O_3 in symmetric angular parameter triangle. M = open minima, M* = ring minimum.

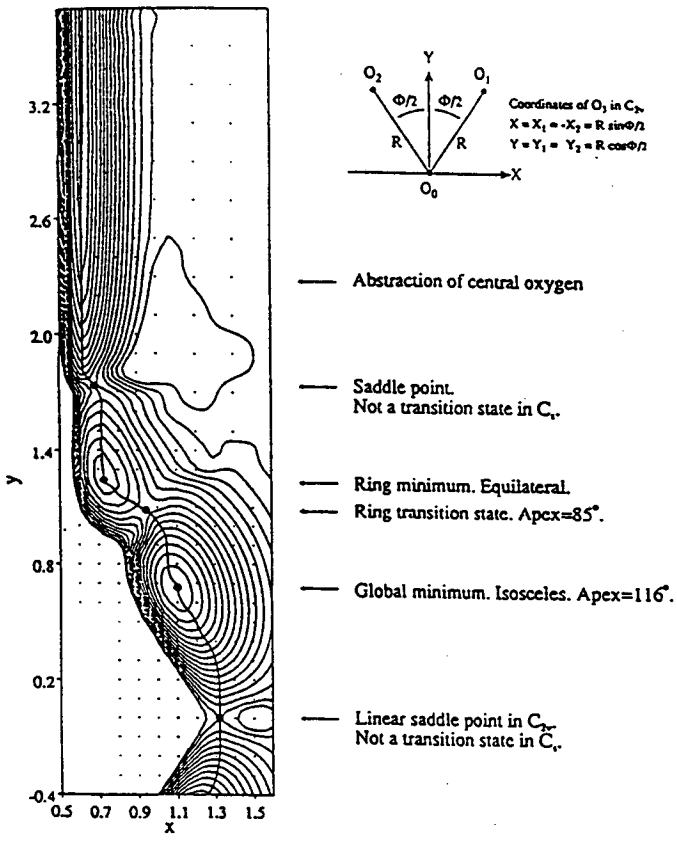

Figure 1. Full ground state potential energy surface of O_3 in C_{2v}. Coordinates defined at upper right. Heavy dots=critical points. Light points: Calculated grid. Heavy line=steepest descent line. Coordinates in Angstrom. Contour increment=0.01 hartree.

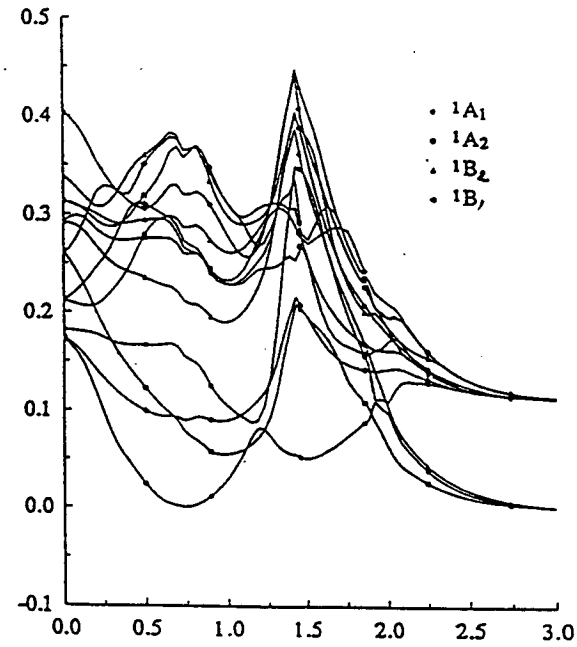

Figure 3. The thirteen lowest singlet states of O_3 along the steepest descent line depicted in Figure 1. Abscissa = path length along this line starting at the linear geometry in Angstrom. Ordinate = Energy difference (E+224.5538) in hartree with -224.5538 being the energy of the global minimum.

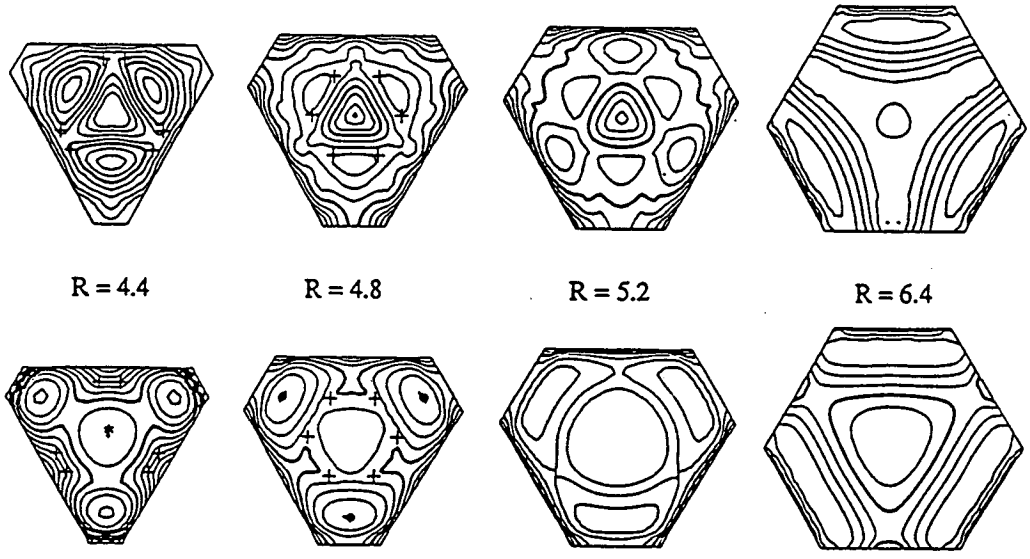

Figure 2. Energy contours of the lowest two $^1A'$ states of ozone. Lower row = ground state, upper row = excited state. On each panel the coordinates, namely ξ_1, ξ_2 with the origin in the center, describe the angular shape of the molecule. The corners of the parameter triangles, corresponding to the smallest bond length being smaller than one angstrom, have been deleted. Each panel corresponds to a fixed value of the molecular circumference R, as indicated. The heavy contours correspond to -224.400 hartree for the ground state and -224.325 for the excited state. The contour increment is 0.025 hartree on all panels. Ring minimum: •; open minima: •; points of intersection between the two surfaces: +.

Tetraethynylethylene, A Molecule with Four Very Short C-C Single Bonds. Interpretation of the Infrared Spectrum.

Buyong Ma, Yaoming Xie, and Henry F. Schaefer III
Center for Computational Quantum Chemistry
University of Georgia
Athens, Georgia 30602

The "enediynes" have been known for many years and are important species in chemistry and biochemistry. However, the attachment of additional acetylene substitutents to the central C=C double bond has proven to be challenging. Nevertheless, last year (1991) the ultimate cross-conjugated π-system tetraethynylethylene

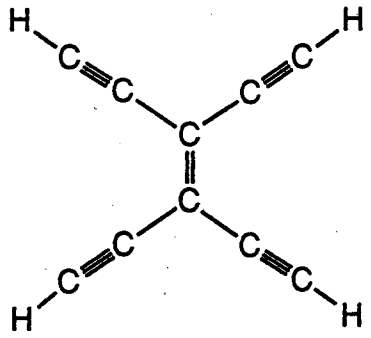

was finally synthesized, by Rubin, Knobler, and Diederich at UCLA. Tetraethynylethylene is fairly soluble in pentane and crystallizes out of this solvent at -10°C as white plates. Tetraethynylethylene is also the first $C_{10}H_4$ isomer to be prepared in the laboratory.

The tetra-substituted molecule with all four hydrogens replaced by trimethylsilyl (TMS) groups $(CH_3)_3Si$ was subjected to a crystallographic study by the UCLA group. Unfortunately, from the chemistry point of view, the structure appears to be very strongly influenced by crystal packing forces. Specifically two of the C-C single bond distances are 1.424Å, while the other two are 1.479Å. Similarly, two of the C≡C triple bond distances are 1.163Å, while the other two are 1.207Å. Presumably all four C-C distances are equivalent in the isolated molecule, as are all four C≡C distances. The solid state deviations of 0.055Å (single bonds) and 0.044 (triple bonds) are seen to be extraordinarily large.

Also very pertinent to the present research is the identification by Rubin, Knobler, and Diederich of four fundamental vibrational frequencies from the infrared spectrum. Three other features in their infrared spectrum (at roughly 1300, 1200, and 1000 cm^{-1}) were not identified. Motivated by the molecular elegance of **1** and its expected future importance in organic chemistry, we have carried out a theoretical study of

tetraethynylethylene. Our immediate goals were the consideration of the molecular structure (severely distorted from D_{2h} symmetry in the crystal structure) and the interpretation of the infrared spectrum. The *ab initio* structure of the isolated molecule displays perfect D_{2h} symmetry. Theoretical vibrational frequencies and infrared intensities make possible an interpretation of the observed IR spectrum. Some attention is given to the molecular orbitals of this the first $C_{10}H_4$ isomer to be prepared in the laboratory.

Research Supported by the U.S. Department of Energy 1990, 1991, 1992.

1. N. L. Allinger, R. S. Grev, B. F. Yates, and H. F. Schaefer, "The Syn Rotational Barrier in Butane", *J. Amer. Chem. Soc.* **112**, 114 (1990).
2. Y. Xie, B. B. Yates, and H. F. Schaefer, "The Wealth of Energetically Low-Lying Isomers for Very Simple Organometallic Systems. The Aluminum-Acetylene (Al-C_2H_2) System", *J. Amer. Chem. Soc.* **112**, 517 (1990).
3. C. P. Blahous, Y. Xie, and H. F. Schaefer, "The Infrared Spectrum of Trimethylenemethane. Predictions of In-Plane Vibrational Frequencies from Correlated Wave Functions", *J. Chem. Phys.* **92**, 1174 (1990).
4. C. Liang, T. P. Hamilton, and H. F. Schaefer, "Classical and non-Classical Forms of the Vinyl Cation: A Coupled Cluster Study", *J. Chem. Phys.* **92**, 3653 (1990).
5. G. E. Scuseria and H. F. Schaefer, "The Concerted Unimolecular Triple Dissociation of s-Tetrazine: Transition State Structural Optimizations Using Configuration Interaction and Coupled Cluster Methods", *John A. Pople Issue, J. Phys. Chem.* **94**, 5552 (1990).
6. Y. Xie and H. F. Schaefer, "Bond Distance Inversion in the Equilibrium Geometry of the Coupled Tricyclo [3.1.0.$0^{2,6}$] Hexyl Molecule $C_{12}H_{14}$. A Puzzling Problem in Molecular Structure", *Chem. Phys. Lett.* **168**, 249 (1990).
7. Y. Xie and H. F. Schaefer, "Aluminirene ($HAlC_2H_2$): The Aluminirane ($HAlC_2H_4$): The Aluminum Substituted Counterparts of Cyclopropene and Cyclopropane", *J. Amer. Chem. Soc.* **112**, 5393 (1990)
8. C. Liang and H. F. Schaefer, "Electronic Structures of Linear C_4, C_6, C_8, and C_{10} Carbon Clusters and a Symmetry Breaking Phenomena", *Chem. Phys. Lett.* **169**, 150 (1990).
9. M. M. Gallo and H. F. Schaefer, "The Infrared Spectrum of Difluorovinylidene, F_2C=C:", *J. Chem. Phys.* **93**, 865 (1990).

10. R. S. Grev, I. L. Alberts, and H. F. Schaefer, "C_3^+ is Bent", *J. Phys. Chem.* **94**, 3379 (1990).

11. G. E. Scuseria and H. F. Schaefer, "Diatomic Chromium (Cr_2): Application of the Coupled Cluster Method Including All Single and Double Excitations (CCSD)", *Chem. Phys. Lett.* **174**, 501 (1990).

12. C. Liang and H. F. Schaefer, "Carbon Clusters: The Structure of C_{10} Studied with Configuration Interaction Methods", *J. Chem. Phys.* **93**, 8844 (1990).

13. S. Q. Jin, Y. Xie, and H. F. Schaefer, "The Characterization of Simple Organoaluminum Fragments: AlCH, $ALCH_2$, and $AlCH_3$", *Chem. Phys. Lett.* **170**, 301 (1990).

14. T. P. Hamilton and H. F. Schaefer, "The Structure and Energetics of $C_2H_4Br^+$: Ethylenebromonium Ion vs. Bromoethyl Cations", *J. Amer. Chem. Soc.* **112**, 8260 (1990).

15. J. D. Goddard and H. F. Schaefer, "Formyl Fluoride Photodissociation: Potential Energy Surface Features of Singlet HFCO", *J. Chem. Phys.* **93**, 4907 (1990).

16. S. Jin and H. F. Schaefer, "The NaSO → NaOS Potential Energy Hypersurface", *J. Chem. Phys.* **93**, 1799 (1990).

17. J. R. Thomas, G. E. Quelch, and H. F. Schaefer, "The Unknown Unsubstituted Tetraines: 1,2,3,4-Tetrazine and 1,2,3,5-Tetrazine", *J. Org. Chem.* **56**, 539 (1991).

18. C. L. Collins, R. D. Davy, and H. F. Schaefer, "Cyclopentadienylidene in Interstellar Space?", *Chem. Phys. Lett.* **171**, 259 (1990).

19. M. M. Gallo, T. P. Hamilton, and H. F. Schaefer, "Vinylidene-The Final Chapter?",*J. Amer. Chem. Soc.* **112**, 8714 (1991).

20. K. S. Kim, H. S. Kim, J. H. Jang, B.-J. Mhin, Y. Xie, and H. F. Schaefer, "Hydrogen Bonding Between the Water Molecule and the Hydroxyl Radical (H_2O OH): The $^2A''$ and $^2A'$ Minima", *J. Chem. Phys.* **94**, 2057 (1991).

21. C. Liang, Y. Xie, H. F. Schaefer, K. S. Kim, and H. S. Kim, "The Vibrational Spectra of Butatriene (C_4H_4) and Pentatetraene (C_5H_4): Is Pentatetraene Bent?" *J. Amer. Chem. Soc.* **113**, 2452 (1991).

22. B. F. Yates, Y. Yamaguchi, and H. F. Schaefer, "The Dissocation Mechanism of Triplet Formaldehyde", *J. Chem. Phys.* **93**, 8798 (1990).

23. C. Meredith, G. E. Quelch, and H. F. Schaefer, "Open-Chain and Cyclic Protonated Ozone: The Ground State Potential Energy Hypersurface", *J. Amer. Chem. Soc.* **113**, 1186 (1991).

24. G. Vacek, B. T. Colegrove, and H. F. Schaefer, "Does Oxirene Exist? A Theoretical Inquiry Involving the Coupled Cluster Method," *Chem. Phys. Lett.* **171**, 468 (1991).

25. A. C. Scheiner and H. F. Schaefer, "Higher Level Theoretical Evidence for the Weak Triple Bond in Benzyne," *Chem. Phys. Lett.* **177**, 471 (1991).

26. T. P. Hamilton and H. F. Schaefer, "Do the Vinyl Isomers of $C_2H_2Cl^+$ and $C_2H_2Br^+$ Exist?", *J. Amer. Chem. Soc.* **113**, 7147 (1991).

27. S. Q. Jin, Y. Xie, and H. F. Schaefer, "The Description of Elementary Organoaluminum Fragments: $AlCH_x$ (x=1,2,3)," *J. Chem. Phys.* **95**, 1834 (1991).

28. I. M. B. Nielsen, C. L. Janssen, N. A. Burton, and H. F. Schaefer," (1,2)-Hydrogen Shift in Monovalent Carbon Compounds: The Methylcarbyne-Vinyl Radical Isomerization", *J. Phys. Chem.*, in press.

29. H. A. Carlson, G. E. Quelch, and H. F. Schaefer, "How 'Stable' is Cyclobutyne? The Activation Energy for the Unimolecular Rearrangement to Butatriene", *J. Amer. Chem. Soc.*, in press.

30. J. D. Goddard, Y. Yamaguchi, and H. F. Schaefer, "The Decarboxylation and Dehydration Reactions of Monomeric Formic Acid", *J. Chem. Phys.* **96**, 1158 (1992).

31. D. A. Horner, W. D. Allen, and H. F. Schaefer, "Sodium Superoxide (NaO_2): $\tilde{X}\,^2A_2$ and $\tilde{A}\,^2B_2$ Potential Energy Surfaces", *Chem. Phys. Lett.* **186**, 346 (1991).

32. A. C. Scheiner and H. F. Schaefer, "Cyclopentadienylideneketene: An Infrared Spectrum Frequently Mistaken for Benzyne", *J. Amer. Chem. Soc.*, in press.

33. M. M. Gallo and H. F. Schaefer, "Methylcarbene: The Singlet-Triplet Energy Separation", *J. Phys. Chem.* **96**, 1515 (1992).

34. T. P. Hamilton and H. F. Schaefer, "The Prototypical Zinc Carbene and Zinc Carbyne Molecules ZnCH2 and HZnCH: Triplet Electronic Ground States", *J. Chem. Soc. (London) Chem. Communications* 621 (1991).

35. B. J. DeLeeuw, R. S. Grev, and H. F. Schaefer, "A Comparison and Contrast of Selected Saturated and Unsaturated Hydrides of Group 14 Elements: C_2H_6, Si_2H_6, Ge_2H_6, and C_2H_2, Ge_2H_2", *J. Chem. Ed.*, in press.

36. J. R. Thomas, G. E. Quelch, E. T. Seidl, and H. F. Schaefer, "The Titane Molecule (TiH_4): Equilibrium Geometry, Infrared and Raman Spectra of the First Spectroscopically Characterized Transition Metal Tetrahydride," *J. Chem. Phys.*

STABILIZATION OF LIFTED TURBULENT-JET FLAMES†

R. W. Schefer

Combustion Research Facility
Sandia National Laboratories, Livermore, CA 94551

Lifted flames are of considerable current interest since they include many of the fundamental mechanisms controlling flame stabilization and extinction in practical burners. Several theories have been proposed to explain the stabilization mechanism of lifted flames. Vanquickenborne and van Tiggelen[1] proposed that in lifted flames the fuel and air are fully premixed prior to ignition and that stabilization occurs where the local flow velocity along the stoichiometric contour is equal to the turbulent flame speed. Peters and Williams[2] have proposed a laminar flamelet concept in which the fuel and air are not premixed at the flame stabilization point and that liftoff can be explained in terms of extinction due to locally-high values of scalar dissipation. The model proposed by Broadwell et. al.[3] considers both large-scale motion and small-scale mixing between the fuel and air. In the proposed model, hot combustion products are carried by large-scale motion from inside the jet to the outer edges where they are subsequently reentrained with outer air and act as an ignition source for unreacted fuel.

Each of these models has had some degree of success in predicting both liftoff height and blowout. Which model is closer to the true physical picture is not clear. In the present study, planar imaging measurements of CH, CH_4 and temperature are used to evaluate the above models in lifted, turbulent CH_4-jet flames. The experimental measurements focus on planar imaging data since insights into both the turbulence structure and its relationship to the flame zone and its location are provided.

The burner consisted of a 5.4-mm diameter fuel jet located in the center of a plate. Methane was injected through the central fuel tube into surrounding still air. Measurements were carried out at jet exit velocities of 21 m/s and 37 m/s, corresponding to fuel-jet Reynolds numbers of 7,000 and 12,100, respectively. At the lower velocity the visible flame was stabilized at an axial position approximately 30 mm downstream of the burner face while at the higher velocity the visible flame was stabilized farther downstream at about 68 mm.

As discussed elsewhere[4], the determination of temperature from Rayleigh scattering is complicated by the variation in Rayleigh scattering cross sections for air, CH_4 and combustion products and generally requires that in addition to the Rayleigh signal, the local gas composition be known. It can, however, be shown that in the present flames simultaneous measurement of Rayleigh scattered light and CH_4 concentration is sufficient to obtain both the temperature and the CH_4 mole fraction. This measurement involves the use of a two-camera imaging system used previously for simultaneous measurement of CH, OH and CH_4[5].

For the measurements, the Combustion Research Facility's flash lamp-pumped dye laser (1.8-μsec pulse duration) was tuned to a wavelength of 444 nm to produce spontaneous Raman scattering from CH_4 at 514 nm. The beam was formed into a 0.3-mm thick sheet of light by a multipass cell consisting of two cylindrical reflectors. The CH_4 Raman-scattering signal was collected at right angles to the laser sheet, passed through a 10-nm bandwidth filter centered at 510 nm, and focussed onto an intensified vidicon camera. The Rayleigh

† Work supported by the Department of Energy, Office of Basic Energy Sciences, Division of Chemical Sciences.

scattered light was collected using identical optics, passed through a filter centered at the laser wavelength, and focussed onto the second camera. A second set of data was obtained in which the combined CH and CH_4 distribution was measured with one camera. The addition of CH data provides information on the relationship between the flame zone and the local turbulence structure. For these measurements, the laser was tuned to a wavelength of 431.5 nm and used to excite the (0,0) band of the $A^2\Delta - X^2\Pi$ system of CH. Fluorescence of the (0,1) transition was observed at 489 nm. Simultaneously, Raman scattering from CH_4 also occurred near 489 nm for the 431.5-nm excitation. The combined CH fluorescence and CH_4 Raman-scattering signals were detected using one camera while the Rayleigh scattering signal was obtained at 431.5 nm using the second camera.

Single-shot images of CH, CH_4 mole fraction and temperature (presented as contour plots) are shown in Fig. 1 for the 7,000 Reynolds number flame. Two images, taken on different laser shots, are presented to illustrate the time-varying aspects of these flames. Flow direction is vertical from the bottom to the top. In each image the highest CH concentrations are indicated by the dark solid regions. The region between 0.05 and 0.15 contour lines (dotted) for CH_4 mole fraction corresponds to fuel-air mixtures within the CH_4 flammability limits, while the 0.3 contour line is included to better indicate the structure of the central jet. The 0.05 and 0.15 contour lines are only apparent upstream of the flame zone since they closely coincide with the high CH region downstream. Temperature levels greater than 1000 K are indicated by the light shaded areas.

In general the flame zone, as defined by the high CH, forms in a narrow region along the outer boundaries of the central fuel jet. In Fig. 1a, the flame zone is convex to the outer flow near the upstream stabilization point. Comparison with the CH_4 distribution (0.3 contour) indicates that the flame is pushed outward in response to an outward bulge in the central jet and that the flame is stabilized along the upstream edge of this bulge. The flame zone in Fig. 1b can be characterized as relatively straight (parallel to the axis) and nearly continuous in the axial direction. Note that in Fig. 1b the central jet boundaries (0.3 CH_4 contour) are also relatively straight and exhibit no outward bulges. The consistency of these patterns in numerous images provides strong evidence for the close coupling between the large-scale jet structure and the flame zone.

A major difference between proposed models for turbulent flame stabilization is the assumption of premixed fuel and air verses the assumption of nonpremixed laminar flamelets. Comparison of the CH and CH_4 distributions in Fig. 1 and in other images shows that the upstream flame stabilization point consistently occurs between the 0.05 and 0.15 CH_4 contours (representing the flammability limits for CH_4). Probability distributions of the CH_4 mole fraction calculated at the instantaneous flame stabilization point statistically verify this observation and clearly show that in both flames the fuel and air are premixed at the stabilization point[4]. This observation is in conflict with the assumptions of Peters and Williams[2] that liftoff can be explained in terms of a nonpremixed laminar flamelet concept.

An important question concerns the role of scalar dissipation, χ, in flame stabilization[2]. From the planar imaging data, χ was calculated directly from the instantaneous CH_4 distributions. Probability distributions of χ at the flame stabilization point are lognormally distributed with a maximum value of about 1 sec^{-1}. This value is significantly lower than the critical stoichiometric extinction value of 12 sec^{-1} estimated from counter-flow diffusion flame data[4]. It is therefore concluded that scalar dissipation is not an important quantity in the stabilization of these flames.

In agreement with the flame stabilization model proposed by Broadwell et. al.[3], the images in Fig. 1 indicate that a close coupling exists between the large-scale jet structure and the flame zone. The experimental results further suggest a model that includes both the large-scale concepts of Broadwell et. al.[3] and premixed turbulent flame propagation[1].

From the images presented, two types of flames are typically seen in these flows. One in which the flame zone is convex to the outer flow near the upstream stabilization point and a second in which the flame zone is relatively straight and continuous along the axial direction. The former indicates a strong interaction between the flame zone and the large scale jet structure while the latter indicates little interaction between the central jet and the flame zone and is more indicative of turbulent flame propagation through a narrow region of premixed flammable gas.

Future work will involve modification of the Diana facility laser to provide two closely-spaced laser pulses with a variable time delay. Images from the two pulses will be used to study the time development of the interaction between large-scale jet structure and flame stabilization.

References

1. Vanquickenborne, L. and van Tiggelen, A.: *Comb. Flame* **10**, 59 (1966).
2. Peters, N. and Williams, F. A.: *AIAA J.* **21**, 423 (1983).
3. Broadwell, J. E., Dahm, W. J. A. and Mungal, M. G.: *Twentieth Symposium (International) on Combustion*, p. 303, The Combustion Institute, 1985.
4. Schefer, R. W., Namazian M. and Kelly, J.: "Stabilization of Lifted Turbulent-Jet Flames", *Combust. Flame*, submitted, 1992.
5. Schefer, R. W., Namazian M. and Kelly, J.: *Twenty-Third Symposium (International) on Combustion* (The Combustion Institute, Pittsburgh, PA), p. 669, 1991.

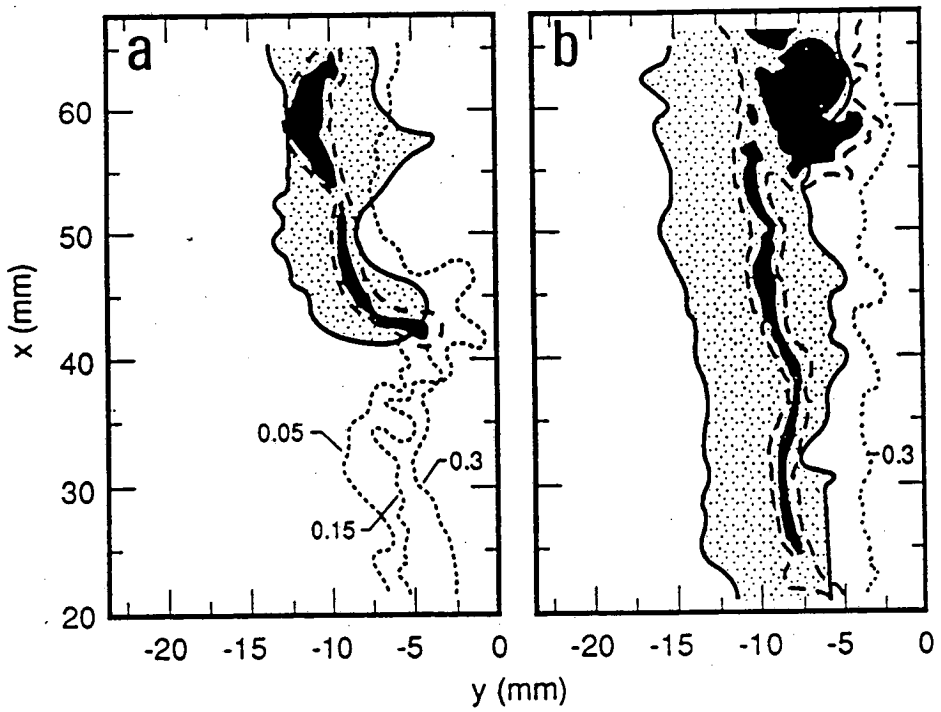

Fig. 1. Planar images of combined CH/CH_4 and temperature distributions in a lifted, turbulent CH_4-jet flame. CH levels are indicated by dark shaded area and dashed line. CH_4 contour levels of 0.05, 0.15 and 0.3 are shown as dotted lines. Regions with temperatures greater than 1000 K are shown as light shaded areas.

R. W. Schefer: Journal Publications Supported by This Program 1990-1992

Namazian, M., Schefer, R. W. and Kelly, J., "Concentration Imaging Measurements in Turbulent Concentric-Jet Flows," *AIAA J.* **30**, No. 2, 384-393 (1992).

Schefer, R. W., Namazian, M. and Kelly, J., "Simultaneous Raman Scattering and Laser-Induced Fluorescence for Multi-Species Imaging in Turbulent Flames," *Opt. Lett.* **16**, 858-860 (1991).

Schefer, R. W., Namazian, M. and Kelly, J., "CO, OH and CH_4 Concentration Measurements in a Lifted Turbulent-Jet Flame," *Twenty Third Symposium (International) on Combustion* (The Combustion Institute, Pittsburgh, PA), 669-676 (1991).

Chen, R., Driscoll, J. F., Kelly, J., Namazian, M. and Schefer, R. W., "A Comparison of Bluff-Body and Swirl-Stabilized Flames," *Combust. Sci. Technol.* **71**, 197-217 (1990).

COMPUTATIONAL AND EXPERIMENTAL STUDY OF LAMINAR FLAMES

M. D. Smooke and M. B. Long
Department of Mechanical Engineering
Yale University
New Haven, CT 06520

Program Scope

Our research has centered on the investigation of the effects of complex chemistry and detailed transport on the structure and extinction of hydrocarbon flames in counterflow, cylindrical and coflowing axisymmetric configurations. We have pursued both computational and experimental aspects of the research in parallel. The computational work has focused on the application of accurate and efficient numerical methods for the solution of the one and two-dimensional nonlinear boundary value problems describing the various reacting systems. Detailed experimental measurements were performed on axisymmetric coflow flames using two-dimensional imaging techniques. In particular, spontaneous Raman scattering and laser induced fluorescence were used to measure the temperature, major and minor species profiles. Our goal during this period has been to obtain a more fundamental understanding of the important fluid dynamic and chemical interactions in these flames so that this information can be used effectively in combustion modeling.

Recent Progress

Our computational research has focused on both one and two-dimensional systems. In one dimension we have developed models for counterflow premixed flames in a cold-reactant/hot product configuration and for cylindrical premixed flames in which a fuel-air mixture is injected radially inward into an open tube. Since both systems admit similarity solutions of the two-dimensional conservation equations, the governing equations in each case can be reduced to a system of one-dimensional two-point boundary value problems. In two dimensions we have concentrated our efforts on the modeling of axisymmetric laminar diffusion flames in which a fuel jet discharges into a coflowing air stream. The fully elliptic form of the conservation equations were solved in cylindrical coordinates. Spontaneous Raman spectroscopy and laser induced fluorescence have been used to measure major and minor species in a methane-air diffusion flame that was designed to match the conditions of the computed flame. The emphasis of the experimental work was on providing the best quantitative information possible on the flow configurations studied. The information obtained in these experiments will help improve the accuracy of measurements in turbulent flames and it will provide better data on the relative applicability of different scattering mechanisms.

Future Plans

During the next three years we hope to expand our research in three main areas. First, we intend to develop a flamelet model for turbulent nonpremixed combustion based upon three different flamelet libraries–the nonpremixed counterflow system, the nonpremixed cylindrical system and the axisymmetric nonpremixed coflow system. Second, we plan on continuing our studies of methane-air coflow flames. In particular, we want to continue our measurements of minor species in the flame and the comparison of these measurements with the computational results. Further, the computations will be modified to include NO_x chemistry and we will investigate (both computationally and experimentally) the reduction of NO_x by modifications to the inlet velocity field. Finally, we plan on extending the coflow model to be able to study time-dependent flames that undergo perturbations of the flow field. Flames of this type are useful in providing a transitional system between laminar and turbulent flames.

References

1. M. D. Smooke and M. B. Long, "Computational and Experimental Study of a Laminar Axisymmetric Methane-Air Diffusion Flame," *Twenty-Third Symposium International on Combustion*, (1991).

2. M. D. Smooke and V. Giovangigli, "Extinction of Tubular Premixed Laminar Flames with Complex Chemistry," *Twenty-Third Symposium International on Combustion*, (1991).

3. M. D. Smooke, J. Crump, K. Seshadri and V. Giovangigli, "Comparison Between Numerical Calculations and Experimental Measurements of the Structure of Diluted Methane-Air Premixed Flames," *Twenty-Third Symposium International on Combustion*, (1991).

4. M. D. Smooke and V. Giovangigli, "Numerical Modeling of Axisymmetric Laminar Diffusion Flames," to be published *Impact of Computing in Sci. and Eng.*, (1992).

5. Y. Xu and M. D. Smooke, "Application of a Primitive Variable Newton's Method for the Calculation of Axisymmetric Laminar Diffusion Flames," to be published *J. Comp. Phys.*, (1992).

6. M. D. Smooke and V. Giovangigli, "A Comparison between Experimental Measurements and Numerical Calculations of the Structure of Premixed Rotating Counterflow Methane-Air Flames," to be published 24th Symposium International on Combustion (1992).

7. M. D. Smooke, Y. Xu, R. M. Zurn, P. Lin, J. H. Frank and M. B. Long, "Computational and Experimental Study of OH and CH Radicals in Axisymmetric Laminar Diffusion Flames," to be published 24th Symposium International on Combustion (1992).

TURBULENT COMBUSTION

L. Talbot and R. K. Cheng

Energy & Environment Division
Lawrence Berkeley Laboratory
Berkeley, CA 94720

Scope

Turbulent combustion is the dominant process in most practical combustors. Compared to combustion in laminar flows, the most significant aspect is that turbulent mixing increases the combustion rate and volumetric power density. Turbulent mixing also has significant influence on the rates of chemical reactions and hence a direct effect on the formation of pollutants and other combustion processes such as ignition and extinction. Thus, a thorough understanding of the physical effect of turbulence on combustion processes and the development of theoretical models capable of predicting these processes is necessary for the design and development of modern combustion systems. This would lead to combustion devices with improved efficiency, minimum pollutant emission characteristics, optimum size, minimum cost, and maximum durability.

The overall objective of this program is to investigate, primarily experimentally, the interaction and coupling between fluid mechanical turbulence and combustion reaction in turbulent flames. The interaction processes are complex and involve scalar and velocity fluctuations at time and length scales spanning several orders of magnitude. In most practical systems, they are also influenced by other factors such as flow and burner geometries. Our approach is to investigate idealized laboratory flames to gain a fundamental understanding of the fluid mechanic of turbulent flames for the advancement of turbulent combustion theory. Laser diagnostic techniques with high spatial and temporal resolution are used to measure in-situ the statistical turbulence properties. The current research goal is to gain a physical description of the changes in turbulence characteristics due to the combustion heat release, and also to quantify the relationship between the burning rate and turbulence intensity. The information is applied to the development of predictive numerical turbulent combustion models. This research is beneficial in the improvement of modern practical combustor design with enhanced efficiency and reduced pollutant emission levels.

Several well-established laser diagnostic techniques with high spatial and temporal resolutions are used to measure statistical moments and correlations of velocity and scalars (i.e. gas density, reaction progress variable). These techniques include laser Doppler anemometry (LDA) for simultaneous measurement of two velocity components and Rayleigh scattering from a focused laser beam for density measurements. Other diagnostics for the scalar properties include laser-induced Mie scattering from silicone-oil aerosol (MSOD) for measuring the reaction progress variable and flame crossing frequencies in premixed flames. Mie scattering is also used for laser sheet imaging of the flame structures by high-speed tomography. Quantitative information of the flame structures is obtained by computer-controlled image processing.

The laboratory scale premixed flame configurations used in this study are idealizations of those found in many practical systems. The first is an unconfined rod-stabilized, plane-symmetric, v-flame propagating in turbulent flow, and the second a large axi-symmetric Bunsen-type conical turbulent flame stabilized by pilot flames at the exit of a 50mm diameter tube. The turbulent flame brushes formed in these burners are oblique to the incident flow and their flowfield can be treated as two-dimensional. The data are then suitable for comparison with the numerical results of the statistical model developed by Bray, Moss and Libby (BML), or with the deterministic models based on Chorin's vortex dynamics technique.

The third configuration is a planar premixed turbulent flame stabilized in a stagnation flow. The flame brush is locally normal to the approach flow around the stagnation point and does not involve a recirculation region for stabilization. Near the stagnation region, this flame satisfies the planar flame criteria specified in statistical models of turbulent combustion. The fourth and most recently investigated is a newly discovered configuration is a freely propagating flame stabilized by weak swirl. This configuration shows great promise as the most convenient means for determining burning speed and may be a useful tool for studying local extinction by turbulence under very lean conditions. In all configurations, turbulence intensities upstream of the flame regions are generated by a grid or a perforated plate. Turbulence intensities produced are typically 5 to 10%. At flow velocities of the fuel/air mixture between 5 to 10 m/s, the turbulence Reynolds number, Re_l, is in the range of about 100. Under these conditions the turbulent flames are characterized as wrinkled laminar flames because the chemical time scales are small compared to those of turbulence.

The theoretical study of premixed turbulent flames involves the development of deterministic models of turbulent combustion. The numerical technique employed is Chorin's vortex dynamics method. In contrast with the statistical modeling approach where the changes in flame turbulence are modeled and used as input parameters, the vortex dynamics model is capable of predicting these changes and other flame phenomena, in particular, the structure of the wrinkled flames.

Recent Progress

We have developed a new configuration for studying premixed turbulent flame propagation. This freely propagating open flame is stabilized by weak swirl. It provides a close approximation to the planar one-dimensional flame of theoretical models and supports stable combustion under very lean conditions. This configuration is, therefore, ideal for future investigation of other combustion processes such as local flame extinction. The burner operates under a much wider flow and mixture conditions than our other configurations. In particular, it supports stable combustion under very lean conditions. This feature can be exploited for application to other fundamental combustion research or to practical systems.

Our investigation of turbulent flamelet structures continues with the analysis of flame curvature deduced from tomography. The tomographic data are determined on planes passing through the flame zone and thus can provide directly only two-dimensional measurements of complex three-dimensional flamelet surface structures. The direct

experimental determination of flame structures in three dimensions presents serious practical difficulties, and the suitability of the present data to test and validate theoretical models is at yet unresolved. To address these issues, the two-dimensional flame front curvatures and orientations obtained for stagnation point flames are compared to the results deduced from direct numerical simulation. The comparison shows that the two-dimensional tomographic results are a reasonably good estimate of the curvatures of the three-dimensional simulation. It is encouraging for continuing comparisons of the present type that computer models are successful in simulating significant features of the geometry of experimental flames.

We have also initiated the study of unsteady flame propagation in an enclosure initiated by ignition. This is one of the classic configurations used for the determination of turbulent burning speed. The experiments performed include Rayleigh scattering measurement of flame propagation in laminar and turbulent environments initiated by three different ignition sources and comparison of burning rates.

Future Plan

Further development and refinement of the swirl burner are planned. The flamelet structures of the swirl stabilized flames will be investigated by tomography, and a series of studies will be conducted to investigate the turbulent burning speed and flame extinction. Development of diagnostics will focus on Particle Image Velocimetry (PIV). The PIV system will be used to determine the interaction between vorticity and flamelet curvature. To extract useful information from this 2D method, data interpretation will be guided by direct numerical simulations. A combustion vessel with six windows will be available to us for use in determining the burning rate of unsteady flame propagation from tomography. The results are expected to provide a direct validation of the relationship between burning rate and area of wrinkled flamelets. The development of new diagnostics and experimental apparatus represents a significant expansion in our capability. The integration of these techniques and apparatus into the system will take several years to complete, and will be implemented as it becomes necessary.

Recent Publications:

1. Shepherd, I. G., Cheng, R. K., and Goix, P. J., "The Spatial Structure of Premixed Stagnation Point Flames," 23rd International Symposium on Combustion, p. 781 (1990).

2. Cheng, R. K., and Shepherd, I. G., "The Influence of Flame Geometry on Premixed Turbulent Flame Propagation," Combustion and Flame, 85, p. 7 (1991).

3. Hertzberg, J. R., Shepherd, I. G., and Talbot, L., "Vortex Shedding in Premixed Turbulent Flames, Combustion and Flame, 86, p. 1 (1991).

4. Ueda, T., and Cheng, R. K., "Interaction of Jet Diffusion Flamelets with Grid Generated Turbulence," Combustion Science and Technology, 80, 1-3, p. 121 (1991).

5. Shepherd, I. G., Cheng, R. K, and Talbot, L. "Experimental Criteria for the Determination of Fractal Parameters of Premixed Turbulent Flames" accepted for publication, Experiments in Fluids (1991).

6. Goix, P. J., and Talbot, L., "Turbulent Counterflow Diffusion Flame Structure and Dilution Effects," Combustion Science and Technology, 79, 4-6 , p. 175 (1991).

Other publications:

1. Shepherd, I. G., Ashurst, Wm. T. "Flame Front Geometry in Premixed Turbulent Flames," Accepted for presentation at the 24th International Symposium on Combustion, (1992).

2. Chan, C. K., Lau, K. S., Chin, W. K., and Cheng, R. K., "Freely Propagating Open Premixed Turbulent Flames Stabilized by Swirl" Accepted for presentation at the 24th International Symposium on Combustion (1992).

3. Tamai, R., Maxson, J. A., Shepherd, I. G., Cheng, R. K., and Oppenheim, A. K., "Rayleigh Scattering Density Measurements of Combustion in an Enclosure" Accepted for presentation at the 24th International Symposium on Combustion (1992).

Single-Shot Measurement of the Intensity and Phase of a Femtosecond Pulse Using the Optical-Kerr Effect

Rick Trebino
Combustion Research Facility
Sandia National Labs
Livermore, CA 94551

Program Scope

The purpose of this program is the development of techniques for the measurement of ultrafast events important in chemistry. Ultrafast spectroscopic methods and ultrashort-pulse laser generation and measurement techniques are the subjects of this work. This year, we discuss a technique for measuring the intensity and phase of an individual femtosecond pulse.

Recent Progress

In studies of intramolecular motion performed with ultrashort laser pulses, the detailed temporal behavior of the excitation pulse's intensity and phase play an important role in determining the precise motion that is excited. For example, a pulse whose intensity is high for less than a vibration period may excite a well-defined wave packet, while a pulse whose intensity persists for much longer will excite a vastly different vibrational wave function. More importantly, a negatively chirped pulse (that is, a pulse whose frequency decreases with time) may excite a wave packet that grows in magnitude as it evolves along a dissociative potential surface, while a positively chirped pulse may lack the specific overlap of frequency vs. time with the wave packet. As a result, it is critical to know the precise intensity and phase evolution of an ultrashort pulse used for such studies. Unfortunately, methods for making such measurements have not been available because no device has sufficient temporal resolution. Indeed, it is ultrashort laser pulses themselves that are usually used to obtain ultrafast temporal resolution.

In response to this problem, we have developed and demonstrated the first technique for measuring the full, time-dependent intensity and phase, E(t), of an individual femtosecond pulse. This new technique, which we call "frequency-resolved optical gating" (FROG), uses the polarization-spectroscopy optical-gate arrangement with an instantaneously responding $\chi^{(3)}$ sample medium, such as glass. Here, however, the pulse is split and one version of the pulse gates the other (see Fig. 1). We then measure the signal spectrum as a function of the delay between the two input pulses. Because the signal pulse is shorter than the input pulses (by a factor of $\sqrt{3}$ for Gaussian pulses), the signal pulse reveals, for a given delay, the frequency of a particular temporal component of the ultrashort pulse (See Fig. 1). For reasonably well-behaved pulses, the output plot of signal intensity vs. frequency and delay graphically displays the pulse instantaneous frequency vs. time

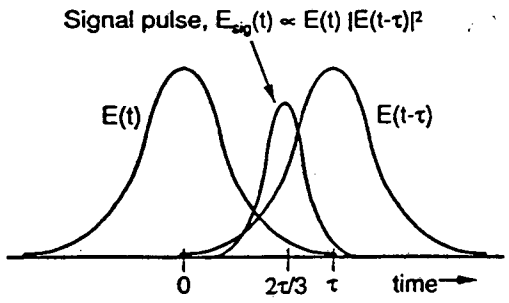

Figure 1. Two input pulses [E(t) and E(t-τ)] and the signal pulse resulting in an optical-gating experiment [$E_{sig}(t,\tau) \propto E(t)\,|E(t-\tau)|^2$]. Note that the signal pulse is centered at the time, ~2τ/3, and that it is narrower than the input pulses. The frequency of the signal pulse thus approximates that of the input pulse, E(t), at that time. The gate pulse, E(t-τ), does not contribute frequency information to the signal pulse because of its squared-magnitude contribution.

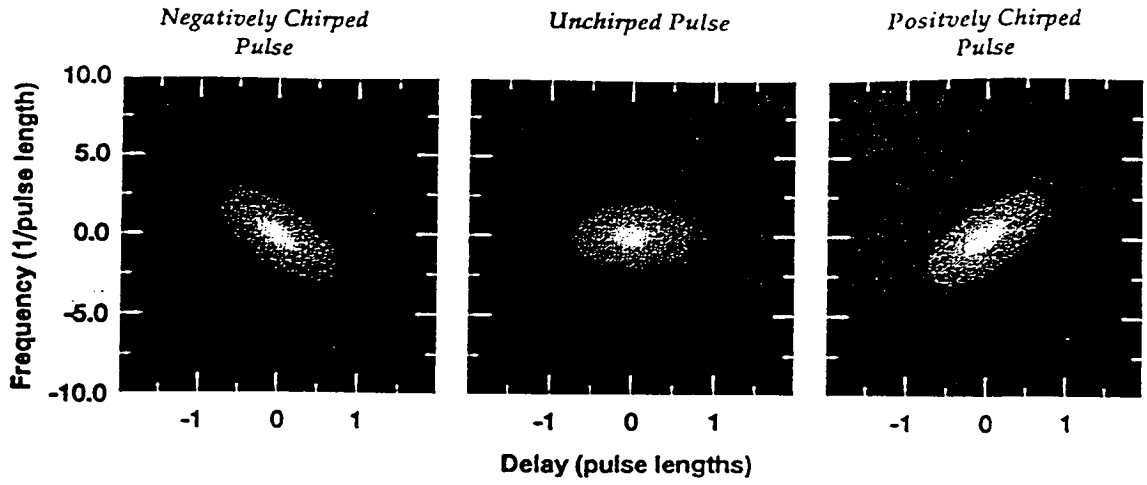

Figure 2. Theoretical FROG signal spot at the output of the spectrometer for negatively chirped, transform-limited, and positively chirped Gaussian pulses. Observe that the shape of the signal-light intensity indicates the instantaneous-frequency-vs.-time curve for the pulse.

(See Fig. 2). More importantly, inversion of $\omega(t)$ to obtain $t(\omega)$, followed by integration of this result, yields the phase vs. frequency, $\varphi(\omega)$. In conjunction with the pulse spectrum, $I(\omega)$, which is also naturally obtained in FROG, this result yields the full amplitude and phase of the pulse field in the frequency domain, $E(\omega)$. Simple Fourier transformation yields $E(t)$. We have demonstrated the method using a microscope slide as a nonlinear medium and ~620-nm, ~200-μJ, nearly transform-limited ~100-fsec pulses and ~200-fsec chirped pulses.

Previous work has achieved multi-shot intensity-and-phase measurement of ultrashort pulses[1], but using a technique that is unlikely to achieve single-shot measurements; is difficult to scale to the UV spectral range; and uses a complex arrangement. The FROG apparatus, on the other hand, is very simple and easy to align. In addition, FROG uses the optical Kerr effect, not second-harmonic generation, so it extends easily into the UV regime, where we have also made single-shot intensity-and-phase measurements (for 308 nm pulses). In addition, FROG appears to have no practical temporal-resolution limit because the pulse measures itself. We have also demonstrated a version of this method using self-diffraction[2] instead of polarization spectroscopy, which appears very well suited for single-shot measurement of few-fsec pulses, where propagation through material should be minimized.

Figure 3 shows an image of the FROG output for a positively chirped ~200-fsec pulse. From this plot, we obtain $\omega(t)$, or its inverse, the pulse time vs. frequency, $t(\omega)$. The phase vs. frequency, $\varphi(\omega)$, is then obtained using $\varphi(\omega) = -\int t(\omega')\, d\omega'$.[1] Figure 4 shows $t(\omega)$ along with the measured pulse spectrum. Inverse-Fourier-transforming the field to the time domain yields $E(t)$ and the pulse intensity vs. time shown in the inset of Fig. 5, which also shows the computed

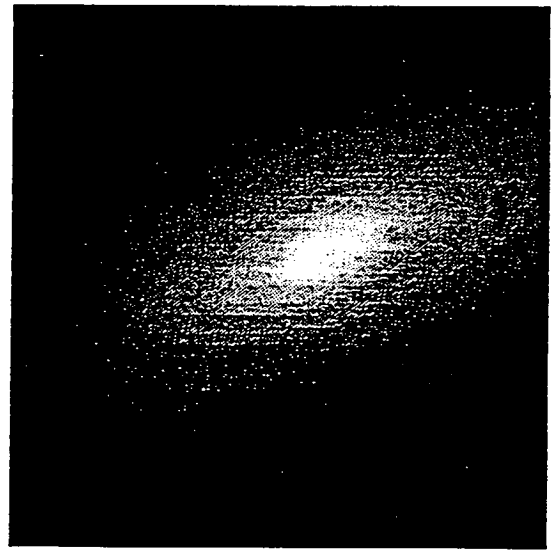

Figure 3. Experimental density plot of single-shot FROG raw signal intensity vs. delay (horizontal axis, increasing) and wavelength (vertical axis, decreasing) for a partially recompressed pulse. The shape indicates the frequency vs. time; here a nearly linear positive chirp (longer wavelengths occurring earlier) is indicated. (The dark spot at left is an artifact.)

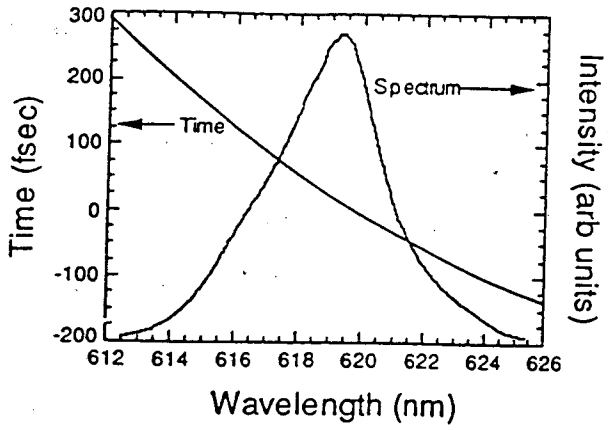

Figure 4. The derived pulse time vs. wavelength and the measured pulse spectrum. These two results yield the full pulse field (up to an unimportant constant phase factor). Observe the positive, nearly linear chirp.

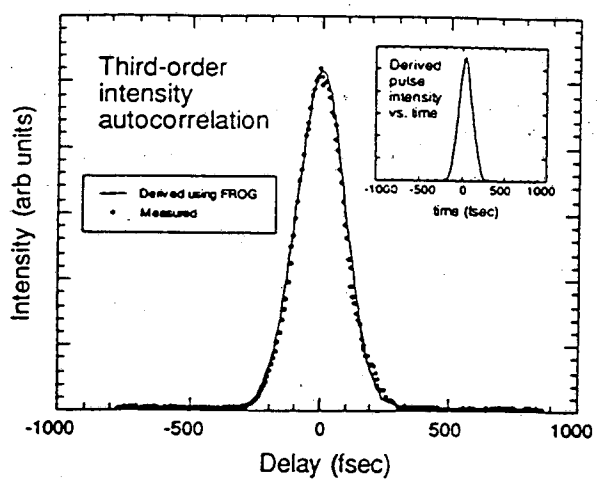

Figure 5. The third-order intensity autocorrelation of the derived pulse and the measured third-order single-shot pulse intensity autocorrelation. (The experimental third-order intensity autocorrelation is obtained by integrating the signal intensity over frequency for a given value of the delay.) Inset: the derived pulse intensity vs. time.

pulse third-order intensity autocorrelation, in good agreement with a simultaneously obtained experimental third-order autocorrelation.

Future Work

We should point out that, while this method is simple and convenient, the simple inversion algorithm described above is only approximate for pathological pulse shapes and phase evolutions. It can be shown, however, that the full pulse field is uniquely determined by the FROG output even for pathological pulse shapes and/or phases, despite the relatively long gate pulse (only a factor of $\sim\sqrt{2}$ shorter than the pulse to be measured). The inversion of the FROG output can be shown to be equivalent to the two-dimensional phase retrieval problem, for which solutions are known to exist:

$$I_{FROG}(\omega, \tau) \propto \left| \int\int E_{sig}(t, \Omega) \exp(-i\omega t - i\Omega\tau) \, dt \, d\Omega \right|^2$$

where $I_{FROG}(\omega, \tau)$ is the measured quantity, and $E_{sig}(t, \Omega)$ is the Fourier transform of the optical-Kerr-effect signal, $E_{sig}(t, \tau) \propto E(t) \, |E(t-\tau)|^2$, with regard to the delay variable, τ. While such solutions can be difficult to find for complex fields, a tremendous additional simplification in FROG is the resemblance of the mathematics to the Gabor transform, which provides an important constraint to assist convergence. Support constraints also exist. We are at present implementing phase-retrieval methods, in order to extract full, exact information in the general case. Preliminary results indicate that these methods work well. In a theoretical simulation, a linearly chirped, nearly square pulse, for example, was easily reconstructed using the theoretical FROG output, the approximate reconstructed initial guess, and a simple inversion algorithm. We are now testing the algorithm using more complex pulse shapes and using it to reconstruct complex experimentally measured pulse shapes obtained in our UV experiments.

References

1. J.L.A. Chilla and O.E. Martinez, Opt. Lett. 16, 39 (1991).
2. D.J. Kane and R. Trebino, submitted to J. Quant. Electron.

Publications 1990-92

C.E. Barker, R. Trebino, A.G. Kostenbauder, and A.E. Siegman, "Frequency-Domain Observation of the Ultrafast Inertial Response of the Optical Kerr Effect in CS2," J. Chem. Phys. 92, 4740 (1990).

R. Trebino and L.A. Rahn, "Calculation of Higher-Order Wave-Mixing Spectra," Opt. Lett. 15, 354 (1990).

C.C. Hayden and R. Trebino, "Coherent Interactions in Two-Beam Excite-Probe Absorption Measurements: Phase Gratings in Flowing Samples," Appl. Phys. B 51, 350 (1990).

R. Trebino and C.C. Hayden, "The Anti-Resonant Ring in Ultrafast Excite-Probe Spectroscopy," in Ultrafast Phenomena VII, eds. C.B. Harris, E.P Ippen, G.A. Mourou, and A.H. Zewail, (Springer-Verlag, Berlin, Heidelberg, 1990), p. 157.

R. Trebino, C.C. Hayden, A.M. Johnson, W.M. Simpson, and A.M. Levine, "Chirp and Self-Phase Modulation in Induced-Grating Autocorrelation Measurements of Ultrashort Pulses," Opt. Lett. 15, 1079 (1990).

R. Trebino and C.C. Hayden, "Velocity Measurement Using the Phase of a Laser-Induced Grating," Opt. Lett. 15, 1397 (1990).

R. Trebino and C.C. Hayden, "Anti-Resonant-Ring Transient Spectroscopy," Opt. Lett. 16, 493 (1991).

J.T. Fourkas, T.R. Brewer, M.D. Fayer, and R. Trebino, "Probing Picosecond Flame Dynamics with Transient Grating Experiments," Proceedings of LASERS '91, in press.

R. Trebino, "Unusual Lineshapes in Higher-Order Dephasing-Induced Wave-Mixing," Laser Spectroscopy X, eds. M. Ducloy, E. Giacobino, and G. Camy (1991) in press.

A.M. Levine, E. Ozizmir, R. Trebino, and C.C. Hayden, "New Developments in Autocorrelation Measurements of Ultrashort Pulses," Laser Spectroscopy X, eds. M. Ducloy, E. Giacobino, and G. Camy (1991) in press.

R.P. Lucht, R.L. Farrow, R. Trebino, and L.A. Rahn, "Nonperturbative Calculations of High-Intensity Effects in Nonlinear Wave-Mixing Processes," Laser Spectroscopy X, eds. M. Ducloy, E. Giacobino, and G. Camy (1991) in press.

J.T. Fourkas, R. Trebino, and M.D. Fayer, "The Grating Decomposition Method: A New Approach for Understanding Polarization-Selective Transient Grating Experiments I. Theory," J. Chem. Phys. (1992) in press.

J.T. Fourkas, R. Trebino, and M.D. Fayer, "The Grating Decomposition Method: A New Approach for Understanding Polarization-Selective Transient Grating Experiments II. Applications," J. Chem. Phys. (1992) in press.

R.P. Lucht, R. Trebino, and L.A. Rahn, "Resonant Multiwave Mixing Spectra of Gas Phase Sodium: Nonperturbative Calculations," Phys. Rev. A (1992) in press.

D.J. Kane and R. Trebino, "Measurement of the Intensity and Phase of Femtosecond Pulses Using Frequency-Resolved Optical Gating," submitted to IEEE J. Quant. Electron. (1992).

D.J. Kane and R. Trebino, "Single-Shot Measurement of the Intensity and Phase of a Femtosecond Pulse," submitted to Ultrafast Phenomena VIII (1992).

VARIATIONAL TRANSITION STATE THEORY

Donald G. Truhlar
Department of Chemistry, University of Minnesota, Minneapolis, Minnesota 55455

This project involves the development and application of variational transition state theory (VTST) and semiclassical transmission coefficients to gas-phase reactions.[R1] The work involves development of the theory and practical techniques for applying the theory to wider classes of transition states, development of new methods for interfacing reaction-path dynamics calculations with electronic structure theory, and applications to specific reactions.

There are two main assumptions in transition state theory, the equilibrium assumption and the dynamic bottleneck assumption. The latter is also called the no-recrossing assumption. If recrossing does occur, classical conventional transition state theory overestimates the accurate classical reaction rate. Therefore, the best approximation to the real rate constant can be obtained by choosing the transition state to minimize the rate. To implement this we define a reaction coordinate s, and for each value of s we define a generalized transition state dividing surface as the hypersurface locally perpendicular to the minimum energy path (MEP) in mass-scaled coordinates. Canonical variational theory (CVT) is obtained by minimizing the rate constant with respect to s.[R2] In addition to energetic effects, CVT also includes the entropic effect on the location of the transition state. In many cases variational transition states are significantly displaced from the saddle point because of zero point and entropic effects that depend on s.

To include quantum effects we quantize the energy levels of the transition state and account for tunneling. We have shown that accurate rate constants can be calculated by using semiclassical transmission coefficients to account for tunneling, but only if "multidimensional effects" are included.[R1,R3,P14] The first such effect is that the effective potential for tunneling must include the adiabatic evolution of vibrational energy in modes transverse to the MEP. Second, there is a nonclassical internal centrifugal effect that causes the tunneling path to lie on the concave side of the MEP. For large curvature of the MEP, one must include contributions from a series of tunneling paths, some of which differ geometrically from the MEP by more than a radius of curvature. We have found that reasonable accuracy can be obtained by carrying out approximate semiclassical calculations by theories developed for the two limiting cases of small curvature (SC)[R4,P20] and large curvature (LC)[R5,P20] of the MEP.

The essential input for VTST and semiclassical tunneling calculations is the potential energy surface of the system under study. We are using two types of electronic structure approach to obtain the requisite potential energy surface information—*ab initio* and semiempirical calculations.

The POLYRATE computer program. POLYRATE[R6,P20] is our portable computer program for applying VTST to polyatomic reactions. Over the last few years we greatly improved the POLYRATE code by including the large-curvature, version 3 (LC3) method for ground-state-to-ground-state and ground-state-to-excited-state tunneling contributions, improved reaction-path following algorithms,[P18] the centrifugal-dominant small-curvature tunneling (CD-SCT) approximation, a hindered-internal-rotator anharmonicity algorithm,[P9] and a convenient mechanism for controlling dimensions.

Optimized reaction-path algorithms . We have systematically optimized and tested ten different algorithms, including higher-order methods and stiff solvers, for following the reaction path and computing vibrational frequencies and free energies of activation along it. We compared the methods in terms of the number of energy, gradient, and hessian calculations required to achieve a given accuracy in the rate constant. As a result of our optimization, a new algorithm called ES1* emerged as generally best for a wide range of ratios of the hessian cost to the gradient cost. In one test case it is four times more efficient than the fourth-order Runge-Kutta algorithm.

Large curvature tunneling including excited states. We have shown in previous years that accurate semiclassical transmission coefficients for VTST may be calculated from the transmission probabilities of reactants initially in the ground state, but—when reaction-path curvature is large—such probabilities must be summed explicitly over final states. The most recent test of the semiclassical methods, for H and D transfer between chlorine atoms in three dimensions, showed agreement within the reliability of the quantal calculations with accurate quantal reaction rates for the same potential energy surfaces in five out of six cases. Extension of this formalism to general polyatomic reactions has now been completed.

Anharmonic quantal partition functions Convenient methods have been developed for calculating the approximate quantum mechanical partition function of a hindered internal rotational

mode of a polyatomic molecule and for including mode-mode coupling in quantum partition functions. The accuracy in both cases is quite satisfactory for VTST.

$Cl^- + CH_3{}^*Cl \rightarrow CH_3Cl + {}^*Cl^-$. (*Cl is a labeled Cl atom.) Correlated calculations of the energies and frequencies at the saddle point, ion-dipole complex, and reactants plus additional energy calculations at selected geometries in the strong interaction region were used to parameterize a multidimensional potential energy function for the degenerate S_N2 reaction of chloride ion with methyl chloride. Semiclassical variational transition-state theory was used to calculate the gas-phase rate coefficient and to determine a value of 3.1 kcal//mol for the semiempirical value of the barrier height. A new potential energy function with this barrier height was created and used to calculate the rate coefficients and phenomenological activation energies over the 200–1000 K temperature range. The activation energy was predicted to show a large temperature dependence.

$Cl^- + CD_3Cl$ and $Cl^-(D_2O)_n + CH_3Cl$, $n = 1,2$. We presented a potential energy surface for the microhydrated S_N2 reaction of a chloride ion with methyl chloride in the presence of one or two water molecules. All degrees of freedom were included, and in particular the potential energy surface for the dihydrated reaction involves 36 degrees of freedom in Cartesian coordinates. We calculated an inverse effect for D substitution at methyl both for bare and microhydrated solute. These KIEs and those for D substitution in water were interpreted in terms of the contributions of individual vibrational modes; in the n = 2 case the solvent KIE is attributable to the breaking of a water-water hydrogen bond and the weakening of a water-chloride hydrogen bond. Detailed factorization of the KIEs led to the identification of important contributions from high-frequency modes that have been invariably neglected in previous work interpreting experimental work. We also drew quantitative conclusions about the contributions of low-frequency modes and about the effect of variational optimization of the location of the transition state on these contributions.

Direct dynamics. The prediction of rate constants by *ab initio* methods is limited by the computational effort of calculating and fitting reactive potential energy surfaces. Further progress can be made using semiempirical molecular orbital theory and direct dynamics, by which we mean the calculation of rates directly from electronic structure information without the intermediacy of fitting the electronic energies to a potential energy function. We have proposed and implemented a new way to use semiempirical molecular orbital theory as a fitting tool by adjusting the coulomb integrals and other parameters neglect-of-diatomic-differential-overlap (NDDO) molecular orbital theory. This provides an implicit potential energy function with less effort than analytic fitting and without the danger of omitting important types of interaction terms in an explicit potential function. We tested this approach for the reaction of Cl^- with CH_3Cl as well as for the microhydrated versions of this reaction. This interface of the molecular orbital calculations with the dynamics calculations was accomplished by the use of a new direct dynamics computer program MORATE. The results were compared in detail to previous calculations based on 18-, 27-, and 36-dimensional semiglobal analytic potential energy functions, and the correspondences between the kinetic isotope effects and their interpretation in terms of specific modes is very encouraging. We conclude that use of NDDO molecular orbital theory with specific reaction parameters should be a very useful technique for modeling potential energy surfaces for polyatomic reactions.

Interpolated VTST. In interpolated VTST[P11,P17] we start with *ab initio* calculations at the stationary points and optionally a *few* other points, and we use these to directly interpolate all reaction path properties needed for VTST and semiclassical multidimensional transmission coefficients. The results we obtained so far are very encouraging. For OH + H_2 and isotopic analogs, the interpolation procedures quantitatively reproduced effects due to variational optimization of the transition state location and tunneling along the MEP and semiquantitatively reproduced the effect of reaction-path curvature in the tunneling calculation.

Correlation of quantized transition state structure in accurate quantum dynamics calculations with adiabatic transition state theory. We have correlated accurate quantum dynamics calculations for H + H_2 and O + H_2 with variational transition state features. This has led to a deeper understanding of the quantum mechanics of transition states.

$F + H_2 \rightarrow HF + H$. A new potential energy surface was presented for the reaction F + H_2 → HF + H. The regions of the surface corresponding to collinear and bent geometries in the F–H–H and H–F–H barrier regions were based on scaled external correlation (SEC) electronic structure calculations. The new surface includes dispersion forces by a double many-body expansion.

$CH_3 + H_2, D_2$, and HD, $H + CD_3H \rightarrow H_2 + CD_3$. VTST calculations with multidimensional semiclassical transmission coefficients were also carried out for this prototype case of α-deuterium secondary kinetic isotope effects (KIEs) in a reaction involving the transformation between sp^3 and sp^2

carbon atoms. We found that the variational transition states lead to significantly different nontunneling KIEs than the conventional ones, e.g., 1.22 vs. 1.07, and the inclusion of multidimensional tunneling effects increases the discrepancy even more. The origins of these variational and tunneling effects were examined in detail in terms of structure, vibrational frequencies, and the curvature of the reaction path.

$Cl^- + CH_3Br \rightarrow CH_3Cl + Br^-$. We reported a molecular modeling study of the kinetic isotope effect (KIE) of a gas-phase S_N2 reaction that has recently been measured over a temperature range of a factor of 2.6; the KIE is inverse and rises 10% over this range. Our molecular modeling calculations employing VTST and direct dynamics yielded an inverse KIE that rises 10% as well. The molecular modeling calculations provide a mode-level interpretation of the inverse KIE.

Optimization of stationary points on potential energy surfaces with constraints. A new approach was presented for performing geometry optimization for stationary points on potential energy hypersurfaces with equality constraints on the internal coordinates of a polyatomic system. The working equations are the same as for unconstrained Newton-Raphson optimization in Cartesian coordinates except that projection operators were applied to the gradient and Hessian to enforce the constraints. Two reactive systems with bond distance and bond angle constraints were treated as examples, and the method performed satisfactorily.

Definition of reaction-path coordinates. We presented equations for generalized-normal-mode vibrational frequencies in reaction-path calculations based on various sets of coordinates for describing the internal motions of the system in the vicinity of a reaction path. We considered three-dimensional atom-diatom collisions with collinear steepest descent paths and reactions of the form $CX_3 + YZ \rightarrow CX_3Y + Z$ with reaction paths having C_{3v} symmetry as examples, and we presented numerical comparisons of the differences in harmonic reaction-path frequencies for various coordinate choices for three such systems. We tested the importance of the differences in the harmonic frequencies for dynamics calculations by using them to compute thermal rate constants using VTST with semiclassical ground-state tunneling corrections. We presented a new coordinate system for the reaction $CH_3 + H_2$ that should allow for more accurate calculations than the Cartesian system used for previous reaction-path calculations on this and other polyatomic systems.

References

R1. For reviews see D.G. Truhlar and B.C. Garrett, Accounts Chem. Res. **13**, 440 (1980); B.C. Garrett, D.G. Truhlar, and R.S. Grev, in *Potential Energy Surfaces and Dynamics Calculations*, edited by D.G. Truhlar (Plenum, New York, 1981), p. 431; D.G. Truhlar, A.D. Isaacson, R.T. Skodje, and B.C. Garrett, J. Phys. Chem. **86**, 2252 (1982); D.G. Truhlar, A.D. Isaacson, and B.C. Garrett, in *Theory of Chemical Reaction Dynamics*, edited by M. Baer (CRC Press, Boca Raton, 1985), Vol. 4, p. 65; D.G. Truhlar and B.C. Garrett, Annu. Rev. Phys. Chem. **35**, 159 (1984); M.M. Kreevoy and D.G. Truhlar, in *Investigation of Rates and Mechanisms of Reaction*, 4th ed., edited by C.F. Bernasconi (John Wiley & Sons, New York, 1986), Pt. 1, p. 13; D.G. Truhlar and B.C. Garrett, J. Chim. Phys. **84**, 365 (1987); S.C. Tucker and D.G. Truhlar, in *New Theoretical Concepts for Understanding Organic Reactions*, edited by J. Bertrán and I.G. Csizmadia (Kluwer, Dordrecht, 1989), p. 291; and refs. P5 and P19.

R2. B.C. Garrett and D.G. Truhlar, J. Chem. Phys. **70**, 1593 (1979).

R3. B.C. Garrett, D.G. Truhlar, and G.C. Schatz, J. Amer. Chem. Soc. **108**, 2876 (1986); G.C. Lynch, D.G. Truhlar, and B.C. Garrett, J. Chem. Phys. **90**, 3102 (1989).

R4. R.T. Skodje, D.G. Truhlar, and B.C. Garrett, J. Phys. Chem. **85**, 3019 (1981).

R5. B.C. Garrett, D.G. Truhlar, A.F. Wagner, and T.H. Dunning, Jr., J. Chem. Phys. **78**, 4400 (1983); D.K. Bondi, J.N.L. Connor, B.C. Garrett, and D.G. Truhlar, J. Chem. Phys. **78**, 5981 (1983); M.M. Kreevoy, D. Ostović, D.G. Truhlar, and B.C. Garrett, J. Phys. Chem. **90**, 3766 (1986); B.C. Garrett, N. Abusalbi, D.J. Kouri, and D.G. Truhlar, J. Chem. Phys. **83**, 2252 (1985); B.C. Garrett, T. Joseph, T.N. Truong, and D.G. Truhlar, Chem. Phys. **136**, 271 (1989).

R6. D.-h. Lu, T.N. Truong, B.C. Garrett, R. Steckler, A.D. Isaacson, S.N. Rai, G.C. Hancock, J.G. Lauderdale, T. Joseph, V.S. Melissas, and D.G. Truhlar, QCPE Bull. **11**, 13 (1991).

Publications, 1990-present

P1. "A Six–Body Potential Energy Surface for the S_N2 Reaction $Cl^-(g) + CH_3Cl(g)$ and a Variational Transition State Theory Calculation of the Rate Constant," S.C. Tucker and D.G. Truhlar, Journal of the American Chemical Society **112**, 3338–3347 (1990).

P2. "The Effect of Nonequilibrium Solvation on Chemical Reaction Rates. Variational Transition State Theory Studies of the Microsolvated Reaction $Cl^-(H_2O)_n + CH_3Cl$," S.C. Tucker and D.G. Truhlar, Journal of the American Chemical Society **112**, 3347–3361 (1990).

P3. "*Ab Initio* Transition State Theory Calculations of the Reaction Rate for OH + $CH_4 \rightarrow H_2O$ + CH_3," T.N. Truong and D.G. Truhlar, Journal of Chemical Physics **93**, 1761–1769 (1990).

P4. "What is the Effect of Variational Optimization of the Transition State on a–Deuterium Secondary Kinetic Isotope Effects? A Prototype: $CD_3H + H \rightarrow CD_3 + H_2$," D.–h. Lu, D. Maurice, and D.G. Truhlar, Journal of the American Chemical Society **112**, 6206–6214 (1990).

P5. "From Force Fields to Dynamics: Classical and Quantal Paths," D.G. Truhlar and M.S. Gordon, Science **249**, 491–498 (1990).

P6. "Global Control of Suprathreshold Reactivity by Quantized Transition States," D.C. Chatfield, R.S. Friedman, D.G. Truhlar, B.C. Garrett, and D.W. Schwenke, Journal of the American Chemical Society **113**, 486-494 (1991).

P7. "Projection Operator Method for Geometry Optimization with Constraints," D.-h. Lu, M. Zhao, and D.G. Truhlar, Journal of Computational Chemistry **12**, 376-384 (1991).

P8. "Solvent and Secondary Kinetic Isotope Effects for the Microhydrated S_N2 Reaction of $Cl^-(H_2O)_n$ with CH_3Cl," X.G. Zhao, S.C. Tucker, and D.G. Truhlar, Journal of the American Chemical Society **113**, 826-832 (1991).

P9. "A Simple Approximation for the Vibrational Partition Function of a Hindered Internal Rotation," D.G. Truhlar, Journal of Computational Chemistry **12**, 266-270 (1991).

P10. "Simple Perturbation Theory Estimates of Equilibrium Constants from Force Fields," D.G. Truhlar and A.D. Isaacson, Journal of Chemical Physics **94**, 357-359 (1991).

P11. "Direct Dynamics Calculations with Neglect of Diatomic Differential Overlap Molecular Orbital Theory with Specific Reaction Parameters," A. Gonzalez-Lafont, T.N. Truong, and D.G. Truhlar, Journal of Physical Chemistry **95**, 4618-4627 (1991).

P12. "The Definition of Reaction Coordinates for Reaction-Path Dynamics," G.A. Natanson, B.C. Garrett, T.N. Truong, T. Joseph, and D.G. Truhlar, Journal of Chemical Physics **94**, 7875-7892 (1991).

P13. "Use of Scaled External Correlation, a Double Many-Body Expansion, and Variational Transition State Theory to Calibrate a Potential Energy Surface for FH_2," G.C. Lynch, R. Steckler, D.W. Schwenke, A.J.C. Varandas, D.G. Truhlar, and B.C. Garrett, Journal of Chemical Physics **94**, 7136-7149 (1991).

P14. "Critical Tests of Variational Transition State Theory and Semiclassical Tunneling Methods for Hydrogen and Deuterium Atom Transfer Reactions and Use of the Semiclassical Calculations to Interpret the Overbarrier and Tunneling Dynamics," B.C. Garrett and D.G. Truhlar, Journal of Physical Chemistry **95**, 10374-10379 (1991).

P15. "Quantized Transition State Structure in the Cumulative Reaction Probabilities for the Cl + HCl, I + HI, and I + DI Reactions," D.C. Chatfield, R.S. Friedman, G.C. Lynch, and D.G. Truhlar, Journal of Physical Chemistry **95**, 57-63 (1992).

P16. "Interpolated Variational Transition State Theory: Practical Methods for Estimating Variational Transition State Properties and Tunneling Contributions to Chemical Reaction Rates from Electronic Structure Calculations," A. Gonzalez-Lafont, T.N. Truong, and D.G. Truhlar, Journal of Chemical Physics **95**, 8875-8894 (1991).

P17. "Temperature Dependence of the Kinetic Isotope Effect for a Gas-Phase S_N2 Reaction: Cl^- + CH_3Br," A.A. Viggiano, J. Paschkewitz, R.A. Morris, J.F. Paulson, A. Gonzalez-Lafont, and D.G. Truhlar, Journal of the American Chemical Society **113**, 9404-9405 (1991).

P18. "Optimized Calculations of Reaction Paths and Reaction-Path Functions for Chemical Reactions," V.S. Melissas, D.G. Truhlar, and B.C. Garrett, Journal of Chemical Physics, in press.

P19. "Variational Transition State Theory with Multidimensional Semiclassical Ground-State Transmission Coefficients: Applications to Secondary Deuterium Kinetic Isotope Effects in Reactions Involving Methane and Chloromethane," D.G. Truhlar, D.-h. Lu, S.C. Tucker, X.G. Zhao, A. Gonzalez-Lafont, T.N. Truong, D. Maurice, Y.-P. Liu, and G.C. Lynch, in *Isotope Effects in Chemical Reactions and Photodissociation Processes*, by J.A. Kaye (American Chemical Society, Washington), in press.

P20. "POLYRATE 4: A New Version of a Computer Program for the Calculation of Chemical Reaction Rates for Polyatomics," D.-h. Lu, T.N. Truong, V.S. Melissas, G.C. Lynch, Y.-P. Liu, B.C. Garrett, R. Steckler, A.D. Isaacson, S.N. Rai, G.C. Hancock, J.G. Lauderdale, T.Joseph, and D.G. Truhlar, Computer Physics Communications, in press.

KINETICS DATA BASE FOR COMBUSTION MODELING

Wing Tsang and John T. Herron
Chemical Kinetics and Thermodynamics Division
National Institute of Standards and Technology
Gaithersburg, Maryland 20899

PROGRAM SCOPE

The aim of this work is to produce a complete set of rate constants for use in the computer simulation of hydrocarbon combustion. The approach has been to begin with small molecules and gradually introduce more complicated species and structural elements. Currently, the data base1-5 contains all the reactions involving the following molecules and radicals; H, H2, O, O_2, OH, CO, CO_2, H_2O, HO_2, H_2O_2, HCO, H_2CO, CH_3, CH_4, C_2H_6, C_2H_5, C_2H_4, C_2H_3, C_2H_2, C_2H, CH_3OO, CH_3O, $^1CH_2$, $^3CH_2$, CH_3OH, CH_2OH, C_3H_8, i-C_3H_7, n-C_3H_7, i-C_4H_{10}, t-C_4H_9, i-C_4H_9, C_3H_6, C_3H_5, 2-C_4H_8, C_4H_7. Work on butadiene, butadienyl, propargyl and allene is nearing completion. All possible reactions are examined and the recommendations are based on either an evaluation of existing experimental results or on a best possible estimate, with the thermodynamics of the process as the boundary condition using appropriate theoretical or empirical methods.

RECENT PROGRESS

Recent work has focussed on the reactions of the larger olefins, the initial products of the decomposition of the larger alkyl radicals, which can have a profound effect on the overall course of the decomposition reaction. The introduction of unsaturated bonds leads to an increase in the number of available reaction channels. Although, in the absence of reliable experimental data a detailed treatment is not possible, we have been able to make recommendations based on very simplified models of the chemistry. In the following we discuss some of the key problems which have arisen in the course of this work.

Unimolecular decomposition. The presence of a double bond leads to a drastic weakening of the bond beta to the site of unsaturation and a strengthening of that adjacent to the double bond, and it is necessary to consider contributions from both bond breaking channels. We have previously carried out such an analysis for propene decomposition where data exist and the fits of the data have proven to be satisfactory in terms of the thermochemistry and the energy transfer parameter. In general, for small olefins, where there are no weak allylic carbon-carbon bonds, the olefins are more stable than the comparable alkanes.

In the case of cis-2-butene the available data is consistent with the direct formation of butadiene[6] under most combustion conditions. Over the whole range of experimental conditions, the reaction mechanism is more complex, including:

cis-butene ⇄ trans-butene → H+2-butenyl
→ CH_3+1-propenyl
→ H_2+butadiene
→ H+2-butenyl
→ CH_3+1-propenyl

A complete RRKM treatment would involve determining steady state distributions of the cis and trans butene isomers. In the absence of that kind of data, we have carried out calculations assuming that either there is complete cis-trans equilibration, or that there is no cis-trans conversion, followed in each case by multiple channel decomposition. We conclude that, in general, the molecular channel will be the most important. Indeed the relative smallness of the A-factor for the molecular channel compared to those for the other channels means that under most combustion conditions the molecular reaction is at the high pressure limit. These results illustrate again the importance of the magnitude of the A-factor in controlling energy transfer in unimolecular reactions. Unfortunately, for the present purposes there is considerable uncertainty in the rate expression for butadiene formation. Thus some caution must be exercised in the use of the recommendations.

In the case of butadiene decomposition, the experimental data, as discussed by Kiefer et al[7], are compatible with a molecular channel at the lower temperatures involving the direct formation of ethylene and acetylene. However, at the higher temperatures the bond breaking reaction to form two vinyl radicals begins to make a contribution. A possible problem in the earlier analysis of Kiefer et al was the failure to take into account contributions from the lower energy molecular channel in the analysis of the higher temperature results. This is consistent with by their need to postulate an extremely low rate constant for vinyl radical decomposition. A multichannel RRKM calculation has now been carried out and more reasonable fits of the data have been obtained. However, as in the case of cis-2-butene decomposition, the analysis is dependent on the rate expression selected for the molecular process.

Radical combination. The greater stability of resonance stabilized radicals means that combination reactions are very important in high temperature systems. There are very good data for the allyl self-reaction[8] and use of the combination to cross-combination rule should yield reasonably accurate rate constants for combination with alkyl radicals. The olefins formed in these reactions can decompose through a 6-membered retro-ene complex, although our RRKM calculation indicate that this is not competitive with stabilization. These processes have small A-factors compared to those for bond breaking and the lower activation energy is apparently not sufficient to make up the difference. This is another manifestation of the importance of the A-factor in determining the magnitude of energy transfer in unimolecular reactions.

The combination of propargyl radical has received much recent attention as a source of benzene in high temperature combustion systems[9]. The possible presence of over ten isomers has been indicated in recent studies[10]. Most of these are the linear isomers which are rapidly converted to more stable cyclic forms. However, the experimental evidence indicates that fulvene is very stable thermally. It may well be that conversion to benzene is largely induced by hydrogen atoms. For the present purposes our recommendation is given as an overall conversion rate of propargyl to form benzene with cautionary warnings

regarding the possible contributions from other reaction channels.

Radical attack on olefins. Unsaturation presents new reactive sites for radical attack. A serious problem is that addition leads to the formation of larger radicals, which under high temperature conditions either will be strongly reversed, or will undergo 1,4 or 1,5 hydrogen migration followed by decomposition, leading to a significantly altered pattern of decomposition products. The overall process is then:

$$\text{radical} + \text{olefin} \rightleftarrows \text{adduct} \rightleftarrows \text{isomerization product} \rightleftarrows \text{products}$$

As in the case of the conversion of cis-2-butene to butadiene, a proper calculation using RRKM theory should yield the pressure dependent rate constants and branching ratios. However, in the absence of accurate data on the isomerization processes for the radicals and the formidable calculational problems, we have assumed that the radicals are equilibrated and estimated branching ratios on the basis of reaction pathway degeneracies and bond energies.

A related problem arises from the addition of resonance stabilized radicals to unsaturated compounds, followed by isomerization to cyclic radicals. This has been confirmed experimentally[11], with recent measurements indicating that although this may be favored at lower temperatures, at combustion temperatures this process is probably slow compared to the reverse decomposition reaction[12]. However, the long life of these radicals in high temperature environments means that even a small rate constant for reaction with stable reactants such as ethylene and acetylene can lead to large product yields.

Data compilation. We continue to compile all publised data on combustion related reactions and the evaluations of the present work as part of the NIST Chemical Kinetics Database[13], for use on personal computers. The PC data base includes data on over 6000 reaction pairs, and new data are being added continuously.

PLANS

In the current year we expect to add to our data base an additional alkyne, propyne. In addition, it is expected that we will begin work on the aromatics. The first molecule to be covered will be benzene. Subsequently, we expect to concentrate on additional reactions of aromatic compounds, specifically those of phenyl, toluene, benzyl and phenol.

REFERENCES

1. Tsang, W. and Hampson R., J. Phys. Chem. Ref. Data, 15, 1087, 1986
2. Tsang, W., J. Phys. Chem. Ref. Data, 16, 471, 1987
3. Tsang, W., J. Phys. Chem. Ref. Data, 17, 887, 1988
4. Tsang, W., J. Phys. Chem. Ref. Data, 19, 1, 1990
5. Tsang, W., J. Phys. Chem. Ref. Data, 20, 221, 1991
6. Alfassi, Z. B., Golden, D. M., and Benson, S. W., Int. J. Chem. Kin., 5, 991, 1973
7. Kiefer, J. H., Mitchell, K. I. and Wei, H. C., Int. J. Chem. Kin., 20, 787, 1988

8. Tulloch, J. M., MacPherson, M. T., Morgan, C. A., and Pilling, M. J., J. Phys. Chem., 86, 3812, 1982
9. Stein, S. E., Walker, J. A., Suryan, M. M. and Fahr, A., 24th Sym. (Int.) on Combustion, (The Combustion Institute, Pittsburgh, Pa.),1990, 85
10. Tsang, W. and Walker, J. A.; "The Thermal Decomposition of Octadiyne as a Source of Propargyl Radicals" in preparation
11. Saito, T., Nohara, D. and Kunugi, T., "A Kinetic Study on the Formation of Aromatics During Pyrolysis of Petroleum Hydrocarbons" in "Industrial and Laboratory Pyrolysis"(L. F. Albright and B. L. Crynes, ed.) ACS Symposium Series 32, American Chemical Society, Washington, DC., pg 152
12. Tsang, W., and Walker, J. A., "Thermal Decomposition of 1,7 Octadiene and the Stability of Allyl and Pentenyl-4 Radicals", submitted to J. Phys. Chem.
13. "NIST Standard Reference Database 17; NIST Chemical Kinetics Database", Version 3.0, Standard Reference Data, National Institute of Standards and Technology, Gaithersburg, MD, April, 1991.

PUBLICATIONS, 1990-1992

1. Tsang, W., Mallard, W. G., and Herron, J. T. "Progress in the Development of a Chemical Kinetic Data Base for Combustion Chemistry" in "Scientific and Technical Data in a New Era" (P. S. Glaeser, ed.), Hemisphere Publishing Co, New York, 1990, pg 167
2. Tsang, W. and Lifshitz, A., "Shock Tube Methods in Chemical Kinetics," Annual Reviews of Physical Chemistry, 1990
3. Tsang, W., "Chemical Kinetic Data Base for Combustion Chemistry. Part IV. Isobutane", J. Phys. Chem. Ref. Data, 19, 1, 1990
4. Tsang, W., "Chemical Kinetic Data Base for Combustion Chemistry. Part V. Propene", J. Phys. Chem. Ref. Data, 20, 221, 1991
5. Slagle, I. R., Batt, L., Gmurczyk, G. W., Gutman, D. and Tsang, W., "The Unimolecular Decomposition of the Neopentyl Radical", J. Phys. Chem., 95, 7732, 1991
6. Tsang, W.,"Chemical Kinetic Data Base for Hydrocarbon Pyrolysis", Ind. Eng. Chem., 31, 3, 1992

Kinetic and Mechanistic Studies of OH- and CH-Radical Reactions

Andrew McIlroy‡ and Frank P. Tully
Combustion Research Facility
Sandia National Laboratories
Livermore, CA 94551-0969

Reactions of OH and CH radicals with fuel and oxidant molecules constitute critical steps in combustion processes. During the past year, we investigated the kinetics of the reactions of (1) OH with perfluoropropene and perfluorobenzene and (2) CH with H_2 and D_2. Pulsed-laser photolysis of the radical precursor initiates chemical reaction within a heated (or cooled) cell; cw, laser-induced fluorescence detection quantifies the evolution of the reaction in time.

We completed detailed kinetic studies of the reactions of OH with hexafluoropropene, $F_3C\text{-}CF{=}CF_2$, and hexafluorobenzene, C_6F_6. These fluorinated species were chosen in order to probe the approach to chemical equilibrium in OH + unsaturated molecule recombination/dissociation reactions, e.g., OH + alkene $\Leftrightarrow$ HO•alkene and OH + aromatic $\Leftrightarrow$ HO•aromatic. In propene and benzene, the temperature range over which the recombination/dissociation reactions may be studied is limited by the onset of direct H-atom abstraction by OH at $T \geq 600$ K and $T \geq 350$ K, respectively. Substitution of F for H eliminates this direct reaction channel on energetic grounds, and we expected the net OH-loss rate $\rightarrow 0$ as the recombination/dissociation balance shifts toward reactants at high T. The results for both reactions surprised us. As seen in Fig. 1 for OH + C_3F_6, we observed, as expected, a decreasing rate coefficient, k, with increasing temperature and biexponential [OH] decays above 528 K, indicative of the approach to steady-state, on the time scale of the experiments, of the recombination/dissociation reactions. Above 650 K, however, k(OH + C_3F_6) increases as T rises, providing evidence for yet another reaction channel, perhaps involving formation of HF + C_3F_5O. As shown in Fig. 2 for OH + C_6F_6, we observed a monotonically increasing k with increasing T, and we did not find biexponential [OH] decays at any temperature. This result implies either that the C-O bond strength in HO•C_6F_6 is dramatically different than that in HO•C_6H_6, or that HO•C_6F_6 does not re-form OH. Continuing studies of OH + unsaturated molecule reactions are planned.

We also began a series of CH-radical kinetics experiments with studies of the reaction

$$\begin{array}{c} CH + H_2 \Leftrightarrow CH_3^* \Leftrightarrow CH_2 + H. \\ \Downarrow M \\ CH_3 \end{array}$$

This is a fundamentally important and theoretically tractable reaction. We measured the pressure dependence of the reaction at 295 K and the temperature dependence of the reaction at P = 8.2 and 750 torr of He. These results are displayed in Figs. 3-5. The buffer-gas pressure dependence results from competition between collisional stabilization

of CH_3^* and dissociation back to reactants. At low pressure, CH-removal due to CH_3^* stabilization becomes less important, and the temperature dependence of the rate coefficient is dominated by the process forming CH_2 + H. Conversely, at 750 torr of He, the temperature dependence for CH-removal mostly reflects the collisional stabilization channel. Preliminary experiments on CH + D_2 indicate that the isotopic exchange channel to form CD + HD is a very significant process. Continued experiments and RRKM/master equation calculations on these reactions are planned.

‡ Sandia Postdoctoral Research Associate

DOE/BES-sponsored publications during the past two years:

1. F. P. Tully, "Catalytic Dehydration of Alcohols by OH. $(H_3C)_3CCH_2OH$. A Limiting Case," *Twenty-Third Symposium (International) on Combustion* (The Combustion Institute, Pittsburgh, PA) pp 147-153 (1990).

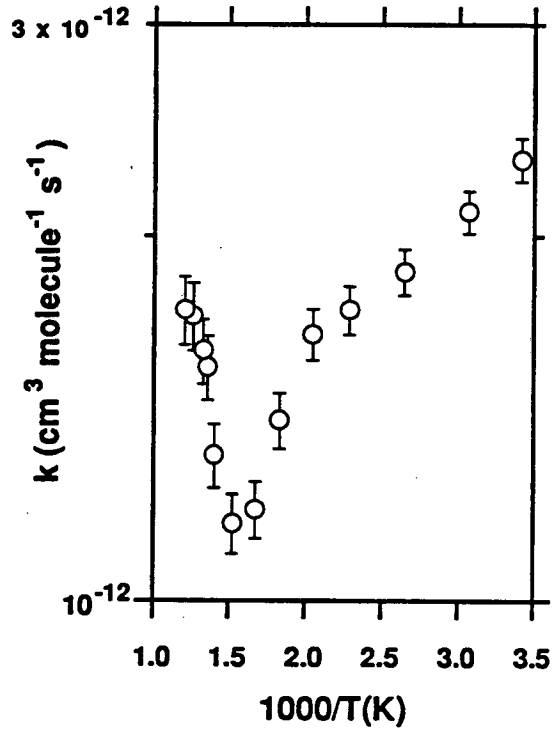

Fig. 1: Arrhenius plot of kinetic data for the reaction OH + C_3F_6 → Products. Points between 528 and 592 K were obtained from initial slopes of biexponential [OH] decays.

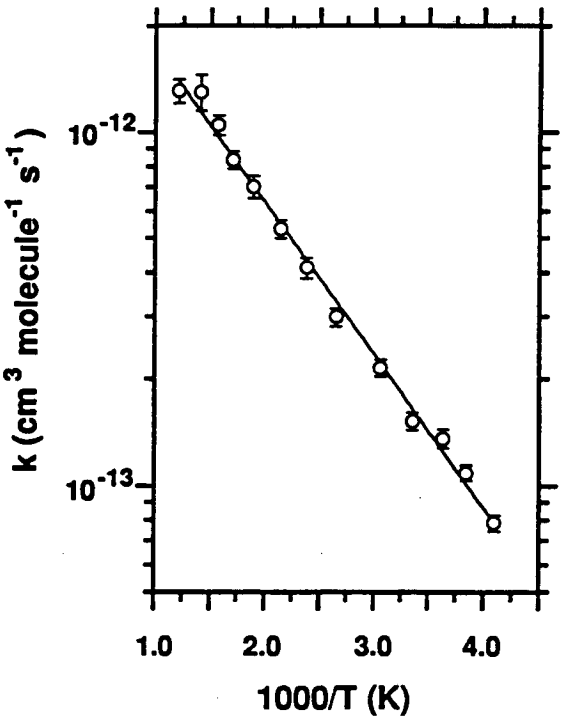

Fig. 2: Arrhenius plot of kinetic data for the reaction OH + C_6F_6 → Products.

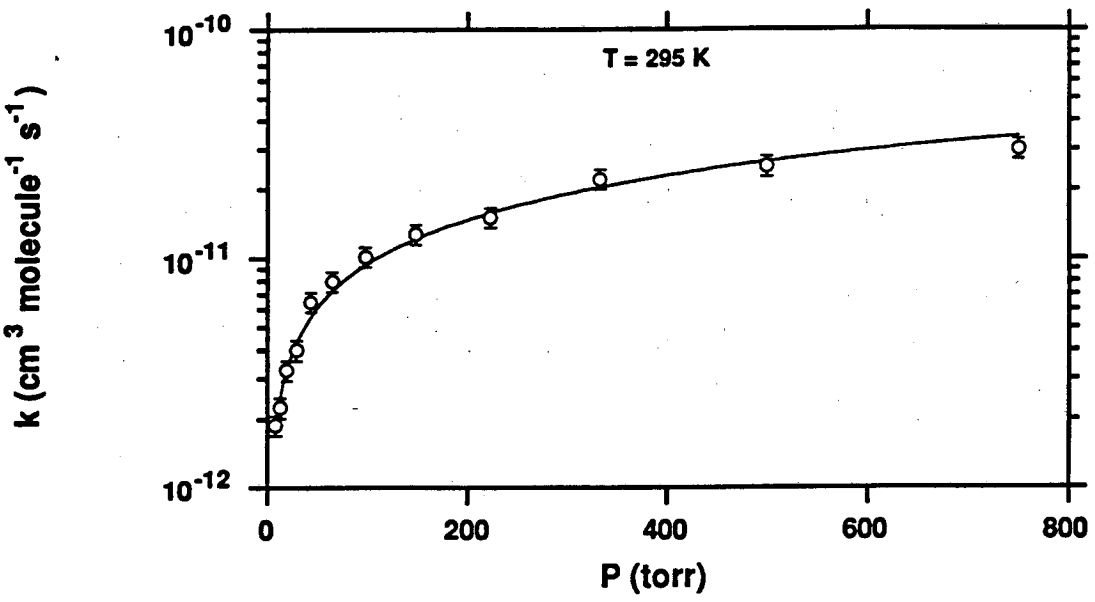

Fig. 3: Rate coefficient for CH-loss in CH + H_2 → Products reaction as a function of He buffer-gas pressure.

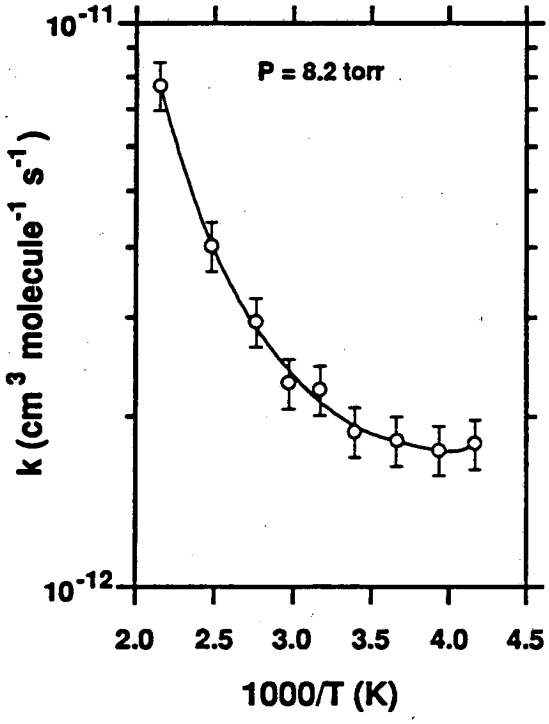

Fig. 4: Arrhenius plot of rate coefficient for CH-loss in CH + H_2 → Products reaction at 8.2 torr He pressure.

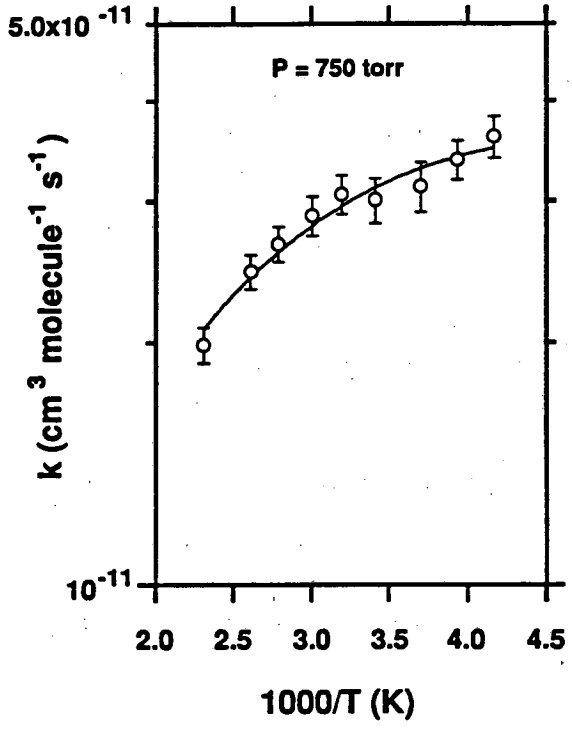

Fig. 5: Arrhenius plot of rate coefficient for CH-loss in CH + H_2 → Products reaction at 750 torr He pressure.

SINGLE-COLLISION STUDIES OF HOT ATOM ENERGY TRANSFER AND CHEMICAL REACTION

James J. Valentini
Department of Chemistry
Columbia University
New York, NY 10027

PROGRAM SCOPE

The emphasis of this research is state-to-state dynamics of reaction and energy transfer in collisions at high kinetic energy or with reactants that are vibrationally excited. Current emphasis is on reactions of free radicals such as H, OH, and CH_3 with H_2, CH_4, H_2O, and other hydrogen-containing molecules. The motivation for the work is the desire to provide a detailed understanding of the fundamental molecular processes involved in the production, utilization, and transformation of energy sources, as in combustion and coal gasification.

The work is primarily experimental, using highly time-resolved laser spectroscopic methods to provide for reactant preparation and product analysis on a single-collision time scale. The primary spectroscopic tool for product state analysis is coherent anti-Stokes Raman scattering (CARS) spectroscopy. CARS is used despite its modest sensitivity because of its generality and because the extraction of quantum state populations from CARS spectra is straightforward. The combination of the generality and easy analysis of CARS makes possible absolute cross section measurements (both state-to-state and total), a particularly valuable capability for characterizing reactive and inelastic collisions. Reactant free radicals are produced by laser photolysis of appropriate precursors. For reactant vibrational excitation stimulated Raman techniques are being developed and implemented.

There is also a significant theoretical component to our research. This involves quasiclassical trajectory calculations of the state-to-state dynamics. The theoretical calculations enable the detailed analysis and interpretation of the experimental results needed to extract the full value of the laboratory measurements. Also, viewed as simulations of the collision dynamics the trajectory calculations make possible the development of phenomenological models of reaction dynamics at high energies.

The focus of this research program is now on reactions involving both polyatomic reactants and polyatomic products. Our objective is to determine how the multitude of degrees of freedom of the reactants and products influence the dynamics of reactions at high energies, that is how the high dimensionality of the reactants/products differentiates such reactions from atom + diatom reactions of the same kinematics and energetics.

RECENT PROGRESS

In this past year we have finished three projects and begun two new ones. Our experimental study of the dynamics of the H + RH → H_2 + R (RH = CH_4, C_2H_6, and C_3H_8) reactions has been completed, and several journal articles describing the results have appeared or will soon appear in print. The biggest surprise of that study was the anomalous positive correlation of H_2 product rotational and vibrational energies. This is unprecedented for a direct, ostensibly simple, bimolecular reaction.

We also completed our study of the photodissociation dynamics of CH_3I. This project was undertaken as a preliminary to an investigation of the state resolved dynamics of reactions (e. g. H + CH_4 → H_2 + CH_3 and OH + CH_4 → H_2O + CH_3) in which we need to characterize the state distribution of the methyl radical product. We used the photolysis of CH_3I to provide a source of methyl radicals that we could use to assign and characterize the fully rotationally resolved CARS spectrum of the radical. This spectroscopy had not been worked out previously, but a knowledge of it is essential to our planned use of CARS to detect, with rotational state resolution, the CH_3 reaction product. A paper on the CH_3 CARS spectroscopy has recently appeared in print.

These experiments also provided an extensive characterization of the uv photodissociation dynamics of CH_3I + hν → CH_3 + I. We determined both the vibrational and rotational state distributions of the CH_3 fragment. In particular, we were able to address very thoroughly the mapping of CH_3I parent rotational angular momenta onto the CH_3 fragment. We did so by effecting photodissociation at different positions in a pulsed free-jet expansion, so as to control the parent CH_3I rotational state distribution. We took advantage of the universality of CARS to determine both the parent rotational state distribution, which in general is not Boltzmann, and that of the fragment, making correlations between them easy to establish. We are now preparing a manuscript describing these results, and will soon submit this for publication.

Also completed this past year are our quasiclassical trajectory studies of the dynamics of the H' + HX → H'H + X / H'X + H reactions (X = Cl, Br, I). Two papers dealing with these studies have already appeared, and another has just been submitted for publication.

One of our newly initiated projects is the extension of our quasiclassical trajectory studies to many-atom systems. Our growing interest in experimental state-to-state dynamics studies of reactions involving polyatomic reactants and products dictates that we develop the capability to carry out theoretical calculations on such systems. Our short-term interest is in the H + CH_4 → H_2 + CH_3 reaction described above, for which we have already completed the experimental studies. To do these quasiclassical trajectory calculations we have written and tested a new code, since nothing available was suitable for our needs. In particular, we have implemented an

adiabatic invariance approach for the quantization of the zero-point energy of the CH_4 reactant. Production runs of the trajectories have just gotten underway.

On the experimental side we are initiating a study of the dynamics of the H + CH_4 reaction with vibrationally excited CH_4 prepared by stimulated Raman excitation. This is being implemented with CARS detection of the CH_3 radical product to assess the flow to vibrational energy from reactants to products in this system.

RESEARCH PUBLICATIONS 1990-1992

1. P.M. Aker and J.J. Valentini, "Quasiclassical Trajectory Studies of H + HX → H_2 + X (X = Cl, Br, I) Reactions at High Collision Energy," Israel Journal of Chemistry, 30, 157 (1990).

2. G. Rumbles, E.K.C. Lee, and J.J. Valentini, "Laser-Induced Fluorescence from Predissociating Formyl Radical. Part 2. Analysis of Dispersed Emission from the A-X Transition," J. Chem. Soc. Faraday Trans. 86, 3837 (1990).

3. G.J. Germann, Y-D. Huh, and J.J. Valentini, "Observation of Anomalous Energy Partitioning to the HD Product of the H + CD_4 → HD + CD_3 Reaction," Chem. Phys. Lett. 183, 353 (1991).

4. J.J. Valentini, P.M. Aker, G.J. Germann, and Y-D. Huh, "Transition State Control of Product Rotational Distributions in H + RH → H_2 + R Reactions (RH = HCl, HBr, HI, CH_4, C_2H_6, C_3H_8)" J. Chem. Soc. Faraday Discuss. 91, 173 (1991).

5. G.J. Germann, Y-D. Huh, and J.J. Valentini, "State-to-State Dynamics of Atom + Polyatom Abstraction Reactions. I. The H + CD_4 → HD(v',J') + CD_3 Reaction," J. Chem. Phys. 96, 1957 (1992).

6. N.E. Triggs, M. Zahedi, J.W. Nibler, P. DeBarber, and J.J. Valentini, "High Resolution Study of the ν_1 Vibration of CH_3 by CARS Photofragment Spectroscopy," J. Chem. Phys., 96, 1822 (1992).

7. P.M. Aker, G.J. Germann, and J.J. Valentini, "Experimental and Theoretical Study of H + HI → H_2 + I Reaction Dynamics at 1.3 eV Collision Energy," J. Chem. Phys., 96, 2756 (1992).

8. G.J. Germann, Y-D. Huh, and J.J. Valentini, "State-to-State Dynamics of Atom + Polyatom Abstraction Reactions. II. The H + C_2H_6 → H_2 + C_2H_5 and H + C_3H_8 → H_2 + C_3H_7 Reactions," J. Chem. Phys., 96, xxxx (1992).

Theoretical Studies of the Dynamics of Chemical Reactions

Albert F. Wagner, Michael J. Davis, Stephen K. Gray, George C. Schatz

Theoretical Chemistry Group, Chemistry Division
Argonne National Laboratory, Argonne, IL 60439

Hierarchical Analysis of Molecular Spectra. A method of analyzing spectra of highly excited molecules has been developed. Such spectra are often very complicated and are difficult to assign in a traditional manner, with statistical methods often used to characterize them. Our methodology combines aspects of traditional and statistical approaches. We have applied our methods to several theoretical and experimental spectra. In the case of experimental spectra we can discern information such as: 1) spectral clustering, 2) dimensionality, and 3) number of time scales implied by a given spectrum. In addition to this, when a theoretically generated spectrum is available, we can use our methods to unambiguously assign smooth spectral features and also to study energy transfer pathways.

The figures on the following page give an overview of our methodology which will be described more fully in the presentation. The plot on the upper left is a vibronic spectrum for NO_2 published by Delon, Jost, and Lombardi [J. Chem. Phys. *95*, 5701(1991)]. The plot on the upper right shows a smoothed version of the spectrum, which shows distinct clumping. Results such as these can be used to generate a hierarchical tree, such as the one in the lower left. This plot was generated by following the evolution of the spectrum as the resolution is changed in a continuous manner. Peaks emerge as resolution is increased and these are represented by the branching of the tree. The tree can be analyzed with several different types of measures. The plot on the lower right shows one type of analysis. This figure measures the importance of each node on the tree. The abscissa is the number of peaks detected at any given resolution and the ordinant shows the log of the variance of the data represented by the tree (roughly, the spacings of the nodes from the previous figure modulated by the branching topology of the tree). The relevant aspects of this plot are the overall magnitude of the variance and the various sudden drops in the variance as more peaks are resolved. The overall size of the variance is related to the complexity and assignability of a spectrum, although this assignability may be quite unusual from a traditional spectroscopic viewpoint. The sudden drops are related to the various time scales present in the molecule, which in turn is related to energy transfer properties of the molecule.

Reactions involving the formyl radical. The reaction

$$H + CO \rightleftharpoons HCO^* \overset{M}{\rightleftharpoons} HCO \qquad (1)$$

is of long-standing interest as a prototype of a simple addition reaction. As last year, this reaction was studied with stabilization [in collaboration with Bowman (Emory)], time-independent quantum dynamics, and time-dependent quantum dynamics calculations. The first two methods were used on total angular momentum J=1 calculations. Significant basis set problems were encountered with either method that are now believed resolved. Results indicate that HCO resonances have a symmetric top pattern with slowly decreasing lifetimes with increasing J. Increasing the bend excitation in the resonance systematically distorts the symmetric top pattern. The fully three dimensional time-dependent quantum dynamics calculations of HCO unimolecular decay for J = 0 were completed. An efficient and novel propagation scheme, generally applicable to other wave packet problems, was developed and used. The positions and linewidths of the sane resonances studied by time-independent scattering and stabilization methods were inferred from relatively short

time propagations with the aid of Prony's spectral method. The CO rotational product distributions were found to exhibit interesting structure, which in turn could be partly understood by inspection of the portions of the wave packet that pass through the transition state region. A video depicting the time evolution of wave packet density in 3D helped develop a mechanistic picture.

In collaboration with Goldfield at the Cornell Supercomputer Facility, a project to examine the wave packet dynamics of the Renner-Teller effect in HCO was initiated. Motivation for this project has been provided by the extensive experimental work of Houston's group on this system. This project involves examining bend excitations on the first excited state of HCO (which is linear) and then probing the formation of H + CO products, which can only result by Renner-Teller interaction with the ground electronic state. The nature of the Renner-Teller interaction is such that overall rotational angular momentum leads to coupling of the (bent) ground and (linear) excited states. It is hoped that the time-dependent calculations will lead to simple mechanistic pictures of this seemingly complicated dynamics.

Thermal Dissociation of HCN. A standard derivation of the bond energy from the measured thermal dissociation rate constant of HCN:

$$HCN \xrightarrow{M} H + CN \qquad (2)$$

is more than 5 kcal/mole lower than the known thermodynamic value. The standard derivation ignores the hindered rotation of H about CN whose barrier is quite high (>40 kcal/mole). However, in collaboration with Kiefer (UIC), we performed an approximate rigid bender calculation of the complete spectrum of hindered rotor states and showed that the density of these states dramatically increased the A factor, allowing the derivation of the correct bond energy. This dynamics is a simpler version of what is inferred in the dissociation of acetylene and other small unsaturated molecules.

Reaction of atomic radicals with hydrogen halides. In continuing centrifugal-sudden distorted-wave and coupled channel hyperspherical quantum dynamics studies of prototypic heavy-light-heavy triatomic reactions, the following reactions have been examined:

$$Cl' + HCl \rightarrow Cl'H + Cl \qquad (3)$$

$$I' + HI \rightarrow HI' + I \qquad (4)$$

$$O(^3P) + HCl \rightarrow OH + Cl\,. \qquad (5)$$

for developing theories of tunnelling and other quantum phenomena including transition state resonances. All three reactions have been examined by transition state photodetachment spectroscopy, and ab initio PESs are recently available for reactions (3) and (5). In addition to assessing the accuracy of these surfaces and comparing approximate dynamical models to our exact quantum calculations on all three reactions, our most intriguing results concern the measurable consequences of the lowest energy transition state resonance for reaction (3). Before our study it was generally assumed that transition state resonance features in any reaction are completely washed out in integral cross sections because of the sum over partial waves provides a source of inhomogeneous broadening. For reaction (3) we found that this was not necessarily true for reactions starting from the v=1 state of HCl, and that, at low temperatures, a single transition state resonance can be dominant in determining the transition state rate constant.

Wave Packet Dynamics of 4-Atom Unimolecular Reactions. A project to study 4-atom wave packet dynamics has been initiated. The initial project involves studying the fragmentation of X_2BC van der Waals clusters (X = noble gas atom, BC = halogen molecule) to X + X+ BC. Such reactions have been studied experimentally by Janda and co-workers. With such time-

dependent calculations it is possible to directly assess the role of sequential ($X_2BC \rightarrow X + XBC \rightarrow X + X + BC$) vs. direct ($X_2BC \rightarrow X + X + BC$) mechanisms, and other interesting dynamical features. A reduced dimension study was completed and work has been initiated on the full (six dimensional) problem.

Markov Shifts in the Henon Family
M. J. Davis, R. S. MacKay, and A. Sannami, Physica D **52**, 171 (1991).

Novel Methods of Spectral Analysis
R. Roy, B.G. Sumpter, G.A. Pfeffer, S.K. Gray, and D.W. Noid, Physics Reports **205**, 109 (1991).

An Ab Initio Theoretical Study of the CH_2+H $\rightleftharpoons$ CH_3 $\rightleftharpoons$ CH+H_2 Reactions
M. Aoyagi, R. Shepard, A. F. Wagner, International Journal of Supercomputing Applications **5**, 72 (1991).

Theoretical Stabilization and Scattering Studies of Resonances in the Addition Reaction H + CO $\rightleftharpoons$ HCO
B. Gazdy, J. M. Bowman, S.-W. Cho, and A. F. Wagner, J. Chem Phys. **94**, 4192-4194 (1991).

The Addition and Dissociation Reaction H + CO $\rightleftharpoons$ HCO. 3. Implementation of Isolated Resonance RRKM Theory with Exact Quantum Studies for J=0
S.-W. Cho, A. F. Wagner, B. Gazdy, and J. M. Bowman, J.Phys. Chem **95**, 9897-9900 (1991).

The Analysis of Muonium Hyperfine Interaction Measurements of Thermal Rate Constants for Addition Reactions
R. J. Duchovic, A. F. Wagner, R. E. Turner, D. M. Garner, and D. G. Fleming, J. Chem. Phys. **94**, 2794-2806 (1991).

Experimental and Theoretical Study of the Recombination Reaction CH_3 + CH_3 $\rightarrow$ C_2H_6
D. Walter, H-H. Grotheer, J. W. Davies, M. J. Pilling, and A. F. Wagner, Twenty-Third International Symposium on Combustion **23**, 107-114 (1990).

Influence of Transition State Resonances on Integral Cross Sections and Product Rovibrational Distributions for the Cl + HCl $\rightarrow$ ClH + Cl Reaction
G. C. Schatz, D. Sokolovski and J.N.L.Connor, J. Chem. Phys. **94**, 4311 (1991).

A Quasiclassical Trajectory Study of the OH + CO Reaction
K. Kudla, G. C. Schatz and A. F. Wagner, J. Chem. Phys. **95**, 1635 (1991).

An Analytical Representation of the Lowest Potential Energy Surface for the Reaction $O(^3P)$ + HCl(X) $\rightarrow$ OH($X\Pi$) + $Cl(^2P)$
G. C. Schatz and M. S. Gordon, J. Chem. Phys. **95**, 6421 (1991).

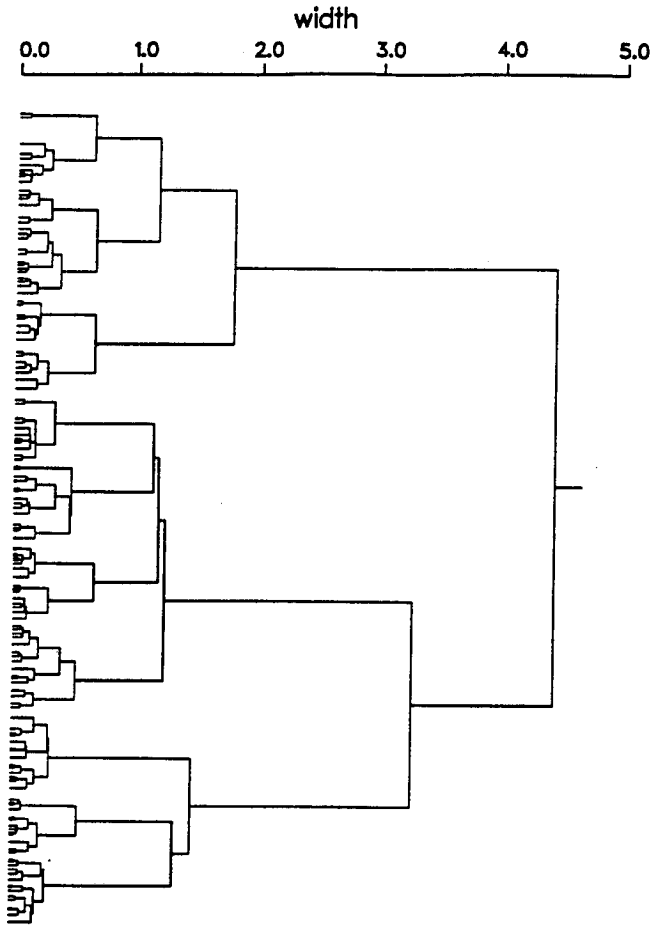
width
0.0
1.0
2.0
3.0
4.0
5.0

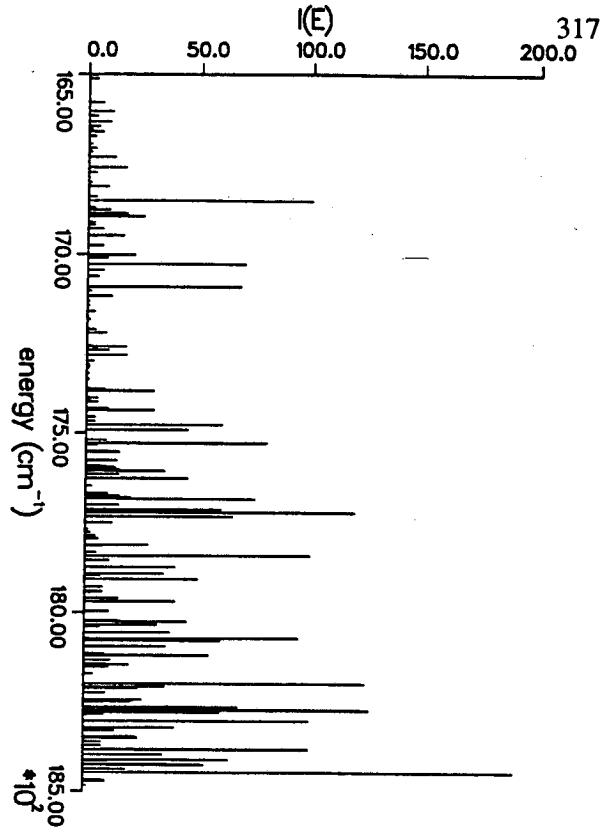
I(E)
0.0
50.0
100.0
150.0
200.0
165.00
170.00
175.00
180.00
185.00
energy (cm⁻¹)
*10²

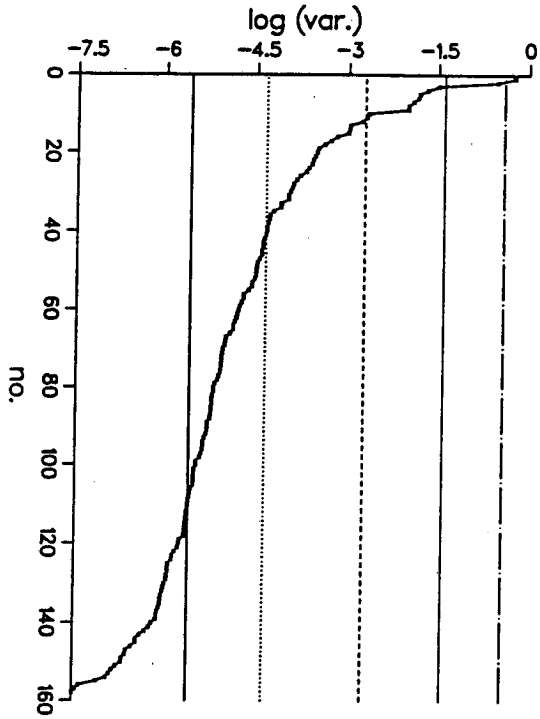
log (var.)
-7.5
-6
-4.5
-3
-1.5
0
0
20
40
60
80
100
120
140
160
no.

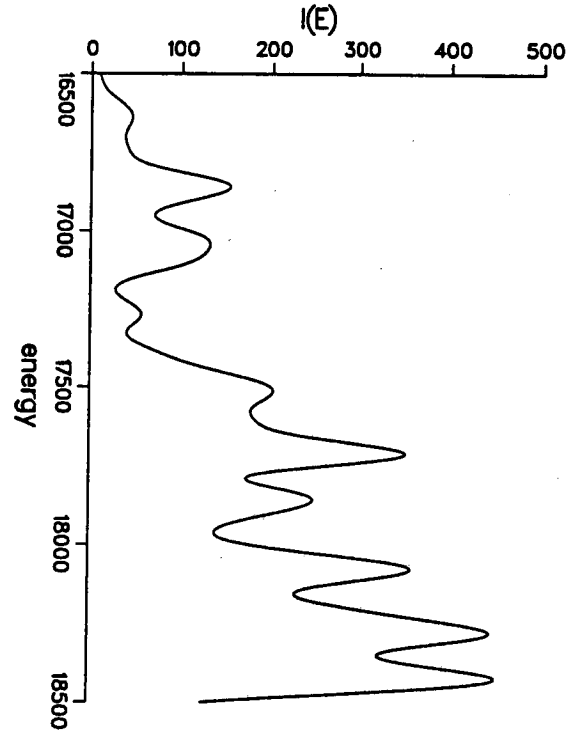
I(E)
0
100
200
300
400
500
16500
17000
17500
18000
18500
energy

CHEMICAL KINETICS MODELING

Charles K. Westbrook and William J. Pitz
Lawrence Livermore National Laboratory
P. O. Box 808, Livermore, California 94550

Our research program emphasizes the development of detailed chemical kinetic reaction mechanisms for the combustion of hydrocarbon and other types of fuels, as well as the application of these mechanisms to the modeling of combustion in practical energy systems. Interactions with other researchers who carry out experimental projects and with industrial programs are essential parts of our work.

During the past year, much of our work has involved development and application of reaction mechanisms to describe engine knock and other low temperature oxidation processes. Abstraction of H atoms from primary, secondary and tertiary sites in the hydrocarbon fuel molecule, addition of molecular oxygen to the alkyl radicals, isomerization of these alkylperoxy radicals via internal H atom transfer, production of OH and other radical species via radical decomposition, and other low temperature oxidation processes were found to be very important in predicting rates of ignition. In particular, in the area of alkylperoxy radical isomerization, ring strain energy and the type of C-H bond being broken were found to be of greatest importance and could be used to interpret most of the available data on the variation of octane rating with molecule size and structure.

We used these kinetic principles to write reaction mechanisms for isomers of pentane, hexane, and heptane and some isomers of octane. Each of these fuels was used within the model to examine its rate of ignition and its implied octane number. In most cases, the computed rate of ignition correlated extremely well with its observed octane number.

Mixtures of different fuels and the use of different proknock and antiknock additives were studied with the numerical model. Although the relationship between ignition rate and octane number was found to be nonlinear, additives and mixtures were still found to act in a predictable and theoretically sound manner. The model clearly describes most of the major features of the knock problem.

We are continuing these studies of knock tendency. We found that a major antiknock additive, methyl tert-butyl ether (MTBE) acts by removing radical species from the radical pool, by inhibiting internal isomerization reactions, and by producing relatively unreactive intermediate species. It is also interesting to note that this mode of operation is much different from that of another strong antiknock compound tetra-ethyl lead (TEL), which inhibits the intermediate temperature ignition that is promoted by HO_2 radicals. Thus our study shows that different antiknock compounds can act in vastly different ways. These studies also suggest modes of activity for screening other possible antiknock additives. In the coming year we intend to focus on the details of the $R+O_2$ reaction, its product distributions, and the relative rates of stabilization, internal isomerization, and thermal decomposition. A question of particular relevance is whether isomerization occurs primarily in the ground state or excited state of RO_2.

Our studies have also emphasized the refinement of submechanisms for smaller hydrocarbon species which are produced and then consumed during the oxidation of larger practical fuels. These species studied as fuels themselves included ethene, propene, and isobutene, all of them important intermediate species in many types of fuel consumption. In addition, we studied oxidation mechanisms of ethanol and propane. In the coming year we hope to develop reaction mechanisms for other alcohol fuels, including isomers of propanol, and for other oxygenated species as well. We also intend to continue our past studies of butane oxidation; while past work emphasized oxidation at atmospheric and lower pressures, our next project will address butane combustion at elevated pressures, which will refine our understanding of the pressure dependence of many reaction rates and other portions of the reaction mechanisms.

We continued to apply kinetic modeling techniques to the analysis of detonation parameters, working in close collaboration with experimental studies. Numerically predicted detonation cell sizes for hexane, decane, and various nitro-alkanes and alkyl nitrates all agreed well with measured values, lending further confidence to the general techniques used to estimate reaction rate parameters and reaction paths. In addition, model predictions of the variation in detonability with initial gas temperature and pressure were found to agree well with experimental results.

We continued to examine the kinetics of hydrocarbon analogs, species in which either H or C atoms are replaced by other atoms. The most common of such species are chlorinated hydrocarbons, which we studied in stirred reactor environments. However, another analog species in silane, and methane analog with C replaced by Si. We examined ignition and oxidation of silane in shock tube and low temperature conditions, focusing on the role of SiH_3O_2 radicals in both excited and ground states. This work was rather speculative, but it was able to interpret existing experimental data and serves as a starting point for subsequent experimental and modeling studies.

We applied our chemical kinetics models to more speculative studies of hydrocarbon and other species consumption under supercritical water conditions. We identified very high pressure falloff behavior of decomposition reactions of species such as HO_2 and H_2O_2, but it also appears as if conventional combustion kinetics are applicable under these conditions. We also examined the chemical engineering problem of oxidative coupling, converting methane to higher hydrocarbons under very rich oxidation conditions. We demonstrated that the same reactions that consume methane also consume the C_2 and higher species, resulting in a fairly rigid limit to the effectiveness of this type of process in converting methane to liquid fuels. Finally, during the past two years, we wrote or co-authored three reviews of kinetic modeling and combustion.

Publications in 1990-1992

1. Hoffman, J. S., Lee, W., Litzinger, T. A., Santavicca, D. A., and Pitz, W. J., "Oxidation of Propane at Elevated Pressures: Experiments and Modelling", Combust. Sci. and Technol. 77, 95 (1991).

2. Miller, J. A., Kee, R. J., and Westbrook, C. K., "Chemical Kinetics and Combustion Modeling", Annu. Rev. Phys. Chem. 1990 41, 345 (1990).

3. Mallinson, R. G., Braun, R. L., Westbrook, C. K., and Burnham, A. K., "Detailed Chemical Kinetics Study of the Role of Pressure in Butane Pyrolysis", Indust. and Engin. Chemistry Research 31, 37 (1992).

4. Tieszen, S. R., Stamps, D. W., Westbrook, C. K., and Pitz, W. J., "Gaseous Hydrocarbon-Air Detonations", Combust. Flame 84, 376 (1991).

5. Papavassiliou, J., Makris, A., Knystautas, R., Lee, J. H., Westbrook, C. K., and Pitz, W. J., "Measurements of Cellular Structure in Spray Detonation", Thirteenth International Colloquium on the Dynamics of Explosions and Reactive Systems, 1991.

6. Westbrook, C. K., "Combustion", Encyclopedia of Applied Physics, in press (1992).

7. Wilk, R. D., Pitz, C. K., Westbrook, C. K., and Cernansky, N. P., "Kinetic Modeling of Ethene Oxidation at Low and Intermediate Temperatures", Twenty-Third Symposium (International) on Combustion, p. 203, The Combustion Institute, Pittsburgh (1991).

8. Wilk, R. D., Pitz, W. J., Westbrook, C. K., Addagarla, S., Miller, D. L., Cernansky, N. P., and Green, R. M., "Combustion of n-Butane and Isobutane in an Internal Combustion Engine: A Comparison of Experimental and Modeling Results", Twenty-Third Symposium (International) on Combustion, p. 1047, The Combustion Institute, Pittsburgh (1991).

9. Britten, J. A., Tong, J., and Westbrook, C. K., "A Numerical Study of Silane Combustion", Twenty-Third Symposium (International) on Combustion, p. 195, The Combustion Institute, Pittsburgh (1991).

10. Cowart, J. S., Keck, J. C., Heywood, J. B., Westbrook, C. K., and Pitz, W. J., "Engine Knock Predictions Using a Fully-Detailed and a Reduced Chemical Kinetic Mechanism", Twenty-Third Symposium (International) on Combustion, p. 1055, The Combustion Institute, Pittsburgh (1991).

11. Griffiths, J. F., Coppersthwaite, D., Phillips, C. H., Westbrook, C. K., and Pitz, W. J., "Autoignition Temperatures of Binary Mixtures of Alkanes in a Closed Vessel: Comparisons Between Experimental Measurements and Numerical Predictions", Twenty-Third Symposium (International) on Combustion, p. 1745, The Combustion Institute, Pittsburgh (1991).

12. Westbrook, C. K., and Pitz, W. J., "Numerical Modeling of Combustion of Complex Hydrocarbon Fuels", in Numerical Approaches to Combustion Modeling, J. P. Boris and E. Oran, eds., Prog. Astr. Aero., vol. 135, American Institute of Aeronautics and Astronautics, Washington (1991).

13. Beeson, H. D., McClenagan, R. D., Benz, F. J., Pitz, W. J., Westbrook, C. K., and Lee, J. H. S., "Detonability of Hydrocarbon Fuels in Air", Prog. Astro. Aero. 133, 19 (1991).

14. Corre, C., Dryer, F. L., Pitz, W. J., and Westbrook, C. K., "Two-Stage n-Butane Flame: A Comparison Between Experimental Measurements and Modeling Results", accepted for publication (1992).

15. Chevalier, C., Pitz, W. J., Warnatz, J., and Westbrook, C. K., "Hydrocarbon Ignition: Automatic Generation of Reaction Mechanisms and Applications to Modeling of Engine Knock", accepted for publication (1992).

16. Curran, H. J., Dunphy, M. P., Simmie, J. M., Westbrook, C. K., and Pitz, W. J., "Shock Tube Ignition of Ethanol, Isobutene, and MTBE: Experiments and Modeling", accepted for publication (1992).

17. Westbrook, C. K., Pitz, W. J., and Leppard, W. R., "The Autoignition Chemistry of Paraffinic Fuels and Pro-Knock and Anti-Knock Additives: A Detailed Chemical Kinetic Study", Society of Automotive Engineers report SAE-912314 (1991).

18. Pitz, W. J., Westbrook, C. K., and Leppard, W. R., "Autoignition Chemistry of C_4 Olefins Under Motored Engine Conditions: A Comparisons of Experimental and Modeling Results", Society of Automotive Engineers report SAE-912315 (1991).

19. Barr, P. K., Keller, J. O., Bramlette, T. T., Westbrook, C. K., and Dec, J. E., "Pulse Combustor Modeling: Demonstration of the Importance of Characteristic Times", Combust. Flame 82 252 (1990).

PROBING FLAME CHEMISTRY WITH MBMS, THEORY, AND MODELING

Phillip R. Westmoreland

Department of Chemical Engineering
University of Massachusetts at Amherst
159 Goessmann Laboratory
Amherst, Massachusetts 01003

Phone (413) 545-1750
FAX (413) 545-1647
BITnet address: "westm@umaecs"
Internet address: "westm@ecs.umass.edu"

Program Scope

The objective is to establish kinetics of combustion and molecular-weight growth in C_3 hydrocarbon flames as part of an ongoing study of flame chemistry. Specific reactions to be studied are (1) the growth reactions of C_3H_5 and C_3H_3 with themselves and with unsaturated hydrocarbons and (2) the oxidation reactions of O and OH with C_3's. Our approach combines molecular-beam mass spectrometry (MBMS) experiments on low-pressure flat flames; theoretical predictions of rate constants by thermochemical kinetics, Bimolecular Quantum-RRK, RRKM, and master-equation theory; and whole-flame modeling using full mechanisms of elementary reactions.

Recent Progress

Work in the first year has focused on measurements in fuel-lean and fuel-rich propene flat flames at low pressures. In parallel to the experimental work, theoretical and modeling research has examined chemically activated reactions important in the propene flame.

Flame measurements. Axial profiles of mole fractions have been measured in the MBMS apparatus built originally by Biordi[1] and modernized by us. The flames were supported on a 10-cm-diameter sintered-bronze burner, positioned relative to a fixed quartz MBMS probe aligned with the flame axis. Formed by supersonic expansion through the 0.125-mm probe orifice and a 10-mm skimmer orifice, the beam was chopped at 555 Hz and introduced into a quadrupole mass spectrometer with electron-impact ionizer. Both analog and pulse-counting signal detection were used. Major species (except H_2O) were calibrated directly, minor species were calibrated by the method of relative ionization cross-sections, and the H_2O calibration was inferred from an O-atom balance in the post-flame gas.

Profiles of area expansion ratio and temperature permit fluxes and net reaction rates to be calculated from the mole-fraction data. Area expansion ratio $A(z)$ was measured by hot-wire anemometry in a cold flow of gas. Using the resistive-heating method of Kent[2] to correct for radiative and convective heat losses, temperatures were measured with 76-μm-diameter Pt/Pt-13%Rh thermocouples, butt-welded and coated with a noncatalytic Y_2O_3-BeO film. These $A(z)$ and $T(z)$ data are also used in the flame modeling, allowing the reaction mechanism to be tested.

Concentration profiles of 20 species (Table 1) have been mapped in a fuel-lean $C_3H_6/O_2/Ar$ flame at a fuel-equivalence ratio of $\phi = 0.229$, pressure of 30.00±0.01 Torr, and burner velocity of 57 cm/s (298 K). Point measurements of five other species were also made. For reference, the maximum temperature was 1935 K, measured at 12.4 mm axial distance from the burner.

Fuel propene was quickly converted to H_2 and CO, which were in turn converted to H_2O and CO_2. H-atom was rapidly formed and destroyed, reaching a maximum mole fraction of 0.001. In contrast, O and OH reached mole fractions of 0.01. Most of the hydrocarbon chemistry occurred in a narrow region from 3 to 6 mm from the burner.

In a fuel-rich $C_3H_6/O_2/Ar$ flame, full profiles of 32 species have been mapped, and point measurements were made for seven species (Table 1). Flame conditions were $\phi = 1.64$, 35.00±0.01 Torr, and 27.3 cm/s velocity. In this flame, the maximum temperature reached 2265 K at 8.0 mm.

The primary flame zone in this flame is much wider, with hydrocarbon chemistry proceeding rapidly in the region from 3 to 12 mm. The balance among H, OH, and O shifted as well, with H and OH reaching mole fractions of 0.0016 and 0.0018 but O so low as to be obscured by CH_4. Notable features of the data set are the complete set of C_3 profiles from C_3H_2 to C_3H_6 and measurements of CH_2, C_2H, and C_2H_3, which have been achieved in few other flames.

Theoretical kinetics. At typical flame temperatures and pressures, we predict[3] that direct propargyl (C_3H_3) combination forms the open-chain C_6H_6 species 1,5-hexadiyne, 1,2,4,5-hexatetraene, and 4,5-hexadienyne in preference to cyclic C_6H_6 species 3,4-dimethylenecyclobutene, fulvene, and benzene ( ,  , and  vs.  ,  , and ). These chemically activated reactions, analyzed by a new Q-formalism of Bimolecular Quantum-RRK, have rate constants and rates that are consistent with C_6H_6 data from a $C_2H_2/O_2/Ar$ flat flame, but the mass 78 signal would be due to linear C_6H_6's rather than to benzene, at least initially. Cyclic C_6H_6's may be generated by thermal isomerizations, as shown in studies of hexadiyne pyrolysis.[4]

Entropy effects interfere with direct chemically activated formation of benzene or of phenyl + H. The energy of propargyl combination is higher than any barriers to rearrangement, which might seem to suggest rapid, barrierless conversion to the most stable C_6H_6 isomer, benzene. However, each rearrangement proceeds via a tight, concerted transition state with consequently low A_∞-factors. At the same time, decompositions of the chemically activated hexadiyne and hexatetraene have high A_∞-factors.

Rate constants at low pressure give the limiting possibility of direct formation of phenyl + H. Collisional energy transfer is necessary to stabilize C_6H_6 isomers at any significant rate, but the collision rate can be made vanishingly small by calculations at very low pressures. As shown in Figure 3, if phenyl + H and C_6H_6 to C_3H_3's are the only decomposition channels left, direct phenyl formation from $C_3H_3 + C_3H_3$ has a low rate constant relative to k_∞. Again, the reason is that reaching a chemically activated benzene state is difficult due to the entropic effects.

Future Plans

Work in the next year will extend and analyze the data set described here. Fluxes and net reaction rates are being calculated from the data for each species, and predictions of flame modeling are being compared to the data. To identify and measure the C_6H_6 isomers, microprobe samples are being drawn from the molecular-weight-growth zone; analyses are by GC and GC/MS. An RRKM code for chemically activated reactions is being developed using the Q-formalism for multiple internal rearrangements, which had been developed using Bimolecular Quantum-RRK theory.[3]

References

1. Biordi, J. C.; Lazzara, C. P.; Papp, J. F. *Combustion and Flame* **1974**, *23*, 73; Biordi, J. C. *Prog. Energy Comb. Sci.* **1977**, *3*, 151.

2. Kent, J. H. *Combustion and Flame* **1970**, *14*, 279.

3. Thomas, S. D., Communal, F., Westmoreland, P. R. "C_3H_3 Reaction Kinetics in Fuel-Rich Flames," Preprints of Div. of Fuel Chemistry, American Chemical Society, **36**, No. 4, 1448-1455 (1991); presented at the Symposium on Combustion Chemistry, 202nd National Meeting of ACS, New York NY, August 25-30, 1991.

4. Stein, S. E., Walker, J. A., Suryan, M. M., Fahr, A. *23rd Symp. (Intl.) on Combustion*, The Combustion Institute, Pittsburgh, 85 (1990).

Table 1. Species measured in low-pressure flat flames of propene/oxygen/argon at fuel-lean (ϕ = 0.229) and fuel-rich (ϕ = 1.64) conditions. In addition, point measurements were made for masses 75, 76, 77, 79, 80, and 92 in the fuel-rich flame.

Species	Fuel-lean	Fuel-rich	Species	Fuel-lean	Fuel-rich
H	Profile	Profile	C_3H_3	Point	Profile
H_2	Profile	Profile	C_3H_4	Profile	Profile
CH_2	Point	Profile	Ar	Profile	Profile
CH_3	Profile	Profile	C_3H_5	Profile	Profile
Mass 16	Profile (O)	Profile (CH_4)	C_3H_6	Profile	Profile
OH	Profile	Profile	CH_3CHO	Point	-
H_2O	Profile	Profile	CO_2	Profile	Profile
C_2H	-	Profile	C_4H_2	-	Profile
C_2H_2	Profile	Profile	C_4H_4	-	Profile
C_2H_3	Point	Profile	Mass 54	Profile (C_3H_2O)	Profile (C_4H_6)
C_2H_4	Profile	Profile	Mass 56	Profile (C_3H_4O)	Profile (C_4H_8)
CO	Profile	Profile	Mass 58	Profile (C_3H_6O)	Profile (C_4H_{10})
Mass 29	Profile (HCO)	Point	C_5H_4	-	Profile
Mass 30	Profile (H_2CO)	Profile	C_5H_5	-	Profile
O_2	Profile	Profile	C_5H_6	-	Profile
HO_2	Point	-	C_5H_7	-	Profile
H_2O_2	Point	-	C_6H_2	-	Profile
C_3H_2	-	Profile	C_6H_6	-	Profile

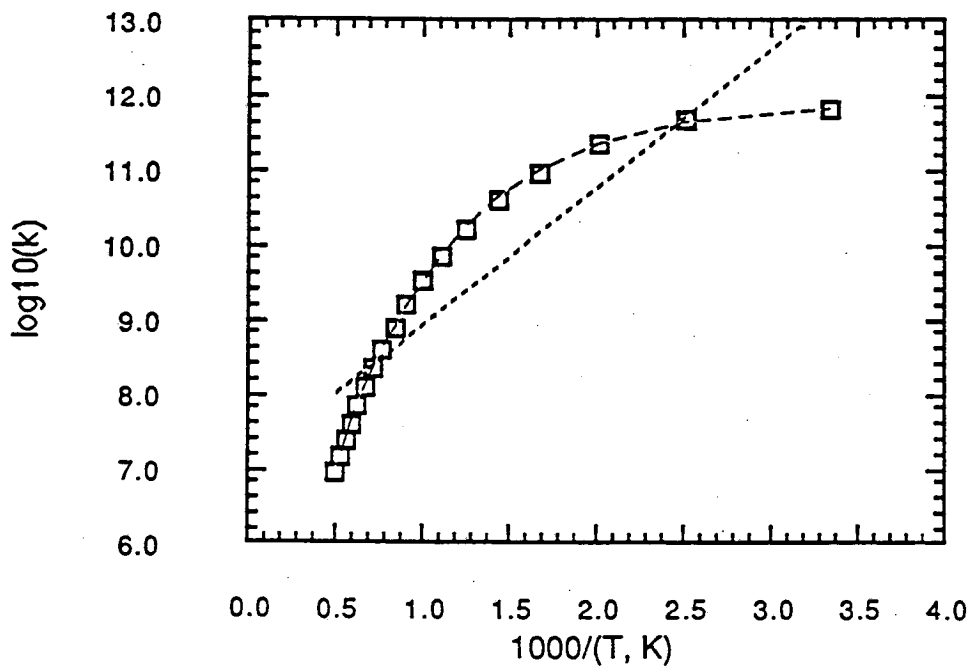

Figure 1. Arrhenius plot of predicted bimolecular rate constant for $C_3H_3 + C_3H_3 \rightarrow$ phenyl + H ($cm^3mol^{-1}s^{-1}$) via hexadiyne at very low pressure, shown as square symbols. Short dashed line is an Arrhenius fit; long-dashed line is a fit to $A \cdot T^b \cdot \exp(-C/T)$.

Time-resolved Diode Laser Studies of Energy Transfer from Highly Vibrationally Excited Molecules

Ralph E. Weston
Chemistry Department
Brookhaven National Laboratory
Upton, NY 11973

Program Scope

The goal of this program is to investigate the details of energy transfer from atoms or molecules with added translational, vibrational, or electronic energy. Typically, the excitation source is a pulsed laser, and the probe is infrared emission or infrared diode laser absorption spectroscopy.

Recent Progress

Collisional deactivation of highly vibrationally excited molecules is a crucial step in the mechanism of many reactions, particularly unimolecular reactions. While vibrational-vibrational energy transfer involving low-lying levels has been extensively studied, it has only recently become possible to study energy transfer from molecules with well-defined and "chemically interesting" amounts of energy. Our approach to this problem differs from the experiments carried out by Barker[1] and by Troe[2] by focussing on the acceptor molecule rather than the excited donor. As in their work, an aromatic donor molecule is excited to the S_1 or S_2 singlet state by pulsed radiation from an excimer laser (KrF, 248 nm). Very rapid internal conversion, instantaneous on the time scale of the collision processes under investigation, returns the molecule to the ground S_0 state with a well-defined amount of vibrational energy. Collisional energy transfer to CO_2 as the bath gas is followed with time-resolved infrared diode laser absorption spectroscopy. Specific rovibrational states can be probed, and because the spectral resolution of the diode is about one-tenth the Doppler width of CO_2 lines at room temperature, the translational energy can also be determined. The diode laser is scanned over the absorption line by frequency locking to a tunable etalon. In our experiments so far, the excited species has been benzene, benzene-d_6, or hexafluorobenzene.

Measurements of the rise time for the population of acceptor molecules in the 00^01 state (the antisymmetric stretch) lead to a rate constant for the relaxation of benzene that is in good agreement with that determined by Barker[3] and coworkers using an entirely different method. A determination of rotational state populations within the 00^01 state indicates that the vibrationally excited molecules are not significantly rotationally excited. Other experiments indicate that the translational energy content is also small. In addition, these experiments show that a very small fraction ($4\text{-}8 \times 10^{-4}$) of the energy in the aromatic molecule appears in the ν_3 mode of CO_2. Toselli and Barker[1], using infrared fluorescence as the probe, report similar results for the efficiency of vibrational excitation.

Other experiments by the Barker and Troe groups show that the average

energy loss from aromatic molecules to CO_2 is a few hundred cm^{-1} per collision, and the question arises as to the partitioning of this energy among the CO_2 degrees of freedom. Our present experiments are designed to probe the ground vibrational state (00^00), which is difficult because of background absorption by both the unexcited sample itself and by carbon dioxide in the atmosphere within the optical path. The goal in these experiments is to determine the rotational and translational energy content of collisionally excited $CO_2(00^00)$ molecules. It has been possible to measure line shapes of molecules in high rotational states (J up to 70), and these are compatible with a translational excitation of ~550 cm^{-1} per collision with hexafluorobenzene. At lower J values near the maximum at the ambient temperature, the line shape appears to be a difference of two Gaussians: an absorption increase due to molecules being scattered into the specific rotational state at a high translational temperature combined with a decrease due to molecules being removed at the ambient temperature. A simple two-temperature model fits the observed rotational population distribution reasonably well, and leads to an estimate of ~450 cm^{-1} of rotational energy transferred per collision.

The contrast between the rotational and translational energy contents of the collisionally excited ground vibrational state and those of the 00^01 excited state is striking. The Born approximation model usually applied to collisional energy transfer provides a qualitative explanation for this difference. It results from the different nature of the collisions responsible for vibration-vibration (V-V) energy transfer compared with those responsible for vibration-translation,rotation transfer (V-T,R). In a collision leading to V-T,R transfer, a relatively large amount of energy, corresponding to a vibrational quantum of the donor molecule, is removed from the excited molecule. According to the model, such an event requires a potential that is changing rapidly as the collision partners approach. This is provided by the steep short-range repulsive part of the potential, which will lead to "hard" collisions producing translational and rotational excitation of the acceptor molecule. On the other hand, V-V energy transfer can be induced by slowly changing long-range multipole-multipole forces when the process is nearly energy resonant (i. e., if vibrational frequencies of the acceptor match those of the donor). The resulting "soft" collisions will not produce rotationally or translationally hot acceptor molecules.

Future Plans

We believe that these initial experiments demonstrate that the diode laser technique provides an unequalled method for studying the details of energy transfer processes. We are extending the investigation of aromatic donor molecules to determine the amount of vibrational excitation in the CO_2 bending mode, which the calculations of Barker and Toselli indicate to be an order of magnitude greater than that of the antisymmetric bend.

The availability of diodes that cover shorter wavelengths, including the C-H stretching region of the spectrum, will enable us to investigate a new class of molecules as acceptors. In particular, it will be interesting to observe directly the effects of molecular size, complexity, and isotopic substitution on energy transfer efficiencies.

References

1. Toselli, B. M. and Barker, J. R. *J. Chem. Phys.* **95**, 8108 (1991) and earlier papers from the Barker group cited therein.

2. Cf., for example, Hippler, H. and Troe, J. in *Adv. Gas-Phase Photochemistry and Kinetics: Bimolecular Collisions.* eds. Ashfold, M. N. R. and Baggot, J. E. Royal Society of Chemistry, London, 1989.

3. M. L. Yerram, J. D. Brenner, K. D. King, and J. R. Barker. *J. Chem. Phys.* **94**, 6341 (1990).

Publications, 1990-present

Sedlacek, A J., Weston, R. E., Jr., Flynn, G. W. Br* + CO_2 revisited: An interrogation of E-V transfer with time-resolved diode laser spectroscopy. *J. Chem. Phys.* **93**, 2812 (1990).

Hewitt, S. C., Hershberger, J. F., Chou, J. Z., Flynn, G. W. and Weston, R. E., Jr. Rotationally and translationally resolved hot atom collisional excitation of the CO_2 Fermi mixed bend/stretch vibrational levels by time-dependent diode laser spectroscopy. *J. Chem. Phys.* **93**, 4922 (1990).

Sedlacek, A J., Weston, R. E., Jr., Flynn, G. W. Interrogating the vibrational relaxation of highly excited polyatomics with time-resolved diode laser spectroscopy: C_6H_6, C_6D_6, and C_6F_6 + CO_2. *J. Chem. Phys.* **94**, 6483 (1991).

Weston, R. E. Chemical reactions. in *Encyclopedia of Applied Physics*, ed. G. L. Trigg, vol. 3, pp. 377-411, VCH Publishers, NY, 1992.

Hall, G. E., Muckerman, J. T., Preses, J. M., Weston, R. E., Jr., and Flynn, G. W.
Time-resolved FTIR studies of the photodissociation of pyruvic acid at 193 nm. *Chem. Phys. Lett.*, accepted.

Weston, R. E., Jr. and Flynn, G. W. Relaxation of molecules with chemically significant amounts of vibrational energy: The dawn of the quantum state resolved era. in *Annual Review of Physical Chemistry*, ed. H. L. Strauss, Annual Reviews, Inc., Palo Alto, CA, submitted.

Khan, F. A., Kreutz, T. G., Flynn, G. W. and Weston, R. E., Jr. Translationally and rotationally resolved excitation of CO_2 by collisions with hot hydrogen atoms. *J. Chem. Phys.*, submitted.

VUV Studies of Photodissociation and Photoionization Dynamics

Michael G. White and J. Robb Grover

Chemistry Department, Brookhaven National Laboratory, Upton NY 11973

Intense VUV synchrotron radiation and laser-generated, coherent VUV radiation are used to study the spectroscopy and dynamics of neutral and ionic molecular species with high internal energy content. Current studies focus on state-resolved measurements of VUV photodissociation and photoionization processes on molecules relevant to atmospheric and combustion chemistry. Dynamical information is inferred from product rovibronic state distributions, kinetic energies and angular distributions obtained from resonant multiphoton ionization and novel photoelectron detection techniques. Parallel investigations of weak molecular clusters are aimed at obtaining mechanistic and dynamical information on the dissociative rearrangement processes of molecular intermediates produced by photoionization. These latter studies make use of the intense and widely tunable VUV radiation from the National Synchrotron Light Source in conjunction with photoionization mass spectroscopy for product identification, mass analysis of molecular beams and measurements of product kinetic energies.

Photoionization dynamics and high resolution cation spectrosopy. High resolution, threshold photoelectron spectroscopy has been used in conjunction with a coherent VUV radiation source to obtain the rovibronic state distributions of molecular ions following single-photon ionization. These measurements probe the dynamical couplings of the photoexcited electron with the molecular ion core and the partioning of energy and angular momentum in the photoionization process. Studies to date have investigated the ionization dynamics of a number of linear molecules (O_2, HCl, N_2O) in which we have characterized the angular momentum constraints in rotational photoionization transitions and examined the influence of resonance phenomena (autoionization and shape) on rotational state branching ratios. More recent work on the H_2X (X = O, S) bent triatomics explored the propensities for rotational photoionization transitions in asymmetric tops. Combined with fully *ab initio* photoionization calculations done in collaboration with McKoy and coworkers at Cal Tech, the H_2X results dramatically demonstrate how the non-isotropic potential of the molecular ion core can "scatter" the escaping photoelectron into final state channels which contradict predictions based on atomic-like analogies. In addition, we have begun a study of simple second-row hydride molecules which are important as reactive intermediates in combustion and atmospheric chemistry and tractable for study by threshold photoelectron spectroscopy and *ab initio* theoretical methods. As an initial study, we obtained the rotationally-resolved threshold photoionization spectra of OH and OD using a flow tube radical source. The fast, exothermic reaction, $NO_2 + H \rightarrow OH + NO$ was used to produce the OH (OD) radicals with near thermal rotational temperatures. Unusual ionization dynamics were observed in which rotational photoionization

transitions with $\Delta J < 0$ are favored over those with $\Delta J > 0$. Theoretical simulations of the cation rotational state distributions by McKoy and coworkers (Cal Tech) using *ab initio* Schwinger variational calculations suggest that the observed asymmetries in branch intensities are not a consequence of the one-electron ionization dynamics. Assignment of the rotational spectra also led to very accurate determinations of the ionization potentials for both OH^+ and OD^+.

Future studies will be directed towards extending our initial work on OH (OD) to other small molecular hydride radicals such as CH, CH_2, NH, NH_2, C_2, C_2H as well as HS and CS. Radical species will be produced by free radical reactions in a flow–tube source or by free-jet, laser photolysis of polyatomic precursor systems. Our present capabilities of synchrotron-based and laser-based VUV radiation sources are ideally suited for investigations of the excited state dynamics of these species at internal energies near and above their ionization thresholds. Using a combination of mass analyzed photoionization and threshold photoelectron spectroscopy, we hope to obtain rotationally-resolved photoionization spectra for a number of second row hydrides with particular emphasis on examining the ionization dynamics and determining very accurate ionization potentials. The latter are extremely useful for obtaining accurate heats of formation used in reaction rate kinetics. Currently, our pulsed ionization technique coupled with a laser-based VUV radiation source can be used to determine ionization potentials to ≤ 2 cm^{-1}, which is at least an order of magnitude better than conventional photoelectron spectroscopy.

Energy Analysis of Dissociative Photoionization of Small Clusters. Measurements were made of the kinetic energy distributions (KED) of $(1,3\text{-}C_4H_6 \cdot SO_2)^+$, $C_4H_6SO^+$, $C_4H_6^+$, and SO_2^+ produced by single-photon ionization in cluster beams generated by expansions of $1,3\text{-}C_4H_6$ + SO_2. For these experiments the high-transmission energy analyzer developed at Brookhaven was used. Examination of the KED's of the monomer and heterodimer ions at photon energies just above their ionization potentials provided measurements of beam translational temperatures. At substantially higher energies the KED of $(1,3\text{-}C_4H_6 \cdot SO_2)^+$ reveals surprisingly large center-of-mass energies (>0.3 eV) at significant intensity. The photon energy and nozzle pressure dependence show that these energetic ions are coming from trimers and/or larger clusters. Such large recoil energies cannot be thermal because the target clusters are cold, about 30-50 K, and it is difficult to understand their origin in terms of van der Waals forces alone. One possible mechanism for coupling sufficient energy is intracluster production of vibrationally excited ions, followed by transfer of the vibrational energy into translational energy via a nonstatistical breakup. The production of $C_4H_6SO^+$, which entails the rupture of the strong S-O bond, is accompanied by significant recoil, the KED of which will be useful in understanding the mechanism of this unexpected reaction.

Mechanisms of Clustering in Jet Expansions. Understanding of cluster production in free jet expansions, especially the formation of small mixed clusters of polyatomic molecules, is essentially non-existent at present. This is due to a dearth of reliable data on the product cluster distributions. However, by application of the near-threshold ioniza-

tion analysis technique developed at Brookhaven our laboratory has now begun to supply the necessary measurements, as exemplified by the following: (1) A comparison was made of the clustering of thiophene seeded 1:9 into helium and argon. The beam densities of dimers and trimers maximize at substantially larger pressures for helium than for argon, by a factor of 2.2-2.3. Pressure scaling rule studies show this scale factor also applies to the low pressure side of the pressure dependencies, and not just to the maxima. Since the gamma-factor (= Cp/Cv) is identical for the two mixtures, this result shows quantitatively how much more effective argon is than helium in removing the heat of condensation; (2) Systematic variation of the composition of the ternary mixture CH_3OH + CF_3Br + Ar showed that the methanol clusters far more easily than the halon. Most likely this is because the dissociation energy of $(CH_3OH)_2$ is larger than that of $(CF_3Br)_2$. However, although the pressure dependence of $(CH_3OH{\cdot}CF_3Br)$ seems consistent with an intermediate dissociation energy, the relative beam density suggests that it is the smallest of the three dimers. Whether the apparent discrepancy is due to dynamics or structure (or both) awaits further experimentation.

A predictive systematics was sought using information on all van der Waals dimers whose pressure dependence in jet expansions has been believably measured to date. There are twenty-two such studies, of which fourteen were done in this laboratory. Attempts to correlate dissociation energies, pressure power laws, beam temperatures, and effective pressure ranges have met with poor success. Such irregularity suggests that dynamical effects are important, because they would be expected to be more sensitive than equilibria to differences between molecules, their resulting cluster structures, and the pathways by which the clusters are formed. On the other hand, it was noticed that whenever more than one kind of dimer is formed in the same expansion, the one with the largest dissociation energy appears at the lowest pressures, and vice versa.

Research Publications 1990–1992

1. Shape Resonance Effects in the Rotationally Resolved Photoelectron Spectra of O_2, M. Braunstein, V. McKoy, S. M. Dixit, R. G. Tonkyn and M. G. White, *J. Chem. Phys. Commun.*, **93**, 5345 (1990).

2. Photoionization Studies of Internally Reactive Small Clusters: The van der Waals Complexes of 1,3-Butadiene with Sulfur Dioxide, J. R. Grover, E.A. Walters, J. K. Newman and M. G. White, *J. Am. Chem. Soc.*, **112**, 6499 (1990).

3. Comparison of Nuclear Bragg Scattering with Mossbauer Spectroscopy from the Measurement of Hyperfine Interactions, J. R. Grover, D. P. Siddons, J. B. Hastings, G. Faigel, L. E. Berman and P. E. Haustein, *Hyperfine Interactions*, **62**, 35 (1990).

4. Production of $C_2H_4Cl^+$ by Dissociative Photoionization of Weak Molecular Complexes

in C_2H_4 + HCl Mixtures, E. A. Walters, J. R. Grover, D. L. Arneberg, C. J. Santandrea and M. G. White, *Zeit. fur Physik*, **D16**, 283 (1990).

5. Chemistry with Synchrotron Radiation, J. M. Preses, J. R. Grover, A. Kvick and M. G. White, *Amer. Sci.*, **78**, 424 (1990).

6. High Resolution Threshold Photoionization of N_2O, R. T. Weidmann, E. R. Grant, R. G. Tonkyn and M. G. White, *J. Chem. Phys.*, **95**, 746 (1991).

7. Proposed UV-FEL User Facility at Brookhaven National Laboratory, I. Ben-Zvi, L. F. DiMauro, S. Krinsky, M. G. White and L. H. Yu, *Nuclear Instrum. Meth.*, **A304**, 181 (1991).

8. Rotationally Resolved Photoionization of H_2O, R. G. Tonkyn, R. T. Wiedmann E. R. Grant and M. G. White, *J. Chem. Phys.*, **95**, 7033 (1991).

9. Vibrational Spectroscopy of Xe_2^+ by Pulsed Field Ionization, R. G. Tonkyn and M. G. White, *J. Chem. Phys.*, **95**, 5582 (1991).

10. ZEKE Threshold Photoelectron Spectroscopy: Photoionization Dynamics and the Level Structure of Molecular Cations, E. R. Grant and M. G. White, *Nature*, **354**, 249 (1991).

11. Cluster Beam Analysis via Photoionization. J.R. Grover, W.J. Herron, M.T. Coolbaugh, W.R. Peifer and J.F. Garvey, *J. Phys. Chem.*, **95**, 6473 (1991).

12. Rotationally Resolved Threshold Photoionization of H_2S, R. T. Wiedmann and M. G. White, *SPIE Proceedings, Conf. 1638 - Optical Methods for Time- and State- Resolved Chemistry, Los Angeles, CA, January 19-25, 1992.*

13. Anomalous Branch Intensities in the Threshold Photoionization of HCl, R. G. Tonkyn, R. T. Wiedmann and M. G. White, *J. Chem. Phys., in press.*

14. Rotational Ion Distributions for Near Threshold Photoionization of H_2O, M. T. Lee, K. Wang, V. McKoy, R. G. Tonkyn, R. T. Wiedmann, E. R. Grant and M. G. White, *J. Chem. Phys. Commun., in press.*

Reactions of Small Molecular Systems

Curt Wittig
Department of Chemistry
University of Southern California
Los Angeles, CA 90089-0482

Recent Progress

H atoms react with N_2O mainly via the highly exothermic channel:[1-8]

$$H + N_2O \rightarrow OH(X^2\Pi) + N_2 \qquad \Delta H_{298} = -21{,}820\ cm^{-1} \qquad (1)$$

Attack at the oxygen side faces an entrance barrier of ~ 7,000 cm^{-1}.[5] Past this, NN-OH bond cleavage occurs without involvement of a long lived intermediate. Attack at the terminal nitrogen, once past a barrier which is smaller than that for oxygen-side attack, leads to an intermediate $HNNO^\dagger$ which lies lower in energy by ~ 5,300 cm^{-1} than the reactants.[5] Then reaction can proceed either via 1,3-hydrogen migration to yield OH + N_2. In the present work, Doppler shift measurements of OH(v=0) suggest a very high degree of N_2 internal excitation, presumably vibrational. This offers a clear view of the role of migration. The large amount of N_2 vibrational excitation is most likely the consequence of an $HNNO^\dagger$ intermediate whose long N-N bond length is projected onto the vibrations of the N_2 product formed from 1,3-hydrogen migration. A simple Franck-Condon model can rationalize the data.

Reactions were initiated in flowing samples of typically 20-30% HI and 70-80% N_2O at 40 mTorr pressure. Photolysis and probe beams were collinear and counterpropagating. Photodissociation yields both ground state $I(^2P_{3/2})$ and excited state $I(^2P_{1/2})$; thus, H atoms are prepared with two different kinetic energies. With 100 ns delay, nascent H atoms undergo ~ 0.3 hard sphere collisions on average and nascent products undergo < 0.1 collisions on average. Changing either the delay time or the total pressure by a factor of 2 did not affect the results.

OH $A^2\Sigma \leftarrow X^2\Pi$ LIF signals were normalized for laser intensities and pressure. Spectra calculated from published line positions and line strengths, convoluted with the experimentally measured line shape, were fitted to the normalized spectra. Rotational distributions for v = 0,1 were obtained from satisfactory fits. OH internal energy is significant, which is not surprising given the considerable amount of energy available. Once past an entrance barrier there is no long-lived intermediate and product distributions will be biased by the large reverse barrier. OH internal excitation has been found to be essentially independent of photolysis wavelength in the range 240-270 nm. The [v=1]/[v=0] ratio is ~ 0.5 for the observed rotational levels, i.e., neglecting v=0 rotational levels above 8,000 cm^{-1}. For Doppler shift measurements, where the signal to noise ratio is critical, only levels with $N \leq 15$ were used. OH(v=0) Doppler profiles were taken using 248 nm photolysis. Delay times were varied between 50 and 300 ns, and Doppler profiles were monitored for the different P, Q, and R rotational branches and for the highest and lowest detectable rotational quantum numbers (3 and 15). No significant changes in lineshape or linewidth were observed for any changes of the parameters mentioned above. Representative data are shown below.

The maximum and mean OH kinetic energies in the CM system were found to be 12,000 ± 4000 cm^{-1} and 7,000 ± 2,000 cm^{-1}, respectively. The uncertainties are liberal. From momentum balance, this corresponds to 19,300 ± 6400 and 11,300 ± 3200 cm^{-1} for the maximum and mean CM kinetic energies, respectively. This is modest considering that the excess energy is approximately 37,600 cm^{-1}, and that the OH(v=0) levels being monitored have low internal energy, i.e., $E_{int}(OH)$ is typically ~ 1000 cm^{-1}. This means that the N_2 fragment associated with the probed OH levels has an average internal energy ~ 25,000 cm^{-1}. We *assume* this is

mostly vibrational. Though this is a remarkable amount of N_2 internal energy, we believe the experimental conclusions are sound. The data simply do not support a higher CM kinetic energy. This will be discussed below within the context of rapid 1,3-hydrogen migration from the nitrogen side to the oxygen side of an $HNNO^{\dagger}$ intermediate that leaves the N-N internuclear separation elongated relative to the diatomic N_2 equilibrium separation.

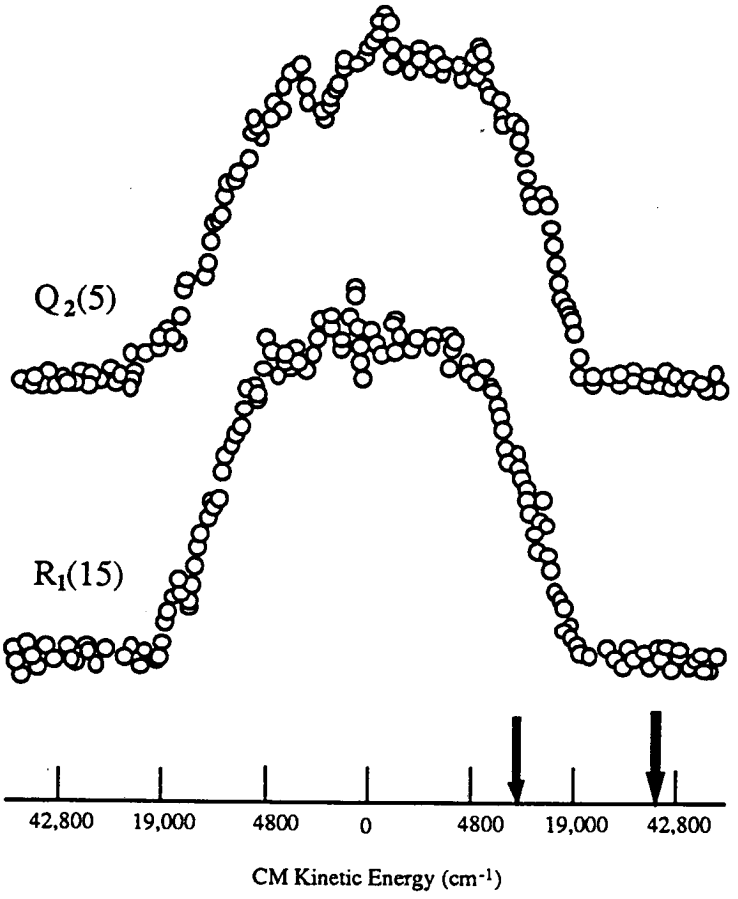

1. Sub-Doppler resolution OH LIF spectra; resolution was ~ 0.05 cm^{-1}. The lineshapes are typical of all transitions monitored. The thin arrow indicates the average CM kinetic energy, ~ 11,000 cm^{-1}; the thick arrow indicates the total available energy, 37,000 cm^{-1}.

As stated above, OH translational energies were measured from Doppler shifts and the profiles were seen to be insensitive to the levels probed. In addition, rotational and vibrational populations did not change over the photolysis wavelength range 263-240 nm, suggesting bias by the reverse barrier. Since incident H atoms strike N_2O molecules with all possible angles and impact parameters, they may attach initially to either the oxygen or the terminal nitrogen. We do not think they attach to the central nitrogen, but this is conjecture; isotopic substitution can resolve this. Intuitively, one might think that attachment at the oxygen is most conducive to forming OH. However, this may not be the case. Specifically, ab initio calculations of portions of the HNNO potential surface indicate a much lower entrance channel barrier for forming an HNNO intermediate than direct attack at the oxygen to form N_2 + OH. Once HNNO is formed, the barrier for 1,3-hydrogen migration to the oxygen side is narrower and slightly lower than the barrier for direct hydrogen addition at the oxygen side (see Fig. 1). Thus, it is believed that HNNO is the precursor to OH, at least at energies near the barrier

heights. Even at higher energies, it may be that the HNNO intermediate is preferred for a democratic set of attack geometries.

The HNNO intermediate may hold the key to understanding the low CM kinetic energies and the corresponding high degree of N_2 vibrational excitation. In going from an HNNO intermediate to the NN-OH exit channel, there is a large change in N-N bond length which can promote significant product N_2 vibrational excitation. In order to see how large this effect might be, Franck-Condon factors were calculated for projections of the elongated N-N coordinate onto an N_2 vibrational basis. This is a rough estimate to see if a reasonable mechanism and sensible molecular parameters can reconcile the experimental findings. An implicit assumption is that hydrogen motion is fast enough so that the N-N bond length does not relax appreciably while hydrogen undergoes the 1,3 shift. Note that a hydrogen atom with ~ 1000 cm^{-1} of translational energy moves 1 Å in ~ 20 fs.

Figure 2 shows the Franck-Condon factors. $\Psi_{N\text{-}N}$ is assumed to peak at an N-N separation of 1.23 Å, i.e., the calculated N-N equilibrium separation in HNNO. Gaussian widths near that of free N_2 were used; changes in these widths by ± 20% did not lead to different conclusions. Given the crudeness of this estimate, it is not worth exploring different N-N separations, Gaussian widths, etc. The distribution shown in Fig. 2 indicates a high degree of N_2 vibrational excitation, in qualitative agreement with the experimental observations. The average N_2 vibrational energy is ~ 15,000 cm^{-1}, which is less than the average N_2 internal energy obtained from the Doppler shift measurements (i.e., ~ 25,000 cm^{-1}). However, the Franck-Condon factors do not account for N_2 rotational excitation, which could easily be several thousand cm^{-1}. To take the comparison one step further, we calculated the corresponding Doppler spectrum (solid line) assuming no N_2 rotational excitation and a spatially isotropic distribution of OH velocities. Agreement is good, lending support to the model.

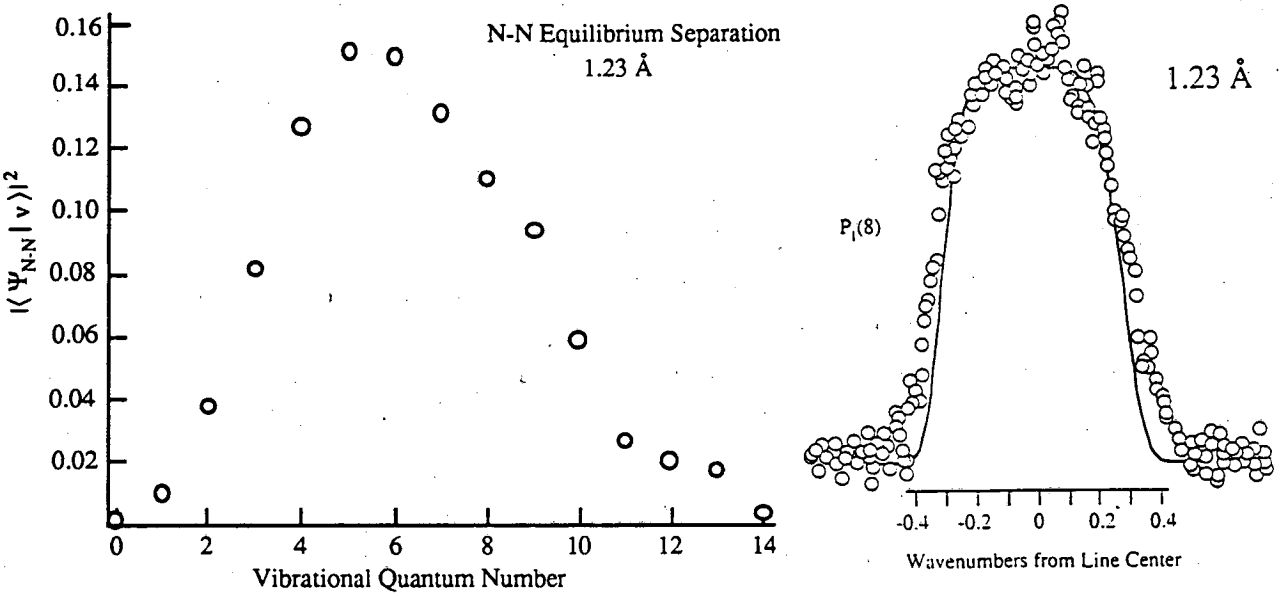

2. Franck-Condon factors ($\Psi_{N\text{-}N}$ is assumed to have a N-N separation of 1.23 Å, the HNNO equilibrium distance) and a comparison between experimental and calculated spectra.

It is easy to manipulate a better agreement. For example, since the HNNO intermediate is highly vibrationally excited, the average N-N distance will be longer than at equilibrium. Maybe this longer N-N length should be used instead of 1.23 Å. In fact, $R_{N\text{-}N}$ = 1.24 Å, corresponding to an average N_2 vibrational energy of 17,000 cm^{-1}, results in an excellent fit. From such agreement, we conclude that for the OH rotational levels monitored reaction proceeds

predominantly via a vibrationally excited $HNNO^{\dagger}$ intermediate. We can think of no other way to get a large amount of energy into the N_2 vibrational degree of freedom.

Future Plans

We plan to continue work on the development of a source of monoenergetic hydrogen atoms having tunable and low kinetic energies. To achieve this, a diatomic precursor such as HBr is excited to v = 2 or 3 with a powerful infrared pulse obtained from a parametric oscillator. An ultraviolet pulse then photodissociates these excited molecules. Much lower regions of the repulsive curve are accessible than from v = 0, so it will be possible to do hot H atom experiments at lower collision energies than has hitherto been possible. We are also exploring inelastic scattering of H atoms from molecules using our Rydberg time-of-flight machine. This has produced several preliminary results which will be presented at the meeting.

References

1. G. Dixon-Lewis and D.J. Williams, in Gas-phase Combustion, Comprehensive Chemical Kinetics, C. H. Bamford & C.F.H. Tipper, Eds., Vol. 17 (Elsevier, Amsterdam, 1977).
2. W.E. Hollingworth, J. Subbiah, G.W. Flynn and R.F. Weston Jr., J. Chem. Phys. 82, 2295 (1985).
3. P. Marshall, T. Ko and A. Fontijn, J. Phys. Chem. 93, 1922 (1989).
4. H. Ohoyama, M. Takayanagi, T. Nishiya and I. Hanazaki, Chem. Phys. Lett. 162, 1 (1989).
5. P. Marshall, A. Fontijn and C.F. Melius, J. Chem. Phys. 86, 5540 (1987).
6. D. Patel-Misra, D.G. Sauder and P.J. Dagdigian, Chem. Phys. Lett. 174, 113 (1990).
7. S.T. Gibson, J.P. Greene and J. Berkowitz, J. Chem. Phys. 83, 4319 (1985).
8. K.M. Errin and P.B. Armentrout, J. Chem. Phys. 86, 2659 (1987).

Publications from DOE Sponsored Research

Translational Energy Distribution from C_2H_2+hν(193.3 nm) → C_2H+H, J. Segall, Y. Wen, R. Lavi, R. Singer and C. Wittig, J. Phys. Chem. 95, 8078 (1991).

Photoinitiated Reactions in Weakly Bonded Complexes, S.K. Shin, Y. Chen, S. Nickolaisen, S.W. Sharpe, R.A. Beaudet, and C. Wittig, *Advances in Photochemistry*, Vol 16, D. Volman, G. Hammond, and D. Neckers, eds., Wiley and Sons, pp. 249-363 (1991).

High Resolution Infrared Diode Laser Spectroscopy of $SO(^3\Sigma^-)$ in a Secondary Slit Supersonic Expansion, Z.S. Huang, J.E. Verdasco, C. Wittig and R.A. Beaudet, Chem. Phys. Lett., in press (1992).

Photoinitiated H- and D-Atom Reactions in the Gas Phase and in N_2O-HI and N_2O-DI Complexes, E. Böhmer, S.K. Shin, Y. Chen and C. Wittig, J. Chem. Phys., submitted (1992).

Infrared Absorption Spectroscopy of the Weakly Bonded CO-Cl_2 Complex, S.W. Bunte, J.B. Miller, Z.S. Huang, J.E. Verdasco, C. Wittig and R.A. Beaudet, J. Phys. Chem., in press (1992).

Infrared Absorption Spectroscopy of the CO-Ar Complex, A.R.W. McKellar, Y.P. Zeng, S.W. Sharpe, C. Wittig and R.A. Beaudet, J. Mol. Spectrosc., submitted (1992).

Infrared Spectroscopy of CO_2-D(H)Br and its Molecular Structure, Y.P. Zeng, S.W. Sharpe, S.K. Shin, C. Wittig and R.A. Beaudet, J. Chem. Phys., submitted (1992).

Theoretical Studies of Nonadiabatic and Spin-Forbidden Processes: Investigations of the Reactions and Spectroscopy of Radical Species Relevant to Combustion Reactions and Diagnostics

David R. Yarkony
Department of Chemistry
Johns Hopkins University
Baltimore, MD 21218

Our research program focusses on studies of spin-forbidden and electronically nonadiabatic processes involving radical species which are relevant to combustion reactions and combustion diagnostics. To study the electronic structure aspects of these processes a unique and powerful system of electronic structure programs, developed over the past six years, the BROOKLYN codes, is employed. These programs enable us to address questions basic to the understanding of elementary combustion chemistry processes which are not tractable using more standard quantum chemistry codes. Particularly relevant to this research program are the capabilities to

(i) treat the spin-orbit interaction with in the context of the full microscopic Breit-Pauli approximation,

(ii) determine the interstate derivative couplings $f_\alpha^{IJ}(\mathbf{R}) = \left\langle \Psi_I^0(\mathbf{r};\mathbf{R}) \middle| \frac{\partial}{\partial R_\alpha} \Psi_J^0(\mathbf{r};\mathbf{R}) \right\rangle_{\mathbf{r}}$ which result in the breakdown of the single surface Born Oppenheimer approximation and

(iii) locate seams of actual/avoided crossings and minimum energy crossings of potential energy surfaces.

We have used these methods to address problems in the following areas:

SPIN-FORBIDDEN RADIATIONLESS DECAY

(a) Spin-forbidden decomposition of $CH_3O^+(^3A_2)$

Motivated by conversations with Dr. J. Berkowitz at the Argonne National Laboratory we have considered[1] the feasibility of the spin-forbidden process

$$CH_3O^+(^3A_2) \rightarrow CH_3O^+(^1A') \rightarrow HCO^+(X^1\Sigma^+) + H_2(X^1\Sigma_g^+)$$

It has been suggested that this radiationless decay process limits the ability to detect CH_3O by photoionization methods. The barrier to this processes occurs at the minimum energy crossing point on the surface of intersection of the lowest $^3A''$ and $^1A'$ potential energy surfaces. The straightforward procedure that has been used in the past to locate the minimum energy point, is referred to as the indirect determination of the minimum energy crossing point. In the indirect method the crossing surface is first characterized and then its minimum is determined. This procedure is computationally costly since for a system with N internal degrees of freedom (here 9) a crossing surface, or seam, of dimension N–1 must be determined and analyzed. Thus the determination of this point represents a significant computational bottleneck. However this bottleneck can be avoided. Fletcher[2] has shown that the minimum energy crossing point can be determined directly, that is, without prior determination of the crossing surface itself, by solving the following Lagrange-Newton system of equations:

$$\begin{bmatrix} \mathbf{W}^{IJ}(\mathbf{R},\lambda) & \mathbf{g}^{IJ}(\mathbf{R}) \\ \mathbf{g}^{IJ}(\mathbf{R})^\dagger & 0 \end{bmatrix} \begin{bmatrix} \delta\mathbf{R} \\ \delta\lambda \end{bmatrix} = -\begin{bmatrix} \mathbf{g}^I(\mathbf{R}) + \lambda \mathbf{g}^{IJ}(\mathbf{R}) \\ \Delta E_{IJ}(\mathbf{R}) \end{bmatrix} \qquad 1$$

where $\delta\mathbf{R} = \mathbf{R}'-\mathbf{R}$, $\delta\lambda = \lambda' - \lambda$, and the energy gradient $\mathbf{g}^{I}(\mathbf{R})$ and energy difference gradient $\mathbf{g}^{IJ}(\mathbf{R})$ are given by

$$g_\alpha^I(\mathbf{R}) = \frac{\partial E_I^0(\mathbf{R})}{\partial R_\alpha} \qquad 2a$$

$$g_\alpha^{IJ}(\mathbf{R}) = \frac{\partial E_I^0(\mathbf{R})}{\partial R_\alpha} - \frac{\partial E_J^0(\mathbf{R})}{\partial R_\alpha} = \frac{\partial \Delta E_{IJ}(\mathbf{R})}{\partial R_\alpha} \qquad 2b$$

and the second derivative matrix, $\mathbf{W}^{IJ}(\mathbf{R},\lambda)$, is given by

$$W_{\alpha\beta}^{IJ}(\mathbf{R},\lambda) = \frac{\partial^2 L_{IJ}(\mathbf{R},\lambda)}{\partial R_\alpha \partial R_\beta} = \frac{\partial}{\partial R_\alpha}\left[g_\beta^I(\mathbf{R}) + \lambda g_\beta^{IJ}(\mathbf{R})\right] \quad . \qquad 3$$

$W_{\alpha\beta}^{IJ}(\mathbf{R},\lambda)$ can be determined using a forward or a centered difference of $g_\beta^I + \lambda g_\beta^{IJ}$, that is:

$$W_{\alpha\beta}^{IJ}(\mathbf{R},\lambda) = \left\{\left[g_\beta^I(\mathbf{R}+\varepsilon\mathbf{I}^\alpha) + \lambda g_\beta^{IJ}(\mathbf{R}+\varepsilon\mathbf{I}^\alpha)\right] - \left[g_\beta^I(\mathbf{R}) + \lambda g_\beta^{IJ}(\mathbf{R})\right]\right\} / \varepsilon \qquad 4a$$

or

$$= \left\{\left[g_\beta^I(\mathbf{R}+\varepsilon\mathbf{I}^\alpha) + \lambda g_\beta^{IJ}(\mathbf{R}+\varepsilon\mathbf{I}^\alpha)\right] - \left[g_\beta^I(\mathbf{R}-\varepsilon\mathbf{I}^\alpha) + \lambda g_\beta^{IJ}(\mathbf{R}-\varepsilon\mathbf{I}^\alpha)\right]\right\} / 2\varepsilon \qquad 4b$$

where $\mathbf{I}^\alpha$ is a unit vector along the direction R_α. In our implementation the gradient and energy difference gradient are evaluated- for MCSCF/CI wavefunctions- without recourse to divided difference differentiation, using analytic gradient techniques.[3] It is important to observe that because analytic gradient techniques are used to evaluate the right hand side of eq. 1 *it is not necessary to limit the number of nuclear degrees of freedom considered in that equation.*

For the methoxy cation it was shown, using CI expansions as large as 2.5 million configuration state functions, that ΔE=15.4kcal/mol, where ΔE is defined as the difference between the energy at minimum energy crossing structure, denoted MEX(^{3}A"–^{1}A'), and the energy at the minimum on the bound state potential energy surface. Thus the indicated reaction provides a low energy decomposition pathway.

The spin-orbit interactions $H_\perp^{so}$ and $H_\parallel^{so}$, where

$$H_\perp^{so} = \left\langle \Psi_{2A'}(^3A'') \middle| H^{so} \middle| \Psi_{1A'}(^1A') \right\rangle \qquad 5a$$

$$H_\parallel^{so} = \left\langle \Psi_{1A'}(^3A'') \middle| H^{so} \middle| \Psi_{1A'}(^1A') \right\rangle \qquad 5b$$

and

$$\Psi_{1A'}(^1A') = \Psi[^1A'(0)] \qquad 6a$$

$$\Psi_{1A'}(^3A'') = i\,\Psi[^3A''(0)] \qquad 6b$$

$$\Psi_{2A'}(^3A'') = i\,\{\Psi[^3A''(1)] - \Psi[^3A''(-1)]\}/\sqrt{2} \qquad 6c$$

$$\Psi_{1A''}(^3A'') = i\,\{\Psi[^3A''(1)] + \Psi[^3A''(-1)]\}/\sqrt{2} \qquad 6d$$

were determined at MEX(^{3}A"–^{1}A'). We found $H_\perp^{so}$=11.3cm^{-1} and $H_\parallel^{so}$=66.4cm^{-1}. Using an approximate Landau-Zener model, it was estimated that vibrational states with energies above the minimum energy crossing will intersystem cross within 1000 vibrational periods, that is 1000

passes through the intersurface crossing. Decay rates for the predissociated levels, that is levels below the minimum energy crossing point energy, cannot be considered in this approximate manner and require a more complete treatment of the decay process.

(b) Predissiciation of the Individual rovibronic levels of $OH(A^2\Sigma^+)$

In situ detection of nascent OH is an important problem in studies of combustion processes. Recently several groups,[4-6] including the very recent work of Gray and Farrow at the Sandia Combustion Research Facility[5] and Crosley and co-workers are SRI International,[6] have considered using the strongly predissociated $OH(A^2\Sigma^+,v=3)$ state in a laser fluorescence detection scheme. This predissociation is induced by the $1^4\Sigma^-$ state and is thus spin-forbidden. Reliable theoretical modelling of the predissociation process requires accurate $A^2\Sigma^+ \sim 1^4\Sigma^-$ spin-orbit couplings, which were not available. We are in the process of determining the requisite couplings and modelling this radiationless decay process. Our initial results in this regard are summarized in the following figure which reports our total decay rate for $OH(A^2\Sigma^+, v=3, N, F_i)$ $\tau^{tot}(F_i)$ and compares it with the results of Gray and Farrow (E1) and Crosley and co-workers(E2). [The *relative* decay rates of Crosley were scaled to agree with our theoretical results for N=0.]

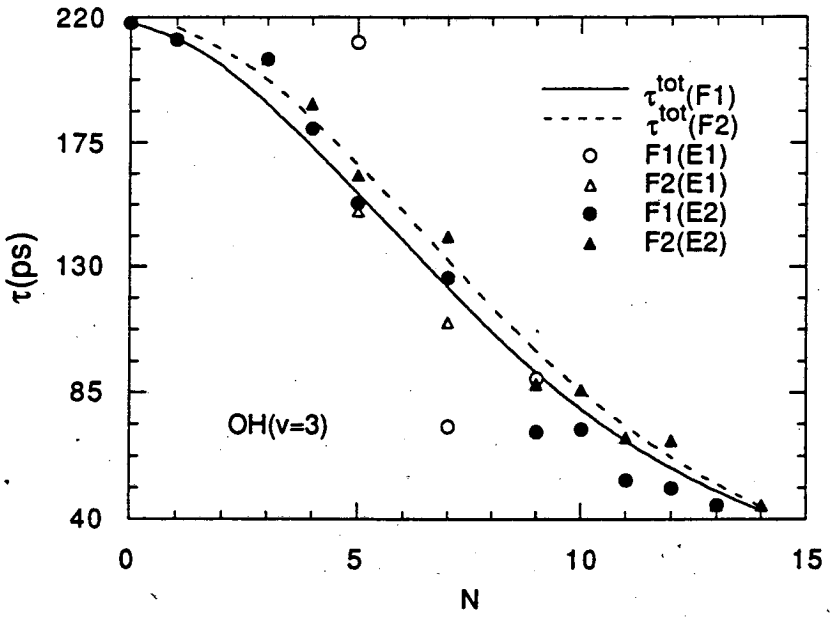

SPIN-FORBIDDEN CHEMICAL REACTIONS

The spin-forbidden radical-molecule reaction

$$CH(X^2\Pi) + N_2(X^1\Sigma_g^+) \rightarrow HCN(X^1\Sigma^+) + N(^4S)$$

is important in the production of NO in flame fronts.[7] The rate constant for this reaction is difficult to measure.[8, 9] Previously we had considered the doublet-quartet intersystem crossing in order to establish the feasibility of this reaction.

As part of this DOE funded research program we have developed[10] the following qualitative model for this reaction based on the intermediate complex model of Tully[11] and of Zahr, Preston and Miller.[12] $CH(X^2\Pi)$ approaches $N_2(X^1\Sigma_g^+)$ along the N_2 perpendicular bisector. Energy transfer from this relative translational mode to the N_2 stretch and other internal coordinates results in a metastable intermediate complex, with the approximate structure  . This

metastable complex repeatedly traverses the doublet-quartet crossing seam in the vicinity of the transition state which occurs at the minimum energy crossing point. In this way the intermediate complex facilitates the intersystem crossing. The geometrical arrangement at the minimum energy crossing point also has the structure  except that the N-N bond is more highly stretched. Those molecules which cross onto the quartet surface proceed, via asymmetric N-N motion, exoergically and irrevocably to the products $HCN(X^1\Sigma^+) + N(^4S)$. See the following figure

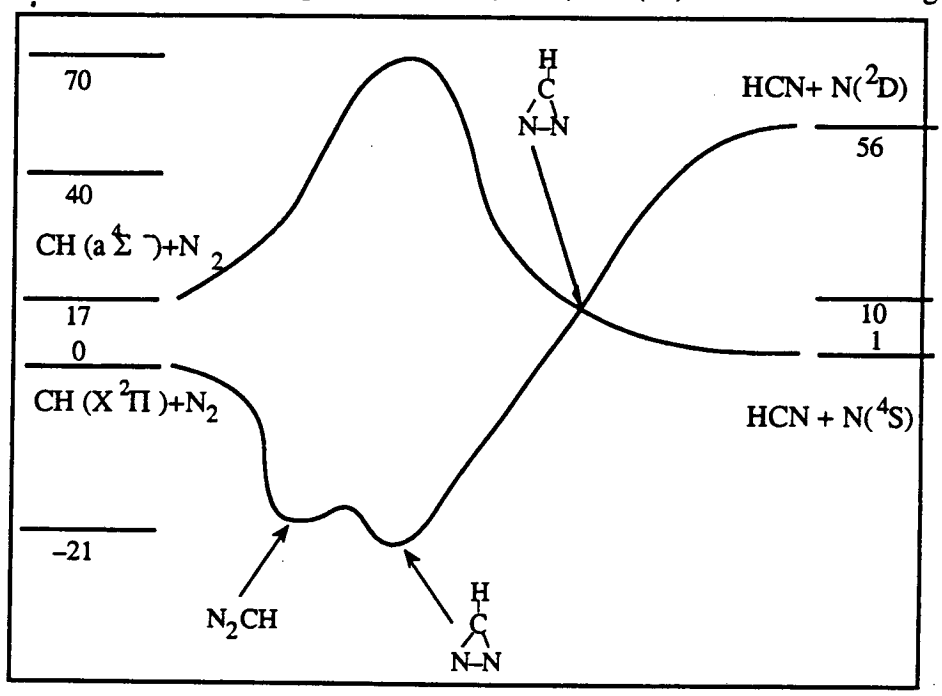

Potential energy surfaces for this reaction are being developed based on high quality *ab initio* electronic structure calculations. These surfaces will be used to consider the rate constant for this reaction.

REFERENCES

References with index in bold/italic are funded by the DOE Office of Basis Energy Sciences

1. D. R. Yarkony, J. Amer. Chem. Soc. (1992), in press.

2. R. Fletcher, *Practical Methods of Optimization*, (John Wiley and Sons, New York, 1981) , Vol. 2.

3. D. R. Yarkony, J. Chem. Phys. **92**, 2457 (1990).

4. P. Andresen, A. Bath, W. Groger, H. Lulf, G. Meijer, and J. t. Meulen, Appl. Opt. **27**, 365 (1988).

5. J. A. Gray and R. L. Farrow, J. Chem. Phys. **95**, 7054 (1991).

6. D. E. Heard, D. R. Crosley, J. Jeffries, G. Smith, and A. Hirano, J. Chem. Phys. (1992), in press.

7. C. P. Fenimore, in *13th Symposium (International) on Combustion*, (The Combustion Institute, Pittsburgh, PA, 1971) , p. 373 .

8. D. Lindackers, M. Burmeister, and P. Roth, *23rd Symposium (International) on Combustion*, (The Combustion Institute, Pittsburgh, PA, 1990) , p. 251 .

9. A. J. Dean, R. K. Hanson, and C. T. Bowman, in *23rd Symposium (International) on Combustion*, (The Combustion Institute, Pittsburgh, PA, 1990) , p. 259 .

10. M. R. Manaa and D. R. Yarkony, Chem. Phys. Lett. **188**, 352 (1992).

11. J. C. Tully, J. Chem. Phys. **61**, 61 (1974).

12. G. E. Zahr, R. K. Preston, and W. H. Miller, J. Chem. Phys. **62**, 1127 (1975).

INDEX

LIST OF INVITEES AND PARTICIPANTS

Dr. William Ashurst
Combustion Research Facility
Sandia National Laboratory
Livermore, California 94551-0609

Prof. Tomas Baer
F1 Jardin aux Fontaines
9 Rue Nazareth
34090 Montpellier
FRANCE

Prof. John R. Barker
Dept. of Atmospheric & Ocean Sci.
244 West Engineering Building
University of Michigan,
Ann Arbor, Michigan 48109-2143

Dr. Robert S. Barlow
Division 8354
Combustion Research Facility
Sandia National Laboratory
Livermore, California 94551-0609

Prof. Robert A. Beaudet
Department of Chemistry
University of Southern California
Los Angeles, CA 90089-0482

Dr. Joseph Berkowitz
Chemistry Division
Argonne National Laboratory
9700 South Cass Avenue
Argonne, Illinois 60439

Prof. Richard Bersohn
Department of Chemistry
Columbia University
959 Havemeyer Hall
New York, New York 10027

Dr. J. Stephen Binkley
Combustion Research Facility
Sandia National Laboratories
Livermore, California 94551-0969

Prof. Joel M. Bowman
Department of Chemistry
Emory University
1515 Pierce Drive
Atlanta, Georgia 30322

Prof. C. Thomas Bowman
Department of Mechanical
Engineering
Stanford University
Stanford, California 94305

Dr. Kenneth Brezinsky
Dept. of Mechanical and
Aerospace Engineering
Princeton University
Princeton, New Jersey 08544

Dr. Nancy J. Brown
Applied Science Division
Lawrence Berkeley Laboratory
University of California
Berkeley, California 94720

Dr. David W. Chandler
Combustion Research Facility
Sandia National Laboratory
Livermore, California 94551-0609

Prof. Peter Chen
Department of Chemistry
Harvard University
12 Oxford Street
Cambridge, Massachusetts 02138

Dr. Robert K. Cheng
Applied Sciences Division
Lawrence Berkeley Laboratory
University of California
Berkeley, California 94720

Prof. Dennis J. Clouthier
Department of Chemistry
University of Kentucky
Lexington, Kentucky 40506-0055

Dr. Norman Cohen
The Aerospace Corporation
Post Office Box 92957
Los Angeles, California 90009-2957

Prof. Phillip Colella
Dept. of Mechanical Engineering
6189 Etcheverry Hall
University of California
Berkeley, CA 94720

Dr. Meredith B. Colket, III
United Technologies Research Center
East Hartford, CT 06108

Prof. Terrill A. Cool
Dept. of Applied and Engineering
Physics
Cornell University
Ithaca, NY 14853-1301

Prof. F. Fleming Crim
Department of Chemistry
University of Wisconsin
Madison, Wisconsin 53706

Dr. David R. Crosley
SRI International
333 Ravenswood Avenue
Menlo Park, California 94025

Prof. Robert F. Curl, Jr.
Department of Chemistry
Rice University
6100 South Main Street
Houston, Texas 77251

Prof. Hai-Lung Dai
Department of Chemistry
University of Pennsylvania
Philadelphia, Pennsylvania 19104

Dr. Michael J. Davis
Chemistry Division
Argonne National Laboratory
9700 South Cass Avenue
Argonne, Illinois 60439

Dr. Anthony M. Dean
Exxon Research & Engineering Co.
Clinton Township, Route 22 East
Annandale, NJ 08801

Prof. Andrew E. DePristo
Inst. for Physical Research & Tech.
Ames Laboratory
Iowa State University
Ames, Iowa 50011-3020

Prof. Frederick L. Dryer
Dept. of Mechanical and
Aerospace Engineering
Princeton University
Princeton, New Jersey 08544

Dr. Joseph L. Durant
Combustion Research Facility
Sandia National Laboratory
Livermore, California 94551-0609

Dr. Alan Eckbreth
Assistant Director of Research,
Propulsion and Flight Systems
United Technologies Research Center
East Hartford, Connecticut 06108

Prof. G. Barney Ellison
Department of Chemistry and Biochemistry
University of Colorado
Boulder, Colorado 80309-0215

Prof. James M. Farrar
Department of Chemistry
University of Rochester
Rochester, New York 14627

Dr. Roger Farrow
Division 8354
Combustion Research Facility
Sandia National Laboratory
Livermore, California 94551-0609

Prof. Peter M. Felker
Dept. of Chemistry and Biochemistry
University of California
405 Hilgard Avenue
Los Angeles, CA 90024-1406

Prof. Robert W. Field
Department of Chemistry
Massachusetts Institute of Technology
Cambridge, Massachusetts 02139

Dr. George A. Fisk
Combustion Research Facility
Sandia National Laboratory
Livermore, California 94551-0609

Prof. George W. Flynn
Department of Chemistry
Box 315, Havemeyer Hall
Columbia University
New York, NY 10027

Prof. Arthur Fontijn
Department of Chemical and Environmental Engineering
Rensselaer Polytechnic Institute
Troy, New York 12180-3590

Dr. Richard Gann
Center for Fire Research
B250 Polymers Building
National Inst. of Standards & Tech.
Gaithersburg, MD 20899

Mr. Charles W. Garrett
FE-14 B-129/GTN
Office of Fossil Energy
U. S. Department of Energy
Washington, D.C. 20545

Prof. W. Ronald Gentry
Department of Chemistry
University of Minnesota
207 Pleasant Street, Southeast
Minneapolis, Minnesota 55455

Prof. Clayton F. Giese
Department of Chemistry
University of Minnesota
207 Pleasant St., S.E.
Minneapolis, Minnesota 55455

Prof. Graham P. Glass
Department of Chemistry
Rice University
6100 South Main Street
Houston, Texas 77251

Prof. Irvin Glassman
Dept. of Mech. & Aerospace Eng.
Princeton University
Princeton, New Jersey 08544

Dr. David Golden
SRI International
333 Ravenswood Avenue
Menlo Park, California 94025

Prof. Robert J. Gordon
Department of Chemistry
4500 Science & Engineering South
Univ. of Illinois at Chicago Box 4348
Chicago, Illinois 60680

Dr. Carl A. Gottlieb
Division of Applied Sciences
Pierce Hall 107C
Harvard University
Cambridge, Massachusetts 02138

Dr. Jeff Gray
Combustion Research Facility
Sandia National Laboratory
Livermore, California 94551-0609

Dr. J. Robb Grover
Chemistry Department
Brookhaven National Laboratory
Upton, New York 11973

Mr. Marvin E. Gunn, Jr.
CE-121 5E-066/FORS
U. S. Department of Energy
Washington, D.C. 20585

Prof. David Gutman
Department of Chemistry
The Catholic University of America
Michigan Ave. at 7th Street, N.E.
Washington, D.C. 20064

Dr. Gregory E. Hall
Chemistry Department
Brookhaven National Laboratory
Upton, New York 11973

Prof. Ronald K. Hanson
Dept. of Mechanical Engineering
Stanford University
Stanford, California 94305

Dr. Lawrence B. Harding
Chemistry Division
Argonne National Laboratory
9700 South Cass Avenue
Argonne, Illinois 60439

Prof. Charles B. Harris
Chemical Sciences Division
Lawrence Berkeley Laboratory
University of California
Berkeley, California 94720

Dr. Stephen J. Harris
Physical Chemistry Department
General Motors Research Laboratories
Box 9055
Warren, Michigan 48090-9055

Dr. Carl C. Hayden
Diagnostics Research Division, 8354
Combustion Research Facility
Sandia National Laboratory
Livermore, California 94551-0609

Dr. Martin Head-Gordon
AT&T Bell Laboratories
Room 1A-360
600 Mountain Avenue
Murray Hill, New Jersey 07974

Prof. M. Heaven
Department of Chemistry
Emory University
1515 Pierce Drive
Atlanta, Georgia 30322

Dr. John Herron
Chemical Sciences & Tech. Lab.
National Inst. of Standards and Technology
Gaithersburg, Maryland 20899

Dr. Jan R. Hessler
Chemistry Division
Argonne National Laboratory
9700 South Cass Ave.
Argonne, Illinois 60439

Dr. Jon T. Hougen
Molecular Physics Division
National Inst. of Standards and Technology
Gaithersburg, MD. 20899

Prof. Paul L. Houston
Baker Laboratory
Department of Chemistry
Cornell University
Ithaca, New York 14853-1301

Prof. Jack B. Howard
Dept. of Chemical Engineering
Massachusetts Institute of Technology
Cambridge, Massachusetts 02139

Prof. Philip M. Johnson
Department of Chemistry
State University of New York
Stony Brook, New York 11794

Prof. Harold Johnston
Chemical Sciences Division
Lawrence Berkeley Laboratory
University of California
Berkeley, California 94720

Prof. M. Kaufman
Department of Chemistry
Emory University
1515 Pierce Drive
Atlanta, Georgia 30322

Prof. Michael E. Kellman
Department of Chemistry
University of Oregon
Eugene, Oregon 97403

Prof. Ralph D. Kern, Jr.
Department of Chemistry
Lakefront Campus
University of New Orleans
New Orleans, Louisiana 70148

Prof. John H. Kiefer
Department of Chemical Engineering
University of Illinois at Chicago
Chicago, Illinois 60680

Dr. R. Bruce Klemm
Applied Sciences Department
Brookhaven National Laboratory
Upton, New York 11973

Dr. Michael L. Koszykowski
Combustion Research Facility
Sandia National Laboratory
Livermore, California 94551-0609

Dr. Andrew Kung
Chemical Sciences Division
Lawrence Berkeley Laboratory
University of California
Berkeley, California 94720

Dr. Allan H. Laufer
ER-141 GTN
Chemical Sciences Division G-236
U.S. Department of Energy
Washington, D.C. 20585

Prof. Yuan T. Lee
Materials and Chemical Sciences Div.
Lawrence Berkeley Laboratory
University of California
Berkeley, California 94720

Prof. Stephen R. Leone
Department of Chemistry
University of Colorado
Campus Box 215
Boulder, Colorado 80309

Prof. Marsha I. Lester
Department of Chemistry
University of Pennsylvania
231 South 34th Street
Philadelphia, Pennsylvania 19104

Prof. William A. Lester, Jr.
Materials and Chemical Sciences Div.
Lawrence Berkeley Laboratory
University of California
Berkeley, California 94720

Prof. Paul A. Libby
Dept. of Applied Mechanics and Engineering Sciences.
University of California, San Diego
La Jolla, California 92093-0023

Prof. John C. Light
The James Franck Institute
University of Chicago
5640 Ellis Avenue
Chicago, Illinois 60637

Prof. Ming-Chang Lin
Department of Chemistry
Emory University
1515 Pierce Drive
Atlanta, Georgia 30322

Prof. Marshall B. Long
Dept. of Mechanical Engineering
Yale University
P.O. Box 1504A Yale Station
New Haven, Connecticut 06511

Dr. David Mann
Army Research
Office Research
Triangle Park, NC 27709-2211

Dr. Peter Mattern
Combustion Research Facility
Sandia National Laboratories
Livermore, California 94551-0969

Dr. J. R. McDonald
Code 6110
Naval Research Laboratory
Washington, D.C. 20375-5000

Dr. Joseph V. Michael
Chemistry Division
Argonne National Laboratory
9700 South Cass Avenue
Argonne, Illinois 60439

Dr. James A. Miller
Combustion Chemistry Div. 8353
Combustion Research Facility
Sandia National Laboratory
Livermore, California 94551-0609

Dr. Richard Miller
Power Branch Office of Naval Research
800 North Quincy Street
Arlington, VA 22217-5000

Prof. William H. Miller
Materials and Chemical Sciences Div.
Lawrence Berkeley Laboratory
University of California
Berkeley, California 94720

Prof. C. Bradley Moore
Materials and Chemical Sciences Div.
Lawrence Berkeley Laboratory
University of California
Berkeley, California 94720

Dr. James T. Muckerman
Chemistry Department
Brookhaven National Laboratory
Upton, New York 11973

Dr. Herbert H. Nelson
Code 6111
Naval Research Laboratory
Washington, DC 20375-5000

Prof. Daniel M. Neumark
Materials & Chemical Sciences Div.
Lawrence Berkeley Laboratory
University of California
Berkeley, California 94720

Prof. Cheuk-Yiu Ng
Inst. for Phys. Research & Tech.
Ames Laboratory
Iowa State University
Ames, Iowa 50011-3020

Dr. Phil H. Paul
Combustion Research Facility
Sandia National Laboratory
Livermore, California 94551-0609

Prof. David S. Perry
Department of Chemistry
University of Akron
Akron, Ohio 44325

Dr. William J. Pitz
L-298 Lawrence Livermore National Laboratory
P.O. Box 808
Livermore, California 94550

Prof. Stephen B. Pope
Dept. of Mech. & Aerospace Eng.
106 Upson Hall
Cornell University
Ithaca, New York 14853

Dr. Jack M. Preses
Chemistry Department
Brookhaven National Laboratory
Upton, New York 11973

Prof. Herschel A. Rabitz
Department of Chemistry
Princeton University
Princeton, New Jersey 08544

Dr. Larry Rahn
Combustion Research Facility
Sandia National Laboratory
Livermore, California 94551-0609

Dr. A. R. Ravishankara R/E/AL2
National Oceanic & Atmospheric Administration
325 Broadway
Boulder, CO 80303

Prof. Hanna Reisler
Department of Chemistry
University of Southern California
Los Angeles, California 90089-0484

Prof. Thomas R. Rizzo
Department of Chemistry
University of Rochester
River Station
Rochester, New York 14627

Dr. Eric A. Rohlfing
Combustion Research Facility
Sandia National Laboratory
Livermore, California 94551-0609

Prof. Klaus Ruedenberg
Inst. for Phys. Research & Tech.
Ames Laboratory
Iowa State University
Ames, Iowa 50011-3020

Dr. Branko Ruscic
Chemistry Division
Argonne National Laboratory
9700 South Cass Avenue
Argonne, Illinois 60439

Prof. Henry F. Schaefer, III
Department of Chemistry
University of Georgia
Athens, Georgia 30602

Prof. George C. Schatz
Department of Chemistry
Northwestern University
2145 Sheridan Road
Evanston, Illinois 60201

Dr. Thomas M. Sebestyen
Advanced Propulsion Div., CE-322
Trnsprt. Tech., Cnsrvtn & Rnw. Enregy. Office
U.S. Department of Energy
Washington, DC 20585

Dr. Robert V. Serauskas
Physical Sciences Department
Gas Research Institute
8600 West Bryn Mawr Avenue
Chicago, Illinois 60631

Dr. Robert Shaw
Army Research Office
Research Triangle Park, NC 27709-2211

Dr. Ron Shepard
Chemistry Division
Argonne National Laboratory
9700 South Cass Ave.
Argonne, Illinois 60439

Prof. Robert Silbey
Department of Chemistry
Massachusetts Institute of Technology
Cambridge, Massachusetts 02139

Prof. Mitchell Smooke
Dept. of Mechanical Engineering
Yale University
P.O. Box 1504A Yale Station
New Haven, Connecticut 06511

Dr. Kermit Smyth
Center for Fire Research
B258 Polymers Building
National Inst. of Standards and Tech.
Gaithersburg, Maryland 20899

Dr. Leon M. Stock
Director, Chemistry Division
Argonne National Laboratory
9700 South Cass Avenue
Argonne, Illinois 60439

Dr. James Sutherland
Applied Sciences Department
Brookhaven National Laboratory
Upton, New York 11973

Dr. Norman Sutin
Chemistry Department
Brookhaven National Laboratory
Upton, NY 11973

Dr. Donald W. Sweeney
Reacting Flow Division 8351
Combustion Research Facility
Sandia National Laboratories
Livermore, California 94551-0609

Prof. Lawrence Talbot
Applied Sciences Division
Lawrence Berkeley Laboratory
University of California
Berkeley, California 94720

Prof. Patrick Thaddeus
Division of Applied Sciences
Pierce Hall 107C
Harvard University
Cambridge, Massachusetts 02138

Dr. Julian M. Tishkoff
Aerospace Sciences
Air Force Office of Scientific Rsrch.
Bolling Air Force Base
Washington, DC 20332-6448

Dr. Jurgen Troe
Institute für Physikalische Chemie
Universität Göttingen
Tammannstraße 6
D-3400 Göttingen GERMANY

Prof. Donald G. Truhlar
Department of Chemistry
University of Minnesota
Minneapolis, Minnesota 55455

Dr. Wing Tsang
Chemical Sciences & Tech. Lab.
National Inst. of Standards and
Technology
Gaithersburg, Maryland 20899

Dr. Frank P. Tully
Combustion Research Facility
Sandia National Laboratory
Livermore, California 94551-0609

Prof. James J. Valentini
Department of Chemistry
Columbia University
116th Street and Broadway
New York, New York 10027

Dr. Albert F. Wagner
Chemistry Division
Argonne National Laboratory
9700 South Cass Ave.
Argonne, Illinois 60439

Dr. Charles Westbrook
L-298 Lawrence Livermore National
Laboratory
P.O. Box 808
Livermore, California 94550

Prof. Phillip R. Westmoreland
Dept. of Chemical Engineering
University of Massachusetts
Amherst, Massachusetts 01003

Dr. Ralph E. Weston
Chemistry Department
Brookhaven National Laboratory
Upton, Long Island, N.Y. 11973

Prof. Curt Wittig
Department of Chemistry
University of Southern California
Los Angeles, California 90089-0484

Dr. Francis J. Wodarczyk
Chemistry Division
Experimental Physical Chem. Prgrm.
National Science Foundation
Washington, DC 20550

Prof. David R. Yarkony
Department of Chemistry
Johns Hopkins University
34th & Charles Streets
Baltimore, Maryland 21218

LAWRENCE BERKELEY LABORATORY
UNIVERSITY OF CALIFORNIA
TECHNICAL INFORMATION DEPARTMENT
BERKELEY, CALIFORNIA 94720